ST. ANNE'S

COLLEGE OF ENGINEERING AND TECHNOLOGY

(Approved by AICTE, Affiliated to Anna University, Chennai)
Anguchettypalayam, Panruti Taluk - 607 110, Cuddalore Dist.

NCRDSET '17

25th February 2017

Volume - I

PROCEEDINGS OF THE 3RD NATIONAL CONFERENCE ON RESEARCH AND DEVELOPMENT IN SCIENCE, ENGINEERING AND TECHNOLOGY

sponsored by

Indian Society for Technical Education

Proceedings of

ISTE sponsored

3rd National Conference on Research and Development in Science, Engineering and Technology

NCRDSET '17

(Volume I)

25th February 2017

Organised by

St. Anne's College of Engineering and Technology

Anguchettypalayam, Panruti – 607110.

PREFACE

We are very pleased to introduce the proceedings of the Third National Conference on Research and Development in Science, Engineering and Technology (NCRDSET '17). The Conference provided a setting for discussing recent developments in a wide variety of topics. The Conference has been a good opportunity for participants coming from various institutions to present and discuss topics in their respective research areas.

This proceeding has been spitted into two volumes one for Branches dealing with circuitry and other non- circuitry viz., circuitry will contains papers in the field of Electrical, Electronics and communications and Non-Circuitry is complied in the area of Computer Science, Mechanical, Civil and Applied Sciences.

This volume of Proceedings for Branches dealing with Circuitry will help the readers in various topics of embedded systems, IOT, power systems, power electronics converters and inverters, simplified and advanced modules of Image and signal processing and many more areas of their respective fields. The level of interest in the subject matter of the conference was maintained from previous events and over 70 suitable papers were submitted for presentation at the conference in this volume. This required the programme to be organized in two parallel sessions, each on a specific theme, to provide each paper with sufficient time for presentation and to accommodate all of them within the overall time allocated.

Finally, it is appropriate that we record our thanks to our fellow members of the Technical Organizing Committee for their work in securing a substantial input of papers in encouraging participation from all over the nation. We are also indebted to those who served as Session Chair persons. Without their support, the Conference could not have been the success that it was. We also acknowledge the authors themselves, without whose expert input there would have been no conference.

V.C. EUGIN MARTIN RAJ
Convenor - NCRDSET'17

25th February 2017

ORGANISING COMMITTEE

CHIEF PATRON

Rev. Sr. Victoria, S.A.T
Secretary
St. Anne's College of Engineering and Technology

PATRON

Dr. R. Arokiadass, M.E., Ph.D.,
Principal
St. Anne's College of Engineering and Technology

CO - PATRON

Sr. Gnana Jency Salate Mary, S.A.T
Vice Principal
St. Anne's College of Engineering and Technology

CONVENOR

Mr. V.C. Eugin Martin Raj,
Assistant Professor & Head
Department of Electrical and Electronics Engineering

CO - CONVENORS

Mr. D. Ommurugadasan,
Associate Professor & Head
Department of Mechanical Engineering

Sr. Anita,
Assistant Professor & Head
Department of Electronics and Communication Engineering

Mrs. D. Pauline Freeda,
Assistant Professor & Head
Department of Computer Science and Engineering

Sr. Avila Therese,
Assistant Professor & Head
Department of Science and Humanities

Prof. D. VELMURUGAN, Ph.D

(Off) 044-22300122
(Res) 044-23762085
(Mob) 98410 75847
E-mail: shirai2011@gmail.com

UGC-BSR Faculty
Centre of Advanced Study in Crystallography and Biophysics
UNIVERSITY OF MADRAS
Guindy Campus, Chennai – 600 025, INDIA

16th Feb 2017
Chennai

I am very much pleased to know that St.Anne's College of Engineering and Technology, Anguchetty palayam , Panruti Taluk is organising the ISTE sponsored 3rd National Conference on Research and Development in Science , Engineering and Technology. R&D in an extraordinary way in the above three areas will definitely lead our country to great heights. The recent launching of 104 satellites through a single rocket shows the capabilities of our Indian Scientists and Engineers and we get the appreciation in global level. Most of the IT industries abroad depend on the talented Indians who work for them from within their countries or from India and most of them are engineering graduates. Even though the college has so far produced only three batches of Engineers , some students in the past obtained university rankings. This clearly proves not only the hard working skills and intelligence of the students from this college but also the training / teaching they received from the able teachers. I wish great success to the Institution and good luck to the students.

(Prof. D. VELMURUGAN)

MESSAGE FROM SECRETARY'S DESK

It gives me immense pleasure that our college St. Anne's College of Engineering and Technology is organizing the 3rd.National Conference on RESEARCH AND DEVELOPMENT IN SCIENCE, ENGINEERING AND TECHNOLOGY [NCRDSET '17] on 25th February 2017. We hope that this small step taken by our college will open up a new horizon.

Engineering and Technology in Research and development is an integral part that helps to understand and provide a fruitful interaction among dynamic research scholars, faculty members and students to disseminate the awareness of the recent developments and latest trends in the field of Science, Engineering and Technology.

I appreciate the consistent effort of NCRDSET'17 to explore new areas of research and dissemination of new ideas, knowledge and technologies covering varied sectors including the Engineering sector. This conference can play an important role to create awareness and will create a platform for making interaction with faculty members and students.

I express my sincere gratitude to all the authors, speakers, committee members, reviewers, sponsors, advisers and other members whose sincere efforts are the key factors for the success of this conference. I appreciate feedback from all the participants. I wish all the success of NCRDSET'17.

Finally, I would like to convey my special thanks to the principal Dr. R. Arokiadass and his powerful team of organizing committee.

I wish the conference a great success.

Sr. Victoria, S.A.T.

Secretary

St. Anne's College of Engineering and Technology

MESSAGE FROM PRINCIPAL'S DESK

I am very glad that our College is organizing a 3rd National Conference on "Research and Development in Science, Engineering and Technology" on February 25, 2017.

I believe the Conference would assuredly support everyone to have the latest updates and progress achieved by the technology development. The conference will provide a platform for academician, researcher, entrepreneur, industrialist and various other professionals to exchange their innovative ideas for the development of self, society and nation.

The gathering will motivate the innovators to enlighten and sharpen their skills and competence and enhance human network and relationship.

My heartfelt wishes to HOD's, staff members and students of our College for their efforts in organizing and participating in this conference.

I wish the conference a grand success.

Dr.R. Arokiadass, M.E., Ph.D.,

Principal

St. Anne's College of Engineering and Technology

MESSAGE FROM VICE-PRINCIPAL

Necessity is the mother of all Invention.

From the beginning of time, humans everywhere have been inventing. In fact, most of what is around us now was invented by someone in the past. An open and curious mind allows an inventor to see beyond what is known. Seeing a new possibility, connection, or relationship can spark an invention. I believe that, this Third National Conference in Research and Development in Science, Engineering & Technology (NCRDSET'17) will explore the research dimensions and thought process on a platform of Intellect and bring quality in academics as well as research and Development. Also this program will be an excellent opportunity for Academicians, Researchers and Students to present their research findings and inventions from different fields. I welcome all the participants and congratulate them for their participation. I also congratulate the organizing committee of this conference and wish them all the success.

"The Lord bless you and keep you; the Lord make his face to shine upon you and be gracious to you." (Numbers 6:24-25)

Sr. Gnana Jency Salate Mary, S.A.T.

Vice Principal

St. Anne's College of Engineering and Technology

TABLE OF CONTENT

33	Power Demand Controller	Mr.K.Veeraragavan	150
34	Performance evaluation of pi Controller based DC-DC resonant converter	Mr.N.Madhanakkumar Mr.P.Mohan	154
35	Design of Dual Proportional Integral Load Frequency Controllers Based on Gravitational Search Algorithm for Nonlinear Hydrothermal Power System	Mrs.S.Lese	157
36	UPQC with fuzzy logic for power quality improvement	Dr.N.Muralikrishnan Ms.G.Sivasankari,	162
37	Asymmetric Three Phase Multilevel Inverter Topologies for Variable Frequency PWM	Mr.Subash Mr.Sasikumar	165
38	Solar Powered Sensor Base Irrigation System With Automatic Control Of Pump	Mr.D.Prabhakaran	169
39	Spectrum Profitability based Channel Allocation for reducing system overhead in Cognitive Radio	Mrs. M. Vaidehi Mrs. D. Umamaheshwari Ms. Mary Amala Jenni	172
40	Implementation of Portable and Economical Real-Time EEG Signal Acquisition System Based on DSP	Mrs. D.Umamaheswari Ms. Mary Amala Jenni Ms. Devika	175
41	Automatic Clothing Pattern Recognition Based on SIFT	Ms.Revathi Jayakumar Ms.S.K.Suriya Ms.C.Adithya	179
42	Android Application for Detection of Plant Syndrome Using Image Processing Techniques	Ms.S.K.Suriya Ms.C.Adithiya Mrs.C.Suganya	183
43	Hardware implementation of iris recognition system based on DSP	Mr.G.Mahendiran Mr.R.Radhakrishnan	189
44	Robotic arm for Pick Place Operation Using Matlab based on offline surface clustering algorithm	Mr.R.Srinivasan Miss.L.Saranya Miss.V. Priyadharshini	191
45	VLSI Design of High Speed Vedic Multiplier for FPGA Implementation	Mr V.Venkatesan Mr R.Radhakrishnan Mr G. Mahindran	195
46	Efficient utilization of electricals In a forum by analyzing the human Movements	Mr D.Kishore	198
47	Implementation Of Weed Detection System With Herbicide Sprayer Robot	Mr.A.Kumaraswamy Mr.S.Logesh	200
48	Daytime Brake Light Detection System Using Monocular Vision	Mr. A.Kumaraswamy Mr.A.C.B.Yokesh Raj	202
49	A Hysteresis Comparator With Voltage Level Shifter Using Current Generators	Mrs. N Saraswathi Mr.Athira Dominic Mr. Mayank Kumar singh Mr.Thejus Raj H	204
50	A wearable patient health Monitoring system using iot	Mr P.Tamilselvan Mr T.Rahul	209
51	Diagnosis of Parkinsons Disease Using Retina Model	Ms R.Vino Ms R.Bhuvana Ms A.Puviarasi	212

Improved Rear Surface Passivation of Cu(In,Ga)Se2 Solar Cells: A Combination of an Al2O3 Rear Surface Passivation Layer and Nanosized Local Rear Point Contacts

Mr.M.Venkatesh
Assistant professor
Department of Electrical and Electronics Engineering
ACT COLLEGE OF ENGINEERING AND TECHNOLOGY .CHENGALPAT

***Abstract*—An innovative rear contacting structure for copper indium gallium (di) selenide (CIGS) thin-film solar cells is developed in an industrially viable way and demonstrated in tangible devices. The idea stems from the silicon (Si) industry, where rear surface passivation layers are combined with micron-sized local point contacts to boost the open-circuit voltage (VO C) and, hence, cell efficiency. However, compared with Si solar cells, CIGS solar cell minority carrier diffusion lengths are several orders lower in magnitude. Therefore, the proposed CIGS cell design reduces rear surface recombination by combining a rear surface passivation layer and nanosized local point contacts. Atomic layer deposition of Al2 O3 is used to passivate the CIGS surface and the formation of nanosphere-shaped precipitates in chemical bath deposition of CdS to generate nanosized point contact openings. The manufactured Al2 O3 rear surface passivated CIGS solar cells with nanosized local rear point contacts show a significant improvement in VO C compared with unpassivated reference cells.**

Index TermsAl2 O3 , atomic layer deposition, copper indium gallium selenide (CIGS), Cu(In,Ga)Se2 , Ga grading, nanosized, passivated emitter, passivated emitter and rear cell (PERC), pho-tovoltaics, point contact openings rear locally diffused cell (PERL), rear surface passivation, Si, solar cells, thin film.

I. INTRODUCTION

T present, rear surface recombination in highly efficient Acopper indium gallium (di)selenide (CIGS) solar cells is limited by using Ga grading to create a back surface field (BSF). World record conversion efficiencies (Eff.) of lab-scale CIGS so-lar cells are around 20%. Some recent outstanding examples are

1) the Japanese thin film manufacturer Solar Frontier, claiming a cadmium-free CIGS solar cell efficiency record of 19.7%, and 2) the Swiss Federal Laboratories for Materials Science and

Technology (EMPA), who have announced a thin-film CIGS solar cell record of 20.4% on a flexible polymer substrate [1][5]. These high efficiencies are achieved by varying the [Ga]/([Ga]+[In]) ratio to obtain different band gaps at different depths in the CIGS film. To reduce rear surface recombination, an increase of this ratio and, thus, bandgap toward the Mo back contact is a standard practice [6]. See, e.g., Fig. 1, which shows a scanning electron microscopy (SEM) cross section of a Mo/CIGS structure (produced adjacent to a 20.0% CIGS solar cell) fabricated by increasing the [Ga]/([Ga]+[In]) ratio toward the Mo/CIGS rear interface [4]. This gradient causes a quasi-electrical BSF that keeps the minority charge carriers away from the Mo/CIGS interface, and effectively reduces rear surface re-combination [6].

In Si solar cell manufacturing, the present-day workhorse is the full aluminum (Al) BSF p-type silicon (Si) solar cell, whose rear structure is very comparable with those high-efficient CIGS cells. Fig. 2(a) represents a sketch of such a traditional full Al BSF cell. At the rear Al/Si interface, a BSF is formed thanks to a highly Al-doped p+ region. In addition, in this case, the purpose of this BSF is to keep photo-electrons

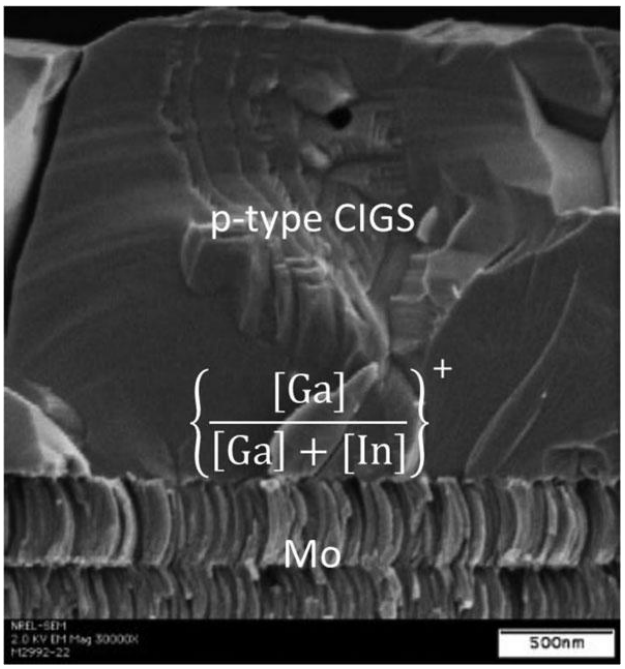

Fig. 1. SEM cross-section picture of a Mo/CIGS structure with a cell efficiency potential of 20.0% (taken from [4]).

away from the metal/semiconductor (Al/Si) interface and, as a result, to reduce rear surface recombination [7].

Nevertheless, more advanced passivated emitter and rear cell (PERC) and analogous cell designs are on their way to substitute conventional aluminum Al BSF Si solar cells [8][10]. Fig. 2(b) represents a sketch of this alternative PERC [7]. As can be seen,

with respect to a conventional Al BSF solar cell production line, only a few extra steps are needed to introduce PERC processing: single-side texturing, local diffusion technologies, passivation layer deposition, and passivation layer opening. The potential of this more advanced cell processing is exposed by referring to the 25% world record cell conversion efficiency for single-junction Si solar cells as this record is achieved applying the passivated emitter, rear locally diffused cell (PERL) design, which is a PERC combined with locally diffused rear point contacts [1], [11].

Compared with conventional Al BSF processing, the rear of those advanced Si cell designs (PERC/PERL) is improved by a combination of an adequate rear surface passivation layer and micron-sized local point contactsas shown in Fig. 2(b). Such

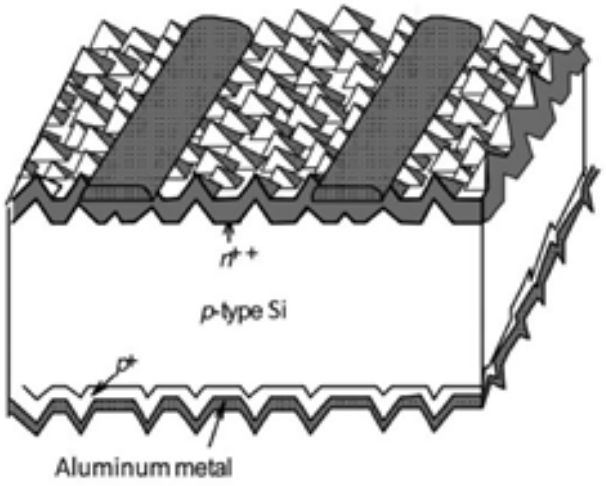

Fig. 2. the conventional full Al back surface field p-type Si solar cell

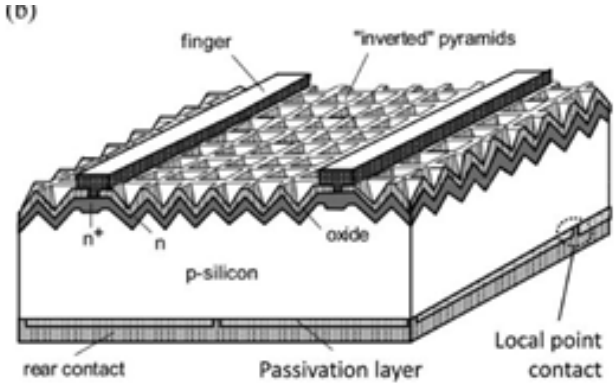

Fig. 3. the passivated emitter and rear p-type Si solar cell (taken from [7]

a passivition layer combines two passivation mechanisms: 1) chemical passivationa low density of interface defects Dit and 2) field-effect passivationcaused by a high density of fixed charges within the passivation layer. Roughly said, the point con-tact opening diameter has to be on the order of 50 to 200 m, with a distance of 400 to 1600 m between contact openings, as the minority carrier diffusion length Ln in industrial p-type Si wafers is in the order of 200 to 800 mdepending on Si material quality and the doping level [8][10], [12]. Characteristic surface passivation layers for p-type Si are a combination of alu-minum oxide (Al2 O3), silicon oxide (SiO2), and hydrogenated silicon nitride (SiNx :H)

are generated industrially by applying laser technology and rep-resent 2 to 5% of the total rear surface area [8][10], [15][17].

Those rear surface passivation technologies are cost-effective for Si solar industry. They increase cell efficiency and allow the use of ever thinner wafers (resulting in a reduction in material cost), by improvements in rear surface passivation and rear inter-nal reflection. In the case of standard full Al BSF solar cells, the rear surface recombination velocity Sb and rear internal reflec-tion Rb generally are in the order of 1 104 to 1 106 cm/s and 60 to 70%, respectively. Unfortunately, this means that for full Al BSF cells a reduction in wafer thickness will decrease cell ef-ficiency, because of 1) a raise in surface recombinationdue to an increased surface-to-volume ratio combined with insufficient surface passivation and 2) a loss in absorptiondue to thinner cells combined with low rear internal reflection. Rear surface passivated cell designs, on the other hand, lead to Sb as low as 1 102 cm/s and Rb above 85% and, hence, enhanced cell efficiencies for thinner Si wafers [8], [14], [18], [19]. Typically, short-circuit current JS C is increased slightly due to higher Rb , while the fill factor FF is reduced somewhat due to more challenging contacting schemes. Nevertheless, due to an absolute improvement in rear surface passivation the open-circuit volt-

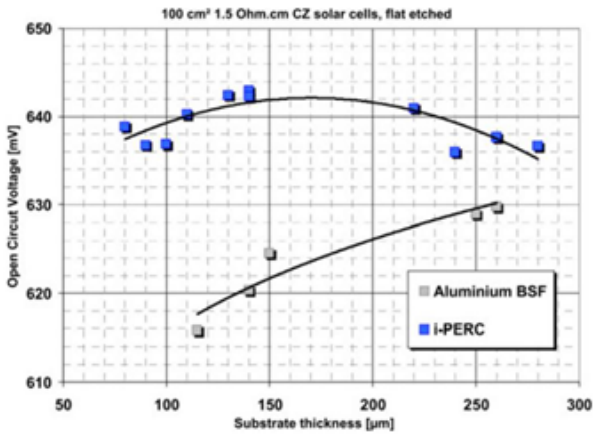

Fig. 4. Comparison of open-circuit voltages as a function of Si substrate thickness for ( ) rear surface passivated industrial PERC (i-PERC) cells and ( ) standard full Al BSF reference cells (taken from [20]).

age VO C is enhanced significantly. See, for example, Fig. 3, which compares VO C of rear surface passivated i-PERC Si solar cells with standard full Al BSF cells as a function of Si wafer thickness [20]. Practically speaking, 300-m-thick standard Al BSF Si solar cells can be substituted by more efficient rear sur-face passivated cells with a thickness between 100 and 200 m.

Therefore, the purpose of this study is to assess the potential of these rear surface passivation technologies in CIGS solar cells. As for Al BSF Si cells, the Mo/CIGS rear surface of normal Ga-graded CIGS cells is known to show high Sb (also between 1 104 and 1 106 cm/s [21][23]) and low Rb (see the next section for Rb as a function of wavelength for the Mo/CIGS interface). Hence, analogous to Si PERC, the proposed cell design combines a rear surface passivation layer and local rear point contacts (LRPC), enabling reduced back contact recombination and, thus, higher efficienciesparticularly for ever thinner CIGS absorber layers. However, thin film solar cells are known to have very short minority carrier lifetimes, which means that LRPC for rear passivated CIGS cells require to be nanosized and closely spaced. Assuming that Ln between 0.75 and 1.50 m is feasible [24], [25], the contact openings targeted are between 200 and 400 nm in diameter with internal spacing between 1.5 and 3.0 m, as scaled from the Si PERC design and keeping the contacting area between 2 and 5% of the total rear surface area. Fig. 4 shows a graphical representation of this proposed cell design.

This novel rear contacting structure for CIGS solar cells is developed in an industrially viable way and its improvement compared with state-of-the-art reference cellsis demonstrated in tangible devices as a function of CIGS absorber layer thickness.

II. METHODOLOGY

The formation and subsequent removal of spherical particles (so-called colloids or precipitates) in chemical bath deposition (CBD) of CdS is applied to generate nanosized point contacts.

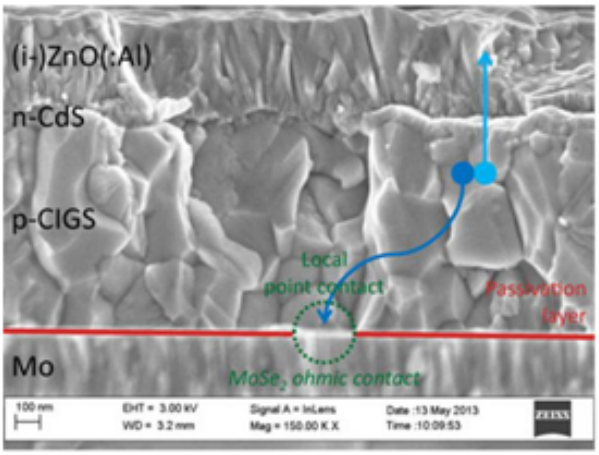

Fig. 5. Proposed CIGS solar cell design to reduce back contact recombination, by combining a rear surface passivation layer and local rear point contacts.

In this study, standard CBD CdS is grown in a solution with 1.136 M ammonia, 0.100 M thiourea, and 0.003 M cadmium acetate, at 60 C. However, to obtain particle-rich CdS deposition conditions, an alternative approach is required: 1) After preparing the CBD solution, soda lime glass (SLG)/Mo substrates are only immersed when the CBD solution reacted for X minduring which time CdS nanoparticles are formed within the solution [26]. 2) Thereafter, the substrates are dipped for Y min, and a thin particle-rich CdS film is grown. By varying time intervals X and Y the particle-density can be varied. Fig. 5 shows top-view SEM pictures of thin particle-rich CdS layers deposited on SLG/Mo substrates before and after removal of these particles [27]; in this case, both X and Y equal 4 min, and an extra layer of CdS is grown to intensify the contrast in Fig. 5(b). Particle removal is established in various ways: via 1) ultrasonic agitation, 2) dry ice (liquid CO2) cleaning, or 3) mechanical wiping. Using numerous SEM measurements, an average particle diameter of 285 30 nm and average point.

opening diameter of 220 25 nm is calculated. In conclusion, to actually create nanosized point openings in rear surface

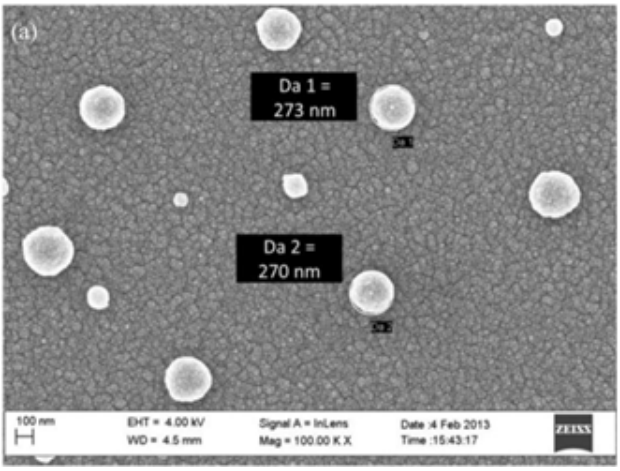

Fig. 6. a particle-rich CdS layer grown on a SLG/Mo substrate

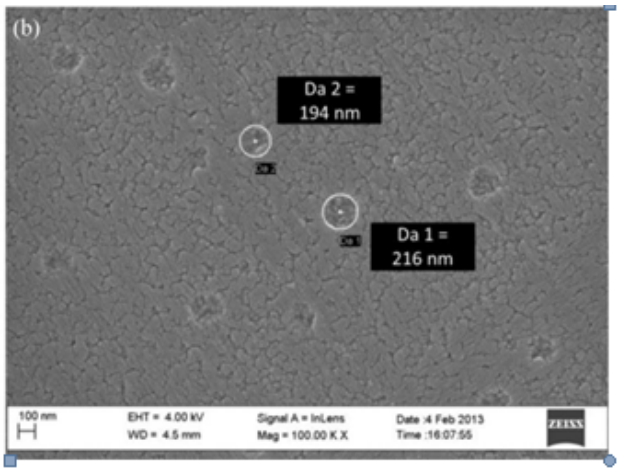

Fig. 7. a particle-rich CdS layer grown on a SLG/Mo substrate

pas-sivation layers for CIGS, the passivation layer is 1) first grown on this particle-rich CdS layer, and 2) subsequently, the particles are removed. This way, a passivation layer with nanosized point openings having a diameter around 220 nm is obtained.

Atomic layer deposition (ALD) of Al2 O3 is applied as CIGS surface passivation layer. In this study, ALD Al2 O3 passiva-tion layers are deposited in a temporal ALD reactor at 300 C, using trimethylaluminum (TMA) and an oxygen source (both water (H2 O) and ozone (O3) are used) as precursors [28]. Pre-viously, Al2 O3 is verified to be an adequate CIGS surface passivation layer, thanks to its 1) chemical passivationfirst principles calculations indicate that the deposition of Al2 O3 re-duces about 35% of the interface defect densityand 2) field effect passivationAl2 O3 exhibits a large density of negative charges, causing a field effect that reduces the CIGS surface minority charge carrier concentration and, hence, passivates the interface effectively [23]. In the same work, an improvement of two orders in magnitude is reported for the integrated pho-toluminescence intensity of Al2 O3 passivated CIGS compared

with unpassivated CIGS. Hence, a significant reduction in Sb is expected for Al2 O3 passivated CIGS surfaces compared with standard Mo/CIGS surfaces. To also have an idea about its opti-cal confinement, Rb at the Mo/(CdS/)Al2 O3 /CIGS interface is calculated as in [29]; applying thickness, refractive index and extinction coefficient of the Al2 O3 layer as mea-sured on an Si substrate using spectrally resolved ellipsometry. In Fig. 6, Rb is depicted as a function of long wavelength and Al2 O3 layer thickness in the case of a Mo/(CdS/)Al2 O3 /CIGS structure. This shows thatcompared with the standard Mo/CIGS interface (equivalent to an Al2 O3 layer thickness of 0 nm)applying a thin layer (e.g., 5 nm) of Al2 O3 as rear surface passivation increases Rb only slightly, while a thicker Al2 O3 layer (e.g., 50 nm) leads to a larger Rb enhancement.

Ungraded CIGS absorber layers are used [30] 1) to allow eval-uation of an obvious improvement in VO C if rear surface passiva-tion is enhanced and 2) to exclude any other surface passivation effects. CIGS layers are deposited in a high-vacuum chamber equipped with open-boat evaporation sources, while evaporation rates are monitored using a mass spectrometer. During CIGS growth, the maximum substrate temperature is 540 C; Se is evaporated in excess; and constant rates of Cu, In, and Ga are ap-plied until a desired CIGS thickness is reached. All studied sam-ples have compositional values of [Cu]/([Ga] + [In]) = 0.90 0.02 and [Ga]/([Ga] + [In]) = 0.30 0.01, which are calculated from X-ray fluorescence (XRF) measurements. CIGS film thick-nesses are measured with a profilometer and are varied between 0.48 0.02 and 1.58 0.04 m. These flat-evaporation-rate-CIGS absorbers with uniform low Ga concentration are fa-vored to assess rear surface passivation, because of their high reproducibility, their characteristic high Ln [24], and to exclude complementary rear surface passivation effects (e.g., a quasi-electrical field created by a Ga gradient causing a slope in the conduction bandas is the case in standard high-efficient CIGS cells). This approach leads to cell efficiencies below 16.5%, but allows an evident boost in solar cell characterization results if the advanced CIGS cell design functions.

Table I gives an overview of all steps required to fabricate rear surface passivated CIGS solar cells with nanosized LRPC. A detailed description of standard CIGS solar cell processing at the Angstrom Solar Center can be found in [31], i.e., excluding the ungraded absorber layer formation and the advanced back contact design. The starting substrate is low-

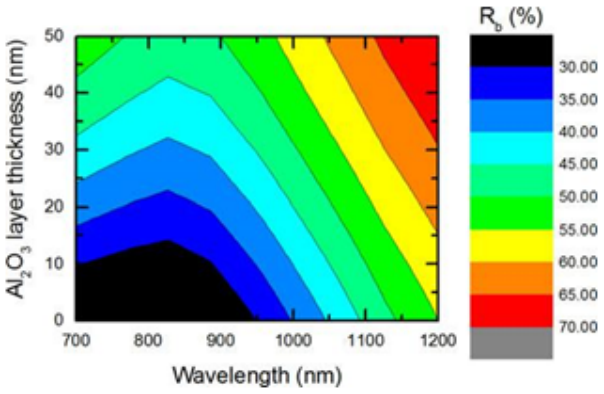

Fig. 8. . Calculated rear internal reflection as a function of wavelength and Al2 O3 layer thickness for a Mo/(CdS/)Al2 O3 /CIGS device.

TABLE I
OVERVIEW OF ALL STEPS REQUIRED TO FABRICATE AL_2 O_3 REAR SURFACE PASSIVATED CIGS SOLAR CELLS WITH NANO-SIZED LOCAL REAR POINT CONTACTS

Step	Description
0	Start: low-iron soda lime glass
1	Glass cleaning
2	Mo rear contact sputtering
3	Particle-rich CBD CdS deposition
4	ALD Al_2O_3 passivation deposition
5	CdS particle removal
6	Ungraded CIGS absorber co-evaporation
7	CBD CdS buffer deposition
8	(i-)ZnO(:Al) window sputtering
9	Ni/Al/Ni front contact evaporation
10	Mechanical scribing of 0.5 cm^2 solar cells

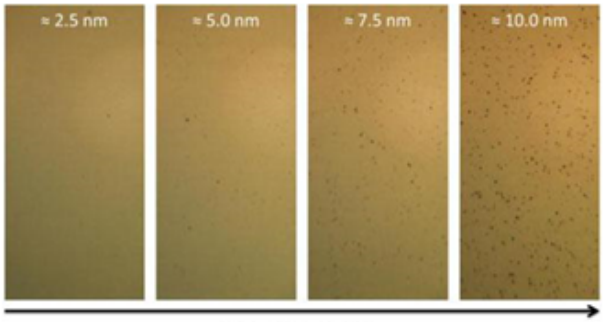

Fig. 9. Top-view optical microscopy pictures after particle removal of SLG/Mo/particle-rich-CdS/Al2 O3 samples as a function Al2 O3 layer thick-ness.

iron SLG with a thickness of 1 mm, which first undergoes a cleaning process. As back contact, a Mo layer is deposited in an inline sputtering system. It has a sheet resistance of 0.6 / and a typical thick-ness of 350 nm. The advanced back contact design combines an ALD Al2 O3 rear surface passivation layer and CBD of CdS to generate nanosized LRPC, as described previously. On top of this rear contact structure, an ungraded CIGS absorber layer of desired thickness is evaporated, al-sodescribed previously. The buffer layer is deposited using a standard CBD CdS process. Next, the shunt reducing intrinsic ZnO layer (i-ZnO) and, sub-sequently, the Al-doped ZnO (ZnO:Al) front contact of the cells are sputtered. As front contact grid, a Ni/Al/Ni stack is deposited by evaporation through a shadow mask. The (i-)ZnO(:Al) and Ni/Al/Ni stack have a total thickness around 400 and 3000 nm, respectively. Finally 0.5 cm2 solar cells are defined by mechan-ical scribing with a stylus. No antireflective coating is used.

Light JV measurements are performed at 25 C under standard AM1.5 G conditions in a home-made system with a tungsten halogen lamp, which is calibrated using a certified silicon photo diode [31].

III. RESULTS AND DISCUSSION

The proposed technique to create nanosized point openings in Al2 O3 passivation layersby removing spherical particles deposited by CBD CdSworks fine for Al2 O3 layers that are not too thick (5 nm). Fig. 7 depicts for various Al2 O3 thicknesses and top-view optical microscopy pictures of SLG/Mo

particle-rich-CdS/Al2 O3 structures after particle removal. These pictures show that for too-thick ALD Al2 O3 films (7.5 nm), the particle removal becomes unsatisfactory. The self-limiting nature of ALD reactions leads to an ideal growth control and the ability to coat high-aspect-ratio structures, as desired for the suggested point opening approach. However, these ALD advan-tages also mean that CdS nanoparticles embedded in too-thick Al2 O3 films become irremovable.

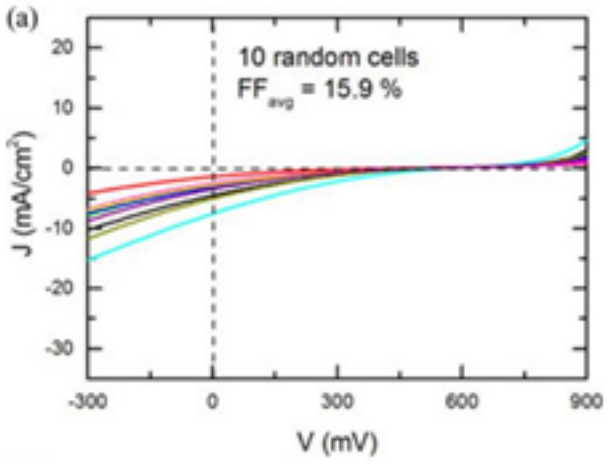

Fig. 10. Al2 O3 rear surface passivated CIGS solar cells without nanosized LRPC

Therefore, 5 nm of Al2 O3 has been used for all passivated cells with LRPC, which are described next.

Al2 O3 rear surface passivated CIGS solar cells require 1) LRPC for appropriate contacting and 2) extra supply of Nasince Al2 O3 layers act as a barrier for Na diffusion from the SLG substrate. Fig. 8(a) shows representative JV curves for ten random Al2 O3 rear surface passivated CIGS solar cells without LRPC. These cells have an average FF of 16%, which 1) proves that there is no appropriate back contacting with-out point contacts and 2) indicates that the passivation layer

is intact after CIGS processing. Fig. 8(b), on the other hand, shows representative JV curves for 10 random Al2 O3 rear surface passivated CIGS cells with nanosized LRPC. The average FF increases to 45%, higher compared with the cells without LRPC but still rather low. In addition, these JV curves show a roll-over effect, characteristic for devices lacking Na [32]. Note that 1) Al2 O3 films are known to be excellent gas dif-

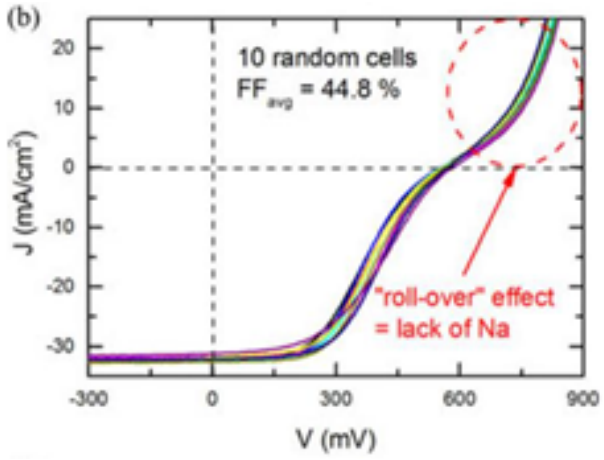

Fig. 11. Al2 O3 rear surface passivated CIGS cells with nanosized LRPC,

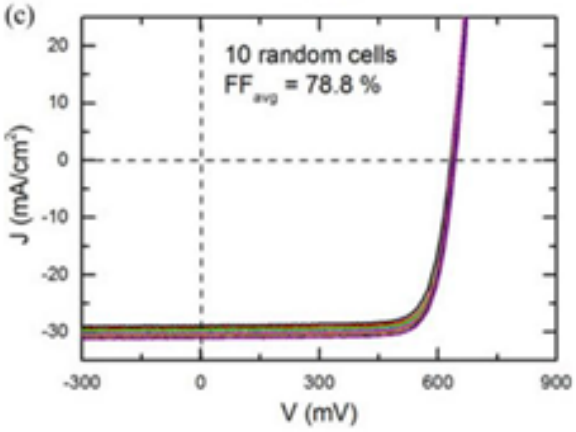

Fig. 12. Al2 O3 rear surface passivated CIGS cells having nanosized LRPC and an additional NaF layer evaporated on top of the Al2 O3 layer (after particle removal). In all examples, the Al2 O3 and CIGS layer thickness are around 5.0 nm and 1.58 m, respectively. In each case, 10 random JV curves are shown, and the average fill factor is given

fusion barriers [33] and that 2) this roll-over effect is not as pronounced as in Na-free cells [32]. Therefore, Fig. 8(c) shows

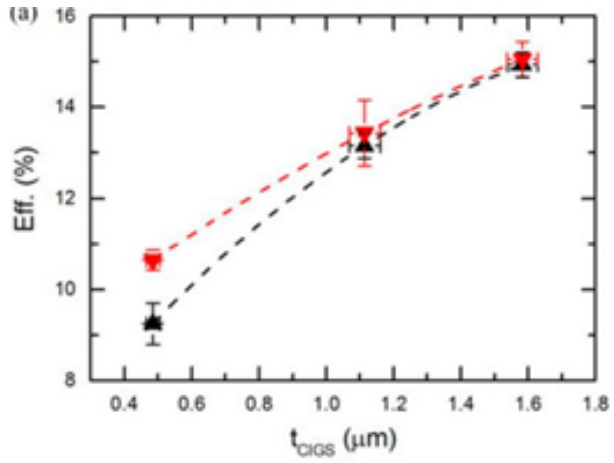

Fig. 13. cell conversion efficiency

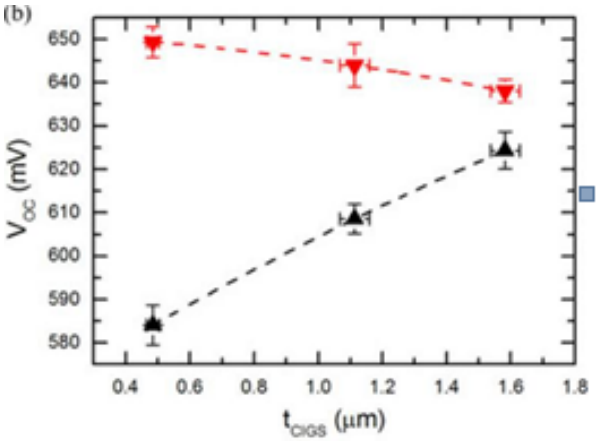

Fig. 14. open-circuit voltage

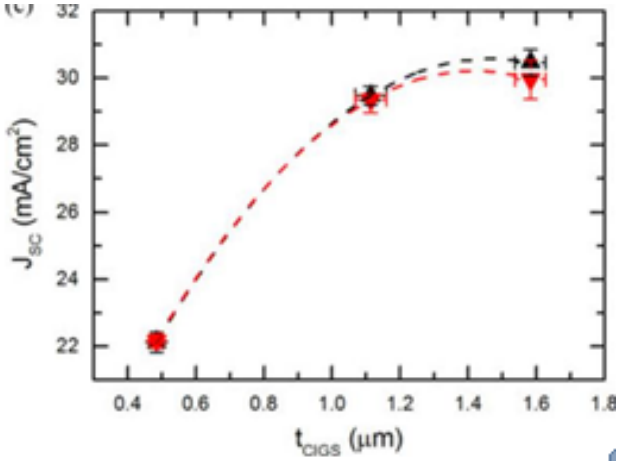

Fig. 15.) short-circuit current as a function of CIGS absorber layer thickness for Al2 O3 rear surface passivated CIGS solar cells having nanosized LRPC compared with unpassivated reference CIGS cells

representative JV curves for 10 random Al2 O3 rear surface passivated CIGS cells having LRPC andafter removal of the CdS nanoparticlesan additional NaF layer evaporated on top of this Al2 O3 layer. Fig. 8(c) proves that the low FFs in Fig. 8(b) are indeed caused by Al2 O3 acting as an Na diffusion barrier. Even more, the combination of LRPC and extra Na supply leads to a high average FF of 79%.

The rear surface of Al2 O3 rear surface passivated CIGS so-lar cells with nanosized LRPC are better passivated compared with unpassivated reference cells, which becomes more obvious in the case of thinner CIGS absorber layers. Fig. 9 shows the average 1) Eff., (b) VO C , and (c) JS C as a function of CIGS ab-sorber layer thickness for Al2 O3 rear surface passivated CIGS solar cells having nanosized LRPC and unpassivated reference CIGS cells. Note that for each CIGS thickness, the same op-timized NaF thickness is used for both the Al2 O3 passivated and the unpassivated reference cells. Fig. 9(a) shows that higher average efficiencies are measured for all the Al2 O3 rear passi-vated cells. In addition, the difference becomes more apparent for the thinnest CIGS layers. Fig. 9(b) demonstrates that this increase in efficiency is obtained thanks to an improvement in VO C for the Al2 O3 rear passivated cells. The most logical explanation for this increase in VO C is a significant enhance-ment in rear surface passivation (=lower Sb) for the Al2 O3 rear-passivated cells [23], [27]. This boost in surface passiva-tion becomes clearer for thinner CIGS absorber layers, as this well-passivated rear surface then gets closer to the space charge region of the cell. In addition, it is remarkable that this change in VO C as a function of absorber layer thickness for rear passivated compared with unpassivated cells is very similar to Fig. 3. Un-fortunately, the average JS C of the passivated and unpassivated cells is similar for all CIGS thicknesses, as seen in Fig. 9(c). This comparable behavior in JS C for passivated and unpassi-vated cells can be explained by a too-small improvement in Rb for only 5 nm of Al2 O3 as rear surface passivation layer, as already shown in Fig. 6.

IV. CONCLUSION AND OUTLOOK

For the first time, the concept of rear surface passivation as used in advanced Si cell technologies (PERC/PERL)is developed for and shown in industrially viable CIGS solar cells: 5 nm of ALD Al2 O3 is used to passivate the CIGS rear surface and the formation of nanosphere-shaped precipitates in CBD CdS to generate point contact openings. The same (VO C) be-havior is shown for rear surface passivated CIGS solar cells compared with unpassivated reference cells [see Fig. 9(b)] as for rear surface passivated Si solar cells compared unpassivated Si cells (see Fig. 3). Thanks to a significant improvement in rear surface passivation, an obvious increase in VO C is measured, especially for ever thinner CIGS absorber layers, as this well-passivated rear surface gets closer to the most active region of the cells.

However, more reflective rear surface passivation layers need to be integrated to increase JS C and, hence, efficiency, even fur-ther. As seen in Fig. 6, 5 nm of ALD Al2 O3 increases

Rb only slightly compared with the referential Mo/CIGS rear interface. Therefore, the focus is now on integrating thicker passivation layers to combine improved rear surface passivation with en-

hanced optical confinement. For that reason, research is ongoing to 1) combine Al2 O3 rear surface passivation with other point contact opening approaches (lithography, laser ablation) or 2) combine the CBD CdS proposed technique to create nanosized point openings with other CIGS passivation layer candidates. The final target iscompared with unpassivated state-of-the-art CIGS solar cells of normal thicknessto develop CIGS cells having improved rear surface passivation and rear internal re-flection, leading to a substantial increase in cell efficiency, even for thinner CIGS absorber layers.

REFERENCES

[1] Onslow A.M.I.E.E.. *Electrical engineers data books (vol. one) lighting, traction and power distribution. Volume compiled*,publishers Ernest Benn ltd, 8 Boverie Street, London. Published 1925.

Monitoring and Controlling of Distribution Transformer Using PLC

Preetheepa. D
UG Scholar
Department of Electrical and Electronics Engineering
IFET College of Engineering, Villupuram.

Priya.S
UG Scholar
Department of Electrical and Electronics Engineering
IFET College of Engineering, Villupuram.

***Abstract*—The Embedded system is designed and developed for monitoring and controlling electrical appliance mainly Transformers using PLC,. Distribution transformers of substation are one of the most important equipment in power system network. Because of, the large number of transformers and various components over a wide area in power systems, the data acquisition, condition monitoring, automatic controlling are the important issues. This paper presents design and implementation of automatic control circuits which is used in PLC automation to monitor as well as diagnose condition of transformers, like load currents, transformer temperatures, voltages, oil level. The proposed on-line monitoring system integrates a solid state device named PLC (programmable logic controllers) and sensor packages. The suggested PLC monitoring system will help to detect the internal fault as well as external fault of transformer and also diagnose these faults with the help of desired range of parameters which is setting by programmer. The developed automation system istestedon Transformer on current load and temperature rise for various load isnoted and Transformer isswitchedoffwhenitstemperaturerisesabove40 oC.**

I. INTRODUCTION

Automationcontrol isu sed for var io us-Control systemsforoperatingequipmentsuch asmachinery,processesinfactories,boilersandhe attreating-ovens,switchingintelephonenetworks ,steeringandstabilization ofshipsor aircraftand other applicationswith minimalor reduced humanintervention1].Someprocesseshavebeen completely automated. The biggest benefit of aut omationis that it saves laborhoweveritisalsousedtosave energy andmaterialsand to improve quality, accuracy and precision. Itessentially involvesleveraging the power of technology toreduce the dependency onhumanpresenceanddecisionmakingforany process[2]. It leverages different electronic equipment (either stand aloneorinter linked with appropriate applications)to control different paramet ersofanyprocessand to use the appliances inasmarterwaytosaveenergy[3]- [4]. It also enable speopletobemore energy consciousbyenablingthem tohavearealtimestatusofelectricappliances [5]- [6]. And making thesystemautomated alsohelpsreducepeakhour powerconsumptionbyenablingpeopletoturnoffa ppliances atwillremotely[7]. This facilitates aconstant power supply byhavingvariedpricingpoliciesfor different times of dayand night. The main concern of this paper with transformer protection is rescued the transformer against internal faults as well as ensuring security of the protection scheme for external faults. Overloading of power transformers beyond the nameplate rating can cause a rise in temperature of both transformer oil and windings. Overloading is nothing but it is an over current fault which occurs on secondary side of distribution transformer. If the winding temperature rise exceeds the transformer limits, the insulation will deteriorate and may fail prematurely. Power system faults external to the transformer zone can cause high levels as well as low level of voltage on transformer. It leads to over voltage fault and under voltage fault.The fault impedance of power line being low, the fault current are relatively high. During the occurrence of faults, the power flow is diverted towards the fault and the supply to the neighbouring zone is affected and voltages become unbalanced. A comprehensive transformer protection scheme needs to include protection againstTransformer overload, over voltage fault and low voltage fault as well as protection for internal faults.Consequently largerevenuelossesandmaintenancecost goeshighduetofailure[1012].Thefigure1givesth edifferenttype-softransformerfailureclassificati onpertainingtothewinding failure, bushing failure,corefailure,andtank failure andcoolingfailure. These failuresgiveraiseto break down of transformer.

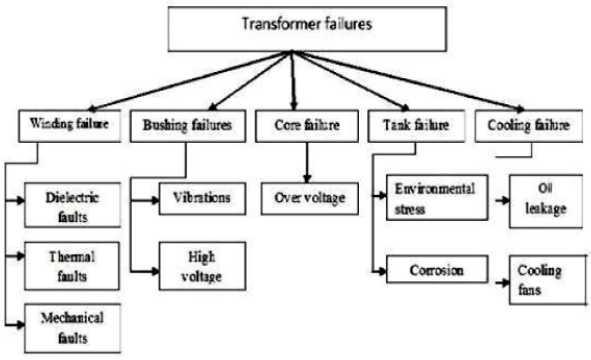

Fig. 1. Different Faultsin Transformer

II. TRANSFORMER FAULT DETECTION

A. A. Under Voltage Fault

When the operating voltage decreases to lower limit of voltage rating, the under voltage fault will occur. This fault can detect by voltage sensor. The rating of this sensor is Input (0 - 300 V) and Output (4 20 mA).

B. B. Over Voltage Fault

There may be always a chance of system over voltage due to sudden disconnection of large load. The magnitude of this voltage is higher than its normal level but frequency is same as it was in normal operating condition over voltage in the power system causes an increase in stress on the insulation of transformer. As we know that, voltage V = 4.44.f.T V , increased voltage causes proportionate increase in the working flux. The increase flux is diverted from the transformer core to other steel structural parts of the transformer. An increase in transformer terminal voltage or a decrease in frequencywill result in an increase in the flux [7].Core bolts which normally carry little flux may be subjected to a large component of flux diverted from saturated region of the core alongside. During this condition, the bolt may be rapidly heated up and destroys its own insulation as well as winding insulation. When the operating voltage increasesto upper limit of voltage rating, the over voltage fault willoccur. This fault can also detect by voltage sensor. Therating of this sensor is Input (0 - 300 V) and Output (4 20 mA).

C. C. Over current fault (Overload)

Over current fault is mainly due to overload in secondary-side of distribution transformer. Over current conditions are typically very short in duration (less than two seconds)because protection relays usually operate to isolate the faults from the power system line. Overload is current drawn by load, a load current in excess of the transformer name-plate rating at secondary side. Current increases the hottest-spot temperature (and the oil temperature), and thereby decreases the insulation life span. When the operating current increases to upper limit of current rating, the over current fault will occur. This fault can detect by current sensor. The rating of this sensor is Input (0 10A) and Output (4 20 mA).

D. D. Under Current Fault

When the operating current decreases to lower limit of current rating, the under current fault will occur. This fault can also detect by current sensor. The rating of this sensor is Input (0 10A) and Output (4 20 mA).

E. E. Over Temperature Fault

Not only over load current may not result in damage to the transformer but also the absolute temperature of the windings andtransformer oil remains within specified limits. Thr ratings of transformer are based on a 24-hour average ambient temperature of 30C (86F). Due to over voltage and over current, temperature of oil increases which causes failure of insulation of transformer winding. When the temperature of transformer increases to upper limit of temperature rating, the over temperature fault will occur. This fault can detect by temperature sensor. The rating of this sensor is Input (0 100C) and Output (4 20 mA).

F. F. Oil leakage

One of the biggest reasons of cooling system failure is leak in the oil/water pipes. This causes the reduction in the fluids which results in low heat exchange which is not good for the transformer. Leakage happens because of environmental stress, corrosion, high humidity and sun radiation.

III. DESIGN OF PLC BASED TRANSFORMER FAULT DETECTION

The schematic block diagram of this model has been shown in figure-2. It consists of different blocks.

The main of the project is to design and develop an automation system for controlling of the transformer using PLC and monitoring the temperature rise, overloading oil level changes and protected it from the windings break down. The block diagram of the experimental set up is shown in above figure 2whenever the transformer is overloaded the temperature and oil level inside the transformer is sensed by the sensors that is when the temperature and oil level cross some certain limits then it give signal to PLC device,thisisamasterdevice which control every action of the system. Whenever the various failures occurs in primary and secondary of the distribution of the transformer then the various values of current and voltage is sensed by current and voltage sensors and it will send signals to the PLC to trip the supply across primary or secondary of the transformer.

A. A. Three Phase Power Supply

In substation, three phase power supply is used for power transmission. A three-phase system is usually more economical than an equivalent single-phase or phase system at the same line to ground voltage because it uses less conductor material to transmit electrical power.

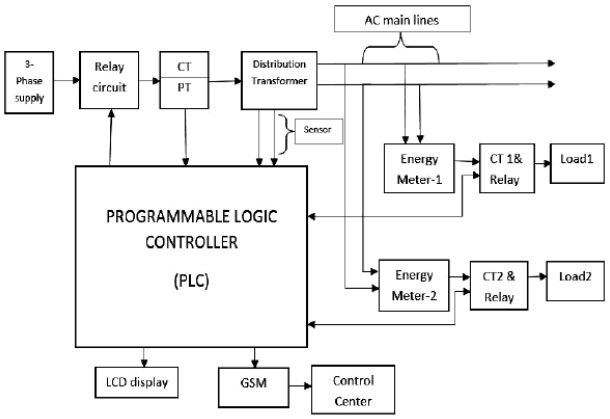

Fig. 2. Block diagram of proposed project

B. B. Relays

A relay is an electrically operated switch. Many relays use an electromagnet to mechanically operate a switch, but other operating principles are also used, such as solid-staterelays. Relays are used where it is necessary to control a circuit by a low-power signal (with complete electrical isolation between control and controlled circuits), or where several circuits must be controlled by one signal.

C. C. Transformer

The transformers are electrical devices used for energy transferred by electromagnetic induction between two or more circuits. The automation of transformer should be done for the robust operation without fail, The Temperature rise due to the various issues in the Transformer will affect the insulation provided for the windings and also the oil level should be monitored so automation should be done to control the temperaturerise, oil level over loading of the transformer.

D. D. PLC System

A Programmable Logic Controller is an industrial automation or computer control system that continuously monitors the state of input devices and makes decisions based upon a custom program to control the state of output devices.

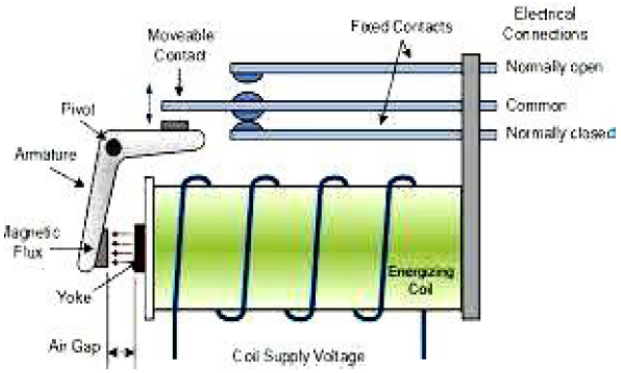

Fig. 3. Electromagnetic relay

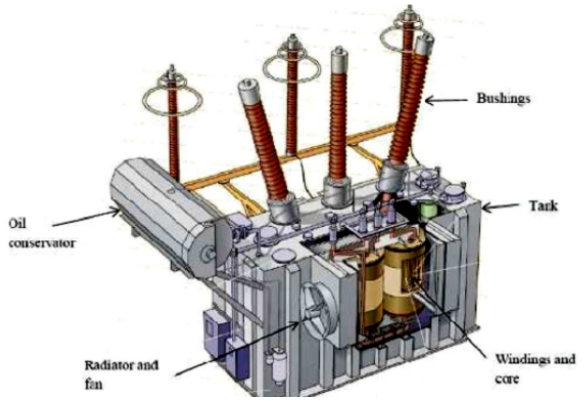

Fig. 4. transformar

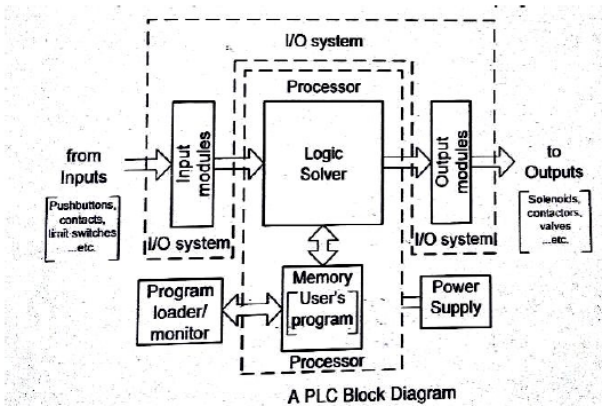

Fig. 5. PLC basic block diagram

Automated system can be a machine or a process and can be called a process control system. Function of a process control system is constantly watched by input devices (sensors) that gives signals to a PLC controller.

E. E. Loads

This load can be used as a LED light which acts as aload in secondary side of transformer. It can also use high load at secondary side of current sensor which is placed in primary of transformer.

IV. CONCLUSION

In this paper we have presented a design of a system based on PLC that is used to monitor and control the voltage, current and temperature and oil level of a distribution transformer in both sides. The proposed PLC system which has been designed to monitor the transformers essential parameters continuously monitors the parameters throughout its operation. When the PLC recognizes any increase or decrease in the level of voltage, current, oil level or temperature values the unit has been made shutdown in order to prevent it from further damages with the help of relays in three phase system. The system not only controls the distribution transformer in the substation by shutting it down, but also displays the values throughout the process for users reference in SCADA system. This claims that the proposed design of the PLC system makes the distribution transformer more robust against some key power quality issues which make the voltage, current or temperature to peak. Hence the distribution is made more secure, reliable and highly efficient by means of the proposed system.

REFERENCES

[1] KarthikShivaram,NikhilRajendra *Power line communication based Automation system using hand held Wi-FiDevice",*,University ofMichigan,USA;StanfordUniversity,2 012ISCE1569550137.

[2] Wong,E.M.C.*A phone based remote controller for home and office automation," Consumer Electronics,*,IEEE Transactions on , vol.40,no.1,pp.28-34,Feb1994 doi:10.1109/30.273654.

[3] Coskun, I.; Ardam, H.; *"A remotecontroller for home and office appliances by telephone,"Consumer Electronics,IEEETransactionson,*,A remote controller for home and office appliances by telephone,"Consumer Electronics,IEEETransactionson.

[4] Koyuncu,B. *"PCremotecontrol ofappliancesbyusingtelephone lines," ConsumerElectronics,*,IEEETransaction s on, vol.41, no.1, pp.201-209,Feb1995 doi:10.1109/30.370328

[5] Zhang X.; Sun J.; Zhou L., *Development of an Internet Home Automation System using Java andDynamicDNSService*,Sixth International Conference onParallelandDistributedComputing, Applications andTechnologies(PDCAT 05)0-7695- 2405-2/05

Power management in stand alone hybrid system using ANFIS and Fuzzy logic controller

Edwinlawrance.M
Assistant professor
, Department of EEE
SSM Institute of Engineering and technology, Dindigul
Manoj3e@gmail.com

Mr. S.PRAKASH
Assistant professor
Department of EEE
SSM Institute of Engineering and technology, Dindigul
lawrancepm@gmail.com

Aarthi.S
UG Scholar
Department of EEE
SSM Institute of Engineering and technology, Dindigul
Aarthiarun27@gmail.com

Indhuja.V
UG Scholar
Department of EEE
SSM Institute of Engineering and technology, Dindigul
Indhu110795@gmail.com

***Abstract*—In This paper a hybrid system consists of PV power module and wind driven Permanent Magnet Synchronous Generator feeds an isolated load through a Boost Converter was proposed. The output voltage Of PV module depends on solar irradiance as well as the output voltage and frequency of the PMSG is variable in nature due to non uniform wind velocities. The fluctuating output is rectified and kept constant by means of a boost converter. A neuro fuzzy logic controller is designed to extract the maximum power from PV also fuzzy logic controller is designed to set the duty ratio of the boost converter and to choose the moment to charge/discharge the battery and the moment to dissipate excess power in a dump load..This converter output is converted to three phase ac using a three phase PWM inverter. The proposed system has been demonstrated using MATLAB Simulink based simulations KeywordsAdapative neuro Fuzzy logic controller , Boost Converter, Permanent Magnet synchronous Generator**

I. Introduction

THE WORLD has known the issues of global warming, and renewable energy is a solution to reduction of greenhouse emissions. The use of renewable energy sources gives a excellent potential for many applications, and particularly, off-grid stand-alone systems have many benets. In remote areas, the energy storage units are needed in order to balance the electric power production and consumption within a system having a many number of renewable energy penetration also to increase the reliability of the system. Many studies have been done to make use of renewable energy sources (e.g. solar, biogas, wind, etc) that are stand alone. Among these, solar and wind energy are two of the most promising renewable power generation technologies. The availability of renewable energy sources has daily and some have seasonal patterns which results in difficulties in regulating the output power production and the load is the major the drawback of standalone power systems .For example, the daily wind speed is not constant and solar irradiation cut-off at night and cloudy days, thus, the solar and wind system cannot supply the load throughout a day. The solar power as well as wind power are available is not continuously for the entire day. solar or wind power systems alone cannot be used on remotely located areas which require constant guaranteed power. Alternative to this is the installation of hybrid energy systems. The hybrid Energy system must need a controller to monitor the power generation and load demand. And it to be performed the necessary action based on hybrid system operating condition.

In this paper, Adaptive Neural Fuzzy Inference System is used to extract the maximum power from the PV system. The PO method is used to develop the MPPT of Wind turbine. Last a Fuzzy logic Controller is designed in such a way it selects the best available energy source(s) and to choose the moment to dissipate excess power in a dump load. MATLAB/Simulink software is used to model for designing of the proposed controller that optimize power generated and consumed and also manage the power of battery on PV-Wind hybrid system

II. Modeling of Hybrid System Components

The present invention relates to a system for controlling the operation of electrical loads. The purpose of the demand controller of this invention is to maintain the total electrical power demand of the load at or below a predetermined peak demand. The concepts of this invention may be used for controlling a single electrical load but are preferably employed in controlling a plurality of electrical loads on a priority basis.

An electrical power demand is metered usually on the basis of a predetermined demand interval which may be, for example, a 15 minute, 30 minute or 60 minute demand interval. During this demand interval the consumption of electrical energy is accumulated and averaged. Thus, in this systems have been devised for maintaining the demand below a predetermined peak value during the demand interval thereby limiting this peak demand charge. Some of these techniques, however, such as a zero-order constant rate

comparison technique had not been totally satisfactory. Accordingly, one object of the present invention is to provide a

demand controller having an improved forecasting technique. Another object of the present invention is to provide a demand control technique that can be implemented relatively simply without the need for excessive complex data processing and logic circuitry

III. STATUS OF TNEB

In this section, the dynamic simulation model for the system is described. The system consists of various units, PV power and wind power units as primary sources of energy, battery bank unit as auxiliary source of energy, dc-dc and dc-ac converters, load unit and control unit.The function of controller unit is to ensure the management of the power, which is delivered by the hybrid system to satisfy the load and to charge the battery. The inverter unit is used to convert the DC generated power from renewable energy sources to feed the load with the required AC power. The excessive charge from the battery will be dumped to the dump load unit. The dump load in this case is the battery storage .

A. The Photovoltaic Module

The operation and the performance of PVgenerator depends to its maximum power,the models describing the PV module's maximum power output behaviorsare more practical for PV systemassessment. The following section describes the mathematical model for estimating the power output of PV. The equivalent circuit of a PV cell is shown in Fig 2. It includes a current source, a diode, a series resistance and a shunt resistance.

The current source Iph represents the cell photocurrent. Rsh and Rs are the intrinsic shunt and series resistances of the cell, respectively. Usually the value of Rsh is very large and that of Rs is very small, hence they may be neglected to simplify theanalysis. PV cells are grouped in larger units called PV modules which are further interconnected in a parallelseries configuration to form PV arrays. The photovoltaic panel can bemodeled mathematically as given in equations below: Module photo-current:

Where Iph is the light generated current in a PV module (A),ISCr is the PV module short-circuit current at 25oC and 1000W/m2, Ki is the short-circuit current temperature co-efficient at ISCr = 0.0017A=oC, T is the module operating temperature in Kelvin, G is the PV module illumination (W/m2) = 1000W/m2. Module reverse saturation current - Irs:

(2) Where q is Electron charge = 1.610-19C, Voc is the open circuit voltage, Ns is the number of cells connected in series, k is Boltzman constant = 1.3805*10 -23J/K, A = B is an ideality factor = 1.6, The module saturation current I0 varies with the cell temperature, which is given by

Where Tr is the reference temperature = 298 K, Io is the PV module saturation current (A), Ego is the band gap for silicon = 1.1 eV. The current output of PV module is (4) Where Np is the number of cells connected in parallel, Vpv is output voltage of a PV module (V), Ipv is output current of a PV module

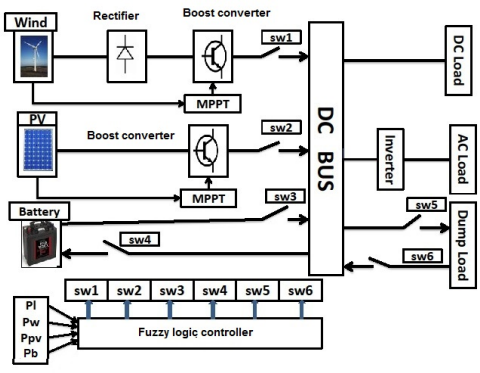

Fig. 1. Block diagram of PV-Wind Hybrid power system with controller

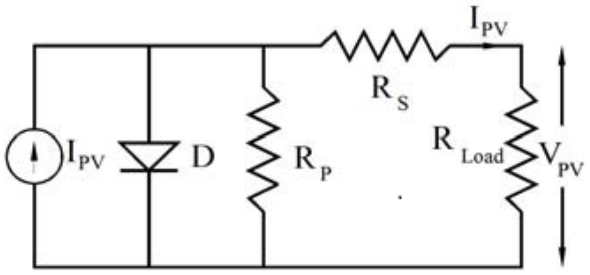

Fig. 2. The equivalent circuit of a PV cell

$$Iph = [ISCr + Ki\ (T - 298)] * G / 1000 \quad (1)$$

Fig. 3.

$$Irs = \frac{Iscr}{\exp\left(\frac{qVoC}{NskAT}\right) - 1}$$

Fig. 4.

$$Io = Irs\left[\frac{T}{Tr}\right]^3 \exp\left[\frac{q*Ego}{BK}\left[\frac{1}{Tr} - \frac{1}{T}\right]\right] \quad (3)$$

Fig. 5.

$$Ipv = Np * Iph - Np * Io\left[\exp\left[\frac{q*(Vpv+IpvRs}{NsAkT}\right] - 1\right. \quad (4)$$

Fig. 6.

(A), Rs is the series resistance of a PV module. Equations (1) - (4) are used to develop the PV model.

B. The Wind Turbine

There are two types of configuration for wind turbine exist, which is the vertical-axis wind turbine (VAWT) configuration and the widely used horizontalaxis wind turbine (HAWT) configuration. Wind turbines operate in two modes namely constant or variable speed. Advantages of constant speed turbine is that eliminates expensive power electronics such as converters and inverters. The main disadvantage is turbine cannot operate at its peak efficiency in all wind speeds. A relationship between the output power and the various variables constitute the mathematical model of the wind turbine. In this paper a model describing HAWT is proposed. For an object having mass m and velocity under a constant acceleration, the kinetic energy Ł is given by

The power in the wind is given by the rate of change of kinetic energy, i.e

Where is the upstream wind velocity at the entrance of the rotor blades in m/s and is the downstream wind velocity at the exit of the rotor blades in m/s. From the mass flow rate, the equation can be written as Where is a fraction called the power coefficient. The power coefficient represents a fraction of the power in the wind captured by the turbine and has a theoretical maximum of 0.593. is often called the Betz limit after the Germany physicist Albert Betz who worked it out in 1919. The power coefficient can be expressed by a typical empirical formula as

Where Ł is the turbine angular speed. Equations (5) - (13) describe the power captured by the turbine and constitute the turbine model.

C. Baterry storage system

Unlike fossil and nuclear fuels, which are concentrated sources of energy that can be easily stored and transported, renewable forms of energy are highly dilute and diffuse.The .lead-acid battery is proposed in this paper for energy storage. Moreover, their supply can be extremely intermittent and unreliable.When the state of charge(SOC) is below 80 percentage then the discharging switch is ON. Based on the model given by Gu H et al [5] and incorporation of the diffusion precipitation mechanism studied by Ekdunge and Simonsson [6] in the reaction kinetics of the negative electrode, Kim and Hong [7] analyzed the discharge performance of a flooded lead acid battery cell using mathematical modeling. Bernardi and Carpenter [8] developed a mathematical model of lead acid batteries by adding the oxygen recombination reaction. Nguyen et al. [9] presented a model analogous to the flooded type and examined the dynamic behavior of the cell during discharge with respect to cold cranking amperage and reserve capacity. Bernardi and Carpenter [8] developed a mathematical model of lead acid batteries by adding the oxygen recombination reaction. Nguyen et al. [9] presented a model analogous to the flooded type and examined the

$$Ww = \frac{1}{2}\mathrm{mv}^2 \quad (5)$$

Fig. 7.

$$Pw = \frac{dWw}{dt} = \frac{1}{2}\frac{dm}{dt}V_W{}^2 \quad (6)$$

Fig. 8.

But the mass flow rate is given by

$$\frac{dm}{dt} = \rho A V_w \quad (7)$$

Where A is the swept area of the turbine, ρ is the density of air. With this expression equation (7) becomes

$$\frac{dm}{dt} = \rho A V_W{}^3 \quad (8)$$

The actual mechanical power Pw extracted by the rotor blades in watts is the difference between the upstream and the downstream wind powers [3], i.e.

$$P_W = \frac{1}{2}\rho A V_W \left(V_u{}^2 - V_d{}^2\right)$$

Fig. 9.

$$\rho A V_{w=}\frac{\rho A(V_u+V_d)}{2} \quad (10)$$

Vw being the average of the velocities at the entry and exit of rotor blades of turbine. With this expression, equation (10) can be simplified and becomes

$$P_w = \frac{1}{2}\rho A V_w{}^3 \quad (11)$$

Fig. 10.

$$C_p = \frac{1}{2}(\lambda - .022\beta^2 - 5.6)e^{-0.17\lambda} \quad (12)$$

Where β is the pitch angle of the blade in degrees and λ is the tip speed ratio of the turbine, defined as

$$\lambda = \frac{V_{w(mph)}}{W_{b\,(rads^{-1})}} \quad (13)$$

Where Wb is the turbine angular speed. Equations (5) - (13) describe the power captured by the turbine and constitute the turbine model.

Fig. 11.

dynamic behavior of the cell during discharge with respect to cold cranking amperage and reserve capacity.Extensive SOC determination methods have been introduced by Sabine Piller et al. [11]. During the charging process, when the total output of PV and wind generators is greater than the load demand, the available battery bank capacity at hour t can be described by [12.

On the other hand, when the load demand is greater than the available energy generated, the battery bank is in discharging state. Therefore, the available battery bank capacity at hour t can be expressed as (15) Where Cbat(t) and Cbat(t-1) are the available battery bank capacity (Wh) at hour t and t-1, respectively, bat is the battery efficiency (During discharging process, the battery efficiency = 1) is self-discharge rate of the battery bank. Epv(t) and EWG(t) are the energy generated by PV and wind generators, respectively; EL(t) is the load demand at hour t and inv is the inverter efficiency At any hour, the storage capacity is subject to the following constraints:

IV. ENERGY MANAGEMENT AND CONTROL SYSTEM

A. ANFIS Based PV MPPT

A typical solar panel can converts only 30 to 40 percent of the incident solar irradiation into electrical energy. Maximum power point tracking technique is used to improve the efficiency of the solar panel. Therefore the MPPT of a photovoltaic array is an essential part of a PV system. Among these techniques, hill-climbing MPPT such as perturb and observe (PO), which is a simple algorithm that does not require previous knowledge of the PV generator characteristics and is easy to implement with analogue and digital circuits.In this technique, first the PV voltage and current are measured and hence the corresponding power is calculated. The peak power point is recognized and hence the corresponding voltage can be calculated [13] [14]. The major drawbacks of PO/hill-climbing are occasional deviation from the maximum operating point in case of rapidly changing atmospheric conditions, such as broken clouds. Also, correct perturbation size is important

$$C_{bat}(t) = C_{bat}(t-1)*(1-\sigma)+(E_{pv}(t)+E_{WG}(t)-\frac{EL(t)}{\eta inv})\eta_{bat} \quad (14)$$

Fig. 12.

$$C_{bat}(t) = C_{bat}(t-1)*(1-\sigma)-(\frac{EL(t)}{\eta inv}-E_{pv}(t)+E_{WG}(t)) \quad (15)$$

Fig. 13.

$$Cbatmin \leq Cbat(t) \leq Cbatmax \quad (16)$$

Fig. 14.

in providing good performance in both dynamic and steady-state response [15]. MPPT achieved very good performances, fast responses with no overshoot, and less fluctuations in the steady state for rapid temperature and irradiance variations [19]. For MPPT, ANFIS input can be PV array parameters like PV voltages and currents, environmental data like irradiance and temperature, or any combination of these, whereas the output signal is the identified maximum power or the duty cycle signal used to drive the electronic converter to operate at the MPP. The ANFIS input and output data are obtained from experimental measurement or model-based simulation results. After learning relation of with temperature and irradiance, ANFIScan track the MPP online [17]. The operating temperature is varied from 15 C to 65 C in a step of 5C and the solar irradiance level is varied from 100 W/m2 to 1000 W/m2 in a step of 50 W/m2, to get the training data sets for ANFIS.

B. FLC BASED WIND MPPT

The amount of power produced by a wind turbine is expressed as shown:

PT = 0.5cpAV3 (1) where is the air density A is the cross sectional area of the turbine V is the wind velocity The coefcient of power(cp) is a value dependent on the ratio

sno	irradiance(w/m^2)	temperature(deg celecius)	voltage(v)
1	900	10	16.6
2	830	35	8.75
3	910	12	16.39
4	850	50	20.36
5	920	30	16.57
6	600	52	20
7	770	47	19.9
8	700	42	19.9
9	950	23.75	17.7
10	980	24.5	17.89
11	985	24.62	17.8
12	995	24.87	18
13	180	30	13.51
14	220	40	16.77
15	825	20.6	17.1
16	925	18	17.4
17	940	20	17.68
18	930	23	17.7
19	650	16	16
20	955	23.87	17.7
21	960	24	17.8
22	970	24.25	17.9
23	975	24.37	17.8
24	100	-40	7.8995
25	100	0	11.74

Fig. 15. ANFIS Training Data

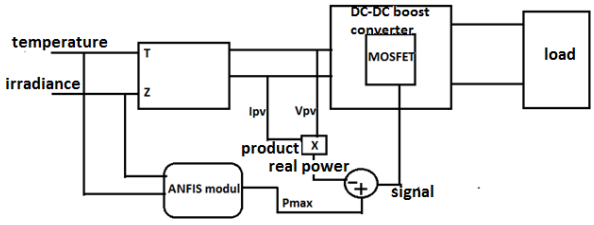

Fig. 16. Proposed ANFIS based MPPT of the PVsystem

between the turbine rotors angular velocity, (T) and the wind speed (V). This ratio is known as the Tip speed ratio (TSR), and is represented by . TSR is given by:

= TR V (2)

where R is the radius of the turbine. A wind turbine is generally characterised by its cp versus curves obtained for different wind speeds, and usually takes the shape. From the relationship between TSR and cp, it is possible to devise a control strategy that ensures that the wind turbine operates around or at the peak point of the curve. Such strategies are commonly referred to as Maximum Power Point Tracking (MPPT) techniques. MPPT techniques fall into two broad categories: Techniques that employ known turbine characteristics Techniques that allow optimization without knowledge of turbine characteristics.

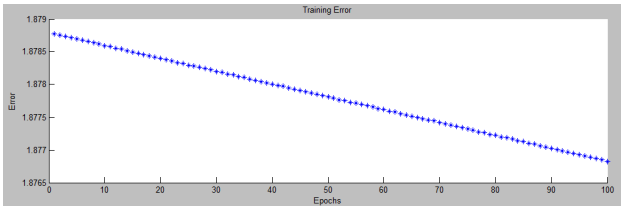

Fig. 17. The ANFIS MPPT Structure

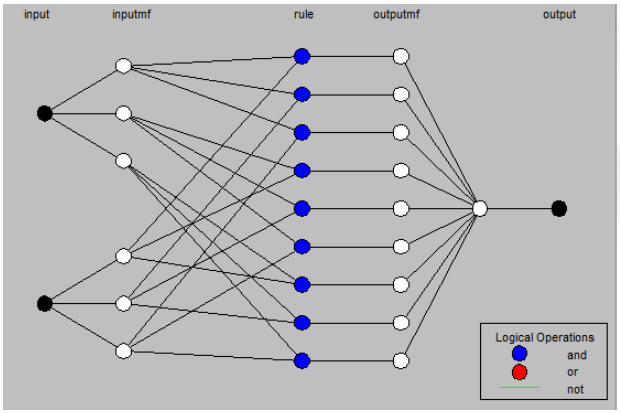

Fig. 18. Solar Irradiance Membership Function.

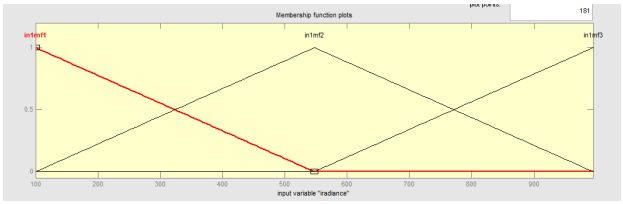

Fig. 19. Solar Irradiance Membership Function.

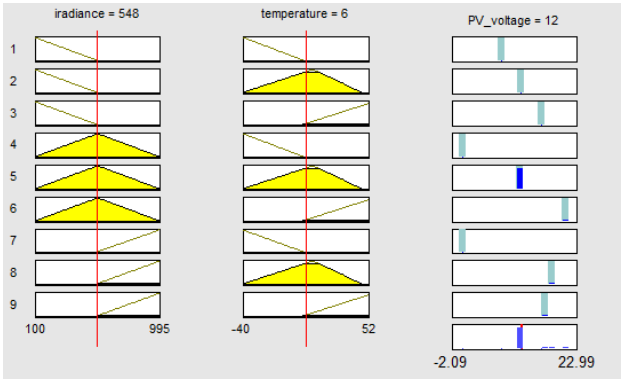

Fig. 20. Temperature membership Function.

C. FLC Based Power Management

The Fuzzy Logic Controller is used to control the power generated by wind source, PV source, Battery and dump load. It will control the battery state of charge (SOC) by activating the charger control switch when there is excess power from primary sources and activates the discharging switch in case of primary sources do not meet the load demand. The controller has four inputs named as Load Power (Pl), Wind turbine power (Pw), Solar PV Power (Ppv) and Battery Power (Pb). The outputs for controller are Wind power switch (SW1), PV power switch (SW2), Battery power switch (SW3), Charger controller switch (SW4), dump load charging switch (SW5) and dump load discharging switch (SW6). All four inputs has three(3) triangular membership function such as Low, Medium and High L,M,H and all output have two membership function (ON and OFF).

For the inputs low is defined from 0-200W, medium range from 200-600W and high considered to range from 600-1000w. All selector switches will be ON when any of the sources is low. The battery state of charge is limited from 20 to 80 which means the battery charging switch will be ON only when the state is below 80 and the discharging switch will

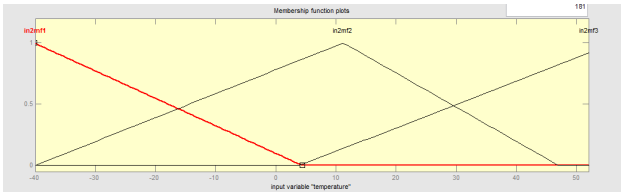

Fig. 21. . 8 Rule View at 548 irradiance and 6 temperature

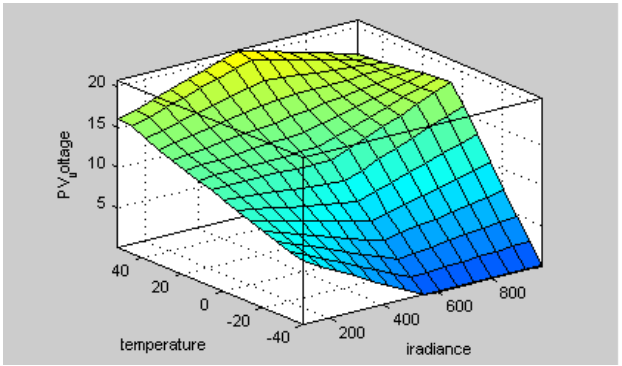

Fig. 22. . 8 Rule View at 548 irradiance and 6 temperature

be ON only when the SOC is above 20. This paper proposes Sugeno type of fuzzy inference system.

V. Simulation results and discussion Evaluation of proposed MPPT

The proposed PV MPPT model has been designed and simulated by MatLab/Simulink software Simulation model of PV-Wind hybrid system with battery storage and Fuzzy Logic controller is developed using MATLAB/Simulink software.

Case 1

Consider the case where all of the renewable sources are sufficient to run the load. The solar selector switch SW1, the wind selector switches SW2, charge control switches (SW4 and SW5) are activated and the other selector switches are turned off. The fuzzy rule that satisfies this condition is: If (Pl is L/M/H) and (Ppv is M/H) and (Pw is M/H) and (Pb is M/H) then (SW1 is ON) and (SW2 is ON) and (SW3 is OFF) and (SW4 is ON) and (SW5 is ON) and (SW6 is OFF). Table 4 show fuzzy rules formed that satisfies this condition.

Component	Rating(w)
Wind Power	1000
PV Power	1000
Battery Power	2000
DC Load	500
AC Load	500

Fig. 23. Rating of hybrid system components

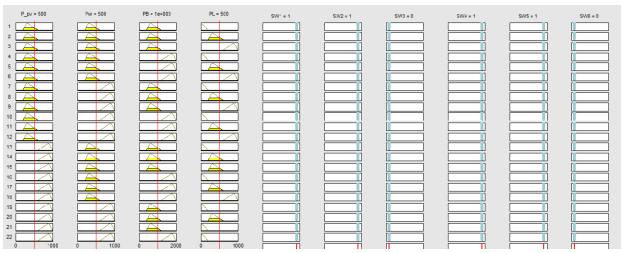

Fig. 24. Simulink model for the ANFIS MPPT

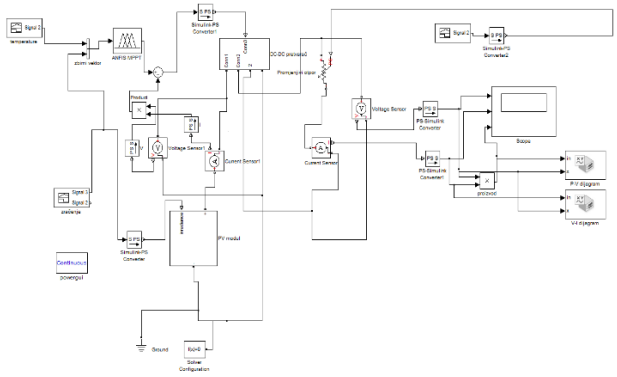

Fig. 25. Fuzzy rules

Ppv	Pw	Pb	P1	SW1	SW2	SW3	SW4	SW5	SW6
M	M	M	L	ON	ON	OFF	ON	ON	OFF
M	M	M	M	ON	ON	OFF	ON	ON	OFF
M	M	M	H	ON	ON	OFF	ON	ON	OFF
M	M	H	L	ON	ON	OFF	ON	ON	OFF
M	M	H	M	ON	ON	OFF	ON	ON	OFF
M	M	H	H	ON	ON	OFF	ON	ON	OFF
M	H	M	L	ON	ON	OFF	ON	ON	OFF
M	H	M	M	ON	ON	OFF	ON	ON	OFF
M	H	M	H	ON	ON	OFF	ON	ON	OFF
M	H	H	L	ON	ON	OFF	ON	ON	OFF
M	H	H	M	ON	ON	OFF	ON	ON	OFF
M	H	H	H	ON	ON	OFF	ON	ON	OFF
H	M	M	L	ON	ON	OFF	ON	ON	OFF
H	M	M	M	ON	ON	OFF	ON	ON	OFF
H	M	M	H	ON	ON	OFF	ON	ON	OFF
H	M	H	L	ON	ON	OFF	ON	ON	OFF
H	M	H	M	ON	ON	OFF	ON	ON	OFF
H	M	H	H	ON	ON	OFF	ON	ON	OFF
H	H	M	L	ON	ON	OFF	ON	ON	OFF
H	H	M	M	ON	ON	OFF	ON	ON	OFF
H	H	M	H	ON	ON	OFF	ON	ON	OFF
H	H	H	L	ON	ON	OFF	ON	ON	OFF
H	H	H	M	ON	ON	OFF	ON	ON	OFF
H	H	H	H	ON	ON	OFF	ON	ON	OFF

Fig. 26.

Case 2 Consider the case where all of the renewable sources are insufficient to run the load. The discharge selector switch (SW3) is activated and the other selector switches are turned off. The fuzzy rule that satisfies this condition is: If (Pl is L/M/H) and (Ppv is L) and (Pw L) and (Pb is M/H) then (SW1 is OFF) and (SW2 is OFF) and (SW3 is ON) and (SW4 is OFF) and (SW5 is OFF) and (SW6 is OFF). Case 1 :Fig .11 shows the output of controller when PV and wind supplies load (1=ON , 0 = OFF).

VI. Conclusion

The photovoltaic and wind hybrid power system is simulated using MATLAB/Simulink software. ANN and FLC MPPT Control is applied for solar and wind sources to make the system efficient. The performance of the MPPT was compared with the classical P O technique. Results indicate that the ANFIS-based model developed in this work can predict the MPP for a PV panel with high accuracy. Moreover the simulation results of the developed Fuzzy logic based Power Management shows that the controller provides uninterrupted power, effective utilization of sources, minimizing usage of battery and hence improve battery life. It was found that the hybrid topology exhibits excellent performance under various operating conditions, and maintain the battery SOC between 20 80. It can be concluded that the controller can satisfactory manage energy supply in a PV-Wind hybrid power system.

References

[1] anesh Kumar Vinayagamoorthy *Dynamic Energy Management Sysytem For A Smart Microgrid , IEEE Transation On Neural Networks And Learning Systems* ,Vol 27 , No 8 ,August 2016.

[2] C.-S. Chiu*T-S fuzzy maximum power point tracking control of solar power generation systems, IEEE Trans. Energy Conv* ,., vol. 25, no. 4, pp. 11231132, Dec. 2010.

[3] M.G.Villalva, J.R.Gazol, and E.R.Filho *M.G.Villalva, J.R.Gazol, and E.R.Filho, Comprehensive Approach to Modeling and Simulation of Photo-voltaic Arrays", IEEE trans. on Power Electronics,*,vol.24, no.5, pp.1198-1208, 2009.

[4] Piller S, Perrin M, Jossen A. *"Methods for state-of-charge determination and their applications.*96(1):113-20,2001.

An Interleaved Half-Bridge Three-Port Converter With Enhanced Power Transfer Capability Using Three-Leg Rectifier for Renewable Energy Applications

A.RICHARD PRAVIN
Assistant professor
, Department of EEE
st annes college of enginnering and tech

***Abstract*—In this paper, an interleaved half-bridge (IHB) three-port converter (TPC) is proposed for a renewable power system. The IHB-TPC is used to interface three power ports: 1) one source port; 2) one battery port; and 3) one isolated load port. The proposed IHB-TPC is derived by integrating two halfbridge TPC modules. A parallel configuration is adopted for the primary side of the two half-bridge modules, while a parallel series configuration is adopted for the secondary side of the two modules. The power can be transferred from the source and the battery to the load within the whole switching cycle with the proposed IHB-TPC. It means there are no additional conduction losses caused by the circulating current or the free-wheeling operation stage. Hence, the voltage gain can be extended, and the output filter can be reduced. Zero-voltage switching is realized for all the four main switches to reduce the switching losses. Two of the three ports can be tightly regulated by adopting pulsewidth modulation plus phase-shift control, while the third port is left unregulated to maintain power balance for the system. The operation principles and the performances of the proposed converter are analyzed in detail. The experimental results are given to verify the feasibility and the effectiveness of the proposed converter. Index TermsDCDC converter, half-bridge converter, multiport converter, renewable power system.**

I. INTRODUCTION

RENEWABLE energy power systems attract more and more attention, because the energy and environmental problems are becoming increasingly serious [1]. A renewable energy system needs to interface several energy sources, Manuscript received April 14, 2015; revised July 9, 2015; accepted September 3, 2015. Date of publication September 11, 2015; date of current version April 29, 2016. This work was supported in part by the State Key Laboratory of Power Systems, Tsinghua University, under Grant SKLD14M01, in part by the National Natural Science Foundation of China under Grant 51377083 and Grant 51577102, and in part by the Natural Science Foundation of Jiangsu Province, China, under Grant BK20140812 and Grant BK2012794. Recommended for publication by Associate Editor Gerry Moschopoulos. (Corresponding author: Kai Sun.) H. Wu, L. Zhu, and Y. Xing are with the Jiangsu Key Laboratory of New Energy Generation and Power Conversion, College of Automation Engineering, Nanjing University of Aeronautics and Astronautics, Nanjing 210016, China (e-mail: wuhongfei@nuaa.edu.cn; lilyzhu@nuaa. edu.cn; xingyan@nuaa.edu.cn).such as photovoltaic (PV) panels and fuel cells with the load along with battery backup [2], [3]. It leads to a supreme need for integrated power converters that are capable of interfacing and controlling several power terminals with low cost and a compact structure [4], [5]. An integrated three-port converter (TPC), instead of several independent two-port converters, finds applications in such systems, because it has the advantages of reduced conversion stages, less component count, lower overall mass, improved reliability, and enhanced dynamic performance due to power stage integration. In addition, since the control and power management of a TPC can be realized using a single controller, the communication that would be necessary in the conventional structure based on multiple two-port converters is not required. Hence, the communication delay and error can be avoided by the centralized control of the TPC [6]. Due to the advantages of an integrated TPC, there have been extensive studies, and a wide variety of topologies have been proposed in the literatures. The TPC topologies can be classified into three categories: 1) fully nonisolated topologies [7][10]; 2) fully isolated topologies [11][14]; and 3) partly isolated topologies [15][21]. Nonisolated TPCs are usually constructed from multiple buck, boost, or buckboost topologies by sharing the switching devices and the storage elements, e.g., the filter inductors [7], [8]. They have the advantages of compact design and high-power density. However, soft switching is not easy to implement for the power devices, and the voltage conversion ratio between the power ports cannot be too high or low. Fully isolated TPCs are usually constructed based on the high-frequency ac-link method, and using multiple bridge circuits and a multiwinding transformer [11][14]. They have the advantages of flexible voltage levels and soft switching due to the use of a highfrequency transformer. They are good candidates for certain critical applications where isolation is required. However, too many active switches have to be used, which leads to complicated driving and control

circuitry. Partly isolated TPCs, which are the main focus of this paper, are usually constructed by integrating a nonisolated buck, boost, or buckboost circuit into the primary-side circuit of an isolated converter, such ascompact design, and soft switching. Besides, they can also satisfy the requirement of the isolation and voltage conversion ratio of the load port using a high-frequency transformer. A bidirectional buckboost converter and a half-bridge converter are integrated to derive a tri-modal half-bridge TPC [18]. Its main advantage is that zero-voltage switching (ZVS) can be achieved for all switches. However, a middle branch is introduced to satisfy the requirement of power control, which leads to a complex topology and additional conduction losses. A family of half-bridge TPCs is proposed based on the integration of bidirectional buckboost, forwardflyback, and half-bridge converters [19]. The main attractive features of these TPCs are simple circuit and high-power density. However, hard switching and the large circulating current caused by the free-wheeling operation stage will increase the switching and conduction losses. Besides, the power rating of the half-bridge converter-based TPCs is limited. Interleaved bidirectional nonisolated dcdc converters and full-bridge converters are integrated to generate a family of TPCs by sharing the switching bridges [16], [17]. ZVS can be easily achieved with these TPCs. However, at least four magnetic components are required, because the filter inductors and transformer are not integrated, which limits the power density of these TPCs. Meanwhile, the large circulating current associated with the free-wheeling operation stage will decrease the conversion efficiency as well. The full-bridge TPCs presented in [20] and [21] are a combination of two halfbridge TPCs. They inherit the advantages of half-bridge and full-bridge TPCs in [17] and [19], such as high integration, high-power density, and ZVS capability. However, the circulating current associated with the free-wheeling operation stage still exists and introduces additional conduction

II. PROPOSED INTERLEAVED HALF-BRIDGE THREE-PORT CONVERTER

The proposed IHB-TPC derived from two IHB TPCs is shown in Fig. 1. The primary-side circuits of the two half-bridge TPCs are in parallel, while the secondary windings of the two transformers are in series, and share a common rectification and filter circuit. Different from the conventional full-bridgerectifier with a full-bridge rectifier, another rectifying leg composed by D5 and D6 is introduced and connected to the common terminal of the secondary windings of the two transformers. Therefore, a three-leg diode rectifier is employed on the secondary side of the proposed IHB-TPC. The three diode legs build three full-bridge diode rectifiers. Leg-1 and Leg-2 build a full-bridge rectifier for the equivalent full-bridge converter composed by the two half-bridge converters. In this case, the secondary windings of the two transformers are in series. Leg-1 and Leg-3 build a full-bridge rectifier for the transformer T1. Leg-2 and Leg-3 build another full-bridge rectifier for the transformer T2. With the three-leg rectifier, the secondary windings of the two transformers can be either in parallel or in series. The three full-bridge rectifiers will work alternately and transfer energy from the primary side to the secondary side within the whole switching cycle. As a result, there will be no free-wheeling operation stage, and the conduction losses associated with the circulating currents in the conventional full-bridge converter are eliminated.

III. OPERATION PRINCIPLES OF THE PROPOSED IHB-TPC

A. *Equivalent Circuit Between Any Two Ports*

Equivalent Circuit Between Any Two Ports The proposed IHB-TPC is applied to a PV-sourced power system with battery backup. In general, there are three power flows in a three-port power system composed by PV, battery, and load: 1) from the PV to the load; 2) from the PV to the battery; and 3) from the battery to the load. The equivalent circuit of each power flow path, or between any two ports, is shown in Fig. 2. It can be seen that the equivalent circuit from the PV to the load is an IHB converter with a three-leg diode rectifier. The equivalent circuit from the PV to the battery is an interleaved buck converter. And the equivalent circuit from the battery to the load is an interleaved forwardflyback converter with a three-leg diode rectifier. B. Working Modes Analysis Ignoring the power loss in the conversion, we have ppv = pb + po (1) where ppv, pb, and po are the power flowing through the

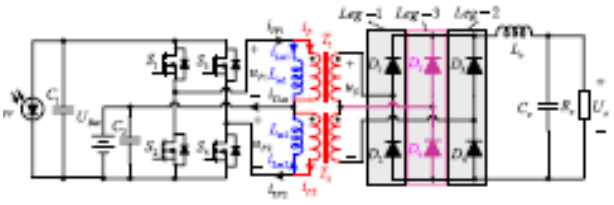

Fig. 1. Block diagram of PV-Wind Hybrid power system with controller

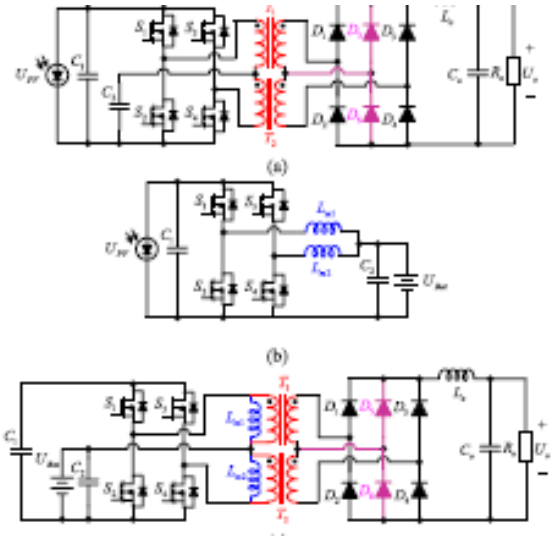

Fig. 2. Block diagram of PV-Wind Hybrid power system with controller

PV, battery, and load port, respectively. As illustrated in Fig. 3, according to the power relations among the power ports in the three-port power system, the IHB-TPC has three work modes: 1) dual-output mode (DOM) with ppv pothe battery absorbs the surplus PV power, and both the load and the battery take power from the PV; 2) dual-input mode (DIM) with ppv ¡ po and ppv ¿ 0the battery discharges to feed the load along with the PV; and 3) single-input single-output mode (SISOM) with ppv = 0the battery supplies power to the load alone. The operation principles of the IHB-TPC in different working modes are similar to each other. The difference among these modes is the value and the direction of the magnetizing currents, iLm1 and iLm2 in Fig. 3, which is dependent on the power relation of ppv, pb, and po. iLm1 and iLm2 are positive in the DOM, because the battery is charged, while they are negative in the DIM and the SISOM, because the battery is discharged. C. Switching States Analysis The equivalent circuit of the presented IHB-TPC is illustrated in Fig. 4, where Lk1 and Lk2 are the leakage inductances reflected to the secondary side. The parameters of the two transformers are the same: Lm1 = Lm2 = Lm and Lk1 = Lk2 = Lk . N is defined as the turns ratio of the transformer N = NS/NP, where NS and NP are the turns of the secondary- and primary-side windings of the two transformers. According to the power balance of thethree-port power system, two of the three ports should be controlled simultaneously, and the third one is used for maintaining the power balance. It means two control variables are needed for the power control. To satisfy the requirement of power control, a pulsewidth modulation (PWM) plus phase-shift modulation scheme is applied to the IHB-TPC. The duty cycles of the primary switches are employed to balance the voltages between the PV and the battery, and to achieve the maximum power point tracking (MPPT) control of the PV or the charging control of the battery. The phase-shift angle between the two switching bridges is employed as another control freedom to regulate the secondary-side output voltage. The waveforms of the IHB-TPC in different working modes are similar, except that the directions and the average values of the currents iLm1, iLm2, and iTLm are different. Only the DOM is analyzed with its key waveforms illustrated in Fig. 5, where D is the duty cycle of the upper switches S1 and S3, and is the phase-shift angle between the gating signals

IV. PERFORMANCE ANALYSIS OF THE PRESENTED CONVERTER

A. *Voltage Conversion Ratio*

Since the equivalent circuit from the PV to the battery is a buck converter, according to the voltsecond balance of the magnetizing inductance, we have UBat = DUPV or UPV = UBatTherefore, the duty cycle of the upper switches can be employed to balance the voltages between the PV and the battery. The voltage of a battery can be treated as a constant, because the variation of the battery voltage is very slow, and the PV power can be controlled by regulating the duty cycle D. Thus, MPPT or battery charging control can be achieved. The output voltage equals to the average value of the rectified voltage uR. The variation range of the phase angle is from zero to . Since the durations of Stages IIV are very narrow, they are ignored to simplify the analysis. There are three possible operation cases according to the relationship between the duty cycle D and the phase angle . The waveforms of the three cases are shown in Fig. 7, where TS is the switching period. By averaging the voltage uR, the output voltage is given by DB. Soft-Switching Performance ZVS soft switching of all the active switches can be achieved thanks to the phase-shift control and the complementary operation of the two switches in one switch leg. The principles of ZVS are similar to those of the IHB converter with a three-leg diode rectifier [22], [23]. However, due to the existence of the dc bias current through the two magnetizing inductances, iLm1 and iLm2, the ZVS conditions of the lower switches, S2 and S4, and the upper switches, S1 and S3, will be changed. When the battery is charged, the dc bias current flowing through the magnetizing inductance is positive. The equivalent circuit of the primary side is a buck converter, and the lower switches S2 and S4 are served as the synchronousrectification switches of the buck converter. In this case, ZVS of the lower switches can be always achieved. However, ZVS of the two upper switches S1 and S3 is determined by the energy stored in the leakage inductance, which is the same as that in the IHB converter with a three-leg diode rectifier [23]. On the other hand, if the battery is discharged, the dc bias current flowing through the magnetizing inductance is negative. In this case, ZVS of the two upper switches S1 and S3 will be much easier with the help of the magnetizing inductances, while ZVS of the lower

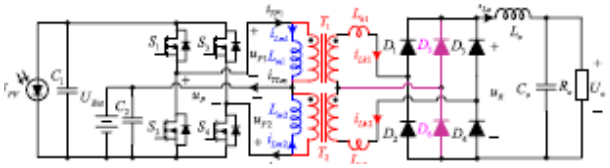

Fig. 3. Block diagram of PV-Wind Hybrid power system with controller

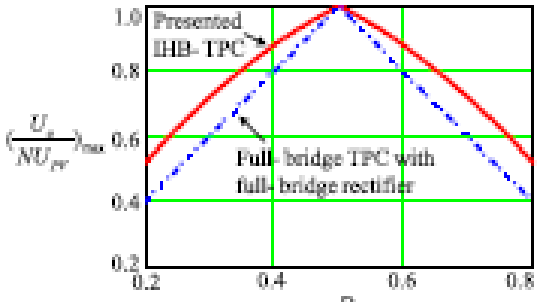

Fig. 4. Block diagram of PV-Wind Hybrid power system with controller

switches is determined by the energy stored in the leakage inductances.

V. EXPERIMENTAL VERIFICATION

A 500-W prototype controlled by an MC56F8245 DSP is built to verify the theoretical analysis. A variable resistor in series with a dc voltage source is used to simulate the PV characteristics. The steady-state waveforms when the IHB-TPC operates in the DOM with uPV = 76 V and uBat = 40 V are shown in Fig. 12. The waveforms agrees with the theoretical analysis pretty well. The voltage oscillation on the rectified voltage uR is caused by the resonance between the leakage inductance and the parasitic capacitance. From the waveform of the rectified voltage uR, it can be seen that the transformer T1 transmits power to the load within the whole switching cycle, and henceThe ZVS turn-ON waveforms of the switches S1 and S2 are shown in Fig. 14(a) and (b). In the experiment, the converter operates in the DOM with half-load power. It can be seen that the ZVS turn-ON of S1 and S2 has been achieved. As analyzed above, S3 and S4 have similar soft-switching performance, and can also achieve ZVS turn-ON. Therefore, all the primary switches can operate with soft switching, which can reduce the switching losses. The working mode transient waveforms are tested and shown in Fig. 15, where the mode transition is triggered by stepping up/down the load power. It can be seen that, when the output load steps up and down, the IHB-TPC switches between the DOM and the DIM smoothly and freely, and the battery switches between the charging mode and the discharging mode to compensate the load power variations while the PV and the load voltage are always kept constant.VII. CONCLUSION In this paper, a novel IHB-TPC is presented to interface three dc power ports: 1) an input source port; 2) a bidirectional storage port; and 3) an isolated load port. A three-leg diode rectifier is adopted in the proposed IHB-TPC on the secondary side, which enables the use of the whole switching cycle. This offers enhanced performances for the IHB-TPC to improve the power transfer capability, extends the voltage transfer ratio, reduces the conduction losses, improves the efficiency, and reduces the filter size. As a result, high efficiency and highpower density can be achieved with the proposed converter. Two degrees of control freedom necessary for the power flow control in a three-port power system are provided by a PWM plus phase angle shift modulation scheme. Besides, all the primary-side switches can realize ZVS soft switching, which reduces the switching losses. The experimental results on a 500-W prototype have verified the feasibility and the effectiveness of the proposed converter. The experimental results indicate that higher efficiency has been achieved by the proposed IHB-TPC

REFERENCES

[1] anesh Kumar Vinayagamoorthy *Dynamic Energy Management Sysytem For A Smart Microgrid , IEEE Transation On Neural Networks And Learning Systems* ,Vol 27 , No 8 ,August 2016.

[2] C.-S. Chiu*T-S fuzzy maximum power point tracking control of solar power generation systems, IEEE Trans. Energy Conv* ,., vol. 25, no. 4, pp. 11231132, Dec. 2010.

[3] M.G.Villalva, J.R.Gazol, and E.R.Filho *M.G.Villalva, J.R.Gazol, and E.R.Filho, Comprehensive Approach to Modeling and Simulation of Photo-voltaic Arrays", IEEE trans. on Power Electronics,*,vol.24, no.5, pp.1198-1208, 2009.

[4] Piller S, Perrin M, Jossen A. *"Methods for state-of-charge determination and their applications.*96(1):113-20,2001.

Simulink Based Pi and Fuzzy Logic Controllers for the Speed Control of DC Motor

Dr.N.Neela
Professor
Department of Electrical and Electronics Engineering
Annamalai university

S.Vetriselvi
PG Scholar
Department of Electrical and Electronics Engineering
Annamalai university

***Abstract*—Intelligent controllers as new technologies have recently been applied to electrical power control systems in general and motor control systems in particular.The Main Role Of This Work Is implementation of a (FLC) system and the conventional (PI) controller for speed control of DC motor.It is based on field programmable gate array (FPGA) circuit. Both FLC and conventional PI controller hardware are synthesized, functionally verified and implemented using Xilinx Integrated Software Environment (ISE) Version 11.1i.The fuzzy control applications with the physical systems require a real-time operation to interface high speed constraints. Fuzzy logic control (FLC) provides an alternative to the PID controller since it is a good tool for the control of nonlinear systems that are difficult in modeling.**

I. INTRODUCTION

The development of high performance motor drives is very important in industrial as well as other purpose applications. The dc motors are used in various applications such as defence, industries, Robotics etc. DC drives, because of their simplicity, ease of application, reliability and favourable cost have long been a backbone of industrial applications. DC drives are less complex with a single power conversion from AC to DC. DC drives are normally less expensive for most horsepower ratings. DC motors have a long tradition of use as adjustable speed machines and a wide range of options have evolved for this purpose. In these applications, the motor should be precisely controlled to give the desired performance. Many varieties of control schemes such as P, proportional integral (PI), proportional derivation integral (PID), adaptive, and fuzzy logic controller (FLCs), have been developed for speed control of dc motors. The proposed controller systems consist of multi-input fuzzy logic controller (FLC) and multi-input integrated fuzzy logic controller (IFLC) for the speed control.

II. DC MOTOR

A machine that converts D.C. power into mechanical power is known as a D.C. motor. Its operation is based on the principle that when a current carrying Magnetic field, the conductor experiences a mechanical force. The direction of this force is given by Flemings left hand rule and magnitude is given by;F = B.I. newtons Basically, there is no constructional difference between a D.C. motor and a D.C. generator. The same D.C. machine can be run as a generator or motor. DC motors consist of one set of coils, called armature winding, inside another set of coils or a set of permanent magnets, called the stator. Applying a voltage to the coils produces a torque in the armature, resulting in motion. If electrical energy is supplied to a conductor lying perpendicular to a magnetic field, the interaction of current flowing in the conductor and the magnetic field will produce mechanical force (and therefore,mechanical energy.

A. POWER ELECTRONICS DEFINED

It has been said that people do not use electricity, but rather they use communication, light, mechanical work, entertainment, and all the tangible benets of energy and electronics. In this sense, electrical engineering as a discipline is much involved in energy conversion and information. Energy is a critical need in every human endeavor. The capabilities and exibility of modern electronics must be brought to bear to meet the challenges of reliable, efcient energy. Power electronics involves the study of electronic circuits intended to control the ow of electrical energy.

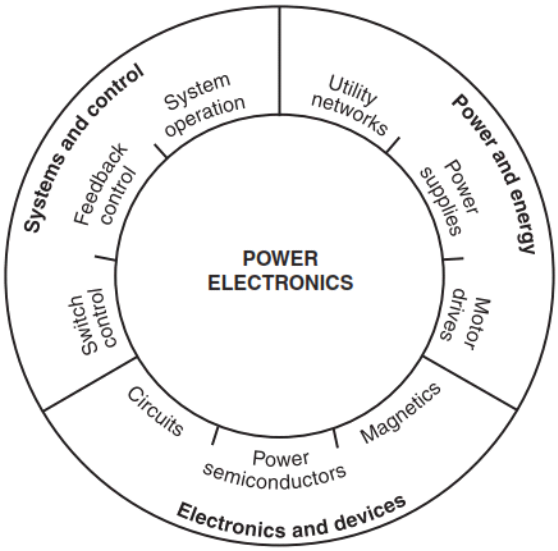

Fig. 1. .Control, energy, and power electronics are interrupted

B. SPEED CONTROL METHODS OF DC MOTOR

Flux control method Armature and Rheostatic control method Voltage control method Multiple voltage control Ward Leonard system

III. METHOD.EXISTING

A. PI CONTROLLER

The PI controller is by far the most common control algorithm. Most practical feedback loops are based on PI control or some minor variations of it. Many controllers do not even use derivative action. The PI controllers appear in many deferent forms, as stand-alone controllers, they can also be part of a DDC (Direct Digital Control) package or a hierarchical distributed process control system or they are built into embedded systems. Thousands of instrument and control engineers worldwide are using such controllers in their daily work. The PI algorithm can be approached from many divergent directions. It can be viewed as a device that can be operated with a few empirical rules, but it can also be approached analytically. Many industrial processes are controlled using conventional controllers like PI, PD, and PID etc. To manipulate the final control element in order to bring the process measurement to the set point whenever the set point is changed, and to hold the process measurement at the set point. The control algorithm must be designed to quickly respond to changes in the set point (usually caused by operator action) and to changes in the loads (disturbances). The design of the control algorithm must also prevent the loop from becoming unstable, that is, from oscillating. There are varieties of control actions that are used, in order to achieve the desired response from the designed process satisfactorily and efficiently.However, the controller performance will deteriorate as the process moves further away from the steady state around which it was linearized. Therefore application of PI controller becomes more attractive for controlling tool wear.

B. STRUCTURE OF PI CONTROLLER

IV. PROPOSED METHODOLOGY

Fuzzy Logic Controller (FLC) is based on fuzzy logic controller and constitutes a way of converting linguistic control strategy into an automatic by generating a rule base which controls the behaviour of the system. Fuzzy control is control method based on fuzzy logic. Fuzzy provides a remarkably simple way to draw definite conclusions from vague ambiguous or imprecise information. It suitable for applications such as the speed control of dc motor which is has non linearities. FLC have some advantages compared to other classical controller such as simplicity of control, low cost and the possibility to design without knowing the exact mathematical model of the process. Fuzzy logic incorporates an alternative way of thinking which allows modelling complex systems using higher level of abstraction originating from the knowledge and experience.

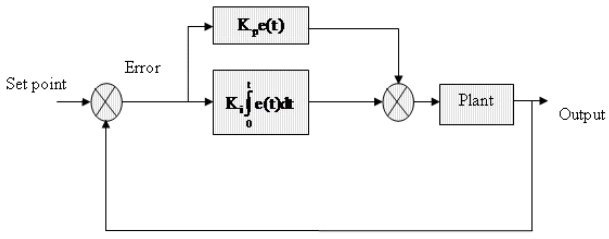

Fig. 2. Basic structure of PI

V. SIMULATION RESULTS

A. SIMULATION RESULTS

VI. PROPOSED SYSTEM

VII. CONCLUSION

The main contribution of this work is to present an Mapproachof real time fuzzy logic controller for DC motor some advantages such as flexible design (the membership functions and rule base can be easily changed), feature accuracy, high reliability, cost improvement, and high speed. The performance of the FLC is compared with the PI controller for referencespeed and load changes. The satisfied ability of the

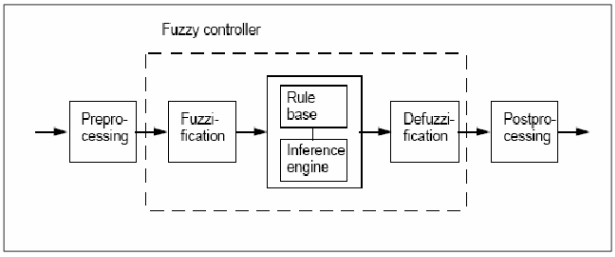

Fig. 3. Structure of fuzzy logic controller

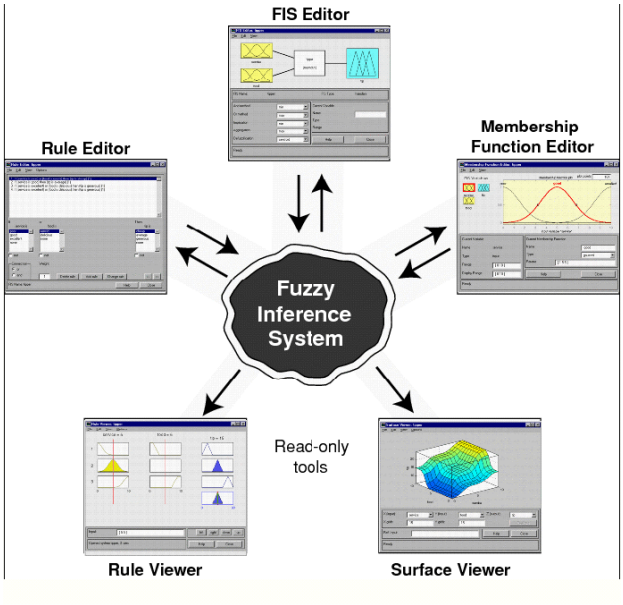

Fig. 4. Fuzzy Inference System

system control with FLC is better than PI controller. In the

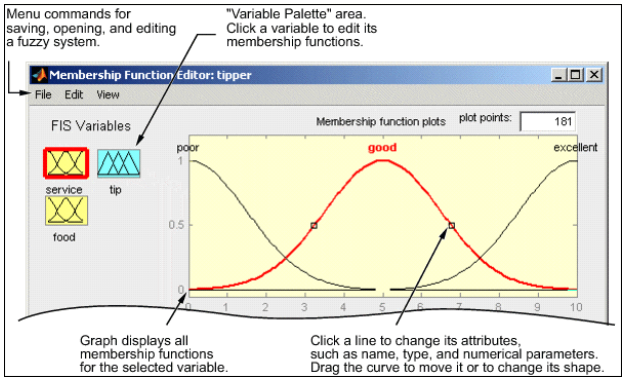

Fig. 5. Membership function

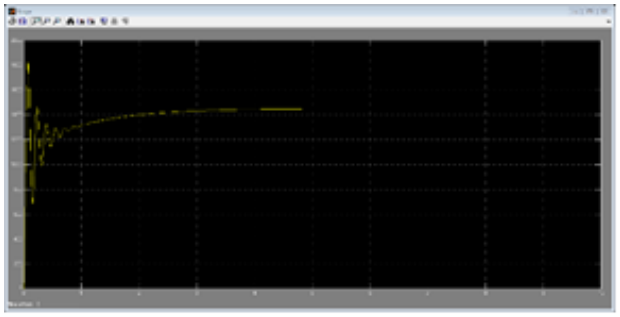

Fig. 6. Simulink model with different pi values

Fig. 7. Simulink model with different pi values

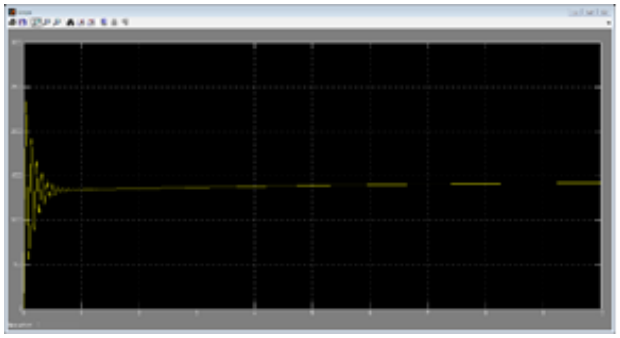

Fig. 8. Simulink model with different pi values

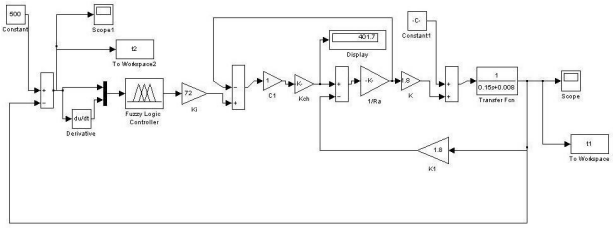

Fig. 9. SIMULINK MODEL

existing system, the pi values will be given in different ranges. The PI controller is used to compare with the FLC. Finally FLC is efficient compared with the PI controller.

REFERENCES

[1] Hammed B, Al-Mobaied M. Fuzzy *PID controllers using FPGA Technique for real time DC motor speed control. Intel Control*,Auto 2011; 2(August):23340.

[2] Millan I, Montel O, Sepulveda R, Castillo O. *Design and Implementation of a hybrid fuzzy controller using VHDL. SoftComputing for hybrid Intel. Systems. Berlin,* ,Springer-Verilog; 2008, SCI 154.

[3] Ngai G, Gharieb W, Binder Z *Application of fuzzy control to a Non-linear thermal process. In: The 31st conference of the IEEE on Decision and control*,Tucson, Arizona, December 1992.

[4] Kumar V, Rana KPS, Kumar V. . *Real time comparative study of the performance of FPGA based PID and fuzzy controllers for a rectilinear plant. In: IEEE conference publications, power electronics (IICPE), 2010 India international conference, 2830,*,January 2011.Embedded system based on a real time fuzzy motor speed controller 407.

[5] Kaur A, Kaur A *Development of neuro fuzzy controller algorithm for air conditioning system. (IJEST) Int J Eng. Sci Techno* ,2012;4(04):166771, ISSN: 0975-5462.

Reconfiguration of Distribution System Network for Loss Reduction Using Group Search Optimization Technique

K. Sriram
Assistant Professor
Department of EEE
St. Annes CET

G. Gnana Sundari
UG Scholar
Department of EEE
St. Annes CET

Dhivya Bharathi.B
UG Scholar
Department of EEE
St. Annes CET

***Abstract*—Network reconfiguration in distribution system is realized by changing the status of sectionalizing switches to reduce the power loss in the system. This paper presents a new method which applies thegroup search optimization algorithm (GSO) for determining the sectionalizing switch to be operated in order to solve the distribution system loss minimization problem. The GSO algorithm is a new population based metaheuristic approach inspired by foraging behaviour of animals. The advantage of GSO algorithm is that it does not require external parameters such as cross over rate and mutation rate as in case of genetic algorithm and differential evolution and it is hard to determine these parameters in prior. The other advantage is that the global search ability in the algorithm is implemented by introducing neighborhood source production mechanism which is a similar to mutation process. To demonstrate the validity of the proposed algorithm, computer simulations are carried out on 33-bus systems and compared with different approaches available in the literature. The proposed method has outperformed the other methods in terms of the quality of solution and computational efficiency. KeywordsDistribution system, Network reconfiguration, Loss reduction, Group Search Optimization Algorithm.**

I. INTRODUCTION

The distribution systems deliver power to the customers from a set of distribution substations and these are normally configured radially for effective co-ordination of their protective systems. There are two types of switches used in primary distribution systems; sectionalizing switches (normally closed) and tie switches (normally open). They are designed for both protection and configuration management in the system. Under normal operating conditions, feeders are frequently reconfigured by changing the open/closed state of each switch in order to reduce line losses or to avoid the overloading network branches. Since there are many candidate-switching combinations possible in a distribution system, finding the operating network reconfiguration becomes a complicated combinatorial, non-differentiable constrained optimization problem. Distribution system reconfiguration for loss reduction was first proposed by Merlin et al [1]. They employed a blend of optimization and heuristics to determine the minimal-loss operating configuration for the distribution system represented by a spanning tree structure at a specific load condition. A branch and bound type heuristic algorithm was suggested byCivanlaret al. [2], where a simple formula was developed for determination of change in power loss due to a branch exchange. In [3][5], the authors suggested to employ a power flow method-based heuristic algorithm (PFBHA) for determining the minimum loss configuration of radial distribution networks. In [6][8], the authors proposed a solution procedure employing simulated annealing (SA) to search an acceptable non-inferior solution. Nara et al. [9] presented an implementation using a genetic algorithm (GA) to look for the minimum loss configuration. Das [10] presents an algorithm based on the heuristic rules and fuzzy multi-objective approach for optimizing network configuration. In this paper, a new algorithm called group search optimization (GSO) algorithm is proposed for the minimization of power losses in the distribution system. The group search optimization algorithm is a new metaheuristic approach, proposed by Karaboga [21]. It is inspired by the foraging behavior of animals. The proposed method is tested on 14, 33 and 119 bus systems and results obtained are effective and encouraging. The rest of this paper is organized as follows: Section II provides mathematical model of the problem; Section III describes overview of GSO algorithm; Section IV provides application of GSO to network reconfiguration problem; Section V provides results and section VI outlines conclusions.

II. FORMULATION OF OPTIMIZATION MODEL FOR LOSS MINIMIZATION

The network reconfiguration problem in a distribution system is to find a best configuration of radial network that gives minimum power loss while satisfying certain operating constraints. The operating constraints are voltage profile of the system, current capacity of the feeder and radial structure of the distribution system.

Because of the complexity of the large scale distribution system, network reconfiguration problem is normally assumed as symmetrical system and constant loads. Therefore, the distribution lines are represented as series impedances and load demand as constant and balanced power sinks $S_L = P_L + jQ_L.Therealandreactivepowerflowsatthereceivingendandthevolta$

Equations (4) (6) are known as the Distflow equations.Hence, at the first node of the network is knownor estimated, then the same quantities at the other nodes canbe calculated by applying the above branch equations successively. This procedure is referred to as a forward update. Similar to forward update, a backward updateis expressed by the following set of recursive equations [4]:

Note that by applying backward and forward update schemes successively one can get a power flow solution. The power loss of the line section connecting between buses i and i+1 is computed as

III. GROUP SEARCH OPTIMIZATION TECHNIQUE(GSO)

Group search optimization (GSO) is a novel stochastic optimization algorithm that was developed by (S. He et al., 2009). This algorithm is inspired by the foraging behaviour of animals. The entire population of the GSO algorithm is termed a group and each individual in the population is called a member. There are three types of members namely: producers, scroungers and rangers. In order to achieve this foraging task the producer- scrounger strategy is engaged. Producing signifies to the action of searching for food and scrounging means joining the group for foraging. Rangers perform random walks in the search space. According to the GSO algorithm only one member is chosen to be the producer and the remaining members are scroungers and rangers. The producer constantly looks and finds the resources and the scroungers just join the producer. During iterations, the member that is found to have the best fitness value is chosen as the producer. The producer scans the environment to look for its resources. Scanning is a vital factor of search orientation.

During iterations a number of group members are selected as scroungers. The scroungers will keep searching for opportunities to join the resources found by the producer. At the $k^{t}iteration, theareacopyingbehaviourofthei^{t}hscroungercanbemo$

Different strategies were adopted by the animals to restrict their searches. GSO algorithm uses a strategy called as bounded search space. According to this strategy if any member is outside the search space it will turn back into the search space by setting the variables that violated the boundary criteria.

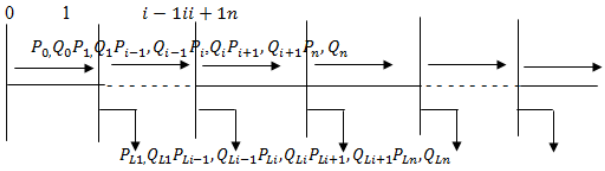

Fig. 1. Single-line diagram of a main feeder

$$P_{i+1} = P_i - P_{Li+1} - R_{i,i+1}.\frac{(P_i^2+Q_i^2)}{|V_i|^2} \quad (4)$$

$$Q_{i+1} = Q_i - Q_{Li+1} - X_{i,i+1}.\frac{(P_i^2+Q_i^2)}{|V_i|^2} \quad (5)$$

$$|V_{i+1}|^2 = |V_i|^2 - 2\left(R_{i,i+1}.P_i + X_{i,i+1}.Q_i\right) + \left(R_{i,i+1}^2 + X_{i,i+1}^2\right).\frac{(P_i^2+Q_i^2)}{|V_i|^2} \quad (6)$$

Fig. 2.

$$P_{i-1} = P_i + P_{Li} + R_{i,i+1}.\frac{(P_i'^2+Q_i'^2)}{|V_i|^2} \quad (7)$$

$$Q_{i-1} = Q_i + Q_{Li} + X_{i,i+1}.\frac{(P_i'^2+Q_i'^2)}{|V_i|^2} \quad (8)$$

$$|V_{i-1}|^2 = |V_i|^2 + 2\left(R_{i-1,i}.P_i' + X_{i-1,i}.Q_i'\right) + \left(R_{i-1,i}^2 + X_{i-1,i}^2\right).\frac{(P_i'^2+Q_i'^2)}{|V_i|^2} \quad (9)$$

Where

$$P_i^i = P_i + P_{Li} \text{and } Q_i' = Q_i + Q_{Li}$$

Fig. 3.

$$P_{Loss}(i, i+1) = R_{i,i+1}.\frac{(P_i^2+Q_i^2)}{|V_i|^2} \quad (10)$$

Fig. 4.

$$P_{T,Loss} = \sum_{i=0}^{n-1} P_{Loss}(i, i+1) \quad (11)$$

Fig. 5.

One point in zero degree:

$$X_z = X_p^k + r_1 l_{max} D_p^k(\varphi^k)$$

One point in the right hand side:

$$X_r = X_p^k + r_1 l_{max} D_p^k(\varphi^k + r_2\theta_{max}/2$$

One point in the left hand side:

$$X_l = X_p^k + r_1 l_{max} D_p^k(\varphi^k - r_2\theta_{max}/2$$

Fig. 6.

$$\varphi^{k+1} = \varphi^k + r_2\,\alpha_{max}$$

Fig. 7.

$$x_i^{k+1} = a.r_1 l_{max}$$

And move to the new point:

$$x_i^{k+1} = x_i^k + l_i D_i^k(\varphi^{k+1})$$

Fig. 8.

IV. . GSO ALGORITHM FOR NETWOK RECONFIGURATION PROBLEM

The proposed artificial bee colony algorithm is summarized as follows: 1.Read the line input data; Initialize MNC Maximum Iteration Count and base case as the best solution; 2.Construct initial Bee population solution xijas each bee is formed by the open switches in the configuration and the number of employed bees are equal to onlooker bees; 3.Evaluate fitness value for each employed bee by using the following the formulae 4.Initialize cycle=1; 5.Generate new population solution vijin the neighborhood of xijfor employed bees using equation and evaluate them; 6.Apply the greedy selection process between xiand vi; 7.Calculate the probability values Pifor the solutions xiby means of their fitness values using the equation 12; 8. Produce the new populations vifor the onlookers from the populations $x_i, selecteddependingonPibyapplyingroulettewheelselectionpr$ $rocessforth$ $cycle+1; 13.Ifcycle < MIC, gotostep5, otherwisegotostep14; 14$

V. TEST RESULTS

The proposed method was tested on 33-bus [17] radial distribution systems and results have been obtained to evaluate its effectiveness. For all these systems, the substation voltage is considered as 1.0 p.u. and all the tie and sectionalizing switches are considered as candidate switches for reconfiguration problem. The algorithm of this method was programmed in MATLAB environment and run on a Pentium IV, 3-GHz personal computer with 0.99 GB RAM. 33- bus system:The 33bus, 12.66 kV, radial distribution system [17] shown in fig. It consists of five tie lines and 32 sectionalize switches. The normally open switches are 33, 34, 35, 36 and 37 and the normally closed switches are 1 to 32. The data of the buses and lines are given Table. The total real and reactive power loads on the system are 3715 kW and 2300 KVAr. The initial power loss this system is 202.71 kW. The lowest bus bar voltage limit is0.9131 p.u which occurs at node 18.

For this test case, the bee colony population size is taken as 50 and the number of employed bees is and onlooker bees. The scout bee is taken as 1. The maximum iteration count (MNC) is taken as 100. Simulations are carried from 10 to 100 iterations and all are converged to same solution after 8 iterations. The CPU time used to get optimal solution is 5.3 seconds. The optimal configuration obtained by the proposed algorithm is 33,14,8, 32, 28, which has a real power loss of 139.5 kW. This amounts to a reduction of 31.2 % in total power loss. The minimum node voltage of the system after reconfiguration improved to 0.9437 p.u (node 33). The results of the proposed algorithm are compared with Genetic Algorithms [14] and Refined Genetic Algorithms [16] and are presented in Table 2. From the results, it is observed that the optimal power loss obtained by the proposed method is 1.1 kW less than GA [14] and is same as RGA [16]. The CPU time used by the proposed method is 5.3 sec only but it is 15.2 and 13.8 in case of GA and RGA methods.

VI. CONCLUSIONS

In the present work, a new population based group search optimization (GSO) has been proposed to solve the network reconfiguration problem in a radial distribution system. The main

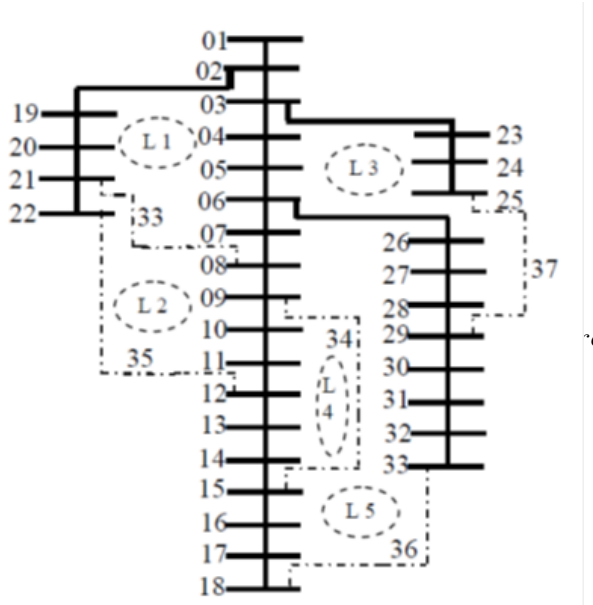

Fig. 9. Bus radial distribution system with loops

Line No.	From Bus	To Bus	R(Ω)	X(Ω)	Load at Receiving End Bus	
					Real Power Load(kW)	Reactive Power Load(kVAR)
1	1	2	0.0922	0.0477	100.0	60.0
2	2	3	0.4930	0.2511	90.0	40.0
3	3	4	0.3660	0.1840	120.0	80.0
4	4	5	0.3811	0.1941	60.0	30.0
5	5	6	0.8190	0.070	60.0	20.0
6	6	7	0.1872	0.6188	200.0	100.0
7	7	8	1.7114	1.2351	200.0	100.0
8	8	9	1.0300	0.7400	60.0	20.0
9	9	10	1.0400	0.7400	60.0	20.0
10	10	11	0.1966	0.0650	45.0	30.0
11	11	12	0.3744	0.1238	60.0	35.0
12	12	13	1.4680	1.1550	60.0	35.0
13	13	14	0.5416	0.7129	120.0	80.0
14	14	15	0.5910	0.5260	60.0	10.0
15	15	16	0.7463	0.5450	60.0	20.0
16	16	17	1.2890	1.7210	60.0	20.0
17	17	18	0.7320	0.5740	90.0	40.0
18	2	19	0.1640	0.1565	90.0	40.0
19	19	20	1.5042	1.3554	90.0	40.0
20	20	21	0.4095	0.4784	90.0	40.0
21	21	22	0.7089	0.9373	90.0	40.0
22	3	23	0.4512	0.3083	90.0	50.0
23	23	24	0.8980	0.7091	420.0	200.0
24	24	25	0.8960	0.7011	420.0	200.0
25	6	26	0.2030	0.1034	60.0	25.0
26	26	27	0.2842	0.1447	60.0	25.0
27	27	28	1.0590	0.9337	60.0	20.0
28	28	29	0.8042	0.7006	20.0	70.0
29	29	30	0.5075	0.2585	200.0	600.0
30	30	31	0.9744	0.9630	150.0	70.0
31	31	32	0.3105	0.3619	210.0	100.0
32	32	33	0.3410	0.5302	60.0	40.0
33*	21	8	2.0000	2.0000		
34*	9	15	2.0000	2.0000		
35*	12	22	2.0000	2.0000		

Fig. 10. Test Data For 33-Bus System

Item	Tie Switches	Power Loss (kW)	Min.Node Voltage (p.u)	Power Loss Reduction (%)	CPU Time (s)
Original Configuration	33,34,35,36 37	202.71	0.9131 (Node 18)	--	--
Proposed Method	33,14,8,32, 28	139.5	0.9437 (Node 33)	31.2	5.3
GA[14]	33,9,34,28 36	140.6	0.9371 (Node 33)	30.6	15.2
RGA[16]	7,9,14,32, 37	139.5	0.9371 (Node 33)	31.2	13.8

Fig. 11. Simulation Result of 33-Bus System

objectives considered in the present problem are minimization of real power loss, voltage profile improvement and feeder load balancing subject to the radial network structure in which all loads must be energized. Simulations are carried on 33 bus systems and results are compared with the other populations based methods such as GA, DE and simulated annealing. The results obtained by the proposed method out perform the other methods in terms of quality of the solution and computation efficiency. The main advantage of GSO algorithm is that it does not require external parameters such as cross over rate and mutation rate etc, as in case of genetic algorithms, differential evolution and other evolutionary algorithms and these are hard to determine in prior. The other advantage is that the global search ability in the algorithm is implemented by introducing neighborhood source production mechanism which is a similar to mutation process. As far as the authors knowledge this is the first application of group search optimization algorithm to network reconfiguration problem in distribution system. This paper demonstrates the capability of group search optimization algorithm in solving network reconfiguration problem. Ideas presented in this paper can be applied to many other power system problems also.

REFERENCES

[1] A. Merlin, H. Back, *Search for a minimal-loss operating spanning tree configuration in an urban power distribution system Proceedings of 5thPower System Computation Conference (PSCC), Cambridge*,UK, 1975, pp. 1-18.

[2] S. Civanlar, J. Grainger, H. Yin, and S. Lee, *Distribution feeder reconfiguration for loss reduction, IEEE Trans. Power Del* ,vol. 3, no.3, pp. 12171223, Jul. 1988.

[3] D. Shirmohammadi and H.W. Hong *Reconfiguration of electric distribution networks for resistive line losses reduction, IEEE Trans.Power Del.,* ,vol. 4, no. 2, pp. 14921498, Apr. 1989.

[4] T. P. Wagner, A. Y. Chikhani, and R. Hackam, *Feeder reconfiguration for loss reduction: an application of distribution automation, IEEETrans. Power Del* ,vol. 6, no. 4, pp. 19221931, Oct. 1991.

[5] S. Goswami and S. Basu, *A new for the reconfiguration of distribution feeders for loss minimization, IEEE Trans. Power Del* ,vol. 7, no. 3,pp. 14841491, Jul. 1992.

[6] H. C. Cheng and C. C. Kou, , *Network reconfiguration in distribution systems using simulated annealing, Elect. Power Syst. Res., simulated annealing, Elect. Power Syst. Res*,vol. 29, pp. 227238, May 1994.

[7] A. K. Nara, A. Shiose, M. Kitagawoa, and T. Ishihara, , *Implementation of genetic algorithm for distribution systems loss minimum World Academy of Science, Engineering and Technology 45 2008 713 reconfiguration, IEEE Trans. Power Syst.,* ,vol. 7, no. 3, pp. 10441051, Aug. 1992.

[8] D. Karaboga, B. Basturk, *A powerful and efficient algorithm for numerical function optimization: artificial bee colony (ABC) algorithm,Journal of Global Optimization,* ,Vol. 39, pp. 459471, 2007.

OPTIMAL AND RELIABLE OPERATION OF MICROGRID USING BIOGEOGRAPHY BASED OPTIMIZATION ALGORITHM

M.PREMALATHA
Assistant Professor
Department of Electrical and Electronics Engineering
St.anne'sCollege of Engineering,panruti

premasadha@gmail.com

***Abstract*—This paper presents a method to minimize the fuel cost during the grid-connected mode of operation and to ensure stable mode of operation after islanding in microgrid. To achieve this, the economic dispatch problem with constraints such as reserve for non-dispatchable DGs, inter-area flow limits and stable island operation are formulated. The constraints for stable island mode operation are in accordance with variable droop power sharing principles. This problem is solved using biogeography based optimization algorithm (BBO). Biogeography deals with how species arise, migrates, extinct in nature. This algorithm searches for the global optimum solution mainly through migration and mutation. The proposed method is tested with three area fifteen units system. The result proposes this technique is better in solving economic dispatch problem in the microgrid.**

Keywords-Economic dispatch, Microgrid, Islanding mode, Grid connected mode, BBO algorithm

I. INTRODUCTION

The electric grid has been undergoing tremendous changes at present due to the addition of distributed energy resources. Connection of distributed energy resources made a path for creation of microgrid. Microgrid consists of small distributed generation units with enough power generation to supply the all load demand. The two modes of operation in microgrid are grid-connected mode and island mode [1]. There are many technical issues related to microgrid operation including interconnection schemes between microgrid and the maingrid [2]. This paper illustrates only the stable islanding operation of microgrid using power sharing principles. DGs are categorized as dispatchable or non dispatchable units based on their active power control [3]. Dispatchable DGs, such as micro turbines using thermal inputs and fuel cells are capable of producing controlled active power on demand. Therefore they are assigned for the task of regulating the voltage and frequency during islanded operation [4]. In contrast, renewable energy based DGs operate according to the maximum power tracking concept whether the microgrid is connected to the maingrid. Solar and wind DGs are non dispatchable since the output power mainly depends on the weather condition rather than load. This paper focuses only on power sharing principle for dispatchable DGs, while non dispatchable DGs are considered to be negative load. Many conventional approaches including Lagrangian multiplier method [6] have been applied to solve economic dispatch problems but these methods require incremental cost curves are monotonically increasing in nature. The dynamic programming [7] method, does not impose any restriction on the nature of the cost curves and solve both convex and non-convex economic dispatch problems but it suffers from increase simulation time. Several methods such as genetic algorithm[8], artificial neural networks [9], evolutionary programming[10], differential evolution [11], bacterial foraging Algorithm [12] etc., have been developed and applied successfully to economic dispatch problems. The conventional economic dispatch problems were solved using many optimization techniques but the optimal scheduling of microgrid ever attempted. Biogeography describe about the distribution of biological organism. It also describes about the species rise, migration and extinct. In BBO, a good solution is analogous to a habitat with high Habitat Suitability Index (HSI) and a poor solution represents a habitat with low HSI. The habitat with high HSI solutions will have less change than the habitat with low HSI solutions. Low HSI solutions tend to copy good features from high HSI solutions. The shared features remain in the high HSI solutions, while at the same time appearing as new features in the habitat with low HSI solutions. BBO works based on two mechanisms: migration and mutation. Like other biology-based algorithms it has the property of sharing information between solutions. The stable operation of microgrid after islanding is maintain by tracking the inter area power flow limits using constant and variable droop power sharing principles. BBO technique is used for minimization of fuel cost during grid connection mode operation of microgrid.

II. PROBLEM FORMULATION

A. FORMULATION MICROGRID ECONOMIC DISPATCH PROBLEM

In an microgrid the primary objective of economic dispatch problem is to minimize the total cost generation while satisfying the power balance and generation limits of the units.The objective function is given as,

POWER BALANCE CONSTRAINTS:The power balance condition is given as the sum power of all units and power from maingrid must be equal to load demand. The effect of non-dispatchable DG is also considered in power balance equation and it is given as, SPINNING RESERVE REQUIREMENT CONSTRAINTS:The load demand and power outputs of the DG vary continuously, so in order to compensate these variations and operate to the system stably additional reserve required. In this microgrid the spinning reserve requirement is given as decrease in the maximum limit and an increase in the minimum limit of the unit which is given by the following equations. For decrease or increase in maximum and minimum limit the condition is given as, In this, it is considered that the load demand varies with in % predicate value and the power output of non-dispatchable DG varies with in % INTER-AREA FLOW LIMIT CONSTRAINTS:The power flow between to area is termed as inter-area flow. It is restricted by physical limits and it is formulated as, assuming that there are p areas,

$$\min T_{FC} = \sum_{u=1}^{K_{gen}} F_u(P_u) \quad (1)$$

The fuel cost function is given by,

$$F_u(P_u) = a_u + b_u P_u + c_u P_u^2 \quad (2)$$

Where

T_{FC} - Total fuel cost

$F_u(P_u)$ - Fuel cost function

K_{ger} - Number of generation units

P_u - Power output of units

Fig. 1.

$$\sum_{u=1}^{K_{gen}} P_u + P_{Maingrid} = \sum_{n=1}^{K_{load}} D_n - \sum_{m=1}^{K_m} P_m \quad (3)$$

Where m – non dispatchable DGs

D – load demand

Fig. 2.

$$P_{jt} \le P_{jt}^{max(min)} - \left(\frac{v}{100} \sum_{n \in S_j} D_n + \frac{w}{100} \sum_{m \in S_j} P_m \right) \quad (4)$$

Where

v - Variation in load demand

w - Power output variation of non-dispatchable DGs

Fig. 3.

B. CONSTRAINTS FOR STABLE ISLANDED OPERATION

During transition power output change in any DG will affect the power flow in the lines and make system unstable. In-order avoid this DGs should have the reserve as much as . Due the increase in reserve there is restriction on flow limits system in stable islanding operation. Such restriction of flow limits will increase the operational cost during the grid-connected operation. Therefore methods for satisfy the above two objectives are cost minimization during the grid connected operation and the stable islanded operation. The following section presents the formulation of this constraint in accordance variable droop power-sharing principle. In constant droop reserve contribution is determined before solving the economic dispatch problem. But when variable droop is applied the power output reference of each DG are determined optimally and the reserve contribution of each DG are calculated according to its operational margin. Hence the output limits of DGs need not to be changed in variable droop power sharing principle but the inter area flow limits should be modified.

C. POWER INITIALLY EXPORTED FROM MICROGRID

If we assume that the output of unit is , the operational margin of this unit is . Therefore, the power shared by unit during the transition can be calculated as follows,

The downward flow limits should be decreased but in variable droop the power shared by each unit is unknown until the economic dispatch problem is solved. Hence the reduced value of the downward flow limits cannot be determined directly as in the case of the constant droop. The power flow from area to area during the grid-connected operation is the sum of the difference between the loads and power outputs of area and the areas downstream from it and it is given as,

D. POWER INITIALLY IMPORTED TO MICROGRID

When the maingrid supplies power to the microgrid, during transition the power output of DGs will be increased and upward power flow limit should be changed. The operational margin of unit in this case is , the amount of power shared by area j can be calculated as,

$$\Delta P_u^{EP} = \frac{P_u - P_u^{min}}{\sum_{i=1}^{K_{gen}} (P_i - P_i^{min})} \cdot \left| P_{Maingrid} \right| \quad (6)$$

The amount of power shared by an area j is given as,

$$\Delta P_{S_j}^{EP} = \frac{P_S - P_S^{min}}{\sum_{i=1}^{K_{gen}} (P_i - P_i^{min})} \cdot \left| P_{Maingrid} \right| \quad (7)$$

Where

S -System area

Fig. 4.

All the variables in equation (11) and (10) can be calculated from system data, and hence before solving the economic dispatch problem the optimal values of inter-area flow limits can be determined.

III. BBO ALGORITHM

A. BIOGEOGRAPHY

Biogeography describes distribution of species in nature also about the rise of species, species migration, extinct. The variables that characterize habitability are called Suitability Index Variables (SIVs). SIVs can be considered as the independent variables of the habitat and Habitat Suitability Index (HSI) can be calculated using these variables. Immigration is a process of migration of some species from one habitat to other habitat. When some species enters into one habitat from any other habitat is known as immigration process. The concept of emigration and immigration can be represented by a probabilistic model. Let us consider the probability that the habitat contains exactly species at time is mathematically given as

IV. BLOCK DIAGRAM

A. BIOGEOGRAPHY-BASED OPTIMIZATION (BBO)

This section describes development of biogeography-based optimization technique and their steps. BBO concept is based on the two major steps migration and mutation. (i) MIGRATION The emigration and immigration rates of each solution are used to probabilistically share information between habitats. Each habitat solution can be modied based on other habitat solutions using habitat modication probability ( ). After selecting the SIV for modication the solutions among the habitat set. Which will migrate randomly chosen SIVs to the selected solution is based on the emigration rates of other solutions. One sort of elitism is used in order to prevent the best solutions from being corrupted by immigration process. Those habitats whose HSI are best are kept as it is without migration operation after each iterations. This operation is known as elitism operation. (ii) MUTATION In BBO sudden change in habitat event is represented by mutation of SIV and species count probabilities are used to determine mutation rates. Each

$$FL_{j-1\_j}^{-} = \sum_{s=1}^{P} \left(D_{s_s} - P_{s_s} \right) (8)$$

Fig. 5.

$$\Delta P_{S_j}^{max} = \frac{P_{S_j}^{max} - P_{S_j}}{\sum_{u=1}^{K_{gen}} \left(P_u^{max} - P_u \right)} \cdot \left| P_{Maingrid} \right| (9)$$

Power balance equation is the sum of power generated by all the units plus the power from the main grid equal to the load and it is given as,

$$\sum_{u=1}^{K_{gen}} P_u + P_{Maingrid} = \sum_{n=1}^{K_{load}} D_n \ (10)$$

Finally, the upward flow limit can be calculated as,

$$-\left(FL_{j-1\_j}^{max} - \left| P_{Maingrid} \right| \cdot \frac{\sum_{s=j}^{P} P_{S_s}^{max} - \sum_{s=j}^{P} D_{S_s} - FL_{j-1\_j}^{max}}{\sum_{u=1}^{K_{gen}} P_u^{max} - \sum_{n=1}^{K_{load}} D_n} \right) (11)$$
$$\leq FL_{j-1\_j}$$

Fig. 6.

$$P_s(t+\Delta t) = P_s(t).(1-\lambda_s \Delta t - \mu \Delta t) + P_{s-1} \lambda_{s-1} \Delta t + P_{s+1} \mu_{s+1} \Delta t \quad (12)$$

Where λ_s and μ_s are the immigration and emigration rates when there are species S in the habitat. This equation holds because in order to have S species at time $(t+\Delta t)$, one of the following conditions must hold:

1. When there is S species at time t, there will be no immigration or emigration occur between t and $t+\Delta t$;
2. When there is $S-1$ species at time t, there will be one species to immigrate;
3. When there is $S+1$ species at time t, there will be one species to emigrate.

The emigration rate λ_k and immigration rate μ_k for k number of species is given as,

$$\mu_k = \frac{Ek}{n} (13)$$

$$\lambda_k = I\left(1 - \frac{k}{n}\right) (14)$$

In case the emigration rate equal to the immigration rate, when value of E=I, then combining equation (13) and (14),

$$\mu_k + \lambda_k = E (15)$$

When immigration rate and emigration rate are equal only one species emigrate or immigrate at a time.

Fig. 7.

Fig. 8. BLOCK DIAGRAM

Area	Fuel cost($/hr)			
	DSM		BBO	
	Without constraint	With constraint	Without constraint	With constraint
A 1	183.74	183.73	168.74	162.88
A 2	164.11	138.76	174.10	159.58
A 3	256.84	289.63	256.84	288.23
Total	**604.68**	**612.12**	**603.68**	**610.69**

Fig. 9. Total cost of each area when power exported

Area	Fuel cost($/hr)			
	DSM		BBO	
	Without constraint	With constraint	Without constraint	With constraint
A 1	92.05	117.93	92.06	115.20
A 2	164.10	124.78	164.30	130.81
A 3	256.84	256.84	252.84	252.88
Total	**512.99**	**499.55**	**509.20**	**498.89**

Fig. 10. Total cost of each area when power imported

habitat member has an associated probability, which indicates the likelihood that it exists as a solution for a given problem. The medium HSI solutions have better chance to create much better solutions after mutation operation. Mutation rate of each set of solution can be calculated in terms of species count probability using the following equation: (16) Where is user-dened variable. This mutation scheme tends to increase diversity among the habitats.

C. BBO Algorithm for Economic Dispatch Problem of Microgrid In this section a new method to solve economic dispatch problem using BBO algorithm is described. The BBO algorithm can be summarized as Representation of SIVs: In economic dispatch problem the decision variables are real power generations, they are used to represent individual habitat. The SIV in a habitat is represented by using real power output of all the generators. The numbers of SIV of BBO algorithm is initialized as and number of habitat Initialization of SIVs: The SIV in each habitat set is initialized randomly with in the effective real power operating limits. The initialization is based on equation (3) for generators Steps of algorithm to solve microgrid economic dispatch problem is given below . Step 1: Initialize number of generator units, maximum and minimum capacity of the distributed generators, power demand and the BBO parameters like habitat modification probability, mutation probability, maximum mutation rate, maximum immigration rate, maximum emigration rate, elitism parameter p and set maximum number of iteration.

Step 2: SIVs of the given habitat is initialized using Initialization of SIV using equation (3). Here for microgrid the SIVs are real power outputs of DGs

Step 3: Calculate the HSI of each habitat for given emigration rate and immigration rate. The fuel cost of the generators in the power system for given power demand is represented by HSI (17) HSI in microgrid economic dispatch problem is fuel cost function given in equation (4)

Step 4: Based on calculated value of HSI value elite habitats are identified. The elite habitats represent the power output of the habitat, which give minimum fuel cost. The number if elite habitat retain will depend on the elitism parameter p.

Step 5: Perform migration operation on SIVs of non elite habitat, selected for migration. The migration is given as i) Select the upper and lower limits for immigration and emigration rate ii) Calculate the species count

Step 6: Then each habitat species count probability is updated using equation in step (6) of BBO algorithm. Mutation operation is performed on non-elite habitats. If the randomly generated number is less than the mutation rate calculated using equation (17) for any habitat, then that particular habitat is selected and mutation operation is performed .Again the limits are verified as in step (5) and the fuel cost is calculated. Step 7: Check for the maximum number of iteration, if condition satisfied stop otherwise go to step (3). After step (5) and (6) all constraints for the microgrid is verified and minimized fuel cost is calculated.

V. RESULTS AND DISCUSSIONS

The test system taken for the analysis of the problem is given in the below table:

The test system consists of 15 distributed generation units and it is divided into three areas each having 5 units. The first unit in each area is considered as FFC mode. To solve this problem, load distribution factor of each area=0.35:0.25:0.40

for $i = 1$ to M
{
if (fuel cost of habitat set $i, HSI_i <$ inf)
{
Species count of habitat $i = M - i$;
}
else
{
Species count of habitat $i = 0$;
}}
end
end

iii) Again calculate value of immigration and emigration rate for each habitat

for $i = 1$ to M
{
$\lambda(i)$ = I*(1-Species count of habitat i /Habitat size M);
$\mu(i)$ = E*(Species count of habitat i /Habitat size M);
}
end

iv) Selection of new SIV for migration operation

for $l = 1$ to M
{
if the randomly generated number is less than the habitat modification probability P_{moc}, then following operation is done as

$\lambda_{Scale} = \lambda_{Lower} + (\lambda_{Upper} - \lambda_{Lower}) * (\lambda(k) - \lambda_{Min}) / (\lambda_{Max} - \lambda_{Min})$

for $k = 1$ to n
{
if the randomly generated number $< \lambda_{Scale}$
{

Fig. 11. BLOCK DIAGRAM

and the load demand is taken as 1500kw. When the 100kw is exported to main grid or imported from maingrid the values of demand, generation with and without constraints in each area is given in below table 2 and 3 respectively. The power generation limits each area for stable island operation when power is initially imported and power is initially exported are calculated. For the stable island operation it is noted the generation limits changes. When power is exported the maximum generation limit is decreased. When power is imported the minimum limit is increased thus it enable stable islanded operation of microgrid. The table 2 and 3 give the calculated values

selectinx = 1;
while (randomnum> select) and (selectinx< M)
selectinx = selectinx +1;
select = select + μ (selectinx);
}
end
newly generated habitat (l, k) = old habitat(selectinx, k);
else
newly generated habitat (l, k) = old habitat (l, k);
}
}
end
end

After migration operation new habitat set is generated. For economic dispatch problem in microgrid, these represent modified power generation (P_u) values of distributed generators in microgrid

v) Operating limit constraint can be satisfied as

if position value of species P_u > maximum position value of species, P_u^{max}

$P_u = P_u^{max}$

else if position value of species P_u < minimum position value of species, P_u^{min}

$P_u = P_u^{min}$

else

$P_u = P_m$

end

vi) Check power balance limit

if (sum of the best position value of each species is added with the power from maingrid should be equal to the sum total load demand supplied y all species minus the value of non dispatchable species

$(\sum_{n=1}^{N_{gen}} P_n + P_{Maingrid} = \sum_{n=1}^{N_{load}} D_n - \sum_{m=1}^{N_{ND}} P_m)$

go to next step

else

repeat above step

Fig. 12. BLOCK DIAGRAM

in which it is noted 40kW of power have been transferred from area 2 to areas 1 and 3 respectively, without the constraint for stable islanded operation. The solutions were altered while considering reserve for stable islanded operation.

For exported power, the download flow from area 2 to area 3 was limited to -0.3kW, where the minus signs indicate power is transferred from area 3 to area 2.On the other hand

DG	Cost data			Output limit(kw)	
	c_g	b_g	a_g	Max	Min
G1	13.526	0.1032	0.0001	300	35
G2	4.0797	0.0792	0.0005	100	20
G3	7.7657	0.0656	0.0004	150	30
G4	1.8505	0.0689	0.0009	80	10
G5	1.091	0.0301	0.0011	100	20
G6	7.5957	0.0346	0.0002	250	60
G7	1.8505	0.0689	0.0009	80	10
G8	4.0797	0.0792	0.0005	100	20
G9	2.4047	0.0134	0.0009	120	30
G10	2.4047	0.0134	0.0009	120	30
G11	11.526	0.1032	0.0001	300	35
G12	6.4976	0.1164	0.0002	150	20
G13	5.4976	0.1164	0.0002	150	20
G14	2.0171	0.0486	0.0013	75	10
G15	2.5442	0.1189	0.0003	100	10
Total				2175	360

Fig. 13. 15-Unit input data

Area	Load (kw)	Generation(kw)		Flow limits			
		Without constraint	With constraint	Area		Limits(kw)	
				From	To	w/o con	W Con
A 1	525	555	545	2	1	40	40
A 2	375	485	454.21	2	3	39	0
A 3	600	561	600.3	3	2	0	0.3

Fig. 14. Power output of DG when exported

Area	Load (kw)	Generation(kw)		Flow limits			
		Without constraint	With constraint	Area		Limits(kw)	
				From	To	w/o con	W con
A 1	525	385	442.30	1	2	0	23
A 2	375	465	401.69	2	3	40	40
A 3	600	555	555	2	1	35	0

Fig. 15. Power output of DG when imported

for imported power the upward flow from area 2 to area 1 was restricted to -23kw. Hence the biogeography based optimization technique is used in this project minimize the cost by 0.011%.The total fuel cost comparing Direct Search Method (DSM)and BBO when power is exported and imported is given in table 4 and 5 respectively. From table 4 it can be said that there is increase of fuel cost by 0.028% from without stable operation constraint for BBO. This increase in cost is not an issue when considering the reliability of power supply.

In the below table the cost reduce by 0.022% from fuel cost without constraints. This reduction in fuel cost can be used from the spinning reserve when power is exported.

It can be also said from the results the proposed method the total cost is minimized compare to the DSM. For power generation of MWs ranges this method can reduce more cost and make stable operation of microgrid during islanding.

VI. CONCLUSION

The economic dispatch problem of microgrid was formulated in accordance with various constraints like i) reserve for non-dispatchable DGs, ii) flow limits between two areas, and iii) reserve for the stable islanded operation to fit the configuration of a microgrid. In this project an additional constraint to ensure the stable island operation of a microgrid are provide with detailed formulation according to the power sharing principle regarding the DGs. The economic dispatch problem of microgrid is solved using BBO algorithm. The cost of generation of power is compared with flow-limits, power importing and exporting from microgrid and vice-versa. This problem is tested with15 distributed generation units system. From the results obtain it can be said that the proposed method have fast convergence rate, avoid premature convergence and best optimum value is obtain. These characteristics BBO method makes it useful for future in solving various economic dispatch related problem to get best solution.

REFERENCES

[1] F. Katiraei, M. R. Iravani, and P. W. Lehn, *Micro-grid autonomous operation during and subsequent to islanding process, IEEE Trans.Power Del.,*,vol. 20, no. 1, pp. 248257, Jan. 2005.

[2] Y. Li, D. M. Vilathgamuwa, and P. C. Loh, *Design, analysis, and real-time testing of a controller for multi bus microgrid system, IEEE.Trans. Power Electron.,* ,vol. 19, no. 5, pp. 11951204, Sep. 2004.

[3] F. Katiraei and M. R. Iravani, *Power management strategies for a microgrid with multiple distributed generation units, IEEE Trans. PowerSyst.,* ,vol. 21, no. 4, pp. 18211831, Nov. 2006.

[4] J. L. Rodriguez-Amenedo, S. Arnalte, and J. C. Burgos, *Automatic generation control of a wind farm with variable speed wind turbines, IEEE Trans Energy Convers.,* ,vol. 17, no. 2, pp. 279284, Jun. 2002.

[5] R.Vijay and C.S. Ravichandran,*Enriched Biogeography based Optimization Algorithm to solve Economic Power Dispatch Problem.Advances in Intelligent and Computing*,Vol.78, pp.879-892,2016.

Design and analysis of 7-level inverter at different modulation indices with a closed loop control

Dr.N .Muralikrishnan
HOD
Department of Electrical and Electronics Engineering
MAILAM ENGINEERING COLLEGE

Mr.G.G.Muthukumar
Assistant professor
Department of Electrical and Electronics Engineering
MAILAM ENGINEERING COLLEGE

Mr.P.Balapriyan
pg scholor
Department of Electrical and Electronics Engineering
MAILAM ENGINEERING COLLEGE

***Abstract*—This paper represents the design, simulation and analysis of a proposed multi level inverter. The proposed multilevel inverter generates seven levels AC output voltage with the appropriate gate signals design. Multilevel inverters have been an important development in recent years, owing to their capability to increase the voltage and power delivered to the motor with semiconductor switches which are available today. The multilevel inverter suitable for high voltage and high power applications, the THD contents in output voltage of inverter is very significant index as the performance of drive depends very much on the quality of voltage applied to drive. The operating principles of the proposed inverter and the voltage balancing method of input capacitors are discussed. The major feature of the proposed topology is the reduction of power components. The THD analysis at different modulation indexes for the proposed topology is also carried out. Index Terms- multilevel, DC to AC inverter, THD, modulation index.**

I. INTRODUCTION

A multi level inverter is a power electronic device built to synthesize a desired AC voltage from several levels of DC voltages .Multi level inverters have been an important development in recent years, owing to their capability to increase the voltage and power delivered to the motor with semi conductors which are available today. Multilevel inverters have gained more attention in high power applications because it has got many advantages .It can realize high voltage and high power output by using semiconductor switches without the use of transformer and dynamic voltage balance circuits. When the number of output levels increases, harmonics of the output voltage and current as well as electromagnetic interference (EMI) decrease. The basic concept of a multilevel inverter is, to achieve higher power by using a series of power semiconductor switches with several lower voltage dc sources, to perform the power conversion by synthesizing a staircase voltage waveform .To obtain a low distortion output voltage nearly sinusoidal, a triggering signal should be generated to control the switching frequency of each power semi conductor switch. In this paper the triggering signals of multi level inverter are designed by using the sinusoidal PWM scheme. A novel multilevel inverter is designed and implemented in this paper. The major feature of the proposed topology is the reduction of power components. The purpose of multilevel topology is to reduce voltage rating of power switch. Therefore, it usually use at high power application. By combining output voltages in multilevel form, it has advantages of low dv/dt, low input current distortion, and lower switching frequency. As a result of advantages of multilevel topology, several topologies have emerged in recent years. The industry demand higher power applications, the specification of power device is higher. Although IGBT has features of high power rating and high voltage stress, it cannot operate at high frequency. And the design of IGBT gate driver is complicated. MOSFET is the appropriate component to operate at high frequency, but power rating is not as good as IGBT. To solve the problem, many different topology of multilevel use low rating component at high power application.

The multilevel approach for DC to AC conversion offers many advantages such as i. The staircase waveform not only exhibits a better harmonic profile but also reduces the dv/dt stresses. Thus, the filter requirements can be greatly brought down (or even eliminated), while electromagnetic compatibility problems can be reduced. ii. The voltage stresses on the semiconductor devices are much lesser as compared to the overall operating voltage. Thus, a high voltage waveform can be obtained with comparatively low voltage rated switches.

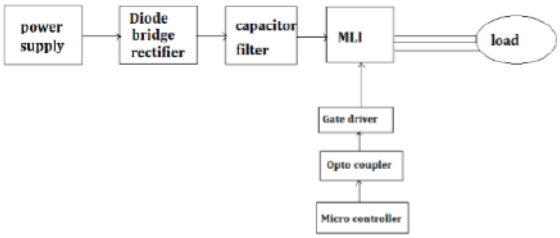

Fig. 1. Basic block diagram of MLI

iii. MLIs produce much smaller common mode voltage and thus the stress in the bearings of a motor connected to a multilevel motor drive can be reduced. iv. Many multilevel topologies offer the possibility to obtain a given voltage level with multiple switching combinations. These redundant states can be utilized to program a fault tolerant operation. v. MLIs can draw input current with low distortion. vi. Renewable energy sources such as photovoltaic, wind, and fuel cells can be easily interfaced to a multilevel converter system and can be controlled for equal load sharing amongst the input sources.

II. CIRCUIT DESCRIPTION

Figure.2 shows the proposed novel topology used in the seven- level inverter. An input voltage divider is composed of three series capacitors C1, C2, and C3. The divided voltage is transmitted to H-bridge by four MOSFET, and four diodes. The voltage is send to output terminal by H-bridge which is formed by four MOSFET. The proposed multilevel inverter generates seven levels AC output voltage with the appropriate gate signals design.The required seven voltage output levels (1/3Vdc, 2/3Vdc, Vdc, 0) are generated as follows: 1) To generate a voltage level Vo = 1/3Vdc, S1 is turned on at the positive half cycle. Energy is provided by the capacitor C1 and the voltage across H-bridge is 1/3Vdc. S5 and S8 is turned on and the voltage applied to the load terminals is 1/3Vdc. 2) To generate a voltage level Vo = 2/3Vdc, S1 and S4 are turned on. Energy is provided by the capacitor C1 and C2. The voltage across H-bridge is 2/3Vdc. S5 and S8 is turned on and the voltage applied to the load terminals is 2/3Vdc. 3) To generate a voltage level Vo = Vdc, S1 and S2 are turned on. Energy is provided by the capacitor C1, C2, and C3. The voltage across H-bridge is Vdc. S5 and S8 is turned on and the voltage applied to the load terminals is Vdc. 4) To generate a voltage level Vo = -1/3Vdc, S2 is turned on at the negative half cycle. Energy is provided by the capacitor C3 and the voltage across H-bridge is 1/3Vdc. S6 and S7 is turned on and the voltage applied to the load terminals is -1/3Vdc. 5) To generate a voltage level Vo = -2/3Vdc, S2 and S3 are turned on. Energy is provided by the capacitor C2 and C3. The voltage across H-bridge is 2/3Vdc. S6 and S7 is turned on, the voltage applied to the load terminals is -2/3Vdc. 6) To generate a voltage level Vo = -Vdc, S1 and S2 are turned on. Energy is provided by the capacitor C1, C2, and C3, the voltage across H-bridge is Vdc. S6 and S7 is turned on, the voltage applied to the load terminals is Vdc. 7) To generate a voltage level Vo = 0, S5 and S7 are turned on. The voltage applied to the load terminals is zero. The Switching Combinations Required To Generate the Proposed Seven-Level Output Voltage Waveform Is Shown Below

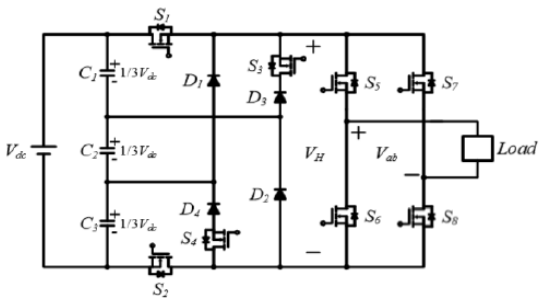

Fig. 2. A novel seven level inverter topology.

III. CONTROL TECHNIQUES

In this paper, several triangular carriers are distributed by phase disposition technique. The advantage of phase disposition technique are uncomplicated to realize and less total harmonic distortion. These carriers compare with a reference sine waveform vsin to get signal of switches. .The frequency of carrier is switching frequency of inverter. Fig. 3 shows the reference sine wave, carriers, and control signals of switches.

The phase disposition technique has all carrier waveforms in phase with same frequency and amplitude, as shown in Fig. . The zero reference is placed in the middle of the carrier sets. For this technique, significant harmonic energy is concentrated at the carrier frequency. The several triangular carriers are distributed by phase disposition technique. The Components Comparison between four different Seven-Level Inverters is shown below.

IV. OPEN LOOP SIMULATION

The simulation circuit for open loop model of the proposed system is shown in the figure.4.Here the input voltage is taken as 240v and the resistive load is taken.

And the simulated output voltage of the open loop simulation obtained is shown in the figure 5

V. CLOSED LOOP SIMULATION

The output voltage of the proposed inverter is compared with reference sinusoidal waveform and the error is given to the PI controller to generate the gating signals. The simulated circuit with PI controller is shown in figure 6.

And the simulated output voltage of the open loop simulation obtained is shown in the figure 7.

	SWITCHING COMBINATIONS							
Output voltage	S1	S2	S3	S4	S5	S6	S7	S8
1/3 Vdc	ON	OFF	OFF	OFF	ON	OFF	OFF	ON
2/3 Vdc	ON	OFF	OFF	ON	ON	ON	OFF	ON
Vdc	ON	ON	OFF	OFF	ON	OFF	OFF	ON
-1/3 Vdc	OFF	OFF	OFF	OFF	OFF	ON	ON	OFF
-2/3 Vdc	OFF	ON	ON	OFF	OFF	ON	ON	OFF
-Vdc	ON	ON	OFF	OFF	OFF	ON	ON	OFF
0	OFF	OFF	OFF	OFF	ON	OFF	ON	OFF

TABLEI: SWITCHING COMBINATIONS REQUIRED TO GENERATE THE PROPOSED SEVEN-LEVEL OUTPUT VOLTAGE WAVEFORM

Fig. 3.

VI. ANALYSIS OF THD AT DIFFERENT MODULATION INDICES

The analysis has been carried out for THD at different modulation indices for closed loop model are represented below .The peak value of reference sine wave is Vsin , and the peak value of carrier wave is Vtri and the modulation index mA is defined as:

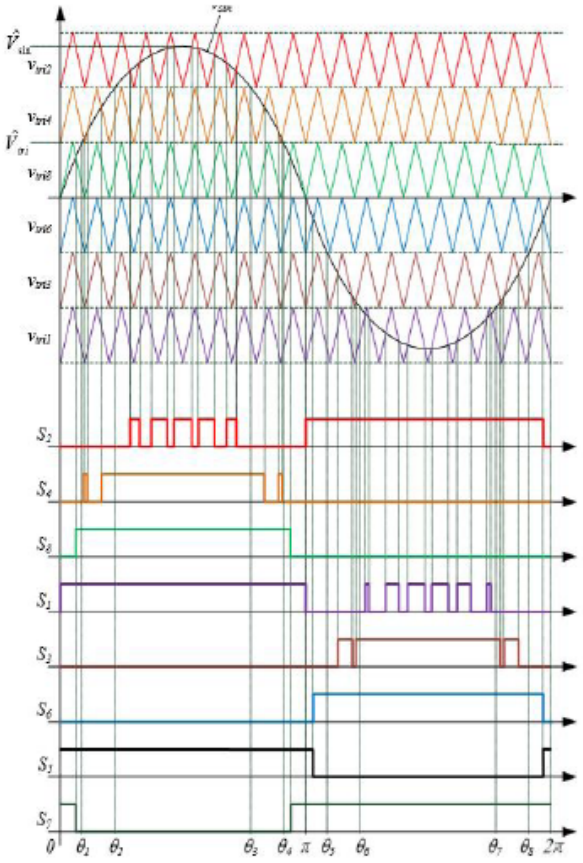

Fig. 4. Reference sine wave, carriers, and control signals of switches.

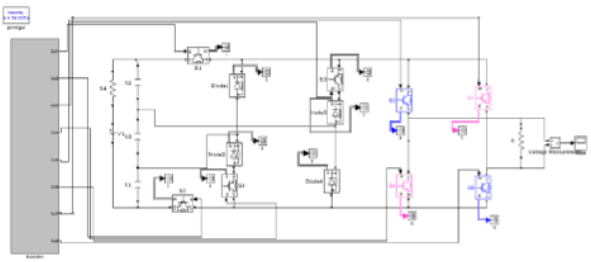

Fig. 5. Simulation circuit for open loop model

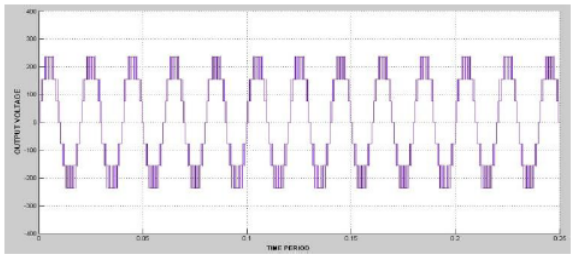

Fig. 6. Simulation circuit for open loop model

VII. CONCLUSION

Thus a seven-level inverter is designed and implemented by using MATLAB in this project. The main idea of the proposed configuration is to reduce the number of power device. The reduction of power device is proved by comparing with traditional structures. The proposed technique can generate stepped waveforms with a wide range of modulation indices (from 0.80 to 1.05), as well as minimized harmonic distortion. Hence from the analysis it can be concluded that modulation index has assorted effect on THD.

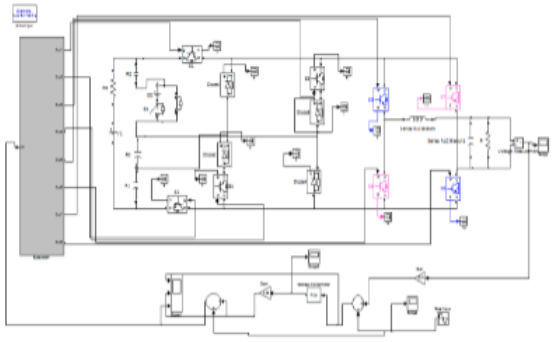

Fig. 7. Simulation circuit of the closed loop model

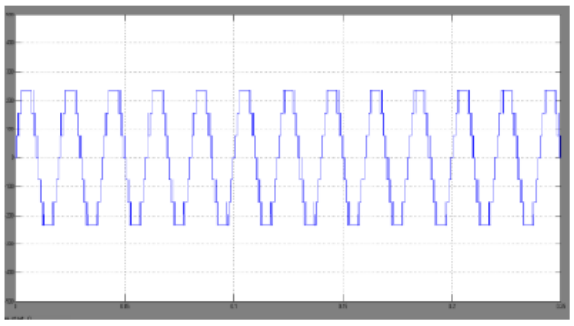

Fig. 8. Simulation circuit of the closed loop model

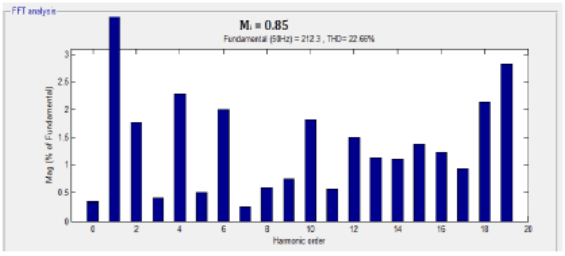

Fig. 9. Simulation circuit of the closed loop model

REFERENCES

[1] Gonzalez.R , Gubia, J. Lopez, and L. Marroyo, *Transformerless Single-Phase Multilevel-Based Photovoltaic Inverter,*,IEEE Trans. on Industrial Electronics, vol. 55, no. 7, pp. 2694-2702, 2008.

[2] S. Daher, J. Schmid, and F. L. M. Antunes,*Multilevel Inverter Topologies for Stand-Alone PV Systems,*,IEEE Trans. on Industrial Electronics, vol. 55, no. 7, pp. 2703-2712, 2008.

[3] W. Yu, J. S. Lai, H. Qian, and C. Hutchens, *High-Efficiency MOSFET Inverter with H6-Type Configuration for Photovoltaic Nonisolated AC-Module Applications,*IEEE Trans. on Power Electronics, vol. 26, no. 4, pp. 1253-1260, 2011.

[4] R. A. Ahmed, S. Mekhilef, and W. P. Hew, *New multilevel inverter topology with minimum number of switches,*,in Proc. IEEE TENCON, pp. 1862-1867, 2010.

An Enhanced Controller for Shunt Active Filter Interfacing Renewable Energy Source and Grid

Mr.R.ajith kumar
UG Scholar
Department of Electrical and Electronics Engineering
ST.ANNE'S COLLEGE OF ENGINEERING AND TECHNOLOGY

***Abstract*—Developing efficient interfacing technologies for the renewable energy source are promising research area now days. The interfacing unit becomes crucial as renewable energy sources when directly connected to grid, can inject harmonic components that may deteriorate the quality of power. This paper proposes a shunt active filter as an interface between renewable energy sources and grid with a modified and efficient control scheme. The shunt active filter with this modified controller controls the real power supplied by the grid (source) to load and remaining load requirements is supported by the renewable energy source in addition to its regular functions such as harmonic current elimination, reactive power compensation and power factor correction. In this paper two types of nonlinear loads are considered and simulated for analyzing the effectiveness of control algorithm to achieve the real power sharing from renewable energy source, grid along with harmonic elimination, reactive power compensation and power factor correction using shunt active filter interface. Keywords- Shunt active; filter inteiface; renewable energy source; AC voltage controller; dynamic and static non-linear loads.**

I. INTRODUCTION

The dependency of electric power generation units on renewable energy sources is increasing day by day. Many research works are still going on in the area of interconnection of these systems to grid. When Distributed Energy Resources (DER) are directly connected to grid, various power quality issues are created. Detailed survey of power quality problems, measurements, analysis and effects of harmonics have been reported in literature. [1, 2, 3] The harmonics have a number of undesirable effects on the distribution system. The harmonic currents are causes additional losses, overheating, and overloading in power system equipments [1]. To mitigate the harmonics and improve the quality of power, two commonly used approaches are the passive filters and active filters [4, 5].The hybrid filters and Improved Power Quality Converters (lPQCs) are also used as solutions to power quality problems[6, 7, 8]. The various interfacing methods are reported in literature for renewable energy source with grid; among those methods the commonly used topologies such as separately connected systems, micro-grids, multi-port converter and custom power devices [9-10]. The shunt active filter interface is a new topology for renewable source, which is proposed in [11-12]. In this paper, a three phase shunt active filter with an enhanced controller is proposed as the interface between a renewable energy source and grid feeding dynamic and static non-linear loads. In the proposed test system, one dynamic and one static load has been considered for analysis purpose. The first test system, AC voltage controller fed induction motor, in which AC voltage controller used as a soft start for induction motor which has been used in various commercial and industrial applications (water pumping systems, conveyors). Although AC voltage controller reduces the starting current, the source current becomes rich in harmonics. The second test system, AC voltage controller fed RL load which is rated same as induction motor load. The diode bridge rectifier load is also introduced along with above mentioned two test system. The harmonics are compensated by the shunt active filter which is used as the interfacing unit between renewable energy source and grid. In addition to normal active filter functions, there is a control over the real power supplied by the grid (source) with the use of shunt active filter based on modified Icos¡l¿ controller.

II. THREE PHASE SHUNT ACTIVE FILTER AS INTERFACE BETWEEN RENEWAB LE ENERGY SOURCE AND GRID

A three phase balanced AC source represents the grid/source is used to supply the non-linear load. The renewable energy source is connected at the point of common coupling through the shunt active filter interface. The output from the renewable energy is considered as DC output, which is connected across the DC link capacitor of shunt active filter. The total load requirement is met by power got from the renewable energy source and source /grid. Here, the grid power is controlled by

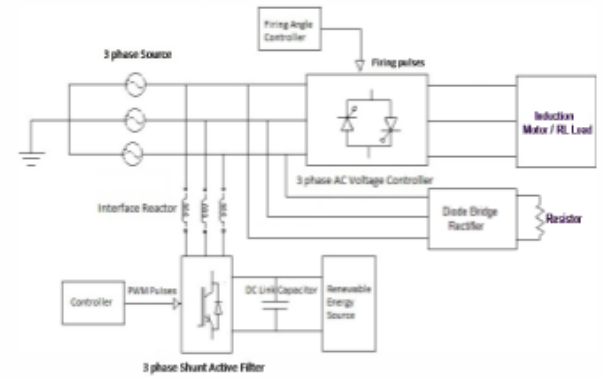

Fig. 1. Schematic of three phase system with shunt active filter as the interface

the proposed controller. Two test systems are being considered in the controller explanation, in test system1 , an AC voltage controller feeds a three phase induction motor of 7.5 hp, 1440 rpm, 400 V, lO A, 0.82p.f, in test system2, the AC voltage controller feeds the three phase RL load of same rating (i.e. PL= 5.6 kW, QL=3.9 kVar).Both these test systems are deploying synchronized 6 pulse generator which generates the pulses for the AC voltage controller. At the time of starting, the firing angle is kept at 110 for reducing the supply voltage to motor .Once the motor starts running; the firing angle of the AC voltage controller is gradually reduced to zero. When the firing angle becomes zero, the full supply voltage appears across the machine and v/f ratio is also maintained constant under steady state conditions. Now a second load of diode bridge rectifier feeding resistive load is introduced at t=3sec. The shunt active filter is traditionally assigned to eliminate the current harmonics, perform reactive power compensation and power factor correction, but in this work it is used as an interfacing unit for renewable energy source. It transfers the real power from renewable energy source to load and grid with modified Icos¡l¿ controller by maintaining unity power factor at the source side. The real power transfer from renewable energy source is regulated by DC-DC converter which maintains the DC link voltage as constant.

III. MODIFIED ICOS¡L¿ CONTROLLER FOR GRID INTEGRATED RENEWABLE ENERGY SOURCE

Various control schemes are used to generate the compensation signals for the shunt active filter, which is used for mitigating power quality issues, they are Instantaneous Reactive Power Theory [13], synchronous detection algorithm [14], DC bus voltage algorithm [15] and synchronous reference frame theory [16] are some of the widely used three-phase shunt active filtering algorithms. Existing control schemes still require fine-tuning to make the computation and the circuit implementations as simple and rugged as possible. A simple and effective control circuit enhances the speed of response and efficiency of the filter. The Icos¡J:¿ algorithm is one such a simple current compensation algorithm to compensate for harmonics in three-phase systems.

A. 1cosCP control algorithm

The Icos¡l¿ algorithm which is reported in [17] is used to provide harmonic, reactive and unbalance compensation in a three phase system with balanced/unbalanced source and load conditions. It uses minimum computational steps and simple circuits and can be applied to practical system conditions like distorted and asymmetrical AC source supplying non-linear unbalanced loads. The current drawn from the source is highly non-linear and reactive when it is supplying a non-linear load such as diode bridge rectifier, thyristor converter, and AC voltage controller. The algorithm aims at limiting the percentage THD in source current within the IEEE standard limits in addition to achieving unity power factor at the source end. In the Icos¡l¿ algorithm, the desired mains/source current is assumed to be the product of the magnitude Icos¡l¿ and a unit amplitude sinusoidal wave in phase with the mains voltage. The mains/source is required to supply only the active portion of the load current as the shunt active power filter is expected to provide compensation for the harmonic and reactive portion of the three-phase load current, and also for any imbalance in the three-phase load currents. Hence, only balanced currents will be drawn from the mains which will be purely sinusoidal and in phase with the mains/source voltages.

B. Modified 1cosCP control algorithm

In general shunt active filters are expected to provide current harmonic compensation, reactive power support and imbalance condition. The real power demanded by the loads is met by the source/grid with power factor maintained close to unity. With renewable energy source backup, real power support can also be extended by the shunt active filter under proper control as and when needed. The modified Icos¡l¿ control algorithm is proposed here to achieve this additional real power support from renewable energy source using shunt active filter. The grid is required to supply only the fraction of active portion of the load curernt as determined by the controller. The remaining load requirement is met by renewable energy source through shunt active filter. The main advantage of this algorithm is that real power sharing is achieved between grid, renewable energy source and load. The reference compensation currents for the shunt active filter are deduced as the difference between the actual load current and the desired source curernt in each phase . i.e.

where K is the load factor which determines how much real power has to be supplied by the source/grid. Va, Vb, and Vc are the unit amplitude templates of the phase to ground source voltages in the three phases respectively.

$$I_{a(comp)} = I_{La} - I_{sa(ref)}; I_{b(comp)} = I_{Lb} - I_{sb(ref)}; \quad I_{Lc(comp)} = I_{Lc} - I_{sc(ref)}; \qquad (1)$$

where, the desired (reference) source currents in the three phases are given as,

$$I_{sa(ref)} = K\left|I_{s(ref)}\right| \times U_a = K\left|I_{s(ref)}\right| \sin\omega t$$

$$I_{sb(ref)} = K\left|I_{s(ref)}\right| \times U_b = K\left|I_{s(ref)}\right| \sin(\omega t - 120°)$$

$$I_{sc(ref)} = K\left|I_{s(ref)}\right| \times U_c = K\left|I_{s(ref)}\right| \sin(\omega t + 120°) \qquad (2)$$

Fig. 2.

$$U_a = 1.\sin\omega t; U_b = 1.\sin(\omega t - 120°); U_c = 1.\sin(\omega t + 120°); \qquad (3)$$

Fig. 3.

The magnitude of the desired source current IIs(ref) I can be expressed as the magnitude of the real component of the fundamental load current in the respective phases .i.e. for phase 'a' it can be written asll 1=IRe(I ll.A zero crossing detector s(ref) La (ZCD) is used to detect the negative going zero crossing of the corresponding phase voltage. The ZCD has been designed with a tolerance of 5% to ensure that any oscillations around the zero-crossing are taken care of The phase-shifted fundamental current goes as the "sample" input and the ZCD output pulse goes as the "hold" input to the "sample and hold" circuit whose output is the magnitude IIcOS¡l¿I=11 I. This magnit ude is s(ref) multiplied with unit amplitude sine wave in phase with input voltage and also desired fraction which determines how much real power is supplied by the source. Difference between load current and reference source current gives the reference filter current. This reference filter current and actual filter current are given to a hysteresis controller to get the pulses for the inverter.

IV. MODELING AND SIMULATION OF SHUNT ACTIVE FILTER WITH MODIFIED ICOS¡P CONTROLLER

The simulations of the above described test systems are carried out in MATLAB /Simulink to check the performance of AC voltage controller as a soft starter for the induction motor and also to verifY the performance of shunt active filter based on modified Icos¡l¿ control algorithm. Three single phase sources which is star connected are considered as grid with voltage of 400V, 50Hz. This grid is connected to non-linear loads. Two types of loads have been considered. (a) AC voltage controller connected to the induction motor. (b) AC voltage controller connected to RL load. Both cases diode bridge rectifier is also switched on along with these loads at t=3 sec. When an induction motor is connected to source through direct on-line starter, the starting current is high. To reduce the starting current, an AC voltage controller is used as a soft start. A three phase AC voltage controller is made up of three back to back connected thyristor pairs that are fired at an interval of 60. The smooth firing angle control is done using control logic and synchronous pulse generator. In such applications, due to the AC voltage controller, rich harmonics are generated and harmonic current drawn from the source/ grid. Since shunt active filter can mitigate the harmonics generated, it has been opted for use in the above mentioned type of load for the given setup. The motor load of 7.5 HP, 1440 rpm, 400 V, 10 A, 0.82 pf ant its equivalent RL load of PL= 5.6 kW, QL=3.9 kVar are connected to test system .The diode bridge rectifier feeding R load with a capacity of IOAkW is also connected in parallel to the system. Shunt Active Filter and Controller A three phase Voltage Source Inverter (VSI) is considered as a shunt active filter for the interfacing unit for the renewable energy source. The pulses for the VSI are derived by the controller using modified Icos¡l¿ control algorithm. The shunt active filter parameters are given in Table I:

A. AC voltage controller as a soft starter

When motor load is connected to supply with direct on-line starter the starting current is almost 90A as seen in Fig. 2 .The starting current, steady state current and current when load is applied (t = 3sec) to motor with direct on-line starter can be noted from Fig. 2 When the induction motor is connected through direct on line starter, the starting current is 90A. Under full load condition, the current is almost lOA. Fig.3 shows the starting current, steady state current and current when full load is applied with soft starter. The firing is done in such a way that, at the time of starting, firing angle is a = 110 and the output voltage of AC voltage controller is thus reduced. This is fed to induction motor which will result in the reduction of starting current. The starting current is reduced to 16A as compared to 90A with direct on line starter. After some time (t=1.2sec), fIring angle a starts gradually reducing and fmally it reaches to OO(t=2sec). At this point, full supply voltage is provided to the machine and it runs under normal conditions i.e the rated voltage and frequency (v/t) ratio maintained constant. Initially the machine is under no load and full load is applied at t=3sec.As mentioned earlier a second non-linear load namely diode bridge rectifIer with resistive load is switched on at this time. The total load power is then 16kW.

B. Shunt active filter with modified lcosr controller as the interfacing unit

The shunt active fIlter used as the interfacing unit should compensate reactive power and harmonics thereby maintaining

Load	Shunt Active Filter Parameters		
	Coupling Inductance	*DC link Capacitance*	*DC Link Voltage*
Test System 1	9 mH	6mF	680 V
Test System 2	8 mH	10mF	680V

Fig. 4. SHUNT ACTIVE FILTER PARAMETERS

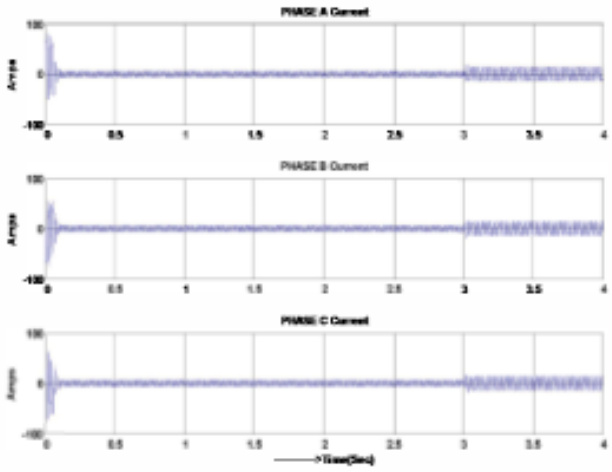

Fig. 5. Wave forms of source current when an induction motor is directly connected to the supply

unity power factor at source side.Fig. 4 shows the waveforms of source voltage, load current, reference fIlter current generated by the controller, actual fIlter current measured from the circuit and desired source current respectively. These are obtained under the dynamic load condition in test system1 (AC voltage controller connected to the induction motor +diode bridge rectifIer feeding resistive load)

High level of harmonics is present in the current wave form as seen. The actual fIlter current and reference fIlter current from the controller are almost same. This implies that the controller is working according to the desired functionalities Fig. 5 shows the source voltage and source current waveform after compensation for all the three phases with three phase shunt active fIlter.

After shunt active fIlter is introduced, unity power factor is obtained and source current became sinusoidal. This implies that the harmonics are considerably reduced by the shunt active fIlter. Fig. 6 shows the waveforms of source voltage, load current, reference fIlter current generated by the controller, actual fIlter current measured from the circuit and desired source current respectively. These are obtained with static load in test system2 (AC Voltage Controller with RL load+ Diode bridge rectifIer feeding resistive load) Before introducing shunt active fIlter source current is distorted and have harmonics. In this case also actual fIlter current follows reference fIlter current. Fig. 7 represents the source voltage and source current waveforms for all the phases under static load after compensation.

It is seen that after introducing shunt active fIlter source current is almost sinusoidal. Table II and III gives the details of real power flow sharing between grid/source and renewable energy resources for both dynamic and static loads. Depending upon the fraction of real power supplied by the source, the above system is simulated and tabulated under different fractions. Depending upon the factor, exact power sharing between gird and renewable energy sources is done. Reactive

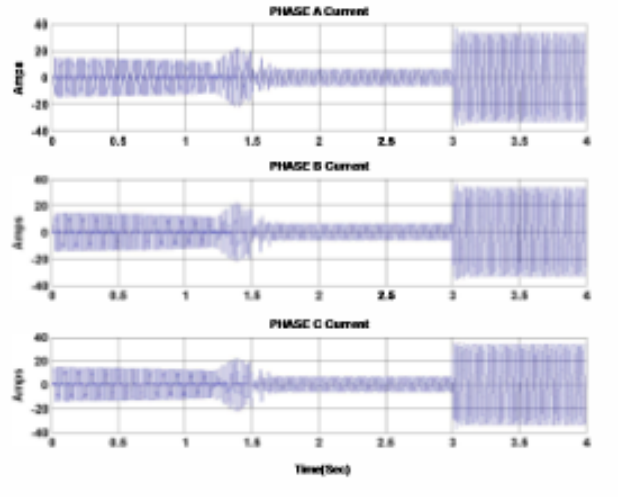

Fig. 6. Wave forms of source current when an induction motor is connected to the supply through AC Voltage Controller as soft start

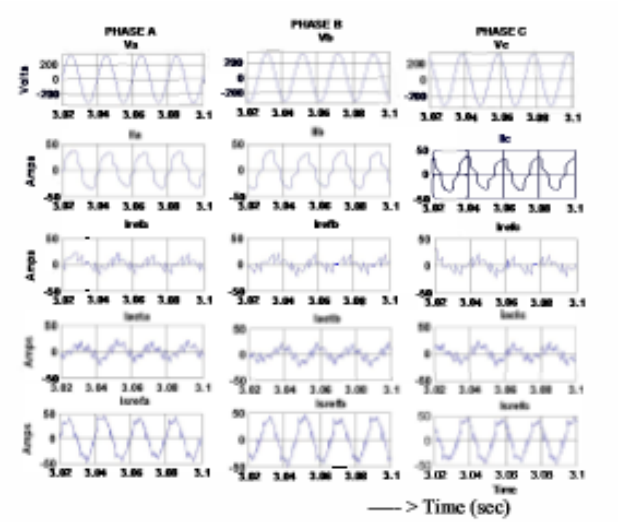

Fig. 7. Wave forms of source voltage, load current, reference filter current, actual filter current and desired source current

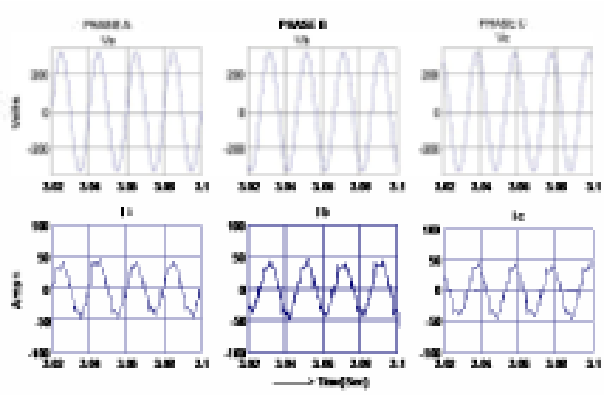

Fig. 8. Source voltage and current wave forms after compensation

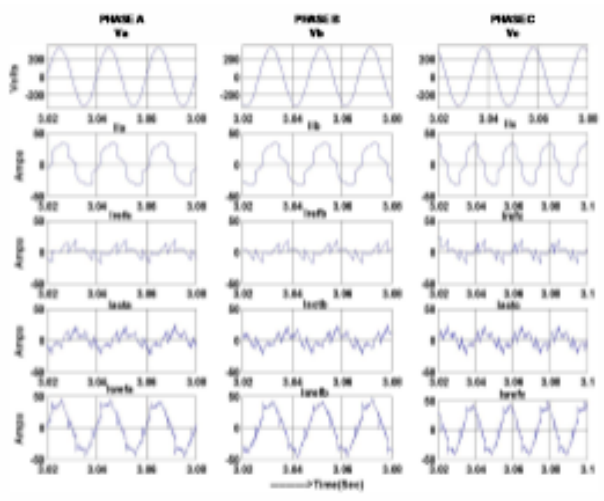

Fig. 9. Wave forms of source voltage, load current, reference filter current, actual filter current and desired source current

power is compensated by the fIlter.

When the load fuctor is 1, the source supplies entire load power. In addition to this, in all the above cases the source is supplying some extra power to compensate the losses taking place in the interfacing unit (approximately 3kW). For different fractions power sharing between gird and renewable energy source is done. For example as in Table II, to meet the load of 16kW with load factor .5,the source should supply 12 kW and renewable energy source should supply 12kW, where source/grid is supplying 15kW to compensate the losses in the interfacing unit. From all the above results it is observed that a shunt active filter when used as the interfacing unit for renewable energy source and grid achieves all compensation requirements effectively in addition to extending real power sharing of load along with the grid.

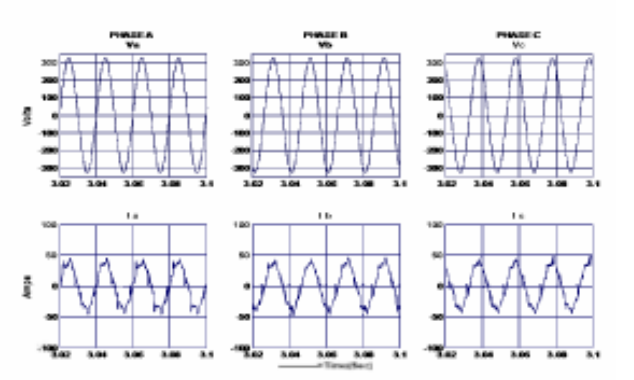

Fig. 10. Source voltage and current wave forms after compensation

L.F	TEST SYSTEM 1		
	Source /Grid Power	*Renewable Energy Source Power*	*Load Power*
1	P=19kW Q=-0.7kVar	P=-3kW(losses) Q= 4.8kVar	P=16kW Q=4.1kVar
0.75	P=15kW Q=-0.8kVar	P=1kW Q=4.9 kVar	P=16kW Q=4.1 kVar
0.5	P=11 kW Q=-0.9 kVar	P=5 kW Q=5.05 kVar	P=16 kW Q=4.1 kVar
0.25	P=7.5 kW Q=-1.1 kVar	P=8.5 kW Q=5.2 kVar	P=16 kW Q=4.1 kVar

Fig. 11. POWER SHARING BETWEEN GRID AND RENEWABLE ENERGY SOURCE

L.F	TEST SYSTEM 2		
	Source /Grid Power	*Renewable Energy Source Power*	*Load Power*
1	P=18.7 kW Q=-0.6 kVar	P=-2.7 kW Q=4.7 kVar	P=16 kW Q=4.1 kVar
.75	P=14.8 kW Q=-0.7 kVar	P=1.2 kW Q=4.8 kVar	P=16 kW Q=4.1 kVar
.5	P=11 kW Q=-0.875 kVar	P=5 kW Q=4.975 kVar	P=16 kW Q=4.1 kVar
.25	P=7.2 kW Q=-1.1 kVar	P=8.8 kW Q=5.2 kVar	P=16 kW Q=4.1 kVar

Fig. 12. POWER SHARING BETWEEN GRID AND RENEWABLE ENERGY SOURCE

V. CONCLUSION

The shunt active filter as an interface between renewable energy sources and grid with an efficient control algorithm has been simulated and the performance has been analyzed. The setup is tested with two types of loads one as dynamic load of AC voltage controller fed induction motor load with diode bridge rectifier and other one as static load which is a combination of AC voltage controller fed RL load along with diode bridge rectifier . The smooth control of the firing angle of AC voltage controller as soft starter is achieved by starting with a large delay angle and gradually reducing it to zero, then full supply voltage is applied by maintain v/f ratio constant for induction motor load and the problems of electromechanical starting can be overcome by this soft starting method. The modified Icos¡D control algorithm for shunt active power filtering was developed and simulated in MA TLAB. The modified Icos¡D controller has control over the real power from the source/grid and the remaining load requirement has been met by the renewable energy source through the shunt active filter interface in addition to the normal functions of such as harmonic elimination, reactive power compensation and power factor correction.

VI. ACKNOWLEDGMENT

This work has been funded by DST SERC under Fast Track Scheme for Young Scientists No: lOO/IFD/2769. The authors are also grateful to Amrita Vishwa Vidyapeetham University, Amrita School of Engineering, Bengaluru campus for extending support for this project.

REFERENCES

[1] W.M.Grady and S.Santoso, *"Understanding Power System Harmonics," IEEE Power Engineering Review,* Vol.21 no.ll,2001, pp. 8-11.

[2] Arrilaga, D. A. Bradley and P.S.Bodger,*"Power Systems Harmonics", Chichester,* UK, Wiley,1985.

[3] L. G. B. Rolim, A. Ortiz, M. Aredes, R. Pregitzer, 1. G. Pinto, Joao L. Afonso, *"Custom Power Interfaces for Renewable Energy Sources",* 1-4244-0755-9/07 IEEE 2007.

[4] Pedro Neves, D Goncalves, J G Pinto, Renato Alves, Joao L. Afonso,*"Single Phase Shunt Active Filter Interfacing Renewable Energy Sources with power Grid".*Vol.21 no.ll,2001, pp. 8-11.

[5] G.Bhuvaneswari, , Manjula G. Nair, *"Design, Simulation and Analog Circuit Implementation of a Three - Phase Shunt Active Filter Using the Icos¡l¿ Algorithm",* IEEE Transactions on power delivery April 2008.

EMBEDDED SYSTEM FOR TRANSFER OF DATA FROM SWITCH YARD TO CONTROL ROOM

Mr.P.KAMALRAJ
UG Scholar
Department of Electrical and Electronics Engineering
MAILAM ENGINEERING COLLEGE

K,PRASATH
UG Scholar
Department of Electrical and Electronics Engineering
MAILAM ENGINEERING COLLEGE

***Abstract*—Data refreshment rate of a present power system is relatively slow and in some cases this slow refreshment rate may not be capable of providing information about dynamic state of power system devices. The use of multi protocol label switching based technique is one option to overcome this problem. A cost effective and simpler detection device is needed for condition monitoring and integrating the sensor signals into the smart grid monitoring system. Remote and on-line monitoring of ultra wide band partial discharge signal in a switch-yard is a new concept in smart grid technology that will help avoid damage of switchyard devices. It is possible to convert the radio frequency partial discharge signal into an equivalent milli-volt or milli-ampere output for remote or centralized monitoring of switchyard devices. Multi Protocol Label Switching based data transfer rate is faster than the conventional data transfer system of a power grid. In this paper a new and technically better method of on-line radio frequency partial discharge monitoring from a remote smart grid control room through multi protocol label switching**

I. INTRODUCTION

The switchyard is a component-based development framework focused on building structured, maintainable services and applications using the concepts and best practices of SOA(service oriented architecture). Switchyard Provides the facilities for switching ,protection Control of electric power. To handle high Voltage power with proper Safety measures. To isolate the noises coming from the grid with true 50Hz power SWITCH YARD IS IMPORTANT PART IN THERMAL PLANT. So in our project, we are planning to design a system for data transfer from switch yard to control room. The cost of structures also is a major consideration while deciding the selection of a substation. For instance, in the case of the strain/flexible bus-bar arrangement, cost of structures is much higher than in the case of rigid bus type. Similarly the form of structures also plays an important part and the choice is usually between using a few heavy structures or a large number of smaller structures. While finalizing the design, size and single line diagram of structures, safety clearance requirements should be ensured. Steel is the most commonly used material in India for substation structures. Normally the steel structures are hot-dip galvanized so as to protect them against corrosion. However, galvanizing sometimes has not 399 proved effective, particularly in substations located in coastal or industrial areas and in such cases painting also becomes essential. In other countries special paints have been developed which are applied within the shop and these paints have been quite effective. Isolating switches are used to isolate equipment for maintenance. Isolating switches on line side are provided earthing blade for connection to earth in off position for safety. Transfer of load from one bus to another by isolators is not recommended. The isolating switches are designed for no load operation. Inadvertent operation of the isolating switch on load will damage the switch. Although a variety of disconnect switches are available, the factor which has the maximum influence on the station layout is whether the disconnect switch is of the vertical break type or horizontal break type.

II. OBJECTIVE:

This system acquires a remote substations parameters like voltage, current, frequency, etc., via embedded system using RF (radio frequency) It allows the remote operator to operate relays, circuit breakers and buzzers, and facilitates the display of various parameters in the LCD that is interfaced to the microcontroller. In this project a microcontroller acts as a central controlling device that accepts the inputs and correspondingly controls the outputs, as shown in the above figure. The microcontroller is programmed in such a way that it sends the input parameters in the field side to a RF, periodically. Similarly, it receives the control signals that are sent from the operators, and in accordance with those signals, it controls the relays and buzzers. At times when current exceeds their limits, the microcontroller automatically trips the circuit breakers and sends that information to the user by SMS. Thus, this is a simple and low-cost type of RF-based project that helps students to get a basic idea about the substation automation. With this system, receive and control the substation equipment.

III. SYSTEM DISCRIBTION

A. *BLOCK DIAGRAM:*

B. *TRANSMITTER:*

C. *RECEIVER UNIT*

IV. CIRCUIT DIAGRAM

A. *TRANSMITTER SECTION:*

B. *RECEIVER SECTION:*

V. CONCLUSION

This system acquires a remote substations parameters like voltage, current, frequency, etc., via embedded system using RF (radio frequency) It allows the remote operator to operate relays, circuit breakers and buzzers, and facilitates the display of various parameters in the LCD that is interfaced to the microcontroller. In this project a microcontroller acts as a central controlling device that accepts the inputs and correspondingly controls the outputs, as shown in the above figure. The microcontroller is programmed in such a way that it sends the input parameters in the field side to a RF, periodically. Similarly, it receives the control signals that are sent from the operators, and in accordance with those signals, it controls the relays and buzzers. At times when current exceeds their limits,

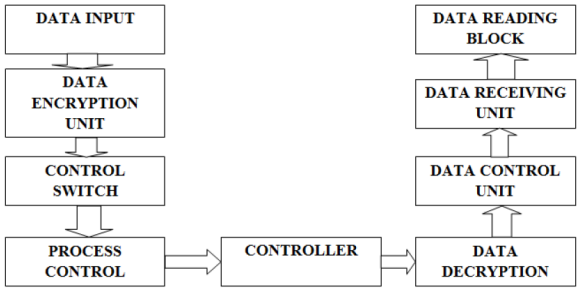

Fig. 1.

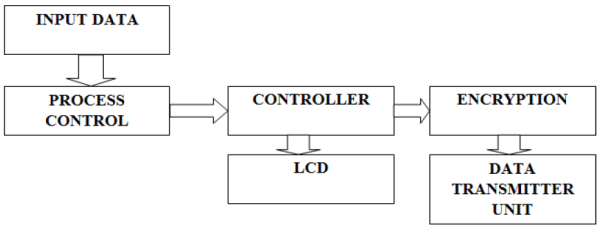

Fig. 2.

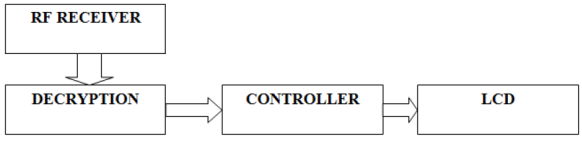

Fig. 3.

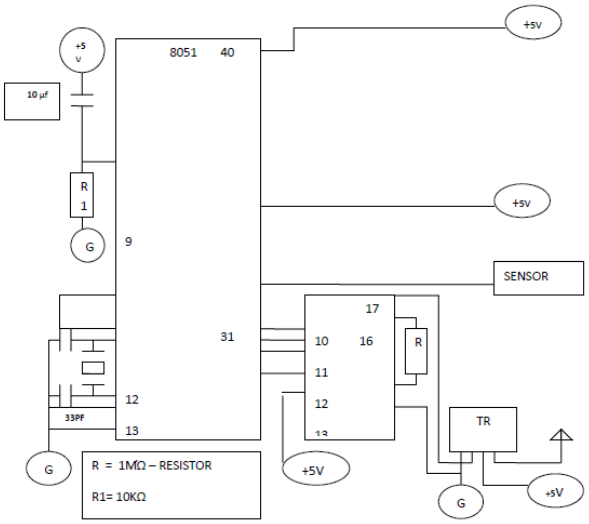

Fig. 4.

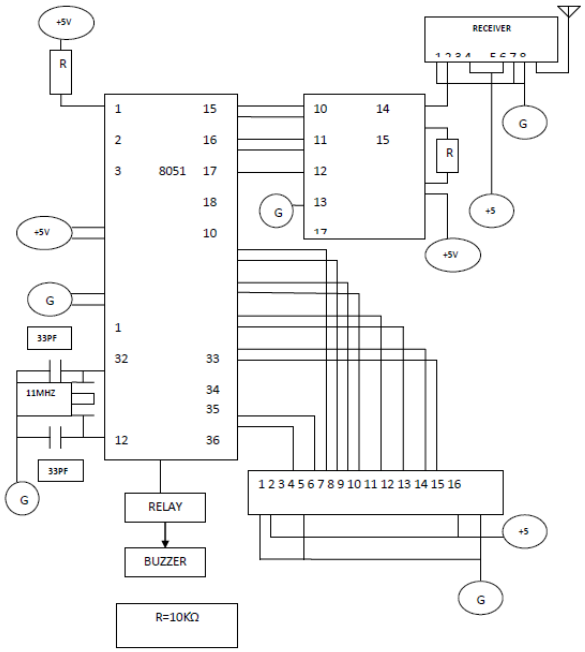

Fig. 5.

the microcontroller automatically trips the circuit breakers and sends that information to the user by SMS. Thus, this is a simple and low-cost type of RF-based project that helps students to get a basic idea about the substation automation. With this system, receive and control the substation equipment.

REFERENCES

[1] Gonzalez.R , Gubia, J. Lopez, and L. Marroyo, *Transformerless Single-Phase Multilevel-Based Photovoltaic Inverter,*,IEEE Trans. on Industrial Electronics, vol. 55, no. 7, pp. 2694-2702, 2008.

[2] S. Daher, J. Schmid, and F. L. M. Antunes,*Multilevel Inverter Topologies for Stand-Alone PV Systems,*,IEEE Trans. on Industrial Electronics, vol. 55, no. 7, pp. 2703-2712, 2008.

[3] W. Yu, J. S. Lai, H. Qian, and C. Hutchens, *High-Efficiency MOSFET Inverter with H6-Type Configuration for Photovoltaic Nonisolated AC-Module Applications,*IEEE Trans. on Power Electronics, vol. 26, no. 4, pp. 1253-1260, 2011.

[4] R. A. Ahmed, S. Mekhilef, and W. P. Hew, *New multilevel inverter topology with minimum number of switches,*,in Proc. IEEE TENCON, pp. 1862-1867, 2010.

HYBRID IMPLEMENTATION OF FACTS DEVICES IN ECONOMIC LOAD DISPATCH USING EVOLUTIONARY ALGORITHMS

Dr.N.Muralikrishnan
ProfessorandHead
Department of Electrical and Electronics Engineering
Mailam Engineerring College, Mailam 604304

G.Alamelumangai
UG Scholar
Department of Electrical and Electronics Engineering
Mailam Engineerring College, Mailam 604304

***Abstract*—Economic load dispatch problem is says that total demand must be shared among the generating units. Economic dispatch is an procedure determine the electrical power to be generated by the committed generating units in a power system so total generation cost of the system is minimized satisfy load demand. Process of allocating generating levels to the generating units so the system is supplied entirely most economic allocation. Depending on load variations the output of generator has to be changed to meet the balance between loads and generation power to make the system efficient. Using evolutionary algorithms is given to the pulse of any facts devices inner thyristor devices .It is used to determine the correct node and improve the performance of the power system. Fit the facts devices and it will useful to reduces the fuel cost. MATLAB is used to verify the results. Keywords- Economic Load Dispatch, EA(EvolutionaryAlgorithm), GA(Genetic Algorithm) Load Demand, Load variations.**

I. INTRODUCTION

Evolutionary Algorithm can be applied on a broad range of problems.EA methods only need the target (fitness) function for a given problem, which is to be optimised. Additional problem specific knowledge can easily be brought into the EA heuristic to improve performance.EA methods do have neglectible demands on the nature. EA methods can be imagined as some kind of toolbox to find high quality solution for complex optimisation problems.

Over the years, many efforts have been made to solve the ELD problem, incorporating different kinds of constraints or multiple objectives through various mathematical programming and optimization techniques. The conventional methods include Newton-Raphson method, Lambda Iteration method, Base point and Participation Factor method, Gradient method etc. However these classical dispatch algorithms require the incremental cost curves to be monotonically increasing or piecewise linear. To solve economic dispatch problem effectively, most algorithms require the incremental cost curves to be of monotonically smooth increasing nature and continuous.

To obtain accurate dispatch results, the approaches without restriction on the shape of fuel cost functions are necessary. Most of conventional methods suffer from the convergence problem, and always get trap in the local minimum. Moreover, some techniques face the dimensionality problem especially when solving the large-scale system In recent years, one of the most promising research fields has been Evolutionary Techniques, an area utilizing analogies with nature or social systems. Evolutionary techniques are finding popularity within research community as design tools and problem solvers because of their versatility and ability to optimize in complex multimodal search spaces applied to non-differentiable objective functions. Several modern heuristic tools have evolved in the last two decades that facilitate solving optimization problems that were previously difficult or impossible to solve. In this paper two different approaches of evolutionary algorithms have been executed and compared i.e. economic load dispatch using quadratic programming and with genetic algorithm for the two test systems

II. LITERATURE SURVEY

Hybrid Partial Gradient Dsecent Simulated Annealing(HPGDSA) method to reduce the CPU time of SA while retaining the main characteristics[2]. Application of mixed-integer linear programming (MILP) in power system planning and expansion and obtained fast and robust behaviours. LP method will be investigated as the approaches to exploit TCSC planning problem with consideration of system loadability[4]. Newton method, have been successfully used to solve the ORPD problem Several disadvantages of these numerical methods exist, such as a lack of ability to find the local and global minimums due to non-linearity and non-convexity[1]. Phase shifter transformer installation considering its advantages can control the value of line power flows obviously. However, because of investment limitations, the installation and usage of phase shifter transformers only based on their advantages will not be economic.

III. EXISITING SYSTEM DRAWBACKS

Mixed integer linear program is used. Divided into two groups relaxation groups and approximations groups. Recursively solving MILP is too time-consuming for large scale systems. Long process for problem solving. This MILP is reformulated as a two-stage linear program.Main problem is computational difficult and has not be properly addressed. Two

stage LP is take more to execute. Deals with the formulation of economic load dispatch problem where the objective function has to be minimized depending upon its equality and inequality constraints. transmission loss plays a major factor and affects the optimum dispatch of generation.

IV. Proposed System

Using evolutionary algorithms determine the correct node. Also find the cost easily. The EA algorithm also used to improve the performance. Fix the facts devices correct place to improve the power system. Instead of Mixed Integer linear program Evolutionary Algorithm is used. In the EA Algorithm in economic load dispatch will reduce the total generation cost of system reduced also satisfies the load demand. In facts device inner thyristor device given pulse is EA algorithm will depends on power factor (reactive power) will increase current is decrease. Depends on this fuel cost will reduced.

V. Operation

In Generating Station side If we generate 200MW means in distribution side we get only 150MW The balance 50MW is loss so we want satisfies that demand the load changes is happening every seconds so maintain the generation constant to prevent the loss. For this prevention we using in this paper Evolutionary Algorithm in Economic Load Dispatch. Here using facts controllers the EA is Programmed in Distribution side to maintain powerfactor and current to reduces the loss. Facts device is an igbt controller EA is programmed to maintain this action. So the Loss is reduced Demand also satisfied.

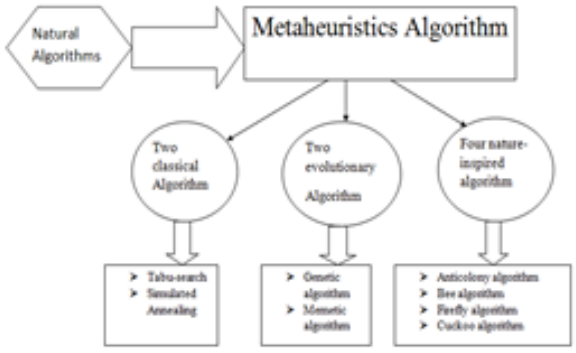

Fig. 1. Classification of algorithm

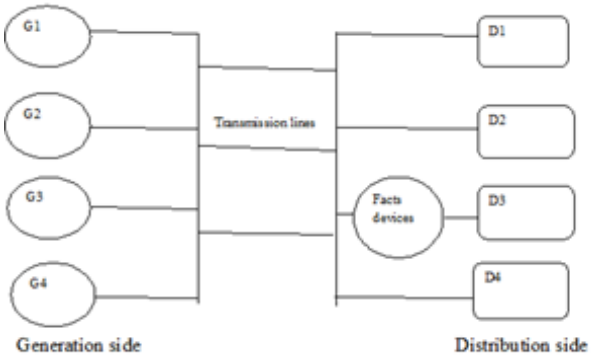

Fig. 2. Operation of system

VI. Evolutionary Algorithm

Evolutionary Algorithms(ED) for combinatorial optimization problems, this paper presents a new versatile optimization algorithm called generalized Evolutionary Algorithms (GED), which can be used to solve the discontinuous, non convex, nonlinear constrained optimization problems. This algorithm is used to solve the complicated, non convex, nonlinear economic dispatch (ED) problem of power systems. Several factors such as, valve-point effects of fuel cost functions, transmission capacity constraints, and system stability constraints are considered in the computation models. Numerical results show that the proposed method is feasible and efficient.

VII. VII. Economic Load Dispatch

Economic Load Dispatch is defined as the sharing of load equally in generating The dynamic economic dispatch problem is a high-dimensional complex constrained optimization problem that determines the optimal generation from a number of generating units by minimizing the fuel cost.The performance of evolutionary algorithms is highly dependent on a number of factors, such as the control parameters, diversity of the population, and constraint-handling procedure used.

Economic Load Dispatch is an integral part of power system generation planning and it is of utmost importance for the electrical utilities and power engineers to explore this area

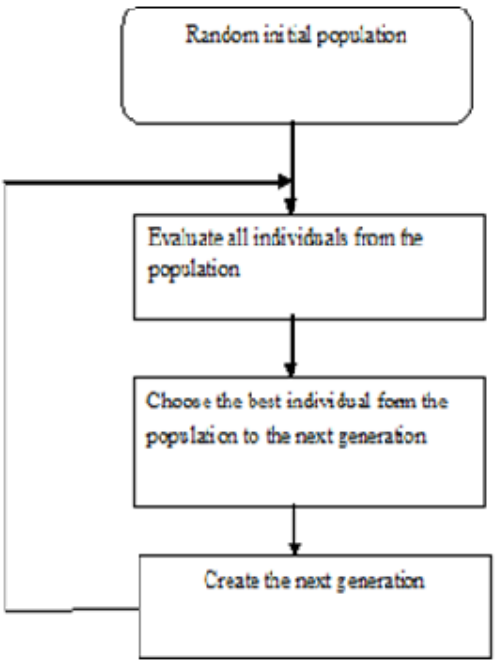

Fig. 3. Proposed EA Process

in short and long term planning scenarios. Load demand requirements subjected to economic feasible solutions matching voltage profile, power demand, minimization of losses, voltage stability and improve the capacity of the system is the need of the hour. Optimization techniques based on evolutionary computing, artificial intelligence, search method finds their applications in the area of economic load dispatch planning to reach global optimal solution for this multi-decision, multi-objective combinatorial problem subjected to different constraints.

For first thing Initialization process Creation of initial population will explains the how many transmission lines to facts devices fit. Only the facts devices will fit either sending end side or the receiving end side. And then Termination point meet Correct place to fit facts devices (either sending or receiving side) is defined terminate point met or not. For example facts devices fitting correct place is obtained means Fix as the best point to fix facts devices and obtained the result (Reduces the fuel cost the Evolutionary Algorithm is given to the pulse of the thyristor used in facts devices).Best Individuals If the correct place is not obtained means in program no will get then check the fitness of the transmission line. If flag is equal to 1 means it is minimum fitness otherwise if flag is equal to 0 means obtain maximum fitness (max and min generation unit. Recombination In recombination is shows combined the transmission line which one is the best transmission line to use (sampling). In Mutation is used to giving better solution of the process. Evaluation off spring in the total yield evaluated. In reinsertion is an revaluation process. Migration process is an to fix the values of facts device. Competition process Competition is process ready to meet termination point and here obtained best point and obtaining the result.

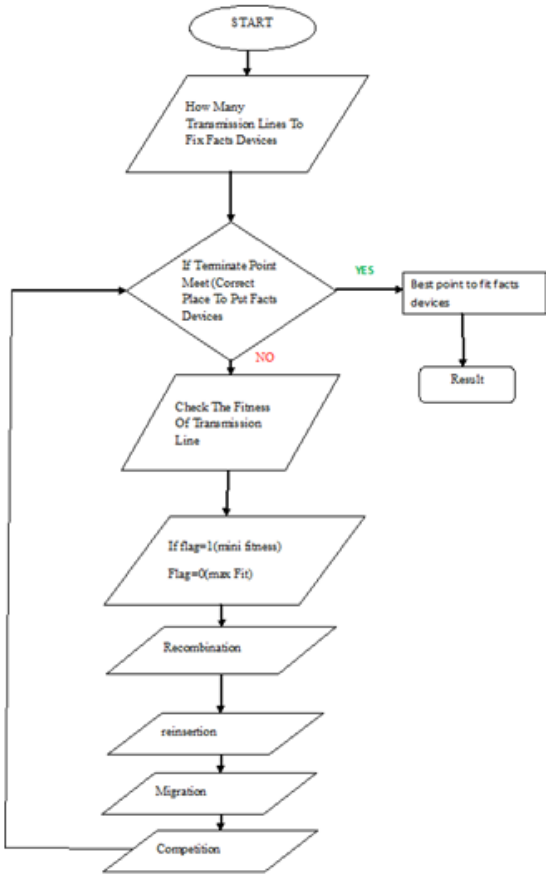

Fig. 4. Flowchart

VIII. Power Factor and Current

Power factor is defined as the cosine of the phase angle between voltage and current. Electric current is a flow of electric charge. In electric circuits this charge is often carried by moving electrons in a wire. Current whenever reduced the power will increase.

IX. Output

The Output Shows Difference between Million and optimization approach also efficiency. In the output

X. Genetic Algorithm

Solving Economic Load Dispatch In Which The Total Cost Of Generating Power Is Minimized With A Valve Point Loading Effect While Satisfying The Load Demand Irrespective Of Transmission Line Losses. These techniques can encounter some difficulties such as getting trapped in local minima, increasing computational complexity and being not applicable to certain objective functions. This calls for developing a new class of solution methods that can overcome these limitations. Heuristic optimization is fast nascent tools that can overcome most of the shortcomings found in derivative based techniques. GA is well suited to and has been extensively applied to solve complex design optimization problems because it can handle both discrete and continuous values. The flowchart depicts the behaviour of genetic Algorithm.

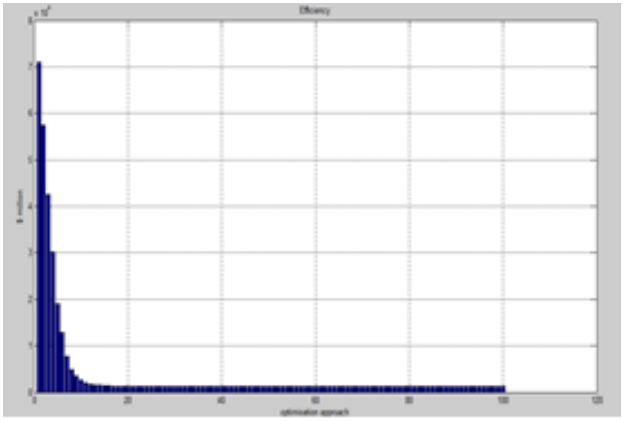

Fig. 5. Output

XI. Economic Dispatch in GA

A. Step 1. Initialization

Initialize population size, maximum generation, stall time limit and read the cost coefficients and B coefficients.

B. Step 2. Formation of population

The initial power search for each generator can be obtained by Pij = Pimin + (Pimax Pimin) / (2l-1)*bij Where, i = number of generator j = number of generation

C. Step 3. Evaluate the fitness function.

The incremental transmission losses denoted as B is calculated as per formula the given below and determines the best fitness and mean fitness values.

D. Step 4. Apply genetic operators

Parent individuals are selected using Roulette Wheel selection procedure and single point crossover is used and finally mutation operator is used for regaining the lost characteristics during the process.

E. Step 5.

Repeat the step 3 and step 4 until the process has been converged or it satisfies the stopping criteria.

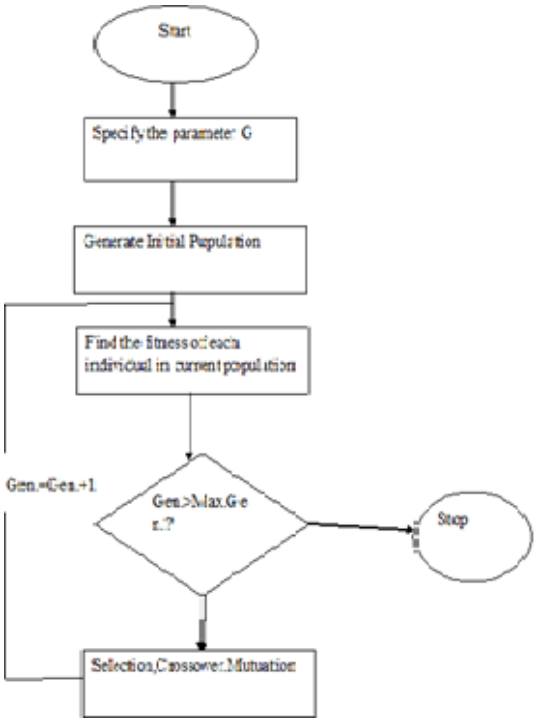

Fig. 6. Flowchart of GA

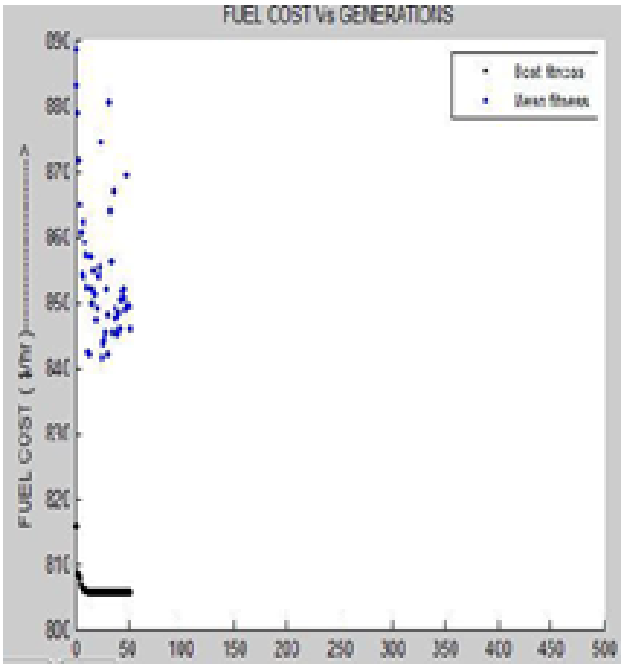

Fig. 7. Fuel cost vs generation in genetic algorithm

XII. Output of System

A. Future work and conclusion

In this paper, we demonstrated that a real-parameter enhanced.GA with a non-uniform mutation and a self-adaptive enhanced DE exhibited superior performances in solving DED problems. In this approach, a random sequential technique was used to consider periodic simpler sub-problems in order to satisfy the equality constraints and dynamic ramp constraints. A dynamic relaxation factor for the equality constraints was set to preserve a few marginally infeasible solutions in order to enhance the convergence rate. Finally using EA algorithm hybrid system performance improves, fuel cost reduced, customer benefit, demand of load will satisfied. In this paper comparison of Evolutionary Algorithm will used to reduce the Fuel cost and reduce the computational cost. Mainly using of facts controller devices aim at increasing the control of power flows in the high-voltage side of the network during both steady state and transient conditions. Also used to satisfies the Load Demands.

References

[1] Wood A.J. and Wollenberg B.F *Power Generation, Operation, and Control.* New York, NY, USA: Wiley, 2012.

[2] Walters D.C. and Sheble G.B., *Genetic algorithm solution of economic dispatch with valve point loading, IEEE Trans. Power Syst.,* vol. 8, no. 3, pp. 13251332, Aug. 1993.

[3] Gaing Z-L, *Particle swarm optimization to solving the economic dispatch considering the generator constraints, IEEE Trans. Power Syst.,* vol. 18, no. 3, pp. 11871195, Aug. 2003.

[4] Xia X. and Elaiw A.M, *Optimal dynamic economic dispatch of generation: A review, Electr. Power Syst. Res.,* vol. 80, no. 8, pp. 975986, 2010.

[5] B. K. Natarajan, *Sparse approximate solutions to linear systems,* SIAM J. Comput., vol. 24, no. 2, pp. 227234, 1995.

Optimal design of energy saving for single phase induction motor

A.Sundara Pandiyan
Assistant professor
Department of Electrical and Electronics Engineering
St.Annes College Of Engineering And Technology

***Abstract*—This project presents the energy conservation and speed control of single phase induction motor using microcontroller. In this project we are designing a circuit for energy conservation for partial load machines. We can implement soft starting and speed control can also be achieved besides doing energy conservation. The advantages of this project are mainly 45-50 percent of energy conservation. Smooth starting of motor is also achieved. Speed control can also be done using this circuit. Our project deals with single phase induction motors, since they are mostly subjected to partial loads. By controlling the amount of voltage supplied to the induction motor and using a microcontroller it is possible to achieve energy saving and speed control.The energy conservation on single phase induction motors is simulated using MATLAB. The circuits for NO LOAD and FULL LOAD are simulated. The simulated results coincide with the experimental results. The voltage supplied to the induction motor is chopped off using the MOSFET, whose firing angle is determined by the microcontroller.The control circuit, power circuit driver circuit are fabricated on general purpose PCB. The required amount of voltage which needs to be supplied when the motor is running at NO LOAD and FULL LOAD can be obtained from the circuits. Also, the simulation results coincide with the hardware results. Index Terms induction motor, microcontroller, chopper , optical sensor,**

I. INTRODUCTION

In electrical power intensive industries like cement, glass, paper, metal etc., where the electricity bill costs more than 30of raw material cost, it is necessary to benchmark the unit consumption per ton of final product output.AC variable speed drive is one of the many well-known solutions to achieve this goal. The growing popularity of ac drives is chiefly due to its ability to control the speed of induction motor, which is most commonly used in industry. Induction motor is the most cost

effective motor. It is considerably smaller, lighter, and more readily available. It is rugged, and virtually maintenance free motor.In Industrial complexes many induction motors may

often be running at no or low partial loads. Irrespective of the load conditions, these motors are however always connected to the mains. Due to the applied rated voltage at stator terminals, rated iron losses have to be supplied constantly to the motors. If it were possible by means of an additional switching device to reduce the terminal voltage of induction motors at no and low partial load, some electrical energy might be saved. Three phase induction motors have high efficiency to less than 50 of load. Large induction motors are inherently very efficient with efficiency as high as 95 at full load. Experiments have revealed that there can be very little advantage in using an energy saving algorithm on anything other than a small inefficient motor.The potential to save energy with a solid-state energy saving device, only becomes a reality when the motor efficiency has fallen. So we have chosen single-phase induction motor.

II. LITERATURE REVIEW

This project is based on the IEEE paper Energy saving operation of Induction motor by voltage reduction at no and low partial load, by Basanta B.Palit, Basle of technology. It gives us the information about the various methods for reducing the terminal voltages to save energy.

III. OBJECTIVE OF THIS PROJECT

The aim of the project deals with energy saving scheme for single-phase induction motor. It includes the following,Control of output voltage by varying the firing angle.Calculation of energy that is being saved.

IV. AIM AND SCOPE OF INVESTIGATION

The aim of this project to simulate AC Chopper system with Induction motor load in closed loop. This is implemented in Hardware with the help of microcontroller.

V. DEMANDSTATUS

VI. ADVANTAGES:

Speed can be varied using firing angle delay. Fast response Input power factor can be improved.

VII. BLOCK DIAGRAM

A. AC SOURCE

AC source is given to the AC Chopper circuit. According to the pulses obtained from the Driver amplifier the Thyristor switch connected between the ac supply and load varying the voltage applied to the Induction motor can controls the power flow in which the motor rotates. When the Thyristor switch starts conduction the current flows in the circuit produces negative pulses which decays the circuit. So to avoid this occurrence Free wheeling diode is used which avoids the unwanted pulses which avoids damage to the motor. Microcontroller is the programming device used here to produce the pulses.5V power supply is given to the microcontroller. The microcontroller used here is 89C51. It is used to produce the delay to firing pulse of the thyristor. The output of the

microcontroller is given to the driver circuit. Driver circuit consists of Opto Coupler which acts as an isolator. The LED of driver circuit initiates Opto Coupler to produce pulses and the output of this OptoCoupler is given to the gate of the Thyristor switch. According to the firing angle thyristor switch of the AC chopper circuit controls the power flow which is used to save the energy.

B. AC CHOPPER CIRCUIT

When a Thyristor Switch is connected between the AC Supply and load varying the voltage applied to the load can control the power flow, and this type of power circuit is known as ac chopper.

The most common applications of this are Industrial heating On-load Transformer connection charging Light control Speed control of polyphase induction motors AC magnet controls

C. INDUCTION MOTOR

Single-Phase Induction Motor is used here. Single-Phase Induction Motor is not Self-starting. However, if the rotor of such a machine is given an initial start in either direction, then immediately a torque arises and the motor accelerates to its final speed.

Advantages of using single-phase induction motor are the following Easy erection and installation Rugged in construction Low maintenance Environmental Compact ability Single-phase induction motor is used for the following Fans, grinders, blowers Centrifugal Pumps Washing machines Refrigerators and air conditioners etc.

D. FREE-WHEELING CIRCUIT

When Thyristor switch conducts the current flows through the circuit produces negative going pulses. To avoid the unwanted negative going pulses free wheeling circuit is used.

E. MICROCONTROLLER

The Microcontroller used here is 89c51.It is used to produce delay to the firing pulse of the thyristor.5V power supply is given to the Microcontroller.

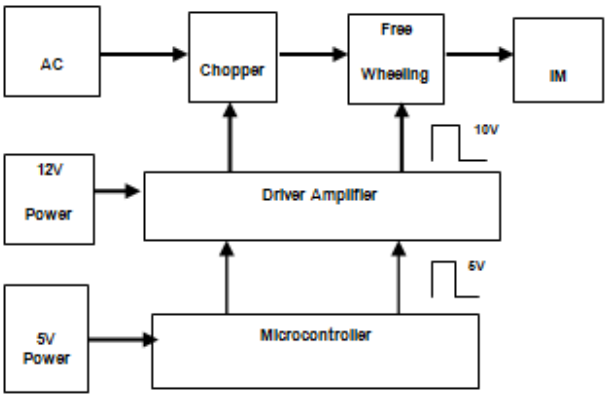

Fig. 1. BLOCK DIAGRAM

F. DRIVER AMPLIFER

The output of Microcontroller is given to the Driver circuit which has Opto Coupler. Opto Coupler is used as an isola-

Under No load Condition

For Speed=1450 rpm; Slip=0.33

Z1=3.46+j2.4 Ω

Z2= (j40.55*(52.42+j1.2))/(52.42+j40.55+j1.2)

=2126.187L91.311/67.0143L38.535

=19.192+j25.263 Ω

Z3= (j40.55*(.88+j1.2))/(.88+j40.55_j1.2)

=60.327L143.76/41.758L88.793

=0.8494+j1.167 Ω

Z=Z1+Z2+Z3

=23.5014+j28.83

=37.159L50.814 Ω

V=230*((((3.6066-2.513).5*sin (2*2.513)-.5*sin (2*3.6066)))/3.14)^.5)

=60.4875V

Fig. 2.

Stator Current I_s =V/Z

=60.4875/37.159

=1.6278A

Fig. 3.

tor. Opto coupler combines an infrared light-emitting diode. According to the LED Glows the Opto Coupler produces the output pulses. The output of the Opto Coupler is given to the gate of the thyristor.

VIII. ANALYSIS OF POWER CIRCUIT AND ITS LOAD

A. NO LOAD OPERATION:

Under no load condition of the Induction Motor the voltage is changed in steps from 20 up to 100 of the rated voltage. At each voltage level the motor is run for sometime, during which the energy is measured. It is clear from the results that the energy consumption is reduced by nearly 50 as the voltage is decreased from rated value to 20 of the rated value.

B. LOW PARTIAL-LOAD OPERATION:

The Energy saving at partial loads will be modest . However, by decreasing the terminal voltage energy can be saved at partial loads between 0 and 20 of the rated value. This, of course is at the cost of the speed, which decreases. On the other hand, there is an improvement in the power factor and the efficiency as we decrease the terminal voltage

Stator copper loss = (1.6278) ^2*3.46

=9.168 watts

Rotor current $I_r = I_s * Z_a / (Z_a + Z_b)$

S= (1.6278*j40.55)/ (j40.55-j1.2_52.42)

=j66.0073/52.42-j41.75

=.985L51.485

Rotor copper loss= (.985) ^2*3.46

=3.357 watts

Iron loss=1.732*60.4875*1.6278*cos (50.814)- 9.168-3.357

=95.253W

Total loss=9.168+3.357+95.253

=107.77 Watts

Fig. 4.

IX. EXPECTED SIMULATION RESULTS

X. CALCULATION OF INDUCTION MOTOR

XI. ENERGY SAVING CALCULATION

XII. CONCLUSION

Energy saver circuit for Induction Motor is simulated using ORCAD PSPICE. A circuit model is developed for simulating closed loop system. This circuit can provide Soft Starting, Speed Control and Energy Saving. The circuit is simulated under no load and full load conditions. The driver circuit, synchronization circuit and power circuit are fabricated on PCB and tested. Later the circuit is tested using PCB system.

From experiment conducted at no load when V=220 volts, the power was found to be 212 watts.

Energy saved = $((W_{rated}-W_{reduced})/W_{rated})*100$

= ((212-107.77)/212)*100%

=49.17%

which is 50% of energy is saved.

Fig. 5.

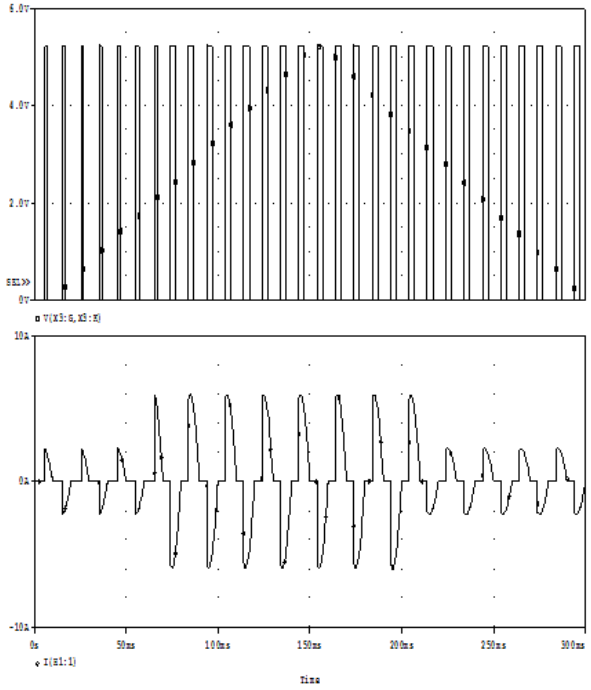

Fig. 6. Output current and triggering pulses

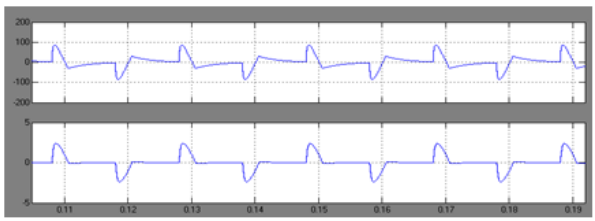

Fig. 7. Voltage and Current Output at =144 Degree

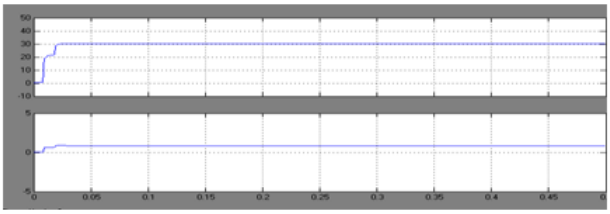

Fig. 8. RMS Voltage and Current Output at =144 Degree

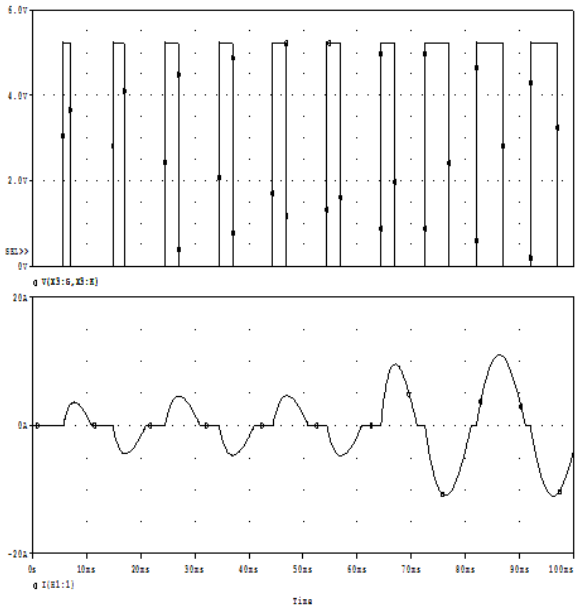

Fig. 9. Output Current and Voltage Waveform

The experimental waveforms coincide with the simulation results. The energy saving of 50 can be obtained only on no-load. The energy saving is applicable only for duty loads. Thus the energy saving is possible only under no-load condition.

REFERENCES

[1] H. W. Beaty and J. L. Kirtley *Electric Motor Handbook,*,1998 :McGraw-Hill.

[2] J. Nagrath and D. P. Kothari, *Electric Machines,* ,1992 :Tata McGraw-Hill

[3] H. Huang, E. F. Fuchs, and J. C. White, *"Optimal placement of the run capacitor in single-phase induction motor designs", IEEE Trans. Energy Convers*,vol. 3, no. 3, pp.647 -652 1988

[4] H. Huang, E. F. Fuchs, and J. C. White, , *"Optimization in single-phase induction motor design, part II: the maximum efficiency and minimum cost of an optimal design",* ,IEEE Trans. Energy Convers., vol. 3, no. 2, pp.357 -366 1988

[5] D. E. Cattermole and R. M. Davis, *"A triac voltage (speed) control for improved performance of split-phase fan motors",* ,IEEE Trans. Power App. Syst., vol. PAS-94, no. 3, pp.786 -791 1975

[6] D. E. Cattermole, R. M. Davis, and A. K. Wallace, *"The design optimization of a split phase fan motor with triac voltage (speed) control",* ,IEEE Trans. Power App. Syst., vol. PAS-94, no. 3, pp.778 -785 1975

[7] J. D. Law and T. A. Lipo, *"A single phase induction motor voltage controller with improved performance",* ,IEEE Trans. Power Electron., vol. PE-1, no. 4, pp.240 -247 1986.

[8] T. A. Lettenmaier, D. W. Novotny, and T. A. Lipo, *"Single-phase induction motor with an electrically controlled capacitor",* ,IEEE Trans. Ind. Appl., vol. 27, no. 1, pp.38 -43 1991

[9] s E. Muljadi, Y. Zhao, T. H. Liu, and T. A. Lipo, *"Adjustable ac capacitor for a single-phase induction motor",* ,IEEE Trans. Ind. Appl., vol. 29, no. 3, pp.479 -485 1993

POWER QUALITY IMPROVEMENT USING SINGLE PHASE NINE LEVEL TRINARY MULTILEVEL INVERTER

R.SIVASANKARI
Assistant Professor
Department of Electrical and Electronics Engineering
St.Annes engineering college
of engineering and technology panruti.

B.PRINCE AMAITHI GANTHI
Assistant Professor
Department of Electrical and Electronics Engineering
St.Annes engineering college of
engineering and technology panruti.

***Abstract*—In this paper represents multicarrier PWM strategies for single phase cascaded nine level Trinary multilevel inverter with separate DC source. Multilevel inverters posses the advantage of reduced harmonics, high power capability and medium voltage level. It focuses on multicarrier single reference Pulse width modulation strategy for the single phase proposed inverter. Performance parameters of single phase cascaded nine level Trinary multilevel inverter have been analyzed. A simulation model of proposed inverter is developed by using MATLAB/SIMULINK 2and its performance has been analyzed**

I. ARTICLE INFO

Article history: Received 14 November 2013 Received in revised form 24 December 2013 Accepted 28 December 2013 Available online 18 January 2014

Keywords: Keyword 1 (Font: Times New Roman 8pt) Keyword 2 Keyword 3 (At least 3 and at most 8 keywords)

II. INTRODUCTION

Recent development of high performance semi conductor power switches such as insulated gate bipolar transistor (IGBT) increase the research interest in high power convertors, such as multi level voltage source increase (VSI)and it is dual ,multi level current source inverters(CSI).Multi level inverter have the capability to deliver higher output power with less-distroded output waveforms resulting is reduction of electromagnetic interference(EMI) noise and size an output filter in distributed power generation application as most renewable energy source, such as photo voltic system deliver dc power, the generated power must be converted to ac power and is fed into through grid connected inverters various standard . Multi level CSI is one effective solution to take such problems. control of the grid connected CSI comparatively similar it is counter part VSI. A grid connected CSI can buffer the output current from the grid voltage fluctuation generates a predetermind current to the power grid without ac current feedback loops and can achieve a high power-factor operation. Its output current is less affected by a grid voltage,and the CSI has inhertent short circuit protection abilities . Moreover ,the discrete diodes connected in series with the power switches to obtain unidirectional power switches in the CSI will be unnecessary because new IGBT with reverse-blocking capability are emerging.

III. PROPOSED TOPOLOGY

Newer Topology of MULTILEVEL inverter We have to reduce the total harmonic distortion as much as possible. By this we can : Increase the performance of drive. Increase the efficiency

IV. TRINARY MULTILEVEL INVERTER

The proposed asymmetric multilevel inverter can be shown in the fig4.1. Each phase consists of three conversion cells and H-bridge. Each cell consists of V1, V2, and V3 voltages connected in cascaded form. This inverter consists of eight switches. Depending upon the switching condition the positive and negative polarity output will be produced by the H-bridge. Expected output voltage level, Vn=3s Where, s=number of stages

V. OPERATION

The new hybrid multilevel inverter consists of full bridge modules which have the relationship of 1v, 3v, 9v..3s-1v for dc link Voltage .The output waveform has 9 levels, + 13, + 12, + 11, + 10, + 9, + 8, + 7, + 6, + 5, + 4, + 3, + 2, + 1,0. The inverter generates 3s different voltage levels (e.g. an inverter with s=3 cells can generate 33=9 different voltage level).The

	Cascaded	Hybrid	New Hybrid
No of level S=No of Stages S=3	2S+1 7 level	$2^{s+1}-1$ 15 level	3^s 9 level
Input DC voltage	V_{dc} $1V_{dc}$	$2^{s-1}V_{dc}$ $4V_{dc}$	$3^{s-1}V_{dc}$ $9V_{dc}$

Fig. 1. Comparison between Hybrid and New Hybrid Inverter

basic hybrid multilevel inverter structure for one phase is illustrated in Fig 4.1 This multilevel inverter is made up of a set of series connected cells. Each cell consists of a 4-switch H-bridge voltage source inverter. The output inverter voltage is obtained by summing the cell contributions. In conventional method, low level inverter is used. Better sinusoidal output was not obtained which is the drawback of the conventional system and the harmonics was high. So increase the levels of the inverter to get high resolution, hence the output wave form is mostly sinusoidal wave formthe cascaded multilevel inverter is prepared by series connection of single phase full bridge inverter. The common function of multilevel inverter is to synthesize a desired voltage from several separate DC sources. Each source is connected to a single phase full bridge inverter. Each inverter is capable of generating three different output voltages, +Vdc, 0 and - Vdc.

VI. Conventional System

Symmetrical cascadedmulti level Inverter was modified to produce 5 level output along with reduced passive components compared to traditional one and improved the efficiency of Cascaded multilevel inverter with 5 level of output. The output voltage was controlled mainly using various PWM Control. It has the property of stepping down or stepping up the input voltage, as a result, the output can be either higher or lower than the input voltage as per requirement

VII. Draw Backs of Conventional System

Large no of switch and switching losses are high. Minimum value of output voltage level. Large amount of harmonics present in the output of inverter. Filter requirement is large

VIII. Proposed Systems

A Trinary multi level inverter used to develop the nine level output voltage with same structure of conventional systems. A multilevel inverter can switch either its input or output nodes (or both) between multiple levels of voltage or current. As the number of levels reaches infinity, the output THD approaches zero. Various new topologies have been developed in the cascaded multi level inverter primarily to improve the efficiency by reducing the number of switches, switching cycles and passive components. To synthesize a desired voltage wave shape from several levels of DC voltages.

IX. MODULATION TECHNIQUES

A. PWM CONTROL STRATEGIES:

This scheme consists of three Bipolar PWM strategies.The reference is the sine signal and carrier is the triangular signal. The multicarrier is positioned above zero level and the carriers are depending upon the output voltage levels. For m level inverter, (m-1)/2 carriers are used.

The three Bipolar PWM strategies are PD(Phase Disposition) APOD(Alternative Phase Opposition Disposition) CO(Carrier Overlapping) VF (Variable Frequency) VA(Variable Amplidute) The advantages of this scheme is Reduces the harmonics Efficiency is high Increase the drive performance

B. BI POLAR SINUSOIDALPHASE DISPOSITION PWM (BSCPDPWM)

BSPDPWM strategy uses (m-1)/2 triangular carriers with the same frequency fc and same peak-to-peak amplitude Ac which are disposed so that the bands they occupy are contiguous. The carrier set is placed above the zero reference. Two modulation waveforms having amplitude Am and frequency fm. and it is centred about the zero level and are used to sample the triangular carriers to generate the gating pulses. The carrier arrangement for nine level inverter using BSPDPWM is shown in Fig.5.1 Amplitude of modulation index can be given by ma=Am/Ac Frequency ratio is mf=fc/fm Where, fc= frequency of carrier signal fm=frequency of reference signal Am=amplitude of reference signal Ac=amplitude of carrier signal

C. BI POLAR SINUSOIDAL ALTERNATIVE PHASE OPPOSITION DISPOSITION PWM (BSAPODPWM):

For m-level inverter, the carriers are arranged in 180 degree out of phase. The carrier arrangement for nine level inverter using BSAPODPWM is shown in Fig.5.2 Amplitude of modulation index can be given by ma=Am/Ac

Frequency ratio is mf=fc/fm Where, fc= frequency of carrier signal fm=frequency of reference signal Am=amplitude of reference signal Ac=amplitude of carrier signal

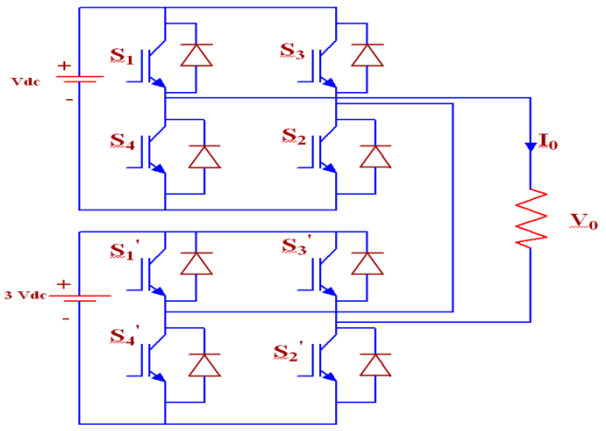

Fig. 2. Circuit Diagram of Trinary MLI

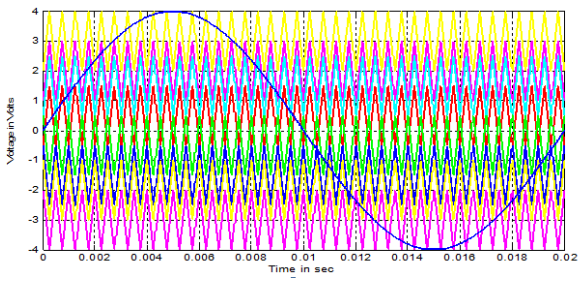

Fig. 3. Carrier arrangement of phase opposition disposition method

X. SIMULATION CIRCUIT

The Three phase Twenty seven level inverter is modelled in SIMULINK using power system block set. Switching signals for single phase multilevel inverter using BSPWM techniques are simulated. Simulations are performed for different values of ma ranging from 0.95 to 1 and the corresponding THD are measured using the FFT block and their values are shown in Table 6.1. Figure 6.3 show the simulated output voltage of single phase MLI and their corresponding FFT plot. Figure 6.2 shows the Nine level output voltage generated by BPDPWM switching strategy and its FFT plot is shown in Figure 6.5. Figure 6.4 shows the nine level output voltage generated by BAPODPWM switching strategy and its FFT plot is shown in Figure 6.5. Tables II to IV show the Crest Factor (CF) for various modulation indices of single phase MLI.The simulation results are obtained by using following parameter such as Vdc1= 10V,Vdc2=30, Vdc3=30 load resistance is 100, carrier frequency fc1 is 3000Hz and fc2 is 2000Hz modulation frequency fmis 50Hz

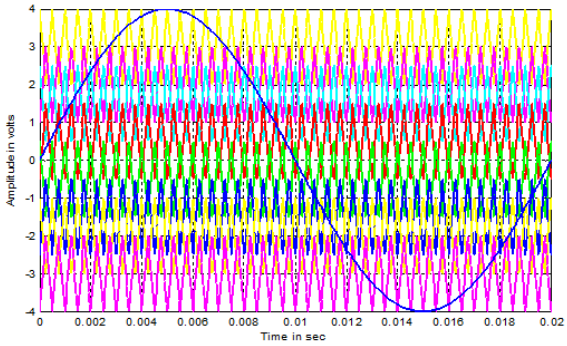

Fig. 4. Carrier arrangement of alternate phase opposition disposition method

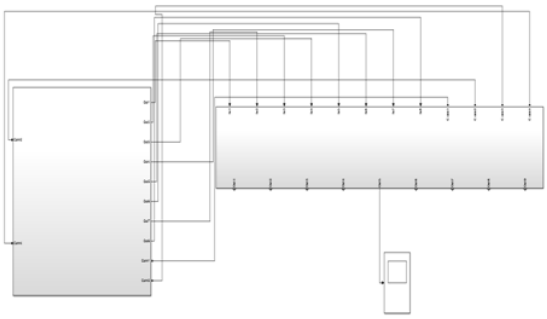

Fig. 5. Simulink model of proposed multilevel inverter

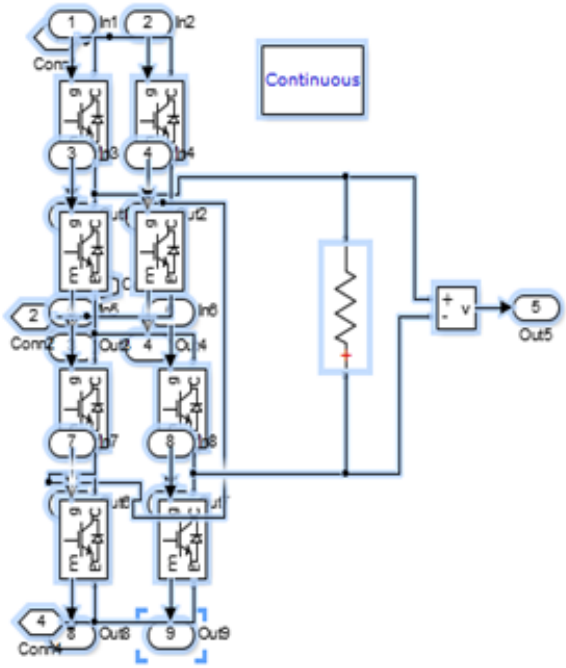

Fig. 6. simulink model of subsystem

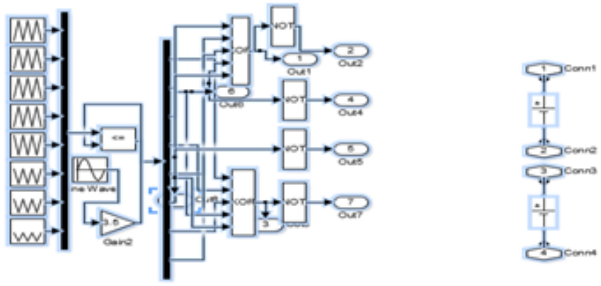

Fig. 7. simulink model of subsystem

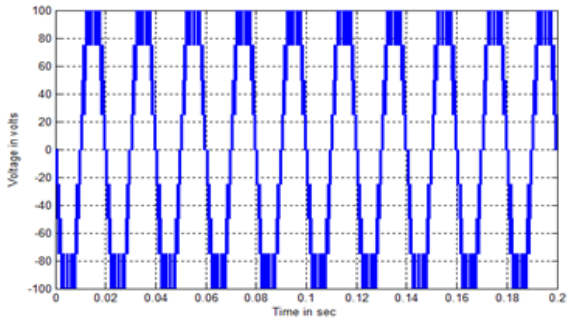

Fig. 8. Output voltage of phase opposition disposition method

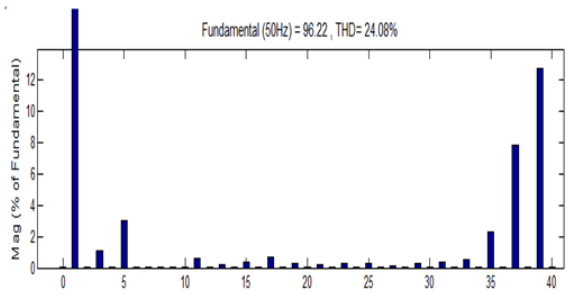

Fig. 9. Fft plot for pod method

XI. ADVANTAGES

Bulky transformers required by conventional multi pulse inverters, Clamping diodes required by multilevel diode-clamped inverters, and Flying capacitors required by multilevel flying-capacitor inverters. The Regulation of DC buses is simple

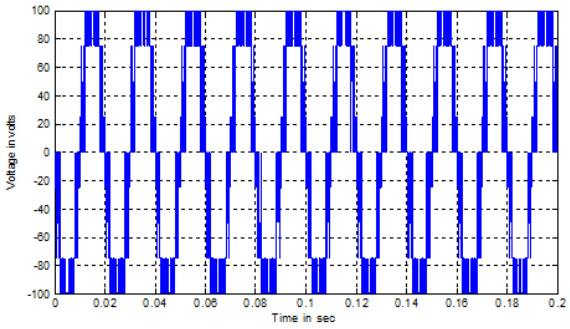

Fig. 10. Output voltage of phase alternate opposition disposition method

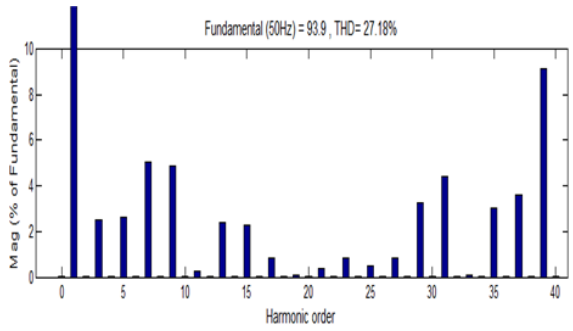

Fig. 11. Fft plot for apod method

Ma	SINE REFERENCE	
	COPOD	COAPOD
1	20.02	22.02
0.95	21.41	23.67
0.9	22.88	25.36
0.85	24.08	27.18
0.8	25.76	29.52

Fig. 12. THD for different kind of modulation indices

XII. FEATURES OF MULTILEVEL CASCADE INVERTER

It is much more suitable to high-voltage, high-power applications than the conventional inverters. It switches each device only once per line cycle and generates a multistep staircase voltage waveform approaching a pure sinusoidal output voltage by increasing the number of levels. Since the inverter structure itself consists of a cascade connection of many single- phase, full-bridge Inverter units and each bridge is fed with a separate DC source, it does not require voltage balance circuits or voltage matching of the switching devices

XIII. APPLICATIONS

UPS Adjustable Speed Drives HVDC System Industrial Application

XIV. CONCLUSION

In this Paper, a Single phase nine level Trinary multilevel inverter has been developed using MATLAB/SIMULINK2013. A proposed symmetric multilevel inverter gives higher output voltage level and pure sinusoidal voltage and harmonic is reduced. The Performance parameters like THD, Vrms, have been analysed and presented. From that the Bipolar Phase

MI	SINE REFERENCE	
	COPOD	COAPOD
1	0.00605	0.00298
0.95	0.00496	0.00192
0.9	0.00337	0.00217
0.85	0.00173	0.00217
0.8	0.00113	0.00556

Fig. 13. Distortion factor for different kind of modulation indices

CF	MI				
	1	0.95	0.9	0.85	0.8
COPOD	1.414	1.413	1.414	1.414	1.414
COAPOD	1.412	1.413	1.414	1.414	1.414

Fig. 14. Crest factor for different kind of modulation indices

Disposition technique provides lower THD and Vrms is higher in Bipolar Alternative Phase Opposition Disposition. From a high voltage level with low distortion performance of resistive load was increased.

REFERENCES

[1] E. Najafi, A. Halim, and M. Yatim, *Design and Implementation of a New Multilevel Inverter Topology,* IEEE Transactions on Industrial Electronics, vol. 59, no. 11, pp. 41484154, 2012.

[2] 2 X. Zhang and J. W. Spencer, *Study of Multisampled Multilevel Inverters to Improve Control Performance,* IEEE Transactions on Power Electronics, vol. 27, no. 11, pp. 44094416, 2012.

[3] E. Esfandiari and N. Bin Mariun *Experimental Results of 47-Level Switch-Ladder Multilevel Inverter,* ,IEEE Transactions on Industrial Electronics, vol. 60, no. 11, pp. 49604967, 2013.

[4] D. A. B. Zambra, C. Rech, and J. R. Pinheiro, *Comparison of Neutral-Point-Clamped , Symmetrical , and Hybrid Asymmetrical Multilevel Inverters,* , IEEE Transactions On Industrial Electronics,, vol. 57, no. 7, pp. 22972306, 2010.

[5] A. Ghazanfari, H. Mokhtari, and M. Firouzi, *Simple Voltage Balancing Approach for CHB Multilevel Inverter Considering Low Harmonic Content Based on a Hybrid Optimal Modulation Strategy,* , IEEE Transactions On Power Delivery, vol. 27, no. 4, pp. 21502158, 2012.

[6] A. Kavousi, B. Vahidi, R. Salehi, M. K. Bakhshizadeh, N. Farokhnia, and S. H. Fathi, *Application of the Bee Algorithm for Selective Harmonic Elimination Strategy in Multilevel Inverters,* ,IEEE Transactions On Power Electronics, vol. 27, no. 4, pp. 16891696, 2012

HARMONIC ELIMINATION AND REACTIVE POWER COMPENSATION USING SHUNT ACTIVE POWER FILTER BASED ON CASCADED TRANSFORMERS

N.Muralikrishnan
Head,
Department of Electrical Engineering
Mailam Engineering college-Mailam

A.Muthuramam
Professor,
Department of Electrical Engineering
Mailam Engineering college-Mailam

E.Tamizhanantham
UG Scholar
Department of Electrical Engineering
Mailam Engineering college-Mailam

***Abstract*—This paper proposes a multilevel shunt active power filter (SAPF) to deal with either harmonic currents compensation or reactive power compensation. Such a device can reduce the harmonic distortion at the grid currents provided by non-linear loads located in stiff systems. The proposed SAPF is based on three-phase bridge (TPB) converters connected to cascaded single-phase transformers. The transformers arrangement permits the compensator to use a single dc-link unit which simplifies the control strategy and number of sensors. The multilevel waveforms are generated by using a suitable PWM strategy associated with the transformers turns ratio. Modularity and simple maintenance make the proposed SAPF an attractive solution compared to some conventional configurations. The model, PWM technique and control strategy, are presented as well as studies considering harmonic distortion and semiconductor losses estimation. Simulation and experimental results are presented in order to validate theoretical approaches.**

I. INTRODUCTION

Distribution power systems are suffering hard impact on their power quality. This is due to the intensive use of non-linear loads added with the growth of renewable energy sources. Such aspects have been leading electrical systems to poor power quality levels. Most common disturbances include: i) harmonic voltages/currents, ii) voltages imbalances, iii) voltage sags/swells, iv) flickers, v) transients and vi) interruptions. Non-linear loads and unbalanced loads are the main reasons of the injected current harmonics and reactive power components at the grid, leading to a low system efficiency with a poor power factor. Extensive surveys have been carried out to quantify these problems, as discussed in [1]. In this way, some custom power devices have been introduced and investigated in the literature. Initially, the harmonic current and reactive power compensations have been treated with passive L-C filters and capacitors. However, this solution has disadvantages associated with fixed compensation and resonance effect on the power system. Then, power companies/industries (e.g., ABB, Siemens, Fuji, Westinghouse, etc) started the development of active power filters (APFs) [1], [2]. There are three types of APFs most applied in the customized power quality market: i) series APF [3]; ii) shunt APF [4][6] and iii) universal APF or unified power quality conditioner (UPQC) [7], [8]. This paper considers the shunt APF (SAPF) technology for applications on three-phase three-wire systems. The shunt active power filter (SAPF) is commonly com-posed by: i) voltage source converter (VSC) or current source converter (CSC), i) dc-link capacitors, iii) optional passive filters, iv) optional isolation transformers and v) protection circuits (e.g., bypass thyristors). In this paper, the SAPF con-sidered is composed by VSC type with isolation transformers. There are several types of topologies to be used in VSC configuration [2], [9][12]. Generally, the two-level (2L) based VSC is commonly used for a 480V voltage rating (i.e., low power applications). Nevertheless, for high power applications, such as distribution voltages levels, the multilevel-based VSC becomes a more attractive solution [13]. In this way, some multilevel configurations have been studied and documented in technical literature [2], [13], [14]. However, those multilevel configurations have disadvantages associated to the high num-ber of dc-link capacitors that, depending on the configuration, can increase the control complexity. For instance, cascaded neutral point-clamped (NPC) and cascaded flying capacitors have issues with imbalance dc-link voltages and power sharing in each cell [14]. Additionally, the lifetime of electrolytic dc-link capacitors is usually shorter than that of other components in power converters [15]. It is usually addressed as one of the most important issues in terms of failure rate in the field operation of power electronic systems [15][17]. Degradation failures occur more often than catastrophic failures (i.e., short or open circuits). In this case, critical failure mechanisms cover electrolytic vaporization and electromechanical reaction (e.g., degradation of oxide layer) [15], [16]. Then, a high number of dc-link capacitors tends to increase the failure probability

of the SAPF. Hence, cascaded transformers can be considered to deal with this issue, maintaining the multilevel feature with a single dc-link capacitor in its configuration. A conventional SAPF used with cascaded transformer coupled with H-bridge (HB) converters was presented in [10]. In this paper, a SAPF based on cascaded transformer coupled with

three-phase-bridge (TPB) converters is proposed, see Fig. 1. Such a structure is generalized for K-stages in which K-transformers are coupled with K-TPB converters. Equivalent multilevel operation is achieved with reduced number of semiconductors devices if compared to conventional HB one [10]. The multilevel waveforms are generated by TPB converters by using suitable PWM strategy associated with the transformers turns ratio. The modularity and simple maintenance makes proposed SAPF an attractive solution in comparison with some conventional configurations. Model and PWM control are presented. Simulation and experimental results are presented for validation purposes.

II. INTRODUCTION

The configuration depicted in Fig. 1 is generalized for K-stages (i.e., K-transformers and K-three-phase-bridge converters). The converters legs are represented by K-power switches (i.e., q1j, q1j, q2j, q2j, ..., qKj, and qKj) in which the subscript j is related to each phase (e.g., j = a; b; c). In addition, power switches q and q are complementary to each other. The conduction state of all power switches is represented by an homonymous binary variable, where q = 1 indicates a closed switch and q = 0 an open one.The converter pole voltages (v1j0, v2j0,..., vKj0), can be expressed as vkj0 = (2qkj 1) vC (1) 2 where k corresponds for each stage (i.e., k = 1; 2; 3; :::; K), j is related for each phase (j = a; b; c) and vC is the dc-link voltage. A previous work in which the converter was considered as a series compensator has been presented in [18]. Since the converter equations are similar to that presented in [18], some equations are not detailed in this paper. Taking into consideration the leakage inductance of a transformer and external interfacing shunt inductance represented by lsh and the load dependent loss of a transformer denoted by rsh, a differential equation for shunt active power filter can be written as where vrj are the resultant voltages of the converter related to the secondary voltages of the scaled transformers and vgs is voltage between the neutral points g and s. From the current node it can be written isj = ilj igj (3) where the load currents ilj are given by the load model. where vrj are the resultant voltages of the converter related to the secondary voltages of the scaled transformers and vgs is voltage between the neutral points g and s. From the current node it can be written isj = ilj igj (3) where the load currents ilj are given by the load model.

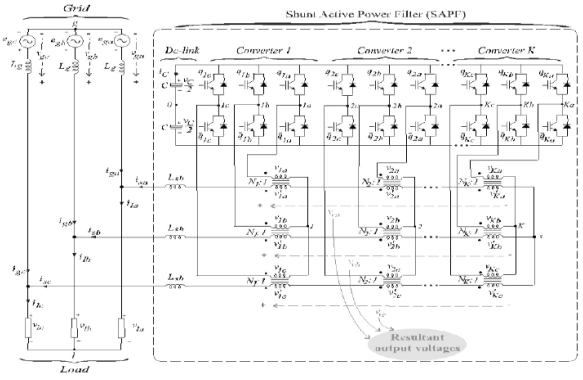

Fig. 1. Proposed SAPF generalized with K-cascaded transformers per phase wye-connected with K-three-phase-bridge converters.

III. HARMONIC DISTORTION ESTIMATION

The resultant output voltages (vrj) have been evaluated by considering the weighted total harmonic distortion (WTHD). Such a parameter permits to quantify the waveform quality that will be processed by the converter of the SAPF. considering a maximum injection of vrj and the filter compensating only reactive power, the WTHD of the voltages vrj for the proposed configuration can be observed in Table I. For this case, the switching frequency (fs) was fixed in 10 kHz. number of stages increases, the WTHD value decreases. The equivalent waveforms for that result, with 1, 2 and 3 stages, are shown in Figs. 3-5, respectively. Such an evaluation werealso presented in [18] but without redundancy case N1 = N2 = 1.

IV. SEMICONDUCTOR LOSSES ESTIMATION

Power switch losses were estimated considering the proposed and conventional SAPF [10] having the same number of power switches (i.e., 6 legs). This leads to the proposed topology operating with 2 stages, whereas the conventional with HB operates with 1 stage. The estimation was implemented by using the thermal module, an existing tool in PSIM v9.0. Such a tool was used with calibration parameters that gives an equivalent loss estimation to that one presented in [20], achieved by experimental tests. The power switch losses model includes:currents iga and igb are obtained by synchronizing their phase with ega and egb, provided by the block Sin in which has its input signal provided by the phase-locked loop P LL block. The PLL used in this work is based on fictitious electrical power (i.e., power-based PLL) and is detailed in [21]. The current controllers Riab define the references voltages vra00 and vrb00 . The dc-link controller RC is a conventional proportional-integral (PI) controller whereas the current controllers Riab are double-sequence controllers (i.e., resonant PI controllers) [22]. From the reference voltages, the PWM strategy defines the state of the switches (q1j, q2j, ..., qKj). a) IGBT and diode conduction losses b) IGBT turn-on losses; c) IGBT turn-off losses; [23]. d) Diode turn-off energy. [24]. This comparison is quite similar to that presented in [18]. However, in the comparative study presented in this paper, the converters were operated for a load power rated at 300 kW . Hence, a reduction up to 82 was observed for proposed configuration compared to the conventional one. Notice that the semiconductor.

V. SIMULATION RESULTS

Simulation results trough PSIM v9:0 are presented in this section. Such outcomes show the resultant output voltages of the converter (vrj) with PWM implementation accordingly to the PWM strategy presented earlier. The first set is shown by considering 1 stage as observed in Fig. 3.

The cases in which the converter operates with 2 stages are shown in Fig. 4. In these cases, only converters 1 and 2 with 2 single-phase transformers and 2 TPB connected in each phase are considered. It can be seen that the result presented in Fig. 4(a) is equivalent to that obtained with 3L-NPC converter or cascaded HB with equal dc-link voltages. It was considered N1 = N2 = 1, which gives more redundant switching states. The cases without redundancy improves the quality of the waveform with more level steps, which leads the voltage vrj to lower harmonic distortion.

Simulation result. Resultant phase-voltage (vra) of converter in phase a for converter operation with 2 stages. (a) Operation with redundancy, having N1 = N2 = 1. (b) Operation without redundancy, having N1 = 1 and N2 = 2.

Simulation result. Resultant phase-voltage (vra) of converter in phase a for converter operation with 3 stages.

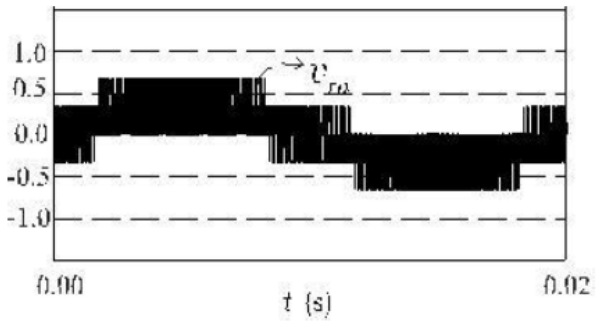

Fig. 2. Simulation result. Resultant phase-voltage (vra) of converter in phase a for converter operation with 1 stage.

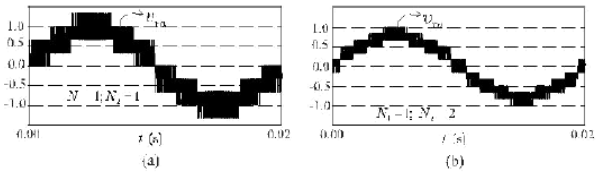

Fig. 3.

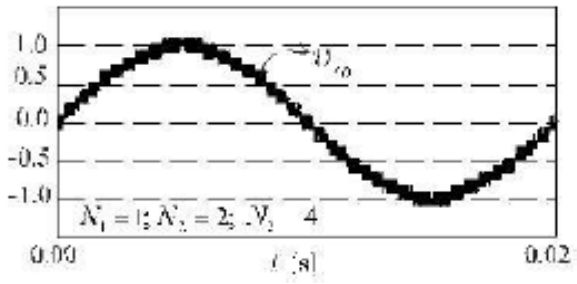

Fig. 4. Simulation result. Resultant phase-voltage (vra) of converter in phase a for converter operation with 1 stage.

VI. EXPERIMENTAL RESULTS

The theoretical approaches were validated experimentally with a downscaled experimental platform, as observed on the left side of Fig. 6. The main components used in this platform include inverters considered as IGBTs from Semikron that are linked with the control strategy by means of a digital signal processor (DSP) TMS320F28335 with microcomputer equipped with appropriate plug-in boards and sensors. A zoomed view of the main devices can be observed on the right side of Fig. 6. The dc-link capacitance used was C = 2200 F with voltage reference fixed as vC = 50V. The switching frequency considered was fsw = 10kHz

Photograph of experimental setup. (On the rigth) Zoomed view of the main devices.

Fig. 7 shows the dynamic operation of the SAPF. In this case a load transient was applied. It can be seen that the dc-link voltage is regulated in its reference value (i.e., vC = 50V) before and after the transient application. The steady state waveforms before the transient can be observed in a zoomed view. The results for the other phases are similar. The power factor at the grid can be observed in Fig. 8. It can be seen that the grid current and grid voltage are in phase, which means a power factor close to the unity.

Proposed SAPF operating with a load transient application. System currents in phase a. Grid current iga. SAPF current isa. Load current ila. Dc-link voltage vC.

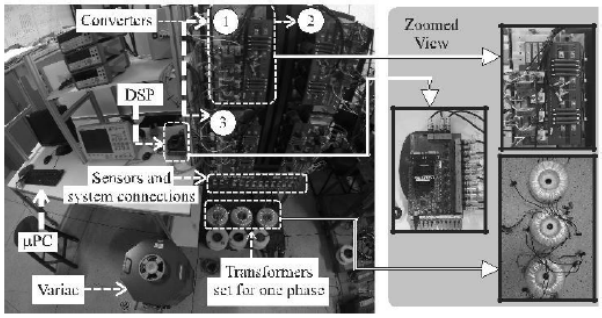

Fig. 5. Downscaled experimental platform.

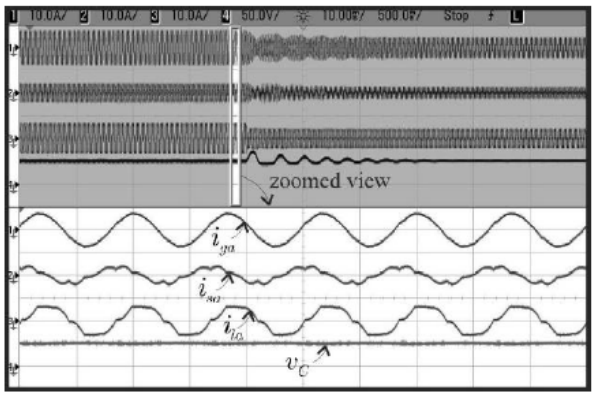

Fig. 6. Experimental results.

Power factor correction at the grid. Grid current (iga) and grid voltage (ega) in phase a. The harmonic spectrum and the total harmonic distortion (THD) of the currents at the grid and at the load can be observed in Fig. 9. It can be seen that SAPF compensation has provided the grid current with THD fixed in 2.58. In this case, the load current THD was 8.10.

(a) Grid current (iga) harmonic spectrum with THD fixed in 2.58. (b) Load current (ila) harmonic spectrum with THD fixed in 8.10.

Fig. 10 shows the PWM implementation with proposed SAPF having 1 stage (i.e., which means using only converter 1). Fig. 11 shows the PWM implementation in which SAPF was considered with 2 stages with N1 = N2 = 1, Fig. 11(a) and with N1 = 1, N2 = 2, Fig. 11(b). Fig. 12 shows similar result, but in this case the SAPF is operating with 3 stages (i.e., with converters 1, 2 and 3). The results for the other phases are similar. Fig. 10. Experimental result with 1 stage in which N1 = 1. PWM converter voltages in phase a. The PWM implementation of proposed SAPF (on the left) and its fundamental signal filtered in oscilloscope (on the right).

Fig. 11. Experimental results with 2 stages. (a) N1 = N2 = 1. (b) N1 = 1 and N2 = 2. PWM converter voltages in phase a with 1 stage in which N1 = 1. The PWM implementation of proposed SAPF (on the left) and its fundamental signal filtered in oscilloscope (on the right).

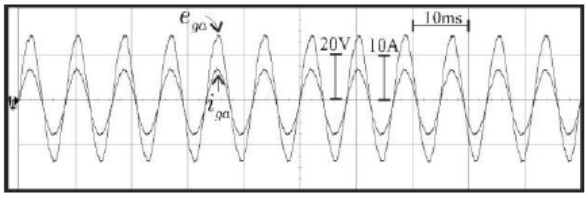

Fig. 7. Experimental results displayed in high resolution.

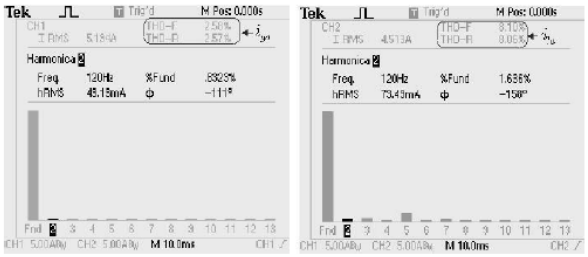

Fig. 8. Experimental results.

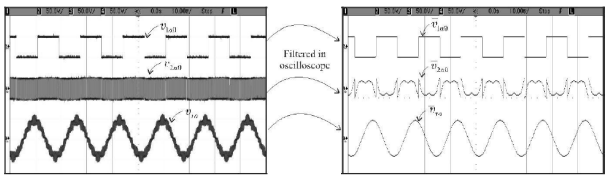

Fig. 9. Experimental results.

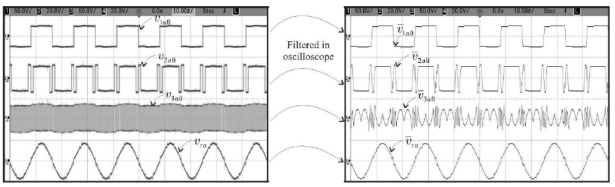

Fig. 10. Experimental results.

Experimental results with 2 stages. (a) N1 = N2 = 1. (b) N1 = 1 and N2 = 2. PWM converter voltages in phase a with 1 stage in which N1 = 1. The PWM implementation of proposed SAPF (on the left) and its fundamental signal filtered in oscilloscope (on the right).

VII. CONCLUSION

A shunt active power filter (SAPF) was studied in this paper. The configuration is based on cascaded transformers coupled with three-phase bridge (TPB) converters. The proposed SAPF has presented lower harmonic distortion content in comparison with the conventional one [10]. Such a reduced harmonic distortion has lead to compare the semiconductor losses by fixing the same WTHD value for proposed and conventional configurations. In this way, the proposed configuration could have its switching frequency decreased to match the same WTHD value obtained with the conventional one. Once the conventional topology considered in [10] has also isolation transformers, a semiconductor losses reduction close to 82A generalization for K-cascaded TPB converters and K-transformers was presented. Such a generalization was validated experimentally for 1, 2 and 3 stages. The proposed SAPF has presented advantages because it provides the improvement of the quality at the signals generated by the PWM converter, by maintaining its modularity features and using simple dc-link control strategy since it need just a single dc-link unity. Another remark is that the number of levels generated at the voltage vrj for the proposed configuration is greater when compared to the conventional one [10], considering the same number of power switches. However, to match the same number of semiconductors losses, the topologies have to operate with different number of stages (i.e., different numbers of transformers). Hence, the proposed configuration will need one additional scaled-transformer for each phase. Nevertheless, such an additional transformer must have lower ratings in comparison with the transformers used for the previous stage. The outcomes have shown its accordance with the theoretical approaches. Detailed analyses comparing the transformer ratings will be investigated for an overall cost estimation between the proposed and conventional solutions.

REFERENCES

[1] B. Singh, K. Al-Haddad, and A. Chandra, *A review of active filters for power quality improvement, Industrial Electronics,*,IEEE Transactions on, vol. 46, pp. 960971, Oct 1999.

[2] H. Rudnick, J. Dixon, and L. Moran, *Delivering clean and pure power, Power and Energy Magazine,*,IEEE, vol. 1, pp. 3240, Sep 2003.

[3] M. Hamad, M. Masoud, and B. Williams,*Medium-voltage 12-pulse converter: Output voltage harmonic compensation using a series apf, Industrial Electronics,*,IEEE Transactions on, vol. 61, pp. 4352, Jan 2014.

[4] P. Jintakosonwit, H. Fujita, H. Akagi, and S. Ogasawara,*Implementation and performance of cooperative control of shunt active filters for harmonic damping throughout a power distribution system, Industry Applications,*,IEEE Transactions on, vol. 39, pp. 556564, Mar 2003.

Implementation of Interleaved Boost Converter Fed DC Drive

N.Dhanasekar M.Arunprakash S.Jagadeeswari S.Nanthitha

***Abstract*—In this paper, the implementation of an interleaved soft switching boost converter fed DC Drive system is presented. This topology is used to increase the efficiency of the AC/DC converter, and it minimizes switching losses by adopting a resonant soft switching method. Detailed analysis of the proposed topology is presented. The overall efficiency of interleaved converter is improved when compared to the conventional boost converter system. Keywords: Boost converter, interleaved, resonant converter, soft-switching, unity power factor.**

I. INTRODUCTION

Power Electronic (PE) converters are now being used in the processing of electrical energy in industrial applications such as adjustable speed drives, SMPSs, UPSs, etc. [1] Therefore, the converters with high power factor are highly required in industries. Most of the PE systems which get connected to AC utility mains use diode rectifiers at the input. The nonlinear nature of diode rectifiers causes significant line current harmonic generation; thus, they degrade power quality, increase losses, failure of some crucial medical equipment, etc. Therefore, power factor correction (PFC) circuits are incorporated in PE systems. Earlier, to reduce rectifier-generated harmonics, expensive and bulky filter inductors and capacitors were installed, but they effectively eliminate only certain harmonics .The active power line conditioners are generally hard switched; hence, the components are subjected to high-voltage stresses which increases further with increase in the switching frequency. Also, hard switching results in low efficiency, large EMI, etc., This paper proposes a high efficiency AC/DC boost converter to control a DC drive .The proposed single-switch type soft-switching boost converter minimizes switching loss by adopting a resonant soft-switching method.[2]-[10] And, no additional switches are needed for soft switching. Also, the proposed model reduces the input current ripple, output voltage ripple, and size of the passive components. The proposed soft-switching interleaved boost converter not only design and analysis of Interleaved Soft Switching Boost Converter Fed DC Drive exploits the interleaved converter but also reduce switching losses through the soft-switching technique.Therefore, the output power can be boosted with high efficiency.

II. OPERATING PRINCIPLE

The circuit shown in Fig.1 is the interleaved boost converter which consists of two single-phase boost converters connected in parallel and then to a single output capacitor. The two PWM signal difference is 180 degree and each switch is controlled in the interleaving method. Since each inductor current magnitude is decreased according to one per phase, the inductor size and Inductance can be reduced and also the input current ripple is decreased.

Initially, the switch is in off state and the DC output of the diode rectifier is transmitted directly to the load through L2 and D10. In this mode, the main inductor voltage becomes (VO VIN). Thus, the main inductor current decreases linearly. If the switch is turned on under zero-current switching because of the resonant inductor L3. As the output voltage is supplied to the resonant inductor L3, the current increases linearly. When the resonant current becomes equal to the main inductor current, the current of the output side diode D10 becomes zero. The resonant inductor L3 and the resonant capacitor C3 resonate and the voltage of C3 decreases from the output voltage VO to zero. The main inductor current iL2 flows through L3 and the switch. When the resonant capacitor voltage VC3 becomes zero, the two auxiliary diodes D5 and D6 are turned on and therefore the resonant inductor current now flows through main inductor L2 and through the two auxiliary diodes. The main inductor current increases linearly. The switch turns off under the zero-voltage

III. SIMULATION RESULTS

The circuit in Fig.2 gives the simulink model of interleaved soft switching boost converter. The graph shown in Fig 2(a) is the AC input voltage .The peak value of AC input voltage is 100V.Fig 2(b) shows the output voltage of rectifier. The DC output of the rectifier is 70V.Switching pulses for the switches M1 and M2 are shown in Fig 2(c).Switching pulses are displaced by 180 degrees.Boosted Output Voltage is shown in Fig 3(a). The voltage is boosted to 190V and current drawn by the load is shown in Fig 3(b).The armature current is 3.9A. Interleaved soft- switching boost converter fed DC drive is

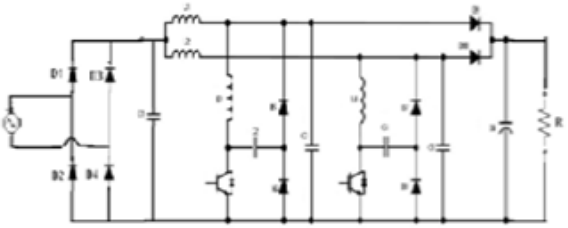

Fig. 1. Interleaved Soft Switching Boost Converter

shown in Fig 4.The speed can be varied over a wide range. The motor speed and Torque are shown in Figures 4(a) and 4(b) respectively. The speed increases and settles at 220 rad/sec condition because of the auxiliary resonant capacitor C2. The current divides it two paths.. One is the L-C3 -VIN loop for which the voltage of the resonant capacitor C3 increases linearly from zero to the output voltage Vo. The other is the L3C2D5 loop for which the second resonance occurs. The energy stored in L3 is transferred to C3. The resonant current decreases linearly and the voltage across C2 reaches maximum. When the resonant capacitor voltage Vc3 is equal to the output voltage VO, the energy flow from L3 to C2 is completed and the resonant current iL3 becomes zero. Then, the voltage of C2 decreases, continuously resonates on the

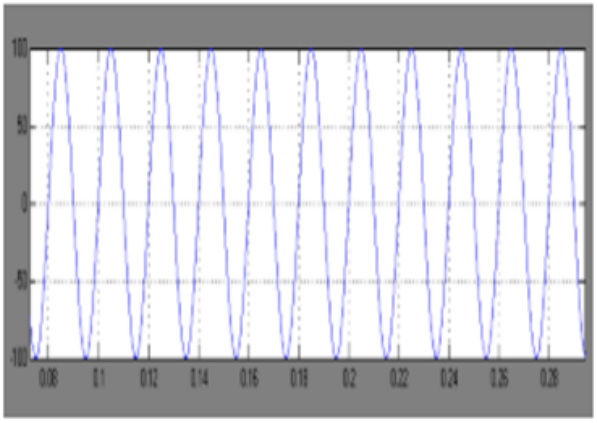

Fig. 2. Simulink model of Interleaved Soft Switching Boost Converter

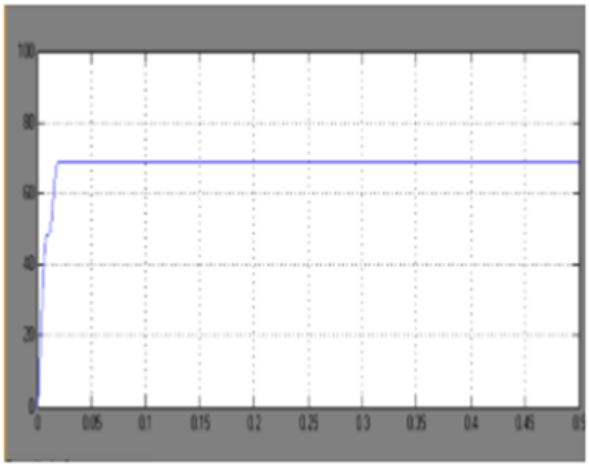

Fig. 3. Simulink model of Interleaved Soft Switching Boost Converter

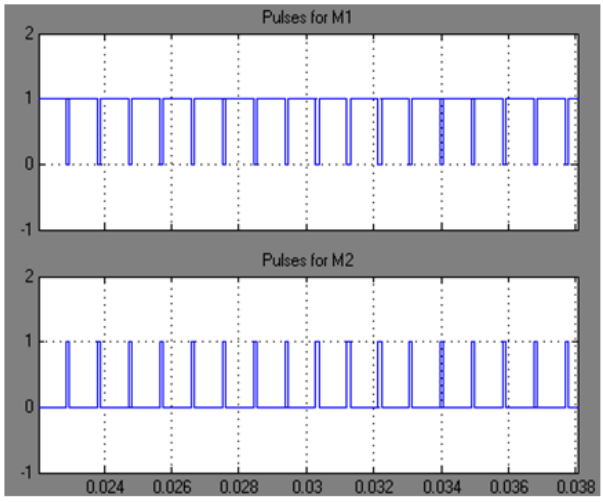

Fig. 4. Simulink model of Interleaved Soft Switching Boost Converter

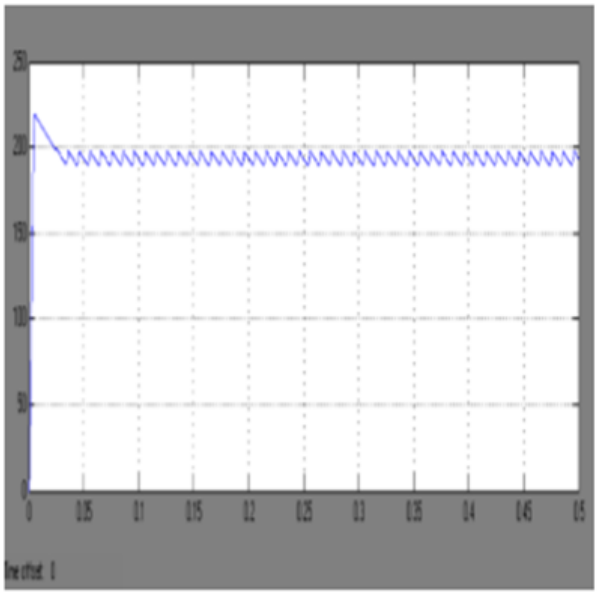

Fig. 5. Simulink model of Interleaved Soft Switching Boost Converter

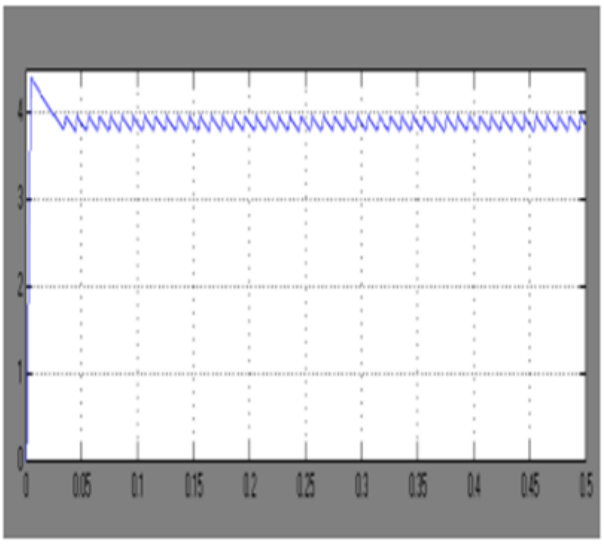

Fig. 6. Simulink model of Interleaved Soft Switching Boost Converter

D6C2L3 D10C6 loop and the energy is transferred from C2 to L3 . When the Vc2 becomes zero, the resonant current reverses its direction. When the voltage of C2 becomes zero, the antiparallel diode of the switch turns on. And now the current flows in two paths. The main inductor current iL2 transmits energy to the output through D10 and decreases linearly. The resonant inductor current iL3 also transmits energy to the load through D10 and flows through the antiparallel diode of the switch.

IV. CONCLUSION

An interleaved converter has been constructed to feed a dc motor. A PI controller has been designed to regulate the speed of the motor. This has accomplished by a closed loop control algorithm through a suitable modification in the duty cycle.A micro controller has been programmed to generate the PWM pulses for the power switches in the converter, besides serving to perform the function of PI controller. It has been shown that the control algorithm works effectively. The scheme has been found to reject the load and source disturbances. The simulation and experimental results have been found to display the capability of the converter to handle transient disturbances and claims its use in sophisticated applications. Their close comparison highlights the merits of this scheme and points out that it will go a long way to explore innovative applications in this domain.

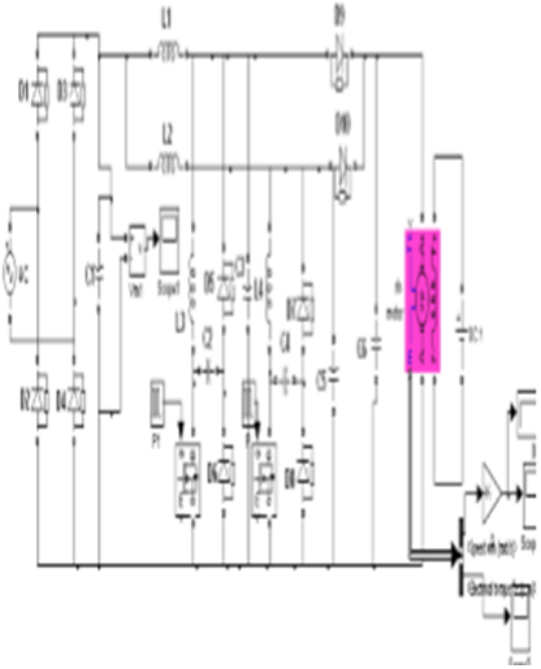

Fig. 7. Interleaved Boost Converter fed DC Drive

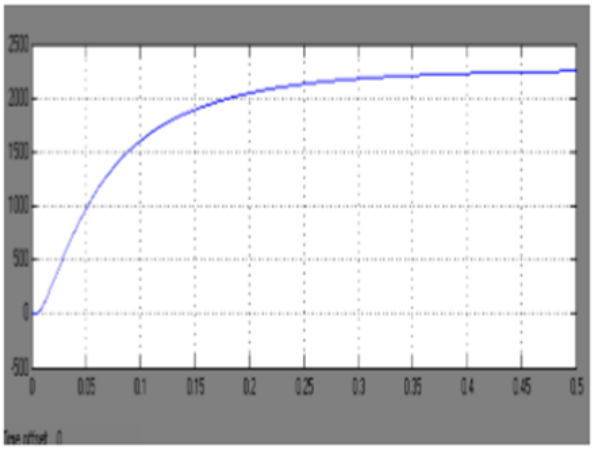

Fig. 8. Motor Speed

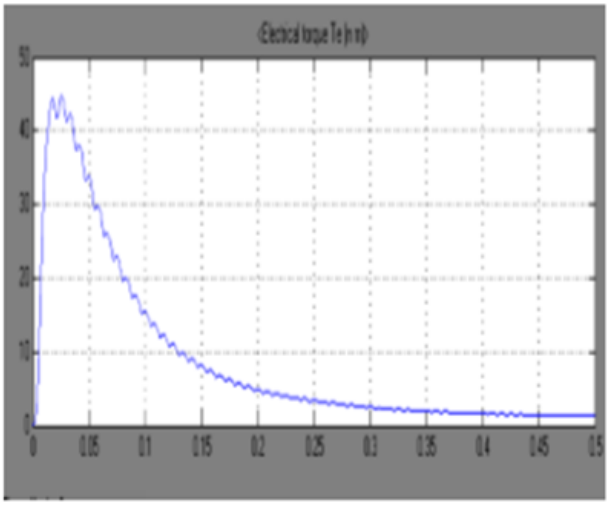

Fig. 9. Torque Developed

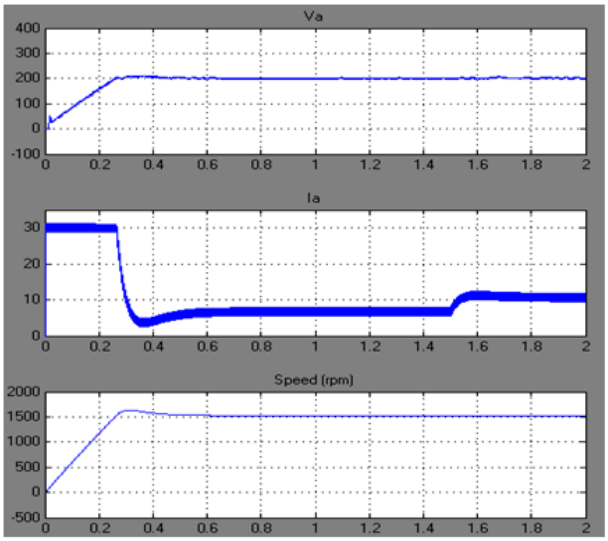

Fig. 10. Performance waveform

REFERENCES

[1] B. Singh, B. N. Singh, A. Chandra, K. Al-Haddad, A. Pandey, and D.P. Kothari, *A review of three-phase improved power quality acdc converters,* ,, IEEE Trans. Ind. Electron., vol. 51, no. 3, pp. 641660, Jun. 2004.

[2] X. Kong and A. M. Khambadkone, *A review of three-phase improved power quality acdc converters,* „Power Electron., vol. 22, no. 2, pp. 543550, Mar.2007.

[3] H. M. Suryawanshi, M. R. Ramteke, K. L. Thakre, and V. B. Borghate *,Unity-power-factor operation of three-phase acdc soft switched converter based on boost active clamp topology in modular approach, IEEE Trans.* Power Electron., vol. 23, no. 1, pp. 229236, Jan. 2008.

[4] H. Mao, O. Abdel Rahman, and I. Batarseh *Zero-voltage-switching dcdc converters with synchronous rectifiers, IEEE Trans.* Power Electron.,vol. 23, no. 1, pp. 369378, Jan. 2008.

[5] B. Singh, B. N. Singh, A. Chandra, K. Al-Haddad, A. Pandey, and D.P. Kothari, *A review of three-phase improved power quality acdc converters,* „ IEEE Trans. Ind. Electron., vol. 51, no. 3, pp. 641660, Jun. 2004.

[6] H. Tao, A.Kotsopoulos, J. L.Duarte, andM.A.M.Hendrix, *Transformer-coupled multiport ZVS bidirectional dcdc converter with wide input range, IEEE Trans.* Power Electron., vol. 2, pp. 771781, Mar. 2008.

[7] M. Borage, S. Tiwari, S. Bhardwaj, and S. Kotaiah, *A full-bridge dcdc converter with zerovoltage-switching over the entire conversion range,IEEE Trans* Power Electron., vol. 23, no. 4, pp. 17431750, Jul. 2008.

ATM SAFTEY AND SECURITY

A.vinayagam
UG Scholar
Department of Electrical and Electronics Engineering
IFET College of Engineering,Gangarampalayam, Villupuram

***Abstract*—ATM security is very important in now a days, in rural area some thief broke the CCTV camera and ATM machine and theft the cash.it occurs mostly in ATM which located in out of cities. My project deals with ARDUINO board and software, PIR which sense the human who are breaking the ATM machines and vibration sensor sense the mechanical vibration, the sensed output drive the motor which control the door (open and close) similarly ultrasonic sensor which placed near the CCTV camera it also control the door (open and close). So the cash is safe and thief is also captured.**

A. Keywords

Automated Teller Machine, ARDUINO software, ARDUINO board PIR sensor, vibration sensor ultrasonic sensor, push to on switch and gear motors

I. INTRODUCTION

Security in the ATM is very necessary because it is widely spread in all areas such as financial, network administration and other important parts of financial network which requires very sensitive handling transmission of data. Manipulating the transmitted data, spoofing and misuse of ATM channels would be very fatal in accounting system. Mostly the ATM transactions should really on the integrity of secure Crypto-processor. Therefore the ATM Forum, developed new standards specification called ATM security specification 1.0 in 1998 and then in March 2001, the ATM Forum developed a new Technical Committee called ATM security specification version 1.1. This paper presents the safety security of the Automated Teller Machine which includes the basic introduction, threats to an ATM network, network security framework.

II. HARDWARE USED

ARDUINO board PIR sensor Ultrasonic sensor Vibration sensor Push to ON switch Motor driver IC Gear motor

III. ARDUINO BOARD

Arduino is an open source electronic platform based on easy to use hardware and software. Arduino board are able to read inputs light on sensor activating a motor. You can tell your board what to do by sending or upload the set of instruction to the microcontroller on the board to do so you use the Arduino programming language and arduino software, based on processing.

IV. PROGRAMMING LANGUAGE

The Arduino programming language is a simplified version of C/C++. If you know C, programming the Arduino will be familiar. If you do not know C, no need to worry as only a few commands are needed to perform useful functions. All sequential programming languages have four categories of instructions. First are operation commands that evaluate an expression, perform arithmetic, toggle states of I/O lines, and many other operations. Second are jump commands that cause the program to jump immediately to another part of the program that is tagged with a label. Jumps are one way to break out of the normal line-by-line processing mode. For example, if you want a program to repeat over and over without stopping, have the last line of the program be a jump command that takes the program back to its first line. Third are branch commands that evaluate a condition and jump if the condition is true. For example, you might want to jump only if a number is greater than zero. Or, you might want to jump only if the state of an i/o line is low. Fourth are loop commands that repeat a section of code a specified number of times. For example, with a loop you can have a light flash on and off exactly six times. Most programming languages contain a relatively small number of commands. The complexity of computers comes from combining and repeating the instructions several million times a second.

V. SPECIFICATION

Microcontroller: ATmega328 Operating Voltage: 5V Input Voltage (recommended):7-12V Input Voltage (limits): 6- 20V Digital I/O Pins: 14 (of which 6 provide PWM output) Analog Input Pins: 6 DC Current per I/O Pin: 40 mA DC Current for 3.3V Pin: 50 mA Flash Memory: 32 KB (ATmega328) SRAM: 2 KB (ATmega328) EEPROM: 1 KB (ATmega328) Clock Speed: 16 MHz

VI. IN EXPENSIVE

Arduino board are relatively in expensive compare to other microcontroller platforms. The least expensive version of arduino is assembled by hand

VII. SIMPLE, CLEAR PROGRAMMING ENVIRONMENT

The Arduino software is easy to use for beginners, yet flexible enough for advanced user to take advantage of as well, its conveniently based on the processing programming environment, so students learning to programing in that environment will be familiar with how the Arduino IDE works.

VIII. PASSIVE INFRA-RED SENSOR

PIR sensors allow you to sense motion, almost always used to detect whether a human has moved in or out of the sensors range. They are small, inexpensive, low-power, easy to use and don't wear out. For that reason they are commonly found in appliances and gadgets used in homes or businesses. They are often referred to as PIR, "Passive Infrared", "Pyro electric", or "IR motion" sensors. PIRs are basically made of a pyro electric sensor (which you can see above as the round metal can with a rectangular crystal in the center), which can detect levels of infrared radiation. Everything emits some low level radiation, and the hotter something is, the more radiation is emitted. The sensor in a motion detector is actually split in two halves. The reason for that is that we are looking to detect motion (change) not average IR levels. The two halves are wired up so that they cancel each other out. If one half sees more or less IR radiation than the other, the output will swing high or low.

IX. WORKING OF PIR

PIR sensors are more complicated than many of the other sensors explained in these tutorials (like photocells, FSRs and tilt switches) because there are multiple variables that affect the sensors input and output. To begin explaining how a basic sensor works, we'll use this rather nice diagram The PIR sensor itself has two slots in it, each slot is made of a special material that is sensitive to IR. The lens used here is not really doing much and so we see that the two slots can 'see' out past some distance (basically the sensitivity of the sensor). When the sensor is idle, both slots detect the same amount of IR, the ambient amount radiated from the room or walls or outdoors. When a warm body like a human or animal passes by, it first intercepts one half of the PIR sensor, which causes a positive differential change between the two halves. When the warm body leaves the sensing area, the reverse happens, whereby the sensor generates a negative differential change. These change pulses are what is detected.

types	cost
At mega around Rs 800	
UNO	around Rs400
NANO	around Rs 450

Fig. 1.

X. ULTRASONIC SENSOR

The ultrasonic wave detection and measurement principle is primarily the reverse operation of ultrasonic wave generation. During ultrasonic wave generation, the transducer element (i.e., piezoelectric) is excited by applying an electrical signal across it. But during ultrasonic wave detection, an electrical voltage signal across the piezoelectric element is monitored. As soon as an ultrasonic wave strikes the transducer, the piezoelectric element vibrates accordingly; thus it generates a voltage signal across its terminals. Figure 2.7 shows a simple conguration of an ultrasonic sensor in a level sensing application. An ultrasonic wave reector (obstacle) oats on the liquid surface. A transducer is mounted at the bottom of the tank and transmits a signal. It determines the uid level by detecting and measuring the time-of-ight of the reected ultrasonic wave.

XI. ULTRASONIC SENSING TECHNOLOGY

A technique known as Interferometry can be used with an ultrasonic sensor to determine uid level. Interferometry consists of diagnosing the properties of two or more waves by studying the pattern of interference created by their superposition. In interferometry, a wave of some specic shape is transmitted and then incoming waves that have the same pattern (i.e., frequencies) are detected. The difference between the two waves (transmitted wave and received wave) is identied. In ultrasonic level sensing systems, the same principle of interferometry can be applied. A simple circuit that can be used to generate a pulse of an ultrasonic wave signal. After transmitting a pulse signal, the circuit listens for any incoming reected echo pulse that has similar features (i.e., frequency) as the transmitted echo. The time difference or time-of-ight is calculated based on the times of transmission and reception of the pulse wave. Paulsen has used the same method for detecting uid levels as described above, in which an ultrasonic transducer driver generates a voltage proportional to the resonant frequency of the ultrasonic transducer. A reference voltage is then generated and the reference voltage and the rst voltage are monitored and compared, and a surface detect signal is generated when the rst voltage drops below the reference voltage

A. Features of Ultrasonic Sensor

(1) Compact and light-weight (2) High sensitivity and high sound pressure (3) High reliability

XII. DIGITAL VIBRATION SENSOR

This basic piezo sensor can be used in anti-theft devices, electronic locks, mechanical equipment vibration detection, sound gesture application and detection range bull's-eye counts vibration sensor occasions. These vibration levels could be given to any controller/processor and necessary decisions could be taken through it. Module triple output mode, digital output simple, analog output more accurate, serial output with exact readings.

XIII. Features

Sensitivity adjustable. The vibration detection has no direction. With analog, digital and TTL level output signal. With mounting holes, firmware installation flexible and convenient. Module triple output mode, digital output is simple, analog output more accurate, serial output with exact readings

XIV. Working of vibration sensor

Digital vibration sensing in the ADIS16220 starts with a wide- bandwidth MEMS accelerometer core that provides a linear motion-to-electrical transducer function. Figure 6 provides a basic physical diagram of the sensing element and its response to linear acceleration. It uses a fixed frame and a moving frame to form a differential capacitance network that responds to linear acceleration. Tiny springs tether the moving frame to the fixed frame and govern the relationship between acceleration and physical displacement. A modulation signal on the moving plate feeds through each capacitive path into the fixed frame plates and into a demodulation circuit, which produces the electrical signal that is proportional to the acceleration acting on the device.

XV. Block Diagram and working

In this project uses arduino board, pir sensor, ultrasonic sensor, vibration sensor and motor .pir sensor which is placed inside the ATM machines and ultrasonic sensor which placed near the CCTV camera and vibration sensor sense the vibration when someone break machine. PIR sensor which sense the human temperature while moving and vibration sensor sense the vibration who break the machine and ultrasonic sensor sense the distance between the camera and ATM machine.

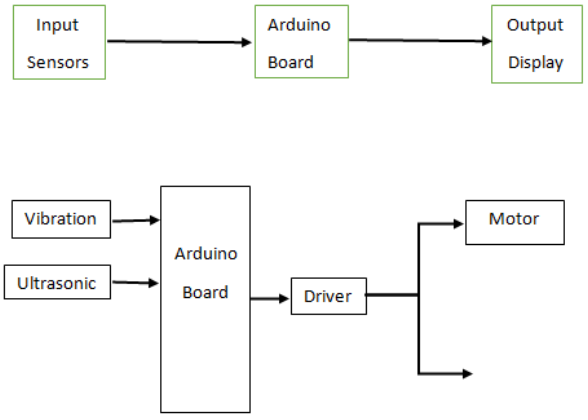

Fig. 2.

Fig. 3.

The sensor output is given as input to the arduino board. Then arduino board drives the motor IC drive to controls both the motor separately according to the output.

XVI. BUFFER AND INDICATOR CIRCUIT

Anyone came to disturb the ATM machinepir sensor sense thehuman temperature and vibrational sensor sense vibration beyond the threshold limit and it confirmed they are thief, like that ultrasonic sensor sense the distance between the abstract. When one came to closer to the ultrasonic sensor in the aim of to break the CCTV camera, when distance is to short, when any two sensor is triggered then suddenly close the door. The thief is captured inside the ATM room and give the alarm. When police become, we provide the switch to open the closed door.

XVII. Future Implementation

Instead of switch use GSM module. By the use of GSM we can operate the arduino board from the bank if we send the signal 0 to open or off the motor and send 1 to on and close the door and arduino board will send the signal or message to bank and police station, when the door is closed in the ATM machine

XVIII. Application

It is used in the various application Based on the safety In ATM In jewelry In home

XIX. Advantage

Arduino board run at 5V so power consumption is less Cost of the total kit is around Rs3000 expect two motor Development of code is very easy while using arduino It is easy to implement Small size and compact

References

[1] Everest FA *The master handbook of acoustics,* ,4th edn. McGraw-Hill, New York 2Bruneau M, Scelo T (2006)

[2] Kumar L *Simmonds Precision Products,* ,Inc. (assignee) (1993) Apparatus and method for discriminating true and false ultrasonic echoes. Patent no. 6046960

[3] Ibrahim RA *Introduction. Liquid sloshing dynamics: theory and applications.* ,publishers Ernest Benn ltd, 8 Boverie Street, London.

[4] Dai L, Xu L *A numerical scheme for dynamic liquid sloshing in horizontal cylindrical containers.* ,ProcInstMechEng Part D J AutomobEng 220(7):901918

Development of RF Energy Harvesting Technique for Li-Fi Application

RICHARD ISRAVELAN J
UG Scholar
Department of Electrical and Electronics Engineering
ST Annes College of Engg and Tech

***Abstract*—This work aims to improve the power generation by applying and experimenting a new technique of Radio Frequency (RF) energy harvesting using products of Powercast. This energy is used to activate a Light-Fidelity (Li-Fi) sample device and charge an energy storage system simultaneously. The final outcome of the system is now able to activate the Li-Fi sample device and charge a battery system at the same time. With the project being improved on a wider scale, many power problems can be solved in such a way that will help all humankind. Keywords RF Energy Harvesting, Powercast, Light Fidelity, Energy Storage System.**

I. INTRODUCTION

Researchers and companies are encouraged to think of new techniques and ideas for driving wireless mobile devices for an enhanced or infinite period of time because of the finite electrical life of batteries. Somehow, the answer lies in capturing the energy from external ambient sources for miniature and mobile electronic devices, this technology is widely known as Energy Harvesting. Fuel is being taken from ambient sources present around us and thereby free to all users by these Energy Harvesters. Some of the types of ambient sources available around us for the technique of energy harvesting are solar, wind, vibration, temperature gradient, electromagnetic, thermoelectric, push buttons, heel strike, and finally, Radio Frequency (RF). So far, known energy harvesting techniques generate small power depending on the used technique. It may be sufficient to drive small electrical devices or devices with low power consumption. But a promotable future is being presented by energy harvesting technology in low power consumption electronic devices and wireless sensor networks [1]. This work focuses on Electromagnetic (EM) energy as one of the energy harvesting techniques, especially RF where it holds a promising future for generating electrical power in a small amount in order to drive partial circuits in wireless communication electronic devices. RF waves' energy used by devices can be harvested and used to operate in more efficient and effective way [2]. Basically, the Li-Fi source needs to be connected to the power grid in order to be able to transfer data and work efficiently. Another problem appears that the Li-Fi device needs to be in a fixed place for the user to have a good connection, meaning that the device cannot be portal. Also, most of today's world technology gadgets are dependent on the battery power. This may create a problem of having the battery constantly charged, which is hard to maintain outdoors

II. PROJECT OVERVIEW

It is essential to adopt green, inexpensive communication strategies because of the growth of popularity, applications of large-scale and sensor-based wireless networks. Deployment of a self-powered nodes network that can harvest energy from many types of sources, either natural or man-made sources, is one of the approaches to develop a sustained network operation. Associated cost of periodic batteries replacement can be significantly reduced by this method. On another hand, battery replacement may not be economically and practically feasible in some deployments according to the location of the sensor. It may even involve risks of high threats to human life. That is why wireless sensor networks (WSN) are now strongly motivated to be enabled to reduce part or all cost of operation by having the capability to harvest energy, thereby taking the first steps towards realizing the vision of perennially operating network [4]. Direct power to electrical battery-free systems, auxiliary power source for rechargeable batteries, battery activation, and remote power with or without battery backup are some of several benefits of implementing a wireless power source that depends on RF Energy Harvesting. Significant flexibility in designing power systems for wireless sensors and interactive devices that is communicating through low power wireless networks is provided by this implementation. High sensitivity of the harvester is needed to enable it to harvest from very low levels of RF energy in order to have the maximum performance, the best design and the flexibility of applications. In order to ensure the most usable power of that harvested energy, high efficiency of the harvester is critically needed. To support a wide range of operating conditions such as input power, load resistance, and output voltage, the range of efficiency should be sufficiently broad. Additionally, to optimize and achieve system power management, smart power management capabilities should be acquired by the harvester. In any surrounding area, many ambient RF power sources are available. Internal sources, anticipated ambient sources, and unknown ambient sources are the three general categories of RF power sources around us, as shown in Fig. 1. Typically, the main components of RF Energy Harvesting circuit are the Antenna with Impedance Matching Circuit, Rectifier, Power Conversion and Energy Storage part as shown in systems that collects RF energy through an antenna, converts it to electrical

energy. This energy (voltage and current) has to pass by a very accurate impedance matching circuit in order to achieve the maximum efficiency of the collected energy. Afterwards, a rectification or a current boost circuits are introduced to the system in order to achieve the desired voltage or current output. By achieving the desired output of the system, it can be used in various applications especially in charging a small battery and turning on the required number of LEDs, as this represents the loading requirement of the Li-Fi device/module. The first stages of receiving the Radio Frequency, impedance matching and rectifying circuitry are managed by thePowercast P2110-EVB Power harvesting evaluation board. Some of the details are indicated as follow.

A. Power Receiving Antenna

In order to radiate and receive electromagnetic (EM) energy, metallic structures known as Antennas are designed. They are used for the guiding device as a transmission line or a wave guide and the free space to be having a transitional structure between them. Time-variant current or acceleration of charge causes a conducting current to radiate. There would be no radiation in the wire with no charge motion in it, since no flow of current occurs [6].

B. Impedance Matching Circuit

In high-frequency circuit design, impedance matching is a critical problem. Its concern is to achieve the maximum power transfer between the two parts by matching one part of the circuit to another one. Impedance matching has many techniques to be done, such as the Q factor approach to matching, L matching circuit, and T matching circuit

C. Rectifier

Rectification is used in order to charge batteries, supply DC motors and so on. There are two types of diode rectifiers: Halfwave and full-wave rectifier. Full-wave rectifier has better performance than half-wave rectifier, yet it needs more number of diodes than the half-wave rectifier

D. Powercast P2110-EVB Power harvester

The Powercast P2110-EVB Power harvesting evaluation board contains a microchip (P2110) used to convert RF to DC power. It also contains proper connections and components for testing and producing the desired output power. It provides power management of RF energy harvesting for micro-power devices. It uses a capacitor as a storage of DC energy to convert from RF energy. The RF input, RFIN as shown in Fig. 3, is an unbalanced input from the antenna. A 50, 902-928 MHz antenna is used to achieve the highest efficiency. It must be isolated from the ground. For the storage capacitor selection, VCAP, an external capacitor needs to be added to the circuit. The value of that exact capacitor is most crucial in determining the amount of energy that can be achieved at the VOUT pin. Leakage current of the capacitor has to be as small as possible, maybe less than 1 A at 1.2 V. The capacitor ESR should be 200 m or less. The smaller the capacitor, the faster the charging, but with shorter operation cycles. And vice versa, the larger the capacitor, the slower the charging, but with longer operation cycles. The minimum required capacitor value of the capacitor can be determined using Eq (1). ON T OUT I OUT C = 15 V (1) Where, VOUT is output voltage, IOUT is output current, and TON is on-time of the VOUT. The importance of the capacitor size decreases while using the RESET function. Since more energy is required, intermittent functions can be facilitated by using a larger capacitor. In order to minimize the required recharge time, some amount of energy need to be removed during the operation from the capacitor by the RESET function. While usingRESET, charge time will not be affected by using a larger capacitor during operation. But to charge from a totally discharge state, more time will be required. VCAP will vary between 1.25 V and 1.02 V during normal operation approximately. Protection of the low voltage super capacitors will require the capacitor's voltage to be internally clamped in case of too large voltage from harvested energy. At approximately 1.8 V, the clamping will begin and the voltage will be limited to less than 2.3 V at the maximum rated input power. As for the DOUT andDSET, the amount of harvested energy is provided by sampling the received signal, which is allowed by the function of the RSSI. Setting the DSET high will direct the harvested DC power to an internal sense resistor, and the DOUT pin will be provided with the corresponding voltage. After a 50 s settling time, the DOUT pin output voltage can be read. Storage of the DC harvested power is not an option during the usage of the RSSI functionality. If the RSSI functionality is not used, DOUT and DSET should be left unconnected. DSET is internally pulled down. Also, Using DOUT and DSET it is possible to collect data from the RF transmitter that is supplying power to the P2110.

As discussed, with DSET high, DOUT will provide a voltage across R3 that can be read by an ADC. However, the voltage on DOUT will also follow the power level of the RF field as the power level changes. If the RF field is being provided by a transmitter that is also communicating by modulating its amplitude, such as the Powercast TX91501-3W-ID transmitter, the data can be read by the P2110. The voltage level is gained up using operation amplifiers and supplied to a device that can read the data pattern supplied by the transmitter. Recharge time back to the activation threshold, VMAX, can be improved by turning off the voltage from VOUT before reaching the lower threshold, VMIN, of the storage capacitor. This can help save energy as well. A microcontroller can be used in order to implement the RESET function. Output voltage, VOUT can be disabled by setting the RESET high after completing the function of the microcontroller. Care should be taken to make sure that the RESET is not inadvertently driven high by the microcontroller during poweron especially. The output voltage will be immediately shut down. Presence of voltage or current at the VOUT pin is digitally indicated by the interrupt function. To bring a microcontroller from a deep sleep mode, an external interrupt can be used. Also, INT can be used in systems with other storage elements. INT pin's digital high level will be

between VMIN and VMAX. A maximum current of 0.1 mA can be provided by the INT pin. In order to set the DC output voltage, an external resistor is to be added to decrease or increase the output voltage using Eq. (2). 10 (2) A resistor calculated by Eq. (3) is used from VSET to VOUT to decrease the output voltage. A minimum of 1.8 V can be achieved. . . (3) A resistor calculated using Eq. (4) may be used from VSET to GND to increase the output voltage. A maximum of 5.25 V can be achieved. . . (4) In minimizing the feed losses, the RF feed line is designed as a 50 trace and should be as short as possible. A via located next to the pads under the receiver is used to connect the GND pins on each side of the RFIN pin to the PCB ground plane. The resistor connected to the VSET pin should be as close as possible to it while setting the output voltage. This pin does not require any addition of any external capacitance. Lo-level analogue voltage signal can be contained by the DOUT pin. An additional filtering capacitance next to the A/D converter may be required in case of connecting a long trace to this pin. The DSET delay time will be increased by introducing an additional capacitance on this pin. To minimize the series resistance of the trace, the trace from VCAP to the storage capacitor should be as short as possible and have a width of greater than 20 mils [9]. The Powercast P2110 functional block diagram is shown in Fig. 3. Fig. 3: Functional Block Diagram of P2110

E. Powercast TX91501-915 MHz Transmitter

The TX91501 Powercast transmitter is designed to provide data and power to RF receivers that contain one of the Powercast harvesters: P2110 or P2110B. It works at 5 V DC. It also has an indicator LED to provide feedback of the connection status. Transmission would stop if there is any obstruction in close proximity. The obstruction has to be removed in order for the transmission to take place again. The output RF power from the TX91501 transmitter is 915 MHz

F. 60H3A3H Ni-MH BUTTON CELL

It is a typical rechargeable nickelmetal hydride (Ni-MH) battery. With a flexible cylindrical shape, it offers 80 mAh capacity with a voltage of 3.7 V. It is a very low cost solution for a project such as this with LEDs usage that does not require high discharge current. Within the battery lies an integrated protection PCB as a protection system to prevent from the overcharge/ over-discharge effects

G. Li-Fi as Loading Requirement

Li-Fi basically consists of Light Emitting Diodes (LEDs). A single p-n semiconductor junction forms the very basic structure of an LED. The p-type and the n-type materials are being charged positively and negatively respectively though a process called Doping. In the n-type material, atoms have extra electrons, while at the p-type material, atoms have empty electron holes. By applying current to this diode, the extra electrons at the n-type material will rush in the direction of the electron holes in the p-type material allowing current to flow though the diode [11]. For the loading requirement of the Li-Fi circuitry, a proposed design of 7 LEDs are to be used. The required voltage would be 1.67 V, and the required current is to be 8 mA.

III. METHODOLOGY

A. Setting up Powercast P2110-EVB RF

As one of the best options, the P2110-EVB is chosen in this work. The board has all the required connections, so there is no need to do any mounting or welding to any component. The main internal components in the board are shown in Fig. 4.

The P2110-EVB consists of two main parts: the P2110 PowerharvesterReceiver, and the 915 MHz Patch Antenna. The P2110 RF energy harvester collects RF energy and converts it into DC power. The microchip stores this DC power in a capacitor to provide an intermittent, regulated voltage output. Connection of the patch antenna is to allow RF input into the P2110 energy harvester receiver. The 915 MHz PCB Patch antenna used with the evaluation board has two layers, with the RF connector located in the middle of the back side of the antenna. The front side should be pointed towards the transmitter with the same polarization. Antenna gain is 6.1 dBi. Referring to Fig. 5, adjustments of switches S2, S3 and S4 are to be made to achieve the desired settings. Here, S2 is set to VCC, S3 to OFF and S4 connects to BATT. Using TX91501-915 MHz transmitter, the distance between the transmitter and receiver has to be less than one (1) meter in order for them to communicate to each other.

B. Configuring Li-Fi Loading

The design approach for the Li-Fi application would require tens of LEDs, yet in this work, only seven (7) red LEDs are used to represent the Li-Fi application. The red LEDs are connected in parallel, so that they can draw the same voltage, and also they can draw the same current each as no other component is connected in parallel with them. For the red LEDs, they need a voltage of 1.67 V to turn on. Meaning that they would require a resistance to be connected in series with the combination of them to decrease the input voltage applied to them either from the P2110-EVB (3.3 V and above) or from the battery system. The value of this resistance can be calculated through Ohm's law as in in Eq.

C. Setting up Energy Storage

In order to make the Li-Fi application portable, a battery (energy storage) system has to be added. This system would consist of two SZJ 80H2A Ni-MH button cell batteries, each of them is 3.6 V/80mAh. Both batteries are connected in parallel in order to have a final battery level with 3.6 V/160 mAh, which is suitable to activate the Li-Fi application effectively and efficiently. This duration is calculated using Eq. (6). whereTd is the discharge time (Hours), Battery capacity is in (mAh), and Id is the discharge current (mA).

IV. RESULTS AND DISCUSSION

A. Overview of the System

The RF Energy Harvesting module for Li-Fi application is divided into three main parts: P2110-EVB power harvesting evaluation board, energy storage system, and Li-Fi load. The main design of the system is shown in Fig. 5. Fig. 5: System Overview The system receives 915 MHz of RF energy via the patch antenna, then it converts to DC power. The resulting voltage shall be introduced to two main switches, S1 and S2. S1 is to connect the Li-Fi application directly to the P2110-EVB output voltage, while S2 is used to connect the P2110-EVB output to the energy storage system. There are six (6) modes of operation for the system which shall be discussed in the following section. The normal output voltage of the system is 3.3 V from the BATT pin. In order to increase that voltage, Eq. (4) is used. The calculated resistance value is R2 = 250 k.

B. Modes of Connection

Mode I: No Connection In this mode, the switches S1 and S2 are open, meaning that there will be no connection between the P2110-EVB and the Li- Fi application nor the battery (energy storage) system. In that case, using a resistor R2 = 250 k, the resulting output voltage at BATT pin is VRF = 4.33 V. Mode II: Battery Charging Only (S2 Closed) During this mode, only switch S2 is closed, allowing the battery system to be recharged using the output power from the RF energy harvester P2110. An illustration of this mode is available in Fig. 6, and the measurements of the system are available in Table I. Parameter Value Remarks VRF (V) 4.33 - VBATTERY (V) X X is increasing, starting from battery's voltage level till 4.33 V IBATTERY (mA) 16.77 Decreasing TCHARGE (hours) 10 With Losses Mode III: Li-Fi Application Only (S1 Closed) In this mode, only switch S1 is closed, while all others are open. The VRF is connected directly to the Li-Fi application circuitry which consists of LEDs and a resistance in order to provide the LEDs with the exact needed voltage for them to illuminate without being damaged by high voltage or current. The R1 value is calculated using Eq. (5). An illustration of this mode is available in Fig. 7, and the measurements of the system are available in Table II. Fig. 7: Mode III Table II. Mode III Parameter Value Remarks VRF (V) 4.33 - VBATTERY (V) 3.6 Considered as fully charged VLi-Fi(V) 4.33 - R1 () 511 - VR1(V) 2.69 - VLED(V) 1.63 Enough voltage to illuminate ILi-Fi (mA) 3.7

Mode IV: Battery Charging and Li-Fi Application (S2 S1/S3 Closed) In this mode, switch S2 and either switches S1 or S3 or both are closed, while switch S4 is open. The VRF is connected to the battery system via switch S2 and also to the Li-Fi application circuitry via both switches S1 and/or S3. In this mode, the battery is charged and at the same time the Li-Fi application is activated. Yet, the battery may take longer time to charge as the withdrawn current is divided between both the battery and the Li-Fi application. An illustration of this mode is available in Fig. 8, and the measurements of the system are available in Table III. Fig. 8: Mode IV Table III. Mode IV Parameter Value Remarks VRF (V) 3.24 - VBATTERY (V) 3.24 Considered as fully charged VLi-Fi(V) 3.24 - R1 () 511 - VR1(V) 1.62 - VLED(V) 1.62 Enough voltage to illuminate ILi-Fi (mA) 2.73 - IBATTERY (mA) 11.94 Decreasing TCHARGE (hours) 13.4 - Mode V: Activating Li-Fi Application using Battery System Only (S3) In this mode, only the switch S3 is closed, while all other switches are open. The Li-Fi application circuitry is connected directly to the battery system via switch S3. In this mode, the Li-Fi application is using the storage of the battery (160 mAh) to be active. This mode can be used in case there is not enough RF power to power up the Li-Fi application alone. An illustration of this mode is available in Fig. 9, and the measurements of the system are available in Table IV. Fig. 9: Mode V Table IV. Mode V Parameter Value Remarks VBATTERY (V) 3.24 Decreasing Voltage (Discharging) VLi-Fi(V) 3.24 Same as Battery, Decreasing R1 () 511 - VR1(V) 1.62 Decreasing VLED(V) 1.62 Enough voltage to illuminate (Last to decrease) ILi-Fi (mA) 3.7 Decreasing TDISCHARGE (hours) 43 - Mode VI: Activating Li-Fi Application using Battery System Only (S4 - High Power) In this mode, only the switch S4 is closed, while all other switches are open. The Li-Fi application circuitry is connected directly to the battery system via switch S4. In this mode, the Li-Fi application is using the storage of the battery (160 mAh) to be active. Using this mode will cause the battery to activate the Li-Fi application directly without passing by the resistance R1. This will cause the LEDs to have higher illumination but at the same time will negatively affect the battery by decreasing the life-time or increasing the discharge rate. Important: Please note that while switch S4 is closed, switch S2 or the combination of switches S1 and S3 must never be closed. An illustration of this mode is available in Fig. 10, and the measurements of the system are available in Table V. Fig. 10: Mode VI Table V. Mode VI Parameter Value Remarks VBATTERY (V) 1.67 Decreasing Voltage (Discharging) VLi-Fi(V) 1.67 Same as Battery, Decreasing VLED(V) 1.67 Enough voltage to illuminate ILi-Fi (mA) 5 Decreasing TDISCHARGE (hours) 32 -

V. CONCLUSION

The Design and the calculations of the Li-Fi application circuitry and the battery (Energy storage) system have been performed accurately. Subsequently, the P2110-EVB has been studied and experimentations have been done on it. Secondly, the Li-Fi application circuitry has been designed and modified as a load requirement. Then the battery system has been sized, implemented with the load and tested. Finally, the whole system was integrated together to construct the complete RF energy harvesting system for the Li-Fi application. The system is installed on a prototype made from plastic to make the outer shape for it. Furthermore, the system has achieved the desired output voltage and current that enables it to charge the battery system and/or activate the Li-Fi application. Eventually, the designing, manufacturing and testing the RF

energy harvesting system for the Li-Fi application has been accomplished successfully.

VI. ACKNOWLEDGMENT

The authors would like to express the utmost gratitude to UniversitiTeknologi PETRONAS for giving financial support to present and publish the work.

REFERENCES

[1] H. Jabbar, Y. S. Song and T. T. Jeong, *"RF Energy Harvesting System and Circuits for Charging of Mobile Devices"*, , IEEE Consumer Electronics Society, p. 247- 253, 2010

[2] A. Sivaramakrishnan and K. J. Jegadishkumar, *"A Highly Efficient Power Management System"*, ,International Journal of Information Technology Convergence and Services, Vol. 1, No. 5, p. 21-30, 2011.

[3] P. Aminov and J. P. Agrawal, *"RF Energy Harvesting"*,,Electronic Components Technology Conference, p. 1838-1841, 2014.

OPTIMAL LOCATION AND SIZING OF DG FOR MAXIMIZING VOLTAGE STABILITY IN A POWER SYSTEM

J.Arul Martinal
Assistant Professor
Department of Electrical and Electronics Engineering
St. Annes College of Engineering and Technology,

***Abstract*—This paper presents the need to operate the power system economically and with optimum levels of voltages has further led to an increase interest in Distributed Generation. In order to reduce the real power losses and to improve the voltage in distribution system, distributed generators are connected to load bus. The most important process is to identify the proper location for fixing and sizing of DGs. The power loss reduction is important factor for utility companies because it is directly proportional to the company benefits in a competitive electricity market, while reaching the better power quality standards is too important as it has vital effect on customer orientation. The proposed method (TLBO) is to use an intelligent technique in order to identify the proper location for fixing and sizing of DGs to reduce the real power losses and to improve voltage stability in distribution system. The impact of increase in DG units is also carried out for various load scenarios. Simulation is carried on a 69 IEEE bus system with out and with the presence of DG and the results are presented and analyzed. Keywords - Distributed generation, Radial distribution system, Voltage improvement, Power loss reduction, Teaching Learning based optimization algorithm.**

I. INTRODUCTION

The modern power distribution network is constantly being faced with an ever growing load demand; this increasing load is resulting into increased burden and reduced voltage. The distribution network also has a typical feature that the voltage at nodes reduces if moved away from substation. This decrease in voltage is mainly due to insufficient amount of reactive power. Even in certain industrial area critical loading, it may lead to voltage collapse. Thus to improve the voltage profile and to avoid voltage collapse reactive compensation is required. The X/R ratio for distribution levels is low compared to transmission levels, causing high power losses and a drop in voltage magnitude along radial distribution lines. It is well known that loss in a distribution networks are significantly high compared to that in a transmission networks. Many arrangements can be worked out to reduce these losses like network reconfiguration, shunt capacitor placement, distributed generator placement etc. The distributed generators supply part of active power demand, thereby reducing the current and MVA in lines. Installation of distributed generators on distribution network will help in reducing energy losses, peak demand losses and improvement in the networks voltage profile, networks stability and power factor of the networks. DG allocation is basically a complex combinatorial optimization issue which requires concurrent optimization of objective. The objective is to determine the optimal location and size of DG units in a distribution network. The optimization is carried out under the constraints of maximum DG sizes, thermal limit of network branches, and voltage limit of the nodes. There are numerous optimization techniques used in the literature. In most of the current works, population based evolutionary algorithms are used as solution strategies. This includes genetic algorithm, evolutionary programming and particle swarm optimization etc. In this project, teaching-learning based optimization, developed by Rao et al., is used to minimize the total system real power loss. Classically, most distribution systems (DSs) are radial in nature, contain only one power source, and serve residential, commercial and industrial loads. DSs are also operated at the lowest voltage levels in the overall power networks [1]. Power is delivered in bulk to substations. The substation is usually where the transmission and distribution networks meet. The backbone of the distribution networks typically is comprised of 3-phase mains. Laterals are tapped off these mains and are usually single-phase (unless 3-phase service is required by a customer) [1-2]. In addition, the lines used for DSs tend to have a higher resistance to impedance ratio (R/X) than the lines in transmission networks [2]. Power loss in distribution networks have become the most concerned issue in power losses analysis in any power networks. In the effort of reducing power losses within distribution networks, reactive power compensation has become increasingly important as it affects the operational, economical and quality of service for electric power networks [3]. The method used a voltage sensitivity index to determine the DG-units optimal location. Then, the DG-unit active and reactive powers were adjusted to obtain maximum voltage support. The weakest bus was identified using Thevenins theorem. Minimizing power loss by finding the optimal size, location and operation point of DG unit was suggested in [4]. A sensitivity analysis relating the power loss with respect to DG-unit current injection was used to identify the DG-unit size and operation point. The

proposed method was tested for constant impedance and a constant current model. The location of the DG-unit was based on the assumption of downstream load buses, which may not be appropriate for different feeder configurations. The authors of [5] employed the GA for optimal power flow (OPF) to minimize the DG-units active and reactive power cost. Two examples of DG-unit optimization cases were considered, with and without reactive power injection. Significant reduction in the search space was attained by eliminating the DG-unit size. However, DG-unit dispatching can cause operational problems in the distribution feeders. An algorithm was offered in [6] to maximize the reduction of load supply costs as well as operational schedules for all feeder load levels exploiting EP. The optimal solution was selected based on maximum cost reduction, which was attained through evaluating the cost of DG-unit supply scenarios based on the base case. The authors of [7] proposed an analytical method to calculate the optimal DG-unit size. In addition, an approximate loss formula to identify the optimal DG-unit placement was suggested. The method offered was based on the exact loss formula. The power flow was employed twice, with and without the DG-unit. The adopted DG-unit injected only active power. In this paper [8], a new optimization approach that utilizes an artificial bee colony (ABC) algorithm to determine the optimal DG-units size, power factor, and location in order to minimize the total system real power loss is proposed. Sample feeder systems are examined, as well as various test cases. The results reveal that the ABC algorithm is efficient, fast-converging, and capable of handling complex optimization problems. The load flow of radial distribution networks employing node-injection to branch-current (BIBC) and branch-current to node-voltage (BCBV) matrices [9]. This paper [10], proposed a methodology for solving the radial load flow for analyzing the optimal capacitor sizing problem. In this method, for each branch of the network three non-linear equations are written in terms of the branch power flows and bus voltages. The number of equations was subsequently reduced by using terminal conditions associated with the main feeder and its laterals, and the Newton- Raphson method is applied to this reduced set. The computational efficiency is improved by making some simplifications in the Jacobian. They have solved the radial distribution network using these three equations by reducing the whole network into a single equivalent. Rao et al. [11] presented Teaching Learning-Based Optimization (TLBO), optimization procedure for mechanical design. The working of this technique is similar to teaching-learning process in the class. The population in this technique is considered as the number of students in a class and the global solution is obtained by the effect of teacher on students and by the interaction of students in class. Rao et al. [12] suggested that proper selection of parameters is essential for other nature-inspired algorithms and otherwise the effectiveness of the algorithm is affected where as TLBO is parameter free algorithm. The enhancement incorporated in to TLBO by Rao and Patel [20] was to exploit the capabilities of multiple teachers into classrooms (learners), adaptive teaching factor, tutorial training and self motivated learning. All these characteristics were thoroughly assessed in solving unconstrained multi-dimensional, linear, and non-linear problems.

II. PROBLEM FORMULATION

One advantage of deploying a DG-unit in distribution networks is to minimize the total system real power loss while satisfying certain operating constraints. In other words, the problem of DG-unit application can be interpreted as finding the optimal size and location of that DG-unit to satisfy the desired objective function subject to equality and inequality constraints. Reliability, accuracy, and flexibility of the DG-unit solution algorithm are influenced by the power flow analysis used. Therefore, the overall algorithm accuracy is highly reliant on that analysis. It can be said that the power-flow analysis is the heart of the DG-unit solution algorithm. Accordingly, the power-flow algorithm is applied in this project. The mathematical formulations of the mixed integer nonlinear optimization problem for the DG-unit application are as follows: The multi objective function is to minimize the total system real power loss and to improve voltage profile in distribution system F=wF1+(1w)F2 (1) where w is weightage factor, w=rand [0,1] Minimization Real Power Loss

The equality constraints are the three nonlinear recursive power-flow equations describing the system

Th Practical concerns in terms of DG-unit sizes and power factors are considered in the proposed method. Since the

$$F_1 = P_{loss} = min \sum_{i=0}^{n} \left(\frac{P_i^2 + Q_i^2}{V_i^2} \right) \times r_{i+1} \qquad (2)$$

- Voltage Profile Improvement

$$F_2 = \sum_{i \epsilon NL} |V_i - V_i^{ref}| \qquad (3)$$

Fig. 1.

$$P_i - \frac{r_{i+1}(P_i^2 + Q_i^2)}{V_i^2} - P_{L_{i+1}} + \mu_P A P_{i+1} - P_{i+1} = 0 \qquad (4)$$

$$Q_i - \frac{x_{i+1}(P_i^2 + Q_i^2)}{V_i^2} - Q_{L_{i+1}} + \mu_Q R P_{i+1} - Q_{i+1} = 0 \qquad (5)$$

$$V_{i+1}^2 = V_i^2 - 2(r_{i+1}P_i + x_{i+1}Q_i) + \left(\frac{(r_{i+1}^2 + x_{i+1}^2)(P_i^2 + Q_i^2)}{V_i^2} \right) \qquad (6)$$

Fig. 2.

rounded-off issues of the DG-units size or p.f. are treated initially in the proposed method, the accuracy of the results is guaranteed. The preselected (discretized) DG-unit sizes are from 10 80 of the total system demands (i.e.,, approximated to integer values with a 100-step interval between sizes. The DG-units p.f. is set to operate at practical values, that is, unity, 0.95, 0.90, and 0.85 towards the optimal result. Moreover, the operating DG-units p.f. (i.e., lagging or leading) must be dissimilar to the buss load p.f. at which the DG-unit is placed. Consequently, the net total of both active and reactive powers of that bus (where the DG-unit is placed) will decrease.

III. TLBO

Teaching-Learning based optimization algorithm is a new optimization technique developed by Rao et al. It is also a population based optimization method like other optimization algorithms and is inspired by the teaching-learning process in a class between teacher and learners. Teachers are considered as the most knowledgeable person and always try to influence the learners to achieve their goal. The quality of a teacher affects the outcome of the learners. Also, the students in the class also improve their knowledge by discussing it with other students in class. The final result of the class is evaluated on the basis of the knowledge that the students have. Teaching-Learning Based Optimization (TLBO) obtain global solutions for continuous non-linear functions with less computational effort and high consistency. The TLBO algorithm is also a population-based algorithm inspired by nature like other algorithms with a pre-defined population size. In all nature-based algorithms, initially the population is generated randomly and an individual in that population represents an optimal solution of the problem. In this algorithm the population refers to the students in a particular class and subjects offered to those students are the design variables of the optimization problem. Thus the objective function value and the design variables constitute the solution representing knowledge of particular students. The teacher for the entire population is the best solution of that population. The design variables are actually the parameters involved in the objective function of the given optimization problem and the best solution is the best value of the objective function

Like genetic algorithm, particle swarm optimization, artificial bee colony and harmony search, teaching-learning based optimization is also a population-based technique which implements a group of solutions to proceed to the optimum solution. The controlling parameters of these algorithms as discussed in are shown in Table 1. The working of TLBO comprises of : (i) Teacher phase and (ii) Learner phase.

IV. Teacher Phase

The first part of the algorithm, where learners increase their knowledge through teacher is known as Teacher Phase. In this phase, the teacher tries to increase the mean result of the class in the subject taught by him or her, depending on his or her capability. The best solution which is defined by the value of its objective function, from the population, is considered as the teacher. The increase in the knowledge of students in a class depends upon the teacher. But practically, for a teacher, it is impossible to increase the knowledge in the students equally because every student possesses different learning levels. So the teacher, after teaching, can only improve the mean level of learners in class to some extent. If the new average grade of the jth subject at kth iteration is newjk , the difference between the existing mean and new mean of the jth subject at the kth iteration may be formulated as, diffjk=rand (newjk-tf jk) (11) where tf is teaching factor which is evaluated randomly by the following equation: tf=round(1+rand(0,1)) (12) The grade of the jth subject of the ith student at (k+i)th iteration is updated by x(i,j)(k+1) = x(i,j)k (13) It may be noted that the random value, in the range[0,1], and teaching factor, tf, affect the performance of the TLBO algorithm. However, the value of tf are generated randomly in the algorithm and are not supplied as input to the algorithm. So the tuning of these parameters are not required by the proposed algorithm unlike the tuning of controlling parameters of other algorithms. Tuning of population size and generation number is required by TLBO algorithm.

V. Learner Phase

A student also learn by interacting with other students in the class. So the phase of learning from the other students of the class is known as the Learner Phase. Learner phase is second part of the algorithm, where learners increase their knowledge by interaction among themselves. A learner further improve the quality of their knowledge by comparing their knowledge with other students if the other learners have

Genetic Algorithm (GA)	Crossover probability, mutation rate and selection method.
Particle Swarm Optimization (PSO)	Learning factor, the variation of weight and the maximum value of velocity.
Artificial Bee Colony (ABC)	Limit value.
Harmony Search (HS)	Harmony memory consideration rate, pitch adjusting rate and number of improvisation.
Teaching-Learning Based Optimization (TLBO)	Mean values of population to update solution.

Fig. 3.

more knowledge. Thus each student randomly choose another student for interaction and learn new things from him if that student has better knowledge than him. Mathematically this learning phenomenon may be expressed as follows:

where x(i,j)(k+1) ; x(i,j)k are the grade point of the jth subject of the ith student at the kth and (k + 1)th iterations; x(l,j)k is the grade point of the jth subject of the lth student (randomly selected) at kth iteration; f(Xl) is the overall grade point of the lth student;

The TLBO algorithm can be implemented in the following steps as in:

Step 1: Define the optimization problem and generate random population according to population size (Pn) (students), number of generations (Gn) and number of design variables (Dn) (subjects) within the limits. This population is expressed as:

Step 2: Teacher Phase Calculate the mean of the population column-wise, i.e. the mean of the subjects of students as:

The best solution for that iteration will act as a teacher Xteacher= X(f(X)=min) The solution obtained, teacher, will always try to change the mean from M(new,D) to X(teacher,D). So, the best solution obtained, Xteacher, will act as a new mean for the iteration. M(new,D)= X(teacher,D) The difference between two means is expressed as

Diff(,D) =r(Mean(new,D) TF M(,D)) The obtained difference is added to the current solution to update its values using X(new,D)= X(old,D)+ Diff(,D) Accept Xnew if it gives better function value. Step 3: Learner Phase In Learner phase as mentioned above, increase their knowledge by mutual interaction with each other and mathematically explained as:

Accept Xnew if it gives better function value. Step 4: Stop if the maximum generation number is achieved; otherwise repeat from Step 2. Two feasible solutions are obtained, i.e. at the end of teacher phase and learner phase, and solution giving better function value (or optimized value) is preferred. The standard procedure of TLBO is shown in flowchart as shown in Figure 1.

$$x_{i,j}^{k+1} = x_{i,j}^{k} + rand * \left(x_{i,j}^{k} - x_{i,j}^{k}\right); if F(X_i) < F(X_i) \quad (14)$$

$$x_{i,j}^{k+1} = x_{i,j}^{k} + rand * \left(x_{i,j}^{k} - x_{i,j}^{k}\right); if F(X_i) > F(X_i) \quad (15)$$

Fig. 4.

$$population = \begin{bmatrix} X_{1,1} & X_{1,2} & \dots & X_{1,D} \\ X_{2,1} & X_{2,2} & \dots & X_{2,D} \\ \vdots & \vdots & \ddots & \vdots \\ X_{pn,1} & X_{pn,2} & \dots & X_{pn,D} \end{bmatrix}$$

Fig. 5.

VI. RESULTS AND DICCUSSIONS

A. TEST SYSTEM

To check the validity of proposed TLBO algorithm, Standard IEEE 69-node Reliability Test System (RTS) was considered in different test cases. In addition, the results of sample feeder systems were compared with those test cases. The proposed TLBO algorithm is implemented in Matlab.

Furthermore, we studied two load scenarios, scenario I and scenario II. For the first scenario, the loads are identical to the values. In other words, the total demands of the 69-bus system are 3802.19kW and 2694.60kVar. Scenario II, on the

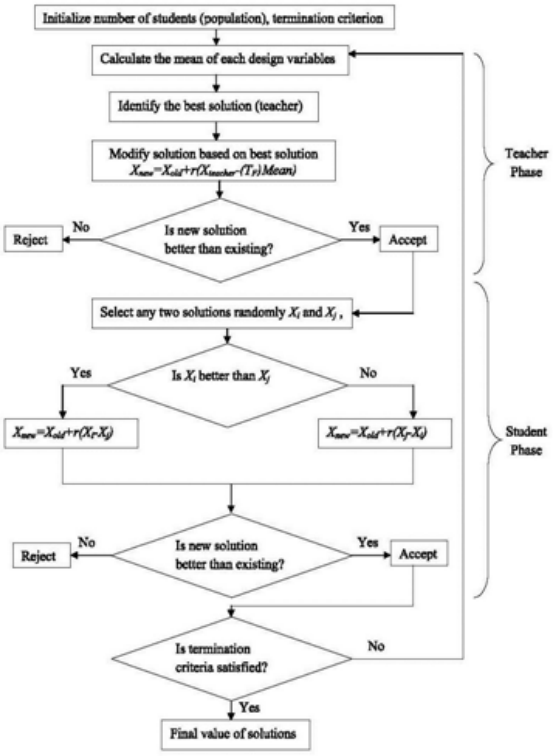

Fig. 6. Flow chart for Teaching-Learning-Based Optimization (TLBO)

$$\begin{aligned} &for\ i = 1{:}popsize \\ &\quad \text{Select two learners randomly } X_i \text{ and } X_l, \text{ where } i \neq l \\ &\quad \text{If } f(X_i) < f(X_l) \\ &\quad X_{new,i} = X_{old,i} + r_i(X_i - X_l) \\ &\quad \text{else} \\ &\quad X_{new,i} = X_{old,i} + r_i(X_l - X_i) \\ &\quad \text{end if} \\ &\quad \text{end for} \end{aligned}$$

Fig. 7.

other hand, represents the situation where the loads of the feeder system increased by 50%. The single-line diagram of the 69-bus feeder system is shown in Figure 2. Table 2 lists the default case results of the chosen feeder system. The substation voltage and load power factors in both scenarios were considered as 1.0 p.u. and lagging p.f., respectively.

The objective functions in all tested cases are to minimize the systems real power loss. However, overall system voltage improvement is considered as an additional goal in test case 2. To avoid over compensation situations, the DG-unit size constraint is set w.r.t. scenario I in all tested cases. In addition, the capacitor size (discrete constraint) is set from 150-4050 kVar with a 150-step interval between sizes. The proposed TLBO algorithm results were obtained after carrying out 30 independent runs.

VII. RESULTS

The test cases conducted were applied at both load scenarios to solve the mixed integer nonlinear optimization problem described in results. Single DG unit Multiple DG unit Single DG unit and a Capacitor

VIII. TEST CASE I - SINGLE DG UNIT

In this test case, an exact solution method was created to verify the results of the proposed TLBO algorithm. Table 3 lists the optimal solutions obtained by the proposed TLBO algorithm for both scenarios. The enhancement results in terms of voltage profiles are illustrated in figure 3 and 4.

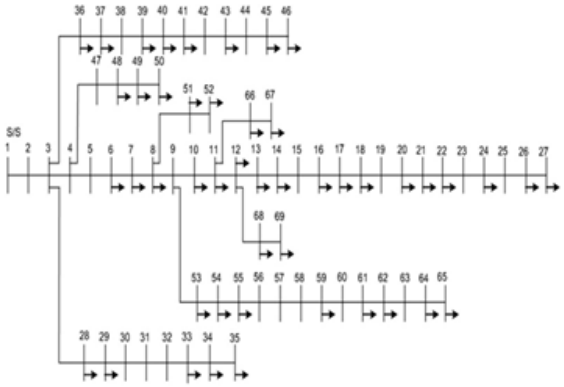

Fig. 8. Single-line diagram of the 69-bus feeder system

Table 2 Optimal result of base case

Load Scenario	I	II
kW loss	224.8	560.34
kVar loss	102.157	252.98
$\|V_{min}\|$, p.u	0.90919	0.85603
$\|V_{max}\|$, p.u	1.0000	1.0000

Fig. 9.

In this test case, the proposed TLBO algorithm successfully achieved the best solutions. Table 4 shows the optimal result of test case II at load scenario I and II respectively. Figure 5 and 6 illustrate the voltage profile for this case.

IX. TEST CASE III SINGLE DG UNIT AND A CAPACITOR

In this test case, we demonstrated the effect of installing (optimally) a reactive power source as well as a DG-unit simultaneously in order to satisfy the objective function. The voltage profile for both scenario of this test case is illustrated in Figure 7 and 8. The proposed TLBO algorithm, as shown in Table 5 for both scenarios, successfully identifies the optimal solutions in each run.

Table 3 Optimal result of test case I

Load Scenario	I Identical load	II 50% increased load
Power Factor	0.85 lead	0.85 lead
DG-unit (KVA)	2000	2000
DG Location	Bus 61	Bus 27
Real Power Loss (KW)	19.8267	48.354
Voltage Profile improvement	1.016	1.018
Objective function	10.4213	24.686

Fig. 10.

Table 4 Optimal result of test case II

Load Scenario	I Identical load	II 50% increased load
Power Factor	0.85 lead	0.85 lead
DG-unit 1 (kVA)	1400	1500
DG-unit 2 (kVA)	1500	2000
DG Location 1	Bus 50	Bus 69
DG Location 2	Bus 61	Bus 61
Real Power Loss (kW)	7.7372	11.5611
Voltage profile improvement	0.9998	1.007
Objective function	4.3685	6.284

Fig. 11.

X. VOLTAGE COMPARATOR

XI. VOLTAGE COMPARATOR

XII. V. CONCLUSION

In this paper, an innovative approach for management of DG power is represented. The proposed method deals with optimal selection of nodes for the placement and size of the

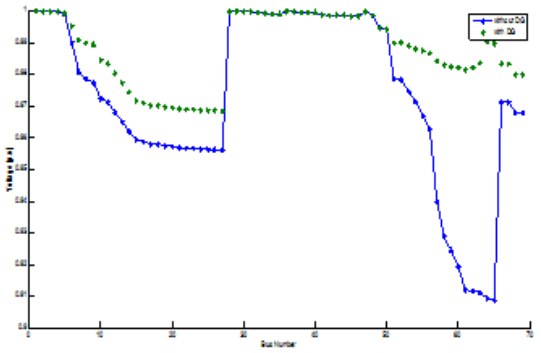

Fig. 12. Voltage profile of test case I at load scenario 1

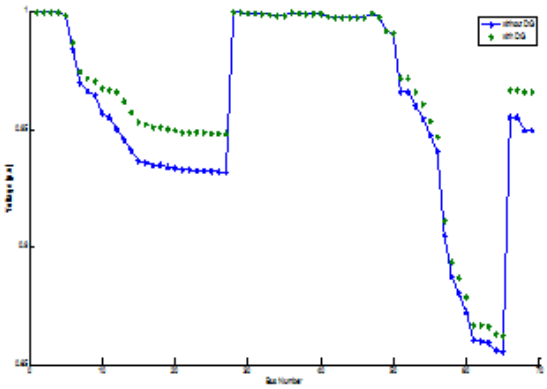

Fig. 13. Voltage profile of test case I at load scenario 2

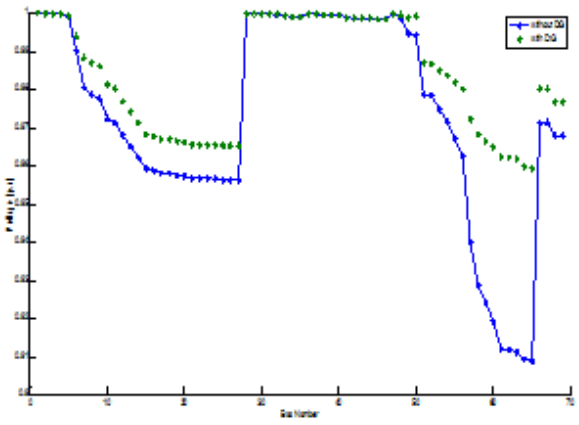

Fig. 14. Voltage profile of test case II at load scenario 1

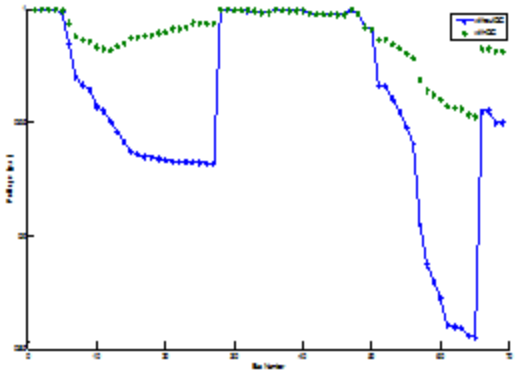

Figure 7 Voltage profile of test case III at load scenario 1

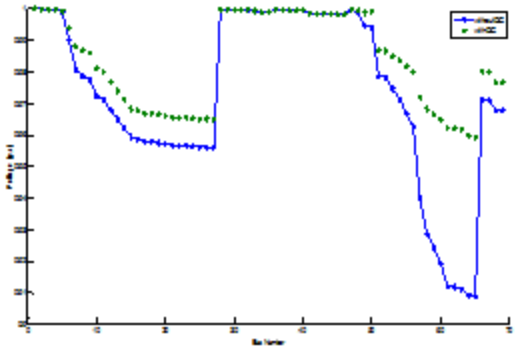

Figure 8 Voltage profile of test case III at load scenario 2

Fig. 15.

Table 5 Optimal result of test case III

Load Scenario	I Identical load	II 50% increased load
Power Factor	0.85 lead	0.85 lead
DG-unit (kVA)	1000	2000
Capacitor (kVar)	1500	1500
DG Location	Bus 11	Bus 11
Capacitor Location	Bus 11	Bus 11
Real Power Loss (kW)	16.253	38.9214
Voltage profile improvement	1.001	1.002
Objective function	8.627	19.9617

Fig. 16.

DG by using TLBO. The load flow problem has been solved by forward/backward load flow methodology. The effectiveness of the approach is demonstrated on the IEEE 69-node reliability test system. If DGs are connected to the system, the simulation results conclude that reduction of real power loss in distribution system is possible and all 1node voltages variation can be achieved within the required limit at various test cases. DGs are connected into the systems power loss and voltage profile is better from when the capacitor bank is connected into the systems, though the DGs are consuming reactive power from the system where extra amount of power loss is occur due to reactive power flow through the line. The results of the proposed TLBO algorithm were compared with those test cases. Among all test cases, test case 2 had the maximum power loss reductions as well as voltage improvement. All mathematical formulation and optimization algorithms have been performed using the Matlab/Simulink program. It is concluded that the implementation of the optimization technique has improved the energy efficiency.

REFERENCES

[1] D. Q. Hung, N. Mithulananthan, and R. C. Bansal, *Analytical expressions for DG allocation in primary distribution networks, IEEE Trans.* ,Energy Convers., vol. 25, no. 3, pp. 814820, Sep. 2010.

[2] Y. M. Atwa, E. F. El-Saadany, M. M. A. Salama, and R. Seethapathy, *Optimal renewable resources mix for distribution system energy loss minimization, IEEE Trans.* Power Syst., vol. 25, no. 1, pp. 360370, Feb. 2010.

[3] M.S. Kandil, M.M. El-Saadawi, A.E. Hassan, and K.M. Abo-Al-Ez *A proposed reactive power controller for DG grid connected systems, Energy Conference and Exhibition (EnergyCon),* ,2010 IEEE International, pp. 446 451, Dec 2010.

[4] R. V. Rao, V. J. Savsani, D. P. Vakharia, *Teaching-learning-based optimization: A novel method for constrained mechanical design optimization problems,* ,Computer-Aided Design, vol. 43, no. 3, pp. 303- 315, 2011.

[5] A.M. El-Zonkoly, *Optimal placement of multi-distributed generation units including different load models using particle swarm optimisation,* ,IET Gener. Trans. Distrib., vol. 5, no. 7, pp. 760771, 2011.

SIMULINK BASED PI AND FUZZY LOGIC CONTROLLERS FOR THE SPEED CONTROL OF DC MOTOR

Dr.N.Neela
Professor
Annamalai university

S.vetriselvi
ME(Embedded system)
Annamalai University

***Abstract*—Intelligent controllers as new technologies have recently been applied to electrical power control systems in general and motor control systems in particular.The Main Role Of This Work Is implementation of a (FLC) system and the conventional (PI) controller for speed control of DC motor.It is based on field programmable gate array (FPGA) circuit. Both FLC and conventional PI controller hardware are synthesized, functionally verified and implemented using Xilinx Integrated Software Environment (ISE) Version 11.1i.The fuzzy control applications with the physical systems require a real-time operation to interface high speed constraints. Fuzzy logic control (FLC) provides an alternative to the PID controller since it is a good tool for the control of nonlinear systems that are difficult in modeling.**

I. INTRODUCTION

The development of high performance motor drives is very important in industrial as well as other purpose applications. The dc motors are used in various applications such as defence, industries, Robotics etc. DC drives, because of their simplicity, ease of application, reliability and favourable cost have long been a backbone of industrial applications. DC drives are less complex with a single power conversion from AC to DC. DC drives are normally less expensive for most horsepower ratings. DC motors have a long tradition of use as adjustable speed machines and a wide range of options have evolved for this purpose. In these applications, the motor should be precisely controlled to give the desired performance. Many varieties of control schemes such as P, proportional integral (PI), proportional derivation integral (PID), adaptive, and fuzzy logic controller (FLCs), have been developed for speed control of dc motors. The proposed controller systems consist of multi-input fuzzy logic controller (FLC) and multi-input integrated fuzzy logic controller (IFLC) for the speed control.

II. DC MOTOR

A machine that converts D.C. power into mechanical power is known as a D.C. motor. Its operation is based on the principle that when a current carrying Magnetic field, the conductor experiences a mechanical force. The direction of this force is given by Flemings left hand rule and magnitude is given by;F = B.I. newtons Basically, there is no constructional difference between a D.C. motor and a D.C. generator. The same D.C. machine can be run as a generator or motor. DC motors consist of one set of coils, called armature winding, inside another set of coils or a set of permanent magnets, called the stator. Applying a voltage to the coils produces a torque in the armature, resulting in motion. If electrical energy is supplied to a conductor lying perpendicular to a magnetic field, the interaction of current flowing in the conductor and the magnetic field will produce mechanical force (and therefore,mechanical energy.

A. POWER ELECTRONICS DEFINED

It has been said that people do not use electricity, but rather they use communication, light, mechanical work, entertainment, and all the tangible benefits of energy and electronics. In this sense, electrical engineering as a discipline is much involved in energy conversion and information. Energy is a critical need in every human endeavor. The capabilities and

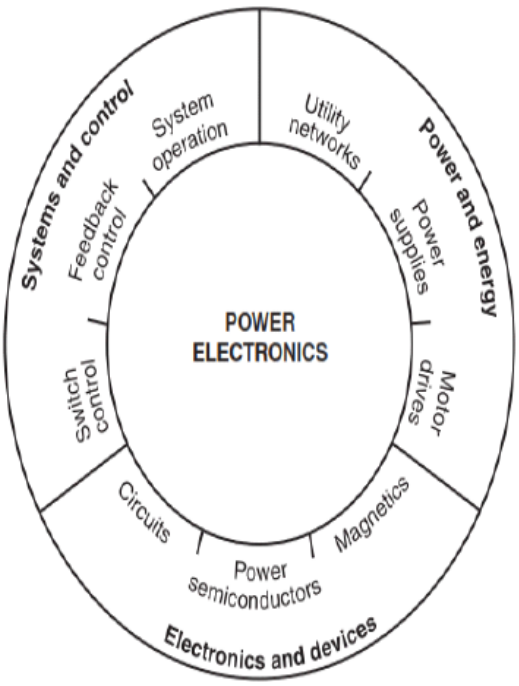

Fig. 1. Control, energy, and power electronics are interrupted

flexibility of modern electronics must be brought to bear to meet the challenges of reliable, efficient energy. Power electronics involves the study of electronic circuits intended to control the flow of electrical energy.

B. SPEED CONTROL METHODS OF DC MOTOR

Flux control method Armature and Rheostatic control method Voltage control method Multiple voltage control Ward Leonard system

III. EXISTING METHOD

A. PI CONTROLLER

The PI controller is by far the most common control algorithm. Most practical feedback loops are based on PI control or some minor variations of it. Many controllers do not even use derivative action. The PI controllers appear in many deferent forms, as stand-alone controllers, they can also be part of a DDC (Direct Digital Control) package or a hierarchical distributed process control system or they are built into embedded systems. Thousands of instrument and control engineers worldwide are using such controllers in their daily work. The PI algorithm can be approached from many divergent directions. It can be viewed as a device that can be operated with a few empirical rules, but it can also be approached analytically. Many industrial processes are controlled using conventional controllers like PI, PD, and PID etc. To manipulate the final control element in order to bring the process measurement to the set point whenever the

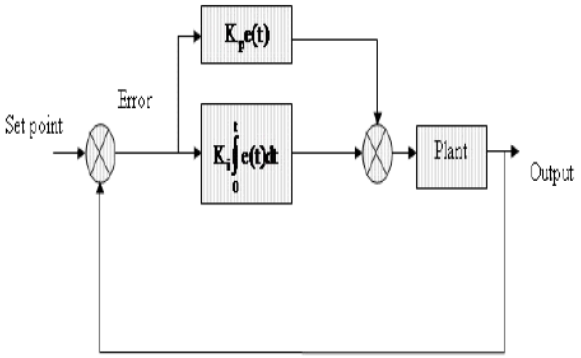

Fig. 2. Basic structure of PI

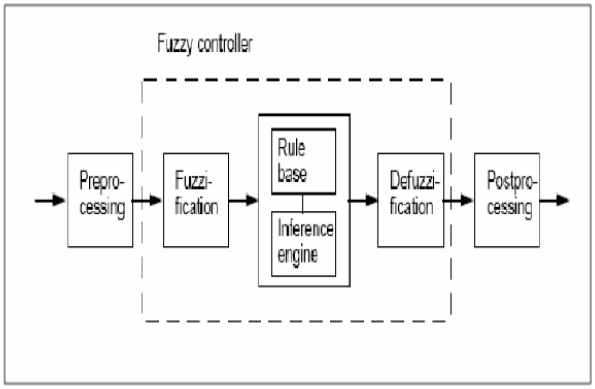

Fig. 3. Structure of fuzzy logic controller

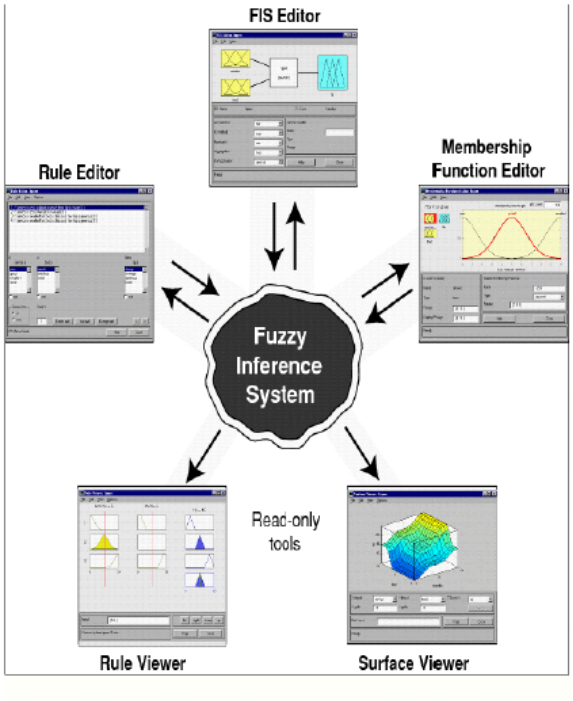

Fig. 4. Fuzzy Inference System

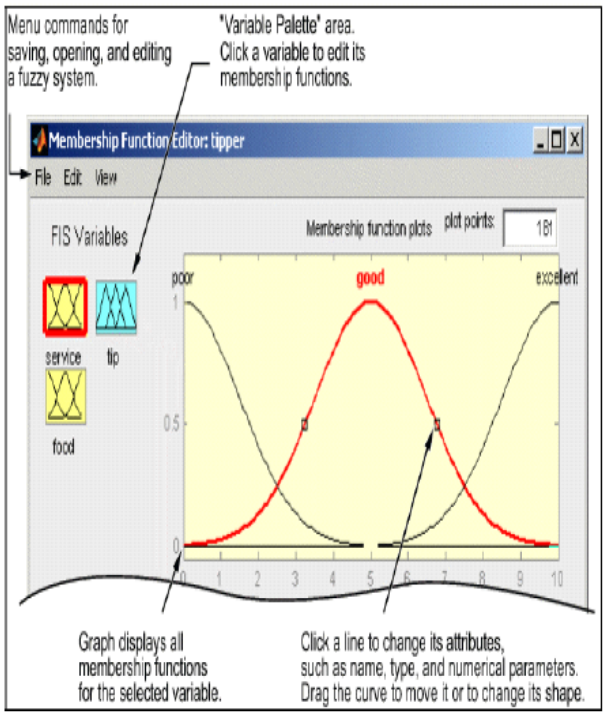

Fig. 5. Membership function

set point is changed, and to hold the process measurement at the set point. The control algorithm must be designed to quickly respond to changes in the set point (usually caused by operator action) and to changes in the loads (disturbances). The design of the control algorithm must also prevent the loop from becoming unstable, that is, from oscillating. There are varieties of control actions that are used, in order to achieve the desired response from the designed process satisfactorily and efficiently.However, the controller performance will deteriorate as the process moves further away from the steady state around which it was linearized. Therefore application of PI controller becomes more attractive for controlling tool wear.

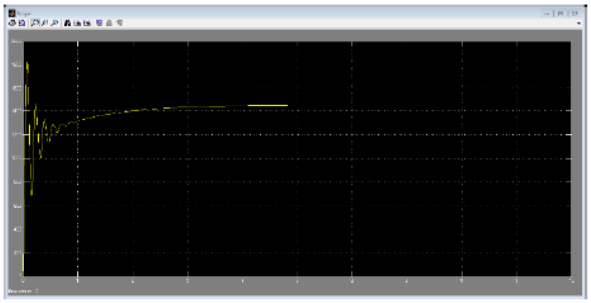

Fig(a)

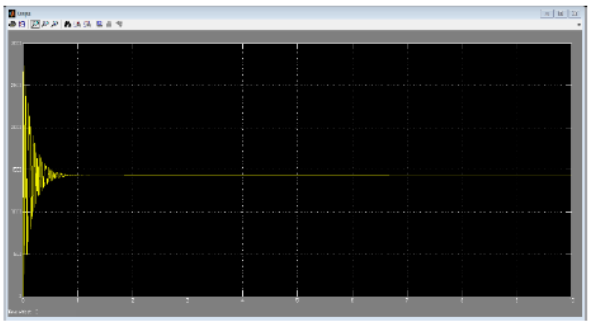

Fig(b)

Fig. 6.

SIMULINK MODEL

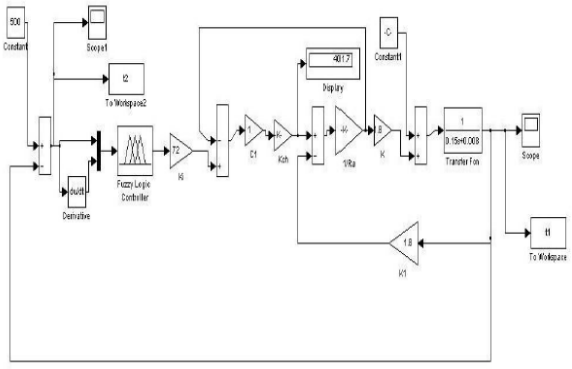

Fig. 7.

B. STRUCTURE OF PI CONTROLLER

IV. PROPOSED METHODOLOGY

Fuzzy Logic Controller (FLC) is based on fuzzy logic controller and constitutes a way of converting linguistic control strategy into an automatic by generating a rule base which controls the behaviour of the system. Fuzzy control is control method based on fuzzy logic. Fuzzy provides a remarkably simple way to draw definite conclusions from vague ambiguous or imprecise information. It suitable for applications such as the speed control of dc motor which is has non linearities. FLC have some advantages compared to other classical controller such as simplicity of control, low cost and the possibility to design without knowing the exact mathematical model of the process. Fuzzy logic incorporates an alternative way of thinking which allows modelling complex systems using higher level of abstraction originating from the knowledge and experience.

V. SIMULATION RESULTS AND EXISTING SYSTEM

A. B.PROPOSED SYSTEM

VI. VI.CONCLUSION

The main contribution of this work is to present an Mapproachof real time fuzzy logic controller for DC motor some advantages such as flexible design (the membership functions and rule base can be easily changed), feature accuracy, high reliability, cost improvement, and high speed. The performance of the FLC is compared with the PI controller for referencespeed and load changes. The satisfied ability of the system control with FLC is better than PI controller. In the existing system, the pi values will be given in different ranges. The PI controller is used to compare with the FLC. Finally FLC is efficient compared with the PI controller.

REFERENCES

[1] Hammed B, Al-Mobaied M. Fuzzy *PID controllers using FPGA Technique for real time DC motor speed control. Intel Control*,Auto 2011; 2(August):23340.

[2] Millan I, Montel O, Sepulveda R, Castillo O. *Design and Implementation of a hybrid fuzzy controller using VHDL. Soft Computing for hybrid Intel. Systems. Berlin,*,Springer-Verilog; 2008, SCI 154.

[3] Kaur A, *Development of neuro fuzzy controller algorithm for air conditioning system. (IJEST) Int J Eng. Sci*,Techno 2012;4(04):166771, ISSN: 0975-5462.

[4] Hammed BM, El-Mohan MS. Fuzzy *Fuzzy controller design using FPGA for sun tracking in solar array system.*Intel Syst Appl 2012; 1(February):4652.

Fuzzy Approach to Voltage Collapse based Contingency Ranking

Karthik.V
UG Scholar
Department of Electrical and Electronics Engineering
St. Annes College of Engineering and Technology

Ajith Kumar.K
UG Scholar
Department of Electrical and Electronics Engineering
St. Annes College of Engineering and Technology

***Abstract*—The importance of preventing the voltage collapse is gaining importance due to increase in dependency on the use of electricity. This has compelled the utilities to maintain high system reliability. The evaluation of a power systems ability to withstand dangerous contingencies and to survive to a normal or acceptable operating point is a prerequisite for security analysis. Fast and accurate security assessment, has become a key issue to ensure secure operation of power system. Steady-state security assessment enables the operating personnel to know which system disturbances or contingencies may cause limit violations and force the system to enter into emergency state. Line outages often cause blackouts due to voltage collapse. Voltage Stability Margin of the system on occurrence of specific contingency gives good information about the severity of the contingency of the system. This paper presents fuzzy approach to voltage collapse based contingency ranking. It uses L index as Voltage Collapse Proximity Indicator. This indicator is used as post contingent quantity in addition to bus voltage profiles to evaluate contingency ranking. The proposed approach is tested under simulated condition on IEEE-30 bus system.**

Keywords: Composite Index, Fuzzy Set, L index, Voltage Collapse Proximity Indicator, Voltage Stability Margin

I. INTRODUCTION

A power system is said to be operating in secure state, if the system remains in a reliable, normal operating state for every contingency case under consideration. Due to time limitation in real-time situations, those contingency cases which are potentially harmful to the system must be picked out and detailed analysis is carried out only for these cases. This process of ranking the contingencies according to their severities is referred to as contingency ranking. In the past, contingency rankings were carried out using the algorithms based on line loadings and bus voltages [1]-[3]. As the recent power systems are experiencing the threat of voltage instability, the contingencies are required to be ranked incorporating this phenomenon. A method based on curve fitting approach is proposed and is compared with continuation power flow method, multiple load flow method and test function method [4]. A new partitioning technique based on tangent vector to the bifurcation manifold is proposed. A tangent vector clustering technique is used for the identification of the critical area with respect to the collapse point at any loading condition. It is used for the computation of new voltage stability index, which speeds

up the computation of the collapse point [5]. The second order information derived from the Singular Value Decomposition analysis of the load flow Jacobian matrix is used to obtain the contingency ranking [6]. The implementation of both Point of Collapse method and Continuation method for the computation of voltage collapse point (saddle-node bifurcations) and its application to detection and solution of voltage stability problem is demonstrated [7]. Fuzzy set theory is a very powerful tool to model uncertainty and to incorporate human experience and heuristics [8]-[13]. A fuzzy set based reasoning approach for contingency ranking is developed using line flows and bus voltage deviations as post contingency quantities to achieve desired contingency list [14].

Line outage often causes blackouts due to voltage collapse. This signifies that reduction in loadability margin under each line outage condition should be given due attention in the ranking process. Voltage Stability margin of the system on occurrence of specific contingency gives good information about the severity of the contingency of the system. Though, the system pre- contingency operating point may be away from the voltage collapse point, contingency will push the system close to proximity to voltage collapse point. Hence, computation of voltage stability margin at this operating point serves as a good indicator of criticality of contingency. The changes in voltage stability margin are computed using static voltage collapse proximity indicator. This paper uses L index as Voltage Collapse Proximity Indicator to rank line outage contingencies. Fuzzy approach is used to combine the effect of voltage collapse proximity indicator and bus voltages to effectively rank the line outage contingencies. The bus voltage profiles and L index are expressed in fuzzy set notation before they are processed by the fuzzy reasoning rules. The severity indices are also divided into different categories based on extensive off-line analysis. The fuzzy rules are used to evaluate the severity of each post contingent quantity. The severity of a contingency is determined by evaluating composite index, which is the summation of severity index of L index and severity of bus voltage profiles. The Fuzzy inference structure FIS is tested in MATLAB 7 Fuzzy Toolbox. The proposed approach is tested under simulated condition on IEEE-30 bus system.

II. L INDEX

L - Index is widely used Voltage Collapse Proximity Indicator for various studies. Among the various indices for voltage-

stability and voltage collapse prediction, the L

index gives fairly consistent results. This is an accurate indicator and is easily computed [15].

A. Mathematical Formulation

Consider a system where n is the total number of buses, with 1, 2, ...g generator buses, and g+1, g+2 g+s SVC buses, g+s+1,.n, the remaining (n-g-s) buses. For a given system operating condition, using the load-flow results, the voltage-stability L - index is computed as,

Where j = g +1,....,n and all the terms within the sigma on the right hand side are complex quantities. The values of Fji are complex and are obtained from the network Y-bus matrix. For a given operating condition, Where IG, IL, VG, and VL represent complex current, voltage vectors at the generator nodes and load nodes. [YGG], [YGL], [YLL] and [YLG] are corresponding partitioned portions of the network Y-bus matrix.

Rearranging, we obtain

For stability, the index L j must not be violated (maximum limit = 1) for any node j. Hence, the global indicator L describing the stability of the complete subsystem is given by L= maximum of L j, for all j load buses. An L index value away from 1 and close to 0 indicates improved system security. For an unloaded system with generator/load buses voltage at 1.00 p.u. the L indices for load buses are closest to zero, indicating that the system has maximum stability margin. For a given network, as the load/generation increases, the voltage magnitude and angles change near maximum power-transfer condition and the voltage-stability index L j values for load buses tend to close to unity, indicating that the system is close to voltage collapse. While the different methods give a general picture of the proximity of the system voltage collapse, the L index gives a scalar number to each load bus. The L indices for given load condition are computed for all the load buses. The maximum of the L-indices gives the proximity of the system to voltage collapse.

III. FUZZY APPROACH TO CONTINGENCY RANKING

Fuzzy logic provides an excellent framework to effectively model uncertainty in human reasoning with the use of linguistic variables with membership function. The use of fuzzy logic is increasing in the power systems problems, as it is an intelligent processing. Many promising applications have been reported in the broad fields of system control, optimization, diagnosis, information processing, decision support, system analysis

and planning. In modern power systems, voltage alone cannot be used for assessing voltage security. Due to increased use of compensating devices which raise voltage to normal levels even when adequate reactive support is lacking, voltage becomes a poor indicator of security. The fuzzy approach uses L index as post contingent quantity in addition to bus voltage profiles to evaluate contingency ranking. The bus voltage profiles and L index are expressed in fuzzy set notation before they are processed by the fuzzy reasoning rules.

quantity. The severity of a contingency is determined by evaluating composite index, which is the summation of severity index of L index and severity of bus voltage profiles. The Fuzzy inference structure FIS is tested in MATLAB 7 Fuzzy Toolbox.

A. Bus Voltage Profiles

The post contingent bus voltage profiles are divided into Where IG, IL, VG, and VL represent complex current, voltage vectors at the generator nodes and load nodes. [YGG], [YGL], [YLL] and [YLG] are corresponding partitioned portions of the network Y-bus matrix.describing bus voltage profile shown in Fig. 1.

IV. L INDEX

The post contingent L index are divided into five categories using fuzzy set notation; very small (VS), 0- 0.18; small (S), 0.24-0.36; medium (M), 0.42-0.56; high (H), 0.62-0.76; very high (VH) 0.82-1.0. Each category represents a severity class of the L index. The boundaries of these categories are fuzzified based on extensive off- line analysis. Fig. 2 shows the membership function of L index.

The fuzzy rules used for evaluation of severity index of bus voltage profiles and L index are given in the following Table 1. Centre of area or gravity method is used for defuzzification.

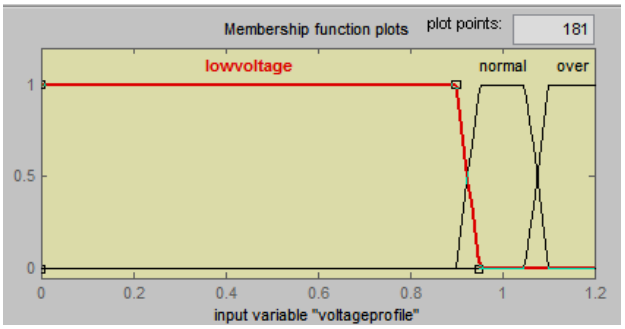

Fig. 1. Membership function for 3 linguistic variables of bus voltage profiles

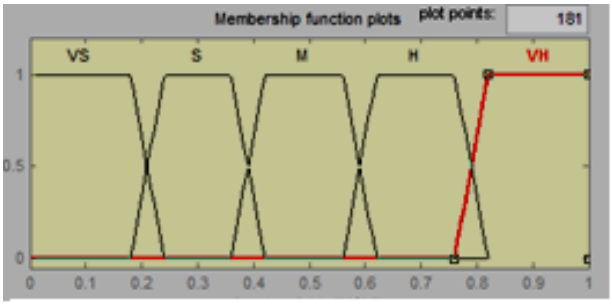

Fig. 2. Membership function for 5 linguistic variables of L index

A. *Severity Index of Post Contingent Quantities*

The output membership functions used to evaluate the severity of bus voltage profile are also divided into three categories using fuzzy set notation. As the linguistic variables are imprecise, each linguistic variable covers a range rather than a single severity index. The boundaries of these categories are fuzzified based on extensive off- line analysis. Trapezoidal membership function is used for describing a linguistic variable.

The output membership functions used to evaluate the severity of L index are divided into five categories using fuzzy set notation. Trapezoidal membership function is used for describing a linguistic variable. The overall severity index (composite index) for a particular line outage is given by CI = SIL + SIVP ; Where, SIL is the severity index of L index for a particular line outage and SIVP is the sum of severity index of all bus voltage profiles for a particular line outage. Thus, the overall severity index indicates the actual severity of the system for a contingency.

V. BLOCK DIAGRAM EXPLANATION

Power demand controller is a current controlling device. This is to be kept in each and every house. The power from energy meter is given to the controller and the output of controller is provided to home loads.

VI. METHODOLOGY

The major steps involved in this approach for contingency ranking is as follows

a) For the given system, considering a line outage at a time, load flow study is performed to determine bus voltage profiles. b) L index is computed using (1) and is used as post contingent quantity. c) Assuming trapezoidal membership function, the bus voltage profiles and L index are represented in fuzzy set notation. d) Severity index of L index and bus voltage profiles are also represented in fuzzy set notation. e) Using Fuzzy-If-Then rules overall severity index for bus voltage profiles and L index is determined. The Fuzzy Inference System is tested in MATLAB 7 Fuzzy Toolbox. f) Composite index is found using the formula CI = SIL + SIVP g) The above procedure is repeated for all the line outages and the contingencies are ranked based on composite index.

Post contingent quantity	Severity index
L index: VS S M H VH	VLS LS BS AS MS
Voltage : LV NV OV	MS BS AS

Fig. 3. Fuzzy Rules

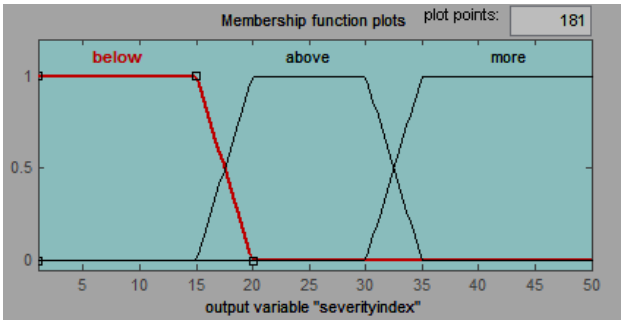

Fig. 4. Membership function for severity index of bus voltage profile

VII. TEST RESULTS

The proposed approach is tested under simulated condition on IEEE-30 bus system. A.C load flow is carried out to select the heavily loaded lines based on Voltage Collapse Proximity Indicator. The IEEE-30 bus system consists of 6 generators, 2 shunt capacitors and 41 transmission lines. Contingency screening is carried out to identify all the heavily loaded lines. On contingency screening total 13 transmission line outages are considered for ranking. The line outages considered for ranking are listed in Table 2.

Simulations were carried out to compute L index and bus voltage profiles for all the contingencies listed in the Table 2. Table 3 and 4 shows the ranking using Fuzzy approach for 100% and 140% load. Fuzzy approach effectively ranks contingencies under different load conditions. Table 5 shows the ranking based on L index and Minimum Singular Value of load flow Jacobian matrix [16] using Fuzzy approach.

From the above results, it can be observed that the contingency ranking obtained using L index and MSV is in close agreement with each other. The proposed fuzzy based composite index is accurate in ranking the contingencies. The contingencies ranked using this index provides very

Contingency no.	Type of contingency	From bus	To bus
1	SLO	1	2
2	SLO	1	3
3	SLO	3	4
4	SLO	2	6
5	SLO	4	6
6	DLO	1	3
		2	4
7	DLO	2	4
		2	5
8	DLO	2	4
		3	4
9	DLO	3	4
		2	5
10	DLO	2	5
		2	6
11	DLO	2	6
		4	6
12	DLO	4	6
		5	7
13	DLO	4	6
		6	7

Fig. 5. List of Line Outage Contingencies in IEEE 30 bus system

Line outages	$SI_{V(SUM)}$	SI_L	CI	Rank
1-2	189.08	31.90	220.98	1
1-3	188.88	14.63	203.51	7
3-4	189.32	11.70	201.02	9
2-6	190.55	6.21	196.76	13
4-6	190.58	9.60	200.18	11
1-3,2-4	184.14	21.10	205.24	5
2-4,2-5	186.45	20.30	206.75	4
2-4,3-4	184.94	20.20	205.14	6
3-4,2-5	185.73	22.40	208.13	3
2-5,2-6	185.06	23.90	208.96	2
2-6,4-6	183.71	19.40	203.11	8
4-6,5-7	191.01	19.90	200.91	10
4-6,6-7	186.45	12.90	199.35	12

Fig. 6. 3 Contingency Ranking Based on L index using Fuzzy Approach: 100 % load

useful information about the impact of the contingency on the system as a whole and helps in taking necessary control measures to reduce the severity of the contingency avoiding possible voltage collapse. The fuzzy approach is very effective in modelling imprecision and uncertainty in power system. Thus, fuzzy reasoning mimics experienced human operator judgement. Fuzzy approach for contingency ranking will serve as a powerful tool for power system operator to foresee the possible occurrence of voltage collapse and initiate appropriate action.

VIII. CONCLUSIONS

Fuzzy approach is used for combining the effect of L index with bus voltage profiles for ranking the contingencies. Fuzzy approach effectively ranks contingencies under different load conditions. The Fuzzy approach is flexible in incorporating human experience and heuristics. It includes the imprecision of linguistic terms associated with voltages and L index translates them into numerical values, which offers more flexibility, better insight into reality than conventional methods. Through proper tuning of membership functions in fuzzy representation, the approach can mimic experienced operators performance in conducting contingency ranking.

REFERENCES

[1] F. Albuyeh, A. Bose and B.Heath *Reactive Power Considerations in Automatic Contingency Selection, IEEE Transactions On Power Apparatus and Systems,*Vol. PAS-101, No. 1, pp.107- 112, January 1982.

[2]].S. Vemuri and R. E. Usher, *On-line Automatic Contingency Selection Algorithms, IEEE Transaction on Power Apparatus and Systems,* ,Vol. PAS-102, pp.346-354, February 1983.

[3]]. D. G. Taylor and L.J. Maahs, *A reactive contingency analysis algorithm using MW and MVAR distribution factors, IEEE Transactions on Power Systems,*Vol. 6, No. 1, pp. 349-355, February 1991.

[4] G.C. Ejebe, G.D. Irissari, S. Mokhtari, O. Obadina, P. Ristanovic, J. Tong, *Methods for Contingency Screening and Ranking for Voltage Stability Analysis of Power Systems, IEEE Transactions on Power Systems*Vol. 11, No. 1, pp. 350-356, February 1996.

Bridgeless SEPIC Converter With a Ripple-Free Input Current

V.Balaji
Asst Professor
Department of Electrical and Electronics Engineering
st.anne's college of engineering and technology

***Abstract*—AbstractConventional power factor correction (PFC) single- ended primary inductor converter (SEPIC) suffers from high con- duction loss at the input bridge diode. To solve this problem, a bridgeless SEPIC converter with ripple-free input current is pro- posed. In the proposed converter, the input bridge diode is removed and the conduction loss is reduced. In addition, the input current ripple is significantly reduced by utilizing an additional winding of the input inductor and an auxiliary capacitor. Similar to the con- ventional PFC SEPIC converter, the input current in a switching period is proportional to the input voltage and near unity power is achieved. The operational principles, steady-state analysis, and design equations of the proposed converter are described in detail. Experimental results from a 130 W prototype at a constant switch- ing frequency of 100 kHz are presented to verify the performance of the proposed converter.**

Index TermsBridgeless converter, coupled inductor, power factor correction (PFC), single-ended primary inductor converter (SEPIC).

I. INTRODUCTION

CCORDING to the demand on high efficiency and low harmonic pollution, the active power factor correction (PFC) circuits are commonly employed in acdc converters and switched-mode power supplies. Generally, these kinds of converters include a full-bridge diode rectifier on an input current path so that conduction losses on the full-bridge diode occur and it will be worse especially at the low line. To overcome this problem, bridgeless converters have recently been introduced to reduce or eliminate the full-bridge rectifier, and hence their conduction losses [1][13]. A bridgeless boost converter is widely used in advantages of reduced input current ripple, but its output voltage should be higher than the peak voltage of the input voltage [1][6]. Relatively low output voltage of PFC converters is required in many applications such as low-voltage switched-mode power supplies. PFC buck converters are more suitable for these ap- plications due to their low output voltage. A bridgeless buck converter was proposed in [7] and [8]. Like conventional PFC buck converters, the output voltage of the converter proposed in [7] and [8] is lower than the peak value of the input voltage.

However, since the input current of the PFC buck converter has dead angles during the time intervals when the input voltage is lower than the output voltage, there is a strong tradeoff be- tween power factor and output voltage selection. On the other hand, a SEPIC PFC converter can provide a high power factor regardless its output voltage due to its step up/down function. In [9][13], several bridgeless single-ended primary inductor converters (SEPICs) were proposed. The efficiency of these converters is improved by removing the input bridge diode. However, bulk input inductor or another LC filter is required to suppress the input current ripple. In Fig. 1, a bridgeless SEPIC PFC converter suggested in [11] is shown. The component count is reduced and it shows high efficiency due to the absence of the full-bridge diode. However, in this converter, an input inductor with large inductance should be used in order to reduce the input current ripple. In addition, the conduction losses on intrinsic body diodes of the switches are caused by using single pulse width modulation (PWM) gate signal. In order to overcome these problems, a bridgeless SEPIC converter with ripple-free input current is proposed in Fig. 2. An auxiliary circuit, which consists of an additional winding of the input inductor, an auxiliary small inductor, and a capacitor, is utilized to reduce the input current ripple. Coupled inductors are

often used to reduce current ripple [14][18]. The shaded area in Fig. 2 represents the auxiliary circuit for achieving the input

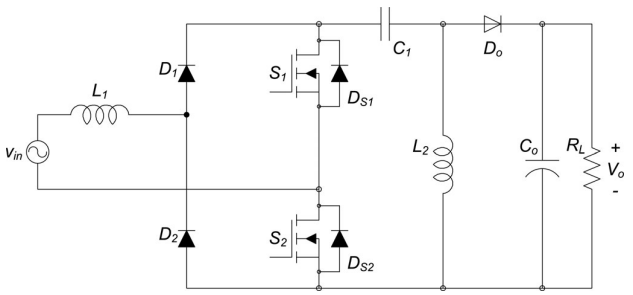

Fig. 1. Bridgeless SEPIC PFC converter in [11].

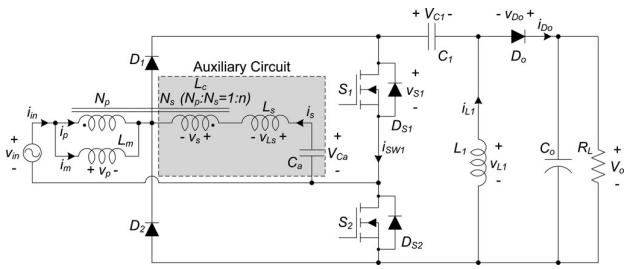

Fig. 2. Proposed bridgeless SEPIC converter.

current ripple cancellation. Fig. 3(b) shows the proposed gate signals for the switches. For a half period of the input voltage, one switch is continuously turned ON and the current via an intrinsic body diode is forced to flow through the channel of the switch. It can reduce the conduction loss on the switch further and the efficiency can be improved.

II. ANALYSIS OF THE PROPOSED CONVERTER

Fig. 2 shows the circuit diagram of the proposed bridgeless SEPIC converter with ripple-free input current. The auxiliary circuit includes an additional winding Ns of the input inductor Lc , an auxiliary inductor Ls , and a capacitor Ca . The coupled inductor Lc is modeled as a magnetizing inductance Lm and an ideal transformer which has a turn ratio of 1:n (n = Ns /Np). The leakage inductance of the coupled inductor Lc is included in the auxiliary inductor Ls . The capacitance of Ca is large enough, so Ca can be considered as a voltage source VCa during a switching period. Since the average inductor voltage should be zero at a steady state according to the volt-second balance law, the average capacitor voltage VCa is equal to the input voltage vin during a switching period. Similarly, the average capacitor voltage VC 1 is equal to vin . Diodes D1 and D2 are the input rectifiers and operate like a conventional SEPIC PFC converter. DS1 and DS2 are the intrinsic body diodes of the switches S1 and S2 . The switches S1 and S2 are operated with the proposed gate so the output diode Do is turned OFF before the main switch is turned ON. The capacitance of the output capacitor Co is as- sumed sufficiently large enough to consider the output voltage Vo as constant. Also, the input voltage is assumed constant and equal to Vin in a switching period Ts . The theoretical waveforms of the proposed converter are shown in Fig. 4. The magnetizing current im varies from its maximum value Im 1 to its minimum value Im 2 . The inductor current is varies from its maximum value Is1 to its minimum value Is2 . The operation of the proposed converter in one switching period Ts can be divided into three modes. Fig. 5 shows the operating modes in the positive input voltage. Before t0 , the switch S1 and the diode Do are turned OFF and the switch S2 is conducting. The input current is the sum of the freewheeling currents Is2 and IL 2 . Mode 1 [t0 , t1]: At t0 , the switch S1 is turned ON and the switch S2 is still conducting. Since the voltage vp across Lm is Vin , the magnetizing current im increases from its minimum value Im 2 linearly with a slope of Vin /Lm as follows:

so the output diode Do is turned OFF before the main switch is turned ON. The capacitance of the output capacitor Co is assumed sufficiently large enough to consider the output voltage Vo as constant. Also, the input voltage is assumed constant and equal to Vin in a switching period Ts . The theoretical waveforms of the proposed converter are shown in Fig. 4. The magnetizing current im varies from its maximum value Im 1 to its minimum value Im 2 . The inductor current is varies from its maximum value Is1 to its minimum value Is2 . The operation of the pro- posed converter in one switching period Ts can be divided into three modes. Fig. 5 shows the

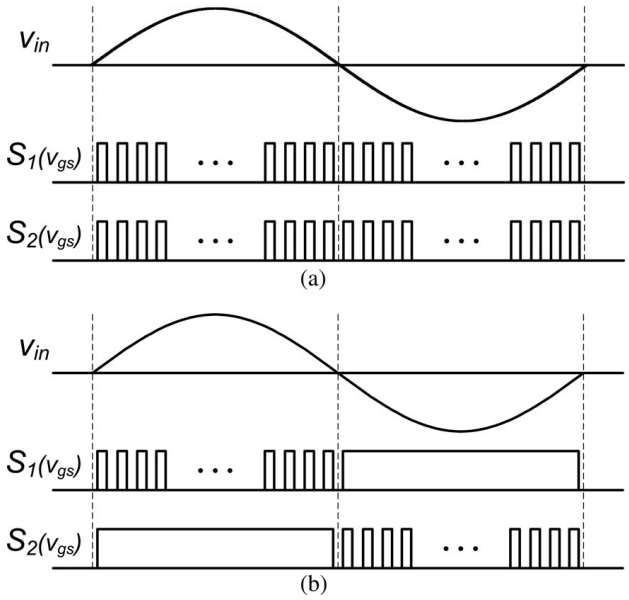

Fig. 3. Gate driving signals. (a) Same gate signals for S1 and S2 . (b) Proposed gate signals for S1 and S2

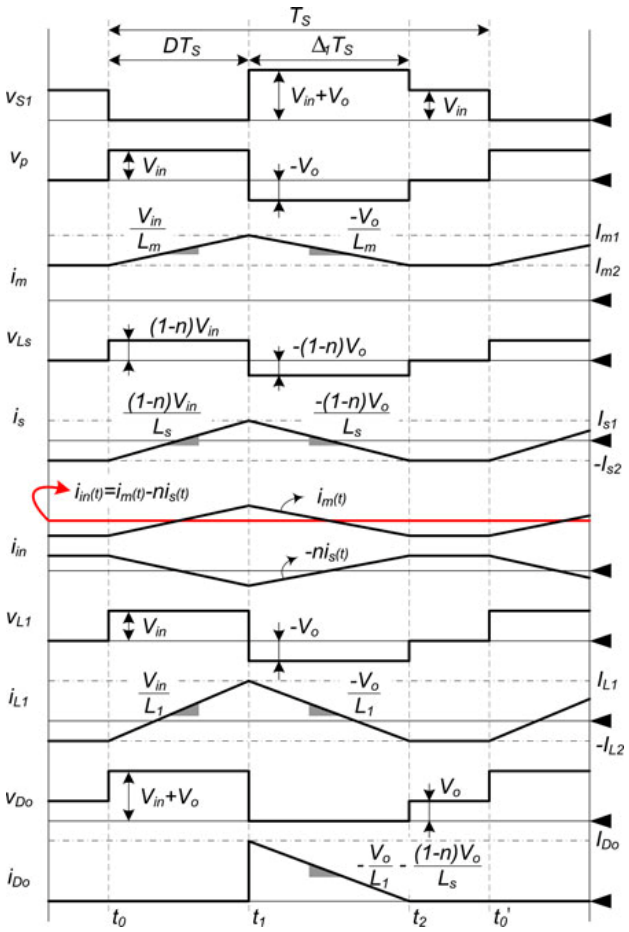

Fig. 4. Gate driving signals. (a) Same gate signals for S1 and S2 . (b) Proposed gate signals for S1 and S2

operating modes in the positive input voltage. Before t0 , the switch S1 and the diode Do are turned OFF and the switch S2 is conducting. The input current is the sum of the freewheeling currents Is2 and IL 2 . Mode 1 [t0 , t1]: At t0 , the switch S1 is turned ON and the switch S2 is still conducting. Since the voltage vp across Lm is Vin , the magnetizing current im increases from its minimum value Im 2 linearly with a slope of Vin /Lm as follows:

III. DESIGN PROCEDURE

A. DESIGN PROCEDURE

Design specifications of the proposed converter are as follows: 1) main voltage range: Vin = 90 Vac 130 Vac ; 2) line frequency: fL = 60 Hz; 3) DC output voltage: Vo = 100 V; 4) maximum output power: Pou t = 130 W; 5) maximum 2fL output ripple: Vo = 6 Vpe a k -pe a k ; 6) switching frequency: fsw = 100 kHz.

$$\overline{L}$$

$$i_m(t) = I_{m2} + \quad (t - t_0). \qquad (1)$$

Fig. 5.

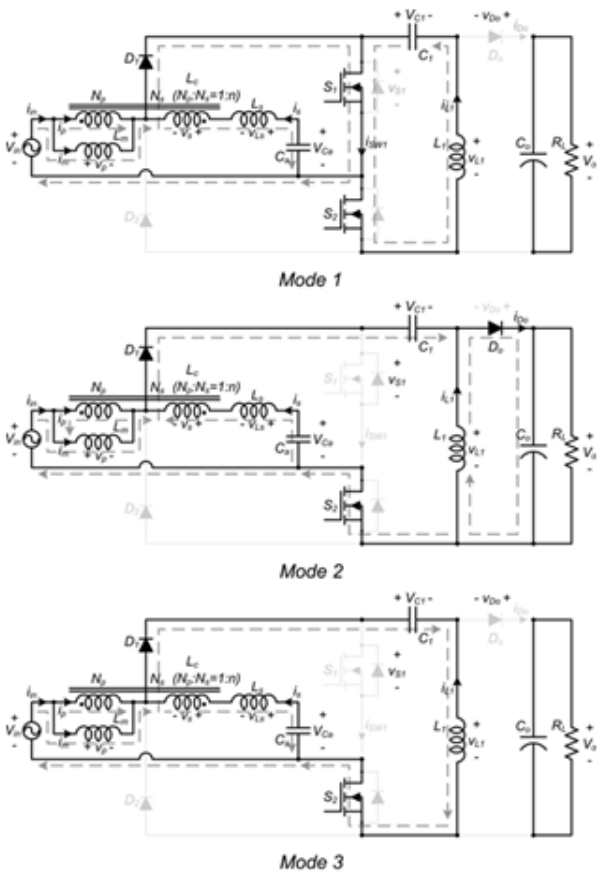

Fig. 6. Operating modes.

B. Input Current

Maximum input current is calculated by the output power and efficiency of the converter as follows:

C. Output Current

The output current in a switching period is equal to the average of the current iDo . From Fig. 4, the output current in Ts is obtained

D. Conditions of Operating in DCM

In order to guarantee the proposed converter to operate in DCM, the inequality of 1 ¡ 1 D must be satisfied. From (9), the duty cycle D is obtained as following inequality:

IV. OUTPUT CAPACITOR

As the output ripple frequency is two times the input line frequency fL , the output capacitor Co must be large enough to minimize the output voltage ripple Vo . Therefore, Co can be obtained from the following equation:

A. Input Voltage Detecting Circuit

In order to reduce the conduction losses by forcing the reverse current of the switches to flow via channel, the input voltage detecting circuit is used. Fig. 6 shows the block diagram of the detection circuit. By using comparators, the sign of the input voltage is detected. Optical couplers are utilized for electrical isolation. Logic gates are employed to make one of the switches conduct continuously and the other operate with PWM signal .

Since $i_{in} = i_m + i_p = i_m - ni_s$ from Fig. 2, the input current i_{in} can be written as follows:

$$i_{in}(t) = I_{m2} + nI_{s2} + \frac{V_{in}}{L_m} - \frac{n(1-n)V_{in}}{L_s} \quad (t - t_0). \quad (3)$$

From (3), the input current ripple can be canceled out and i_{in} can be constant as $I_{m2} + nI_{s2}$ by satisfying the following condition:

$$L_s = n(1-n)L_m \ . \qquad (4)$$

Mode 2 [t_1, t_2]: At t_1 , the switch S_1 is turned OFF and the switch S_2 is still conducting. Since the voltage v_p across L_m is $-V_o$, the magnetizing current i_m decreases from its maximum value I_{m1} linearly with a slope of $-V_o$ /L_m as follows:

$$i_m(t) = I_{m1} - \frac{V_o}{L_m}(t - t_1). \qquad (5)$$

The voltage v_{Ls} across L_s is $-(1-n)V_o$, so that the current i_s decreases from its maximum value I_{s1} linearly with a slope of $-(1-n)V_o$ /L_s as follows:

Fig. 7.

B. Efficiency Improvement

To verify the efficiency improvement of the proposed converter, power dissipation of the reduced components is theoretically calculated with the assumption that the forward voltage is ignored due to the very small RDS (o n) . If the turn ratio n = 0.7 and the magnetizing inductance Lm = 600 H, the maximum value of L1 can be obtained by (19)

At first, the case when the same gate signals in Fig. 3(a) are applied to the switches is considered. When the both switches are turned ON, one diode of rectifier is omitted in the input current path. When the both switches are turned OFF, one of the the average power dissipation, which is saved during a line From the ripple-free condition of (4), the auxiliary inductor Ls = 127 H is obtained.

From (5) and (6), the input current i_{in} can be written as follows:

$$i_{in}(t) = I_{m1} - nI_{s1} + \left(-\frac{V_o}{L_m} + \frac{n(1-n)V_o}{L_s}\right)(t - t_1). \quad (7)$$

With the ripple-free condition of(4), the input current ripple in this mode can be canceled out and i_{in} can be constant as $I_{m1} - nI_{s1}$.

Mode 3 [t_2, t_0]: At t_2, the current i_{Do} becomes zero, and the diode D_o is turned OFF. Since $i_{in} = i_m - ni_s = -i_s - i_{L1}$ in this mode, the input current i_{in} is the sum of freewheeling currents I_{s2} and I_{L2} as follows:

$$I_{in} = I_{m2} + nI_{s2} = I_{s2} + I_{L2}. \quad (8)$$

Since the average voltage across L_m should be zero under a steady state, the timeratio Δ_1 is obtained by

$$\Delta_1 = \frac{V_o}{V_{in}} D \quad (9)$$

where D is the duty cycle.

In a switching period T_s, the maximum current of each inductor is rewritten as follows:

$$I_{m1} = I_{m2} + \frac{V_o}{L_m}\Delta_1 T_s \quad (10)$$

$$I_{s1} = -I_{s2} + \frac{(1-n)V_o}{L_s}\Delta_1 T_s \quad (11)$$

$$I_{L1} = -I_{L2} + \frac{V_o}{L_1}\Delta_1 T_s \quad (12)$$

From (8), (9), (11), and (12) the maximum current of the output diode I_{Do} can be obtained by

$$I_{Do} = I_{in} + I_{s1} + I_{L1} = \left(\frac{1}{L_s} + \frac{1}{L_1}\right) V_{in} D T_s. \quad (13)$$

Fig. 8.

$$I_{in} = I_{in,peak}\sin(\omega t) = \frac{2P_o}{\eta V_{in,peak}}\sin(\omega t). \quad (14)$$

Fig. 9.

V. Maximum Ratings of Switching Devices

In this converter, the voltage stresses of all switching devices are equal to the sum of the maximum input voltage and output

$$i_{Do,avg} = \frac{1}{2} I_{Do}\Delta_1. \quad (15)$$

By substituting (9) and (13) into (15), the output current can be rewritten by

$$i_{Do,avg} = \frac{1}{2}\left(\frac{1}{L_1} + \frac{1}{L_s}\right)\frac{V_{in}^2}{V_o} D T_s. \quad (16)$$

The average output current in one half of the line cycle is obtained by (4) and (16) as follows:

$$\frac{1}{\pi}\int_0^{\pi} i_{Do,avg}\, d\omega t = \frac{1}{4}\left(\frac{1}{L_1} + \frac{1}{nL_m}\right) D T_s - \frac{V_{in,peak}^2}{4L_e V_o}. \quad (17)$$

where $L_e = nL_1 L_m/(L_1 + nL_m)$.

Fig. 10.

$$D < \frac{V_o}{V_{in,peak} + V_o}. \quad (18)$$

When the input voltage $v_{in} = 90$ V_{ac}, D must be smaller than 0.44 for operating in DCM.

Using (17) and (18), the maximum value of L_e is calculated as follows:

$$L_e < \frac{V_{in,peak}^2 D}{4V_o I_{o,avg} f_{sw}}. \quad (19)$$

If the turn ratio $n = 0.7$ and the magnetizing inductance $L_m = 600\ \mu$H, the maximum value of L_1 can be obtained by (19)

$$L_1 < \frac{nL_m \times L_e}{nL_m - L_e}$$

From the ripple-free condition of (4), the auxiliary inductor $L_s = 127\ \mu$H is obtained.

Fig. 11.

$$C_o = \frac{P_o}{4f_L V_o \Delta V_o} = 902\ \mu\text{F}. \quad (21)$$

Fig. 12.

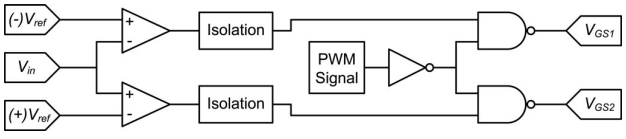

Fig. 13. Input voltage detecting circuit block diagram.

In the case when the proposed gate signals in Fig. 3(b) are applied to the converter, one diode of a rectifier, including the intrinsic body diode, is omitted in a switching period. So, the efficiency improvement of the proposed converter is obtained.

VI. SIMULATION RESULTS

The proposed converter is simulated by PSpice with the spec- ifications and parameters as follows: vin = 130 Vac , fL = 60 Hz, fsw = 100 kHz, D = 0.25, Lm = 600 H, n = 0.7, Ls = 127 H, L1 = 63 H, Ca = 0.3 F, C1 = 0.4 F, Co = 880 F, and RL = 77 . Fig. 7(a) shows the input voltage and current at full load. The input current is a perfect replica of the input voltage and is exactly in phase with that. Fig. 7(b) shows vs1 , iin , is , and iDo at positive input voltage. It is clear that the input current ripple is completely removed by utilizing a coupled inductor which has a small magnetizing inductance. And because of operating in DCM, the output diode Do is turned OFF under zero-current switching condition.

$$V_{D\ max} = V_{SW\ max} = V_{in\ peak} + V_o = 284\,\text{V}. \quad (22)$$

From (13) and (17), the maximum stresses $I_{D,\max}$ and $I_{sw,\max}$ of the diodes and switches are given by

$$I_{D\ max} = I_{SW\ max} = \frac{1}{L_s} + \frac{n}{L_1} \sqrt{\frac{4P_o L_e}{f_{sw}}} = 4.41\ \text{A}. \quad (23)$$

Fig. 14. Input voltage detecting circuit block diagram.

$$P_{D,\,avg} = \frac{1}{T}\int_0^T 2V_D I_D D\,dt = 0.62\,\text{W} \quad (24)$$

where $T = \pi$, $V_D = 0.5$ V, $I_D = 2.27\sin(\omega)$, and $D = 0.428$. Thus, the efficiency improvement of the proposed converter with the same gate signals shown in Fig. 3(a) at $v_{in} = 90$ V_{ac} and 130-W load can be calculated by

$$\Delta\eta_{conventional} = \frac{P_{D,avg}}{130} = 0.48\%. \quad (25)$$

Fig. 15. Input voltage detecting circuit block diagram.

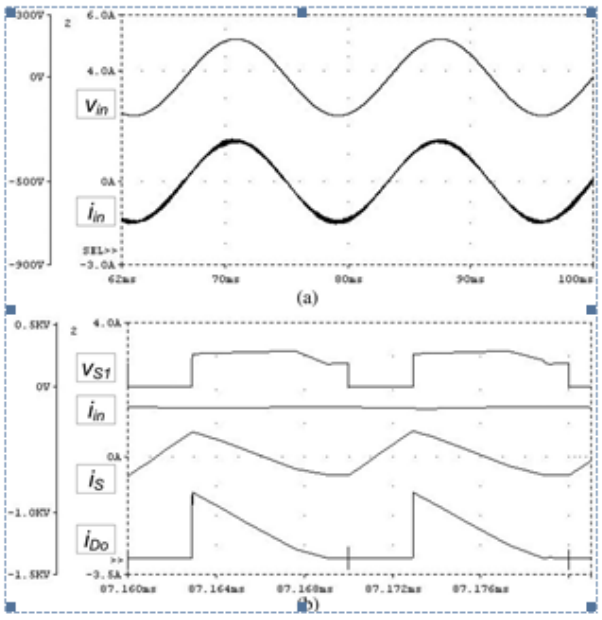

Fig. 16. vS1 , iin , iS , and vDo .

The prototype of the proposed converter is implemented with the same specifications of the simulation in order to verify the theoretical analysis and simulation results. The switching devices, IRFPS43N50K for switches and RF2001T3D for all diodes, are used in this converter. The control circuit is implemented with a constant frequency pulse width modulation controller KA7552 from Fairchild. The controller power consumption is not considered in the laboratory prototype. For the magnetic devices, ferrite EI Core EI3329S from SAMHWA Electronics and Litz wire (32/0.12) are used.

Fig. 8(a)shows the experimental results of the input voltage and current at full load. The phase of the input current is similar to the one of the input voltage and its shape is fully sinusoidal so that a unity power factor is achieved. The experimental wave- forms vs1 , iin , is , and iDo during a few switching periods are shown in Fig. 8(b). The input current ripple is almost removed and the current iDo falls to zero that is alleviating reverse- recovery problem of the output diode Do . Fig. 9(a) shows the gate-source voltages of S1 and S2 according to the input volt- age. For a half period of the input voltage, the switch S1 or

S2 is continuously turned ON and its drain-source voltages are measured as shown in Fig. 9(b). Fig. 10(a) shows the measured efficiency of the conventional SEPIC PFC converter and the proposed SEPIC converter at full load 130 W. In this

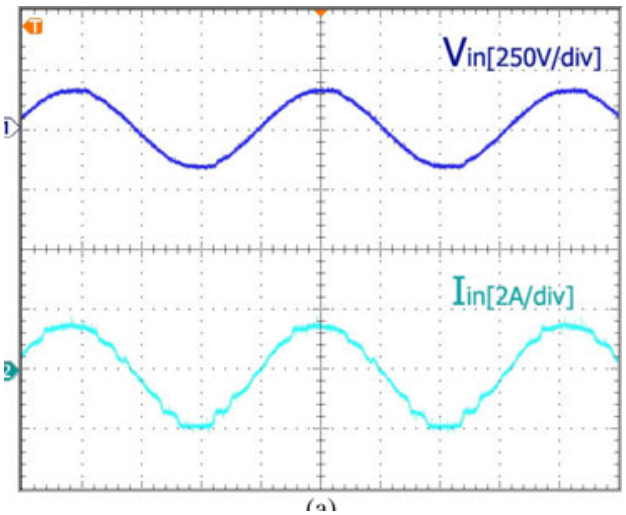

Fig. 17. vin

figure, the efficiency of the proposed converter is improved approximately maximum 190 Vac , compared with the conventional SEPIC PFC converter. The power factor is measured more than 0.995 in both convert- ers as shown in Fig. 10(b). In addition, Fig. 10(c) shows the measured efficiency of the

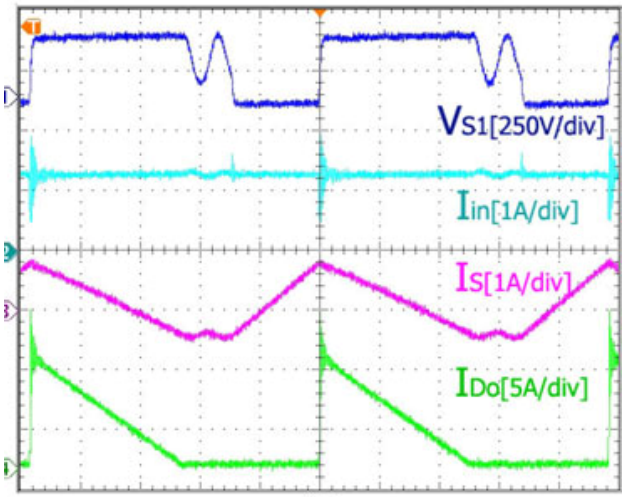

(b)

Fig. 18. vS1 , iin , iS

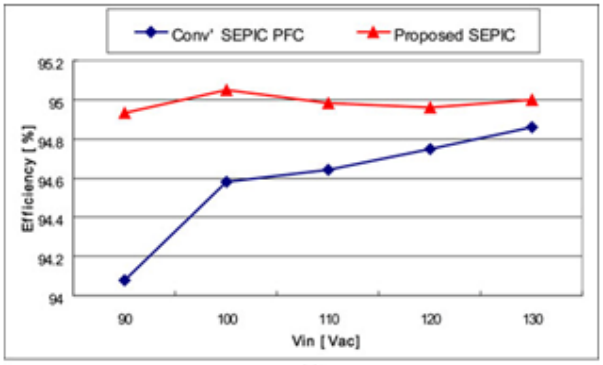

(a)

Fig. 19.) Measured efficiency at load = 130 W.

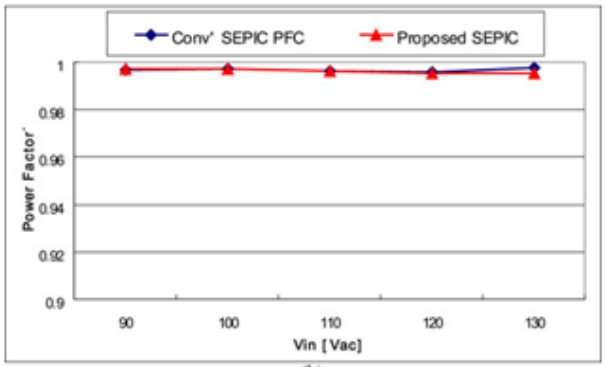

(b)

Fig. 20. Measured power factor at load = 130 W

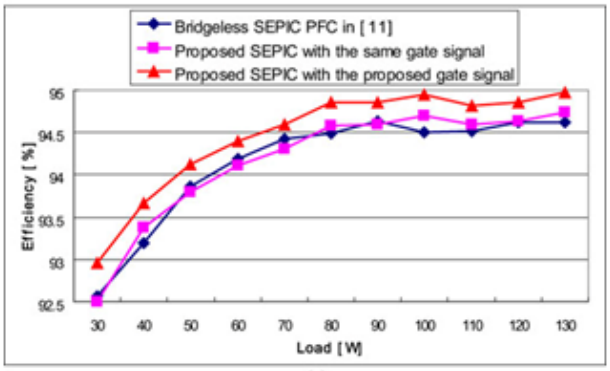

(c)

Fig. 21. Measured efficiency at vin = 100 Vac

bridgeless SEPIC PFC in [11] and the proposed converter at vin = 100 Vac . When the same gate signals in Fig. 3(a) are applied to the switches, the efficiency of the proposed converter is similar to that of the converter in [11]. When the proposed gate signals as shown in Fig. 3(b) are applied to the switches, the efficiency is improved by 0.45% compared with the converter in [11]. Fig. 11 shows the photograph of the prototype.

VIII. CONCLUSION

A bridgeless SEPIC converter with ripple-free input current has been proposed. In order to improve the efficiency, the input full-bridge diode is eliminated. With the proposed gate driving method, the efficiency is improved by 0.45%. In addition, the input current ripple of the proposed converter is significantly re- duced by utilizing an auxiliary circuit consisting of an additional winding of the input inductor, an auxiliary small inductor, and a capacitor. The major disadvantage of the proposed converter is that it has three magnetic components. The theoretical analysis, simulation results, and experimental results were provided.

REFERENCES

[1] W.-Y. Choi, J.-M. Kwon, E.-H. Kim, J.-J. Lee, and B.-H. Kwon, *Bridgeless boost rectifier with low conduction losses and reduced diode reverse-recovery problems, IEEE Trans. Ind. Electron.,*, vol. 54, no. 2, pp. 769780, Apr. 2007.

[2] L. Huber, Y. Jang, and M. M. Jovanovic, *Performance evaluation of bridgeless PFC boost rectifiers, IEEE Trans. Power Electron*vol. 23, no. 3, pp. 13811390, May 2008.

[3] Y. Jang and M. M. Jovanovic *A bridgeless PFC boost rectifier with optimized magnetic utilization,*IEEE Trans. Power Electron., vol. 24, no. 1, pp. 8593, Jan. 2009.

[4] J.-L. Kotny, X. Margueron, and N. Idir*High-frequency model of the coupled inductors used in EMI filters,*IEEE Trans. Power Electron., vol. 27, no. 6, pp. 28052812, Jun. 2012.

Home Automation Using Internet of Things

Vijayaragavan.M
Assistant Professor
Department of Electrical and Electronics Engineering
Mailam Engineering College,Mailam,Tamilnadu

Rajalakshmi.S
Assistant Professor
Department of Electrical and Electronics Engineering
Mailam Engineering College,Mailam,Tamilnadu

Azhagiya Manavalan.P
UG Scholar
Department of Electrical and Electronics Engineering
Mailam Engineering College,Mailam,Tamilnadu

***Abstract*—The main aim of the project is to develop a system that will provide remote control of home appliances and also provide security against the mishaps when the home host is not at home. This paper is mainly concerned with the automatic control of light or any other home appliances using internet. It is meant to save the electric power and human energy. This project is made with the help of controller and raspberry pi. The various appliances connected to the micro controller and sensor is connected using wireless network.**

Key Words: wireless Home automation System (WHAS), Internet of Things (IoT), Wi-Fi network, Microcontroller

I. INTRODUCTION

A. Overview

Homes of the 21st century will become more and more self -controlled and automated due to the comfort it provides, especially when employed in a private home. A home automation system is a means that allow users to control electric appliances of varying kind.

Many existing, well-established home automation systems are based on wired communication. This does not pose a problem until the system is planned well in advance and installed during the physical construction of the building. But for already existing buildings the implementation cost goes very high. In contrast, Wireless systems can be of great help for automation systems. With the advancement of wireless technologies such as Wi-Fi, cloud networks in the recent past, wireless systems are used every day and everywhere.

B. Advantages of Home automation systems over wired system

TIn recent years, wireless systems like Wi- Fi have become more and more common in home networking. Also in home and building automation systems, the use of wireless technologies gives several advantages that could not be achieved using a wired network only.

Reduced installation costs: First and foremost, installation costs are significantly reduced since no cabling is necessary. Wired solutions require cabling, where material as

well as the professional laying of cables (e.g. into walls) is expensive.

1. System scalability and easy extension: Deploying a wireless network is especially advantageous when, due to new or changed requirements, extension of the network necessary. In contrast to wired installations, in which cabling extension is tedious. This makes wireless installations a seminal investment. 2. Aesthetical benefits: Apart from covering a larger area, this attribute helps to full aesthetical requirements as well. Examples include representative buildings with all-glass architecture and historical buildings where design or conservatory reasons do not allow laying of cables.

3. Integration of mobile devices: With wireless networks, associating mobile devices such as PDAs and Smartphones with the automation system becomes possible everywhere and at any time, as a device's exact physical location is no longer crucial for a connection (as long as the device is in reach of the network).

For all these reasons, wireless technology is not only an attractive choice in renovation and refurbishment, but also for new installations.

II. RELATED WORK

[1] Sirsath N. S, Dhole P. S, Mohire N. P, Naik S. C Ratnaparkhi N.S

This paper proposes a Home Automation system that employs the integration of multi-touch mobile devices, cloud networking, wireless communication, and power-line communication to provide the user with remote control of various lights and appliances within their home. This system uses a consolidation of a mobile phone application, handheld wireless remote, and PC based program to provide a means of user interface to the consumer.

[2] Basil Hamed

The main objective of this Paper is to design and implement a control and monitor system for smart house. Smart house

system consists of many systems that controlled by LabVIEW software as the main controlling system in this paper. Also, the smart house system was

supported by remote control system as a sub controlling system. The system also is connected to the internet to monitor and control the house equipments from anywhere in the world using LabVIEW. [3] Deepali Javale, Mohd. Mohsin, Shreerang Nandanwar The prime objective of this paper is to assist handicapped/old aged people. It gives basic idea of how to

control various home appliances and provide a security using Android phone/tab. The design consists of home automation website, Raspberry pi B, ATMEGA8 microcontroller. User can interact with the website and send control signal to the Raspberry pi kit which in turn will control other embedded devices/sensors.

III. SYSTEM ANALYSIS

A. Problem Definition

Many people are always on the move from place to place due to business demands. Some people can spend a couple of days away from their home leaving all their household appliances without any kind of monitoring and control. Some devices are left plugged into power sockets whereas others are supposed to be plugged into and out of power sockets at different intervals depending on the time of the day. All this requires an individual to manually attend to each of the devices independently from time to time. All such monitoring and control can be done without necessarily being around or inside the home. Some devices if not controlled properly consume a lot of energy which leads to extra expenditure on electricity. Therefore we propose to design an internet based home automation system which will enable one to remotely manage his/her appliances from anywhere, anytime.

B. Proposed System Feature

As we enter the 21st century, the interaction between humans and computer is breaking old barriers and entering a new realm. In the highly technology driven world of todays mobile phones have become a part of our Lifestyles. Mobile phones are not just communication tool. Our project tries to derive solution providing better control on home appliance with help of cell phone. The Existing System consists of physical appliances in our home that are been controlled through switches. These devices can be switched ON OFF manually whenever needed. This system is less secured and prone to electrical hazards. Also the wastage of electricity tends to be a major factor of concern. The proposed project is conceived networking our mobile phone to all appliances via a smart logic circuit. The proposed system consists of Smart Logic Circuit connected to the appliances. Status of all home appliances could be controlled by user from remote location with help of users mobile phone.

IV. SYSTEM DESIGN AND IMPLEMENTATION

A. Proposed Home Automation System

The end user can use their mobile phone to log into the system. An initial check is performed for whether the hardware device is ON or not. Only if the Hardware is authorized and ON then the user is Authenticated. Once the authentication is done successfully the user is able to send the control signals to the Hardware machine. At the hardware machine the SL driver program will continuously track for the change in the status will accordingly send the signals to the Circuit. When a user select a change in the status for any of the device [i. e .. ON or Off], the data from the handheld is sent to the Web Server in a string format, where the Web site is hosted. On the server the status is stored in the database in their respective device field. At the Hardware end, the circuit drive program a web page is [retrieve.aspx] is used to retrieve the status of the devices in a timely pattern [every 10sec]. These changes come in to form of cookies [temporary internet files] from the webserver are stored on the computer in the name of the web site. Hence every 10 sec as the page refreshes the new cookie values are updated. The cookie values are read from the program using the VB component GETINERNETCOOKIE after a fixed delay. As the program receives any change in the Device values it send the control signal [binary data] accordingly to the required data pin of the parallel port.

B. Proposed Home Automation System Functions

The proposed home automation system has the capabilities to control the following components in users home and monitor the following alarms:

Temperature and humidity
Gas leakage detection
Control appliances

The proposed home automation system can control the following appliance:

Lights on/off/dim
Fan on/off
On/off different appliance
Leakage of gas

V. SOFTWARE DESIGN FRONT END DESIGN

HTML is a format that tells a computer how to display a web page. The documents themselves are plain text files with special "tags" or codes that a web browser uses to interpret and display information on your computer screen. HTML stands for Hyper Text Mark-up Language; an HTML file is a text file containing small mark -up tags. The mark-up tags tell the Web browser how to display the page. An HTML files must have an htm or html file extension. Database Storage: The gas sensor LM35 is placed in the kitchen to detect any gas leakage, if any leakage is detected the alarm in the hall is raised. Relay is used to switch the electrical appliances like light, fan etc. The

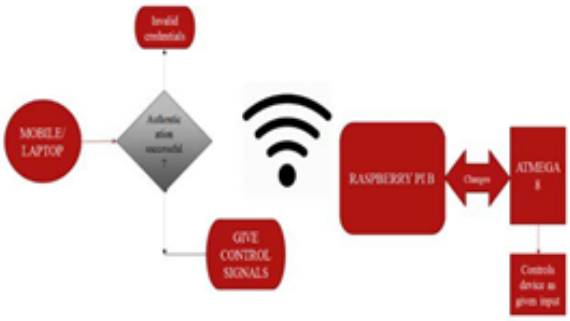

Fig. 1. Proposed model of Home automation system

Intel Galileo is placed in store room or garage. The Raspberry PI B is connected with WiFi or LAN for the connectivity with internet.

A. *Implementation Setup*

Figure 2 illustrates the sequence of activities in the WHAS. When the connection is established it will start reading the parameters of sensors like fan, tube light, gas sensor etc. The threshold levels for the required sensors are set as t1, t2, and t3 etc. The sensor data are sent to the web server and stored in the cloud. The data can be analysed anywhere any time. If the sensor parameters are greater than the threshold level then the respective alarm a1, a2, a3 etc. will be raised and the required actuation is done for the controlling of the parameters.

A model house is built for the home automation system and is as shown in the figure . Light 1 will turn on automatically when light sensor detects the darkness. A cooler/Fan will turn on when the room temperature exceeds the set threshold and in turn reduces the room temperature. The gas sensor LM35 is placed in the kitchen to detect any gas leakage, if any leakage is detected the alarm in the hall is raised. Relay is used to switch the electrical appliances like light, fan etc. The Intel Galileo is placed in store room or garage. The Raspberry PI B is connected with WiFi or LAN for the connectivity with internet.

VI. RESULTS

After the successful connection to the server, the data of sensor are sent to the web server for monitoring of the system. The figure 3 shows the web server page which will allow us to monitor and control the system. By entering the assigned URL address in the web browser this web server page will appear. The web server gives the information about the temperature in different places of the house. It also gives the status of the various electrical appliances like light, fan etc. which we can control remotely. Power demand controller is a current controlling device. This is to be kept in each and every house. The power from energy meter is given to the controller and the output of controller is provided to home loads.

. All the required data is stored in the database. The stored data can be analyzed at anytime and anywhere. The figure 4 shows the temperature in degree Celsius stored at different time intervals. And also it shows the state of the motion detector along with the time. It also provides information about time of motion detected and how many times as well. All this information is stored in the cloud which can be checked by the user any time when away from home.

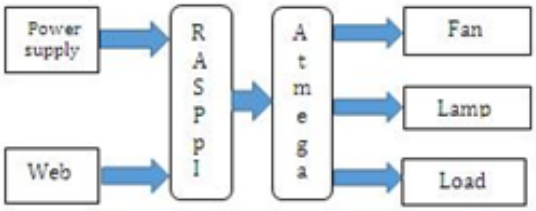

Fig. 2. sequence of activities in WHAS

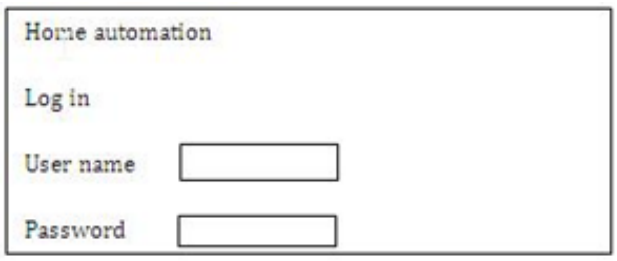

Fig. 3. Web server page

VII. CONCLUSION AND FUTURE WORK

A. *Conclusion*

The home automation using Internet of Things has been experimentally proven to work satisfactorily by connecting simple appliances to it and the appliances were successfully controlled remotely through internet. The designed system not only monitors the sensor data, like temperature, gas, light, motion sensors, but also actuates a process according to the requirement, for example switching on the light when it gets dark. It also stores the sensor parameters in the webpage (database) in a timely manner. This will help the user to analyze the condition of various parameters in the home anytime anywhere.

VIII. FUTURE WORK

Using this system as framework, the system can be expanded to include various other options which could include home security feature like capturing the photo of a person moving around the house and storing it onto the cloud. This will reduce the data storage than using the CCTV camera which will record all the time and stores it. The system can be expanded for energy monitoring, or weather stations. This kind of a system with respective changes can be implemented in the hospitals for disable people or in industries where human invasion is impossible or dangerous, and it can also be implemented for environmental monitoring.

IX. ACKNOWLEDGEMENT

We acknowledge the efforts and hard work by the experts who have contributed towards development of the different home automation systems.We take this opportunity to express our profound gratitude and deep ragards to our guide Prof.Amit kukreja and prof.Sagar Matre for his exemplary guidance ,monitoring and constant encouragement throughout the course of this project.

Fig. 4. Data base of the sensors data stored in the cloud

REFERENCES

[1] Sirsath N. S, Dhole P. S, Mohire N. P, Naik S. C Ratnaparkhi N.S*Department of Computer Engineering, 44, Vidyanagari, Parvati, Pune-411009, India University of Pune, Home Automation using Cloud Network and Mobile Devices*,Published 1925.

[2] Deepali Javale, Mohd. Mohsin, Shreerang Nandanwar *Home Automation and Security System Using Android ADK in International Journal of Electronics Communication and Computer Technology (IJECCT)* ,Volume 3 Issue 2 (March 2013).

[3] Charith Perera, Student Member, IEEE, Arkady Zaslavsky, Member, IEEE, Peter Christen, and Dimitrios Georgakopoulos, *Context Aware Computing for The Internet of Things: A Survey. IEEE COMMUNICATIONS SURVEYS TUTORIAL* Published 1925.

[4] S.P.Pande, Prof.Pravin Sen, *Review On: Home Automation System For Disabled People Using BCI in IOSR Journal of Computer Science* ,(IOSR-JCE) e- ISSN: 2278-0661, p-ISSN: 2278-8727 PP 76-80

[5] Basil Hamed, *Design Implementation of Smart House Control Using Lab VIEW at International Journal of Soft Computing and Engineering (IJSCE) ISSN: 2231-2307*,Volume-1, Issue-6, January 2012.

TIDAL POWER GENERATION THROUGH SIMPLE GEAR MECHANISM

V.Narmadha,
Asst.Prof/EEE
Department of Electrical and Electronics Engineering
St.Annes College of engineering and technology ,

***Abstract*—Now a days, the major problem existing in and out of the nation is power demand. So, the thermal and hydro sectors are in compulsion to meet the necessity of the public. The power generation can be achieved by two modes (Renewable and non-Renewable). The major drawback of using non-Renewable resources is causing pollution. Therefore, renewable resources like hydro, tidal, solar, wind, geo-thermal natural gas and bio-mass mechanism can be used as a source to generate power. The renewable resource makes the environment pollution free. So, our wish is to generate power from renewable resources. Our proposal is an alternative way for the production of power from tidal energy using crank mechanism. This technique consists of two major parts (floating plate and gear mechanism). The floating plate is placed over the sea. Depending upon the movement of waves, the floating plate moves up and down. Those mechanical motions are converted into mechanical rotation by using gear mechanism. That mechanical rotation is converted into electrical power with the help of generator.**

I. INTRODUCTION

Now a day, the big problem in our Nation is power demand. So, we need to generate a power from renewable or non- renewable resources. The Non-Renewable resource causes more pollution. So, our intend is to generating power from renewable resources because pollution free. The renewable resources are, 1) Hydro power generation, 2) Wind power generation, 3) Solar power generation, 4) tidal power generation, 5) Geo-thermal power generation, 6) And, we are creating another one renewable resource. That is based on Tidal energy. The plant is designed in Gear mechanism. The gear mechanism is consists of three main parts. There are driver1, driver2 and follower or prime mover. The Tidal energy is converted into Mechanical upwards and downward motion. The Mechanical upward and downward motion is converted into the Mechanical rotations with the help of CRANKSHAFT. Those mechanical rotations are converted into Electrical energy. Shaft structure and civil construction 1. Gear structure, 2. Key structure, 3. Structure of floating material, 4. Civil structure and prime mover, 5. Structure of bearings, 6. Structure of gear mechanism,

II. GEAR STRUCTURE

The gear structure is mainly depends upon the wave height and length. That is prepared by stainless steel.

III. KEY STRUCTURE:

The key is made up of stainless steel. It is placed between the cranks. It is a movable part.

The key is made up of stainless steel. It is placed between the cranks. It is a movable part.

IV. PRIME MOVER STRUCTURE AND CIVIL CONSTRUCTION:

V. STRUCTURE OF THE PLANT:

1. Gears dimensions 2. Generator dimensions

Where, D1 is the diameter of the driver (gear A and gear B) D2 is the diameter of the follower gear (shaft) D is the diameter of the rotating key motion

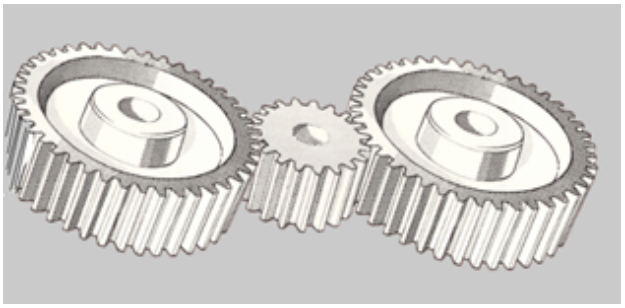

Fig. 1. gears structure

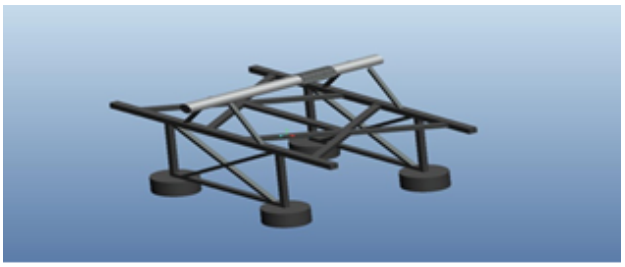

Fig. 2. key structure

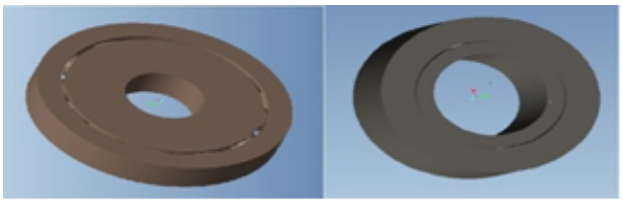

Fig. 3. STRUCTURE OF BEARINGS

The diameter of the key motion (D) is approximately equal to the height of the wave (Hw). The key is movable part. The key is moving in the Keyway based on the wave height. When, the wave height is increase and also increases the diameter of the key motion. The diameter of the key motion in gear A gear B (D) Hw————— (1) Where, D is the diameter of the key motion in the gear A and B Hwis the height of the wave.

A. GENERATOR DIMENSIONS:

The generator dimension and size is depends upon the wave size. i. At minimum wave velocity, the size of the generator is very large and also developing minimum output power. ii. At maximum wave velocity, the size of the generator is small and it developing more amount of output power

i. At minimum wave velocity,(refer page no, 6)

Generator specifications, 500KW, 150rpm, 40 poles 50Hz, permanent magnet synchronous generator is used to generate a power. ii. At maximum wave velocity,(refer page no. 6)

VI. FOUR QUADRANT OF OPERATION

This mechanism is operates at four quadrands in one cycleper one rotation in the gear A and gear B. In above four quadrant of operation is consists of two floating plates (F1 and F2) and two gears (A and B), prime mover with gear. That are named as driver and follower. In Quadrant I and II has operate as same principle. It require to control the gear A with the help of gear B. In these two quadrant, the floating plate F1 is push to rotate the gear A and F2 is pull to rotate the gear B. The gear B act as driver and gear A, prime mover are act as follower. In Quadrantn II and IV operation of the gear mechanism, the floating plate F1 and F2 has attain a same position in the sea waves. In Quadrant III and IV operation of the gear mechanism is require to control the gear B with the help of gear A. the floating plate F1 is pull to rotate the gear A and the floating plate F2 is push to rotate the gear B. The gear A can act as driver and another one gear, prime mover is act as follower.

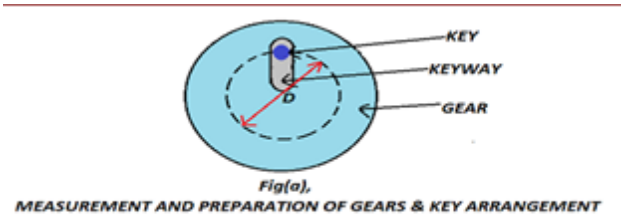

Fig. 4. plant structure

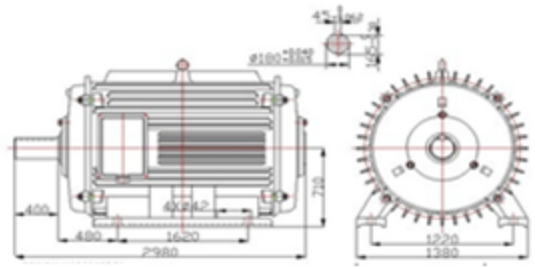

Fig. 5. GEAR DIMENSIONS

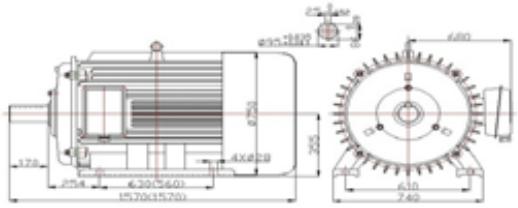

Fig. 6. dimension of generator at minimum wave velocity

VII. TIDAL BRIDGE

The series of gear mechanism is showing a fig (d) that is used to generate a power and to reduce the soil erosion in the sea shore.

VIII. ADVANTAGES

1) Initial cost only needed and no running cost 2) Less maintenance 3) Efficiency is higher than the solar, wind power plants 4) The fuel cost is totally absent 5) The efficiency does not change with age 6) Pollution free plant 7) Power can be generate at all time 8) The variable load does not affect the efficiency 9) To reduce the soil erosions in the sea shores

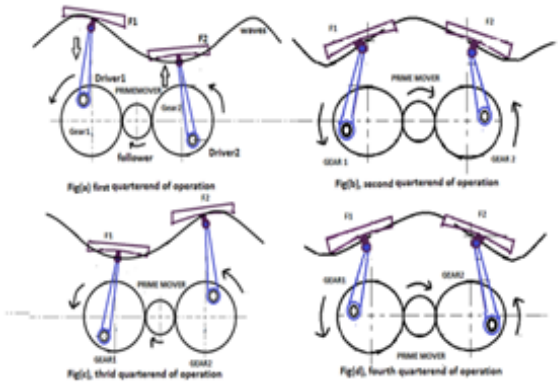

Fig. 7. Four Quadrants of operation

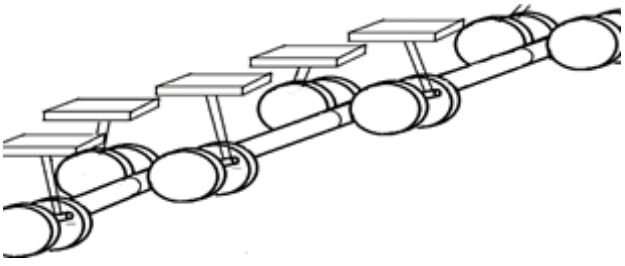

Fig. 8. bridge type of tidal power generation

IX. DISADVANTAGES

1. Initial cost of the plant is high 2. Difficult to construct the plant 3. The gear mechanism must be covered because the living thinks can be affected.

X. CONCLUSION

Finally, we are concluded on this paper. It was tested in the miniature level. The tested level the output will come.so it would be implemented in the real life it helps to generate the power with free of cost.Dont waste the all renewable resource. Save all renewable resources in the world.

REFERENCES

[1] Bernshtein LB *Korea Ocean Research and Development Institute(KORDI).*(1996) Tidal Power Plants.
Christopher D. Hall - *Virginia Polytechnic Institute and State University, Blacksburg, Virginia* Virginia 24061.

Optimal Inductor Current in Boost DC/DC Converters Regulating the Input Voltage applied to Low-Power Photovoltaic Modules

A.RICHARD PRAVIN
Assistant Professor/EEE
Department of Electrical and Electronics Engineering
St.Annes College of engineering and technology ,

***Abstract*—In energy-harvesting applications, inductor-based switching dc/dc converters are usually employed to regulate the operating voltage of the energy transducer and to transfer the harvested energy to a storage unit. In such a context, this paper analyses the optimal inductor current of the converter that leads to maximum power efficiency. This is evaluated assuming a lowpower photovoltaic (PV) module connected to a boost dc/dc converter operating in burst mode so as to reduce the switching losses. The theoretical analysis and the experimental results reported herein prove that this optimal inductor current does not depend on the power generated by the PV module provided that the control circuit is powered from the output, but it does on the output voltage level of the storage unit. Experimental tests with a commercial boost dc/dc converter show that the use of this optimal inductor**

I. INTRODUCTION

switching dc/dc converters are generally employed to regulate their output voltage, they can also be used to regulate their input voltage, which is of interest in energy harvesters that power, for instance, the nodes of a wireless sensor network in smart cities and buildings. In the first case, the dc/dc converter is placed between the energy source (e.g. a battery) and the electronic circuitry (e.g. sensors, amplifiers, microcontrollers and/or transceivers) with two objectives: (i) to power the electronics with a stable supply voltage, and (ii) to transfer the energy from the battery to the electronics in an efficient way. In the second case, the dc/dc converter is placed between an energy transducer (e.g. a PV module) and a storage unit (e.g. a rechargeable battery) with again two goals: (i) to maintain the operating voltage of the energy transducer around its maximum power point (MPP) [1], and (ii) to transfer the energy from the transducer to the storage unit efficiently.control strategy applied to the switching transistors is selected according to the output power demanded by the electronic circuitry. Under light-load conditions (i.e. for load currents of a few mA), which is quite usual in sensor nodes, the wellknown pulse-width modulation (PWM) is not recommended because the fixed switching frequency causes significant switching losses and, hence, reduces the efficiency [2]. Such efficiency can be increased by dynamically adjusting the gate driving voltage [3], the size of the switching transistors [4,5], and the number of active phases in multiphase dc/dc converters [6]. Another way to improve the efficiency is the use of a hybrid control whereby the converter operates in PWM at heavy loads, but it switches to a variable-frequency mode at light loads so as to reduce the switching losses. A first example of that is the pulse-frequency modulation (PFM) where the switching frequency is scaled down with the load current. Constant [7] or adaptive [8] on-time, and constant peak inductor current [9] are two common control techniques based on PFM. A second example is the burst mode (BM) where the transistors are cyclically switched on and off at a fixed frequency (the same as in PWM) during an active period, but they are permanently in off-state during an inactive period, which becomes longer as the load current decreases [10]. During the active period, it is advisable to transfer the energy from the battery to the electronics at an optimal value of inductor current processing circuit for a PV module based on a synchronous boost dc/dc converter is shown in Fig. 1. The converter relies on an inductor (L) and two power MOSFET transistors (MN and MP). The corresponding gate control signals (vc1 and vc2) are generated by a control circuit with two loops [13]: (i) a voltage loop that monitors the input voltage (vin) using a comparator with a hysteresis of Vhys and with a reference voltage (Vin) equal to the MPP voltage determined by a MPPT controller [1], and (ii) a current loop that monitors the inductor current (iL) by either a shunt resistance in series with L or the voltage drop across MN or MP. At the input of the converter, the PV module provides a DC current (Iin) and has a high-value input capacitor (Cin)

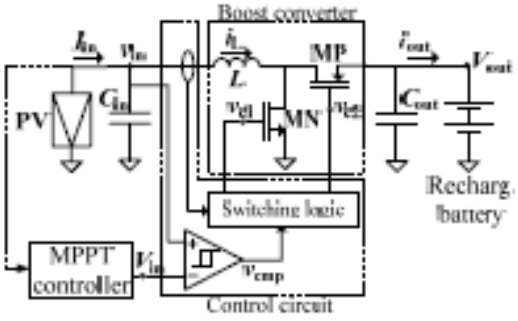

Fig. 1. power processing circuit

in parallel that temporarily stores the energy. On the other hand, the output of the converter is connected to a rechargeable battery in parallel with an output capacitor (Cout) that filters out the highfrequency components of the output current.

II. OPERATING PRINCIPLE

Assuming no losses, the average output current injected to the battery is VinIin/Vout, where Vout is the DC voltage level of the battery. The input voltage (vin) in Fig. 1 is regulated around the desired DC voltage (Vin) by operating in BM. This operating principle involves two stages (inactive and active) that last tinactive and tactive, respectively, and an overall duty cycleDT = tactive/TT, where TT = tinactive + tactive, as shown in Figs. 2(a) and 2(b). In the inactive stage, the converter is deactivated (i.e. MN and MP are off) and Iin charges Cin, thus increasing vin. When vin = Vin + Vhys, the comparator output (vcmp) changes to a high logic level and brings the converter to the active stage. Then, the energy accumulated in Cin is transferred to the output and vin decreases. When vin = Vin Vhys, vcmp toggles to a low logic level, the converter is deactivated and the process starts again. This operating principle based on initially storing the energy in Cin is very appropriate for low-power PV modules since (i) the converter remains inactive most of the time, which reduces the power losses, and (ii) Cin provides an operating voltage equal to the MPP voltage, which ensures a good impedance matching with the equivalent impedance of the PV module regardless of the operating conditions of the converter in active mode. Power processing circuits without a high-value Cin where the converter is always activated and the impedance matching is carried out by adjusting the duty cycle of the switching transistors [22] are more appropriate for medium- and high-power PV modules. In order to transfer the energy from the input to the output during the active stage, a burst of on/off pulses under PWM control is applied to the gate of the transistors, as shown in Fig. 2(c) and with more details in Fig. 2(d) for vc1; vc2 is the same as vc1 but with some dead time between them to prevent vc1 has an on-time (ton), an off-time (toff), a switching period Ts (= ton + toff), a switching frequency fs (= 1/Ts) and a duty cycle D (= ton/Ts). During ton (MN on, MP off), the energy previously accumulated in Cin is stored in L and iL increases, whereas during toff (MN off, MP on), the energy accumulated in L is transferred to the output and iL decreases. A currentprogrammed mode control in continuous conduction mode (CCM) is assumed so that iL has an average of IL0 and a ripple of IL, as shown in Fig. 2(e). In such an operating mode, we have D = 1Vin/Vout, being the efficiency. The optimal value of IL0 to carry out such energy transfer at maximum efficiency is analyzed next considering the main power losses.

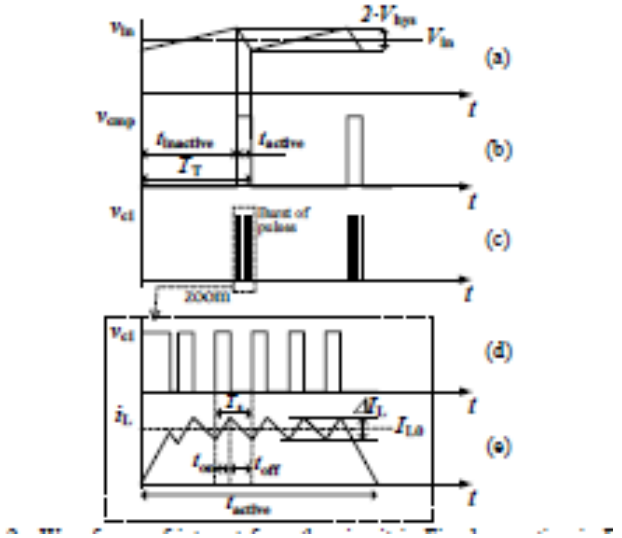

Fig. 2. waveform from the circuit

III. THEORETICAL ANALYSIS

The power efficiency of the circuit in Fig. 1 is theoretically analyzed using the same equivalent circuit model proposed in [11] and represented in Fig. 3. This circuit includes the parasitic resistance (RL, RCi, RCo, RN, and RP) of the main components (L, Cin, Cout, MN, and MP, respectively), and the parasitic capacitance (CA, CG1, and CG2) of the main nodes (node A, gate of MN and MP, respectively); RS is a shunt resistance employed in some dc/dc converters to sense iL. Moreover, the control circuit has a current consumption of IQ,a in active mode and IQ,i in inactive mode, where IQ,i ¡¡ IQ,a. The optimal inductor current is theoretically found in two different scenarios that take into account the trade-off between conduction losses and gate-driving losses at different gatedriving voltages [3]. First, we assume that the control circuit is powered from the output, as shown in Fig. 3. This involves a high gate-driving voltage (i.e. Vout) that decreases the onresistances of MN and MP and, hence, the conduction losses. Second, we consider that the control circuit is powered from the input. In such a case, the gate-driving voltage is lower (i.e. Vin) and, therefore, losses related to the charge-discharge process of CG1 and CG2 are also lower.

A. Control circuit

powered from the output Table I summarizes the power losses (fixed, conduction, and switching losses [11]) present in Fig. 3 in both active and inactive modes when the control circuit is powered from the output. In active mode, the equivalent parasitic resistance is Req,a = RCi + RS + RL + RND+ (RP + RCo)(1 D) . This is assuming that iL

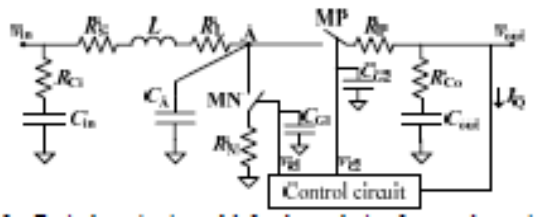

Fig. 3. equivalent circuit

is mostly provided by Cin since IL0 ¿¿ Iin, and that the current through MP is much higher than the average output current injected to the battery. In inactive mode, the equivalent parasitic resistance is eq,i Ci CoB. Control circuit powered from the input Table II summarizes the power losses in both active and inactive modes when the control circuit is powered from the input. In comparison with Table I, we have three main changes: (i) fixed losses are lower since they depend on Vin instead of Vout; (ii) conduction losses in active mode are caused by a higher parasitic resistance, ' eq,a R ¿ eq,a R , because the on-resistances of MN and MP are higher; and (iii) switching losses due to the charge-discharge process of the gate capacitances, G G1 G2 C = C +C , are lower since the gate voltage swing is lower. Following now the same procedure explained in Section III.A, we can find a new expression for the efficiency, the optimal value of IL0 and the maximum

IV. MATERIALS AND METHOD

A commercial boost dc/dc converter, TPS61252 from Texas Instruments [24], has been employed to experimentally prove the concept of optimal inductor current. This converter has a control circuit powered from the output and its IL0 is adjustable from 100 to 1500 mA by an external resistor (RLIM). The inductor current is measured during the off-time through the voltage drop across MP, and a valley current-mode control is applied that cleverly adjusts the valley current limit to achieve the desired average inductor current. In order to have the BM-CCM operation shown in Fig. 2, an external ultralowpower comparator, LTC1440 from Linear Technology, with Vhys = 50 mV was placed before the feedback (FB) input of the converter, as shown in Fig. 5. Using this circuit, when vin becomes higher than the desired voltage, the comparator output changes to a low level, which brings the converter to active mode and, then, iL is regulated around IL0. Otherwise, when vin becomes lower than the desired voltage, the comparator output toggles to a high level and the converter enters into inactive mode. The circuit in Fig. 5 was tested using the operating conditions, instrumentation, and components indicated in Table III. The values of Iin and Vin were selected using as a reference a commercial ultra-thin low-power PV module, SP3- 37 from PowerFilm, that will be under test in Section VI. At standard test conditions (STC) involving a solar irradiance of 1000 W/m2, this PV module has a typical MPP current/voltage/power of 22 mA/3 V/66 mW, which is adequate to power, for instance, a microcontroller-basedautonomous sensor [27]. Note that the maximum MPP current generated by the PV module (22 mA) is clearly lower than the minimum value of IL0 that can be regulated (100 mA), so the approximation indicated in Section III.A is valid. The input power was calculated as VinIin, whereas the average output power (Pout) was measured by a power analyzer, Yokogawa WT310, with a sampling frequency of 100 kSa/s and an update rate of 5 s. With the aim of generalizing the concept of optimal inductor current to other dc/dc converters with different power losses, we also added some external components around the TPS61252, as shown in Fig. 5, so as to raise its fixed, conduction and switching losses. Fixed losses were increased by connecting a resistor (Ri) between Vout and the comparator

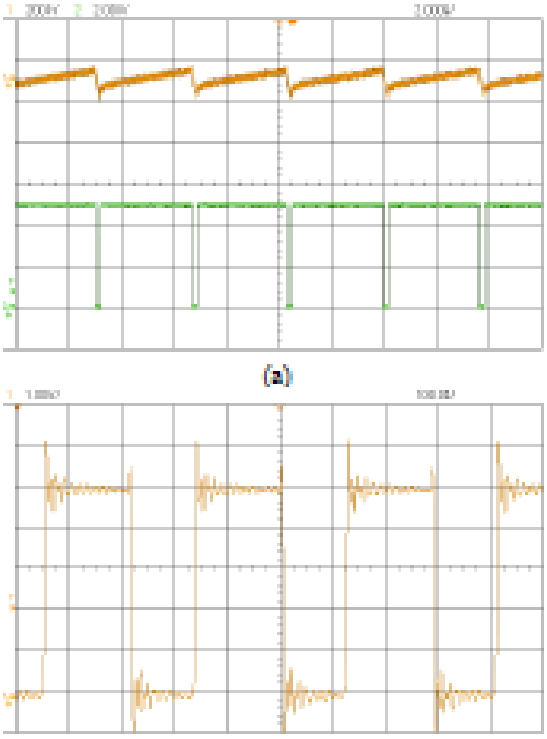

Fig. 4. application circuit basedtsps61252

V. EXPERIMENTAL RESULTS AND DISCUSSION

Before evaluating the efficiency of the circuit in Fig. 5, we tested its operating principle by monitoring the voltage waveform at the main nodes, as shown in Fig. 6 for Vin = 3.0 V, Iin = 22 mA, Vout = 5.0 V, and IL0 305 mA. Fig. 6(a) shows the input voltage and the comparator output for several active and inactive periods; the latter is the complementary of that represented in Fig. 2(b) because this signal is then inverted by the on-chip error amplifier. According to the comparator output, we had DT = 6fairly agrees with that predicted by Iin/IL0. On the other hand, Fig. 6(b) shows the voltage at the switching node A within one active period; this signal is also the complementary of that represented in Fig. 2(d) since it is inverted through MN. In Fig. 6(b) we measured

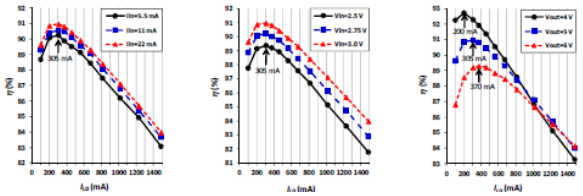

Fig. 5. experimental waveforms

fs = 3.5 MHz, instead of the nominal value of 3.25 MHz, and D = 44calculated by 1 Vin Vout assuming = 91in Fig. 7). Furthermore, D was very stable during the active period, which means that the inductor current was well regulated around IL0. Fig. 7 shows the experimental results of efficiency versus IL0 for different values of (a) Iin, (b) Vin, and (c) Vout, using Iin = 22 mA, Vin = 3.0 V, and Vout = 5.0 V as default values. The higher the value of both Iin and Vin, the higher the efficiency, although the effects of the latter were clearly major. However, the higher Vout, the lower the efficiency. Such effects of Iin, Vin, and Vout on the efficiency agree with (2). Moreover, IL0,opt was independent of both Iin [Fig. 7(a)] and Vin [Fig. 7(b)], but it increased (from 200 to 370 mA) with increasing Vout [Fig. 7(c)], which was already predicted by (3). With respect to the case with minimum efficiency that was found at the maximum value of IL0, the efficiency increased by 7Figs. 7a, 7b, and 7c, respectively, when IL0,opt was applied. In order to quantitatively evaluate the model proposed in Section III, the efficiency was also calculated from (2) and represented in Fig. 8 for the same operating conditions discussed before. Note that Ceq and tc were unknown and were extracted by fitting (2) to a set of experimental results, and that RN and RP were assumed to be dependent on the gate

In a practical implementation, taking into account that the exact value of some variables involved in (3) or (6) can be unknown, the optimal value of IL0 can be automatically determined through a control algorithm, such as the perturb and observe method [17], carried out by a microcontroller. The basic idea would be to slightly perturb the value of IL0 and then observe how the output power changes, assuming the input power constant during the control cycle. If the output power increases, the perturbation should be kept in the same direction; otherwise, it should be reversed. For the TPS61252 under test, the value of IL0 could be perturbed using a digital potentiometer instead of RLIM in Fig. 5. On the other hand, the output power could be observed by sensing: (a) the average output current via a shunt resistor and an amplifying low-pass filter [15,28], or (b) the increment of voltage across a small output capacitor connected in parallel with the main storage device that would be disconnected for a short and known time interval [29].

VI. APPLICATION TO A LOW-POWER PV MODULE

The concept of optimal inductor current has been further proved using a commercial low-power PV module, SP3-37 from PowerFilm. This was first characterized under irradiance-controlled laboratory conditions to achieve the power-voltage (P-V) curve as follows. The PV module was subjected to three irradiance levels (identified as I25, I50, and I100) through a LED array, BXRA-C1202 from Bridgelux, powered at different DC currents and placed at 3 cm [17]. The levels I25, I50, and I100 approximately correspond to an irradiance of 250, 500, and 1000 W/m2, respectively, in terms of power generated by the PV module at the MPP. At each irradiance level, the current generated by the PV module was measured at different applied voltages (from 0 V to 4 V in steps of 100

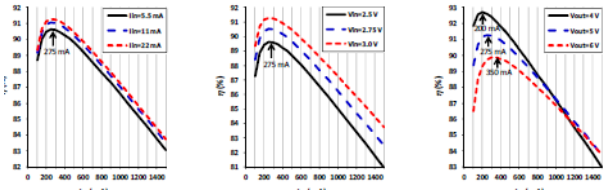

Fig. 6. effiency calculated waveform

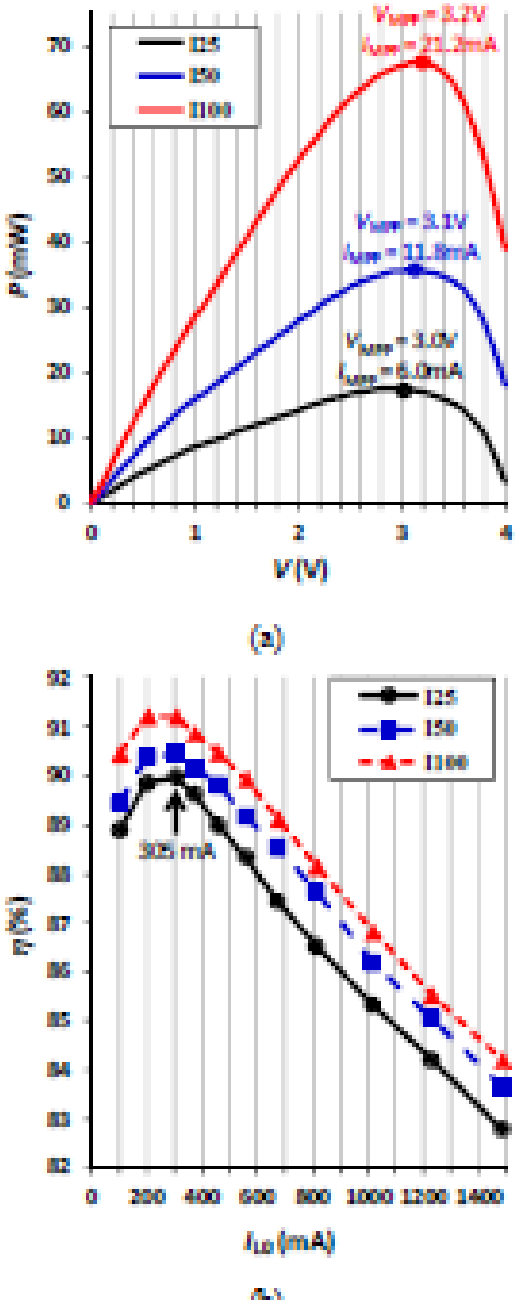

Fig. 7. output waveformsircuit

mV) using a source-measurement unit, Agilent B2901. The experimental results of such a characterization are represented in Fig. 12(a) showing the MPP at each irradianceirradiance level. After characterizing the PV module, this was connected to the power processing circuit shown in Fig. 5 instead of the ideal input current source. Using the same methodology explained in Section IV, the efficiency of the circuit was measured at different values of IL0 and for the three irradiance levels indicated before. At each irradiance level, Vin in Fig. 5 was set to the VMPP value indicated in Fig. 12(a) so as to extract the maximum power from the PV module. The experimental results of efficiency are shown in Fig. 12(b) for Vout = 5.0 V. Note that the efficiency increased with increasing the irradiance level. This is because the higher the irradiance, the higher the value of both VMPP and IMPP (and, hence, Vin and Iin in Fig. 5) and, therefore, the higher the efficiency, as shown before individually in Figs. 7(a) and 7(b). The resulting value of IL0,opt, which was around 305 mA, was the same for the three irradiance levels. Accordingly, as previously suggested in Section III.A, the value of IL0,opt seems to be independent of the power generated by the energy transducer, thus facilitating

VII. CONCLUSION

This work has gone a step further in the field of power processing circuits based on switching dc/dc converters by proposing an optimal inductor current to carry out the energy transfer from a low-power energy transducer to a storage unit. If the control circuit is powered from the output, this optimal inductor current is independent of both the input voltage and the input current. Consequently, this optimal current does not depend on the power generated by the energy transducer, which has been experimentally proved using a commercial low-power PV module subjected to different irradiance levels. However, such a current depends on the output voltage, i.e. the voltage level of the output batteries. Experimental tests with a commercial boost dc/dc converter have shown that the use of this optimal inductor current provides up to 10increase in efficiency. Therefore, this is a simple but effective way to improve the autonomy of sensor nodes powered by low-power PV module.

REFERENCES

[1] H.M. SENH. Kim, S. Kim, C. K. Kwon, Y. J. Min, C. Kim, and S. W. Kim, *An energy-efficient fast maximum power point tracking circuit in an 800- W photovoltaic energy harvester,"*IEEE Trans. Power Electron., vol. 28, no. 6, pp. 2927-2935, June 2013.

[2] C. Lee, Y. Oh, K. Na, Y. Kim, and N. Kim, *Integrated BiCMOS control circuits for high-performance DCDC boost converter,"* IEEE Trans. Power Electron., vol. 28, no. 5, pp. 2596-2603, May 2013.

[3] M. D. Mulligan, B. Broach, and T. H. Lee, *"A constant-frequency method for improving light-load efficiency in synchronous buck converters,"* IEEE Power Electron. Lett., vol. 3, no. 1, pp. 24-29, March 2005.

Home Automation Using Internet of Things

Vijayaragavan.M
Assistant.proffesor
Department of Electrical and Electronics Engineering
MAILAM ENGINEERING COLLEGE

Rajalakshmi.S
assistant.proffesor
Department of Electrical and Electronics Engineering
MAILAM ENGINEERING COLLEGE

Azhagiya Manavalan
UG Scholar
Department of Electrical and Electronics Engineering
MAILAM ENGINEERING COLLEGE

***Abstract*—The main aim of the project is to develop a system that will provide remote control of home appliances and also provide security against the mishaps when the home host is not at home. This paper is mainly concerned with the automatic control of light or any other home appliances using internet. It is meant to save the electric power and human energy. This project is made with the help of controller and raspberry pi. The various appliances connected to the micro controller and sensor is connected using wireless network.**

I. INTRODUCTION

A. a.overview

Homes of the 21st century will become more and more self -controlled and automated due to the comfort it provides, especially when employed in a private home. A home automation system is a means that allow users to control electric appliances of varying kind.

Many existing, well-established home automation systems are based on wired communication. This does not pose a problem until the system is planned well in advance and installed during the physical construction of the building. But for already existing buildings the implementation cost goes very high. In contrast, Wireless systems can be of great help for automation systems. With the advancement of wireless technologies such as Wi-Fi, cloud networks in the recent past, wireless systems are used every day and everywhere.

B. B. Advantages of Home automation systems over wired system

In recent years, wireless systems like Wi- Fi have become more and more common in home networking. Also in home and building automation systems, the use of wireless technologies gives several advantages that could not be achieved using a wired network only.

Reduced installation costs: First and foremost, installation costs are significantly reduced since no cabling is necessary. Wired solutions require cabling, where material as

well as the professional laying of cables (e.g. into walls) is expensive.

1. System scalability and easy extension: Deploying a wireless network is especially advantageous when, due to new or changed requirements, extension of the network necessary. In contrast to wired installations, in which cabling extension is tedious. This makes wireless installations a seminal investment. 2. Aesthetical benefits: Apart from covering a larger area, this attribute helps to full aesthetical requirements as well. Examples include representative buildings with all-glass architecture and historical buildings where design or conservatory reasons do not allow laying of cables.

3. Integration of mobile devices: With wireless networks, associating mobile devices such as PDAs and Smartphones with the automation system becomes possible everywhere and at any time, as a device's exact physical location is no longer crucial for a connection (as long as the device is in reach of the network).

For all these reasons, wireless technology is not only an attractive choice in renovation and refurbishment, but also for new installations.

C. II. RELATED WORK

[1] Sirsath N. S, Dhole P. S, Mohire N. P, Naik S. C Ratnaparkhi N.S

This paper proposes a Home Automation system that employs the integration of multi-touch mobile devices, cloud networking, wireless communication, and power-line communication to provide the user with remote control of various lights and appliances within their home. This system uses a consolidation of a mobile phone application, handheld wireless remote, and PC based program to provide a means of user interface to the consumer.

[2] Basil Hamed

The main objective of this Paper is to design and implement a control and monitor system for smart house. Smart house

system consists of many systems that controlled by LabVIEW software as the main controlling system in this paper. Also, the smart house system was

supported by remote control system as a sub controlling system. The system also is connected to the internet to monitor and control the house equipments from anywhere in the world using LabVIEW. [3] Deepali Javale, Mohd. Mohsin, Shreerang Nandanwar The prime objective of this paper is to assist

handicapped/old aged people. It gives basic idea of how to control various home appliances and provide a security using Android phone/tab. The design consists of home automation website, Raspberry pi B, ATMEGA8 microcontroller. User can interact with the website and send control signal to the Raspberry pi kit which in turn will control other embedded devices/sensors.

II. III. SYSTEM ANALYSIS

A. A. Problem Definition

Many people are always on the move from place to place due to business demands. Some people can spend a couple of days away from their home leaving all their household appliances without any kind of monitoring and control. Some devices are left plugged into power sockets whereas others are supposed to be plugged into and out of power sockets at different intervals depending on the time of the day. All this requires an individual to manually attend to each of the devices independently from time to time. All such monitoring and control can be done without necessarily being around or inside the home. Some devices if not controlled properly consume a lot of energy which leads to extra expenditure on electricity. Therefore we propose to design an internet based home automation system which will enable one to remotely manage his/her appliances from anywhere, anytime.

B. B. Proposed System Feature

As we enter the 21st century, the interaction between humans and computer is breaking old barriers and entering a new realm. In the highly technology driven world of todays mobile phones have become a part of our Lifestyles. Mobile phones are not just communication tool. Our project tries to derive solution providing better control on home appliance with help of cell phone. The Existing System consists of physical appliances in our home that are been controlled through switches. These devices can be switched ON OFF manually whenever needed. This system is less secured and prone to electrical hazards. Also the wastage of electricity tends to be a major factor of concern. The proposed project is conceived networking our mobile phone to all appliances via a smart logic circuit. The proposed system consists of Smart Logic Circuit connected to the appliances. Status of all home appliances could be controlled by user from remote location with help of users mobile phone.

III. IV. SYSTEM DESIGN AND IMPLEMENTATION

A. A. Proposed Home Automation System

Fig. 1. : Proposed model of Home automation system

IV. DEMANDSTATUS

The end user can use their mobile phone to log into the system. An initial check is performed for whether the hardware device is ON or not. Only if the Hardware is authorized and ON then the user is Authenticated. Once the authentication is done successfully the user is able to send the control signals to the Hardware machine. At the hardware machine the SL driver program will continuously track for the change in the status will accordingly send the signals to the Circuit. When a user select a change in the status for any of the device [i. e .. ON or Off], the data from the handheld is sent to the Web Server in a string format, where the Web site is hosted. On the server the status is stored in the database in their respective device field. At the Hardware end, the circuit drive program a web page is [retrieve.aspx] is used to retrieve the status of the devices in a timely pattern [every 10sec]. These changes come in to form of cookies [temporary internet files] from the webserver are stored on the computer in the name of the web site. Hence every 10 sec as the page refreshes the new cookie values are updated. The cookie values are read from the program using the VB component GETINERNETCOOKIE after a fixed delay. As the program receives any change in the Device values it send the control signal [binary data] accordingly to the required data pin of the parallel port.

V. B. Proposed Home Automation System Functions

The proposed home automation system has the capabilities to control the following components in users home and monitor the following alarms:

Temperature and humidity
Gas leakage detection
Control appliances

The proposed home automation system can control the following appliance:

Lights on/off/dim
Fan on/off
On/off different appliance
Leakage of gas

Front End Design:]C. Software design
Front End Design:

Database Storage::]
Database Storage::

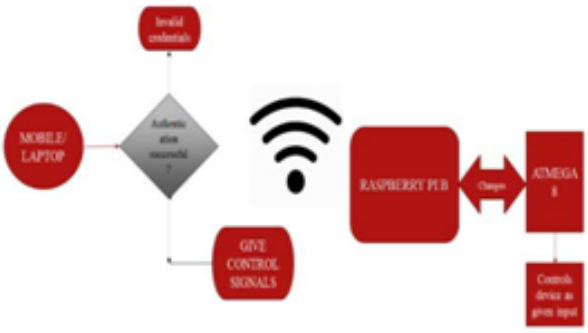

Fig. 2. sequence of activities in WHAS

VI. D. Implementation Setup

VII. EXPLANATION

Figure 2 illustrates the sequence of activities in the WHAS. When the connection is established it will start reading the parameters of sensors like fan, tube light, gas sensor etc. The threshold levels for the required sensors are set as t1, t2, and t3 etc. The sensor data are sent to the web server and stored in the cloud. The data can be analysed anywhere any time. If the sensor parameters are greater than the threshold level then the respective alarm a1, a2, a3 etc. will be raised and the required actuation is done for the controlling of the parameters.

A model house is built for the home automation system and is as shown in the figure . Light 1 will turn on automatically when light sensor detects the darkness. A cooler/Fan will turn on when the room temperature exceeds the set threshold and in turn reduces the room temperature. The gas sensor LM35 is placed in the kitchen to detect any gas leakage, if any leakage is detected the alarm in the hall is raised. Relay is used to switch the electrical appliances like light, fan etc. The Intel Galileo is placed in store room or garage. The Raspberry PI B is connected with WiFi or LAN for the connectivity with internet.

VIII. V. RESULTS

After the successful connection to the server, the data of sensor are sent to the web server for monitoring of the system. The figure 3 shows the web server page which will allow us to monitor and control the system. By entering the assigned URL address in the web browser this web server page will appear. The web server gives the information about the temperature in different places of the house. It also gives the status of the various electrical appliances like light, fan etc. which we can control remotely

All the required data is stored in the database. The stored data can be analyzed at anytime and anywhere. The figure 4 shows the temperature in degree Celsius stored at different time intervals. And also it shows the state of the motion detector along with the time. It also provides information about time of motion detected and how many times as well. All this information is stored in the cloud which can be checked by the user any time when away from home

IX. VI. CONCLUSION AND FUTURE WORK

A. A CONCLUSION

The home automation using Internet of Things has been experimentally proven to work satisfactorily by connecting simple appliances to it and the appliances were successfully controlled remotely through internet. The designed system not only monitors the sensor data, like temperature, gas, light, motion sensors, but also actuates a process according to the requirement, for example switching on the light when it gets dark. It also stores the sensor parameters in the webpage (database) in a timely manner. This will help the user to analyze the condition of various parameters in the home anytime anywhere.

Fig. 3. Web server page

Fig. 4. Data base of the sensors data stored in the cloud

B. Future work

Using this system as framework, the system can be expanded to include various other options which could include home security feature like capturing the photo of a person moving around the house and storing it onto the cloud. This will reduce the data storage than using the CCTV camera which will record all the time and stores it. The system can be expanded for energy monitoring, or weather stations. This kind of a system with respective changes can be implemented in the hospitals for disable people or in industries where human invasion is impossible or dangerous, and it can also be implemented for environmental monitoring.

C. ACKNOWLEDGEMENT

We acknowledge the efforts and hard work by the experts who have contributed towards development of the different home automation systems.We take this opportunity to express our profound gratitude and deep ragards to our guide Prof.Amit kukreja and prof.Sagar Matre for his exemplary guidance ,monitoring and constant encouragement throughout the course of this project.

References

[1] irsath N. S, Dhole P. S, Mohire N. P, Naik S. C Ratnaparkhi N.S Department of Computer Engineering *Home Automation using Cloud Network and Mobile Devices*,publishers Department of Computer Engineering, 44, Vidyanagari, Parvati, Pune-411009, India University of Pune,

GRID INTEGRATION OF RENEWABLE ENERGY RESOURCES

K.SURIYANARAYANAN
UG SCHOLOR
Department of Electrical and Electronics Engineering
IFET COLLEGE OF ENGINEERING

R.VENGADAKRISHNAN
UG SCHOLOR
Department of Electrical and Electronics Engineering
IFET COLLEGE OF ENGINEERING

***Abstract*—There is growing interest in renewable energy around the world. Since most renewable sources are intermittent in nature, it is a challenging task to integrate renewable energy resources into the power grid infrastructure. In this grid integration, communication systems are crucial technologies, which enable the accommodation of distributed renewable energy generation and play an extremely important role in monitoring, operating, and protecting both renewable energy generators and power systems. In this article, we review some communication technologies available for grid integration of renewable energy resources. Then we present the communication systems used in a real renewable energy project, Bear Mountain Wind Farm in British Columbia, Canada. In addition, we present the communication systems used in photovoltaic power systems. Finally, we outline some research challenges and possible solutions about the communication systems for grid integration of renewable energy resources.**

I. INTRODUCTION

As concerns about climate change, rising fossil fuel prices, and energy security increase, there is growing interest around the world in renewable energy resources.Since most renewable energy sources are intermittent in nature, it is a challenging task to integrate a significant portion of renewable energy resources into the power grid infrastructure. Traditional electricity grid was designed to transmit and distribute electricity generated by large conventional power plants. The electricity flow mainly takes place in one direction from the centralized plants to consumers. In contrast to large power plants, renewable energy plants have less capacity, and are installed in a more distributed manner at different locations. The integration of distributed renewable energy generators has great impacts on the operation of the grid and calls for new grid infrastructure. Indeed, it is a main driver to develop the smart grid for infrastructure modernization [1], which monitors, protects, and optimizes the operation of its interconnected elements from end to end with a two-way flow of electricity and information to create an automated and distributed energy delivery network. Communication systems are crucial technologies for grid integration of renewable energy resources. Two-way communications are the fundamental infrastructure that enables the accommodation of distributed energy generation and assists in the reconfiguration of network topology for more efficient power flow. Many types of equipment in the grid (meters, sensors, voltage detectors, etc.) should be monitored and controlled, which will enable important decision support systems and applications, such as supervisory control and data acquisition (SCADA), energy management system (EMS), protective relaying for high voltage lines, mobile fleet voice and data dispatch, distribution feeder automation, generating plant automation, and physical security. These applications are vitalin monitoring, operating, and protecting both renewable energy generators and power systems. There are several communication options available for the grid integration of renewable energy resources. These options include a hybrid mix of technologies, such as fiber optics, copper-wire line, power line communications, and a variety of wireless technologies. There is currently on-going debate surrounding what will emerge as the communications standard of choice. Since utilities want to run as many applications as possible over their networks, issues of bandwidth, latency, reliability, security, scalability and cost will continue to dominate the conversation. In addition, distinct characteristics in the electric grid pose new challenges to the communication systems for grid integration of renewable energy resources.In this article, we review some communication technologies available for grid integration of renewable energy resources. Then we introduce a real renewable energy project, Bear Mountain Wind farm (BMW) in British Columbia, Canada, with 34 ENERCON wind turbine generators and a generation capacity of 102 MW. Particularly, we present the communication systems used in BMW. In addition, we describe the communication systems used in photovoltaic power systems (PPSs). For both wind and PPSs, we outline some research challenges and possible solutions about the communication systems for grid integration of these renewable energy resources. The rest of this article is organized as follows. We describe an overview of communication systems for grid integration of renewable energy resources. We present the communication systems and some research challenges for grid integration of wind farms. We present the communication systems and some research challenges for grid integration of photovoltaic power systems. Finally, we conclude the paper.

II. OVERVIEW OF COMMUNICATION SYSTEMS FOR GRID INTEGRATION OF RENEWABLE ENERGY RESOURCES

A typical electric grid communication system consists of a high-bandwidth backbone and lower-bandwidth access

networks, connecting individual facilities to the backbone. Fiber optics and/or digital microwave radio are usually the technologies for the backbone, whereas the access may use alternatives such as copper twisted-pair wire lines, power line communications, and wireless systems. In this section, we introduce some communication technologies and related standards that are particularly interesting for grid integration of renewable energy resources.

A. POWER LINE COMMUNICATIONS

Power line communications (PLCs) are to use existing electrical wires to transport data. Recently, new PLC technologies are available that allow high bit rates of up to 200 Mb/s. PLC can be used in several important applications: broadband Internet access, indoor wired local area networks, utility metering and control, real-time pricing, distributed energy generation, and so on [2]. From a standardization point of view, competing organizations have developed specifications, including HomePlug Powerline Alliance, Universal Powerline Association and HD-PLC. ITU-T adopted Recommendation G.hn/G.9960 as a standard for high-speed power line communications. In IEEE, P1901 is a working group developing PLC medium access control and physical layer specifications. National Institute of Standards and Technology (NIST) has included HomePlug, ITU-T G.hn and IEEE 1901 as Additional Standards Identified by NIST Subject to Further Review for the smart grid in the USA [1]. The primary advantage of PLC arises from the fact that it allows communication signals to travel on the same wires that carry electricity. However, since power line cables are often unshielded and thus become both a source and a victim of electromagnetic interference (EMI). Another issue is the price. A PLC module is usually more expensive than a wireless module, such as ZigBee, which will be introduced in the next subsection. In addition, wireless is also more practical in some applications, such as water/gas meters powered by batteries without power lines.

B. WIRELESS HOME LOCAL AREA NETWORKS

A leading standard for the wireless home network communications is ZigBee. The Zigbee Smart Energy standard builds on top of the ZigBee Home Automation Network (HAN) standard. HAN provides a framework to automatically control lighting, appliances, and other devices at home. ZigBee Smart Energy provides a framework to connect HAN devices with smart meters and other such devices. This will enable the energy utility to directl y communicate with the end consumers of energy. Wi-Fi is often used as a synonym for IEEE 802.11 wireless local area network (WLAN) technologies. Recently, Wi-Fi became a standard for laptops and subsequently phones due to its high data rate. When using it in utilities, however, Wi- Fis power consumption is an issue that needs to be considered carefully. The ZigBee Alliance and Wi-Fi Alliance also consider collaborating on applications for energy management and networking. The initial goal will be to get Smart Energy 2.0, a standard promoted by ZigBee, to work on Wi-Fi.

III. WIRELESS WIDE AREA NETWORK

Public cell phone carriers have great interest in using wireless wide area networks to connect household smart meters directly with the utilitys systems. A major advantage of this approach is the reduction of the costs (by not having to build a new network and by leveraging the expertise of the telecom world). However, since public wireless cellular networks are not specialized in the machine-to-machine area, some requirements in utilities may not be met by cellular networks. Others argue that if the public wireless giants want to get into this business, they will do whatever it takes to meet the requirements to win these large-scale multi-year utility contracts. WiMAX is based on the IEEE 802.16 standard, enabling the delivery of wireless broadband communications. Unlike the now popular wireless networking technologies using unlicensed spectrum (e.g., those used by Silver Spring and Trilliant), WiMAX uses licesed wireless spectrum, which is arguably both more secure and reliable. The primary disadvantage of using a licensed network is that it is more expensive. In addition, compared to cellular technologies, WiMAX has yet to be deployed at scale, which means some risks when applied to utilities.

A. INTEROPERABILITY OF DIFFERENT COMMUNICATION SYSTEMS

Without a framework of interoperable standards for communications, it would be very difficult to integrate renewable energies into the grid. Since the potential standards landscape is very large and complex, interoperable standards adoption is challenging. Many utilities and regulatory groups are collectively trying to address interoperability issues through workgroups such as the GridWise Architecture Council and Open Smart Grid (Subcommittee of the Utility Communications Architecture International Users Group) as well as through policy action from NIST. In June 2009, NIST announced an interoperability project via IEEE P2030, which seeks to define interoperability of energy technology and information technology operations with electric power systems and end-user applications and loads [3].

B. COMMUNICATION SYSTEMS FOR GRID INTEGRATION OF WIND FARMS

Wind energy has become an increasingly significant portion of the generation mix. Large-scale wind farms are normally integrated into power transmission networks so that the generated electric power can be delivered to load centers in remote locations. Small-scale wind farms can be integrated into power distribution networks to meet local demands. Because of high variability and intermittency, wind farm operations become a great challenge to power systems [4]. Communication systems are fundamental infrastructure that transmits measured information and control signals between wind farms and power systems. Well designed communication systems can better explore the wind potentials and facilitate farm controls, helping shaving peak load and providing voltage support for power systems. Any deficiency in communication systems

could compromise the system observability and controllability, which would negatively impact system security, reliability, and safety. In this section, we present the communication systems used in a real renewable energy project, BMW in British Columbia, Canada.

IV. INTRODUCTION TO BEAR MOUNTAIN WIND FARM

Located in the Peace River area of northern interior British Columbia, Canada, BMW consists of 34 ENERCON wind turbine generators with a generation capacity of 102 MW. It is the first large-scale wind farm that has been integrated into British Columbias transmission network [5]. In commercial operation since December 2009, BMW is a typical project in the sense that it integrates large-scale wind resources into bulk power systems by adopting up-to-date technologies. The reliable and flexible operation of BMW, including active power coordination, reactive power control, wind farm protection, and system protection, has been supported by the communication infrastructure specifically designed for this project. Figure 1 shows a high-level scheme of grid integration of BMW to the bulk power system, where information flow and energy flow among BMW, transmission system, distribution system, and generation system are summarized in an illustrative way. It can be seen that a modern power system is composed of high-power equipment and communication networks. Energy flows through the power grid to meet customer demand, while information flows through the communication system to monitor the system status, control the dynamic energy flows present in the grid, and transfer the information collected from an internet of smart devices for sensing and control across the power grid

V. COMMUNICATION SYSTEMS FOR BMW SUPERVISORY

Control and Data Acquisition Inside BMW, the wind farm SCADA system is used for data acquisition, remote monitoring, and open-loop and closedloop control for both individual wind turbines and the whole farm. BMW SCADA also provides a platform for the customer, the manufacturer (ENERCON), and the utility (BC Hydro) to access the operating state and analyze sampled event data. Moreover, authorized users can use the SCADA to modify parameters of wind energy converter (WEC) controllers, voltage control system (VCS), and so on. This feature is of special importance because wind farm controllers need to be tuned to achieve optimized performance under varying power system conditions. The closedloop control to regulate the voltage at point of interconnection (POI) is another desired SCADA feature, which coordinates wind turbine outputs and provides reactive power support for the utility system. Figure 2 shows a high-level design of the wind farm SCADA communication system and interface with external communication systems, briefly explained as follows: SCADA REMOTE: Used for remote monitoring of wind farm data. Authorized users may access the SCADA database and modify controller parameters. Process data interface (PDI): Used for exchanging real-time wind farm data with external communication systems. Grid data acquisition (GDA): Used to measure electrical variables at the point of interconnection. Substation control unit (SCU): Used for monitoring electrical states and for remote switching operation within the substation of wind farm.

VI. EXPLANATION

VCS: Used for controlling the dynamic voltage at the point of interconnection by utilizing reactive power capability of wind turbines online. METEO: Used for collecting meteorological data such as wind speed, wind direction, and temperature. The status data and measured data are transmitted by SCADA using standard formats such as OPC XML-DA or IEC 60870-5-101(or 104). BMW SCADA cyclically queries the operating and status data from wind turbines via the data bus. The SCADA calculates the average values over 10-minute, day, week, month, and year periods, together with minimum and maximum values. Status data is updated up to

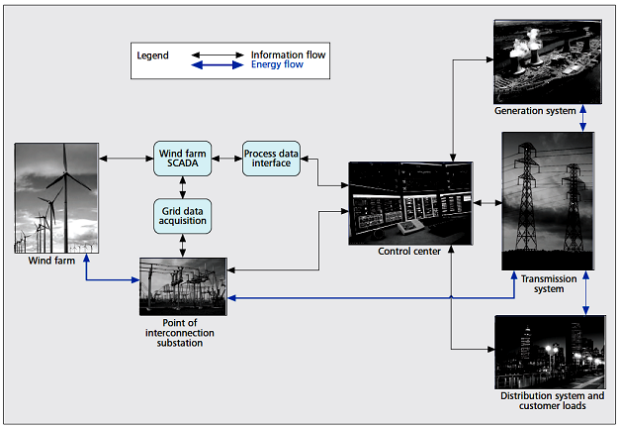

Fig. 1. Grid integration of a wind farm Photo courtesy of BC Hydro

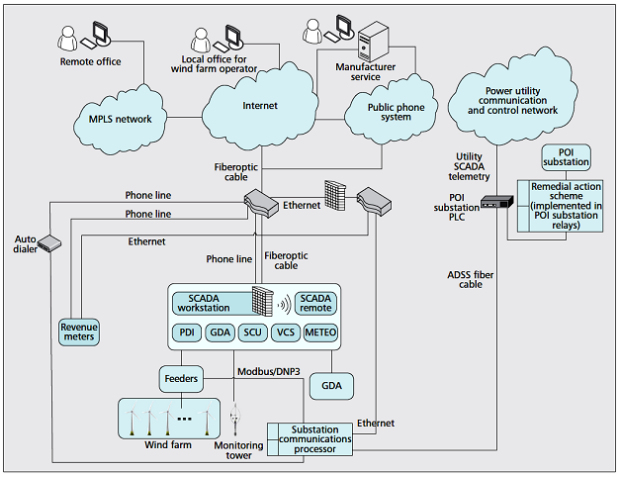

Fig. 2. A typical SCADA communication system in a wind farm.

four times per second. The internal data bus system normally uses fiber optical cables to guarantee the communication speed. When the SCADA communication system is forced out of service or control signals to/from individual wind turbine/generators are interrupted, each affected generator output will automatically default to autonomous voltage control at 15 percent of its capacity and 1.0 power factor. It should be emphasized here that the SCADA system response in the event of communication breakdowns has to be determined case by case.

VII. COMMUNICATION SYSTEM FOR POWER SYSTEM PROTECTION CONTROL AND REMEDIAL ACTION SCHEMES

The grid integration of BMW involves the construction of a new 138 kV substation at the POI. The existing 138 kV line, 1L362 between Chetwynd (CWD) and Dawson Creek (DAW), has been looped in and out of the new station and has been split into two new lines: 1L358 and 1L362. At the CWD and DAW substations, the existing protection, control, and metering devices for the old 1L362 line has been replaced with new protection and control equipment. At CWD, a remote terminal unit (RTU) using a 2400 b/s continuous SCADA channel will be installed. All protection information is transferred from SEL relays to the new RTU via a SEL 2032 Communication processor, and then sent to the utility control center from this RTU through power line carriers. To facilitate the new protection devices and transfer control/ telemetry/alarm data, new PLC systems are installed at the POI substation, CWD, DAW, and neighboring Peace Canyon substation. Another important protection system implemented for BMW is the Remedial Action Scheme (RAS) [6]. Generally speaking, the RAS is a specialized protection system that reacts to predictable power system contingencies by using preplanned control actions. The purpose of the RAS is to mitigate unwanted consequences of the initiating condition or disturbance. Unlike a traditional protection system that only protects a single unit of equipment from local faults, RAS can protect multiple equipment units located remotely from the initiating condition, and can improve reliability on a whole system level. Nowadays, power system reliabilityhighly relies on the dependable performance of theRAS; and again, the RAS functionality largely depends on the robustness of the communication systemscommunication system is designed to facilitate RAS implementation as follows. The communication channels provided for the RAS scheme consist of single mode fiber optic pairs on the ADSS line between POI and BMW. SEL 2800 series media converters are used for transmission of the Mirrored Bits information between the SEL 421 relays. Another fiber pair on the same ADSS cable is utilized for the BMW SCADA channel using the SEL 2800 series media converters. The BMW SCADA channel is crossconnected to the ETL 600 Power Line Carrier Link in the direction from CWD to GMS substation where it cross connects to the Alcatel 3600 DACS and microwave radio in the direction of Williston, which provides aggregate function for all the northern utility SCADA channels. The aggregated traffic is then directed to the utility control center. BMW data together with protection information and line telemetry data are transmitted to the system control center through ADSS fiber cable and power line carrier. Every 4 s, the data will be updated. Figure 3 illustrates part of BMWs information visualized in the Energy Management System in BC Hydros control center.

VIII. RESEARCH CHALLENGES

A. Standardization of protocols

As we can see from the above description, there are many different communication devices for different purposes in a wind farm. A uniform communication platform for monitoring, control, and operation of wind farms is needed such that the communication barriers arising from many proprietary protocols used by different manufacturers could be reduced to a minimum level [7]. Scalability and interoperability among communication equipment will minimize the maintenance effort and improve communication availability.

B. Implementation of synchronized phasor measurement

A normally overlooked technology for wind farm applications is the synchronous phasor measurement. Wind energy is highly variable and intermittent, which requires high-speed accurate power system dynamic control to counteract sudden changes in wind output. Correct real-time control relies on accurate estimation of system states, which is impossible without synchronous phasor measurement units [8]. Developing a communication framework for synchrophasors and management of the synchrophasor data will be one of the major challenges to be resolved.

C. Application of wireless technologies:

So far the grid integration of wind energy mainly utilizes wired communications such as PLC, optical fiber, and copper wires. Using wireless communications for distributed monitoring, authorization, and control may significantly improve wind generation reliability and efficiency, and reduce the life cycle cost of wind power projects.

D. Make use of full capabilities of wind farm SCADA and wind turbine reactive capability:

Many advanced applications in wind farm SCADA (e.g., VCSs) are often unexplored by utilities because of communication barriers. Developing robust two-way communications can activate these useful functions so that wind energy efficiency, control speed, and support to the grid can be greatly improved.

E. Enhance communication systems reliability:

Communication systems failure can result in limited operation of wind farms. The wind farm output may have to be reduced in order to guarantee power system reliability and safety. Therefore, high reliability of communication systems can increase the wind energy yield, which is beneficial for not only wind farm owners, but also utilities and customers.

F. Islanding detection and operation through communication systems:

Islanding detection and operation through communication systems: An electrical island forms when a portion of the power system becomes electrically isolated from the rest of the system, while it continues to be energized by wind farms or other distributed generators. An energized island may cause severe safety hazards and must be effectively detected before some control measures can be taken to fix the problem. The traditional method for islanding detection is to monitor the frequency and/or voltage drifts, which may not function properly or fast enough. Using wireless communications or PLC could be a fast and accurate means for island detection and control.

IX. COMMUNICATION SYSTEMS FOR GRID INTEGRATION OF PHOTOVOLTAIC POWER SYSTEMS

A. INTRODUCTION TO PHOTOVOLTAIC POWER SYSTEMS

The first application of photovoltaic power was as a power source for space satellites. Today, the majority of photovoltaic modules are used for utility-interactive power generation. Grid-connected solar systems are typically classified in three categories: residential, commercial, and utility scales. Residential scale is the smallest type of installation and refers to all installations less than 10 kW, usually found on private properties. The commercial capacity ranges from 10 to 100 kW, and are commonly found on the roofs of commercial uildings. Utility scale is designed for installations above 100 kW, which are traditionally ground-based installations on fields (also known as solar farms or plants).

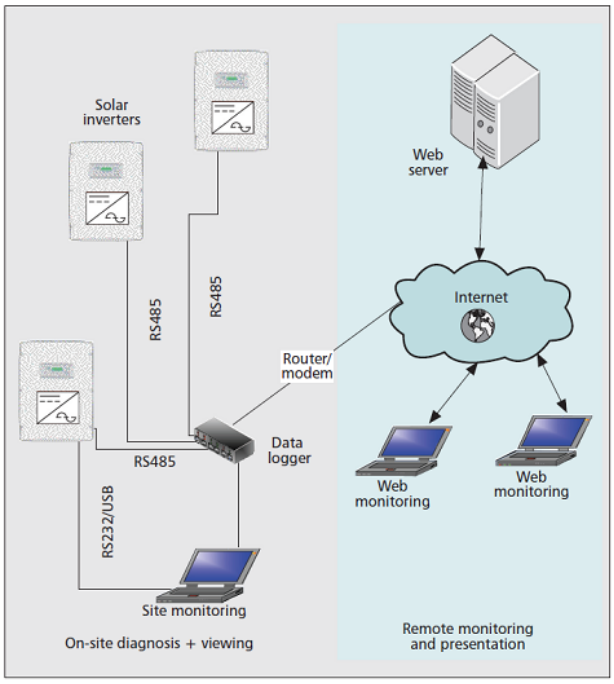

Fig. 3. A typical monitoring application of grid-tied photovoltaic power systems.

B. COMMUNICATION SYSTEMS FOR PPS SUPERVISORY CONTROL AND DATA ACQUISITION

Data acquisition was originally found in the utility scale solar power systems for monitoring connection status, real and reactive power output, and voltage at the interconnection point. With the spread of the Internet, web-based tools have been developed to give photovoltaic system owners access to the current and historical data of their systems. Since then, the communication system becomes cost-effective and applicable to small-scale power systems. As shown in Fig. 4, the monitoring interface gets electrical generation data from the inverters and transmits it to the server via the Internet. Some systems also provide sensors to collect data of ambient temperatures, solar irradiance, total generation, and usage data from the electrical panel. RS-485 is widely used as the protocol between the inverters and the data logger. Ethernet and Internet are typically the media for local and remote monitoring. An RS232 or USB interface is handy for the on-site debug, configuration, or monitoring for one-inverter systems. These systems normally monitor the following variables: the solar array power production, inverter output, inverter status, AC grid conditions, weather station data, temperature of key components, solar irradiance, and so on. The owners or operators can follow the real-time details of system operation. Some monitoring data are metering-quality and used for feed-in tariff.

C. COMMUNICATION SYSTEMS FOR PPS ADVANCED APPLICATIONS: FAULT DIAGNOSIS

A photovoltaic cell is a device that converts light energy into electrical energy. Photovoltaic cells are often encapsulated as a module. Most solar power installations are made up of several strings, each of which includes two or more photovoltaic modules. Strings are then interconnected to create an array with the desired current or power. It is shown in [9] that non-optimal conditions, such as minor shading, can cause a major reduction in solar power output of the photovoltaic array. Nonoptimal conditions are sometimes unavoidable and complicated as they are caused by many different conditions: partial shading, soiling, dust collection, cell damage, cell aging, and so on. As a result, it is very difficult to detect a non-optimal condition by reading the power output or sensing the output terminal of a photovoltaic array. A recent development is to integrate communication systems into the photovoltaic panel, sense the voltage, current, and temperature of each module, and send the information data to the monitoring interface. The solar power monitoring can be classified as three categories: system-level, string-level, and module- level. Figure 5 shows the three-level monitoring based on wireless communication systems. The system will monitor the status of solar modules, solar strings, and solar inverters based on the IEEE 802.15.4-2003 ZigBee standard. Either star or mesh topology can be used.With this wireless monitoring capability,

each solar module status is visible. In practical systems, this is very useful because most solar panels are installed in areas that are not readily accessible. Otherwise, the troubleshooting of solar modules is very difficult.

X. RESEARCH CHALLENGES

A. Power consumption of the end device:

A major challenge of photovoltaic power systems is to reduce the power dissipation losses. Power losses may be caused by non-optimal operational conditions or communication systems (e.g., wireless transmission and receiving). Developing an energy-efficient communication network for solar power integration will significantly reduce the life cycle cost of solar projects.

B. Reliability, coverage, and flexibility:

A reliable communication system is the foundation for effective photovoltaic control. Although wireless communications provide great flexibility to photovoltaic power systems control, the communication may be unreliable due to interference, shadowing, fading, and so on. Moreover the coverage of a wireless network changes dynamically in practice. These uncertainties in wireless communications can cause severe problems in photovoltaic power systems. The trade-off among power consumption, reliability, coverage, throughput, latency, and so on merit further investigation for the wireless communications used in photovoltaic power systems.

C. Addressing and localization:

A solar power system consists of many photovoltaic panels, which are vulnerable to failures and have high maintenance demands. How to identify the failed panel quickly is an interesting research topic. Similar problems exist in wireless sensor networks, where a variety of addressing and localization algorithms have been designed.Adopting those addressing and localization algorithms for the communication systems used in photovoltaic power systems could provide possible solutions.

D. Islanding detection

Photovoltaic power systems face the same challenge of island detection as wind power systems do. Using wireless communications or PLC could be a fast and accurate means for island detection and control in photovoltaic power systems

XI. CONCLUSIONS

Two-way communications are the fundamental infrastructure that enables the accommodation of distributed renewable energy generation. In this article, we review several communication technologies available for the grid integration of renewable energy resources. Since a hybrid mix of technologies will be used in the future, interoperable standards are very important. We show the Bear Mountain Wind Farm project, particularly its communication systems for supervisory control and data acquisition, as well as power protection and control. In this paper how the communication systems used in photovoltaic power systems. Distinct characteristics in integration of renewable energy resources pose new challenges to the communication systems, which merit further research and improvement of technologies.

Fig. 4. Three-level monitoring of photovoltaic power systems based on wireless communication technologies.

REFERENCES

[1] NIST, U.S. Dept. of Commerce, NIST Framework and Roadmap for Smart Grid Interoperability Standards, Release 1.0 (draft), Jan. 2010 *Home Automation using Cloud Network and Mobile Devices*,publishers Department of Computer Engineering, 44, Vidyanagari, Parvati, Pune-411009, India University of Pune,

[2] [S. Galli and O. Logvinov, *Recent Developments in the Standardization of Power Line Communications Within the IEEE,* ,IEEE Commun. Mag., vol. 46, no. 7, July 2008, pp. 6471.

[3] IEEE, P2030 Draft Guide for Smart Grid Interoperability of Energy Technology and Information Technology Operation with the Electric Power System *(EPS), and End-Use Applications and Loads, Dec. 2010.*

[4] A. J. Sguarezi Filho, M. E. de Oliveira Filho, and E. Ruppert Filho *A Predictive Power Control for Wind Energy,* ,IEEE Trans. Sustainable Energy, vol. 2, no. 1, Jan. 2011, pp. 97105.

[5] P. Zhang, , *: Bear Mountain Wind Farm,* Proc. Intl. Wksp. Wind Energy Development, Cairo, Egypt, Mar. 2010.

[6] P. M. Anderson and B. K. LeReverend *Industry Experience with Special Protection Schemes, IEEE Trans. Power Systems*vol. 11, no. 3, Aug. 1996, pp. 116679.

Reactive power compensation using pi and fuzzy controller for grid interactive cascaded pv system

Dr.N .Muralikrishnan
HOD of EEE dept
Department of Electrical and Electronics Engineering
mailam engineering college

Mr.S.Balasubramanyan
Associate professor
Department of Electrical and Electronics Engineering
mailam engineering college

Mr.M.Thirunavukarasu
pg scholar
Department of Electrical and Electronics Engineering
mailam engineering college

***Abstract*—The power mismatch from cascaded individual PV converter modules can bring in voltage and system operation issues. Reactive power mismatch occurs due to the presence of non- linear loads used in domestics, industrial and also as line parameters. This paper addresses these issues, explores the effects of reactive power compensation and optimization on system reliability and power quality, and proposes coordinated active and reactive power distribution to mitigate this issue. The relationship between power and voltage is analyzed with a wide operation range. So we implement the compensation network for the reactive power compensation. Here through comparison of two network the optimized way can be analyzed. The controlling technique used are PI and fuzzy logic controller. Compare to PI controller, fuzzy logic controller maintain the accuracy, high voltage stability and reduce the stability time of capacitor. A comprehensive control system with PI and fuzzy logic controller is designed to achieve effective power distribution and dynamic voltage regulation.**

I. INTRODUCTION

World wide renewable energy resources, especially solar energy, are growing dramatically in view of energy shortage and environmental concerns [1] [3]. Large-scale solar photovoltaic (PV) systems are typically connected to medium voltage distribution grids, where power converters are required to convert solar energy into electricity in such a grid- interactive PV system [4][14]. To achieve direct medium-voltage grid access without using bulky medium-voltage transformer, cascaded multilevel converters are attracting more and more attraction due to their unique advantages such as enhanced energy harvesting capability implemented by

distributed maximum power point tracking (MPPT), improved energy efficiency, lower cost, higher power density, scalability and modularity, plug-N- power operation, etc. [11][14]. Although cascaded multilevel converters have been successfully introduced in medium- to high-voltage applications such as large motor drives, dynamic voltage restorers, reactive power compensations, and flexible ac transformation system devices [15][28], their applications in PV systems still face tough challenges because of solar power variability and the mismatch of maximum power point from each converter module due to manufacturing tolerances, partial shading, dirt, thermal gradients, etc. In a cascaded PV system, the total ac output voltage is synthesized by the output voltage from each converter module in one phase leg, which must ful fill grid codes or requirements. Ideally, each converter module delivers the same active power to grid; hence, symmetrical voltage is distributed among these modules. However, in the event of active power mismatch from these modules, the converter module with higher active power generation will carry more proportion of the whole ac output voltage, which may result in over modulation if the system is not oversized design. In serious scenario, the synthesized output voltage may not be enough to meet the system requirement. As a result, the active power mismatch may not only result in losses in energy harvesting but also system instability and unreliability due to the inadequate output voltage or over modulation issues. Motivations are toward addressing the aforementioned issues and approaching to mitigate the negative effect of active power mismatch. In [29][31], MPPT is achieved for each module in these approaches to enhance energy harvesting. However, only unity power factor control was considered and the inherent reactive power compensation capability of the cascaded PV system is ignored. As a result, the PV system still surfers from the degraded power quality and system reliability.

It is recognized that reactive power compensation is able to provide strong voltage support in a wide range [18], [32]. Proper reactive power compensation can significantly improve the system reliability, and in the meantime help the MPPT implementation for the cascaded module under unsymmetrical condition as well as comply with the system voltage requirement simultaneously. All of these have spurred growing interest in reactive power compensation for the cascaded PV system. A reactive power compensation strategy is integrated in the control system of the cascaded PV system in [33]. However, this approach fails to consider the effect of voltage or current distortion caused by unsymmetrical active power on the power detection and distribution, and the converter module with high active power generation is not required to provide reactive power, which has limited the capability of reactive power compensation. Therefore, optimized solutions have yet

to be found and it is very critical to develop an effective reactive power compensation strategy for the grid interactive cascaded PV system. This paper proposes an reactive power compensation method using advanced controller and evaluates the effect of reactive power compensation on system reliability and power quality in the grid- interactive PV system with cascaded converter modules. A proper reactive power compensation and distribution is considered to eliminate the over modulation caused by unsymmetrical active power. In the proper reactive power management, one first emphasizes that the output voltage from the cascaded PV system must to meet the grid code. The maximum reactive power compensation will be activated to mitigate this issue once active power mismatch occurs and voltage and current distortion are detected. In this way, correct active and reactive power can be calculated, and MPPT for each module can be achieved and grid code can be met simultaneously. However, overcompensation of reactive power may be provided, which increases the system burden. Therefore, reactive power compensation among modules is optimized and redistributed considering their respective active power contribution on the premise that MPPT can be achieved and grid code is fulfilled. As a result, the system reliability will be enhanced. The rest of this paper is organized as follows. In Section II the cascaded PV system configuration is presented and a vector diagram is first derived to help illustrate the principle of active and reactive power distribution between each module. Correspondingly, the relationship between power and output voltage for each module is analysed under different conditions. A reactive power compensation algorithm (RPCA), which is inherently suitable for different types of cascaded PV system, is developed in Section III to improve system operation performance in view of point of common coupling (PCC) voltage range and MPPT implementation. Accordingly, a control system with the proposed RPCA is designed to achieve dynamic voltage regulation and optimized power distribution. The proposed reactive power compensation method is implemented in the MATLAB/ Simulink and PSIM simulation platform and a 10 kVA grid-interactive laboratory prototype. Simulation and experimental results at 2 kVA are given to confirm the validity of the proposed reactive power compensation method in Sections IV and V, respectively, followed by conclusion in Section VI.

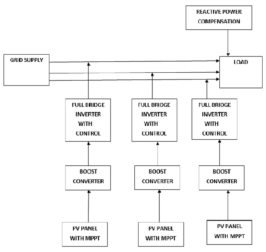

Fig. 1. Block diagram of grid connected PV system with controller.

II. SYSTEM CONFIGURATION AND POWER VOLTAGE DISTRIBUTION

A. System Configuration

Fig. 1 describes the system configuration of one two-stage grid-interactive PV system with n cascaded converter modules for each phase, which is very suitable for the medium/high voltage application. It can be immune to the leakage current and PV potential induced degradation issues. In this paper, three phase PV converters are connected in wye configuration. They also can be connected in delta configuration. The variables in Fig. 1 are defined in Table. In the two-stage PV system, the first-stage dc/dc converters with high voltage insulation can achieve the voltage boost and MPPT for the segmented PV arrays [34], [35]. The second stage three-level H-bridge converter modules are cascaded to augment the output voltage, deliver active power to grid, and provide reactive power compensation. The dc-link voltage can be controlled to be constant and the same in each converter module. For the low voltage application, single- stage system configuration can be considered, where the dc/dc converters in Fig. 1 can be replaced by Quasi-Z-Source network or be removed according to system requirement [7], [29], [30], [32]. The single-stage PV system features simple configuration and fewer devices integration in each module. However, additional methods need be developed to solve the leakage current issues. In addition, the system may need to be oversized to accommodate the wide input voltage variation [25], [30], [32]. In these configurations, unsymmetrical active power may be harvested from the cascaded modules due to PV module mismatch, orientation mismatch, partial shading, etc. In this case, improper power distribution and control are prone to an intrinsic instability problem if MPPT is still desired, which results in a limited operation range for the system [36]. Moreover, it may also seriously deteriorate the system reliability and power quality. Particularly, appropriate reactive power compensation is very helpful to improve the operation of the cascaded PV system. Considering active power is produced by PV arrays and reactivepower injection or absorption is regardless of PV arrays, one expects an independent active and reactive power control for each module. By this way, effect of reactive power compensation on system reliability and power quality can be investigated. In this paper, efforts are focused on the intelligent reactive power compensation method and optimized reactive power distribution from each module using PI and FUZZY controller.

B. Power and Voltage Distribution Analysis

In the cascaded PV system, the same ac grid current flows through the ac side of each converter module. Therefore, the output voltage distribution of each module will determine the active and reactive power distribution. In order to clarify the power distribution, four modules are selected in the cascaded PV converters in each phase as an example. Vector diagrams are derived in Fig. 2 to demonstrate the principle of power distribution between the cascaded converter modules in phase

a [14]. The same analysis can be extended to phases b and c. It means that active and reactive power will be independently controlled in each phase. Therefore, a discrete Fourier transform phase locked loop (PLL) method is adopted in this paper, which is only based on single-phase grid voltage orientation and can extract fundamental phase, frequency, and amplitude information from any signal [8]. Considering that the PCC voltage is relatively stable, vga is first used as the PLL synchronous signal of the cascaded PV system as shown in Fig. 2(a). vga is transformed into stationary reference frame quantities vga and vga which is the virtual voltage with /2 phase shift to vga . They are converted to vga d and vga q in the dq synchronous reference frame, where vga is aligned with the d-axis by PLL control [8]. Ideally, vga d is equal to the magnitude of PCC voltage Vga and vga q is zero.Once the phase-shift angle iga between vga and grid current iga is detected, the new dq synchronous reference frame can be defined. In this frame, iga is aligned with the daxis. Therefore, the daxis component vsa dof the whole PV system output voltage vsa directly decides the active power Injection. The contribution of each module output voltage on qaxis component vsa q is closely related to the reactive power compensation. illustrates voltage distribution of four cascaded converter modules under unsymmetrical active power generation in phase a. The output voltage of the total converter Vsa is synthesizedby the four converter module output voltage with different amplitude and angles. The voltage components of each module in dqframe, vja d and vja q (j = 1, 2, . . . , 4), can be independently controlled to implement the decoupled active and reactive power control. Because of the same gridcurrent through each convert module, the distributed daxis and qaxis voltage components in dq frame determine the active and reactive power distribution in these converter modules, respectively. The v1a d ¿ v2a d¿ v3a d ¿ v4a dindicates that module 1 generates the maximum active power and module 4 generates the minimum active power.The v1a q = v2a q = v3a q = v4a q reveals that the same reactive power is provided by these modules. The previous analysis further clarified the relationship between the previous voltage components and power distribution.

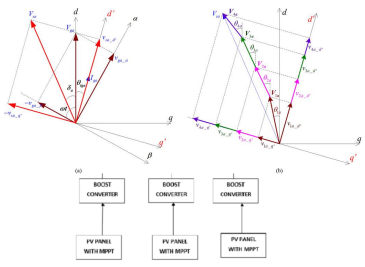

III. PROPOSED REACTIVE POWER COMPENSATION METHOD

A. *RPCA*

As aforementioned, appropriate reactive power compensation will enhance the cascaded PV system reliability and improve power quality, especially for unsymmetrical active power generation. Fig. 9 shows the proposed RPCA for the cascaded PV system in phase a. The same algorithm can be used in phases b and c. The reactive power compensation requirement Q ga is associated with modulation index of output voltage from cascaded PV converter modules, PCC voltage, and MPPT control implementation which will determine the active power reference Pga . In the initial state, MPPT control for each PV converter module is enabled and unity power factor is implemented considering symmetrical operation condition acts on these cascaded modules. In this scenario, Q ga is zero and P ga is derived from the sum of maximum active power from the individual PV arrays n j=1 Ppvja subtracting power loss, which is defined as k1Pga rated. Considering the known Pga rated, k1 can be calculated as P ga/Pga rated. It is determined bythe MPPT control and dc voltage control, which will be introduced in Section III-B. During the system operation, unsymmetrical active power may be generated from these modules due to PV module mismatch, orientation mismatch, partial shading, etc. A a result, over modulation may occur on the PV converters output voltage, especially for the converter module with higher active power output, which seriously impairs the MPPT of each module and system reliability. Once the over modulation is identified, the intentional reactive power compensation is activated to mitigate the over modulation with grid code authorization. If PCC voltage is high, maximum reactive power will be absorbed from grid to bring down the PCC voltage with the normal voltage range according to the IEEE Std. 1547, as well help possible MPPT implementation for each converter module simultaneously. k2 = 1 is designated to achieve the maximum reactive power absorption. The PV system operates like an inductor. Otherwise, the maximum reactive power is injected into grid to provide the PCC voltage support. k2 = 1 is designated to execute the maximum reactive power injection. The PV system operates like a capacitor. maximum reactive power compensation still cannot eliminate the over modulation, MPPT control will be disabled to ensure the security and stability of the cascaded PV system. Instead, reactive power compensation can be optimized, that is the selection of k2 , to reduce the risk of overvoltage or under voltage caused by the maximum reactive power compensation. There are different ways to optimize reactive power distribution in the cascaded PV converter modules [14], [33]. In either way, the limited condition as shown in (6) must be satisfied to avoid the over modulation. It is noted that the selected dc voltage and allowed voltage ripple will also impact on the reactive power compensation optimization. In this paper, the boundary condition in (6) is selected to achieve the optimized reactive power distribution, which can limit the unity modulation

voltage output for the converter module with high active power generation, even help to possible equivalent apparent power being extracted from each PV converter module. The selection of k2 is related to k1 and the level of unsymmetrical active power, which can be obtained based on Fig. 8 and (6). A specific example in Fig. 8 will be provided to demonstrate the proposed RPCA in Section II.

B. Control System Design

A cascaded PV control system with the proposed RPCA in phase a is depicted in Fig. 10. The same control system is applied

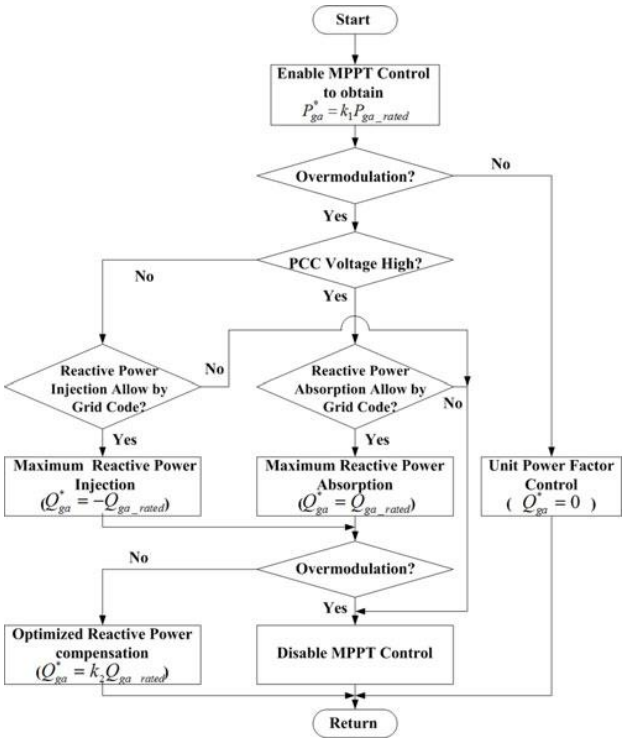

Fig. 3. Flowchart of the proposed RPCA.

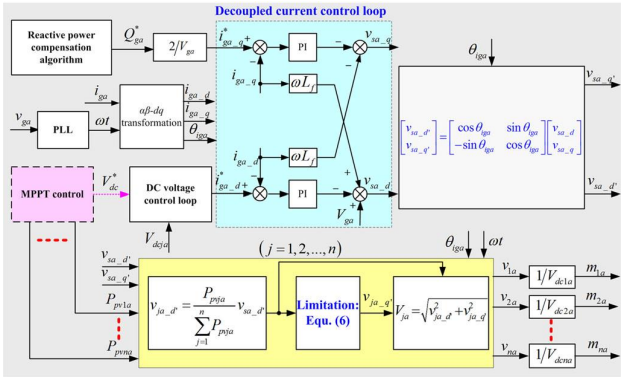

Fig. 4. Block diagram of cascaded PV control system with the proposed RPCA in phase a.

IV. SIMULATION RESULTS

In order to explore the performance of grid- interactive cascaded PV system with the proposed reactive power compensation approach, simulations were first conducted in a co simulation platform fMATLAB/Simulink and PSIM. A 3 MW/12 kV three-phase two-stage cascaded PV system as shown in Fig. 1 is applied in this paper. The system parameters in simulation are summarized . Figs. 11 and 12 illustrate the active and reactive power distribution, grid voltage and current change, voltage distribution among four cascaded PV converter modules with reactive power injection and absorption during different scenarios in phase a, respectively. Fig. 11(a) shows the power distribution with reactive power injection considering the low grid voltage. At the beginning, the MPPT control is enabled and each module harvests maximum power from the segmented PV arrays. At 0.5 s, the active power from four modules P1aP4a , changes from 50 kW to 250 kW. Active power to grid Pga increases from 200 MW to 1 MW. The grid current magnitude Iga increases from 40 A to 200 A in Fig. 11(b). The system does not need the reactive power compensation because the symmetrical active power can equalize the output voltage from these modules. There is no overmodulation, and grid current and PCC voltage have good quality as shown in Fig 11(b) and (c). The modulation indices from our modules, m1a m4a , are within [1, 1]. At 1 s, different active power is generated from the four modules due to the different irradiation. Modules 1 and 2 keep 250 kW active power output but the active power from modules 3 and 4 reduces to 50 kW, which results in big power fluctuation during transient. Moreover, the overmodulation caused by the unsymmetrical active power seriously distorts the grid current ig and degrades system operation The module indices from modules 1 and 2, m1a and m2a , are in the range [1, 1]. After 1.5 s, 1 MVAR reactive power Qga is injected to grid, which means that k2 = 1, and reactive power from four modulesQ1aQ4a is controlled to the same first. It shows that the dynamic performance of reactive power is poor, which is caused by the distorted grid current and measurement module in PSIM. By the reactive power compensation, the system returns to the steady operation although active power distribution among the four modules is still unsymmetrical. Pga keeps at 600 kW, which means that k1 = 0.6. Once the system operates in safety and steady status, the maximum active power output from the four modules can be accurately controlled and detected. The dynamic performance of grid current, PCC voltage Vga , and individual dc voltage, Vdc1aVdc4a , can be seen in Fig. 11(e). performance as shown

It takes 5 cycles to bring the system back to be stable. At 2 s, the reactive power from the four modules is redistributed and optimized to reduce the risk of over voltage. Fig. 11(f) shows the voltage and current waveforms before and after reactive power compensation optimization. The reactive power injection can improve system reliability but also increase the grid voltage magnitude Vga from 9.7 to 10 kV. In order to limit the voltage rise, the optimized reactive power injection

is reduced to 600 kVAR, that is, k2 = 0.6 which is obtained from Fig. 8. In this case, the unsymmetrical reactive power is arranged between the four modules, Q1a = Q2a = 95 kVAR and Q3a = Q4a = 220 kVAR. The filter inductor loss is also provided by the PV system. By the reactive

power optimization Vga decreases from 10 to 9.9 kV; the grid current still has good quality and total harmonic distortion (THD) is less than 5Fig. 12(a) shows the power distribution with reactive power absorption considering the high grid voltage. The same active power as ones in Fig. 11 changes in each stage. At 1.5 s, 1MVAR reactive power Qga , that is, k2 = 1, is absorbed from grid to eliminate the over modulation andQ1aQ4a is controlled to the same first. Pga keeps at 600 kW, which means that k1 = 0.6. Once the maximum active power P1aP4a is accurately captured at new steady system, Q1aQ4a is rearranged to reduce the risk of under voltage at 2 s. The reactive power absorption can improve system reliability but also lower the grid voltage magnitude Vga from 9.9 to 9.7 kV as depicted in Fig. 12(b)(f). In order to limit the voltage drop, the total reactive power injection is reduced to 700 kVAR, that is, k2 = 0.7 which is obtained from Fig. 8. In this case, optimized reactive power distribution can be derived based on (6): Q1a = Q2a = 100 kVAR and Q3a = Q4a = 230 kVAR. The filter inductor loss is provided by a grid. By the reactive power optimization, Vga increases from 9.7 to 9.8 kV, good grid current is guaranteed, and THD is less than 5

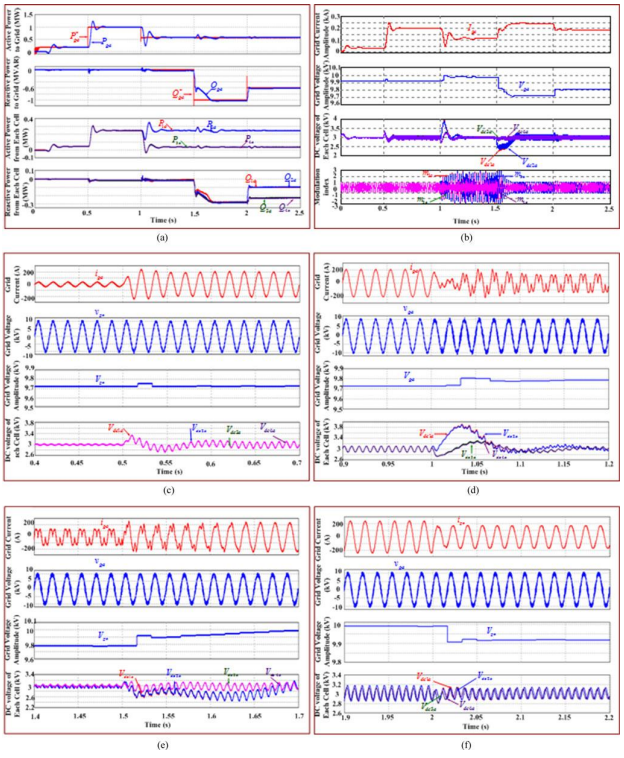

Fig. 5. simulation results

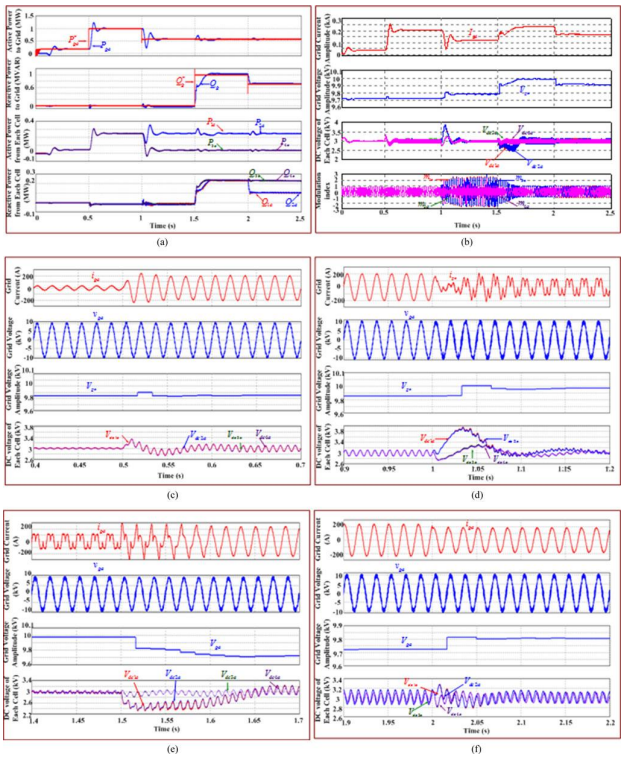

Fig. 6. simulation results

V. CONCLUSION

This paper addressed the effect of reactive power compensation on system operation performance in grid-interactive cascaded systems. The system stability and reliability issue caused by unsymmetrical active power was specifically analyzed. Reactive power compensation and distribution was introduced to mitigate this issue. The output voltage of each module was verified to directly determine the power distribution. The relationship between voltage distribution and power distribution was illustrated with a wide power change range. From the analysis fuzzy logic controller having better stability in capacitor voltage compare to PI controller. Correspondingly, the control system (with PI and fuzzy) technique gives optimized reactive power compensation which can be developed and validated by the simulation and experimental results under different scenarios. The proposed approach was demonstrated to be able to effectively enhance system operation stability and reliability, and improve power quality.

REFERENCES

[1] Y. Bo, L. Wuhua, Z. Yi, and H. Xiangning, Design and analysis of a grid connected photovoltaic power system, *IEEE Trans. Power Electron., vol. 25*, no. 4, pp. 9921000, Apr. 2010

[2] M. R. Islam, Y. Guo, and J. Zhu *A high- frequency link multilevel cascaded medium-voltage converter for direct grid integration of renewable energy systems,* ,, IEEE Trans. Power Electron., vol. 29, no. 8, pp. 4167 4182, Aug. 2014.

[3] X. She, A. Q. Huang, and X. NInteroperability *Current sensorless power balance strategy for dc/dc converters in a cascaded multilevel converter based solid state transformer,*.IEEE Trans. Power Electron., vol. 29, no. 1, pp. 1722, Jan. 2014.

[4] A. J. Sguarezi Filho, M. E. de Oliveira Filho, and E. Ruppert Filho *A Predictive Power Control for Wind Energy,* ,IEEE Trans. Sustainable Energy, vol. 2, no. 1, Jan. 2011, pp. 97105.

[5] Y. Shi, L. Liu, H. Li, and Y. Xue *: A single- phase grid-connected PV converter with minimal dc-link capacitor and low-frequency ripple-free maximum power point tracking,*in Proc. 5th IEEE Energy Convers. Congr. Expo., Denver, CO, Sep.1519, 2013, pp. 23852390.

[6] C. D. Townsend, T. J. Summers, J. Vodden, A. J. Watson, R. E. Betz, and J. C. Clare *IOptimization of switching losses and capacitor voltage ripple using model predictive control of a cascaded H- bridge multilevel STATCOM*, IEEE Trans. Power Electron., vol. 28, no. 7, pp. 30773087, Jul. 2013.

A Novel Approach of Economic Load Dispatch Problems Using Improved Atmosphere Clouds Model Optimization Algorithm

J.Ramesh
Assistant Professor
Department of Electrical and Electronics Engineering
St. Anne's College of Engineering and Technology

R.Gowtham A.Sureshkumar
UG scholar
Department of Electrical and Electronics Engineering
St. Anne's College of Engineering and Technology

S.Balamurugan
UG scholar
Department of Electrical and Electronics Engineering
St. Anne's College of Engineering and Technology

***Abstract*—The growing costs of fuel and operation of power generating units warrant improvement of optimization methodologies for Economic Load Dispatch (ELD) problems. The practical ELD problems have non-convex objective functions with equality and inequality constraints that make it much harder to find the global optimum using any mathematical algorithms. Modern optimization algorithms are often meta-heuristic, and they are very promising in solving nonlinear programming problems. This paper presents a novel approach to determining the feasible optimal solution of the ELD problems using the recently developed Atmosphere Clouds Model Optimization Algorithm (ACMOA). Many nonlinear characteristics of power generators, and their operational constraints, such as generation limitations, prohibited operating zones, ramp rate limits, transmission loss, and nonlinear cost functions, were all contemplated for practical operation. To demonstrate the efficiency and applicability of the proposed method, we study four ELD test system (IEEE 30 Bus Test Case) having non-convex solution spaces and compared with some of the most recently published ELD solution methods.**

I. INTRODUCTION

Since an engineer is always concerned with the cost optimization problem, which isdifficult to solve using the of products and services, the efficient optimum economic traditional methods. operation and planning of electric power generation system have always occupied an important position in Literature Survey: Economic dispatch (ED) is an the electric power industry. A saving in the operation of optimization problem where optimal generation for each the system of a small percent represents a significant generator is determined to minimize total fuel costs, reduction in operating cost as well as in the quantities of subject to equality constraints on power balance and fuel consumed. The classic problem is the economic load inequality constraints on power outputs. Moreover, dispatch of generating systems to achieve minimum transfer losses, generation rate changes and line flows operating cost. Traditional algorithms like lambda may also be considered. iteration, base point participation factor, gradient method A variety of techniques may be used to solve ED and Newton method can solve this ELD problems problems; some are based on classical optimization effectively if and only if the fuel-cost curves of the methods, such as linear or quadratic programming [1-2], generating units are piece-wise linear and monotonically while others use artificial intelligence or heuristic increasing. Practically the input to output characteristics algorithms. Classical techniques are highly sensitive to a of the generating units are highly non-linear, non-smooth selection of the starting point and often converge to a and discrete in nature owing to prohibited operating local optimum or even diverge altogether. LinearDirect Search methods, in contrast to more standard More recently, heuristic search techniques such as optimization methods, are often called derivative-free as particle swarm optimization (PSO) [4-6] and genetic they do not require any information about the gradient algorithm (GA) [7] have also been considered in the (or higher derivative) of the objective function when context of ED. In addition, differential evolution searching for an optimal solution. Therefore Direct algorithms were implemented to solve the ED problem Search methods are particularly appropriate for solving [8-10]. Differential evolution (DE) is a stochastic search non-continuous, non-differentiable and multimodal based method, which can present a simple structure, (i.e. multiple local optima) optimization problems, such as convergence speed, versatility and robustness. However, the economic dispatch.The main objective of this study is DE fast convergence might lead the direction of the to introduce a new Atmospheric Cloud Model search toward a local optimal and premature solution. Optimization (ACMO) [19] in the context of power system Finally, the use of harmony search (HS) method to find economic dispatch problem with a valve-point effect. the global or near global solution for the ED problem can The results are obtained from an IEEE 30 bus 5 machine be found in [11, 12]. HS is considered as a stochastic system solved with different methods in the literature. random search method, which does not need any The resulting optimal solution values are compared with information about the derivative. Nevertheless, HS has the solution values in the literature and the results are some insufficiencies associated with the premature discussed.

A. Atmosphere Clouds Model Optimization

ACMO algorithm is abstracted methods are Tabu Search (TS), Particle Swarm from the generation behavior, move behavior and spread Optimization (PSO) and Sequential Quadratic behavior of cloud in the search space. Programming (SQP) (referred to as a hybrid TS-PSO-SQP). The abstract process of ACMO algorithm is as TS is used to solve the combinatorial subproblem of the follows: UCP. In [16], the modified sub gradient (MSG) and the Firstly the whole search space is divided into many harmony search Sequential (HS) algorithms were disjoint

regions according to some rules and each combined into a single algorithm and used on 3, 5 and 6 region has its own humidity value and air pressure thermal units whose incremental fuel cost functions value;

The behavior of clouds must follow rules listed characteristics (Ex, En, He) and the droplets number n, below: where Ex (Expected value), En (Entropy) and He (Hyper Clouds can only be generated in regions whose entropy) of one cloud express the center position of humidity values are higher than one certain cloud, the cover range of cloud and the thickness of cloud threshold; respectively. Suppose there are m clouds in iteration t, the Under the action of wind, clouds move from regions expression of which is: with higher air pressure value to regions with lower air pressure value; In the moving process, the droplets of one cloud would spread or gather according to the air pressure The droplets numbers of clouds can be expressed as: difference between the region where this cloud locates before move behavior and region where cloud locates after move behavior;

where CNT function is used to do the statistics of data Line Flow Constraints: One important constrain of EED meeting requirement. The specific optimization process of problem is determinate of constrain of Line, because any ACMO algorithm is addressed in details as follows. line have a limit capability for current power, the limit can The flowchart of ACMO algorithm is shown in Fig. 1. checking after load flow for power system. Therefore, this paper discussed the solution of EED problem with line Problem Description: The main objective of ELD is to flow constraints through the application of supposed minimize the total generation cost of the power system algorithm. Its constrains can be modeled by

B. Prohibited Operating Zone Constraints

generators themselves or in the associated auxiliaries Objective Constraints such as boilers, feed pumps, etc., may cause instability in Equality Constraints: Power balance is equality certain ranges of generator power output. Consequently, constraint. In other word, the total power generation must discontinuities are produced in cost curves cover the total demand (PD) and total real power loss in corresponding to the prohibited operating zones. So, transmission lines (Ploss). The condition of equality there is a quest to avoid operation in these zones in order constrain can be expressed

zones constitute the following constraint for ED.

Environmental Objective: The atmospheric pollution Table Comparison of the optimum generator schedule, caused by the fossil fired generator contains sulfur oxides voltage and fuel costs with valve point effects (SOx), nitrogen oxides (NOx), carbon dioxide (CO2) and so on. For simplicity, the total emission of these pollutants is expressed as a sum of a quadratic and exponential function.

C. System Spinning Reserve Constraints:

Spinning reserve is the amount of synchronized generation that can be used to pickup source contingencies or load increase. The available system reserve should be at least equal to the system requirement to overcome contingencies. The system spinning reserve constraint can be formulated factor is 0.7. To demonstrate the effectiveness of the as follows: proposed algorithm, was tested and compared with Evolutionary Programming [20], Tabu Search [21], (15) Hybrid Tabu Search/Simulated Annealing [22], Improved Tabu Search [23], Improved EP [24] and Self Adaptive Differential Evolution with Augmented Lagrange Multiplier Method [25] based on fuel cost characteristics where Si is the spinning reserve of unit i; SR is the system like the valve point effect. spinning reserve requirement; Simax is the maximum spinning reserve contribution of unit i; is the set of all Cost Function with Valve Point Effect: In a steam turbine online units and is the set of units with prohibited zones. with multi stage inputs by a number of valves, the cost Note that for unit with prohibited operating zones, these curve is not smooth. Fuel cost calculated using the zones strictly limit the unit to regulate system load quadratic cost curve will not be accurate as it considers because load regulation may result in its falling into a the curve a smooth one. A sine function is added with the certain prohibited operating zones. As a result, a unit quadratic function to take into account the effect of valve which has prohibited operating zones does not contribute points

raphics[width=0.45] 01

Fig. 1. flow chart

II. RESULTS AND DISCUSSION

The efficiency of the ACMO based method is tested It is lower than the cost reported in the recent literatures on IEEE-30 bus system. The algorithm is coded in shown in references. MATLAB 7.8 environment. A Core2 Duo processor based The line flows under non smooth cost functions are PC is used for the simulations. The base load condition also shown in Table 2. The respective MVA flow of each is taken for the simulation and the system bus and line line with its corresponding MVA rating is also given in data are obtained from standard test case archive. The this table. Figure 2 shows that the algorithm has algorithm is run for 50 iterations with population of 100, converged to a better result and stays in the optimal fuel number of droplets in one cloud of 50 and the threshold

It is recognized that reactive power compensation is able to provide strong voltage support in a wide range [18], [32]. Proper reactive power compensation can significantly improve the system reliability, and in the meantime help the MPPT implementation for the cascaded module under unsymmetrical condition as well as comply with the system voltage requirement simultaneously. All of these have spurred growing interest in reactive power compensation for the cascaded PV system. A reactive power compensation strategy is int to eliminate the over modulation caused by unsymmetrical active power. In the proper reactive power management, one first emphasizes that the output voltage

$$P_j \in \begin{cases} P_{j\min} \le P_j \le P_j^{LB_z} \\ P_j^{UB_{z-1}} \le P_j \le P_j^{LB_z} \\ P_j^{UB_*} \le P_j \le P_{j\max} \end{cases} \quad j = 1,2,\ldots,N_g$$

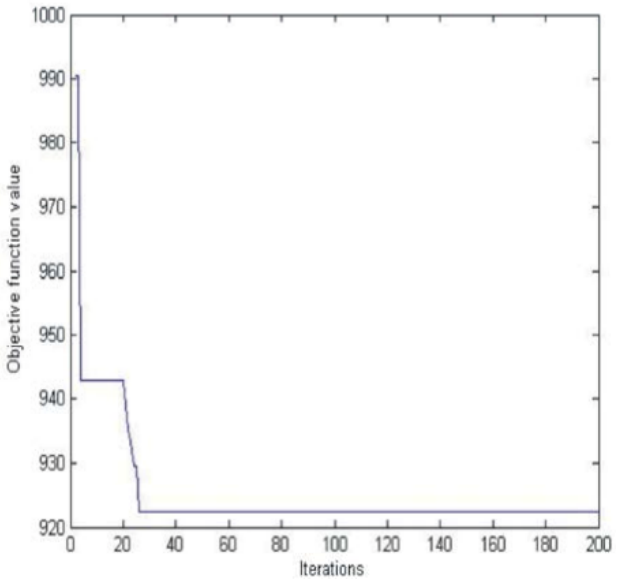

Fig. 2. Convergence of ACMO with valve point effect

from the cascaded PV system must to meet the grid code. The maximum reactive power compensation will be activated to mitigate this issue once active power mismatch occurs and voltage and current distortion are detected. In this way, correct active and reactive power can be calculated, and MPPT for each module can be achieved and grid code can be met simultaneously. However, overcompensation of reactive power may be provided, which increases the system burden. Therefore, reactive power compensation among modules is optimized and redistributed considering their respective active power contribution on the premise that MPPT can be achieved and grid code is fulfilled. As a result, the system reliability will be enhanced. The rest of this paper is organized as follows. In Section II the cascaded PV system configuration is presented and a vector diagram is first derived to help illustrate the principle of active and reactive power distribution between each module. Correspondingly, the relationship between power and output

III. CONCLUSION

In this work, a new nature inspired algorithm is economic dispatch optimization with generator implemented for the ELD problem. The numerical results constraints, Energy Conservation and Management, clearly show that the proposed algorithm gives better results. The ACMO optimization algorithm outperforms 9. Noman, N. and H. Iba, Differential evolution the recently reported algorithms. The strength of the for economic load dispatch problems, Electrical algorithm is proved with the non smooth objective Power System Research, functions,

REFERENCES

[1] Adler, R.B. and R. Fischl, 1977. Securityconstrained economic dispatch with participation factors based on worst case bus load variations ***IEEE Transaction on Power Apparatus Systems, 96(1): 347-56.***

[2] Bui, R.T. and S. Ghaderpanah, 1982 ***Bui, R.T. and S. Ghaderpanah, 1982. Real power rescheduling and security assessment*** **IEEE Transaction on Power Apparatus Systems, PAS 101(1): 2906-2915. . Power Electron., vol.29, no. 8, pp. 4167 4182, Aug. 2014.**

[3] Pancholi, R.K. and K.S. Swarup, 2004. ***Pancholi, R.K. and K.S. Swarup, 2004. Particle swarm optimization for security constrained economic dispatch,.*** **IEEE Trans. Power Electron., vol. 29, no. 1, pp. 1722, Jan. 2014.**

[4] A. J. Sguarezi Filho, M. E. de Oliveira Filho, and E. Ruppert Filho ***A Predictive Power Control for Wind Energy,*** **,IEEE Trans. Sustainable Energy, vol. 2, no. 1, Jan. 2011, pp. 97105.**

[5] Y. Shi, L. Liu, H. Li, and Y. Xue ***: A single- phase grid-connected PV converter with minimal dc-link capacitor and low-frequency ripple-free maximum power point tracking,*** **in Proc. 5th IEEE Energy Convers. Congr. Expo., Denver, CO, Sep. 1519, 2013, pp. 23852390.**

Online Fault Diagnosis of Motor Bearing via Stochastic-Resonance-Based Adaptive Filter in an Embedded System

J.Ramesh
Assistant Professor
Department of Electrical and Electronics Engineering
St. Anne's College of Engineering and Technology

N. Praveenraj
UG Scholar
Department of Electrical and Electronics Engineering
St. Anne's College of Engineering and Technology

***Abstract*—Digital signal processing algorithms are widely adopted in motor bearing fault diagnosis. However, most algorithms are developed on desktop platforms, and their focus is on the analysis of offline captured signals. In this paper, a simple and easily implemented algorithm running on an embedded system is proposed for the online fault diagnosis of motor bearing. The core part of the algorithm is a stochastic-resonance-based adaptive filter that realizes signal denoising and adaptation of the filter coefficient. Processed by the filter, the period of the purified signal is obtained, and then the fault type of the motor bearing is identified. The proposed method has distinct merits, such as low computational cost, online implementation, contactless measurement, and availability for various speed motors. This paper provides a simple, flexible, and effective solution for conducting motor bearing diagnosis on an embedded/portable device. The algorithm proposed is validated by a brushless dc motor and a brushed dc motor fabricating with defective/healthy support bearings.**

Index TermsAcoustic signal processing, adaptive filters, ball bearings, brushless motors, dc motors, digital signal processing, embedded software, fault diagnosis, optimization methods, stochastic resonance (SR).

I. INTRODUCTION

EARING is a vulnerable key component of a rotating motor that usually works in harsh environments, such as strong vibration, humidity, high temperature, and dust. A liter- ature survey indicates that almost Manuscript received July 10, 2015; accepted January 14, 2016. This work was supported in part by the Natural Science Foundation of Anhui Province under Grant 1608085QE110, in part by the National Natural Science Foundation of China under Grant 11274300 and Grant 51475441, and in part by the Program for New Century Excellent Talents in University under Grant NCET-13-0539. This paper was recommended by Associate Editor G. Biswas.methods include motor current signature analysis [6], vibra- tion monitoring [7], [8], temperature measurement [9], and acoustic measurement [10]. These methods have successfully diagnosed/isolated different types of bearing faults in many kinds of motors, such as induction motor [11], permanent magnet synchronous motor, brushless dc motor (BLDCM), and brushed dc motor (DCM) [12]. In principle, when a fault occurs in a bearing, the fault-induced signatures can be revealed by analyzing the measured current, vibration, or acoustic signals through digital sig- nal processing techniques, such as envelope analysis [13], empirical mode decomposition (EMD) [14], wavelet analysis [15], [16], and stochastic resonance (SR) [17][19]. However, the undesired noise from the running machine and the background environment may disrupt the weak and transient signature gained from the defective bearing. Therefore, signal filtering is often used as a preprocessing tool to purify the acquired noisy signal [20], [21]. However, several parameters need to be configured manually in the sophisticated procedures of the current filtering algorithms. For instance, a wavelet filter is used for denois- ing in bearing prognostic applications [22], but the optimum wavelet and threshold should be selected on the basis of a spe- cific signal. An EMD-based filter is used to extract signatures from the defective signal [23], but the selection of the effec- tive intrinsic mode functions (IMFs) needs priori knowledge. Correlation filtering method was introduced for transient mod- eling and parameter identification in the rotating machine fault diagnosis application in [24], but the automatic selection of a suitable model still requires improvement. A filtering process that uses advanced notch filters to remove constant frequency components present in the current of an induction motor was proposed for induction motor diagnosis [25]. However, the sophisticated time-frequency (TF) features related to the struc- tural fault should be recognized and affirmed by the human eye. Recently, several SR-based signal filtering approaches have been studied [7], [10], [20], [26], but several issues on online bearing fault diagnosis have yet to be addressed. For instance, the method in [10] cannot be used in a system with high sampling frequency nor with insufficient sampled points. The method in [7] requires a priori knowledge related to the deepest signal decomposition level and adequate computing resources to achieve multiobject optimization. The method in [26] cannot process nonstationary, amplitude-modulated signals such as defective bearing signals.n summary, the abovementioned filters, including finite

split into two first-order ones as

impulse response (FIR), infinite impulse response (IIR), wavelet-based, EMD-based, and SR-based filters, are either sophisticated or developed and implemented on a desktop

dy dz dt = z, dt

= ay by3 z + x(t). (3)

platform that provides adequate computing resources for executing the complex operations, such as convolution, Fourier transform, and TF transform. Computational resources are limited in middle- and small-sized electrical machines. Therefore,

II. SR-BASED FILTER

SR is a nonlinear phenomenon which is described as a particle that oscillates within a bistable potential in the presence of noise and periodic force, and the weak periodic particle

Fig. 1 indicates that the SNR decreases with the increase

where mean(DZCP) =
1

III. SR-BASED ADAPTIVE FILTER

A. *Concept of the SRAF*

As indicated in Section II, the filtering effect of the SR-based filter can be improved by tuning the injected noise intensity. However, noise is usually involved in the acquired/sampled signal in advance in practice. Alternatively, the SRAF can be achieved by tuning the parameters of the filter [26], as illustrated in Fig. 2. In this regard, the SR filter is responsible for signal denoising, and the adaptive algorithm added in the feedback route of the adaptive filter is used to tune the filter coefficients until the optimal output signal is achieved.

B. *SRAF Indicator*

The SRAF processes the input noisy signal and outputs the purified signal. The denoising effect is dominated by the filter parameters for the existing noisy signal. Therefore, an indicator is needed to construct the optimal SRAF through which the noisy signal is purified to an extreme. The most com- monly used indicator is the SNR in the research of SR-based filters [7], [26]. However, the calculation of SNR requires the exact frequency of the target signal as shown in (7), and such a demand is hardly satisfied in practice. Therefore, a new indi- cator, denoted as the SRAF indicator (SRAFI), is proposed to evaluate the purity of the SRAF output signal in this paper in Algorithm 1 [30]. Indeed, the SRAFI reflects the regularity of the periodic- ity of the output signal. That is, a smaller SRAFI obtains better periodicity of the signal (SRAFI = 0 for a pure single-frequency sinusoid).

C. *SRAF Parameter Selection*

SRAFI is a function of parameters (a, b, h, and , which are all subject to +). The optimal output can be achieved according to the following objective function: a, b, h, arg min SRAFI(a, b, h,) (8)

where ()* is the corresponding optimal value. The proposed algorithm can finally be implemented in the embedded system, and fixing several parameters can improve computational efficiency. For simplicity, both a and b are set to 1 in this paper. Then, the optimization problem becomes h, arg min SRAFI

in D for the linear IIR filter. However, the SR-based filter generates a nonmonotonic SNR curve. That is, the SNR first increases and reaches the maxima, and then decreases with the continuous increase in D. Nevertheless, the output SNR can be improved with the help of proper noise [29]. Such a distinct noise-assisted feature benefits weak signal detec- tion, especially when the target signal frequency is involved in the noise bandwidth SNR of the SRAF output signal is also calculated and plotted in Fig. 3. The SRAFI curve shows a nonmonotonic tendency with the increase in h or . This result indicates that the minimal SRAFI can be obtained by tuning the parameter h or . Moreover, the tendency of SRAFI is approximately opposite that of SNR, which confirms that the minimal SRAFI (which corresponds to the maximal SNR) represents the purest out- put signal with the least noise interference. Fig. 3 shows that both h and can be adjusted to generate the minimal SRAFI value. Tuning only one parameter (h or) is more efficient than tuning both (h and). Subsequently, a study is conducted to assess the parameter to be selected. We search the optimal value of the varying parameter that yields the minimal SRAFI value under differ- ent driving frequencies (25 to 250 Hz). The results with error bars are plotted in Fig. 4 (100 independent realizations for each point). The increase in parameter h shows better linearity with the increase in driving frequency compared with the increase in parameter . Furthermore, the overall error bars in Fig. 4(a) are shorter than those in Fig. 4(b), and this observation means that the parameter h is stable in the parameter-tuning process. According to the above analysis, parameter h is tuned and parameter is fixed to 0.5 for conve- nience. Finally, this paper considers the following simplified optimization problem:

D. *Parameter Optimization Algorithm*

To accelerate the parameter searching speed, a commonly used 1-D search method called the advance and retreat opti- mization (ARO) algorithm is applied in this paper. The ARO flowchart is shown in Algorithm 2. Using the ARO algorithm, the optimal calculation step h* that generates the minimal SRAFI can be obtained

E. *Performance Evaluation*

In this section, a simulation study is conducted to evaluate the performance of the proposed SRAF. The parameters are configured as fs = 5 kHz, fd = 100 Hz, AGWN = 10 dB, h0 = 0.02, l = 0.002, and = 0.0005. As demonstrated in Fig. 5(a), from t = 0 to t = 5 s, the sinusoid is blurred by the injected AWGN [zoomed-in view is plotted in Fig. 5(b)]. At the t = 5 s moment, the SRAF is triggered, and then major- ity of the high-frequency noise is wiped out immediately [see corresponding time-frequency distribution (TFD) in Fig. 5(e)]. However, h has yet to reach the optimal value, and thus the ZCP interval T 1 , T 2 , and T 3 are apparently unequal. Therefore, the output signal

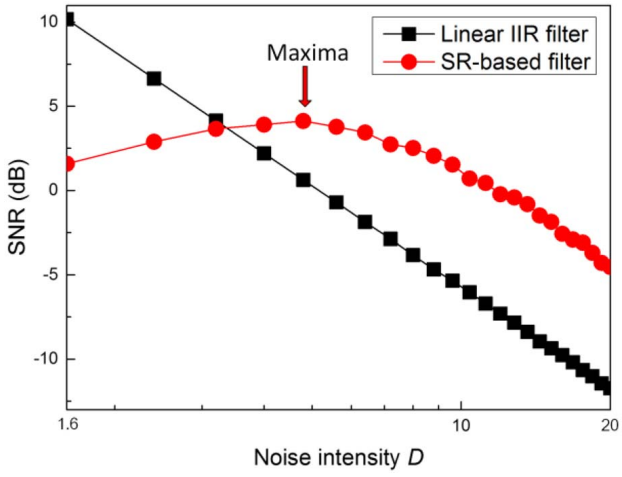

Fig. 1. filter effect

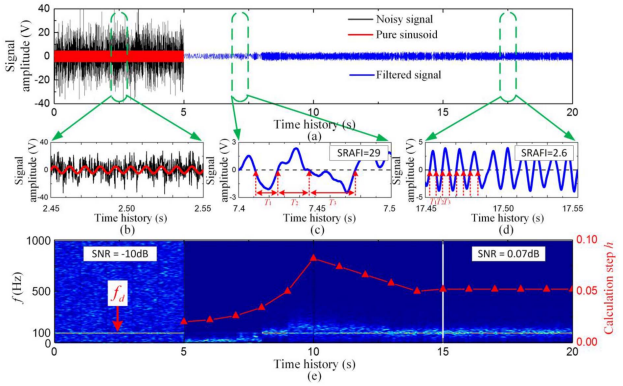

Fig. 2. srafi

is unstable in this stage, as confirmed in Fig. 5(c). Processed by the ARO algorithm, the optimal step h* is obtained, and finally the purified output signal is shown in Fig. 5(d). The sinusoid is almost recovered from the noisy signal as T1 T2 T3 . Fig. 5(c) and (d) shows lated SRAFIs for different stages. A small SRAFI represents

IV. SRAF FOR MOTO R BEARING FAU LT DIAGNOSIS

A. Online Signal Demodulation

Generally, when a fault appears in a bearing, the colli- sion among the outer raceway, the inner raceway, the rolling element, and the cage induces the periodic impulses that can be detected in the acquired vibration or acoustic sig- nal. If the period of the fault-induced impulses can be measured, the fault type of the bearing can be determined. However, the machine vibration frequency is modulated by the fault-induced impulse signal. Therefore, demodulation or

enveloping is usually applied to the acquired signal to better reveal the periodicity of the impulses [31]. Commonly used demodulation techniques include the Hilbert transform (HT)

(2h + l) will all be wiped out when a low-pass filter with a cutoff frequency lower than (2h 2l) is applied on U (t). Therefore, the filtered signal is obtained as

and the TeagerKaiser energy operator (TKEO) [32]. HT is

a complex convolution algorithm, and TKEO is sensitive to the dc component of the signal. In this regard, these two demod-

U (t) = low pass filtering 2 2 2

U (t)

ulation methods are unsuitable for fast online applications.

= Al Ah cos (l t) + 2CAl Ah cos(l t) + C Ah

2 2

Therefore, an online enveloping method called the squaring and low-pass filtering envelope (SLPFE) method is introduced to demodulate the acquired signal, as introduced as follows.

= Ah (Al cos(l t) + C) . (13) Finally, the square root of the filtered signal is computed, and the envelope signal is achieved as

First, a standard modulated signal U(t), which is the product of a low-frequency signal Ul (t) and a high-frequency carrier

Ue (t) = sqrt U (t)

= Ah (Al cos(l t) + C). (14)

enveloping is usually applied to the acquired signal to better reveal the periodicity of the impulses [31]. Commonly used demodulation techniques include the Hilbert transform (HT)

(2h + l) will all be wiped out when a low-pass filter with a cutoff frequency lower than (2h 2l) is applied on U (t). Therefore, the filtered signal is obtained as

and the TeagerKaiser energy operator (TKEO) [32]. HT is

a complex convolution algorithm, and TKEO is sensitive to the dc component of the signal. In this regard, these two demod-

U (t) = low pass filtering 2 2 2

U (t)

ulation methods are unsuitable for fast online applications.

= Al Ah cos (l t) + 2CAl Ah cos(l t) + C Ah

2 2

Therefore, an online enveloping method called the squaring and low-pass filtering envelope (SLPFE) method is introduced to demodulate the acquired signal, as introduced as follows.

= Ah (Al cos(l t) + C) . (13) Finally, the square root of the filtered signal is computed, and the envelope signal is achieved as

First, a standard modulated signal U(t), which is the product of a low-frequency signal Ul (t) and a high-frequency carrier

Ue (t) = sqrt U (t)

= Ah (Al cos(l t) + C). (14)

signal Uh (t), is expressed as

B. Variable Frequency Signal Detection

As indicated in Section III, the SRAFI can reach the mini- mal value (denoted as SRAFI-min) only when the calculation step is configured to be matched with the driving frequency.

1 2 2

1 2 2

Once h* is configured, the SRAFI value fluctuates in a narrow

= 2 Al Ah [1 + cos(2l t)] + 2 Al Ah cos(2h t) 1 2 2 + 4 Al Ah [cos((2h 2l)t) + cos((2h + 2l)t)] + CAl A2 [cos((2h + l)t) + cos((2h l)t)] 2 2 2 2

range centered at SRAFI-min because the defective bearing signal is nonstationary. However, if the motor rotating speed changes, the driving frequency of the acquired bearing sig- nal changes as well. In this case, the original h* becomes unsuitable for the present signal and the SRAFI al, h ¿¿ l . Under this circumstance, the frequency components 2h , (2h 2l), (2h + 2l), (2h l), and

V. EXPERIMENTAL VERIFICAT ION AND DISCUSSION

A. Hardware System

To verify the effectiveness of the proposed method, two motor bearings with localized faults and one healthy bearing are tested in this section. The hardware system for algo- rithm implementation is illustrated in Fig. 7. The bearing signal is recorded in an acoustic form by a microphone (INV 9206, COINV Inc.). The signal conditioner consists of an operational amplifier MAX9632

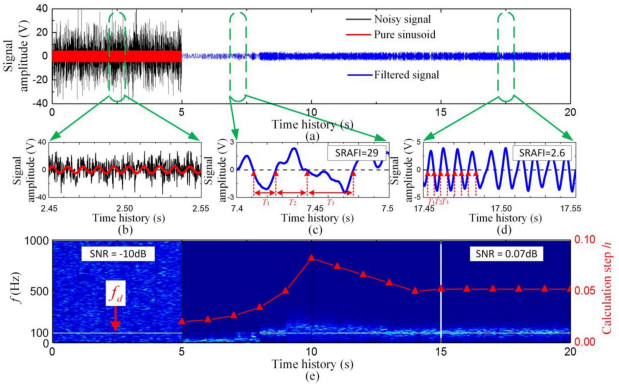

Fig. 3. time history

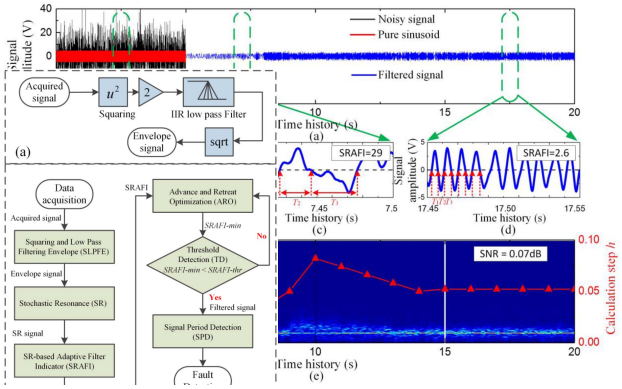

Fig. 4. algorithm

(Maxim Inc.) and an IEPE module that provides the 4 mA current source for the microphone. A 16-bit serial output, analog-to-digital con- verter type of MAX1300 (Maxim Inc.) acquires and quantizes the sound pressure signal. To balance the general-purpose input/output ports, the memory, the computational load, the two 32-bit micro controller units (MCUs) featured with float point units, and the digital signal processor instructions are allocated for the algorithm implementation. MCU1 of the type STM32F407VGT6 (STMicroelectronics Inc.) operating at 168 MHz runs the SLPFE and the SR algorithms. The results

B. Experimental Setup

In accordance with this principle, a threshold detection (TD) strategy is introduced in this paper to automatically inspect the variation of the rotating speed. Specifically The experimental

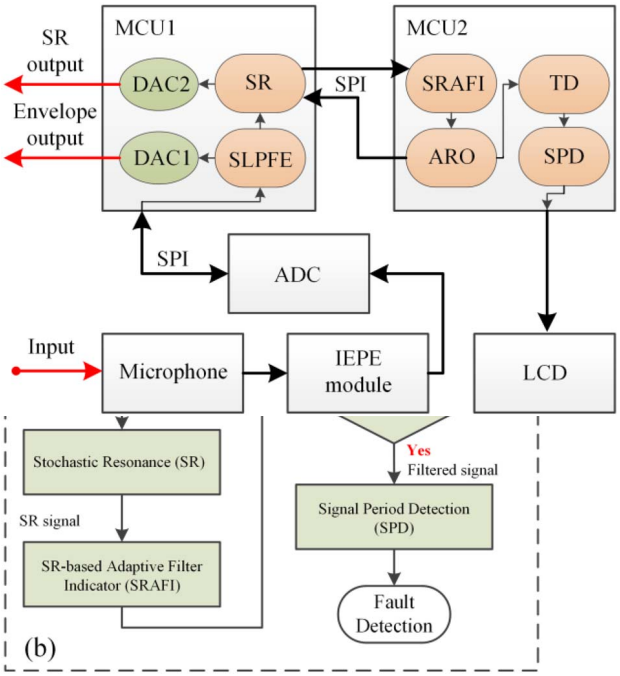

Fig. 5. block diagram

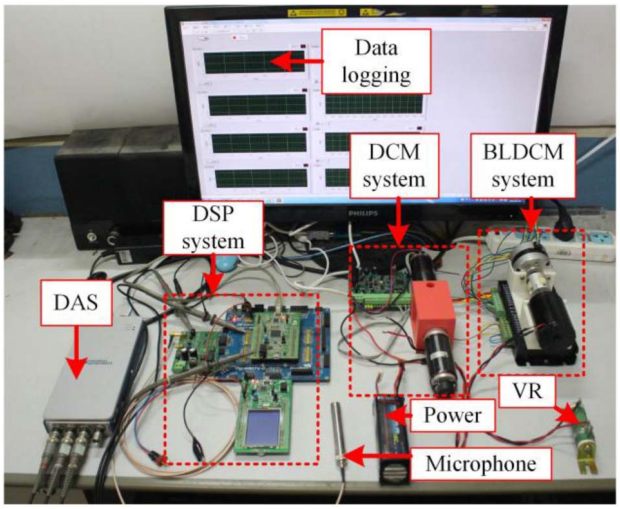

Fig. 6. hardware

setup is shown in Fig. 8. The acquired raw signal, the envelope signal, and the SRAF output signal are recorded by a data acquisition system with the combined types of NI-9234 plus NI cDAQ-9181 (National Instruments Inc.). The sampling frequency is set to 25.6 kHz in the experiment. These data are logged and stored in a PC for analysis and display. The two motor systems of DCM and BLDCM systems that fabricate the defective/healthy support bearings are tested separately. Moreover, a variable resistance (VR) configured at 50 is used separately as the electrical load for the two tests.

C. . Case Study:

used in the present and the following experiments. The pro-files of the fault-induced impulses can be recognized after signal envelope and low-pass filtering, and the characteris- tic frequency fBPFI is emphasized in the spectrum. However, the noise interference remains obvious in both time and fre-

nr fr D1

fBPFI = 2

1 + cos 2

(15)

quency domain, and it could affect the automatic diagnosis of the bearing. In comparison, the outputs of the SRAF are

D. Case Study: Healthy Bearing in DCM

The above two sections reveal the SRAF performance in enhancing the periodic fault signal. In practice, most bear- ings work in healthy conditions, and the fault detection algorithm should not give a fault alarm in this case. To examine the robustness of the SRAF algorithm, a healthy bearing fabricated in the DCM is tested, and the results are demonstrated in Fig. 13(a)(f). The shaft speed is set to 2400 rpm, and the shaft

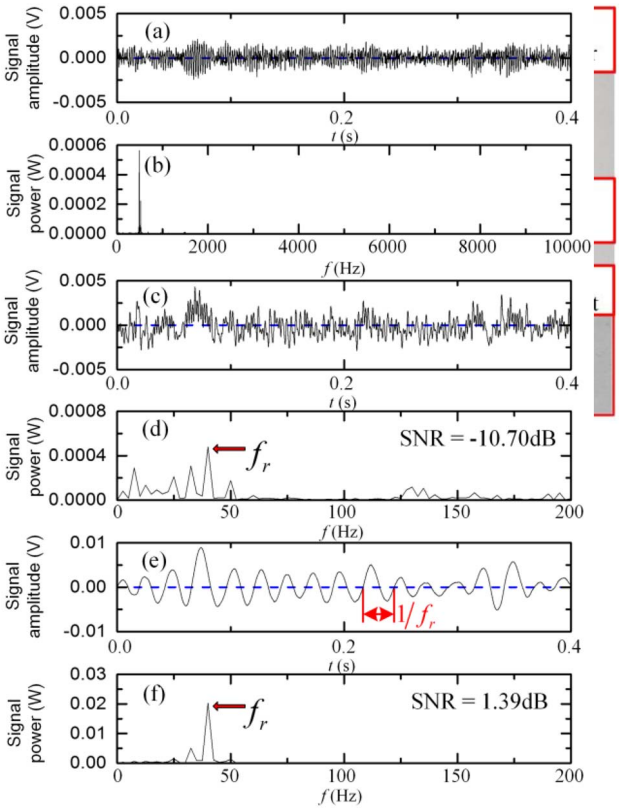

Fig. 7. hardware

frequency fr is 40 Hz. Fig. 13(a) indi- cates that the signal amplitude is relatively lower than that in the fault bearings [Fig. 12(a) and (g)]. The spectrum in Fig. 13(b) shows that the system resonance band is located at around 500 Hz. For the envelope signal spectrum, the shaft frequency fr has higher energy than other frequency com- ponents. Fig. 13(e) and (f) shows the SRAF output signal and spectrum, respectively. The noise is filtered out, and the fr is automatically retained. The above experimental results can be summarized as follows: 1) when a fault exists in the

fBPFO = 2

1 cos 2

. (16)

bearing, the SRAF amplifies the periodic fault-induced char-

In this test, the initial rotating speed is set to 2000 rpm, and later the motor accelerates to 4000 rpm. Accordingly, the fBPFO calculated using (16) shifts from 72 to 144 Hz. Fig. 12(a)(f) shows the raw signal, the envelope signal, and the SRAF output signal together with the corresponding spec- tra at 2000 rpm. Clearly, the periodicity of the purified signal shown in Fig. 12(e) is regular and clear, and these charac- teristics enable the bearing fault frequency to be estimated immediately according to the interval of the impulses even though the fault-induced impulses are blurred by the noise [Fig. 12(a)]. Similarly, the results at the 4000 rpm working condi- tion are exhibited in Fig. 12(g)(l). The proposed method shows a stable capacity to extract the periodical weak signal from the background noise in different working conditions. The advanced SNRs for these two conditions are 9.34 and 10.98 dB, respectively. Fig. 12(m) shows the iterations of parameters h and the SRAFI, and the horizontal threshold line of SRAFI-thr = 100. Both SRAFI-min values for 2000 and 4000 rpm are below the SRAFI-thr. However, once the rotat- ing speed changes, the SRAFI increases because the original h* is unsuitable for the present signal. In this case, the MCU detects the overflow of SRAFI with respect to SRAFI-thr, and then resets the ARO algorithm to search for another h*, as indicated in Section IV-B. Moreover, the online calculation step h, the period, and the frequency of the SRAF output

acteristic frequency and 2) when the bearing has no fault, the SRAF tends to amplify the periodic shaft frequency containing higher energy to other frequency components. Fault detection (whether a fault exists or not) and fault isolation (the kind of fault in the bearing) can be accomplished using the designed SRAF algorithm [33], [34]. To verify if the proposed method triggers no false alarm, a test is conducted in which

where nr is the number of rollers, fr is the rotating frequency of the shaft, D1 and D2 are the diameters of one rolling element and the pitch diameter of the bearing, respectively, and is the bearing contact angle (= 0 for this bearing). In this test, the rotating speed is set to 2500 rpm, and the fBPFI is calculated as 184.4 Hz. Fig. 10(a) shows the acquired signal from the bearing with an inner raceway fault. The fault-induced impulses corrupted by the background noise are barely seen in the waveform. Fig. 10(b) presents the power spectrum of the raw signal, which shows that the resonance peak of the machine is located at around 5200 Hz. However, the defective frequency cannot be measured from the sideband of the peak because of the significant noise interference. Fig. 10(c) and (d) shows the demodulated signal and the corresponding spectrum, respec- tively, processed by the SLPFE algorithm. A third-order Butterworth low-pass filter with cutoff frequency of 300 Hz is

more favorable than those of the envelope, as indicated in Fig. 10(e) and (f). In particular, the interval of the demodulated impulses can be measured directly from the waveform through zero crossing detection. The power spectrum also confirms that the characteristic frequency fBPFI plays the dominant role and provides undeniable evidence that the bearing fault occurs in

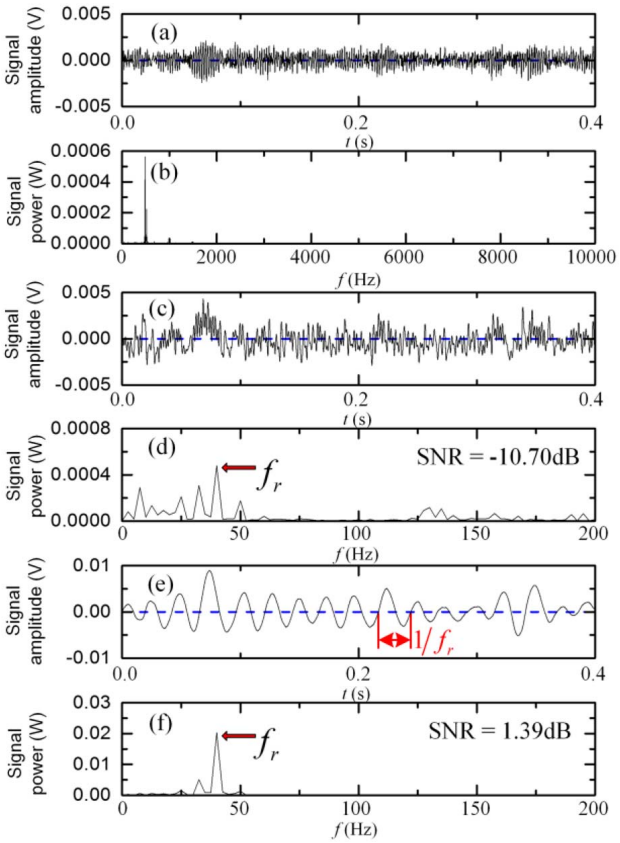

Fig. 8. output

the inner raceway. The iterations of the adjustable parameter h and the corresponding SRAFI are presented in Fig. 10(g). The SRAFI tends toward stability after several iterations, and h* finally converges to 0.124. The advanced SNR is 7.36 dB, which indicates the signal enhancement capacity of the SRAF

VI. Case Study: Bearing Fault Detection in DCM

where CNT function is used to do the statistics of data Line Flow Constraints: One important constrain of EED meeting requirement. The specific optimization process of problem is determinate of constrain of Line, because any ACMO algorithm is addressed in details as follows. line have a limit capability for current power, the limit can The flowchart of ACMO algorithm is shown in Fig. 1. checking after load flow for power system. Therefore, this paper discussed the solution of EED problem with line Problem Description: The main objective of ELD is to flow constraints through the application of supposed minimize the total generation cost of the power system algorithm. Its constrains can be modeled by

A. Prohibited Operating Zone Constraints

generators themselves or in the associated auxiliaries Objective Constraints such as boilers, feed pumps, etc., may cause instability in Equality Constraints: Power balance is equality certain ranges of generator power output. Consequently, constraint. In other word, the total power generation must discontinuities are produced in cost curves cover the total demand (PD) and total real power loss in corresponding to the prohibited operating zones. So, transmission lines (Ploss). The condition of equality there is a quest to avoid operation in these zones in order constrain can be expressed

B. Comparison With Other Methods

In this section, the proposed method is compared with the other established methods to investigate its computational efficiency. The comparative methods are the EMD-based envelope spectrum analysis method (EMD method for short) and the IIR filter. The details of the EMD method are in [35]. The IIR filters are the third-order Butterworth band-pass filters with fixed bandwidths but with variable lower and upper cutoff frequencies. The bandwidth is set to 50 Hz, with the range of the : A criterion, which can be SNR, LMS, or information entropy, needs to be added to the feed- back route of the adaptive filter to guide the algorithm and to obtain the optimal filter coefficients [39]. In this paper, the proposed criterion SRAFI is calculated on the basis of the evaluation of signal regularity. In other words, the opti- mal output signal should have good periodicity because the input signal is periodical. Therefore, the SRAFI converges to a small value. To its vital merit, SRAFI requires no priori knowledge related to the signal structure or any desired reference signals. In this regard, the proposed algorithm based on the SRAFI is data driven, and this merit makes the algorithm pragmatic in application. Nevertheless, the work described here depends mainly on emulational and experimental ver- ification. More efforts should be made to obtain a deeper insight into the nonlinear SRAF (e.g., convergence condition, stability, and parameter selection). From another aspect, more experiments should be performed to evaluate the robustness of the algorithm (e.g., applying this method to diagnose bear- ing fault/health of a high-power industrial motor subjected to strong interference in a field trail). These works will be continued in the future.

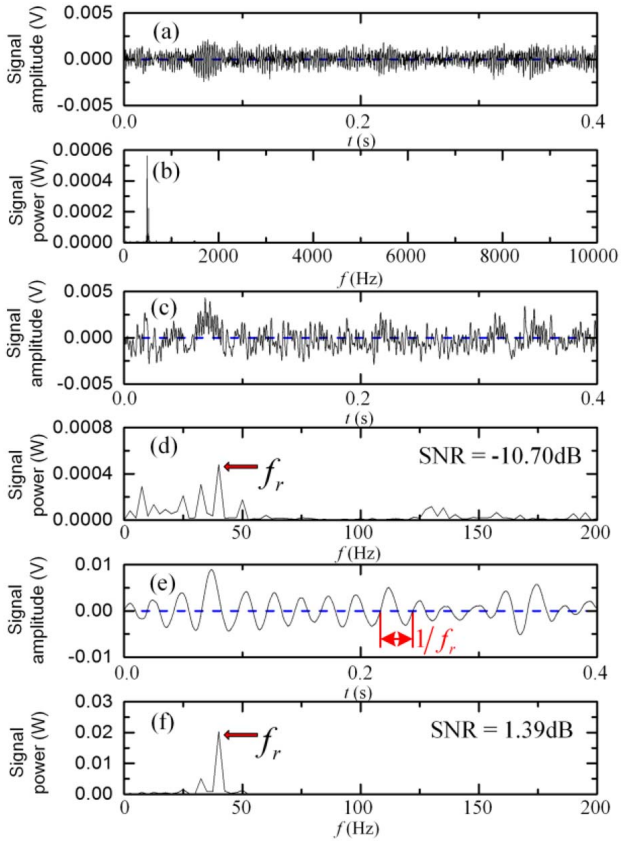

Fig. 9. output

VII. CONCLUSION

An SRAF-based signal filtering method is proposed for online fault detection of motor bearing. The method consists of four parts: 1) the SLPFE algorithm for online demodulation of the acoustic bearing signal; 2) the SR algorithm for denoising and weak periodical signal enhancement; 3) the ARO algo- rithm for the adaptation of the SRAF parameter; and 4) the zero crossing detection algorithm for directly measuring the signal period. With the above steps, the fault-induced impulses that may be blurred by the background noise are demodulated and purified, and the fault type of the bearing can be directly ascertained in accordance with the signal period. The effectiveness and the practicality of the method are validated by both simulated and experimental studies considering the BLDCM test rig and the DCM test rig with defective/healthy support bearings. On the premise of effectiveness, the design objective of this paper is simplicity. A simple algorithm is the most suitable. The obtained results indicate that this objective has been accomplished. Compared with the established filters used in the motor bearing fault diagnosis, the proposed method has several distinct merits, such as low computational cost, online implementation, contactless measurement, and availability for motors with various speeds. In this regard, the principle of the method may also be suitable for online detection/isolation of a periodical fault in the gearbox, rotor system, or other rotat- ing machines. Additionally, the algorithm framework is clear and simple, and these characteristics enable the method to be easily implemented in general-purpose MCUs embedding in low-power portable devices.

REFERENCES

[1] S. Nandi, H. A. ToliyatSecurity Condition monitoring and fault diagnosis of electrical motorsA review, , *IEEE Trans. Syst., Man, Cybern. C, Appl. Rev., vol. 42, no. 6, pp. 11351139, Nov. 2012*

[2] S. A. Huang and K. K. Tan, 1982 *Fault simulator based on a hardware-in-the-loop technique* IEEE Transaction on Power Apparatus Systems, PAS 101(1): 2906-2915. . Power Electron., vol.29, no. 8, pp. 4167 4182, Aug. 2014.

[3] P. Chen, T. Toyota, and Z. J. He, 2004. *PAutomated function generation of symptom parameters and application to fault diagnosis of machinery under variable operating conditions,* IEEE Trans. Syst., Man, Cybern. A, Syst., Humans, vol. 31, no. 6, pp. 775781, Nov. 2001. IEEEhowto:kopka A. J. Sguarezi Filho, M. E. de Oliveira Filho, and E. Ruppert Filho *A Predictive Power Control for Wind Energy,* ,IEEE Trans. Sustainable Energy, vol. 2, no. 1, Jan. 2011, pp. 97105.

[4] D. He, R. Y. Li, and J. D. Zhu *:Plastic bearing fault diagnosis based on a two-step data mining approach*, IEEE Trans. Ind. Electron., vol. 60, no. 8, pp. 34293440, Aug. 2013

A High Step-Up Converter with Voltage-Multiplier Modules for Sustainable Energy Applications

Sivaraman

***Abstract*—In our paper a novel isolated high step-up converter for sustainable energy applications. Through an adjustable voltage-multiplier module, the proposed converter achieves a high step-up gain without utilizing either a large duty ratio or a high turns ratio. The voltage-multiplier modules are composed of coupled inductors and switched capacitors. Due to the passive lossless clamped performance, leakage energy is recycled, which alleviates a large voltage spike across the main switches and improves efficiency. Thus, power switches with low levels of voltage stress can be adopted for reducing conduction losses.**

I. Objectives:

To increases a voltage spike across the main switches and improves efficiency of power without using a battery storage device. A voltage stress can be adopted for reducing conduction losses. An energy can be used for any home application

II. Introduction:

Energy is essential to our society to ensure our quality of life and to underpin all other elements of our economy. However, many developed countries have widely employed fossil fuels for the development of industry, economy and technology, which increase carbon emissions and the international price of oil. Hence, renewable-energy sources are becoming increasingly important and are being utilized worldwide to solve energy-shortage problems and to alleviate environmental-protection issues. We use a sustainable energy of solar energy the rated voltage of renewable-energy sources such as photovoltaic sources or fuel-cell stacks are at low levels, so that an intermediate converter with a sufficiently high step-up conversion and high efficiency is essentially required in this kind of system for high step-up DC/DC converters have been proposed and are widely utilized in many renewable-energy applications

III. Existing System:

In existing system, we use a battery setup for high voltage multiplier using a renewable energy. But in this system a storage device is used to store energy. Due to this the energy is leakage and alleviating large voltage spikes on the power switches. The adoption of low-voltage-rated semiconductor devices is used for storing energy in battery power.

Since the environmental conditions influence PV array voltage and the battery voltage depends on its charge level, the output dc-link voltage Vdc is also influenced by the same. However, the PV array voltage exhibits narrow variation in voltage range with wide variation in environmental conditions.

IV. Proposed System

The proposed system of high step-up converter with voltage-multiplier modules is used for sustainable energy applications.

The isolated step-up converters of pulse-width modulation (PWM) control. Then the energy can be retrieved from solar panel and it is used for the sustainable home application without any battery supply of storage device.

V. Advantage

Voltage-multiplier modules make the voltage gain higher and voltage stresses lower.

Then the performance of voltage multiplier is high then the life time of the input source is good.

VI. Block Diagram

VII. Circuit Diagram

A. Solar panel

A solar panel is a set of solar photovoltaic modules electrically connected and mounted on a supporting structure. A photovoltaic module is a packaged, connected assembly of solar cells. The solar module can be used as a component of a larger photovoltaic system to generate and supply electricity in commercial and residential applications.

VIII. Voltage Regulator circuit

A voltage regulator is designed to automatically maintain a constant voltage level. A voltage regulator may be a simple "feed-forward" design or may include negative feedback control loops. It is used an electromechanical mechanism .A voltage regulator generates a fixed output voltage of a preset magnitude that remains constant regardless of changes to its input voltage or load conditions. There are two types of voltage regulators: linear and switching

IX. 12 Volt Wiper motor

Wiper Motor, the power source of the wiper blade, is the core of the whole wiper system. Therefore, the quality of the wiper motor must be guaranteed to ensure its performance. The wiper motor is a permanent-magnet direct current (DC) one. It is equipped on the front windscreen glass with the mechanical parts of the worm gear. The worm gear functions

to slow down and increase torque. Its output shafts spur four-bar linkage, by which the movement is changed from rotary to swinging.

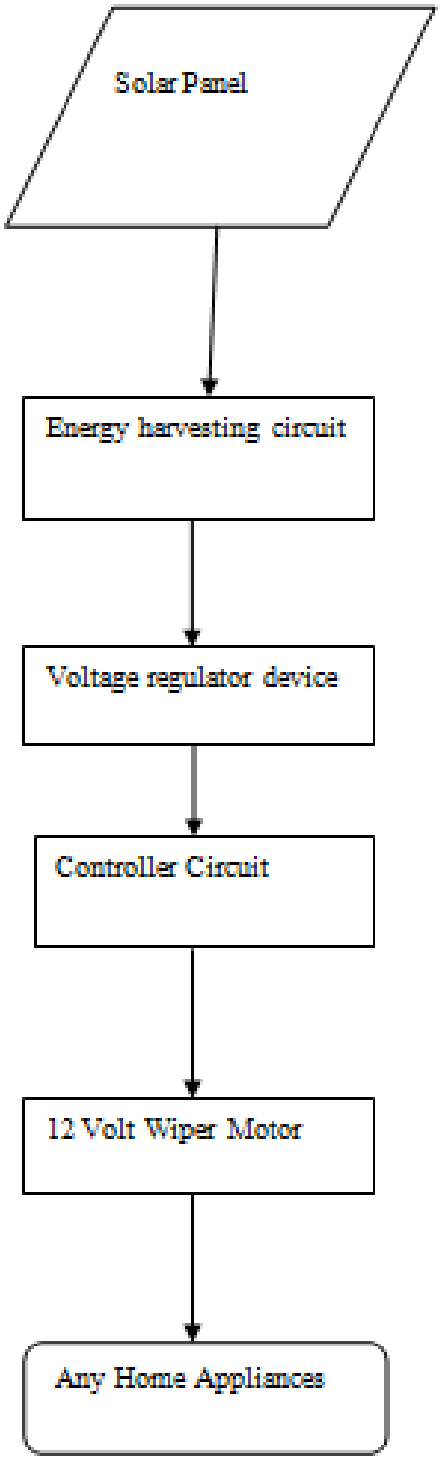

Fig. 1.

X. Energy harvesting circuit

Energy harvesting (also known as power harvesting or energy scavenging) is the process by which energy is derived from external sources (e.g. solar power, thermal energy, wind energy, salinity gradients, and kinetic energy), captured, and stored for small, wireless autonomous devices. Energy from the sun, solar energy, is harvested in two methods. Semiconductor technology called Photo-Voltaic (PV) converts light energy into electricity. Thermal energy from the sun is harvested through heat absorption. Both types of captured

Fig. 2.

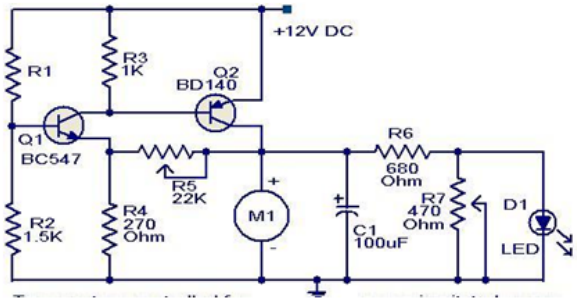

Fig. 3.

Fig. 4.

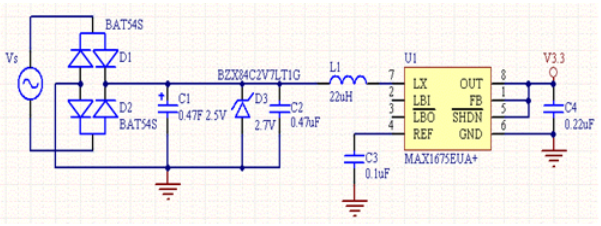

Fig. 5.

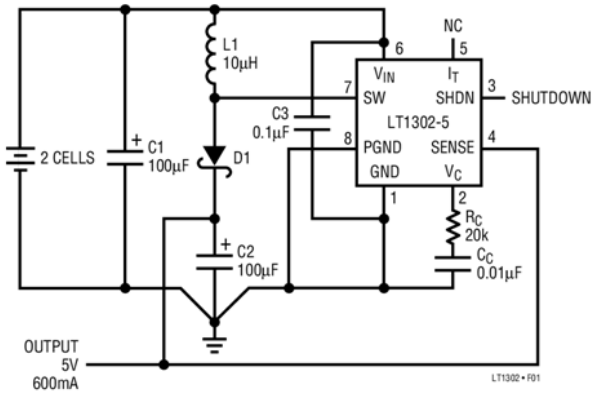

Fig. 6.

energy can be used immediately or stored for later use

XI. Controller circuit

It provides a constant 12 volts output. A fixed voltage regulator can be a positive voltage regulator or a negative voltage regulator. A positive voltage regulator provides with constant positive output voltage.

A voltage regulator is an electronic device that produces a steady and fixed output voltage, independently of its input voltage and output current. In reality, any voltage regulator has a range of input voltages for which it works, a certain level of efficiency and a limited amount of power it can handle.

XII. Conclusion

This paper presents the steady-state and experimental results for the proposed converter, which successfully demonstrates its performance. A prototype isolated converter has been successfully implemented with a high step-up ratio and high efficiency for sustainable energy applications. The presented circuit topology inherently makes the input current continuous and smooth, which decreases the conduction losses, lengthens the life time of the input source. Thus, we use the renewable-energy applications that need high step-up conversion and have electrical-isolation requirements for home application.

References

[1] T. Kefalas, and A. Kladas, *Analysis of transformers working under heavily saturated conditions in grid-connected renewable energy systems,* ,Trans. Ind. Electron., vol. 59, no. 5, pp. 23422350, May 2012.

[2] Jonghoon Kim, Jaemoon Lee, and B. H. Cho, , *Equivalent circuit modeling of pem fuel cell degradation combined with a lfRC,* ,, IEEE Trans. Ind. Electron., vol. 60, no. 11, pp. 50865094, Nov. 2013.

[3] Prasanna U R, and Akshay K. Rathore *Extended range zvs active-clamped current-fed full-bridge isolated dc/dc converter for fuel cell applications: analysis, design, and experimental results*, IEEE Trans. Ind. Electron., vol. 60, no. 7, pp. 26612672, July 2013.

[4] Shih-Jen Cheng, Yu-Kang Lo, Huang-Jen Chiu, and Shu-Wei Kuo, *High-efficiency digital-controlled interleaved power converter for high-power pem fuel-cell applications*, IEEE Trans. Ind. Electron., vol. 60, no. 2, pp. 773780, Feb. 2013.

RECENT TRENDS IN POWER SYSTEM

T.Viswanath
UG Scholar
Department of Electrical and Electronics Engineering
IFET college of engineering Villupuram.

***Abstract*—This paper is intend to the power system which includes generation, transmission and distribution of the electrical energy. This gives the overview of generation which tells about the recent energy production in the world. It explains about the production of energy and source of energy of top 20 countries in the world, also gives the statistical data about the sources available in India and other countries. The overall electrical energy review in 2015 also explained here. Electrical energy transmission tells about the recent trends present in it and transmission development issues also given here. It tells about the future expansion in transmission system and the reason for going into increasing the voltage level high. The investment in the transmission system also explained here. The only one control system for the five national regions of grid is present in Gurgaon it is named as NTAMC. This also explains the energy distribution present in India with the recent technology includes smart grid, SCADA etc. Additionally it tells about the POSOCO with PGCIL and the improvement in the power system by implementing the smart grid very effectively in India.**
keywords: OECD Organization for Economic Co-Operation and development, TWh-Terawatthour

I. Introduction

Electrical Energy is the basic economic development of a country. It exists in different forms in nature but the most important form is the Electrical energy. In this modern society use of electrical energy has become a part and parcel of our life. An electric power system is a network of electrical components used to generate, supply (distribute), transfer (transmit) and use electrical energy. Here grid plays an important role in supplying uninterrupted supply to all the regions in our country. Grid interconnects all the five regions of our country and now it has been made into one grid, one nation, and one frequency in India. Though we generate only 11KV from the generating side it is not sufficient to transmit the power. So we go for transmission where increasing of high voltages in HVAC, HVDC transmission system. Then we distribute the power to the consumers by reducing the voltage levels. Recently the generation of power is increased drastically India using coal and wind energy. In transmission we go for high voltage transmission to reduce loss i.e., I2R losses and corona. The transmission of high voltage exists in India is till 765KV transmission. This transmission made very sophistication by introducing the SCADA systems into the transmission system. The SCADA system makes the man work more easier way where in control room only two PC are present where the all available datas are feed into it. In few years, there is a vast development in the generation and transmission of energy in India.

II. Energy Production

The energy is produce from the generating stations using the available resources either renewable or non-renewable sources. The worlds total production of electrical energy is 23,536,500 GWh till 2014. In this India stands third largest electricity production in the world. It produces about 1,208,400 GWh till 2014*-. The following table represents the top 20 electricity producing countries 2014 -2015.

World electricity generation grew by 0.9% in 2015, slightly below the growth of primary energy (1.0%) Growth was down on 2014 (2.4%) and remained well below the 10-year trend (2.8%). OECD electricity grew by 0.2%, after four consecutive years of declining generation. Non-OECD electricity generation grew by 1.4%, significantly slower than 2014 (4.9%) and well below the 10-year trend (5.5%). The slowdown was most marked in China, the worlds largest electricity generator, with growth of just in 2015, compared to 6.7% in 2014. The worlds second largest generator, the US, posted a decline America was the only region to show a decline in electricity generation (0.1%). India, the third-largest generator, grew by 4.1% to record the largest volumetric growth in generation.

III. Electricity generation in India

There are various renewable and nonrenewable resources present in India. They are wind, oil, nuclear, Hydroelectric, Gas, Coaletc. In the last decade there is an increase in the generation of electricity using coal as a source and next wind energy falls the second in its generation followed by the gas.

Rank	Country/Region	Electricity production (GWh)	Date of information
N/A	World Total	23,536,500	2014[1][2]
N/A	European Union	3,166,000	2014[3]
1	China	5,810,500	2014[3]
2	United States	4,297,300	2014[3]
3	India	1,208,400	2014[3]
4	Russia	1,054,100	2014[3]
5	Japan	1,051,200	2014[3]
6	Canada	615,400	2014[3]
7	Germany	614,600	2014[3]
8	Brazil	562,600	2014[3]
9	France	555,700	2014[3]
10	South Korea	517,800	2014[3]
11	United Kingdom	356,800	2013[3]
12	Mexico	293,600	2013[3]
13	Saudi Arabia	292,200	2013[3]
14	Italy	288,400	2013[3]
15	Spain	265,300	2013[3]
16	Turkey	264,100	2015[4]
17	Iran	263,400	2013[3]
18	South Africa	256,100	2013[3]
19	Taiwan	252,600	2013[3]
20	Australia	244,800	2013[3]

Fig. 1.

The following graph represents the statistical data of electricity generation,

Production and sources of the top 20 countries in the world, Here from the above table we can see that India places 14_th among source available countries which produces 1,052.3TWh of electricity. The sources available in India are 67.9% of coal, 10.3% of Natural gas, 1.2% of oil, 12.4% of Hydropower, 5% of other renewable sources.

The following chart represents the world electricity production from all energy sources (TWh) in 2014

IV. Energy transmission

Electric power transmission is the bulk movement of electrical energy from a generating site, such as a power plant, to an electrical substation. Electricity is a concurrent subject in India i.e, both the central and state governments are responsible for the development of the electricity sector. NTPC, NHPC, THDC, NEEPCO, SJVNL, NLC etc. are the central generation utilities and POWERGRID is the Central Transmission Utility. At the State level, there are Gencos and Transco in the respective States. The country has been demarcated into five electrical Regions viz. Northern (NR), Eastern (ER), Western (WR), Southern (SR) and North Eastern (NER). However, NR, ER, WR and NER have been synchronously interconnected and operating as single grid Central Grid (capacity about 110,000MW). The Southern region is asynchronously connected to the Central Grid through HVDC links.

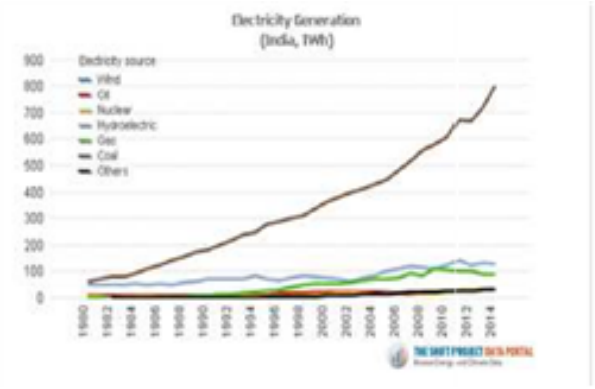

Fig. 2. statistical data of electricity generation

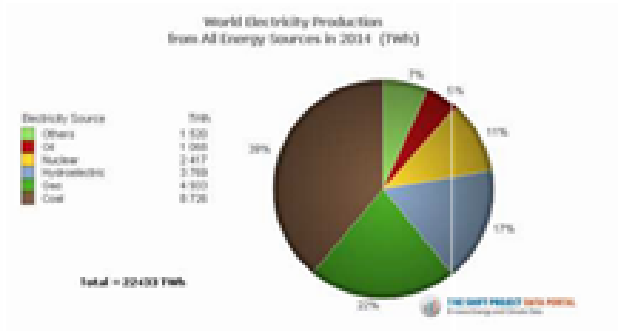

Fig. 3.

V. Transmission System Development Issues

As mentioned above, in order to meet growing requirement, development of strong transmission system between pit-head/resource generation complex and bulk consumption centers are required. However, development of transmission system Involves following issues: - Minimization of Right of Way Protection of flora fauna, wild life Creation of long distance high capacity transmission corridors to enable minimum cost per MW transfer as well as Optimal Transmission losses -Minimal Impact on Environment -Strengthening of National Grid

VI. Future Plan in Transmission

In order to address above issues, high capacity transmission corridors comprising 765kV AC and 800kV 6000MW HVDC system along with 400kV AC have been planned to facilitate transfer of power from remotely located generation complexes to bulk load centers

VII. High Density Transmission Corridor: Increase in voltage

In order to optimize right-of-way, high density transmission corridors (MW per meter ROW) either by increasing voltage level or current order or both i.e. increase in voltage and current are need to be developed. Power intensity at different voltage Level is tabulated in Table below:

Towards development of high intensity transmission corridor, there is a plan to develop 800 kV, 6000 MW HVDC system as a part of evacuation of bulk power from North Eastern Region (NER) to Northern Region (NR) over a distance of around 2000 kms. In addition, increasing the AC voltage level at 1200kV level has been planned. It is to mention that we are aiming towards use of 1100kV equipments for 1200kV operation by optimizing their protective level with the help of high energy level Surge arrester so as to achieve economy in respect of 1200kV UHV system development. Research work for 1000kV HVDC system has also been commenced.

Transmission Lines	Addition by 2012 (Ckm)	Addition by 2017 (Ckm)
765 kV	7,612	25000-30000
HVDC Bipole	11,078	4000 - 6000
400 kV	1,25,000	50000
220 kV	1,50,000	40000
Total	2,93,852	119,000 – 126,000
Substations	**Addition by 2012**	**Addition by 2017**
HVDC	14,700 MW	16,000 -22,000 MW
765 kV	53,000 MVA	1,10,000 MVA
400kV	1,45,000 MVA	80,000 MVA
220 kV	2,30,000 MVA	95,000 MVA
Total Capacity	4,28,000MVA	2,85,000MVA
Inter Regional Transfer Capacity	38,000 MW	75,000 MW

Fig. 4.

VIII. Upgradation of transmission line

power grid has successfully implemented upgrading of 220kV DC Kishenpur Kishtwar line in JK to 400 kV Sc first time in India. It has resulted in increase of power transfer intensity of the transmission corridor with marginal increase in ROW (from 35m to 37m) but far less than standard 400kV line (46 m). Upgradation of 400kV DC lines to 400500kV HVDC bipoles are also under exploration.

IX. Upgradation of HVDC Terminal

POWERGRID has been seamlessly upgraded Talcher (ER) Kolar (SR) HVDC terminal from 2000MW to 2500MW without changing of any equipment. That has been achieved with enhanced cooling of transformer and smoothing reactor with meager cost. The payback period is about 2-3 years.

X. 1200kV Test Station

In order to increase the power density of the corridor, development of 1200kV AC system as next higher AC voltage level has been decided. However, 1200kV AC technology is relatively a new one in the world. Therefore, to develop this technology indigenously, a unique effort has been made by POWERGRID through a collaborative research between POWERGRID and Indian manufacturers to establish a 1200kV UHVAC Test Station. This endeavor shall benefit the Indian Power sector and manufacturers as availability of 1200KV class equipment within country will not only enable optimization of transmission cost, but also help in during OM phase. In this direction, POWERGRID along with Indian manufacturers is establishing a 1200kV UHVAC Test Station at BinaIin the State of M.P) where a 1200KV test line (Sc+Dc) is being constructed along with two nos. 1200KV test bays in which the leading manufacturers are providing main equipment like transformers, surge arresters, circuit breakers, CTs, CVTs and transmission line hardware etc. POWERGRID shall provide space, civil foundation, 1200kV line, control protection system, various testing equipment, auxiliaries fire protection system, 1200kV bushing etc. These test bays and test line shall be used by the manufacturers and POWERGRID for various field tests so that the results and feedback can be used for developing field proven equipment of 1200KV system in India as well as gain initial operational experience. Development of this test station is in advance stage and likely to be commissioned by 2010.

XI. NATIONAL TRANSMISSION ASSET MANAGEMENT CENTRE (NTAMC)

i. The emphasis on the power sector to ensure the growth in GDP has brought in many changes in the business environment of Power Sector. The transmission sector being the integral part of is also facing multiple challenges like competitive bidding for transmission project, lack of experienced manpower, stringent demands by the regulator etc. ii. The technological development couple with falling prices of communication system and information technology provides us the opportunity for virtual manning of Substation thereby optimizing the requirement of skilled manpower and managing the asset with the available skilled workforce. iii. Thus, state of the art computerized control centers NTAMC & RTAMC with associated telecommunication system and adapted substation for enabling remote centralized operation, monitoring and control of POWERGRID Transmission system has been proposed. iv. The aim is to have completely unmanned substation except security personnel. The operations of the substations will be done from a remote centralized location i.e. NTAMC. The RTAMC will co-ordinate the maintenance aspect of the substation from a centralized location and will act as a backup to the NTACM for operation. The maintenance activities would be carried out by maintenance service hub (MSH). One MSH will cater to the requirements of 3-4 substations in its vicinity in coordination with the respective RTAMCs.

v. The substations and various control centers will be connected by redundant broadband communication network through POWERGRID (Telecom) communication links. vi. Telecom Department to provide high speed communication links between NTAMC, RTAMCs and Sub-stations. vii. The Connectivity Status has been finalized in association with LD&C department and NTAMC group. More links have to be planned by LD&C for total protection. Bandwidth requirement and Connectivity Scheme finalized. At stations where this connectivity is not possible, leased lines will be hired from other telecom operators up to the nearest connection point. viii. Total 192 Substation connectivity will be planned in 2 phases. * Phase-I 120 Sub Stations * Phase-II 72 Sub Stations

XII. POSOCO

Power System Operation Corporation Limited (POSOCO) is a wholly owned subsidiary of Power Grid Corporation of India Limited (PGCIL). It was formed in March 2010 to handle the power management functions of PGCIL. It is responsible to ensure the integrated operation of the Grid in a reliable, efficient and secure manner. It consists of 5 Regional Load Dispatch Centers and a National Load Dispatch Centre (NLDC). The subsidiary may eventually be made a separate company, leaving the parent firm with only the task of setting up transmission links. The load dispatch functions, earlier handled by PGCIL, will now come up to POSOCO. They

Fig. 5.

maintain 99.9% of online without interruption of power supply to the grid, even at worse cases.

XIII. POWER GRID TRANSMISSION NETWORK FAILURE

The Northern Region Grid, which provides power to nine states in northern India including Delhi, experienced a widespread outage due to a grid disturbance that occurred at about 2.35 a.m. on 30 July 2012. Restoration work started immediately under the direction of CEO, POSOCO and POWERGRIDs Chairman Managing Director. A team of engineers tried to find out a way for restoring the normal supply of power immediately, so that railways, Metro, airports and other power users deemed essential could get immediate restoration of electricity. With the coordinated efforts of the whole team of engineers and constituent state utilities, power supply to the essential services and other essential loads in northern India was restored by about 8.00 a.m. and about 60% of load of the Northern Region was restored by 11:00 a.m. This was possible by gearing up the power supply from hydroelectric sources and also extending power from the Eastern and Western regions for start-up supply for thermal generating units of the Northern Region. Thus the associated problems for want of power supply could be partially overcome by this time. Later, power supply was restored progressively and by 12:30 p.m. power was extended to most of the cities and towns through POWERGRID substations. The Northern Grid was brought back to normalcy to meet the demand of about 30 GW at 7:00 p.m. On 31 July 2012, the northern grid collapsed for a second time, hours after the power supply was restored in the entire northern region following a disruption on the previous day. The eastern transmission lines also failed, disrupting power supply in Delhi, Uttar Pradesh, Haryana, West Bengal, Assam and Punjab, among other states.

POSOCO mainly comprises - *National Load Despatch Centre (NLDC) *Five Regional Load Despatch Centres *Northern Regional Load Despatch Centre (NRLDC) *Western Regional Load Despatch Centre (WRLDC) *Eastern Regional Load Despatch Centre (ERLDC) *Southern Regional Load Despatch Centre (SRLDC) *North-Eastern Regional Load Despatch Centre (NERLDC)

XIV. ENERGY DISTRIBUTION

An electric power distribution system is the final stage in the delivery of electric power; it carries electricity from the transmission system to individual consumers. Distribution substations connect to the transmission system and lower the transmission voltage to medium voltage ranging between 2 kV and 35 kV with the use of transformers. Primary distribution lines carry this medium voltage power to distribution transformers located near the customer's premises. Distribution transformers again lower the voltage to the utilization voltage of household appliances and typically feed several customers through secondary distribution lines at this voltage. Commercial and residential customers are connected to the secondary distribution lines through service drops. Customers demanding a much larger amount of power may be connected directly to the primary distribution level or the sub transmission level.

XV. OVERVIEW OF THE EXISTING SYSTEM

The distribution segment continues to carry electricity from the point where transmission leaves off, that is, at the 66/33 kV level. The standard voltages on the distribution side are therefore 66kV, 33 kV, 22 kV, 11 kV and 400 to 230 volts, besides 6.6 kV, 3.3 kV and 2.2 kV. Depending upon the quantum of power and the distance involved, lines of appropriate voltages are laid. The main distribution equipment comprises HT and LT lines, transformers, substations, switchgears, capacitors, conductors and meters. HT lines supply electricity to industrial consumers while LT lines carry it to residential and commercial consumers.

XVI. STATE-OF-THE-ART SCADA/EMS SYSTEM

SCADA system which is the sensory organ of grid operator measures vital system variables through RTU (Remote terminal Unit) or SAS (Substation automation system) installed at all the important locations in the grid. The recorded data is transmitted through modern communication channels and displayed in the operator consoles in load dispatch centers It provides real time control and monitoring of energy management facilities to optimize system reliability, load dispatch, voltage control, system restoration, switching operations, planned maintenance outage, data recording, load flow, analyses of existing & future system conditions and thereby optimize operation to each constituent in particular and the Region as a whole. Effective visualization techniques and tools are used to empower the system operator in facilitating quick response under critical conditions. Techniques used by the Indian grid operators are Tabular presentation, Bus Diagrams, Flow gate Illustration, Control Area Tie Line Representation, Geographical Displays, Contouring, Three Dimensional Representations, and Animation.

XVII. SMART GRID

The complexity of Grid is increasing continuously due to Growing number of interconnections within and across the regions. The real time information available today through conventional SCADA/EMS system is limited to analog and status data from the remote terminal units. Information, such as indications of protective control actions, event/fault records, device settings are not available. System dynamics are not taken in real time evaluations. Emergency controls such as load shedding do not consider system-wide conditions. Protective relay settings are static no intelligence is embedded to allow adaptation to the changing system conditions To take care of above complexities and to ensure safe, secure and reliable operation of large interconnected Indian Grid, system operation in future would be equipped with an Intelligent/Smart Grid with placement of Phasor Measurement Unit, Wide Area Monitoring, SelfHealing, and adaptive islanding features etc. with an intent to quickly evaluate system vulnerability with

respect to cascaded events involving faults, device malfunctions and provide remedial action. Initiatives have been taken to implement Smart Grid pilot projects for grid security of Indian grid. (a) Implementation of Pilot project for installation of PMUs (Phasor Measurement Units) in Northern Region (b) Implementation of CSIR approved Project Intelligent Monitoring & Control of the Interconnected Electric Power Grid using WAMS. To keep track of new technology development POWERGRID is also a member of International group VLPGO (Very Large Power Grid Operators) with other international utilities .VLPGO is a common platform where worldwide large Grid Operators come together for mutual benefit, sharing common problems and solution.

XVIII. Smart Grid

The regulatory environment is steadily moving towards increasing competition in the electricity market allowing several new players in addition to traditional utilities and independent power producers such as captive power producers, merchant power producers, renewable energy generators, etc., on the one hand and customers requiring access to the grid on a nondiscriminatory basis on the other. With full open access in the distribution segment, the consumer will no longer be captive to one discom but will have greater choice in getting power from any of the new entities connected to the grid. If the smart grids are implemented very effectively in India, it will be very useful to meet out the power demands. The regulatory environment too has now become stable with multi-year tariffs becoming a norm in states.

References

[1] anesh Kumar Vinayagamoorthy *Dynamic Energy Management Sysytem For A Smart Microgrid , IEEE Transation On Neural Networks And Learning Systems* ,Vol 27 , No 8 ,August 2016.

[2] C.-S. Chiu*T-S fuzzy maximum power point tracking control of solar power generation systems, IEEE Trans. Energy Conv* ,., vol. 25, no. 4, pp. 11231132, Dec. 2010.

[3] M.G.Villalva, J.R.Gazol, and E.R.Filho *M.G.Villalva, J.R.Gazol, and E.R.Filho, Comprehensive Approach to Modeling and Simulation of Photo-voltaic Arrays", IEEE trans. on Power Electronics,*,vol.24, no.5, pp.1198-1208, 2009.

[4] Piller S, Perrin M, Jossen A. *"Methods for state-of-charge determination and their applications.*96(1):113-20,2001.

NEW CASCADED SWITCHED CAPACITOR MULTILEVEL INVERTER WITH REDUCED NUMBER OF SWITCHES FOR PV BASED APPLICATIONS

Mr. G.PREMSUNDER
Associate Professor
Department of Electrical and Electronics Engineering
MAILAM ENGINEERING COLLEGE

Dr. N.MURALIKRISHNA
HOD Of EEE Dep
Department of Electrical and Electronics Engineering
MAILAM ENGINEERING COLLEGE

Ms. R. PRIYADHARSINI
PG Scholar
Department of Electrical and Electronics Engineering
MAILAM ENGINEERING COLLEGE

***Abstract*—The aim of this study is to present a new structure for switched-capacitor multilevel inverters(SCMLIs) which can generate a great number of voltage levels with optimum number of components for both symmetric and asymmetric value of dc voltage sources. A new cascaded multilevel inverter topology which is able to increase the number of output levels without using any full H-bridge cells. To reduce the number of involved components in the current path, value of blocked voltages, the variety of isolated dc voltage sources and as a result the overall cost by less number of switches in comparison with other presented topologies. The validity of the proposed SCMLI has been carried out by several simulation and experimental results. Key words- multilevel inverter, symmetrical and asymmetrical topology.**

I. INTRODUCTION

Power-electronics inverters are becoming popular for various industrial applications. In recent years also high-power and medium-voltage drive applications have been installed. To overcome the limited semiconductor voltage and current ratings, some kind of series and /or parallel connection will be necessary .Due to their ability to synthesize wave forms with a better harmonic spectrum and attain higher voltages, multilevel inverters are receiving increasing attention in the past few years. Multilevel inverter was introduced as a solution to increase the converter operating voltage above the voltage limits of classical semiconductors. The multilevel voltage source inverter is recently applied in many industrial applications such as AC power supplies, static VAR compensators, drive systems, etc. One of the significant advantages of multilevel configuration is the harmonic reduction in the output waveform without increasing switching frequency or decreasing the inverter power output. A multilevel inverter is a power electronic device that has been given more attention since introduced early in 1980s[1]. The desired output voltage of multilevel inverters is synthesized by several discrete DC sources [2]. With increasing the number of DC sources, the number of levels in output waveform increases and the output voltage approaches nearly sinusoidal waveform while employing a fundamental frequency-switching method [3]. The multilevel inverters are used in various applications such as renewable energy interfaces circuit [4, 5], flexible alternating current transmission devices [6, 7] and high voltage direct current [8, 9]. For the purpose of comparison with the traditional two-level configuration, it is needed to mention to both merits and demerits together. Multilevel inverters have more advantages with respect to the traditional two-level configurations; nevertheless, just more important ones are mentioned here: high-power quality [10,11]. However, the main disadvantages of multilevel structures against the traditional two-level configuration are more number of required elements and so the inverter circuit and control scheme will be complex. Therefore the cost of inverter is increased and its reliability is reduced[12]. Therefore reducing the number of circuit devices is the main concern from the point of design. The initial prototype of multilevel inverters is three-level neutral point clamped (NPC) inverter [13]. In NPC, the desired output voltage is attained by combinations of series capacitors voltage. The NPC inverters have some problems, such as clamping diodes and the balance of the DC-link capacitors while the number of output voltage level is increased [14]. An alternative for NPC was a new topology based on the interconnection of several modular structures, called cells, in different paths which were named multicell topology. Many sub topologies and hybrid topologies including their own control scheme based on multicell topologies have been derived. Cascaded multicell (CM) and flying capacitor (FC) are the main inspired from traditional multicell configuration [1517]. The FC employs floating capacitors to clamp the voltage levels. In FC, more number of steps in output voltage

can be produced by clamping several DC

voltages of FCs. However, to maintain the FCs voltage at target values there is a need to more complex control scheme [18, 19]. The multi cell topologies are simply scalable, and present some benefits while operating at internal fault states because of the existence of redundant states [20]. Also CMs are more attractive because of their modular nature, and uncomplicated control scheme and simpler implementation [21]. In this paper, a new modular configuration for cascaded multilevel inverters that generates a large number of steps with a low number of circuit devices is proposed. The proposed topology can be used as asymmetric and symmetric multilevel inverters. The proposed topologies control scheme is as simple as the cascaded multilevel inverter. In addition, to calculate the required magnitudes of DC voltage sources two different are proposed. In general, there are three categorized conventional types for MLI configurations realized by diode clamped (DCMLIs) [5], flying capacitors (FCMLIs)[6]-[7] and cascade H-Bridge (CHB) [8]-[9]. The main condition for generating various number of voltage levels at the output is to use the multiple isolated dc power supplies or virtual dc links such as capacitors or transformers with contribution of several switching devices [4]. However, these requirements create a great limitation for MLIs in industrial applications and it is not preferred on the facet of commercial utility. In recent studies, researchers have tried to obviate these aforementioned limitations through introducing the new developed MLI structures. Nevertheless, generating more output voltage levels with minimum number of isolated dc power supplies and other accompanying components such as gate drivers and power switches likewise, is counted as a main challenge for researchers [10]-[14]. One of the suitable approaches to decrease the number of required dc power supplies is to use of capacitors.Using the redundancy switching states (RSS) can be counted as a helpful way to obviate the discharging problems in the conventional types of MLIs and their modified topologies like flying-capacitor multicell converters (FCMCs).

II. CIRCUIT DESCRIPTION

In this case, all of the switches are driven by fundamental switching frequency whereas the sinusoidal reference voltage is compared with some available dc voltage levels and create the related gate switching pulses. The most advantage of this switching method is referred to low switching frequency which yields to reduction of switching loss [29],[30]. Details of fundamental switching modulation strategy are not objective of this paper. In addition from table V, it is clear that, to generate each of output voltage levels, only five switches are being involved in the current path. At this stage, to determine the capacitance of and , two assumptions are considered which one is related to output sinusoidal load current with phase difference between output voltage and current and the other is contribute to same duration in each step of staircase output voltage. Thus, the maximum discharging amount of each capacitor can be defined as (30) in one half cycles: Where , and are period of one cycle, frequency of output voltage and amplitude of load current, respectively and also is time interval corresponded to the longest discharging cycle (LDC) of each capacitors. On the other hand, in proposed 17-level inverter, this time interval varies for and . According to Table V, the LDC for and are illustrated by Fig.1.Thus, with considering the as maximum allowable voltage ripple, the optimum value of capacitors.

In this paper, initially a new switched-capacitor dc/dc converter (SCC) is presented which can switch as conventional series/parallel conversion and generate multiple dc link voltages with optimum components. In this case, voltage of all capacitors is filled by binary asymmetrical pattern without using any auxiliary circuits. At the next, a new sub-multilevel inverter topology presents which is performed based on proposed SCC unit and without using full H-bridge cell. In addition, this

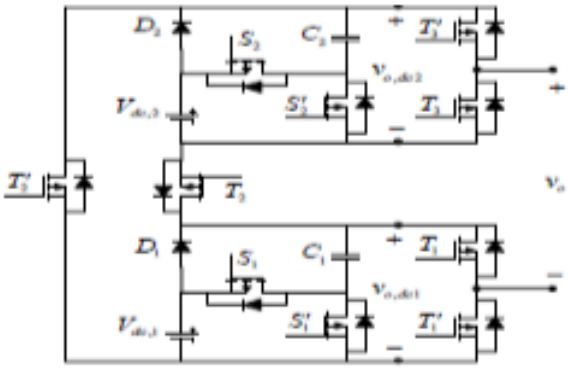

Fig. 1. proposed 17 level inverter topology

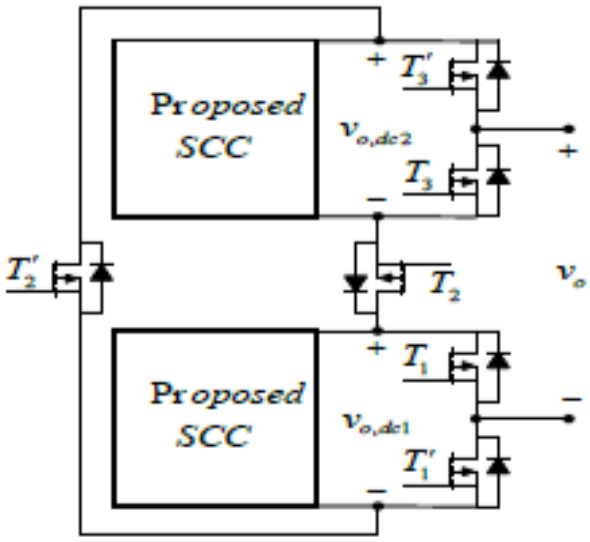

Fig. 2. proposed SMLI configuration

structure is suitable for an inductive load with capability to pass the reverse current. After that, proposed sub-multilevel modules are cascaded with each other and create more output voltage levels. Therefore most of the parameters such as number of required switches, diodes, maximum current path components and value of total blocked or standing voltage are improved. In order to prove the performance of the proposed circuit, variety number of comparisons with other recently suggested topologies has been done in fair conditions and also analysis of theoretical power losses is given. Finally validity of the proposed topology is shown by several experimental and simulation results. Table I: different switching and capacitors states of proposed 17-level inverter .

Switching State		ON Switches	v_o	C_1	C_2
	1	$T_1T_2T_3T_4'S_1S_2$	$4V'_{dc}+v_{c,1}+v_{c,2}$	D	D
	2	$T_1T_2T_3T_4'S_1'S_2$	$4V'_{dc}+v_{c,2}$	C	D
	3	$T_1T_2T_3T_4'S_1S_2'$	$3V'_{dc}+v_{c,2}$	C	D
	4	$T_1T_2T_3T_4'S_1'S_2'$	$4V'_{dc}+v_{c,1}$	D	C
	5	$T_1T_2T_3'T_4'S_1'S_2'$	$4V'_{dc}$	C	C
	6	$T_1T_2T_3'T_4'S_1'S_2'$	$3V'_{dc}$	C	C
	7	$T_1T_2T_3T_4S_1'S_2'$	$V'_{dc}+v_{c,1}$	D	C
	8	$T_1T_2T_3T_4'S_1'S_2'$	V'_{dc}	C	C
	9	$T_1T_2T_3T_4S_1'S_2'$ $T_1'T_2'T_3'T_4'S_1'S_2'$	0	C	C
	10	$T_1'T_2'T_3'T_4S_1'S_2'$	$-V'_{dc}$	C	C
	11	$T_1'T_2'T_3'T_4S_1S_2'$	$-V'_{dc}-v_{c,1}$	D	C
	12	$T_1'T_2'T_3'T_4S_1'S_2'$	$-3V'_{dc}$	C	C
	13	$T_1'T_2'T_3'T_4'S_1'S_2'$	$-4V'_{dc}$	C	C
	14	$T_1'T_2'T_3'T_4'S_1S_2'$	$-4V'_{dc}-v_{c,1}$	D	C
	15	$T_1'T_2'T_3'T_4'S_1'S_2$	$-3V'_{dc}-v_{c,2}$	C	D
	16	$T_1'T_2'T_3'T_4'S_1S_2$	$-4V'_{dc}-v_{c,2}$	C	D
	17	$T_1'T_2'T_3'T_4S_1S_2$	$-4V'_{dc}-v_{c,1}-v_{c,2}$	D	D

Fig. 3. different switching and capacitors states of proposed 17-level inverter

	Symmetrical Inverter	Asymmetrical Inverter	
		Binary	Temaary
N	2N+1	2^{N+1}	3^N
DC source number	N	N	N
Switches number	4N	4N	4N

Fig. 4. Comparison of multilevel inverters

III. SINUSOIDAL PULSE WIDTH MODULATION SCHEME

This scheme consists of three unipolar PWM strategies. The reference is the sine signal and carrier is the triangular signal. The multicarrier is positioned above zero level and the carrier are depending upon the output voltage levels. For m level inverter, (m-1)/2 carrier are used.

IV. SIMULATION CIRCUIT AND RESULTS

The simulation circuit for the seventeen level topology is shown below.

The firing pulses for the power components in the proposed inverter are generated by comparing the carrier and the reference signals as shown in the figure.

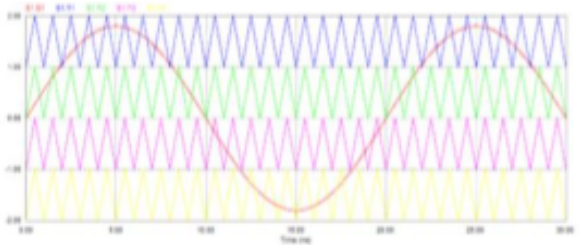

Fig. 5. inphase disposition pwm scheme

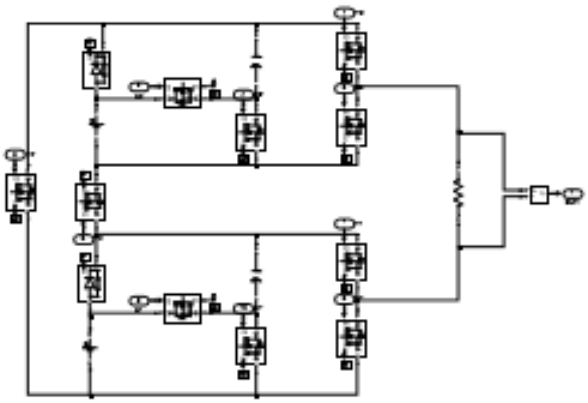

Fig. 6. simulation circuit for 17 level topolog

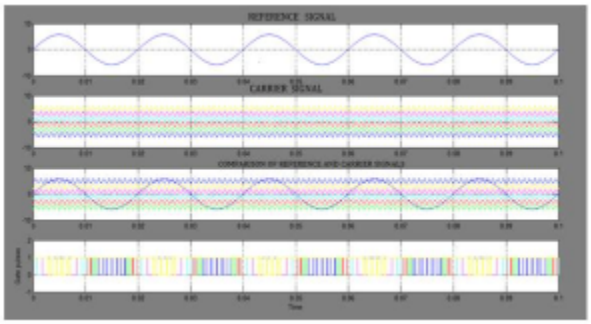

Fig. 7. simulation circuit for 17 level topolog

V. CONCLUSION

In this paper, a new structure was proposed to the multilevel inverter which can generate all the voltage levels at the output. In the conventional output H-bridge cell the number of required MOSFET and other involved components, are more. But in the proposed system the number of required capacitors and other components are less to generate maximum number of output voltage levels. Its associated advantages like better fundamental output voltage, better harmonic performance and easier to implementation.

REFERENCES

[1] J. Chavarria, D. Biel, F. Guinjoan, C. Meza, and J. J. Negroni, *Energy balance control of PV cascaded multilevel grid-connected inverters under level-shifted and phase-shifted PWMs,* IEEE Trans. Ind. Electron. vol. 60, no. 1, pp. 98111, Jan. 2013.

[2] A five-level single- phase grid-connected converter for renewable distributed systems, IEEE Trans. Ind. Electron., vol. 60, no. 3, pp. 906918, Mar. 2013.

[3] J. Rodriguez, L. J.Sheng, and P. Fang Zheng, *Multilevel inverters: A survey of topologies, controls, and applications,* IEEE Trans. Ind Electron., vol. 49, no. 4, pp. 724738, Aug. 2002.

POWER DEMAND CONTROLLER

K.VEERARAGAVAN
PG Scholar
Department of Electrical and Electronics Engineering

***Abstract*—This letter proposes a hybrid multicarrier pulse width modulation (H-MCPWM) technique to reduce leakage current in a transformerless cascaded multilevel inverter for photovoltaic (PV) systems. The transformerless PV inverter topology has the advantages of simple structure, low weight and provides higher efficiency. However the topology makes a path for leakage current to flow through parasitic capacitance formed between the PV module and the ground. Modulation technique has significant impact to reduce the leakage current without adding any extra component. The proposed H-MCPWM technique ensures low leakage current in the transformerless PV inverter system with simplicity in implementation of the modulation technique using lesser number of carriers. Experimental prototype developed in the laboratory demonstrates the performance of the proposed modulation technique in reducing the leakage current.**

I. INTRODUCTION

he total power generation from the photovoltaic (PV) system is relatively small as compared to other common energy resources due to its high installation cost. Reducing the PV system cost and increasing its efficiency has attained greater research interest. One of the solutions to reduce the cost of the PV power system is to remove transformer required in the output of the PV inverter [1-3]. Most of the national electricity regulatory authority made it compulsory to use transformer above certain threshold power in the system because it ensures galvanic isolation. However the use of transformers increases weight, size, and cost of the PV system and reduce the power conversion efficiency. This has motivated the research community to work in the transformerless PV system. The advancement of power electronics technology has made the use of transformerless PV inverter popular in kilo watt (kW) range by imposing standards such as DIN VDE 0126-1-1 [4], [5]. However removal of the transformer intro- duces harmful leakage current to flow through the parasitic capacitance which exists between the PV module and the ground. This leakage current may increase the system losses, total harmonic distortion in the grid current, electromagnetic- inferences and safety concerns [6]-[9]. The factors used to limit magnitude of the common mode voltage include nature of the output pulsewidth of the inverter, number of commuta- tion and grounding of the PV system [10]. The commercial transformerless centralized PV inverter has been successfully connected in roof-top projects with ratings above 10 MW and it is recognized by IEEE 1547 and other standards. This encourages the possibility to use transformerless inverter topology for high power applications [13]. Next-generation PV inverter has reached higher power ratings with modularity, and redundant topologies will be adopted in the design for reliability of the inverter. Traditional two and three-level inverters are unable to provide high efficiency and grid code requirements for higher power and voltage ratings, therefore converter topologies for medium-voltage and megawatt-scale PV inverters are moving towards the multilevel structures. Among various multilevel inverters, cascaded H-bridge multilevel inverter has various advantages compared to other topologies [14]. This use of cascaded H-bridge multilevel inverter opens up the option to eliminate the transformer from the PV system. In general, following two well established modulation techniques are available for the multilevel inverter topologies which provide constant common mode voltage: space vector modulation (SVM) and multicarrier pulse width modulation (MCPWM). The SVM technique is more constructive from the view of switching timings. The switching sequence and modulation can be decided by the users, but it requires regress effort for implementation [15]-[18]. In [19], the author has demonstrated the use of SVM to reduce the leakage current in transformerless PV inverter topology by placing zero active vectors at appropriate switching instants. However selection of switching states is not easy for practical implementation. The MCPWM technique eliminates the problem of common mode voltage applied in neutral clamped multilevel inverter, which increases the computational burden due to more number of carrier signals [20]. In [21], the authors have reported the effect of common mode voltage using bipolar and unipolar modulation schemes on neutral point clamped multilevel inverter and cascaded H-bridge multilevel inverter. As the level of cascaded H-bridge multilevel inverter increases it is expected to get reduction in leakage current, and further studies are required to know the relation between the modulation strategy and the leakage current. The cascaded H-bridge multilevel inverter has the advantages of less leakage current as compared to the conventional single H-bridge inverter due to reduced value of DC link voltage per bridge. The common multicarrier modulation tech-

niques used in the transformerless cascaded H-bridge multile- vel PV inverter topologies introduces common mode voltage. This letter proposes a hybrid multicarrier pulse width modula- tion (H-MCPWM) technique to reduce leakage current in transformerless cascaded H-bridge multilevel inverter for pho- tovoltaic (PV) systems. When the common mode voltage changes in a large step value it induces high leakage current in the PV system through the parasitic capacitance between the PV module and the ground. The reduced voltage transition in the common mode voltage reduces the leakage

current. It is easy to implement the proposed modulation technique without much complexity and require half the number of carriers as required in the conventional MCPWM techniques.

II. CARRIER MODULATION SCHEME FOR CONSTANT COMMON MODE VOLTAGE

Fig. 1 shows the PV supported single phase five-level cascaded H-bridge inverter topology, where two H-bridges are connected in cascade and provides a common output. The con- figuration of two cascaded H-bridges adds the output voltage of the upper and lower bridges to generate five-level stepped output voltage at the AC side, i.e., VPV, VPV/2 , 0, -VPV/2 and - VPV. It is assumed that the grid does not contribute common mode voltage in the system [9]. The converter topology and modulation method have significant contribution in leakage

Where, VN and VN are the voltages between the mid-point of the upper H-bridge inverter legs to the negative terminal of the dc link, V is the voltage between the mid points of the two legs of the lower H-bridge inverter, and let Vo is the output voltage across the load. The leakage current mainly depends upon the magnitude of the inverter common mode voltage. In order to derive the expression of the common mode voltage in the cascaded multilevel inverter the following equations can be written from Fig.1.

current generation. Therefore the transformerless cascaded multilevel inverter shown in Fig. 1 is connected to a simple resistive load for evaluation of the proposed modulation technique. The leakage current is generated in the parasitic capa-

citance formed between the PV module and the ground, where common mode voltage is also induced at the same point as shown in Fig. 1. The common mode voltage of any electrical circuit is the mean value of voltage between the outputs and a common reference point.

Where, VN and VN are the voltages between the mid-point of the upper H-bridge inverter legs to the negative terminal of the dc link, V is the voltage between the mid points of the two legs of the lower H-bridge inverter, and let Vo is the output voltage across the load. The leakage current mainly depends upon the magnitude of the inverter common mode voltage. In order to derive the expression of the common mode voltage in the cascaded multilevel inverter the following equations can be written from Fig.1.

Now considering convention that the leakage current will flow from PV module to ground or vice versa as per the standards IEEE 80 [22], the sign of common mode voltage can be re- versed as Vcm = Vcm and abbreviated now onwards as CMV in this paper. The equation (5) is useful for determining the common mode voltage in various intervals of the reference period. To minimize the leakage current flow through the parasitic capacitance the common mode voltage is required to be main- tained minimum during the switching instances. The minimum step value of the common mode voltage is defined by VPV/(n- 1) in MCPWM technique [18]. In phase disposition multicar- rier pulse width modulation (PD-MCPWM), the common mode Vcm varies in the band range of VPV/2. However in this modulation method total (n-1) number of carrier signals

are used, where n is the inverter level. The proposed H-MCPWM is the modified version of the phase opposite disposition (POD) pulse width modulation technique, where the number of carriers required is half of that required in POD PWM and therefore computational burden is reduced. In this modulation method the carrier signals used are in-phase with each other. The phase of all the carriers is shifted by 180 after each half cycle. Table.I shows the different switching instants and their corresponding magnitude of CMV. It has six switching instants, in which one instant has zero CMV, three instants have 2VPV/4 and two instants have VPV/4, CMV. There is no voltage transition in zero CMV. The CMV may take the values depending upon the inverter switch states selected. Since the voltage source inverter cannot provide pure sinusoidal voltages and has discrete output voltage levels synthesized from the output voltage of the PV [10], [22]. The voltage transition depends upon the direction of the current in the inverter, hence the proposed H-MCPWM modulation technique ensures the reduced common mode voltage generation in the band limit of maximum VPV/4. The switching pattern of the proposed H-MCPWM technique for five-level cascaded multilevel inverter is illustrated in Fig. 2. The operation of the proposed H-MCPWM is divided into two mode of operation, i.e.,

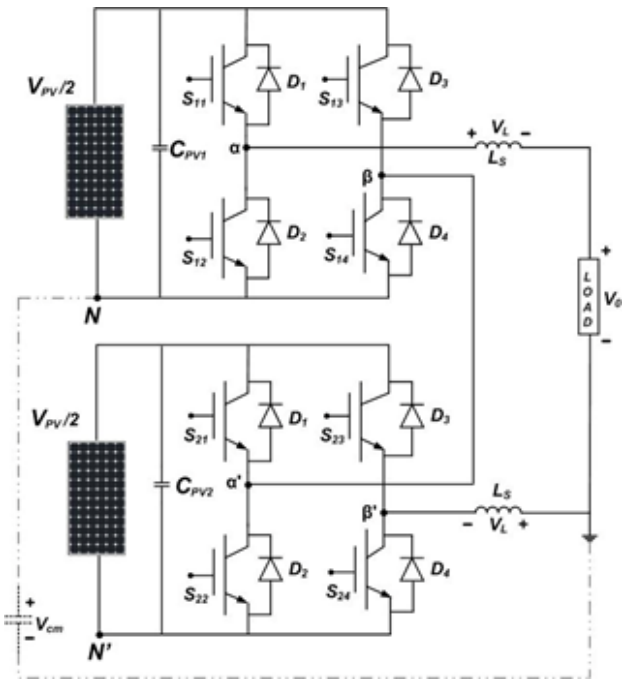

Fig. 1. PV supported transformerless single phase five-level cascaded

$$V_{cm} + V_{\alpha N} - V_L - V_O = 0 \quad (2)$$

$$V_{cm} + V_{\beta N} + V_L - V_{\alpha'\beta'} = 0 \quad (3)$$

Fig. 2.

mode-1 and mode-2, as explained below.

In this mode, all the carrier signals are in-phase with each other, the three level voltages, i.e., 0, VPV/2 and VPV, are generated using following switching scheme.

(i) When the reference signal Vref is smaller than the carrier signals Vc1 and Vc2, then the switches S11, S14, S23, S22, are turned ON and the complimentary switches, S13, S12, S21, S24, are turned OFF. In this situation VN = VPV/2, VN = 0, and the output voltage is V = +VPV/2.

(ii) When the reference signal Vref is greater the carrier signal Vc2, and lesser than the carrier signal Vc1, then the switches S14, S12, S23, S22 are turned ON and the complimentary switches S11, S13, S21, S24 are turned OFF. In this situation VN = 0, VN = 0, and the output voltage is V = 0. (iii) When both the carrier signals Vc1 and Vc2, are smaller than the reference signal Vref, then the switches, S13, S12, S23, S22, are turned ON and the complimentary switches, S11, S14, S21, S24, are turned OFF. In this situation VN = 0, VN = VPV/2, and the output voltage is V = -VPV/2.

B. Mode-2 (T/2 to T) In this mode all the carrier signals are phase shifted by 180, the three level voltages, i.e., 0, +VPV/2 and +VPV, are gen- erated using following switching scheme.

(i) When the reference signal Vref is smaller than the carrier signals Vc1 and Vc2, then the switches, S11, S14, S23, S22, are turned ON and the complimentary switches, S13, S12, S21, S24, are turned OFF. In this situation VN = 0, VN = +VPV/2, and the output voltage is V = -VPV/2. (ii) When the reference signal Vref is greater the carrier signals Vc1, and lesser than the carrier signal Vc2, then the switches, S11, S14, S21, S23, are turned ON and the complimentary switches, S13, S12, S22, S24, are turned OFF. In this situation VN = +VPV/2, VN = +VPV/2, and the output voltage is V = 0. (iii) When both the carrier signals Vc1 and Vc2, are smaller than the reference signal Vref, then the switches S11, S14, S21, S24, are turned ON and the complimentary switches, S13, S12, S23, S22, are turned OFF. In this situation VN = VPV/2, VN = 0, and the output voltage is V = +VPV/2.

The summary of the switching instants employed in two modes of operation is presented in Table I. It is clearly visible from the above discussion that the proposed H-MCPWM technique is able to generate five-level inverter output voltage and attain reduced common mode voltage in the band of maximum VPV/4, which is superior to the conventional MCPWM technique.

III. RESULT AND DISCUSSION

To validate the proposed H-MCPWM technique, a prototype model is developed in the laboratory. The system parameters used for the experimental studies consists of four AKSHAYA ASP-1250 solar PV modules (each module is rated for 50 W), DC link capacitance (2200 F), ground resistance (10), parasitic capacitance (100 nF), switching frequency (3 kHz), inductance (5 mH). The Mitsubishi make intelligent power modules (IPM), PM50RSD120 having IGBT switches are chosen for the H-bridge inverter. The multicarrier modulation techniques are implemented on XILINX XC3S1400A, field programmable gate array (FPGA), which generates the gating signals for the switches of the IPM. Fig. 3 (a), (b) and (c), shows the inverter output voltage, common mode voltage, output current and leakage current, respectively, for the PD-MCPWM, POD-MCPWM and pro- posed H-MCPWM techniques, for the five-level inverter. It can be seen from the figure that the output voltages of the in- verter has five voltage steps, i.e., +40 V, +20 V, 0, 20 V and40 V. It can be observed from Fig. 3 (a) and (b), respectively, that the CMV is 35.2 V (peak) in the PD-MCPWM technique and 26.0 V (peak) in the POD-MCPWM technique.

It is in good agreement with the theoretical aspects explained in the previous section that the PD-MCPWM technique varies in the band range of VPV/2 and hence, further reduction of CMV is not possible due to uncontrolla- ble switching states. The H-MCPWM offers reduced mag- nitude of CMV to the band limit of maximum VPV/4. The proposed H-MCPWM provides reduced CMV during all the switching instants; hence it renders low leakage cur- rent flow through the parasitic capacitance.

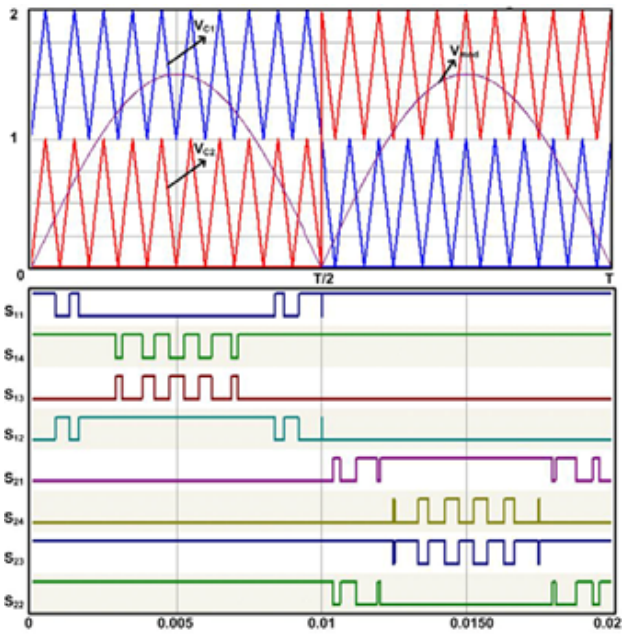

Fig. 3. Switching pattern of proposed H-MCPWM technique for five-level cascaded multilevel inverter.

Logic Conditions	*Switches on Upper H-Bridge*				*Switches on Lower H-Bridge*				*Common Mode Voltage*
Mode-1: (0 to T/2)	S_{11}	S_{14}	S_{13}	S_{12}	S_{21}	S_{24}	S_{23}	S_{22}	V'_{cm}
$V_{c1} > V_{ref} < V_{c2}$	1	1	0	0	0	0	1	1	$2V_{PV}/4$
$V_{c1} > V_{ref} > V_{c2}$	0	1	0	1	0	0	1	1	$V_{PV}/4$
$V_{c1} < V_{ref} > V_{c2}$	0	0	1	1	0	0	1	1	$2V_{PV}/4$
Mode-2: (T/2 to T)	S_{11}	S_{14}	S_{13}	S_{12}	S_{21}	S_{24}	S_{23}	S_{22}	-
$V_{c2} > V_{ref} < V_{c1}$	1	1	0	0	0	0	1	1	$2V_{PV}/4$
$V_{c2} > V_{ref} > V_{c1}$	1	1	0	0	1	0	1	0	$V_{PV}/4$
$V_{c2} < V_{ref} > V_{c1}$	1	1	0	0	1	1	0	0	0

Fig. 4. SWITCHING INSTANTS OF H-MCPWM TECHNIQUE FOR CONSTANT COMMON MODE VOLTAGE

tage, leakage current magnitude and number of carrier requirements, is shown in Table II. The parameters used in simulation are: PV output voltage of 120 V across the DC link of each H-bridge, parasitic capacitance (0.1 F), modulation index (0.9), filter inductance (1.8 mH) and load (20). The table clearly shows the advantage of the proposed H-MCPWM as compared to the other multicarrier PWM techniques. Also the proposed H-MCPWM has less computational burden, as compared to the conventional MCPWM. To show this the digital processor utilization summary report for

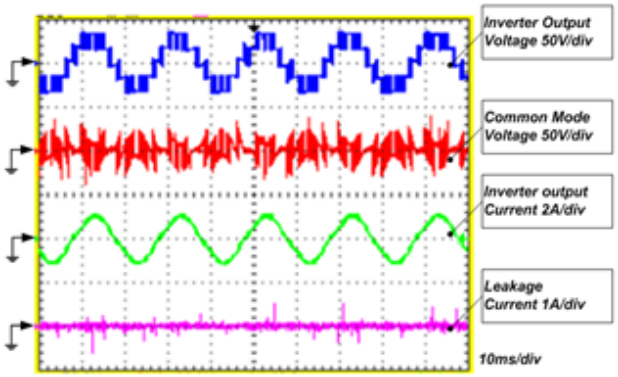

Fig. 5. PD-MCPWM

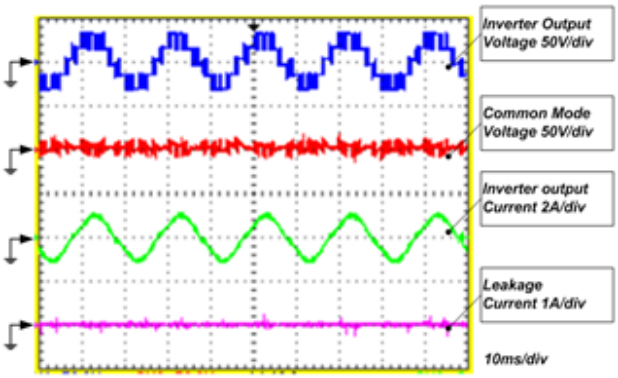

Fig. 6.) POD-MCPWM

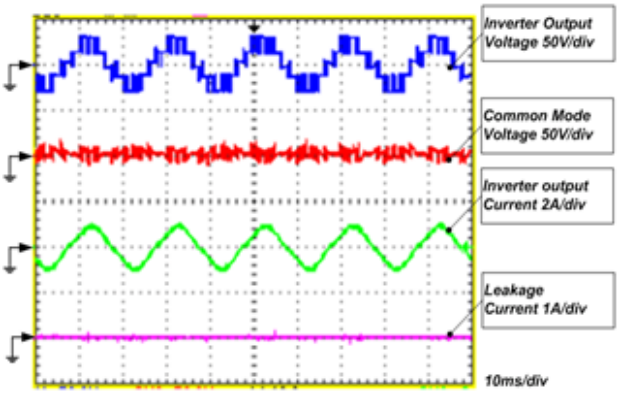

Fig. 7. proposed H-MCPWM techniques.

Device Utilization Summary			
Logic Utilization	**Used**	**Available**	**Utilization**
Number of Slice Flip Flops	296	9,312	3%
Number of 4 input LUTs	605	9,312	6%
Number of occupied Slices	454	4,656	9%
Number of Slices containing only related logic	454	454	100%
Number of Slices containing unrelated logic	0	454	0%
Total Number of 4 input LUTs	662	9,312	7%
Number used as logic	365		
Number used as a route-thru	57		
Number used as Shift registers	240		
Number of bonded IOBs	10	232	4%
Number of BUFGMUXs	1	24	4%
Average Fanout of Non-Clock Nets	2.36		

Fig. 8. MCPWM (both PD and POD) techniques,

Device Utilization Summary			
Logic Utilization	**Used**	**Available**	**Utilization**
Number of Slice Flip Flops	181	9,312	1%
Number of 4 input LUTs	424	9,312	4%
Number of occupied Slices	311	4,656	6%
Number of Slices containing only related logic	311	311	100%
Number of Slices containing unrelated logic	0	311	0%
Total Number of 4 input LUTs	460	9,312	4%
Number used as logic	304		
Number used as a route-thru	36		
Number used as Shift registers	120		
Number of bonded IOBs	6	232	2%
Number of BUFGMUXs	1	24	4%
Average Fanout of Non-Clock Nets	2.75		

Fig. 9. proposed H-MCPWM technique

XILINX XC3S1400A FPGA is shown in the Fig.4 (a) and (b), respectively, for the MCPWM (same for both PD and POD) and for the proposed H-MCPWM, techniques.

IV. CONCLUSIONS

This letter proposes hybrid multicarrier pulse width modulation technique employed in transformerless cas- caded multilevel inverter for the PV systems. The proposed modulation technique attains reduced common mode vol- tage with simplicity in implementation of the modulation technique. It has been illustrated that the proposed modula- tion technique has less leakage current as compared to the two and three-level inverters. It is also observed that the proposed H-MCPWM offers less total harmonic distortion as compared to the conventional modulation methods. It uses only two carrier signals to generate the five-level in- verter output which otherwise is four in other multicarrier modulation techniques.

REFERENCES

[1] R. Gonzalez, J. Lopez, P. Sanchis and L. Marroyo*"Transformerless Inverter for Single-Phase Photovoltaic Systems,"*,," IEEE Trans. on Power Electron., vol.22, no.2, pp.693-697, March 2007.

[2] T. Kerekes, R. Teodorescu, P. Rodriguez, G. Vazquez, and E. Aldabas,*"Transformerless Inverter for Single-Phase Photovoltaic Systems,"*,," IEEE Trans. on Power Electron., vol.22, no.2, pp.693-697, March 2007.

[3] Z. Li, S. Kai Sun, F. Lanlan, W. Hongfei, X. Yan*"*A Family of Neutral Point Clamped Full-Bridge Topologies for Transformerless Photovoltaic Grid-Tied Inverters,",IEEE Trans. on Power Elec- tron.vol.28, no.2, pp.730-739, Feb. 2013.

[4] G. Xiaoqiang, M.C Cavalcanti, A.M Farias and J.M Guerrero, *"Single-Carrier Modulation for Neutral-Point-Clamped Inverters in Three-Phase Transformerless Photovoltaic Systems,"* ,IEEE Trans. on Power Electron., vol.28, no.6, pp.2635-2637, June 2013.

PERFORMANCE EVALUATION OF PI CONTROLLER BASED DC-DC RESONANT CONVERTER

P.Mohan
PG Scholar,
Department of Electrical and Electronics Engineering
MAILAM ENGINEERING COLLEGE

N.Madhanakkumar
Research Scholar,
Department of Electrical and Electronics Engineering
MAILAM ENGINEERING COLLEGE

***Abstract*—In this paper, the closed loop control of resonant DC-DC converter topology is presented. DC-DC converter plays an important role in power conversion. They are used in many applications like telecommunications, IT equipments, it is likely that critical electronic loads, switching mode regulators etc. Control action of our converters involves maintaining constant output voltage in the presence of change in load and change in supply voltage conditions. Traditional controllers have limitation in control action whenever the changes are rapid in nature. In this paper design and simulation using MATLAB/SIMULINK of dc-dc resonant converter output voltage using PI control is presented. Comparison analysis and Simulation results are presented to prove that the steady state deviations of PI controller. KeywordsPI controller; DC-DC resonant converter; closed loop control;**

I. INTRODUCTION

Now-a-days, the LLC resonant converter is also used by consumer electronics on the interest of high power applications and for DC drive applications due to their high power packing density and high efficiency. The high power density which can be achieved by increasing the switching frequency range. The controllable switches are operated on hard switched mode or soft switched mode to achieve this high power density with high efficiency. The hard switching mode is obtained by the pulse generation in PWM converters. But in that mode the power switches suffers from turn on and turn off switching losses when the frequency is increased. The soft switching mode overcome this drawback and reduces the switching losses in resonant converter. So the resonant converter is used alternative than PWM converters in high power applications. The analysis; control and stabilization of the switching converters are the main factors that need to be considered and a suitable controller structure is always in demand for most industrial and high performance applications. The pulse width modulated (PWM) voltage mode control scheme in which the duty cycle is altered, based on the error between the set voltage and the measured output voltage such that the output voltage of the converter is very nearly equal to the desired value is well documented and widely used. The main objective in this work is to illustrate a closed loop model of the buck converter to obtain the desired voltage of the DC load with high accuracy regardless of unregulated input voltage source. Simulation of the buck converter model associated with controller is carried out via MATLAB/SIMULINK program to investigate the performance characteristics and to display the result.

II. DC-DC RESONANT CONVERTER

A. Related Work

The proposed resonant converter consists of two MOSFET switches and two diodes on the input side or primary side of the transformer under the control of ZVS converter. The LLC Resonant converter provides isolation between circuits with the help of transformer. The control is provided using the controller circuit on the output side of the transformer to achieve constant output voltage or wide load range of the converter.

B. DC-DC Converter

The block diagram of resonant DC-DC converter with PI controller is shown in Figure 1.2. The resonant tank consisting of three reactive energy storage elements (LLC) against the conventional resonant converter that has only two elements. Power from the resonant circuit is taken either through a transformer in series with the resonant circuit or series in the capacitor comprising the resonant circuit. In both cases the high frequency feature of the link allows the use of a high frequency transformer to provide voltage transformation and ohmic isolation between the DC source and the load. In LLC the load voltage can be controlled by varying the switching frequency .The phase domain control scheme is suitable for wide variation of load condition because the output voltage is independent of load.

(i) DC input source: 110v and This ZVS output acts as input to the resonant converter. (ii) The ZVS is used instead of ZCS is that it is used to eliminate the capacitive turn on loss. (iii) The single PI controller is used to control the circuit of Resonant converter. (iv) Due to this, the output on the input side and output side is controlled efficiently. (v) Thus, the output of the resonant converter is obtained as 48volt.

III. PI CONTROLLER BASED DC-DC RESONANT CONVERTER

The controller is provided by the design of closed loop system. There are many types of controller and the generally used controller for the control of the system are proportional (P) controller, proportional integral (PI) controller and proportional integral derivative (PID) controller. The controller is provided as feedback control which is often referred as closed loop control system. In a closed loop system, the actuating error signal which is the difference between input signal and feedback signal is fed to the controller so as to reduce the error and bring the output of the system to a desired value. The PI controller has proportional and integral error but derivative (D) of the error is not used. The PI controller is a special case of controller, which is using in abundant for controlling the system. The limitations of PI controller in the closed loop system when compared open loop controller are as follow: The PI controller generates oscillations with peak overshoot. The settling time is also increased in the PI controller. There is also increase in the steady state error when operated under PI controller operation. The output produced makes less sensitive to the sudden line and load disturbance of the system with some oscillations.

A. Simulation studies

The simulation model is done as computer simulation using the MATLAB software. The computer simulation is the most important tool to simulate any system using their respective models. The computer simulation provides the accurate result, reduces the time of operation and easy to control than physical or manual work. As the technology is growing the operation by means of computer simulation is also increasing. Nowadays, in every field there is a role of computer simulation. Thus for electrical and electronics studies there are many types of computer simulation as MATLAB, PSPICE, CAD, etc. In this work, the MATLAB software is used to form the SIMULINK model of the computer simulation. The ZVS buck converter output is the boosted voltage of DC source which produces the output of 48Volt. The pulse to each MOSFET is fed from the pulse generator with the proper time delay to each switching pair. Then the DC output is fed through the tank circuit on the primary side of the transformer. The secondary of the transformer consists of output diode, output capacitor and resistive load.. The repeated sequence triangular wave in the comparator. The comparator has the relational operator which produces the pulsed output signal to MOSFET switches on upper switch and the lower switches is controlled by the inverted output with the help of NOT gate logical operator. Thus the PI controllers are used to control the output voltage. With the help of these control action, the desired output of 48Volt is obtained at the resistive load. The line and load disturbance can be applied to this closed loop Resonant converter with the help of the subsystem created at the input source side and load side. These subsystems consist of the required components to change both the line and load value alternatively so that at their particular time the disturbance is applied and the desired output is obtained.

B. SIMULATION RESULTS

The simulation result for the Resonant converter for start up, under sudden line disturbance and load disturbance are obtained using the SIMULINK model. Using the above models for LLC Resonant converter, the start up as well as transient of both open loop and closed loop PI controller under small signal step disturbances in supply and load are shown in figure (2) to (3). The figure 1(a),1(b) shows the open loop and closed loop PI control responses of LLC Resonant converter start - up output voltage and current with set point of 110V and nominal load of 38.4 respectively. The figure 2(a),2(b) and shows their responses of output voltage and current in open loop and closed loop control under sudden line disturbance (110V 105V 110V) at 2.5sec with nominal load of 38.4 respectively. The figure 3(a),3(b) shows their responses of output voltage and current in open loop and closed loop control under sudden load disturbance(38.4 33.4 38.4) at 1sec with set point of 110V respectively The PI controller regulates the output voltage of the resistive load within a maximum under

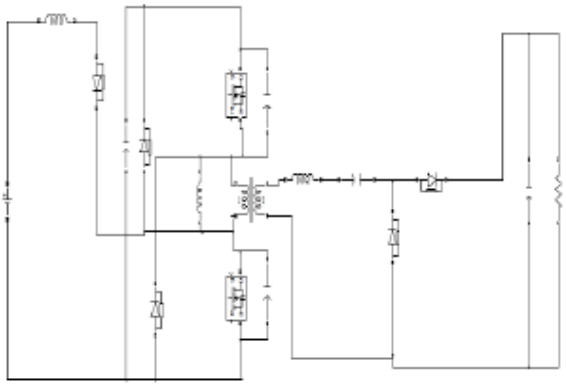

Fig. 1. DC-DC resonant converter circuit

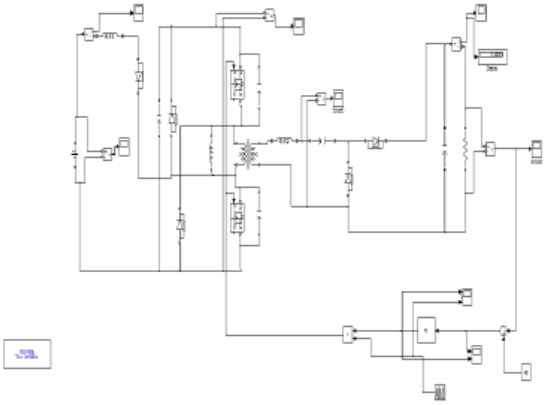

Fig. 2. Model of DC-DC Resonant converter in closed loop

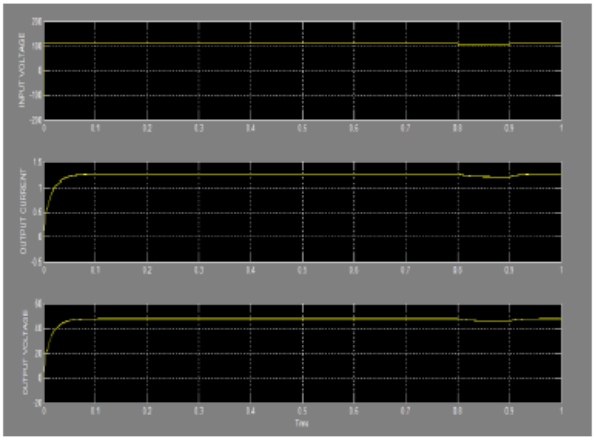

Fig. 3. Simulated output voltage of Resonant converter with sudden line disturbance of (110V 105V 110V) and nominal load 38.4 at t = 0.8sec (open loop)

both line and load disturbance making the controller very less sensitive to these disturbances than the conventional open loop control. So, from the simulation result it is used to understand that the closed loop system is better than the conventional open loop system.

IV. COMPARISION ANALYSIS OF OPEN LOOP AND CLOSED LOOP SYSTEM

With these simulation results, the comparison TABLE II is drawn to clearly predict the performance of the resonant converter and the controller importance in the system.the comparison of simulated performance of open loop and closed loop system for Resonant converter.

Thus the simulation results and comparison analysis, it is proved that the closed loop Resonant converter provides output with reduced rise time, less sensitive to the disturbances and settled soon than the open loop Resonant converter.

V. CONCLUSION

Thus, the performance analysis on open loop and closed loop resonant DC-DC converter model has been done and simulation models are obtained using Matlab/Simulink software and the obtained results are much closed to the particular values. The proposed converter to obtain the desired voltage of the DC load with high accuracy regardless of unregulated input voltage source. The PI controller is the intelligent controller yield better dynamic performances with fast speed response. The proper controller structure of PI controller is tuned using the trial and error method. The system execute better performance under sudden line and load disturbance. To improve the stability of an unstable system, the closed loop control is used to reduce the systems sensitivity, and to produce a reliable and repeatable performance of the system. The open loop and closed loop resonant DC-DC converter characteristic performance was compared and shows that the closed loop control is most efficient. template is designed so that author affiliations are not repeated each time for multiple authors of

TABLE II

Performance evaluation of open loop and closed loop dc-dc resonant converter

System	LINE DISTURBANCE					
	100v		110v		120v	
	V_{In}(V)	V_o(V)	V_{In}(V)	V_o(V)	V_{In}(v)	V_o(V)
Open loop	100	43.4	110	47.8	120	52.3
Closed loop	100	48	110	48	120	48

System	LOAD DISTURBANCE					
	33.4Ω		38.4Ω		43.4Ω	
	I_o(A)	V_o(V)	I_o(A)	V_o(V)	I_o(A)	V_o(V)
Open loop	1.34	44.8	1.24	47.8	1.17	50.9
Closed loop	1.43	48	1.25	48	1.10	48

Fig. 4.

the same affiliation. Please keep your affiliations as succinct as possible (for example, do not differentiate among departments of the same organization). This template was designed for two affiliations.

REFERENCES

[1] Sin-Woo Lee and Hyun-Lark Do, *Soft-Switching Two-Switch Resonant ACDC Converter With High Power Factor*,IEEE transactions on industrial electronics, vol. 63, no. 4, april 2016.

[2] Zhang, Fan, Lei Du, Fang Zheng Peng, ZhaomingQian, *"A new design method for high-power high-efficiency switched-capacitor dcdc converters"*,"A new design method for high-power high-efficiency switched-capacitor dcdc converters"

[3] Abdel-Rahim, Omar, Mohamed Orabi, *Switched inductor boost converter for PV applications*,,In Applied Power Electronics Conference and Exposition (APEC), pp. 2100-2106, 2012.

Design of Dual Proportional Integral Load Frequency Controllers Based on Gravitational Search Algorithm for Nonlinear Hydrothermal Power System

Mrs.S.Lese
Assistant professor
Department of Electrical and Electronics Engineering
St.Annes College of Engineering and Technology, Panruti, Tamilnadu, India.

***Abstract*—This paper considers the design of Dual Proportional-Integral (DPI) Load Frequency Control (LFC), using gravitational search algorithm (GSA). The design is carried out for nonlinear hydrothermal power system where generation rate constraint (GRC) and governor dead band are considered. Furthermore, time delays imposed by governor-turbine, thermodynamic process, and communication channels are investigated. GSA is utilized to search for optimal controller parameters by minimizing a time-domain based objective function. GSA-based DPI has been compared to Ziegler-Nichols based PI, and Genetic Algorithm (GA) based PI controllers in order to demonstrate the superior efficiency of the proposed design. Simulation results are carried for a wide range of operating conditions and system parameters variations.**

KeywordsGravitational Search Algorithm (GSA), Load Frequency Control (LFC), Dual Proportional-Integral (DPI) controller

I. INTRODUCTION

Load frequency control represents a very imperative issue in large-scale power systems. It plays an important role in the power system by maintaining the system frequency and tie-line power flow at scheduled values [1]-[3]. There are two different control loops used to accomplish LFC in an interconnected power system, namely primary and supplementary speed control. Primary control is done by governors of the generators, which provide control action to a sudden change of load. The secondary control adjusts the frequency at its nominal value by controlling the output of selected generators. In last years, many control strategies have been suggested based on the conventional linear control theory. The conventional controller is simple in structure, but its performance deteriorates in the case of most complex systems [4]. For example, the conventional PI controller has some advantages such as small overshoot but settling time is large. Conversely, the conventional I controller has slightly smaller settling time than PI control and larger overshoot [4], [5]. Control system performance can be improved by allowing the controller to switch from one mode to another. For instance, for certain linear systems switching from a proportional controller to an integral controller in a feedback loop may provide a fast response and small overshoot [6]. Based upon the above-mentioned facts, it is desirable to adopt a dual mode controller concludes both proportional and integral controller. In [5] the rate of change of the error is used as switching criteria between proportional and integral controller. The proportional controller acts when the rate of change of the error is sufficiently large, whereas the integral controller would be the better one when the rate of change of the error is small. In [7]-[9], the error is used as switching criteria between proportional and integral controller. The proportional controller is used when the error is large, the integral controller acts when the error is small. The main problem which faces dualmode controller in [5] - [9], it is the switching condition. This paper proposes to solve this problem by make relation between the switching condition and the summation of disturbance on the system. If the summation of disturbance on the system increases the switching condition increase. In order to get better performance from any controller, its parameters need good optimization. The conventional methods face some difficulties to achieve this purpose, such as complex mathematical equations for large systems. Several approaches such as optimal, Genetic Algorithm (GA), Particle Swarm Optimization (PSO), Bacterial Foraging Optimization (BFO), etc., for the design and optimization of the LFC system, have been reported in the literature [10] - [21]. Modern optimal control concept for AGC designs of interconnected power system was firstly presented by [10], [11]. Genetic algorithms (GAs) have been extensively considered for the design of AGC. Optimal PID and fractional-order PID control parameters have been computed by the GAs technique for interconnected, equal non-reheat and reheat type two generating areas [12], [13]. In [14] the Parameters of PID sliding-mode used in LFC of multi-area power systems with nonlinear elements are optimized by GA. In [15], GA is used to compute the decentralized control parameters to achieve an optimum operating point for a realistic system comprising generation rate constraint (GRC), dead band, and time delays. AGC by an integral controller and PI controller based on PSO is reported in [16]. In [17] the parameters of PI controller are designed by PSO

with the new objective function and compared their results with [16]. In [18], a robust PID controller based ICA is used for LFC application. The authors of [19], [20] have proposed bacterial foraging optimization algorithm (BFOA) for designing PI and PID-based load frequency control for a two-area power system with and without GRC. Application of BFOA to optimize several important parameters in AGC of an interconnected three unequal area thermal systems such as the integral controller gains, governor speed regulation, and the frequency bias parameters, has been reported in [21]. In [22] a new optimization algorithm based on the law of gravity and mass interactions is introduced. In the algorithm, the searcher agents are a collection of masses which work with each other based on the Newtonian gravity and the laws of motion. This paper proposes the GSA for optimal tuning of dual PI controller in two area interconnected power system to damp out power system oscillations. The dual PI controller design is formulated as an optimization problem and GSA is employed to search for optimal controller parameters by minimizing a candidate time-domain based objective function. The performance of the proposed dual PI controller- based GSA is evaluated by comparison with a conventional PI controller and PI-based GA. Simulations results on a two-area test system are presented to assure the superiority of the proposed method compared with PI-based GA and conventional one.

II. GRAVITATIONAL SEARCH ALGORITHM

Gravitational Search Algorithm (GSA) is a novel heuristic algorithm inspired by the Newtonian laws of gravity and motion [22]. In GSA, agents are considered as objects and their performance is evaluated by their masses. All these objects attract each other by the force of gravity and moves toward the objects with a heavier mass. The heavy masses correspond to the good solution, and this guarantees the exploitation step of the algorithm. In GSA, each mass (agent) has four representations: position, inertial mass, active gravitational mass and passive gravitational mass. The position of the mass represent a solution of the problem and its gravitational and inertia masses are determined using a fitness function. In other words, each mass presents a solution and the algorithm is run by properly adjusting the gravitational and inertia masses. By lapse of time, it is predictable that masses be attracted by the heavier mass. This mass will represent an optimum solution in the search space. GSA is representing a small artificial world of masses obeying the Newtonian laws of gravitation and motion. Masses obey the following laws [22]-[24]. A. Law of Gravity Each agent attracts every other agent and the gravitational force between the two agents is directly proportional to the product of their masses and inversely proportional to the distance between them R. It has been concluded in the literature that R provides better results than $R^2 in all experiment cases [22]. B. Law of Motion The current velocity$ $ious velocit$

where n is the space dimension of the problem and, xid is the represents the position of ith agent in the dth dimension. At a specific time t, the force acting on mass i from mass j is defined as:

where Maj is the active gravitational mass related to agent j, Mpi is the passive gravitational mass related to agent i, G(t) is gravitational constant at time t, is a small constant, and Rij(t) is the Euclidian distance between two agents i and j:

To give a stochastic characteristic to algorithm, it is supposed that the total force that acts on mass i in a dimension d be a randomly weighted sum of dth components of the forces exerted from other agents:

where randj is a random number in the interval [0,1]. Hence, by the law of motion, the acceleration of the mass i at time t,and in dth direction, aid (t) is given as:

where randi is a uniform random variable in the interval [0,1]. The gravitational constant G is initialized at the beginning and will be reduced with time to control the search update. In other words, G is a function of the initial value (G0) and time (t) as:

Where fiti(t) present the fitness value of the agent at time t, and worst(t) and best(t) are defined as (for a minimization problem): To achieve a good compromise between exploration and exploitation, the number of objects is reduced with lapse of (4) and therefore a set of objects with bigger mass are used for applying their force to the other.

III. DUAL PI CONTROLLER

The control law employed depending upon the magnitude of the rate of change of the error signal.where, ACE(t) is an error signal at a particular instant, is a small positive

$$X_i = \left(x_i^1, \ldots, x_i^d, \ldots, x_i^n\right), i = 1,2,\ldots,n \quad (1)$$

Fig. 1.

$$F_{ij}^d = G(t)\frac{M_{pi}(t) \times M_{pi}(t)}{R_{ij}(t) + \varepsilon}\left(x_j^d(t) - x_i^d(t)\right) \quad (2)$$

Fig. 2.

$$R_{ij}(t) = \left\| x_i(t), x_j(t) \right\|_2 \quad (3)$$

Fig. 3.

$$F_i^d(t) = \sum_{j=1, j \neq i}^{n} rand_j (F_{ij}^d) \quad (4)$$

Fig. 4.

$$v_i^d(t+1) = rand_i \times v_i^d(t) + a_i^d(t)$$

$$x_i^d(t+1) = x_i^d(t) + v_i^d(t+1)$$

Fig. 5.

constant indicating the specified limit of rate of change of the error signal, Ui the control signal to ith area and KPr is the proportional gain.where Ki is the integral gain. Then if the parameters Kpr, Ki and Kc are suitably selected, one can ensure a high-quality transient response. By choosing a suitable value of Kpr, one makes sure that speed of the system is high. Whenever the rate of change of error falls within the specified bound d(ACE(t)/dt , the integrator starts accumulating the error. But if the error exceeds the bound

the integrator resets to zero. The GSA is proposed in this paper to get the best value of Kpr, Ki and Kc. The proposed control scheme

$$M_{ai} = M_{pi} = M_{ii} = M_i, \quad i = 1, 2, \ldots, N$$

$$m_i(t) = \frac{fit_i(t) - worst(t)}{best(t) - worst(t)}$$

$$M_i(t) = m_i(t) / \sum_{j=1}^{N} m_j(t)$$

Fig. 6.

$$best(t) = \max_{j \in \{1,2,\ldots,N\}} fit_j(t)$$

$$worst(t) = \min_{j \in \{1,2,\ldots,N\}} fit_j(t)$$

Fig. 7.

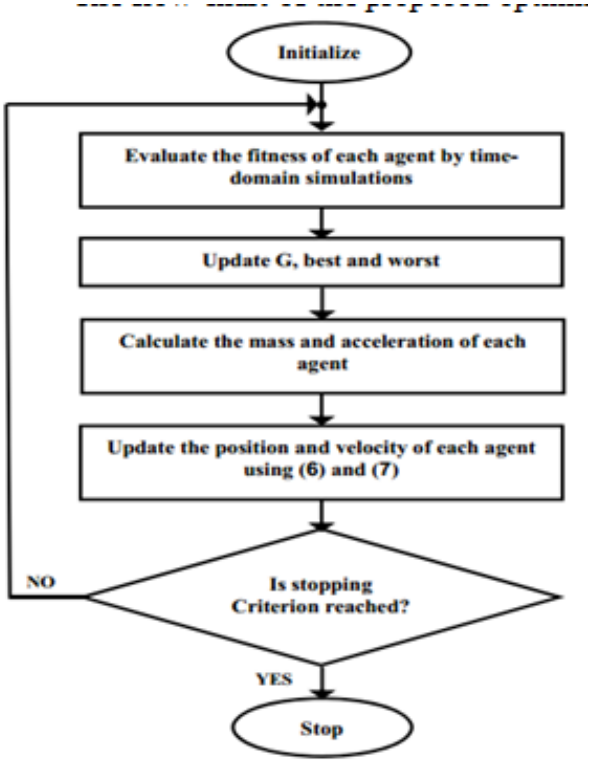

Fig. 8.

IV. TWO AREA HYDRO-THERMAL POWER SYSTEM

A model of controlled hydro-thermal plants in a two-area interconnected power system with nonlinearities and boiler dynamics is shown in Fig. 3 where the system abbreviations and symbols are defined in Table I.

The speed governor dead band has a significant effect on the dynamic performance of the system. For this analysis, in this paper backlash non-linearity of about 0.05% for thermal system and the dead band non-linearity of about 0.02% for hydro system are considered. The system is provided with single reheat turbine with suitable GRC, for thermal area 0.0017MW per sec and hydro area 4.5% per sec for rising generation and 6% for lowering generation. The boiler is used to producing steam under pressure. In this study, the effect of the boiler in a steam area in the power system is also considered and detailed scheme is shown in Fig. 4 given in [25]. The objective function which selected in this paper can be defined by (19). (19) This study focuses on the optimal tuning of controllers for LFC using GSA. The aim of the optimization is to search for the optimum dual PI controller parameters that improve the damping characteristics of the system under all operating conditions and various loads and finally designing a low order controller for easy implementation.

V. SIMULATION RESULTS

In this section, different comparative cases are examined to show the effectiveness of the proposed GSA method for optimizing controller parameters of dual PI controller. Table II

$$\text{For } \left|\frac{d(ACE(t))}{dt}\right| \le \varepsilon$$

$$U_i = -K_i \int ACE(t)dt$$

Fig. 9.

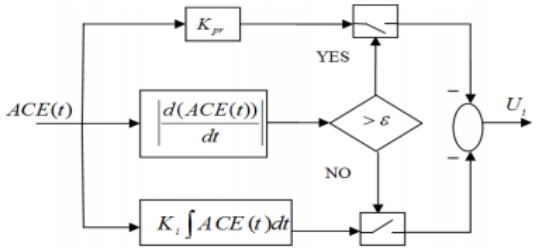

Fig. 2 Block diagram for the proposed dual PI controller

Fig. 10.

gives the optimum values of controller parameters for different methods. The PI controller parameters of the conventional controller due to [26]. Case 1. A 1% step increase in demand of the first area (PD1), the second area (PD2) simultaneously and time delay equal 2 seconds are applied (nominal test case). The change in frequency of the first area f1, the change in frequency of the second area f2, and change in tie-line power of the closed loop system are shown in Figs. 5 7. Remarkably, the response with conventional PI controller has high settling time and undesirable oscillations. Also compared with PI-based GA the proposed method is indeed more efficient in improving the damping characteristic of the power system.

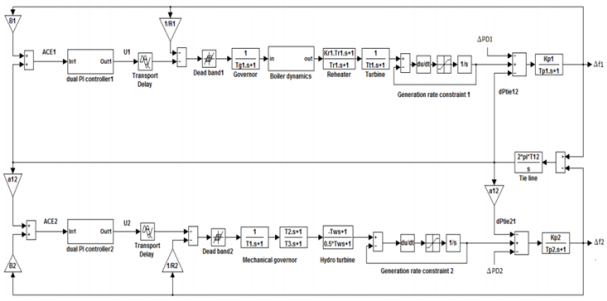

Fig. 11. Two-area interconnected power system

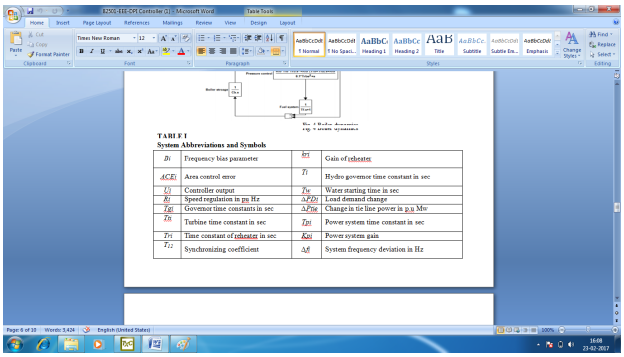

Fig. 12. Boiler dynamics

TABLE I
System Abbreviations and Symbols

Bi	Frequency bias parameter	kri	Gain of reheater
$ACEi$	Area control error	Ti	Hydro governor time constant in sec
Ui	Controller output	Tw	Water starting time in sec
Ri	Speed regulation in pu Hz	ΔPDi	Load demand change
Tgi	Governor time constants in sec	$\Delta Ptie$	Change in tie line power in p.u Mw
Tti	Turbine time constant in sec	Tpi	Power system time constant in sec
Tri	Time constant of reheater in sec	Kpi	Power system gain
T_{12}	Synchronizing coefficient	Δfi	System frequency deviation in Hz

Fig. 13.

TABLE II
Controller Parameters, And Objective Function (J)

	Conventional PI	GA-PI	dual PI
Controller Parameters	K_{pr1}= K_{pr2}=0.3, K_{i1}= K_{I2}=0.12	K_{pr1}=0.9795, K_{i1}=0.0399, K_{pr2}=1.0719, K_{i2}=0.0440	K_{pr1}=0.1845, K_{i1}=0.0496, K_{c1}=0.7672, K_{pr2}=0.2512, K_{i2}=0.0288, K_{c2}=0.4189,
J	14.1752	8.0265	7.1108

Fig. 14.

Case 2. A 1.5% step increase is applied as a change of demand in first area (PD1), the second area (PD2) simultaneously and time delay equal 2 seconds. The change in frequency of the first area f1, the change in frequency of the second area f2 and change in tie-line power of the closed loop system are shown in Figs. 8, 9. From these figures, the response with the conventional controller is unstable. Moreover, the proposed method outperforms and outlasts PI-based GA in damping oscillations effectively and reducing settling time. Hence compared to the conventional controller, and PI-based GA, dual PI controller based GSA greatly enhances the system stability and improves the damping characteristics of the power system. Because of the large values of conventional PI controller response, a sub figure of this part is shown beside the main response.

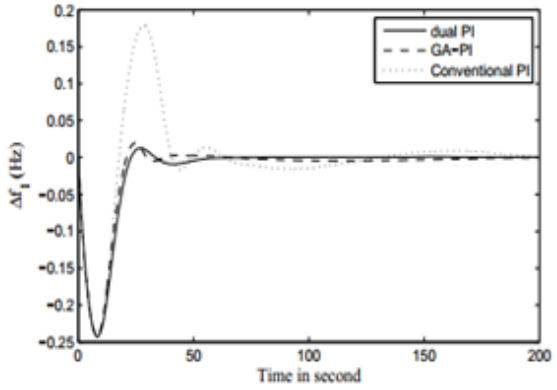

Fig. 15. Change in f1 for case 1

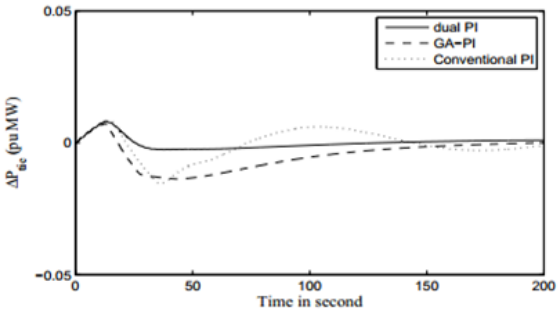

Fig. 16. Change in Ptie for case 1

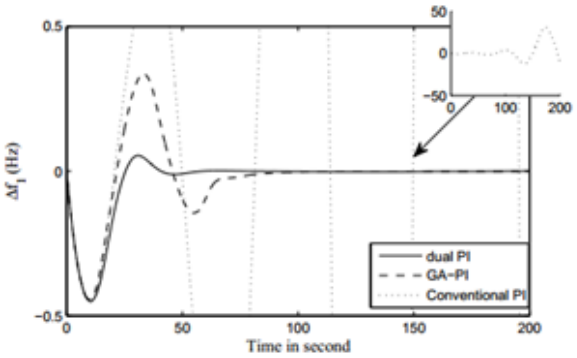

Fig. 17. Change in f1 for case 2

VI. CONCLUSION

This paper presents the application of the GSA algorithm as a new artificial intelligence technique in order to optimize the AGC in a two-area interconnected power system. GSA algorithm is proposed to tune the parameters of dual PI controller. A two-area power system is considered to demonstrate the proposed method. The simulation results emphasis that the designed dual PI controller -based GSA is robust in its operation and gives a superb damping performance for frequency and tie line power deviation compared to conventional PI controller, and PI-based GA. Besides the simple architecture of the proposed controller, it has the potentiality of implementation in real-time environment.

REFERENCES

[1] T. A. N. Wen, *Load frequency control: Problems and solutions,* ,Control Conference (CCC), 2011 30th Chinese. IEEE, 2011..

[2] S. K. Pandey, S. R. Mohanty, and N. Kishor, *A literature survey on loadfrequency control for conventional and distribution generation power systems,* Renewable and Sustainable Energy Reviews, vol.25 no.1, pp. 318-334, 2013.

[3] R. Esmat, Hossein Nezamabadi-Pour, and Saeid Saryazdi,*GSA: a gravitational search algorithm,* ,Information sciences, vol. 179, no.13, pp. 2232-2248, 2009.

[4] R. Esmat, Hossien Nezamabadi-Pour, and Saeid Saryazdi*Filter modeling using gravitational search algorithm,* ,Engineering Applications of Artificial Intelligence, vol.24, no.1, pp. 117-122, 2011.

UPQC WITH FUZZY LOGIC FOR POWER QUALITY IMPROVEMENT

Dr.N.Muralikrishnan
HOD
Department of Electrical Engineering
Mailam Engineering college-Mailam

Ms.G.Sivasankari,
Professor,
Department of Electrical Engineering
Mailam Engineering college-Mailam

***Abstract*—This paper proposed on one of these FACTS devices, the nine-switch unified power quality conditioner (UPQC) with fuzzy logic. UPQC is a recent power electronic module which guarantees better power quality mitigation as it has both series-active and shunt-active power filters (APFs). Maintaining similar power rating compared to the conventional UPQC, the nine-switch UPQC functions during normal, sag and swell operation while utilizing three less semiconductor switching devices. The equivalent power rating of its semiconductor switching devices, with respect to the conventional counterpart, results in reduced losses and cost of the entire system. The shunt and series terminal controllers are accurate and fully utilize the nine- switch UPQC dc-link voltage. As a result, the nine- switch UPQC simultaneously mitigates current and voltage harmonics, provides power factor correction and compensates sag and swell voltage variations.**

KeywordsDiscontinuous pulse-width modulation, nine switch converter, power conditioner, power quality.

I. INTRODUCTION

Since its first introduction, static power converter development has grown rapidly with many converter topologies now readily found in the open literature. Almost always, these two converters are connected in a back to-back configuration, using 12 switches in total and sharing common dc-link capacitor, as reflected by the configuration drawn in Fig. 1(a). Where available, a micro source can also be inserted to the common dc link, if the intention is to provide for distributed generation in a micro grid, without significantly impacting on the long proven proper functioning of the back-to-back configuration. Even though facing no major operating concerns at present, improvements through topological modification or replacement of the back-to back configuration to reduce its losses, component count, and complexity

would still be favored, if there is no or only slight expected tradeoff in performance.

Due to the use of harmonic detectors, the accuracy and response of the control scheme can be adversely impacted. In addition, the dual controller is regularly used in these control schemes due to its simple and robust characteristics. Inspire of its fast response, it has several shortcomings: first, due to the variation of switching frequency, the design of the output filters for converters is very difficult.

II. PROPOSED SYSTEM

One of them is the nine-switch converter that was first proposed in the system. The advantage with respect to the back-to-back topology, it has attracted attention towards its applications and its performanc. comparison with the conventional ones . Fuzzy based nine switch converter operating principles and describes proposed fuzzy based nine switch power conditioner, control strategies i.e., space vector modulation scheme for generating gating signals, series control and shunt control blocks for compensation problems.

III. TOPOLOGY CHARACTERISTICS AND SWITCHING LOGIC

The nine-switch converter can be considered as a combination of two parallel connected three-phase three-leg VSCs as well-known as the back-to-back topology. As a result of this new arrangement, the total number of switches was reduced from twelve to nine with respect to its counterpart. Moreover, both the back-to-back topology and the nine-switch converter are able to generate and control two sets of three-phase signals

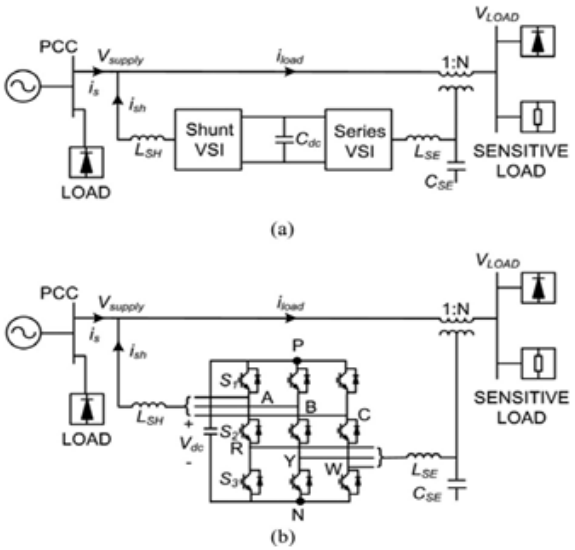

Fig. 1. .Representations of (a) back-to-back and (b) nine-switch Power conditioners.

with different amplitude, frequency and phase shift whether they are currents, voltages or combination of both. Although, the nine- switch converter experiences its own structural limitations that is usually the case for converters. The nine switch converter is formed by tying three semiconductor switches per phase, giving a total of nine forrn all three phases. The nine switches are powered by a common dc link, which can either be a micro source or a capacitor depending on the system requirements under consideration. Like most reduced component topologies, The nine switch converter is formed by tying three semiconductor switches per phase, giving a total of nine for all three phases. The nine switches are powered by a common dc link, which can either be a micro source or a capacitor depending on the system requirements under consideration Where is logical XOR operator .Signals obtained from equation 1, when applied to the nine-switch converter, and then lead to those output voltage transitional diagrams drawn in Fig.3.1 for representing Van and Vrn per phase. Together, these voltage transitions show that the forbidden state of Van= 0V and Vrn=Vdc is effectively blocked off.

A. SERIES CONTROL

The series terminals of the nine- switch UPQC are given two control functions that can raise the quality of power supplied to the load under normal and sag operating conditions. For the former, the series terminals of the conditioner are tasked to compensate for any harmonic distortions that might have originated at the PCC. Spontaneously, the series modulating reference fed to the pulse-width modulator would change from a small harmonic wave pattern to one with fundamental frequency and much larger amplitude, determined solely by the extent of voltage sag.

B. SHUNT CONTROL

The shunt terminals of the nine-switch power conditioner are programmed to compensate for downstream load current harmonics, reactive power, and to balance its shared dc-link capacitive voltage. The sum of outputs from the filter and PI regulator then forms the control reference for the measured shunt current to track. Upon tracked properly, the source current would be sinusoidal, and the load harmonics and reactive power would be solely taken care of by the proposed power Conditioner

IV. SIMULATION RESULTS AND ANALYSIS

The development of MATLAB/SIMULINK simulation model of fuzzy based nine switch Power conditioner and its space vector selection using MATLAB/SIMULINK for harmonic reduction and power factor improvement. It also discusses the simulation procedure for implementing the Simulink model of proposed system.The required voltage for the line under the fault to compensate the voltage sags determined by the pulses. Then the universal bridge draws required voltage to convert it into alternative voltage and it feeds to the filters. The inductive filters and capacitive filters are filtered the harmonics and provide the alternating voltage to the line through the transformers. Here the fault is created and the fault block is connected. The fault which is selected is three phase fault..

To generate time varying, 60 Hz sinusoidal signal with estimated phase angle, the MATLAB function blocks are used. The sine and cosine signals, at unity magnitude from the Phase Locked Loop (PLL)are used to maintain the synchronization

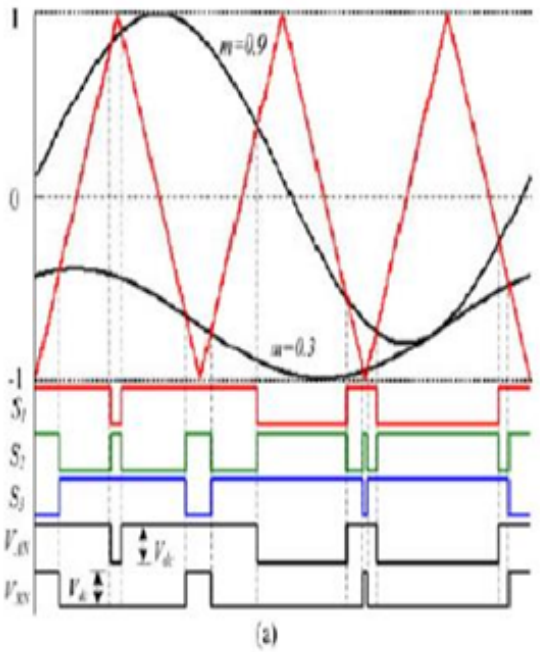

Fig. 2. Arrangementsof Reference having (a)the same frequency but different amplitudes,

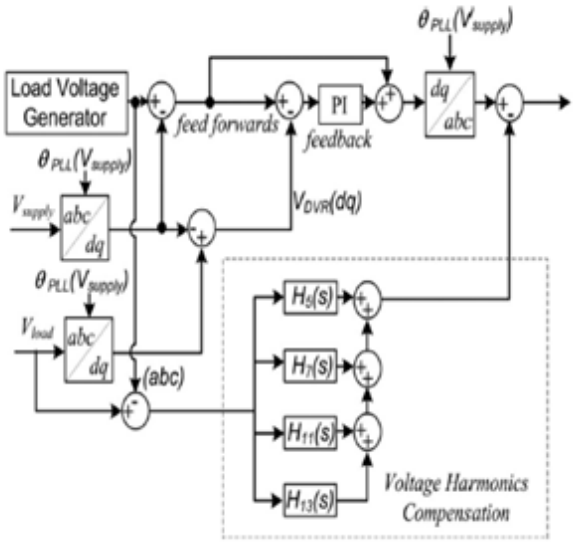

Fig. 3. 1 series control

between the generated reference signal and the supply voltage. This signal multiplied with computed series voltage magnitude gives the required series injected voltage signal with desired phase angle shift.

beginfigure[!t]

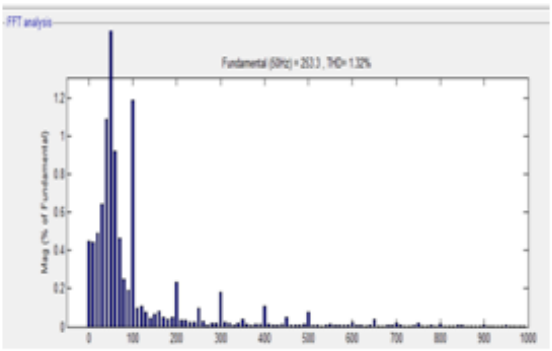

A. CONCLUSION

Thus fuzzy based nine switch converter is simulated using MATLAB/SIMULINK. It effectively reduces the current and voltage harmonics. The increased use of non-linear loads at the industrial and domestic level, which use power semiconductor switching devices, have degraded PQ within the UG and/or distribution networks .A 120 degree modulation scheme is presented for reducing the overall commutation count by 33%. It is also compensated for voltage sags, total harmonic distortion with proper series and shunt controls. Since the number of switches required is less compared to conventional converter, the switching losses are less.

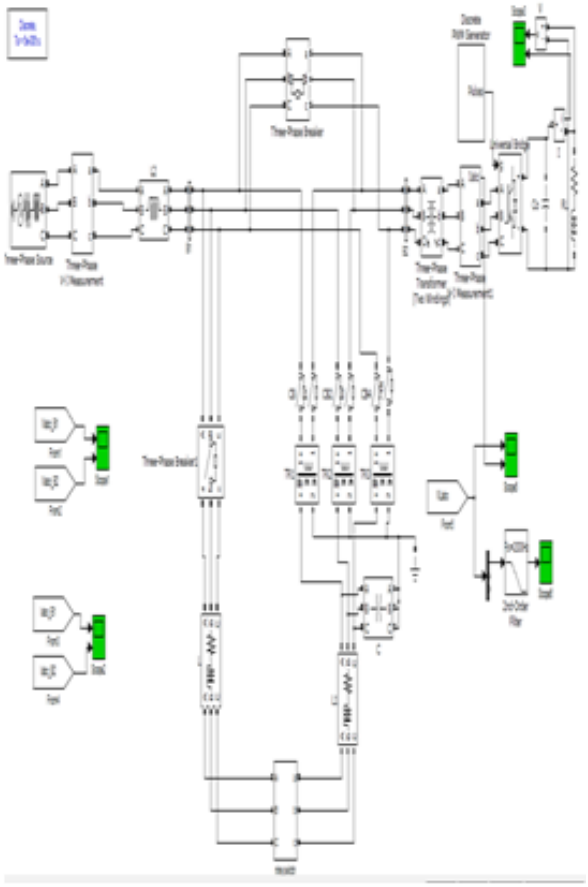

Fig. 4. 1simulation circuit of the proposed system

REFERENCES

[1] Edward. F. Fuchs, Mohammad. A. S. Masoum*Power Quality in Power Systems and Electrical Machines,* ,ISBN-970-0-12-369536, Elsevier Inc., 2008.

[2] Alexander kusko and Marc.T.Thompson, *PoweQuality in Electrical Systems,* The McGraw-Hil Company, Inc.2007.

[3] B.W. Frana, L.F. Silva, M. A Aredes, and M., Aredes, *An improved iUPQC controller to provide additional grid- voltage regulation as a STATCOM,* ,IEEE Trans. Ind. Electron., , vol. 62, no. 3, pp. 1345-1352, Mar. 2015.

[4] R. A. Modesto, S. A. O. Silva, and A. A., Oliveira, *Power quality improvement using a dual unified power quality conditioner/uninterruptible power supply in three- phase four-wire systems,* ,IET Power Electronics, vol. 8, no. 3, pp. 1595-1605, Sept. 2015.

Asymmetric Three Phase Multilevel Inverter Topologies for Variable Frequency PWM

Mr.Subash
UG Scholar
Department of Electrical and Electronics Engineering
Krishnasamy ENGINEERING COLLEGE

Mr.Sasikumar
UG Scholar
Department of Electrical and Electronics Engineering
Krishnasamy ENGINEERING COLLEGE

***Abstract*—Asymmetric three-phase Multilevel Inverter which can achieve reduced harmonics and superior root mean square (RMS) values of the output voltage is proposed. This topology can achieve cascaded full bridge inverter operation with different DC Source and it is fired by using variable frequency pulse with modulation technique as a switching strategy. This pulse width modulation switching strategy has a newly adopted multicarrier single reference technique. The performance parameter factors like Form Factor (FF), Crest Factor (CF), Total Harmonic Distortion (THD) and Fundamental RMS output voltage (VRMS) are estimated by using Proposed asymmetrical three phase cascading multilevel inverter for several modulation indices (0.8-1).The research study carries with it MATLAB/SIMULINK based simulation and experimental results obtained using appropriate prototype (test board) to prove the viability of the proposed concept.**

Keywords: Multilevel Inverter, Variable Frequency Pulse width modulation, Total Harmonic Distortions, Distortion Factor.

I. Introduction

Multilevel Inverter has a strained incredible interest in high-power and medium voltage applications, because it has several benefits: It has high voltage and high power output over the use of power semiconductor switching devices without the use of a transformer. Whenever, the quantity of the output voltage level increases, the total harmonic distortion of the output voltage and current waveform of a multilevel inverter will reduce. A new approach for a modulation of an 11 level cascade multilevel inverter using selective harmonics elimination technique [1]. Introduced a digital control of a three - phase three - stage hybrid multilevel inverter with 18 level output voltage containing minimum switching losses [2]. Develop a fresh type of multilevel inverters using cascading of a two three phase three level inverters [3].The control of cascaded asymmetrical multilevel inverters using only one DC source [4]. Single-phase multilevel inverter with battery balancing operation with reduced harmonic are introduced [5]. Multilevel inverter using direct drive wind turbine grid interfacing are discussed [6].Described three-stage 27-level inverter using H converter is analyzed for average and high-power machine drive applications [7].Trinary 81-level multilevel inverter for STATCOM application [8].Introduced the inverted sine PWM technology for asymmetrical cascaded multilevel inverter [9]. The Neutral Voltage Modulation technique for multilevel cascade inverters under unbalanced dc-link conditions has been proposed [10].Design and implementation of cascaded multilevel inverter operating in current mode [11]. A three-level common-mode voltage eliminated inverter with only one DC supply source using flying capacitor inverter and cascaded H-bridge [12]. Modular multilevel cascaded inverter based on double-star bridge cells using experimental verification [13]. A single-phase photovoltaic (PV) system integrating segmented energy storages (SES) using cascaded multilevel inverter [14]. The proposed topology is obtained by using cascading a five-level flying capacitor multilevel inverter with a flying H-bridge power cell in each phase using a single DC source [15]. A hybrid five-level inverter topology with common-mode voltage elimination for induction motor drives [16]. Novel single-phase five-level inverters develop a five level output voltage with only one DC source using coupled inductors [17]. Design and implementation of a new asymmetrical cascaded multilevel inverter is a series connection of several inverters [18]. Develop a new technology of an improved PWM topology for chopper-cell-based modular multilevel converters [19]. A single phase seven level Asymmetrical Multilevel Inverter fed resistive load using carrier overlap PWM technique with different reference [20]. Asymmetrical cascaded Half-bridge multilevel inverter for 3hp fuel cell electric vehicle (FCEV) with Direct Torque Control Space Vector Modulation scheme (DTC-SVM) based electric drive (induction motor) has been implemented [21].Fresh topologies for a cascade transformer sub-multilevel inverter with every sub-multilevel inverter consists of two DC voltage source with six power semiconductor switches to attain five level output voltage [22]. A new converter configuration based on cascaded converter family unit is offered. The recommended multilevel highly developed cascaded converter has settlement such as lessening in number of Power semi conductor switches and its losses [23]. A fifteen level Photovoltaic fed cascade multilevel inverter for the removal of certain harmonic orders is urbanized for the power quality development [24]. A generalized power loss algorithm for multilevel neutral-point clamped pulse width modulation technique is offered, which is appropriate to any level number of multilevel inverter [25].This paper proposes a asymmetric three phase cascading Trinary-DC source multilevel inverter. The suggested topologies are gained by cascading a full bridge inverter with uneven DC source. These topologies have several new patterns adopting the variable switching frequency. Multi-carrier pulse width modulation techniques are established and

simulated for the preferred three phase asymmetric cascaded multilevel inverter. Finally, the proposed asymmetric three-phase cascading multilevel inverter is demonstrated through experimental results based on the research laboratory (test board) prototype model.

II. Proposed Trinary Multilevel Inverter

The three-phase multilevel inverter is being used for a large number of industrial applications due to their capability of high-power accompanying with lesser output harmonics and switching losses. Multilevel inverter has grown into an active and applied resolution for increasing output power and decreasing total harmonics distortion of AC load system.

The proposed Trinary cascaded multilevel inverter contains three single phase unit. Each single phase unit consists of two full bridges with dissimilar voltage source. The first full bridge contains the DC source of 1Vdc and the second full bridge contains the DC source 3Vdc as presented in Fig. 1. Each DC source is connected to a proposed three phase inverter. Each inverter produces a three dissimilar output voltage levels, such as positive, zero and negative levels by different groupings of the four power semiconductor switches S1, S2, S3 and S4. Whenever the switches, S1 and S4 is turned ON, then the output voltage is positive level (+Ve); whenever the switches S2 and S3 is turned ON, then the output voltage is negative level (-Ve) ;whenever either pair of switches (S1 and S2) or (S3 and S4) is turned ON, then the output voltage will be at zero level (0).

III. Variable Frequency Pulse Width Modulation Techniques

It is usually accepted that the presentation of any multilevel inverter, with any switching control tactic can be correlated to the harmonic contents of its inverter output voltage. There a numerous control technique reported in journalism for a cascaded asymmetric multilevel inverter. But the traditionally used modulation control method is the multicarrier Pulse width modulation technique (MCPWM). In this research paper, changeable switching frequency pulse width modulation technologies such as

i) Variable frequency in phase disposition pulse width modulation system (VFIPDPWM).

ii) Variable frequency phase opposition disposition pulse width modulation system (VFPODPWM).

iii) Variable frequency alternate phase opposition disposition pulse width modulating system (VFAPODPWM).

Which is projected which uses the predictable sinusoidal reference signal and the triangular carrier signals with variable frequency. To put into action of an m-level inverter with (m-1) triangular carrier are used. There are eight separate triangular carriers with variable frequency and with the same magnitudes all carriers; for the eight triangular carrier signals each pair which has a different frequency. The triangular carrier signal C1 and C8 have same frequency and C2 and C7 have another set of same frequency and C3 and C6 have another set of same frequency and C4 and C5 have another set of same frequency. The firing pulses are produced when the amplitude of the reference signal (modulating signal) is superior to that of the triangular carrier signal.

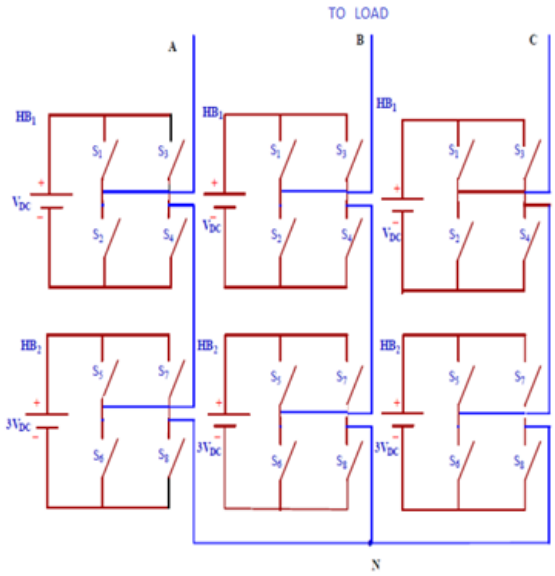

Fig. 1. The Proposed Trinary Cascaded Multilevel Inverter

IV. Variable Frequency In Phase Disposition Pulse Width Modulation System

The vertical offset of carriers for a nine level Trinary DC source multilevel inverter with variable frequency in phase disposition pulse width modulation techniques are illustrated in Fig. 2 and 3. In phase disposition pulse width modulation technique (IPD), all carriers are in phase with each other and it has same amplitude. In this system for an N level inverter, (N-1) carriers with the unlike frequency (2000Hz and 1500Hz) and equal amplitude are prearranged such that the bands they occupy are continuous.

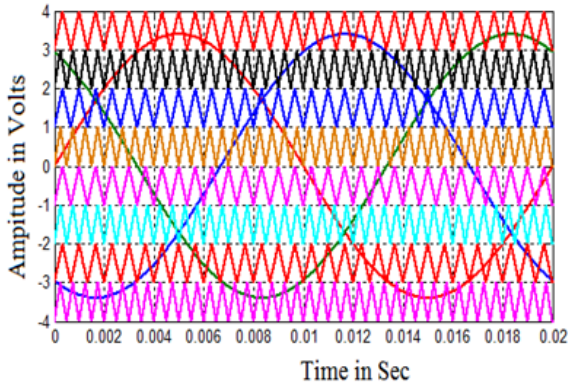

Fig. 2. Carrier and reference wave arrangement of a VFIPD PWM control (ma=0.85 and mf1 = 2000hz and mf2=1500hz)

V. Variable Frequency Phase Opposition Disposition Pulse Width Modulation System

The carriers for a nine level Trinary-DC source, multilevel inverter with variable frequency phase opposition disposition pulse width modulation technique is illustrated in Fig. 3. In this topology, all the carriers are divided uniformly into two groups according to the positive/negative standard levels. These two groups are opposite and 180 degrees out of phase width those below the zero values. 180 degrees out of phase with each other while maintenance in phase within the group phase opposition disposition pulse width modulation topology. In this system for an N level inverter, (N-1) carriers with the unlike frequency (2000Hz and 1500Hz) and equal amplitude are prearranged such that the bands they occupy are continuous.

VI. Variable Frequency Alternate Phase Opposition Disposition Pulse Width Modulation System.

The carriers for a nine level Trinary DC source multilevel inverter with variable frequency alternate phase opposition disposition pulse width modulation techniques are illustrated in Fig.4. In this topology, the carriers are 180 degree alternate phase displace from each other. It may be recognized as pulse width modulation with amplitude overlapping, and neighboring phases are interleaved carriers. In this system for an N level inverter, (N-1) carriers with the unlike frequency (2000Hz and 1500Hz) and equal amplitude are prearranged such that the bands they occupy are continuous.

VII. Simulation Results

A three-phase asymmetric cascading Multilevel Inverter produces nine-level output voltage with a different input DC Source. These three-phase nine level cascaded multilevel inverters with Trinary - DC Source are modelled in MATLAB/ SIMULINK using power systems block set is shown in Fig. 5.

The proposed multilevel inverter contains three single phase unit with uneven voltage Source. These each single phase unit has two full bridges. The first full bridge contains the DC source of 1Vdc and the second full bridge contains the DC source of 3Vdc as presented in Fig. 1. Each DC source is

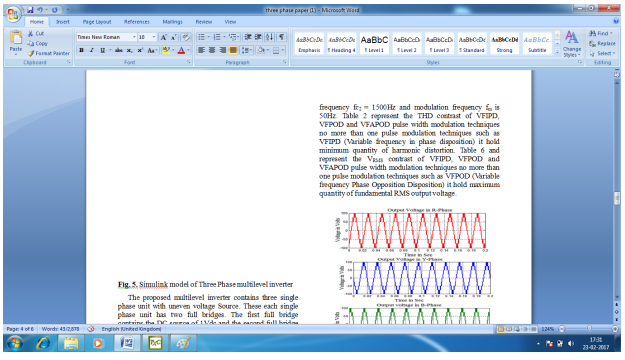

Fig. 3. Simulink model of Three Phase multilevel inverter

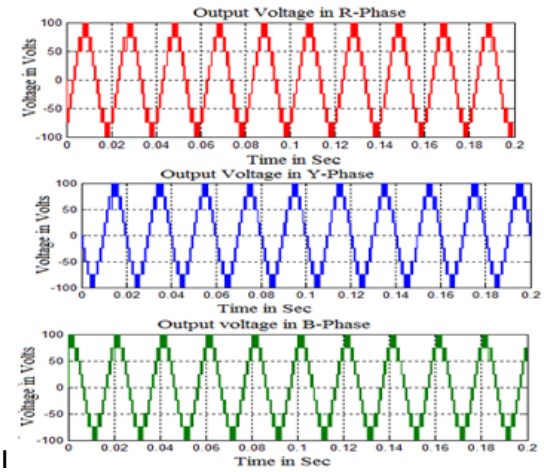

Fig. 4. Output voltages generated by variable frequency in phase disposition PWM control with sinusoidal reference

Table 1. % THD for Different Kind of Modulation Indices

M_a	Sine Reference		
	VFIPD	VFPOD	VFAPOD
1	12.99	13.01	13.74
0.95	15.22	15.32	15.55
0.9	16.06	16.62	16.35
0.85	17.39	16.70	16.20
0.8	16.10	16.75	16.66

Table 2. Fundamental RMS Voltage for Different Kind of Modulation Indices

Ma	VFIPD	VFPOD	VFAPOD
1	70.71	70.83	70.73
0.95	67.18	67.32	67.17
0.9	63.60	63.64	63.62
0.85	60.69	60.71	60.16
0.8	56.57	56.66	56.58

Fig. 5.

connected to a proposed three phase inverter. Each inverter produces a three dissimilar output voltage levels, Such as positive, zero and negative levels by different groupings of the four switches S1, S2, S3 and S4. This circuit is developed by using MATLAB/SIMULINK. The Switching signals of a nine level multilevel inverter using bipolar pulse width modulation technology are simulated. Simulations are performed for a choice of ma assorted from 0.8 to 1 and the resultant %THD is measured using the FFT blocks and their values are exposed in Table 1. Table 2 display the fundamental VRMS of inverter output voltage for similar values of modulation indices. Fig. 6-11 show the simulation output voltage and FFT plot of a nine level cascaded multilevel inverter with different DC source, and their appropriate harmonic order of a spectrum

with bipolar pulse width modulation technology. But only one sample of the modulation indices is shown. For modulation indices (ma=0.85) it is observed from the Fig. (7, 9, and 11) the harmonic energy level is governing in: Fig. 7. represent the harmonic energy level in VFIPD PWM techniques show 40th order of harmonic. Fig.9 represents the harmonic energy level in VFPOD PWM techniques shows 38th 40th order of harmonic.Fig.11 represents the harmonic energy level in VFAPOD PWM techniques shows 29th, 31st, 39th order of harmonic.

Simulations are performed for various values of ma ranges from 0.8 to 1 and the results are obtained by using following parameter such as Vdc = 25V , 3Vdc = 75V, load resistance is 100, carrier frequency fc1 is 2000Hz, carrier frequency fc2 = 1500Hz and modulation frequency fm is 50Hz. Table 2 represent the THD contrast of VFIPD, VFPOD and VFAPOD pulse width modulation techniques no more than one pulse modulation techniques such as VFIPD (Variable frequency in phase disposition) it hold minimum quantity of harmonic distortion. Table 6 and represent the VRMS contrast of VFIPD, VFPOD and VFAPOD pulse width modulation techniques no more than one pulse modulation techniques such as VFPOD (Variable frequency Phase Opposition Disposition) it hold maximum quantity of fundamental RMS output voltage.

VIII. Conclusion

Asymmetric three-phase Multilevel Inverter with variable frequency pulse width Modulation techniques has been developed. The topology has been established that the VFIPD PWM strategy, sinusoidal reference with triangular carrier offers lesser value of total harmonic distortion. VFPOD strategy, sinusoidal reference with triangular carrier is established to perform superiorly since it offers relatively higher fundamental RMS (VRMS) output voltage.

References

[1] F. Filho, H. Z. Maia, T. H. A. Mateus, B. Ozpineci, L. M. Tolbert and J. O. P. Pinto, *Adaptive Selective Harmonic Minimization Based on ANNs for Cascade Multilevel Inverters With Varying DC Source,* ,Transactions on Industrial Electronics, vol. 60, no. 5, pp. 19551962, 2013.

[2] K. A. Corzine, M. W. Wielebski and F. Z. Peng *Control of Cascaded Multilevel Inverters,* IEEE Transaction on power electronic, vol. 19, no. 3, pp. 732738, 2004.

[3] Dixon, J. Pereda, C. Castillo, and S. Bosch, *Asymmetrical Multilevel Inverter for Traction Drives Using Only One DC Supply,* ,IEEE Transactions On Vehicular Technology, vol. 59, no. 8, pp. 3736

[4] C. Young and N. Chu, *A Single-Phase Multilevel Inverter with battery balancing,* , IEEE Transactions on Industrial Electronics, vol. 60, no. 5, pp. 19721978, 2013. [6] M. A. Parker, L. Ran

SOLAR POWERED SENSOR BASE IRRIGATION SYSTEM WITH AUTOMATIC CONTROL OF PUMP

D.Prabhakaran
UG Scholar
Department of Electrical and Electronics Engineering
IFET College of engineering

***Abstract*—this paper throws light on development procedure of an embedded system for solar based Off-Grid irrigation system. Solar power is absolutely perfect for use with irrigation systems. Using Solar Panel, the sun energy will converted to electrical power and saves in to batteries. When the sun is rising and shining, the solar panel will absorb the energy of the sun and the energy will keep in the battery. Light Detecting Resistors (LDRs) are placed on the solar panel which helps in tracking maximum intensity of sunlight. For generation of maximum energy, it is important to maintain solar panels face always perpendicular to the sun. This tracking movement of the panel is achieved by mounting the solar panel on the stepped motor. This stepped motor rotates the mounted panel as per signal received from the programmed microcontroller. The microcontroller used in this project is from AVR family. Soil moisture sensor is placed inside soil to sense the moisture conditions of the soil. Based on moisture sensor values, the water pump is switched on and off automatically. When moisture level of the soil is reaches to low, the soil moisture sensor is sending the signal to microcontroller to start the pump by using stored solar energy. Same time, using GSM technique microcontroller is sending message on farmers mobile about pump status. The microcontroller completes the above job as it receives signals from the soil moisture sensors, and these signals functions as per program stored in ROM of the microcontroller. The LDRs values, soil moisture values, condition of the pump i.e., on/off are displayed on a 16x2 LCD which is interfaced to the microcontroller. Keywords Solar panel, Light Dependent Resistors (LDRs), Soil moisture sensor, AVR microcontroller**

I. INTRODUCTION

In India, agriculture plays a very important role to development of country as our economy mainly based on it. India ranks second worldwide in farm output. The most important factor for the agriculture is timely and ample supply of water. But due to uncertain rainfall and water scarcity in land reservoirs, we are not able to make proper use of agricultural resources. Also unplanned used of water results in to wasting of water on large proportion. With the increase in agricultural activity and competitive demand from different sectors, it has become important to economize on the use of water. We can optimize use of water by adopting sensor base irrigation system. There is different irrigation systems are used nowadays to reduce dependency of rain. Due to the lack of electricity and mismanagement, in the manual control irrigation system many times crops are dry or flooded with water. So to avoid this problem sensor base irrigation system is used. In manual system, farmers usually control the electric motors observing the soil, crop and weather conditions by visiting the sites. Soil moisture sensor base irrigation system ensures proper moisture level in the soil for growing plants in all season. In this system, sensor is sensing the moisture content of soil and accordingly switches the pump motor on or off. Soil moisture sensor is find the soil condition whether the soil is wet or dry. If soil is dry the pump motor will pump the water till the field is wet which is continuously monitored by the microcontroller. The main advantage of soil moisture sensor is to ensure accurate measurements and farmer doesnt have to visit his farm to operate the pump. Same time, using GSM technique microcontroller is sending message on farmers mobile about pump status. For operation of sensor base irrigation system, pump motor requires energy for pumping. In day to day life there is increasing demand for energy but there is continuous reduction in existing sources of fossils and fuels. According to the survey conducted by the Bureau of Electrical Energy in India in 2011, there are around 18 million agricultural pump sets and around 0.5 million new connections per year are installed with average capacity 5HP. Total annual consumption in agriculture sector is 131.96 billion KWh (19% of total electricity consumption). So, solar power is only an answer to todays energy crisis. It is perfect source of energy in the world as it is environment friendly and its unlimited availability. In fact the amount of the Suns energy that reaches the Earth every minute is greater than the energy that the worlds population .

II. PROBLEM DEFINITION

Nowadays, even though irrigation systems are used in agricultural field to reduce dependency of rain, most of them are either regulated manually or having time based automation. In these types of system water is applied to field on the basis of fixed intervals which required high manpower for monitoring and also it reduces the field efficiency. In addition, this fixed interval operation leads to over irrigation than the actual plant requirement and under irrigation when plants required more water in their peak periods. Retardation of crop growth rate, late flowering and reduction of the yield are the major events caused due to water deficiency. Moreover, over irrigation in the root zones leads to ill health of the root zones and vegetation, additional cost for farmer, wasting of water and time wastage.

Also salinity of the soil can be increased by continuous supply of excess water. For operation of irrigation system, electricity is required. So use of solar energy for power generation is essential to tackle current energy crisis. One of the major weaknesses of the fixed panel solar system is that due to rotation of the sun, it is not able to extract maximum energy from the sun.

III. PROPOSED METHODOLOGY

In the proposed system single axis solar tracking system is used for the irrigation along with GSM. Four LDRs are placed on solar panels helps to track maximum intensity of sunlight and thus helps to collect more electricity. Produced electricity is stored in DC battery which is used to pump the water for irrigation system. The analog values from LDR sensors and soil moisture sensor are converted in to digital values by using ADC Converter. The digital values then provided to AVR Microcontroller as an input. Microcontroller is interfaced with DC Pump, LCD, and GSM Module. When moisture content of soil will low, pump will start automatically and farmers can get the information on his mobile through GSM module.

Following are the major components from which proposed system is fabricated. 1. AVR Microcontroller 2. Solar panel 3. Soil Moisture Sensor 4. GSM 5. Liquid Crystal Display (LCD) 6. Light Dependent Resistor (LDR) 7. Battery 8. DC Motor 9. LED 10. RF Radio Frequency Wireless Communication 11. Relay Finally, complete content and organizational editing before formatting. Please take note of the following items when proofreading spelling and grammar:

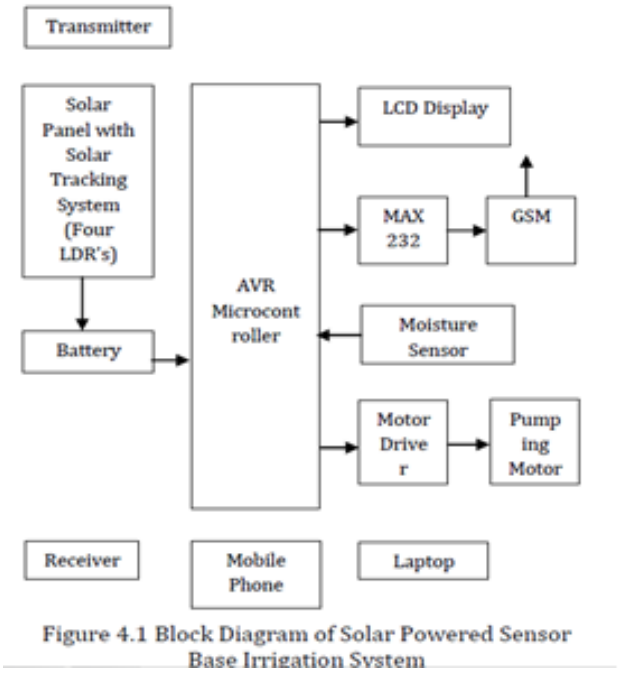

Figure 4.1 Block Diagram of Solar Powered Sensor Base Irrigation System

Fig. 1.

A. Solar Tracking System

The basic idea of developing solar tracking system in this project is to get maximum sunlight from the sun throughout the day, by tracking the movement of the sun. Here the solar cell panel is moved according to the position of the sun. By tracking the movement of the sun, maximum sunlight is obtained; further this energy will be stored in a 12 V DC battery. The solar cell panel will be mounting on a rotating structure. This structure will have DC motors that will help the structure to rotate. Here we are going to implement the LDR for detection of the sunlight. The LDR will be detecting the sunlight and send the data to the microcontroller. We are going to use four LDRs in the project. One at each direction from East to West. As long as the sunlight is in the perimeter of the LDR the solar panel will remain in the same direction. Once the sunlight is out of the perimeter of the LDR, it will stop sending data to the microcontroller. But at the same time the sunlight will be in the perimeter of the next LDR, as we have installed the LDRs in such a pattern. Now the next LDR will start sending the data to the microcontroller. Upon getting the data from the next LDR the microcontroller will send a command to the DC motor. After receiving the command from the microcontroller now the DC motor will get started and the panel will move to the corresponding direction of the next LDR. Again similar procedure will continue for remaining LDRS. This is how we are going to track the sunlight and adjust the solar panel in a position where it will receive maximum sunlight

B. Automated Irrigation System

Now moving to the second part of the project, the energy generated through the solar panel will be sent to a DC battery. The battery will store the energy for further applications. Now we are connecting a water pump to the battery so that the motor should run on the power generated by the solar panel. In this system the water supply will be an automated one that means the pump will supply the water only when the land needs it. In order to achieve this task we are making use of soil moisture sensor and a GSM module. The soil moisture sensors will be placed inside the field, and it will be connected to the microcontroller. The moisture sensor will be continuously sensing the moisture content of the soil and sending it to the microcontroller, where moisture content value will be compared with predefine level. Now whenever the moisture level becomes less than the predefined level, microcontroller will send a command to activate the water pump. Same time microcontroller will activate GSM module, which will send a feedback message to user, stating that the Pump on. After the motor gets started and starts supplying water to the field; simultaneously the moisture sensor will be sensing the moisture content and sending the data to the microcontroller. Since the field is getting water supply now the moisture level of the field will start increasing, this increase in the moisture content will again will be compared with a predefined moisture level. When it will reach the predefined moisture level, pump will automatically off. Again GSM module will

send feedback message stating that Pump off. This water pump also works manually by pressing the key. This is how the system will become an automated system also we are using maximum power from the sunlight. The source program for the microcontroller is written in C language

IV. ADVANTAGES

The main advantages of this proposed system are as follows. 1. By using soil moisture sensors in the field, this system provides water for plants according to the crop water requirement and operates according to the soil moisture condition of the root zone of the plant. This leads to saving of water by avoiding excess irrigation. 2. The system has designed to operate using solar energy; hence it could be used for the areas where the electricity is not available. Further, use of this renewable energy does not affected by the energy crisis. This renewable energy produces little or no waste products such as carbon dioxide or other chemical pollutants, so it has minimum impact on environment. 3. The proposed system controls amount of water use for irrigation in the agricultural fields. Thus it reduces excessive pressure on farmers to pay additional water tariff on water. In addition to this controlled irrigation also save additional cost for water pumping, reduces the conveyance and distribution losses in the field level. Moreover, energy consumption on water pumps could be reduced by efficient water allocation based on the crop water requirement. 4. This solar powered automated irrigation system does not require man power for operation. This intelligent system can detect the soil moisture conditions and perform automatically based on pre-defined moisture conditions. 5. This system reduces run off from over watering saturated soils, avoid irrigating at the wrong time of the day, which will improve crop performance by ensuring adequate water and nutrient balancing. Further, it prevents Salinity of agricultural lands which cause for poor productivity and land degradation. 6. In addition, this system helps in time saving, removal of human error in adjusting available soil moisture level and to maximize their net profit. 7. By using solar tracking system as compared to fixed panels, energy output is increased. 8. Proposed system makes easy to adopt advanced crop systems and technologies, those are complex and are difficult to operate manually.

V. APPLICATIONS

By implementing proposed system, there are various benefits to both government as well as farmers. For the government solution to energy crisis and water shortage is proposed. Main application of the proposed system is for irrigation of agriculture fields. Even we can apply this system in agriculture research stations, greenhouses where high precision soil moisture control is required. Use of solar energy in the proposed system allows us to use this system in remote areas where electricity is not available.

VI. CONCLUSION

In this paper, a solar powered sensor base automated irrigation model is proposed. We designed this model considering low cost, reliability, alternate source of electric power and automatic control. As the proposed model is automatically controlled, it will help the farmers to properly irrigate their fields. The model always ensures the sufficient level of water in the soil. Thus, this system avoids over irrigation, under irrigation, top soil erosion and reduce the wastage of water. Solar power provides sufficient amount of power to drive the system. To overcome the necessity of electricity and ease the irrigation system for our farmers, the propose model can be a suitable alternative.

REFERENCES

[1] Alsayid B, Jallad J, Dradi M and Al-Qasem O, *Automatic Irrigation System with PV Solar International Journal of Latest Trends in Computing,* ,Volume 4, Number 4, December 2013.

[2] Anuraj A and Gandhi R *Solar Tracking System Using Stepper Motor, International Journal of Electronic and Electrical Engineering*Volume 7, Number 6: 561-566, 2014.

[3] Gutirrez J, Villa-Medina J F, Nieto-Garibay A and Porta-Gndara M A, *Solar Powered Smart Irrigation System, Advance in Electronic and Electric Engineering,* 2013.

[4] Harishankar S, Kumar R, Sudharsan K P, Vignesh U and Viveknath T, *Automatic Irrigation System with PV Solar Tracking, International Journal of Latest Trends in Computing,* Volume 4, Number 4: 341-346, 2014.

Spectrum Profitability based Channel Allocation for reducing system overhead in Cognitive Radio

Mrs. M. Vaidehi
Assistant Professor
Department of ECE
St.Annes CET,

Mrs. D. Umamaheshwari
Assistant Professor
Department of ECE
St.Annes CET,

Ms. Mary Amala Jenni
Assistant Professor
Department of ECE
St.Annes CET,

***Abstract*—In older days, the spectrum is divided into portions and each portion is used by separate organizations. This is called static spectrum allocation. But, the organizations do not use the spectrum, fully both in case of time and in the case of bandwidth. The scarce resource spectrum is wasted. So, dynamic spectrum allocation is introduced. In this technique, the communication is done through the bandwidth which is free. So, wastage of bandwidth is reduced partially.**

In Mobile networks, there are two types of users. Primary licensed users, and secondary unlicensed users. Primary users pay and buy a portion of bandwidth and use it. Secondary users use the bandwidth whenever the bandwidth of the primary users is idle. Thus, usability of the electromagnetic spectrum is increased. Base Station acts as the centralized control of the network. It makes the process of channel allocation and routing among the nodes.

The strategies used for channel allocation and routing now are causing overhead to the system thereby increasing the physical cost. In this work, a combined framework for routing and channel allocation is introduced. It combines the process of routing and channel allocation by monitoring and controlling the shadow price of the nodes in the network.

In the proposed strategy, the channel allocation is based on the spectrum profitability which is the difference between the reward for serving the request and the physical cost. If the difference is positive, then the channel will be allocated else not. Also if the channel is allocated and when a primary user enters the channel, it again checks the capacity of the channel, capacity required by the primary user. If the spectrum overloads, connection with secondary users will be disconnected and transferred to alternate path if available. This will increase the spectrum usability and reduces the system overhead.

I. INTRODUCTION

Cognitive (or smart) radio networks are an innovative approach to wireless engineering in which radios are designed with an unprecedented level of intelligence and agility. This advanced technology enables radio devices to use spectrum (i.e., radio frequencies) in entirely new and sophisticated ways. Cognitive radios have the ability to monitor sense and detect the conditions of their operating environment, and dynamically reconfigure their own characteristics to best match those conditions.

The main scope of the work is to maximize the profitability of network using the combined framework of routing and channel allocation. The profit of a network is determined by the difference between the cost of serving a request and the revenue obtained from serving that request. In order to increase the profitability, the physical cost of the system to compute the route and to make decisions about the spectrum allocation should be reduced. In this paper an economic framework for reducing the complexity of routing and channel allocation is proposed.

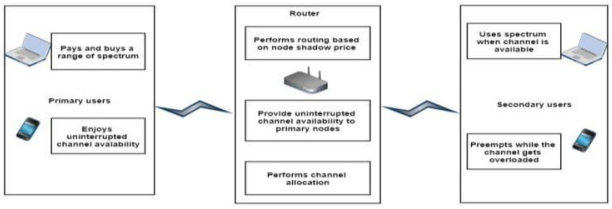

Fig. 1. Data flow diagram of IoT based smart parking assistance.

II. PROBLEMS IN EXISTING SYSTEM

In the existing system, the channel allocation and routing are two separate processes and both has high overhead. They require complex computations to be performed. So overhead of the system is increased. In the existing system, the connection of the secondary user is terminated at once the primary user is online. So, reward for serving the secondary user node will not be obtained. Also in systems like multi hop routing will not assure uninterrupted channel availability for primary users. The algorithm used in the existing system is based on the architecture of the network. The two types are centralized and decentralized. The algorithm used for centralized architecture does not suit decentralized network and vice versa. The shadow price of edges is taken into account in the existing algorithm for routing. But the edge price will fail in the arrival of the primary user. The channel availability for primary users is affected due to the wrong decision on spectrum allocation by the base station.

III. PROPOSED SYSTEM

In the proposed system, the routing and channel allocation is done combined. The complexity of the proposed algorithm is low when compared to the existing algorithms. The algorithm is mainly based on the shadow price of nodes not the edges. So, channel allocation and routing are effective. It assures the uninterrupted channel availability for primary users. It checks the capacity of the channel before rerouting the secondary

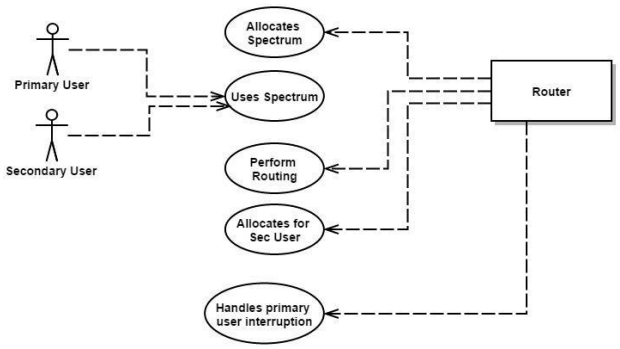

Fig. 2. Use Case Diagram Of Proposed System

user connection. If the capacity is enough for the primary user and secondary user connection, the there is no rerouting. The usability of spectrum is reasonably improved when compared to the existing system. Also the status of primary user is accurately detected by simple automated entry and exit notification so that the channel availability for primary user is certain. The algorithm responds equally for networks of different size. It does not require any prior information other than the shadow price of nodes which is the primary input of the algorithm. The status of the network is tracked and this information will be useful for speeding up the algorithm.

IV. System Architecture

A simple architecture with one primary user, one secondary user and one router is used in this work as shown in Fig.1.

V. Use case diagram

Use case diagram is the primary system model that will show the user interaction of the user with the system. Figure 2 shows the use case diagram of the proposed work as shown in the figure router handle spectrum allocation for the primary and secondary user and also the primary user interrupt to the secondary user allocated spectrum apart from the routing task.

VI. Use case diagram

Let the node at which we are starting to be called the initial node. Let the distance of node Y is the distance from the initial node to Y. Dijkstra's algorithm will assign some initial distance values and will try to improve them step by step.

1. Assign to every node a tentative distance value: set it to zero for our initial node and to infinity for all other nodes.

2. Mark all nodes unvisited. Set the initial node as current. Create a set of the unvisited nodes called the unvisited set consisting of all the nodes.

3. For the current node, consider all of its unvisited neighbours and calculate their tentative distances. Compare the newly calculated tentative distance to the current assigned value and assign the smaller one. For example, if the current node A is marked with a distance of 6, and the edge connecting it with a neighbour B has length 2, then the distance to B (through A) will be 6 + 2 = 8. If B was previously marked with a distance greater than 8 then change it to 8. Otherwise, keep the current value.

4. When we are considering all of the neighbours of the current node, mark the current node as visited and remove it from the unvisited set. A visited node will never be checked again.

5. If the destination node has been marked visited (when planning a route between two specific nodes) or if the smallest tentative distance among the nodes in the unvisited set is infinity (when planning a complete traversal; occurs when there is no connection between the initial node and remaining unvisited nodes), then stop. The algorithm has finished.

6. Select the unvisited node that is marked with the smallest tentative distance, and set it as the new "current node" then go back to step 3.

The performance of the algorithm is evaluated by increasing the no of nodes in the network. Figure 4 shows that the packet delivery of the proposed scheme at 2 node alone is around 99

End to end delivery delay is another performance metric for the routing algorithm. figure 5 shows the secondary user packet delivery delay of the secondary user with the increased no of node in the network. From the graph we can observe that at worst case the proposed algorithm provide around 50ms delay when no of node is 60.

Function Djikstra (Graph, source):

dist. [source] := 0 // Distance from source to source for each vertex v in Graph: // Initializations

ifv source

dist[v] := infinity // Unknown distance function from source to v

previous[v] := undefined // Previous node in optimal path from source

end if

add v to Q// All nodes initially in Q (unvisited nodes) end for

whileQis not empty: // The main loop

u := vertex in Q with min dist[u] // Source node in first case remove u from Q

for each neighbor v of u: // where v has not yet been removed from Q. alt := dist[u] + length(u, v)

ifalt¡ dist[v]: // A shorter path to v has been found dist[v] := alt

previous[v] := u end if

end for end while

return dist[], previous[] end function

VII. Conclusion and Future Work

This work finds the most efficient path to travel the packets over a network. It allocates the bandwidth for both primary user and secondary user. The algorithm does not consider Byzantine attacks. But it can be controlled by integrating adaptive reputation based clustering in decision making. The usability of spectrum is not increased to hundred percent. Once the decision is made, other secondary users would not get channel though they have equal priority. To avoid this, scheduling can be done, but it will increase the overhead of

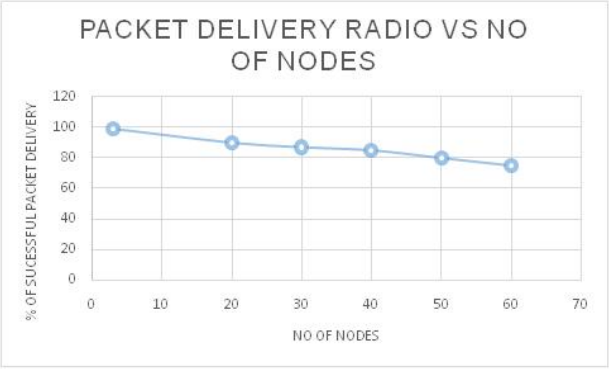

Fig. 3. radio vs no of nodes

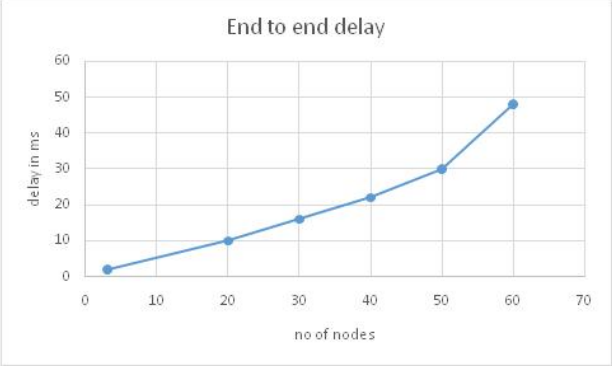

Fig. 4. delay vs no of nodes

the system. A simple scheduling algorithm that should not increase the overhead at the same time, it should not make the nodes to starve in the queue.

REFERENCES

[1] Cabric D, Mishra S, Brodersen R. *Implementation issues in spectrum sensing for cognitive radios. In: Proc Asilomar conf on signals, systems and computers*; November 2004. p. 772-6.

[2] A. Ghasemi, E.S. Sousa, *Collaborative spectrum sensing for opportunistic access in fading environments, in: IEEE Symposium, New Frontiers in Dynamic Spectrum Access Networks (DySPAN05)*, Baltimore, USA, 2005, pp. 131-136

[3] Akyildiz IF, Lee WY, Vuran MC, Mohanty S. *NeXt generation/dynamic spectrum access/cognitive radio wireless networks*: a survey. J Comput Netw (Elsevier) 2006;50:2127-59.

[4] S.M. Mishra, A. Sahai, R. Brodersen, *Cooperative sensing among cognitive radios*, in: IEEE International Conference in Communications (ICC06), Turkey, vol. 4, 2006, pp. 1658-1663.

[5] G. Ganesan, Y.G. Li, *Cooperative spectrum sensing in cognitive radio part II: multiuser networks, IEEE Trans*. Wireless Commun. 6 (6) (2007) 2214-2222.

[6] Y. Chen, *Optimum number of secondary users in collaborative spectrum sensing considering resources usage efficiency*, IEEE Commun. Lett. 12 (12) (2012).

[7] A. Mesodiakaki, F. Adelantado, L. Alonso, C. Verikoukis, *Energy-efficient contention-aware channel selection in cognitive radio ad-hoc networks*, in: Proceedings of the IEEE CAMAD, 2012.

Implementation of Portable and Economical Real-Time EEG Signal Acquisition System Based on DSP

Mrs. D.UMAMAHESWARI
Assistant Professor
Department of ECE
St.Annes CET

Ms. MARY AMALA JENNI
Assistant Professor
Department of ECE
St.Annes CET

Ms. DEVIKA
Assistant Professor
Department of ECE
St.Annes CET

***Abstract*—EEG apparatus are expensive and bulky. Their real-time performance is weak, and EEG signals are easy to be distorted. In this paper, a low-cost portable EEG signal acquisition system based on DSP is developed. By a noninvasive method with bipolar leads, weak EEG signals are induced to the pre-processing circuits, where they will undergo multi-level amplifying and filtering. Then, the analog signals are converted into digital signals using ADS8320. These digitized signals are filtered in DSP (TMS320VC5509) so that the power interference and physiological artifacts are removed with LMS (Last Mean Square) algorithm and ICA (Independent Component Analysis) algorithm. Experimental results demonstrate that the system can acquire weak EEG signals in real time, display and save the processing results. The acquisition system has the advantages of usableness and portability, and helpful to the popularity of community- based and family-based EEG diagnostic equipments.**

I. INTRODUCTION

EEG is a kind of significant bioelectricity signal with abundant physiological and psychological information [1]. By recording EEG, cerebral activities can be monitored for position, diagnosis, and treatment of a wide range of cerebral diseases [2]. At present, most of Chinese EEG equipments are imported from foreign countries [3, 4]. These equipments are expensive and bulky[5][6]. These disadvantages limit the further development of the EEG diagnostic equipment in China [7]. EEG is very weak, whose amplitude is under 100uV and frequency is less than 100Hz [8]. Besides, it is easily interfered from human body and ambient environment [9][10]. So, a variety of factors should be considered in EEG signal acquisition system. For the traditional EEG signal acquisition system, signals sampled by acquisition circuits are converted into digital signals generally [11]. Then the digital signals are transferred to the PC by the way of a wired or wireless transmission [12]. Data can be performed filtering in PC. Their real- time performance is weak inevitably, and they are not convenient for moving [13]. With the development of mobile health, it is demand to develop community-based and family-based EEG diagnostic equipments [14]. Therefore, a low-cost portable real-time EEG signal acquisition system based on DSP is designed and implemented in this paper.

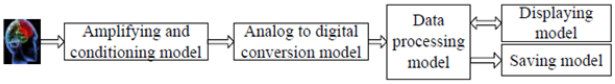

Fig. 1. The Overall Structure Diagram

II. SYSTEM DESIGN

The EEG signal acquisition system includes signal amplifying and conditioning model, analog to digital conversion model, data processing model, displaying and saving model and others modules. Structure diagram is shown in Figure 1. EEG signals are very weak, and it is vulnerable to external interference. Besides, the body's impedance is high, and the body condition is always in change. So the amplification factor of EEG signal acquisition systems is usually in the range of 5000 to 30000. Firstly, multi-level amplifying and filtering, shield guard and Right Leg Drive are used in the system to improve the input impedance and CMRR (Common Mode Rejection Ratio) for avoiding waveform distortion. Then, the analog signals are converted into digital signals using ADS8320. And the digitized signals transfer to the DSP to filter the power interference and physiological artifacts (EOG artifacts).

III. HARDWARE DESIGN

The hardware of system is consisted of the analog circuits (the preprocessing circuits) and the digital circuits (DSP and its periphery circuits). EEG signals are induced when biological electrodes have good contact with skin, then they can be amplified and filtered in the preprocessing circuits. The functions of DSP and its periphery circuits involve acquiring digital signals, performing digital filtering and achieving human-computer interaction. The hardware structure chart is shown in Figure 2.

3.1. Buffer Filtering and Amplifier

The buffer filtering circuit protects circuit away from overshoot current and overshoot voltage. It utilizes the property that current passing through capacity cannot change suddenly

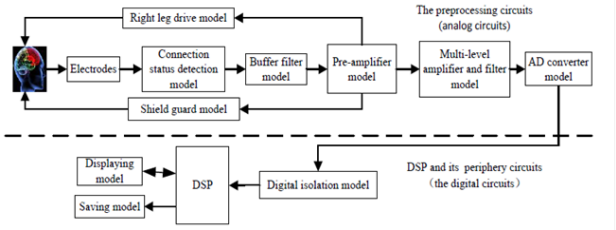

Fig. 2. The Hardware Structure Diagram

$$G = 1+\frac{50k}{R_G}=1+\frac{50k}{100}=501 \quad (1)$$

Fig. 3.

$$G_1 = 1+\frac{100k}{10k}=11 \quad (2)$$

Fig. 4.

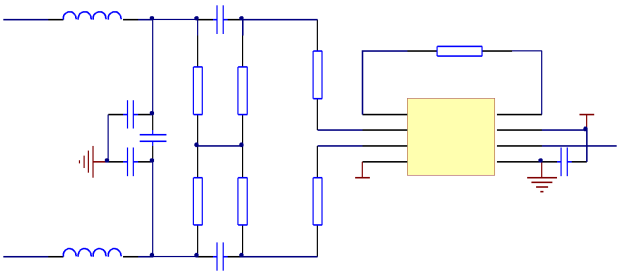

Fig. 5. The Buffer Filter, the Passive High-Pass Filter and the Pre- Amplifier Circuit

to restrain current rate of change, and the property that inductance voltage cannot change dramatically to restrain voltage rate of change. The passive high-pass filter is used to eliminate interference from the mV level polarization potential of electrodes. Otherwise, the polarization voltage will make pre-amplifier saturating. It also improves the post-stage amplifier gain, and provides the opportunity to enhance the CMRR of circuits. The circuits coupling resistances and capacities are comprised of C110, R147 and C111, R148 which constitute the passive high-pass filter.

Two aspects need to be considered for selecting pre-amplifier: 1. Signals as a differential mode signal input obtained from the scalp contain a large number of common-mode component .It requires pre-amplifier with high common-mode rejection ratio. 2. EEG signal is a weak source of high internal resistance, and it requires amplifier with a high input impedance. INA121 is selected as the pre-amplifier in the system. It's common-mode rejection ratio up to 120dB and the input impedance up to 1010 .The pre- level amplification factor G may be described as formula (1), R G =100

OPA130 is selected as the post-amplifier, and the post-amplification factor G1 may be described as formula (2). Buffer filter circuit, the passive high-pass filter circuit and pre-amplification electric circuit is shown in figure 3.

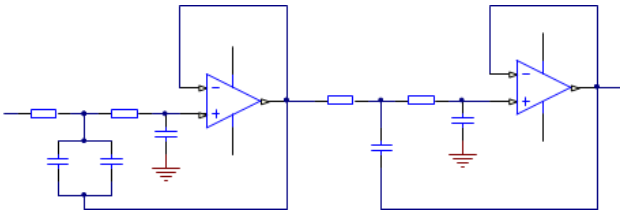

Fig. 6. The Fourth-Order Low Pass Filter

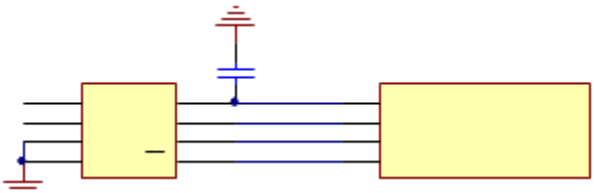

Fig. 7. The Connection of ADS8320 and TMS320VC5509

3.2. Electrode Connection Status Detecting and the Design of Filters

The input signals inducted by electrode are amplified and compared to result a high low level. The low level represents bad connection, and the high level represents good connection. Because EEG concentrated in the low frequency band, it is necessary to design a low-pass filter to filter out high frequency noise. Filters usually have the transition bandwidth. For reducing transition bandwidth, many filters can be cascaded to increase the filter orders. The second-order voltage controlled active filter is used in the system, and it is cascaded to make a fourth-order low pass filter. The low pass filter is shown in Figure 4.The different parameters are adopted in the two second-order low pass filter to acquire good dampening characteristics. The standard form of transfer function of the second-order low pass filter is described as formula (3):

3.3. The Design of Digit Circuits

The digital signal processing is implemented in TMS320VC5509A which is produced by TI. It is C55X series of a high performance, lowest-power DSP. The DSP applies to process algorithms and data. Signals must be converted into digital signals before the digital signal processor. So, ADS8320 is used in the system. The ADS8320 is a high-speed, 14bit resolution option, serial ports. The high speed magnetic isolation chips ADUM2400 and ADUM2401 is used to implement 5000V voltage isolation. The connection of ADS8320 and TMS320VC5509 is shown in Figure 5.

IV. Data Processing Algorithms

The power interference often fluctuates with changes in the power supply system. The fixed bandwidth notch filter cannot completely filter the power interference, and the EEG near the band may be filtered out. The adaptive filter is employed for tracking and processing the power interference. The adaptive filter can automatically adjust parameters according to the fluctuations in the power system. Assume that the power interferences reference input is x(n), the original signals is

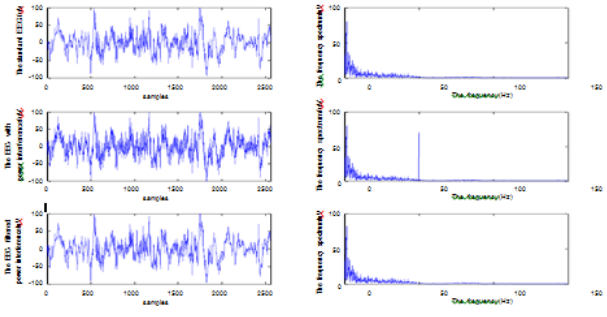

Fig. 8. Comparison between Before and After Filtering

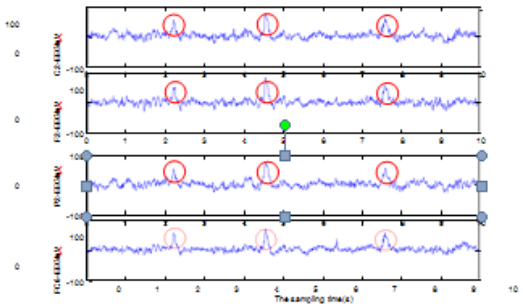

Figure 7. The EEG Signals with EOG Artifacts

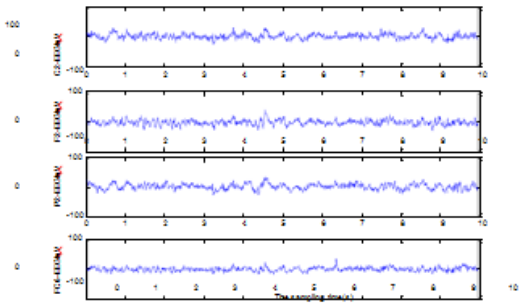

Figure 8. The EEG Signals Filtered EOG Artifacts

Fig. 9.

d(n), the weight vector is w(n), then the output of filter can be represented:

The standard EEG signal downloaded from MIT database is used to verify the effectiveness of the method. Firstly, the power interference is combined with standard EEG signal. And then the EEG signal with power interference is filtered using the LMS algorithm. The frequency spectrums of original signal, the EEG signal with power interference, and filtered signal are demonstrated in Figure 6. As you can see, the power interference component is removed. And there is little impact on the EEG.

EEG has the strong time-varying sensitivity, so it is vulnerable to the interference from human body.EOG is low-frequency signal, and its frequency range is contained in the EEG signals frequency range. Therefore, EOG artifacts seriously influence EEG signals. Independent component analysis method can effectively extract ingredient statistical independence from mixed signals. EOG and EEG can be considered a different signal source generates, i.e., they are independent of each other. Therefore, ICA is used to decompose the acquired EEG signals in the system. The fixed-point FastICA algorithm using negentropy has higher computation efficiency. Therefore, it is used to decompose EEG signal in order to increase computational efficiency. The separate matrices W can be obtained by multiple iterations using independence measurement and optimization algorithm.

are separated into many independent components ui (t) using above formula, and U(t) is the set of ui (t) . The correlation between EOG as a reference signal come from EOG-lead and each individual component is analyzed. The major relevance component is as EOG artifacts and set to 0, others invariability.

Firstly, the above algorithm simulation using MATLAB is shown in Figure 7 and Figure 8. The EEG signals with EOG artifacts are shown in Figure 7, where the red circle marks indicate EOG artifacts. The EEG signals filtered EOG artifacts is shown in Figure 8. Comparing the two figures is easy to see EOG artifacts have obviously been removed and good filtering effect. And then the algorithm is implemented in DSP by CCSLink in order to ensure the systems real-time performance and portability.

V. Experimental Result

The electrode cap is more expensive and not portable, so dots mounted on the head is used to test the system. Three dots are placed on the less muscle place to reduce physiological artifacts interference. Red dot and green dot make up of measuring circuits, and the yellow one is reference dot. As shown in Figure 9, the yellow dot is placed on the ramp above of brow, the green dot is placed on the cheekbone and the red dot is placed on the middle of forehead. EEG acquired using the system is shown in Figure 10. Experimental results show that the system can smoothly and accurately acquire and display EEG. The system meets the design requirements.

VI. 4. CONCLUSION

Aiming at the situation that the acquisition technology of EEG is required to improve continually, a DSP-based low-cost portable real-time EEG signal acquisition system is designed and implemented using technologies of analogue signal processing and digital signal processing. The system can stably acquire EEG, and it may provide a technical support for portable brain health and real-time mobile monitoring

References

[1] T. Jiang and Y. Zhou, *Shanghai Archives of Psychiatry*, vol. 1, no. 24, (2012).

[2] C. Del Percio, C. Babiloni and M. Bertollo,*J. Human brain mapping*, vol. 11, no. 30, (2009).

[3] S. Leino, E. Brattico and M. Tervaniemi, *J. Brain Research*, vol. 10, no. 12, (2001).
[4] F. Di Russo, S. Pitzalis and T. Aprile, *J. Medicine and Science in Sports and Exercise*, vol. 9, no. 37, (2005).

Automatic Clothing Pattern Recognition Based on SIFT

Ms.Revathi Jayakumar
Assistant Professor
Department of ECE
St.Annes CET

Ms.S.K.Suriya
Assistant Professor
Department of ECE
St.Annes CET

Ms.C.Adithya
UG scholar
Department of ECE
St.Annes CET

***Abstract*—Choosing clothes with complex patterns and colours is a puzzling task for visually impaired people. Automatic clothing pattern identification is also a challenging research problem due to rotation, scaling and illumination. Developed camera-based prototype system that recognizes clothes in four categories and identifies the clothes colours depending upon the image type. The system integrates camera and the software implemented in computer for the identification and description of clothing patterns and colours. A camera is used to capture clothing images. The clothing patterns and colours are described to blind users verbally once after implementing this developed algorithm with the embedded part. This paper proposes a schema to remove statistical properties from wavelet sub-bands to capture global features and combined with local features to recognize complex clothing patterns. This method achieves high recognition accuracy and outperforms the state-of-the-art texture analysis methods on clothing pattern recognition.**

I. INTRODUCTION

An Image is defined as 2D function, f(x,y) that carries some info, where x and y are known as plane coordinates. Digital image processing is the use of computer process to perform image processing on digital images. The 2D image is divided into rows and columns. The joint of a row and a column is known as pixel. A finite number of pixels form a digital image. The image can also including depth, color and time. An Image given in the form of an photograph or an X-ray is digitized and stored as a binary digits in computer memory. The digitized image can then be processed and displayed on a monitor. For display, the image is stored in a rapid-access buffer,which refreshes the monitor at a level of 25 frames per second to create a visually continuous display.

1.2 Operation console The operator console contains of equipment and preparations for verification of intermediate results and for changes in the software as and when need. The operator is capable of checking for any resulting faults and for the entry of requisite data.

1.3 Display Popular display devices produce spots for each pixel: Cathode ray tubes Liquid crystal displays Printers.

1.4 IMAGE PROCESSING FUNDAMENTAL

Digital image processing means processing of the image in digital form. Modern cameras may directly take the image in digital form but generally images are originated in visual form. They are captured by video cameras and digitalized. The digitalization method contains sampling, quantization. Then these images are processed by the five fundamental processes.

1.5 FUNDAMENTAL STEPS IN IMAGE PROCESSING

1. Image acquisition 2. Image preprocessing 3. Image segmentation 4. Image representation 5. Image description 6. Image recognition 7. Image interpretation

1.6 IMAGE ACQUISITION

First we want to produce a digital image from a paper envelope. This can be done using either a CCD camera, or a scanner

1.7 IMAGE PREPROCESSING

This is the stage taken before the major image processing task. The problem here is to perform some basic tasks in command to render the resulting image more suitable for the job to follow. In this case it may involve enhancing the contrast, removing noise, or finding regions likely to contain the postcode.

1.8 IMAGE SEGMENTATION

Segmentation is the method of splitting a digital image into multiple segments.The aim of segmentation is to simplify and/or change the demonstration of an image into something that is more meaningful and easier to examine. Image segmentation is typically used to identify objects and boundaries (lines, curves, etc.) in images image segmentation is the process of sharing a label to every pixel in an image such that pixels with the same label share certain visual characteristics.

1.9 IMAGE REPRESENTATION

Image process is the process of convert the input data to a form suitable for computer processing

1.10 IMAGE DESCRIPTION

Image description is the process of extract features that result in some quantitative information of interest or features that are basic for separating one class of objects from another.

1.11 IMAGE RECOGNITION

Image recognition is the process of assign a label to an object based on the information provided by its descriptors.

1.12 IMAGE INTERPRETATION

Image interpretation is the process of assign meaning to an ensemble of recognized objects.

1.13 DISADVANTAGES OF EXISTING SYSTEM

Traditional texture methods cannot achieve the same level of accuracy in the context of clothing pattern recognition. The conventional systems are not able to automatically recognize clothing patterns. The key details of their implementation are missing. The robustness and security level of the systems is weak. The techniques and the algorithms used for that recognition was not so robust and they leads to mismatching of final output

Texture is important property of images. Texture is a powerful regional descriptor that helps in the retrieval process. Texture, on its own does not have the ability of finding similar images, but it can be used to classify textured images from non-textured ones and then be joined with another visual attribute like color to make the retrieval more effective. Texture has been one of the most significant characteristic which has been used to classify and recognize objects and have been used in ruling similarities between images in multimedia databases.

II. PROBLEM DESCRIPTION

Existing texture analysis methods mainly concentration on textures with large changes in view point, orientation and scaling, but with less intra-class pattern and variations. Liu et al. built a clothing recommendation system for specific occasions (eg. Wedding or dating)Hidayati el al. proposed a method for genre classification of upper wear clothes.Yuan et al. established a system to assist blind people to match clothes from a pair of dress images. A lot of techniques and computer vision modules are offered for blind navigation assistance[1].the two parallel SIFT feature extraction algorithm using general multicourse processors, as well as some techniques to optimize [2] the performance of multicourse. Blind people can able to identify the bank note. A process of finding banknote was implemented in paper [10]. But it was also not successful. Old-style procedures cannot achieve the same level of accuracy in the context of clothing pattern recognition. The conservative systems are not able to automatically recognize clothing patterns. The key particulars of their implementation are missing. The robustness and security level of the system is weak. The techniques and the algorithm used for that recognition was not so robust and they leads to mismatching of final output.

III. METHODOLOGY

3.1 SCALE-INVARIANT FEATURE TRANSFORM

SIFT generates one of the popular local image features widely used to match objects in different images. Because of its performance, it is used for various applications such as object recognition, image edging and robot navigation. However, complex calculation and excessive memory access make it problematic to process SIFT operation for a large size audiovisual in real time.

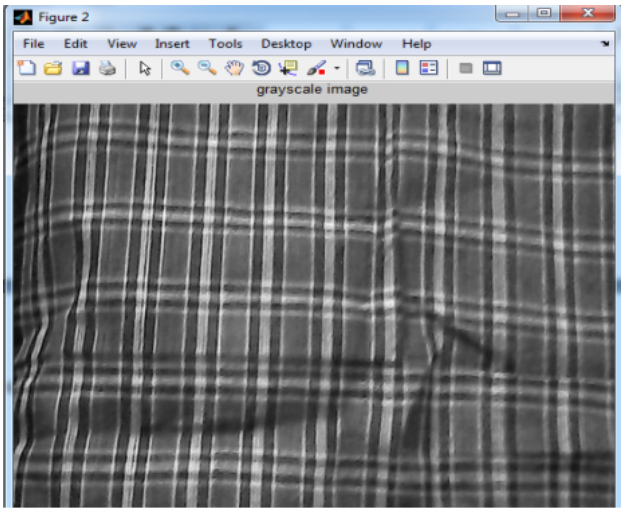

Fig. 1. Gray scale conversion

SIFT is an approach for detecting and extracting local feature descriptors from images. In order to generate the set of image features, the algorithm contains of five major computation steps: Building Gaussian Scale Space, Localization, Key Point Detection, Orientation Assignment, Key Point Descriptor and Matrix Operations. Building Gaussian Scale Space, Key point candidates for SIFT features are obtained possibly from local extreme of difference-of-Gaussian pyramid.

IV. IMPLEMENTATION

MATLAB offers a high-level language and development tools that let you quickly develop and analyze your algorithms and applications. Matlab is a program that was originally designed to simplify the implementation of numerical linear algebra routines. It has grown into something much bigger, and it is used to implement numerical algorithms for a wide collection of applications. The basic language used is very similar to standard linear algebra notation, but there are a few extensions that will likely cause you some problems at first.

4.1 IMAGE RGB to GRAY SCALE CONVERSION The cloth images which are captured by the camera are given as the input for this process. Since it was in color (RGB) form, the 3-band monochrome was converted into single-band monochrome data (grayscale image). This process is known as RGB to gray conversion

4.2 PREPROCESSING The converted grayscale image was further enhanced to improve the quality of the image since the input image was affected by noise due to illumination variations. So it is necessary to remove the noise. This process is known as noise removal. The filters can be used for removing the noise. The Enhancement techniques such as Adaptive Histogram Equalization can be used for further enhancement.

4.3 WAVELET TRANSFORM

The enhanced image was decomposed using the wavelet transform. We can use both Discrete Wavelet Transform

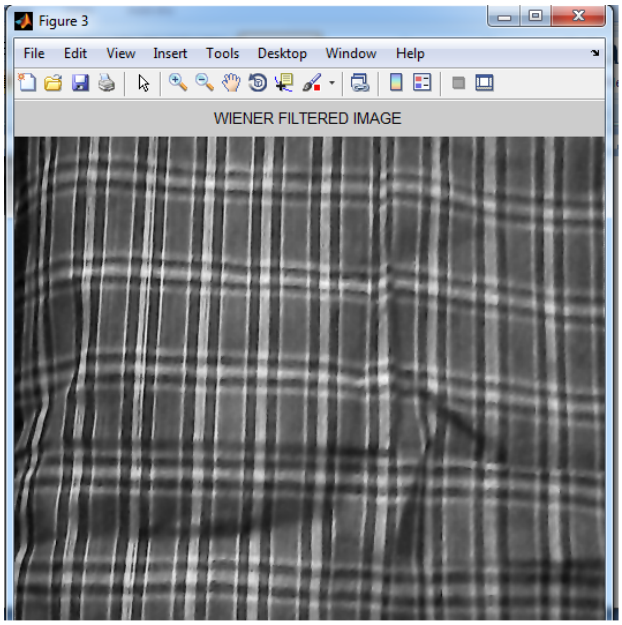

Fig. 2. Weiner filter

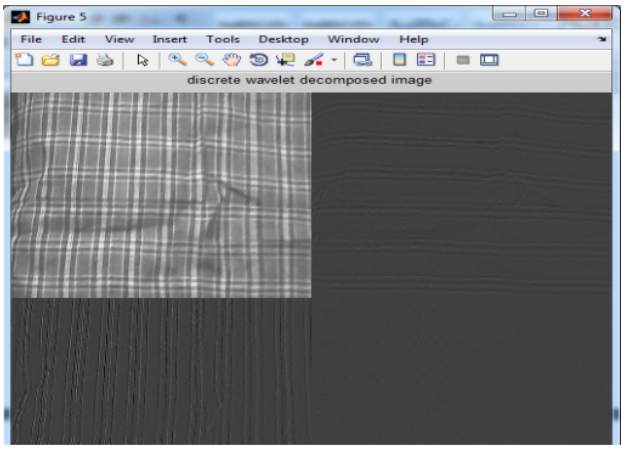

Fig. 3. DWT decomposed image level I

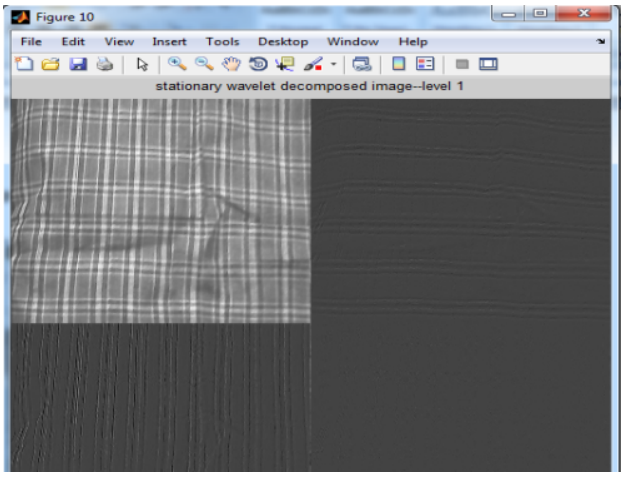

Fig. 4. SWT decomposed image 1

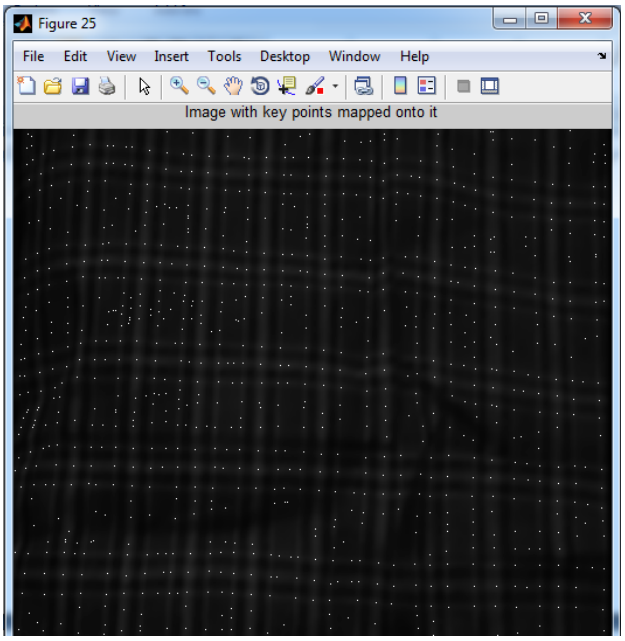

Fig. 5. Feature point detection image (SIFT)

(DWT) and Stationary Wavelet Transform (SWT) for statistical feature analysis. Out of these, SWT is more preferable since there will be no pixel losses while decomposing into several bands

4.4 FEATURE EXTRACTION The decomposed cloth image was given as the input for feature extraction stage. Here SIFT algorithm is used for extracting the features. SIFT is an approach for identifying and extracting local feature descriptors from images. In order to generate the set features of image, the algorithm consists of five major steps: Building Gaussian Scale Space, Localization, Orientation Assignment, key point detection,Matrix Operations. Building Gaussian Scale Space Key point candidates for SIFT features are obtained theoretically from local extrema of difference-of-Gaussian (DoG) pyramid.

4.5 CLASSIFICATION The different cloth pattern images was classified based on the extracted features from the SIFT. Finally the images were classified as Plain, Checked, Patternless and Irregular.

V. RESULT

This work proposed, a system to recognize clothing patterns and colors to help visually impaired people in their daily life. We employ STA to extract the global statistical features on wavelet sub bands; and SIFT to represent the local structural features. The arrangement of multiple feature channels provides complementary information to improve recognition accuracy, Based on a review and a proof-of-concept evaluation with blind users, we have collected a dataset on clothing pattern including four-pattern categories of plaid, checked, patternless, and irregular. Experimental results prove that our

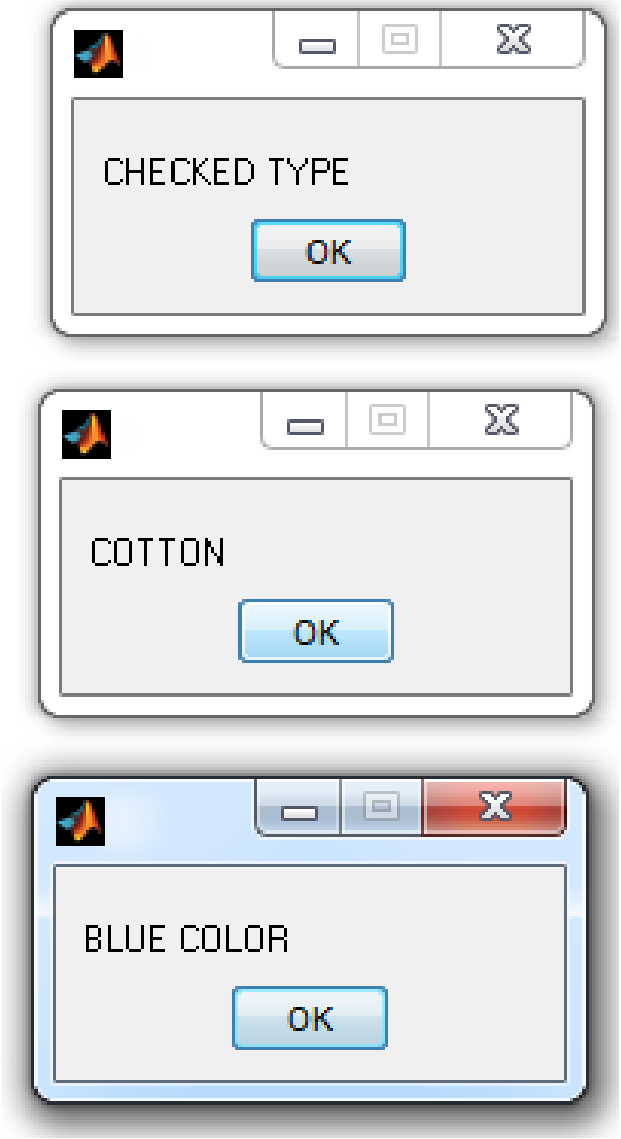

Fig. 6. Finalised output

proposed method outperforms the state-of-the-art methods in clothing pattern recognition.

REFERENCES

[1] Gnana Praveen.R and Roy P Paily (2013) Blind Navigation Assistance for Visually Impaired Based on Local Depth Hypothesis from a Single Image.

[2] Jie Jiang, Xiaoyang Li and Guangjun Zhang, (2014),SIFT Hardware Implementation for Real Time Image Feature ExtractionIEEE Transactions on Human-Machine Systems.

[3] Krystian Mikolajczyk and Cordelia Schmid, (2005),A Performance Evaluation of Local Descriptor IEEE transactions on Pattern Analysis and Machine Intelligence.

[4] Kourosh Jafari-Khouzani and Hamid Soltanian-Zadeh (2005) *Radon Transform Orientation Estimation for Rotation Invariant Texture Analysis*,IEEE transactions on Pattern Analysis and Machine Intelligence.

Android Application for Detection of Plant Syndrome Using Image Processing Techniques

Ms.S.K.Suriya
Assistant Professor
Department of ECE
St.Annes CET

Ms.C.Adithiya
Assistant Professor
Department of ECE
St.Annes CET

Mrs.C.Suganya
Assistant Professor
Department of ECE
St.Annes CET

***Abstract*—Plant pathologists detect syndromes directly with the naked eye. However, such detection usually requires continuous monitoring, which is time overwhelming and very expensive on large farms. The disease diagnosis is limited by the humans visual abilities because most of the first symptoms are microscopic. Therefore, seeking rapid, automated, economical, and accurate methods of plant syndrome detection is very important .This project deals with the image processing techniques, used to identify and classify the disease symptoms affected on different agriculture crops. Plant diseases are mainly caused by bacteria, fungi, virus, nematodes, etc., of which fungi is the main infection causing creature. The magnitude and eminence of plant products gets reduced by plant diseases. The goal is to detect, to categorize and to accurately quantify the main symptoms of plant diseases using the disease affected leaf image by extracting the features like MSERF and SURF of diseased leaf part which is useful for the classification of syndromes.**

I. I INTRODUCTION

India is an agronomic country. Farmers have wide range of diversity to handpicked suitable fruit and vegetable crop. Images are captured by digital camera mobile and processed using image processing techniques, then the portion of the leaf sport has been used for the classification purpose for the detection of diseases. Two major steps involved in the reclamation process are feature extraction and classification. Considerable research is carried out in the area to automatically categorize the leaves. MATLAB is being used as a dais for laboratory exercises and the problems modules in the Image Processing partial of the Computer Graphics and Image Processing progress unit. This handout defines the MATLAB development environment you will be using, you are projected to have read it and be conversant with it before endeavoring the Laboratory and Coursework Obligations. The first step in MATLAB image processing is to recognize that a digital image is self-possessed of a two or three dimensional matrix of picture elements. Individual pixels contain a numbers representing what grayscale or color value is allotted to it. Color depictions generally contain three epochs as much statistics as grayscale pictures, depending on what pigment representation structure is used. Therefore, shade pictures take three epochs as much computational power to process. The method for conversion from color to grayscale will be validated and all processing will be done on grayscale images. However, in order to comprehend how image dispensation works, we will begin by analyzing undemanding two dimensional 8-bit matrices. Loading an Image numerous times you will want to practice a precise image, other times you may just want to experiment a filter on an arbitrary template. If you choose to do this in MATLAB you will need to load the image so you can begin dispensation. If the image that you have is in tint, but color is not imperative for the current solicitation, then you can modify the image to grayscale. This makes dealing out much simpler since then there are only a third of the pixel standards present in the new-fangled image. Color may not be essential in an image when you are trying to localize a specific object that has good contrast with its surroundings. Then the features of the gray scale image are extracted for the further classification.

II. II RELATED WORK

D. Moshoua, C. Bravoa, R. Obertib, J. Westc, on Plant syndrome detection based on data fusion . Kohonen maps are used for hyper and multi-spectral fluorescence imaging, mainly deals with the ground-based real-time remote sensing system for discovering diseases in arable cropsunder field conditions and in an each stage of syndrome development, before it can visibly detected. This was consummated throughsensor fusion of hyper-spectral replication facts between 450 and 900nm and fluorescence imaging. The work explained here used yellow rust (Pucciniastriiformis) disease of winter wheat as a sculpt system for taxing the featured technologies. Hyperspectralreflection images of vigorous and infested plants were occupied with an imaging spectrograph under field statuses and ambientlighting circumstances.

Multi-spectral fluorescence pictures were taken instantaneously on the same plants using Ultraviolent- blue excitation. Through appraisal of the 550 and 690nm fluorescence images, it was probable to detect disease existence. The fraction of pixels inone image, foreseeable as diseased, was set as the final fluorescence infection variable called the lesion index (LI). A haunted reflection method, centered on only three wavebands, was recognized that could discriminate disease from healthy with anlargelyburden of concerning 11.3

E. Nurnadiaha, W. Aimruna, M.S.M. Amina, A.S. Idrisb on Preliminary Study on Detection of Basal Stem Rot (BSR) Disease at Oil Palm Tree by means of Electrical Resistance, BSR disease affects oil palm in Malaysia instigated by Ganodermaboninense which resulted in the devastation of basal

tissues of the place in the ground. The study was aimed to notice an infected tree by with electrical resistance (ER). LandMapperERM-2 was used to distinguish the diseases by assembling ER data at eight positions neighboring the trunk at three different levels of height for each tree. Tree which is contaminated gives low ER measurements between 0 to 24.9 while for the in fine fettle tree have 25 to 150.

Reza Ghaffari, Fu Zhang, Daciana Iliescu, Mark Leeson, Richard and John Clarkson Early Detection of Diseases in Tomato Crops: An Automated racket and Intelligent system Approach Abstract Sensor arrays also known as Electronic Noses(ENs) have been worn to visualize the Volatile Organic Compounds (VOCs) of both strong and infected tomato (Solanumlycopersicum) crops. Statistical and intellectual systems techniques were engaged to process the data collected by an EN. K-Means clustering and Fuzzy C-Mean (FCM) clustering were practical to evaluate any clusters within the dataset. In addition, Multi-Layer Perceptron model in AAN and Radial Basis Function (RBF) based Artificial Neural Network (ANNs) were charity to acquire to pigeon-hole and hence categorise the datasets. With the RBF, MLP and LVQ techniques were reached upto 94, 96 and 98

Arti N. Rathod, Bhavesh Tanawal, Vatsal Shah on Image Processing Techniques for Detection of Leaf Disease, In agriculture research of involuntary leaf infection detection is essential research subject as it may provide evidence benefits in perceiving large pitches of crops, and thus automatically perceive symptoms of syndrome as soon as they give the impression on plant vegetation. The term syndrome is usually used only for devastation of live shrubberies.

This paper provides various approaches used to study of leaf disease detection using image processing. The methods are recycled for increasing output and reduction subjectiveness arising from human experts in detecting the leaf disease. Digital image handling is a technique used for amelioration of the image. To improve agricultural products instinctive detection of symptoms is beneficial.

III. III PROPOSED WORK ANDROID ARCHITECTURE

Android provides an open source development platform that offers developers the strength to build extremely powerful applications. Android help Developers to take free advantage of the device hardware, access location information, run background services, divert call and messages, etc.For developing key application developers take the advantages of same framework APIs. Application architecture use reusability features of components. Once the application has been published, its capabilities are reuse by other applications. Thus it allows the one component to replace by others components. Below listed all applications are a set of services and systems use in developing this application, including To build an application consists of buttons and textboxes used rich set of Views. The lifecycle of application and navigation back stack is manages by an Activity Manager . To receive intents send by other application into our own application can by managed by Broadcast method of Broadcast Receiver service. Using this method events raised by any application can be handle by our application. Now in our system, we take the diseases information for Kharif (summer, monsoon) and Rabi (winter crops). Then depending upon the crop, various types of diseases information like how that diseases occur, what are precaution required to cure that diseases, which pesticides and in how much quantity is it is apply to the crops, How to apply pesticides are presents in an audio form in our system. After whenever farmer required that information, they just used the system and retrieved it just used the keypad of their android phone.

IV. IMAGE PROCESSING TECHNIQUES

Color image to gray

First, the image is converted to the grayscale image. The function of G =rgb2gray (Z) is used to convert into the grayscale image. Then, the intensity of image is adjusted by calling function that specifies the lower and upper picture elements each of one percent that are used for dissimilaritystretching the grayscale image.

V. THRESHOLDING

The simplest approach to segment an image is using thresholding. To make segmentation more robust, the porch should be automatically preferred by the system. Knowledge about the objects, the relevance, the impression should be used to desire the threshold automatically. BW = im2bw(R, level) converts the grayscale image R to a binary image. The output image B Winter changes all pixels in the keyre presentation with luminance greater than echelon with the value 1 (white) and replaces all other pixels with the value 0 (black). Symbolizelevel in the range [0,1]. This range is proportional to the signal levels possible for the image's class. Therefore, a level assessment of 0.5 is equidistant between black and white, regardless of class. To estimate the level dispute, you can exploit the function gray thresh. If you do not stipulatelevel, im2bw uses the value 0.5.

Fig. 1. Sample input images

VI. Filtering image

Median filtering is a nonlinear method used to remove noise from images. It is widely used as it is very effective at eliminating noise while preserving edges. It is particularly operational at removing salt and pepper type blare. The median filter works by poignant through the reflection pixel by pixel, replace each value with the nucleus value of bordering pixels. The blueprint of neighbors is called the "window", which slides, pixel by way of pixel over the all-inclusive image2pixel, image. The median is calculated by first cataloging all the pixel values from the window into arithmetic order, and then exchanging the pixel being deliberated with the middle (median) pixel value.

A median filter is more operative than convolution when the goal is to concurrently reduce blare and preserve edges.B = medfilt2(l, [m n]) implements median filtering of the milieu l in two measurements. Each output pixel contains the median value in the m-by-n communal around the equivalent pixel in the input image. Medfilt2 waddings the image with s on the edges, so the norm values for the point within [m n]/2 of the edges might appear inaccurate. B = Medfilt2(A) achieves median filtering of the matrix A using the defaulting 3-by-3 locality.B = medfilt2(A, 'indexed', ...) processes A as an indexed image, wadding with 0s if the category of A is uint8, or 1s if the class of A is double = medfilt2(..., padopt) gear stick how the matrix margins are padded. padopt may be 'zeros' (the default), 'symmetric', or 'indexed'. If padopt is 'symmetric', A is correspondingly prolonged at the boundaries. If padopt is 'indexed', A is padded with ones if it is twice over; otherwise it is padded with zeros.

VII. MORHPOLOGICAL METHODS

Morphology is a broad set of image processing maneuvers that process images based on shapes. Morphological operations apply a structuring element to an input illustration, creating an productivity image of the equivalent size. In a morphological operation, the value of each pixel in the harvest image is based on a judgment of the corresponding pixel in the input image with its neighbors. By indicating the size and shape of the neighborhood, you can create a morphological operation that is sensitive to unambiguous shapes in the participation image. The most basic morphological operations are dilation and erosion. Dilation increases pixels to the restrictions of objects in an illustration, while erosion eliminates pixels on object restrictions. The number of pixels added or impassive from the stuffs in an image depends on the size and shape of the structuring element used to development the image. In the morphological dilation and erosion operations, the state of any specified pixel in the output representation is determined by applying a rule to the analogous pixel and its neighbors in the input image. The regulation used to process the pixels defines the maneuver as a dilation or an erosion.

The input image to be administered (grayscale, binary, or packed binary image).

A structuring constituent object, reimbursed by the structural element function, or a binary matrix describing the neighborhood of a constituting element imdilate also accepts two optional influences: SHAPE and PACKOPT. The SHAPE disputedisturbs the size of the output image. The PACKOPT argument make certain the input image as packed dualistic. (Packing is a method of constricting binary images that can speed up the dispensation of the appearance).

VIII. VOLTAGE COMPARATOR

Sur features

SURF is a stout local article detector, and can be used in computer vision responsibilities like object recognition or 3D restoration. It is partly inspired by the SIFT descriptor. Therefore, harmoniously to SIFT algorithm, the feature point revealing of SURF set of rules still is based on scale space principle. In contrast, SIFT algorithm embraces Difference of Gaussians (DoG) to extract feature-points, while SURF uses an integer evaluation as the element of Hessian blob detector, which can be computed tremendously quickly with an integral image.

As for a pixel point with scale in image. In order to speed up the multiplication in SIFT algorithm, the Box riddle is used to in the region of substitute the Gaussian filter. In addition, SIFT algorithm simplify the reckoning of determinant, which no longer gauges the weight of each region unconnectedly, thus the determinant can be obtained. Due to the use of fundamental image and the Box filter, the size of the filter is only transformed in the scale-space accumulated by the SURF algorithm, while the image size is perpetual.

In contrast, the clarified image is unrelenting to be riddled in SIFT filtering algorithm. SURF algorithm rulerintergalactic is divided into several orders, and each order encirclements a number of layers. Commonly speaking, the numeral of orders is set to four, each order has four layer scale images, where the bottom image of each regulate is creative image. The size of the filter in each layer is ij2 , where i is the order of the image and j is the layer of the doppelgnger.

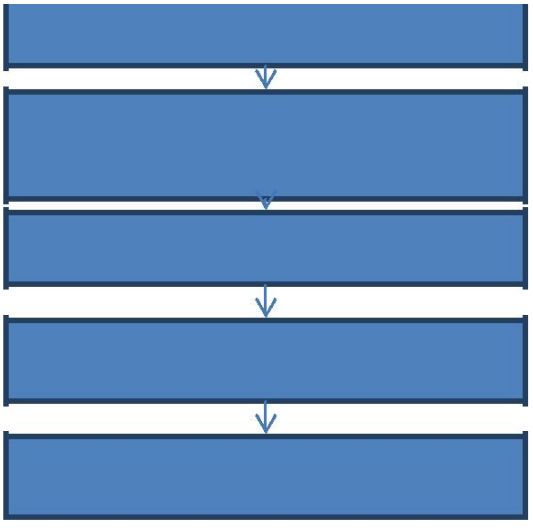

Fig. 2. Work flow

For occurrence, the strainer sizes of the first-order image are 9,15,21,27, respectively.

The transformed value of the bulk is only 6 in the first mandate, while the different in other order is 12, 24, and 48. The consistent scale of each image is s 2 , where s is the side length of the filter in the existing image. After the deviousness of the Hessian matrix determinant is obtained in each layer, the non-maximum dominance is performed in neighborhood. Therefore, the point can be nominated as a feature argument when only the value of the current point is bigger (smaller) than the value of 26 points everywhere the pixel. Because the Box filter is used to approximately exchange the Gaussian filter and integral image is used to fast-track the incorporation process, it is probable to improve the swiftness of operation in the case of high accuracy.

Mser features

MSER is a method for blob detection in images. The MSER algorithm abstracts from an image a quantity of covariant regions, called MSERs: an MSER is a stable attached constituent of some gray-level sets of the image.

MSER is based on the idea of taking regions which stay nearly the equivalent through a wide assortment of thresholds.

Altogether the pixels below a given threshold are white and all those upstairs or equal are black If we are shown a categorization of thresholded images It with frame corresponding to beginning , we would perceive first a black image, then white adverts corresponding to local intensity smidgens will appear then grow grander. These white adverts will eventually amalgamate, until the whole image is white.

The set of all connected apparatuses in the sequence is the conventional of all extremal regions. Optionally, elliptical frames are fervently involved to the MSERs by fitting contractions to the regions. Those regions descriptors are retained as features.

The term extremal refers to the property that every picture elements inside the MSER have either advanced (bright extremal regions) or subordinate (dark extremal regions) concentration than all the pixels on its outer borderline. This operation can be achieved by first categorization all pixels by gray value and then incrementally adding pixels to each associated component as the threshold is transformed. Over a large assortment of inceptions the local binarization is constant and shows some invariance to affine transformation of image intensities and scaling.

IX. B CLASSIFICATION

Classification is done by comparing the values of area, perimeter and centroid values For calculating the perimeter of an binary image ,BW2 = bwperim(BW1) returns a binary image encompassing only the perimeter pixels of objects in the input image BW1. A pixel is part of the perimeter if it is nonzero and it is associated to at least one zero-valued picture elements. The default connectivity is 4 for two dimensions, 6 for three measurements and conndef(ndims(BW), 'minimal') for higher dimensions. BW2 = bwperim(BW1, conn) specifies the desired connectivity. For calculating the area of an binary Image, total = bwarea(BW)assessments the area of the substances in dualistic image BW. total is a scalar whose value corresponds jaggedly to the total number of on pixels in the image, but potency not be exactly the identical because different patterns of pixels are subjective differently.

X. IV RESULT AND CONCLUSION MSERF AND SURF FEATURES EXTRACTED

For normal leaf:

71x1 MSER Regions array with properties: Count: 71

Location: [71x2 single] Axes: [71x2 single] Orientation: [71x1 single] PixelList: 71x1 cell

For diseased leaf:

5x1 MSER Regions array with properties: Count: 5

Location: [5x2 single] Axes: [5x2 single] Orientation: [5x1 single] PixelList: 5x1 cell

In this paper we describe our work bothered with the perception between vigorous and diseased plant leaf using an features extracted from the diseased leaf part. By calculating the area, centroid and perimeter of the diseased leaf part and features like MSERF(Maximal Stable Extremal regions) and SURF(speeded up robust) are extracted and compared. The diseased plant leaves are classified based on the extracted features and thenthe diseases with their treatments are displayed in the form of text file.

XI. CAPTURING AND UPLOADING AN IMAGE

The input image from various part can be captured and uploaded into the server for the detection of disease. Then the uploaded image will be downloaded at any time and the diseased leaf image is feature extracted and classified for the disease detection.

REFERENCES

[1] [2] Jagadeesh D. Pujari, Rajesh Yakkundimath,Abdulmunaf S Byadgi ,*Image processing based detection of fungal disease in plants Procardia computer science 46*(ICICT 2014).

[2] [3] ElhamOmrani A, Benyamin Khoshnevisan A, ShahaboddinShamshirband B, HadiSaboohiC, Nor BadrulAnuar D, MohdHairulNizam*MdNasir e Potential of radial bias function based vector regression for apple diseas detection*Measurement 55(IEEE 2014).

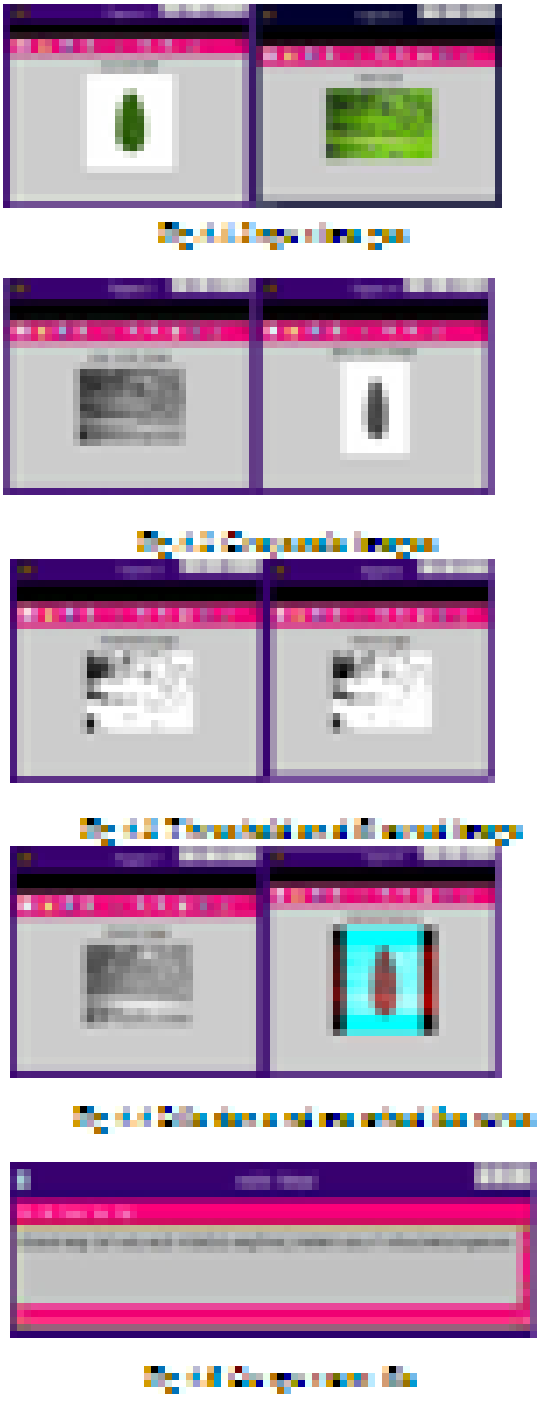

Fig. 3. Output text file

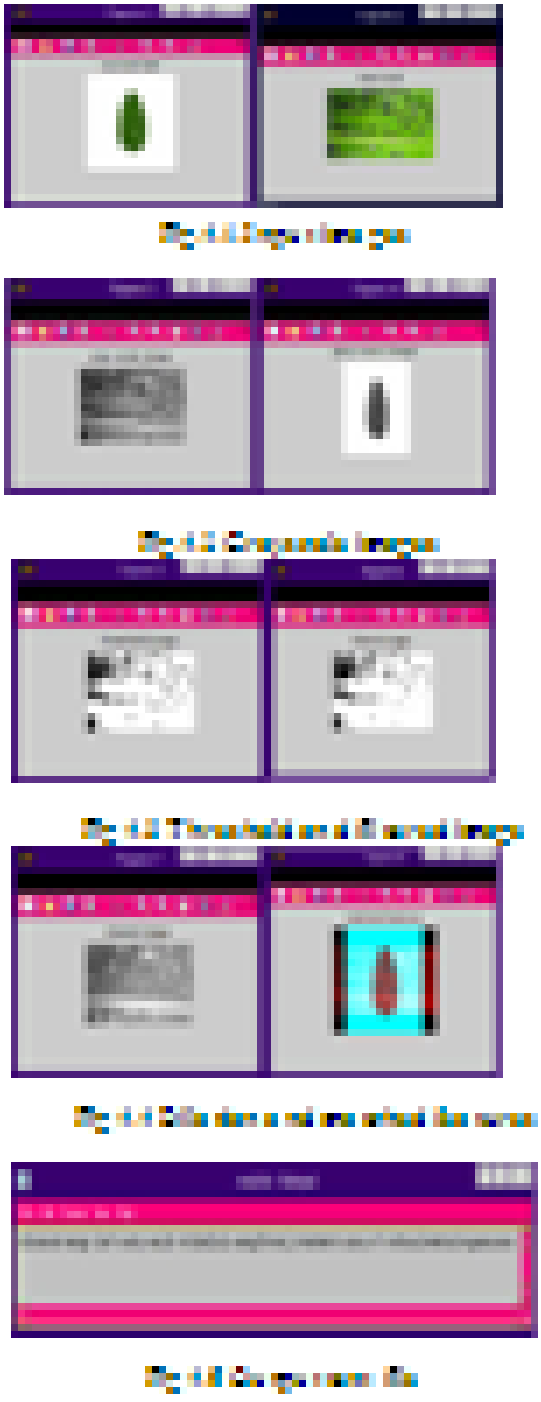

Fig. 4. Capturing the image

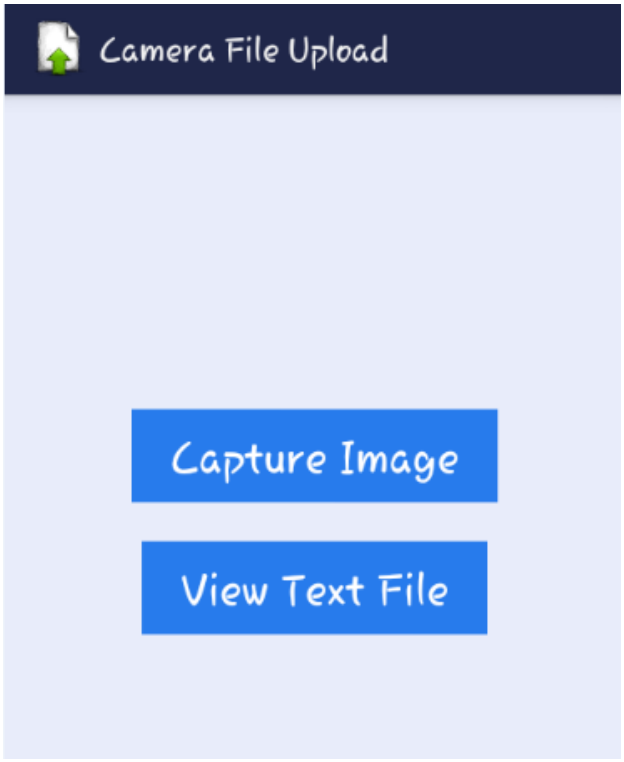

Fig. 5. Uploading the image

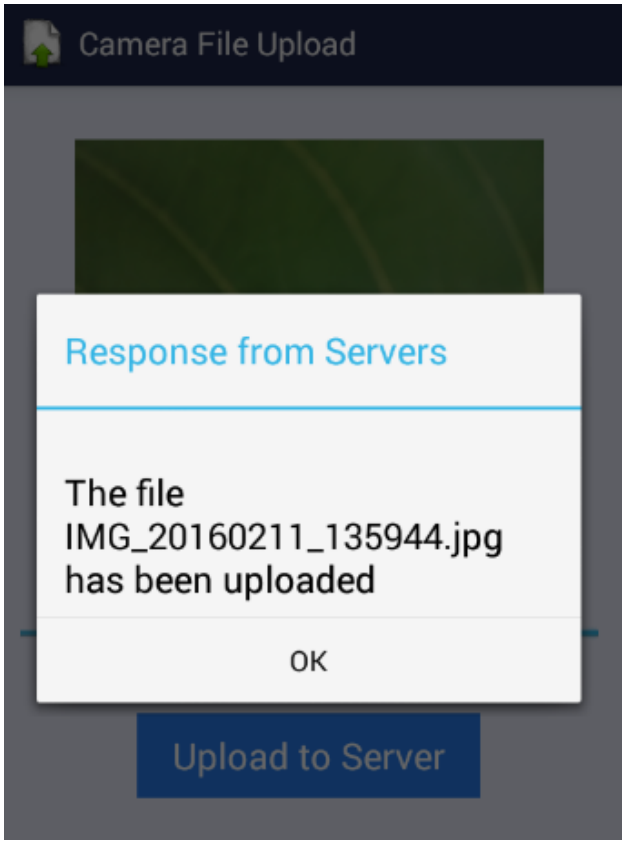

Fig. 6. Response from the server

Hardware implementation of iris recognition system based on DSP

Mr.G.Mahendiran
Assistant Professor
Department of ECE
St.Annes CET

Mr.R.Radhakrishnan
Assistant Professor
Department of ECE
St.Annes CET

***Abstract*—Iris recognition as the new century the most research value and send potential development, biological feature recognition technology, the biological characteristics of knowledge don't technology intends to compare the high accuracy, high stability, high anti-counterfeiting and pick a non touch. In this paper, the hardware system design of iris recognition based on TMS320C6713b floating point DSP is proposed, and the structure, function and working principle of each part are introduced in detail.**

I. INTRODUCTION

As an emerging biometric technology, iris recognition has been paid more and more attention because of its good stability, high accuracy and high accuracy. In recent years, the research and application of iris recognition technology has made considerable progress, and show a broad prospect and market. As shown in Figure 1, the human eye is composed of three parts: the scleral, the iris and the pupil. The iris is the second layer of the eyeball wall, the front part of the pigment film, which is in the shape of a circular disc, and the surface of the iris is in a radial arrangement with high and low level, and the texture of the color is uneven. The iris is the only internal organ that can be seen from outside. In the iris features visible on the connection organization pectinate ligament, matrix collagen, ciliary body, contraction folds, crypt, around the pupil ring pigment, and sometimes to spot, so you can see the obvious texture. The iris texture feature with complex structure, therefore, iris recognition is regarded as the highest reliability of biological recognition technology determination.

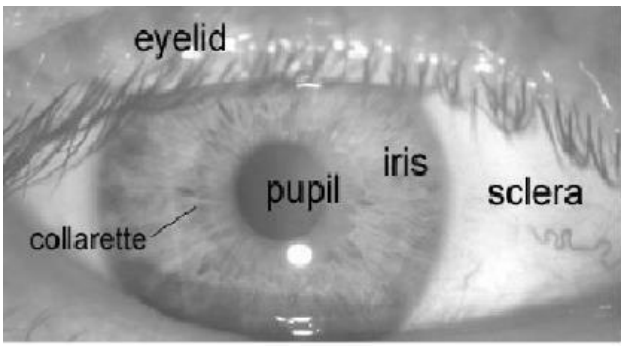

Fig. 1. eye appearance

II. THE BASIC PRINCIPLES OF IRIS RECOGNITION

Iris recognition does not in iris color information as the basis, but on those similar to the stripes, spots, coronal, filaments and other shapes intertwined fine features, these features are called texture features of the iris. Iris recognition is to these texture characteristics as the basis for identification. After obtaining an iris image, iris information systems acquired quality assessment and pre-processing, and according to some preprocessing algorithm for iris feature extraction and subsequent realization of coding, characterized by iris has been stored in the database matches complete the identification process. A

complete process including iris recognition iris image acquisition, image quality assessment, image preprocessing (iris location, normalization, image enhancement, etc.), feature extraction, pattern matching coding and five parts, which is a feature extraction and recognition algorithm coding core.

III. THE DESIGN OF THE SYSTEM OVERALL PLAN

Iris recognition algorithms can be used to implement the system, there are two, one is connected to the PC's large-scale applications, an iris recognition system is based on embedded microcontrollers. Connecting a PC for large-scale application system has a flexible system architecture, computing capability, and multiple systems can share a single iris recognition device, you can build large-scale database applications, to achieve mass iris recognition. Embedded system is a complete system relatively independent, it does not need to connect to other devices or computers to complete the iris recognition function independently, and its function is single, commonly used in places with high requirements for flexibility.

The system implemented iris recognition system is embedded systems. The embedded system is the most critical is the application and development of embedded microprocessor. The system consists of six parts: power monitoring and management and reduction, iris image acquisition, iris image processing, system memory, human-computer interaction (LCD and keyboard) and USB2.0 host communication interface for data transfer. The system adopts + 5V DC power supply. As shown in Figure 2, the hardware structure of the embedded iris recognition system platform is shown in Figure.

Each part of the specific work as follows: TI company's linear DC voltage stabilized source TPS70302 +5V DC-DC

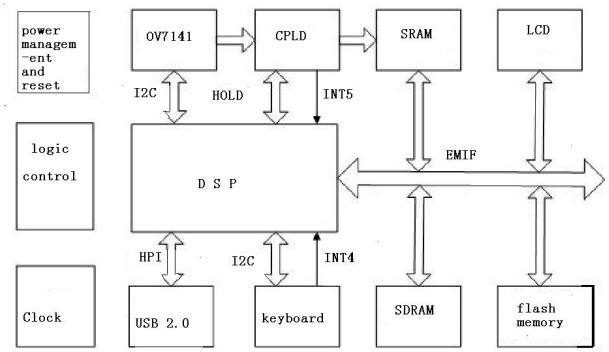

Fig. 2. hardware structure of embedded iris recognition system

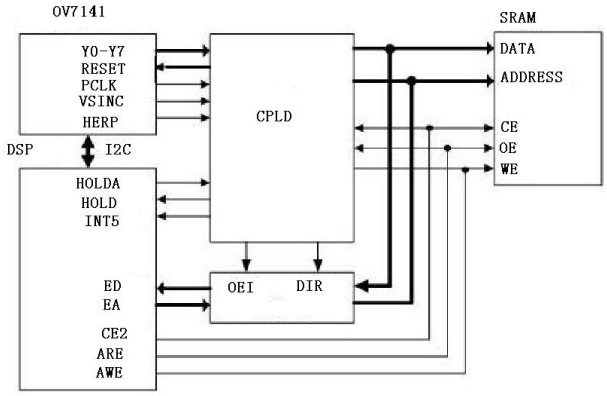

Fig. 3. design of iris image acquisition hardware system

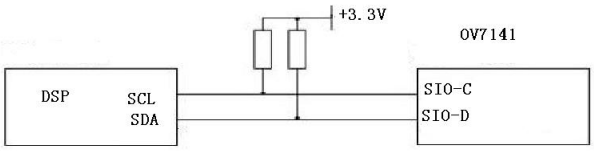

Fig. 4. schematic diagram of DSP and OV7141 hardware interface

to provide +3.3V and +1.26V level. In addition, the OV7141 needed for the +2.5V level by +5V for DC-DC to get the TPS767D325. CMOS image sensor OV7141 responsible iris physical sensing, and outputs the digitized video stream iris image signal. SDRAM system memory for executing programs and temporary data. FLASH MEMORY for storing program code and iris signatures. The human computer interface is provided with a keyboard and a liquid crystal. 4 * 4 small keyboard for input user ID and control system working condition. System operation prompt and iris recognition result display on the liquid crystal module (LCD). USB2.0 host communication data transmission interface to achieve communication between the system and the PC, complete the PC upload / download iris feature database, image data, code program, and so on.. DSP is the core of the system, it is not only to complete the iris recognition algorithm and digital image processing, but also responsible for the control of other external devices (OV7141, keyboard controller, LCD, etc.).

IV. Design of System Hardware Circuit

4.1 Image acquisition circuit

As shown in Figure 3 for the iris image acquisition hardware system wiring diagram. CPLD generation DSP communication with HOLD bus handshake. Iris image data received and stored in SRAM allocated by the CPLD. When one frame iris image acquisition is completed, CPLD generate an external interrupt signal (INT5) of EDMA trigger DSP operation, the notification will be stored in the SRAM DSP iris bitmap copied to the iris recognition algorithms for processing in the SDRAM memory space specified.

4.2 Interface circuit design of image acquisition module

This system is responsible for the design of DSP image sensor OV7141 settings. Using SCCB provided by the OV7141 interface, by setting the OV7141 internal registers, to complete the set of its working state, working mode, the size of the sensor window, scanning mode and data output format, etc.. Figure 4 shows the schematic diagram of the hardware interface between DSP and OV7141.

4.3 Device of DSP peripheral memory The system makes full use of EMIF DSP interface, designed to connect the SDRAM, FLASHMEMORY SRAM and other large capacity of peripheral storage devices.

SRAM is an asynchronous static memory. The system selection of SRAM is IS61LV10248, with 1MByte storage space. CPLD connection with the CPLD to receive and store image data. Connected with DSP, occupy the CE2 space of its EMIF.

SDRAM is a synchronous dynamic random access memory. This system uses a Micron company's 32 bit MT48LC2M32B2 SDRAM with in the DSP processing the iris data storage.

FLASH also called flash memory, is a kind of high density, non-volatile EEPROM. In this system, there are two main functions of FLASH: First, the stored system code, after the power on the DSP will be stored in the Flash code copied to the SDRAM run, another role is to preserve the iris feature points extracted by the iris processing algorithm as well as some user information. This system uses the FLASH chip for the SST39LF160 company's SST, its capacity is 2M bytes, can work under the 3V 3.6V voltage, the access speed is 70ns.

V. Conclusion

The embedded iris recognition system developed in this paper has the characteristics of fast speed, high stability, small size, low power consumption, which provides a good platform for the iris recognition algorithm.

References

[1] John Daugman. *How iris recognition works, IEEE transactions on circuits and system for video technology,*, 2004,16(1):6-16.

[2] Jain A K, Ross A, Pankanti S . Biometrics:*a Tool for In formation Security[J]. IEEE. Transactions on Information Forensics and Security,* 2006 ,1(2): 125 -1 43.

Robotic arm for Pick Place Operation Using Matlab based on offline surface clustering algorithm

Miss.V. Priyadharshini
PG Student
Embedded System Technologies
Krishnasamy College of Engineering & Technology
Cuddalore, Tamil Nadu.

Miss.L.Saranya
Assistant Professor
Department of ECE
KCET
Cuddalore, Tamil Nadu.

Mr.R.Srinivasan
UG Scholar
Department of ECE
KCET
Cuddalore, Tamil Nadu.

***Abstract*—The industry is moving from current state of automation to Robotization, to increase productivity and to deliver uniform quality. The main objective of this paper is to perform an object detection and its pose estimation for robotic pick and place operation using offline surface clustering algorithm. The pick and place robot is a microcontroller based mechatronic system that detects the object, picks that object from source location and place it at desired location. RGBD Sensor provides depth information beyond visual data. In the present situation the detection part is mainly based on the recent template-based linemod approach for object detection. Offline surface clustering algorithm was introduced to overcome the difficulties that occur in present situation and it improves the correct detection rate compared to linemod approach, hence suitable for robotic applications. Object detection by image processing algorithms is done using MATLAB software. Hardware implementation of robotic pick place task for detected object is done using PIC microcontroller.**

Keywords: Object detection, RGBD Sensor, linemod approach, offline surface clustering algorithm, robotic arm.

I. INTRODUCTION

Image processing is a method to convert an image into digital form and perform some operations on it, in order to get an enhanced image or to extract some useful information from it. It is a type of signal dispensation in which input is image, like video frame or photograph and output may be image or characteristics associated with that image. Usually Image Processing system includes treating images as two dimensional signals while applying already set signal processing methods to them. It is among rapidly growing technologies today, with its applications in various aspects of a business. Image Processing forms core research area within engineering and computer science disciplines too. Image processing basically includes the following steps: Importing the image with optical scanner or by digital photography, Analyzing and manipulating the image which includes data compression and image enhancement and spotting patterns that are not to human eyes like satellite photographs, Output is the last stage in which result can be altered image or report that is based on image analysis.

The modern world is enclosed with gigantic masses of digital visual information. To analyze and organize these devastating oceans of visual information image analysis techniques are major requisite. In particular, useful would be methods that could automatically analyze the semantic contents of images or videos. The content of the image determines the significance in most of the potential uses. One important aspect of image content is the objects in the image. So, there is a need for object recognition techniques. Object recognition is an important task in image processing and computer vision. It is concerned with determining the identity of an object being observed in an image from a set of known tags. Humans can recognize any object in the real world easily without any efforts; on contrary machines by itself cannot recognize objects[2]. Algorithmic descriptions of recognition task are implemented on machines; which is an intricate task. Thus, object recognition techniques need to be developed which are less complex and efficient.

Many successful approaches that address the problem of general object detection use a representation of the image objects by a collection of local descriptors of the image content. Global features provide better recognition. Color and shape features can also be used. Various object recognition techniques are available. Difficulties may arise during the process of object recognition, and they are lightning, positioning, rotation, mirroring, occlusion, scale. The robust and efficient object recognition technique using image processing algorithm can be developed by taking into account these difficulties and overcoming them. The image processing algorithms used in this system are linemod algorithm and offline surface clustering algorithm which can detect an object efficiently and accurately for robotic pick place operation.

II. METHODOLOGY

This system consists of image acquisition phase, image processing phase and image transmission using communication protocol. The image is acquired by means of a camera and this phase is known as image acquisition phase, this captured image is processed in the Personal Computer by efficient image processing algorithms. Thus, the objects can be detected at this phase and this phase is known as image processing phase, Finally, the detected objects are transmitted towards the microcontroller unit using the communication protocol Zigbee for performing robotic arm pick place task.

III. Object Recognition Using Image Processing Techniques

In this process image processing algorithms are used to detect an object. The two image processing algorithms used in this paper for object recognition are:-

1. Linemod algorithm.
2. Offline surface clustering algorithm.

Linemod Algorithm

Linemod is an object detection and pose estimation pipeline which receive input as 3D mesh object model[5]. From the model, various viewpoints and features from multiple modalities (RGB gradients, Surface normal) are sampled. The features are filtered to a robust set and stored as a template for the object and the given viewpoint. This process is repeated until sufficient coverage of the object is reached from different viewpoints.The detection process implements a template matching algorithm followed by several post processing steps to refine the pose estimate. The approach was designed specifically for texture-less objects, which are notoriously challenging for pose estimation methods based on colour and texture. Linemod uses gradient finding in template matching algorithm. Linemod algorithm fully depends on the template matching Strategy. The flow chart of linemod algorithm is given below for object recognition.

IV. Camera

Image which is to be processed for object recognition is captured using a camera. This is the image acquisition phase.

A. RGB Image

An RGB image, sometimes referred to as a truecolor image, is stored as an m-by-n-by-3 data array that defines red, green, and blue color components for each individual pixel. RGB images do not use a palette. The color of each pixel is determined by the combination of the red, green, and blue intensities stored in each color plane at the pixel's location. Graphics file formats store RGB images as 24-bit images, where the red, green, and blue components are 8 bits each. This yields a potential of 16 million colors.

B. Grayscale Image

In photography and computing, a grayscale digital image is an image in which the value of each pixel is a single sample, that is, it carries only intensity information. Images of this sort composed exclusively of shades of gray, varying from black at the weakest intensity to white at the strongest.

C. Gradient Finding

An image gradient is a directional change in the intensity or color in an image. Image gradients may be used to extract information from images. Each pixel of a gradient image measures the change in intensity of that same point in the original image, in a given direction. One of the most common uses is in edge detection.

D. Template Matching

Template matching is a technique for finding small parts of an image which match a template image [2]. It is a straightforward process. In this technique template images for different objects are stored. When an image is given as input to the system, it is matched with the stored template images to determine the object in the input image. Templates are frequently used for recognition of characters, numbers, objects, etc. It can be performed on either color or gray level images. Template matching can either be pixel to pixel matching or feature based. In feature based the features of template image is compared to features of sub-images of the given input image; to determine if the template object is present in the input image. Dataset consists of collection of images stored as template and the captured image is compared with that stored template and by this technique object is detected in linemod algorithm. Thus, the matched object is detected and transmitted to microcontroller unit for performing pick

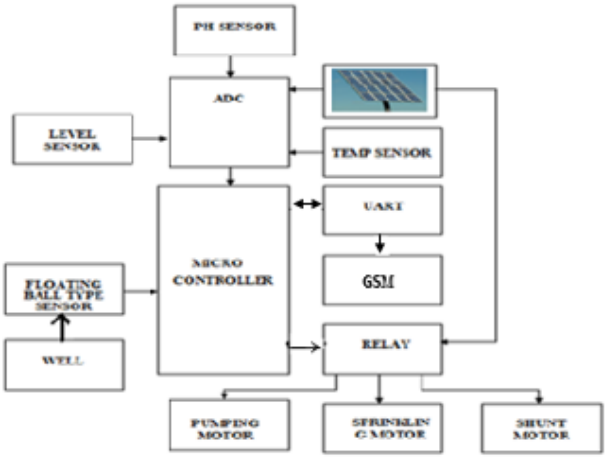

Fig. 1. Block diagram for Object Recognition

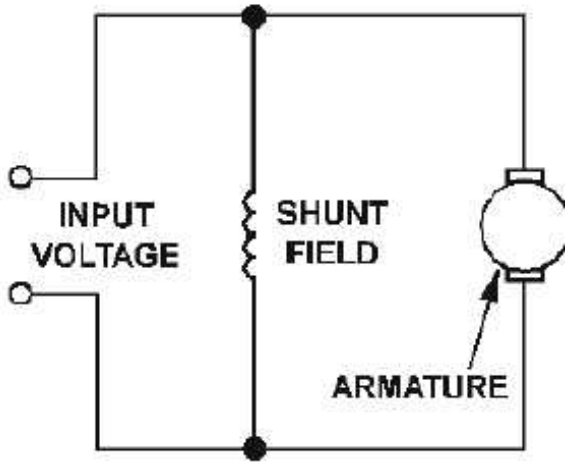

Fig. 2. Flowchart of Linemod Algorithm

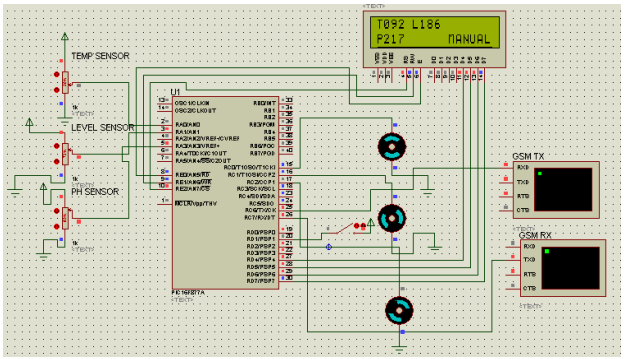

Fig. 3. Flowchart of Offline Surface Clustering Algorithm

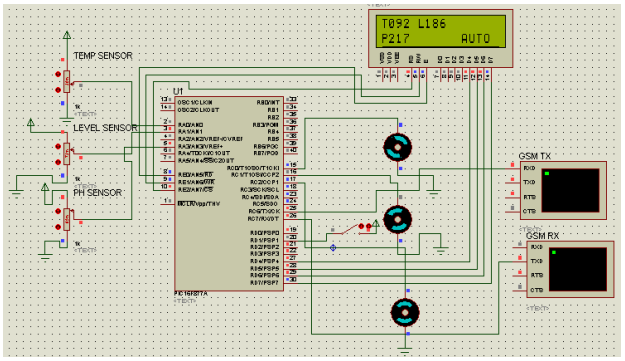

Fig. 4. Block diagram for Robotic arm pick place task

place operation using zigbee. The template matching technique requires large database of image templates for correct object recognition. Hence it must be used only when limited objects are to be detected and it will not provide accurate results in detecting curved objects hence offline surface clustering algorithm is used.

E. Offline Surface Clustering Algorithm

This section describes the offline clustering method of the polygon models of the object and the environment [1]. We will briefly explain the overview of the basic algorithm of the clustering method. In the clustering algorithm, we first calculate the initial set of clusters where each cluster is composed of a few triangles. Then, we consider iteratively merging a neighbouring cluster as far as the cluster can be approximated by a planar region. When searching the object posture, we consider that the surface of the object maintains contact with the surface of the environment.

F. Cluster Analysis

Cluster analysis or clustering is the task of grouping a set of objects in such a way that objects in the same group called a cluster are more similar in some sense or another to each other than to those in other groups clusters. Cluster analysis itself is not one specific algorithm, but the general task to be solved. It can be achieved by various algorithms that differ significantly in their notion of what constitutes a cluster and how to efficiently find them. The flow chart of Offline surface clustering algorithm is given below for object recognition.

V. Binary Image

A binary image is a digital image that has only two possible values for each pixel. Typically, the two colors used for a binary image are black and white, though any two colors can be used. The color used for the objects in the image is the foreground color while the rest of the image is the background color. A point is selected for the binary image and the triangular representation is made from that point to boundaries of the image. The triangle is further extended with neighbouring triangles and the cluster is obtained. Now identify the number of individual cluster obtained. Then project the line and merge the similar cluster pixels together to form

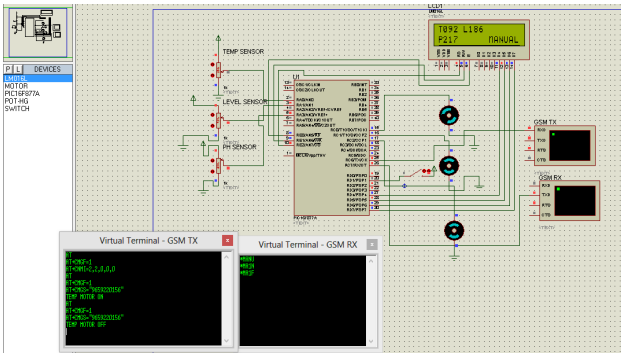

Fig. 5. Image Captured and Converted for Object Detection

a boundary. This boundary formation provide efficient object recognition and the detected object is transmitted towards the microcontroller through zigbee unit. By means of forming the cluster through generating centroid for represented triangles using region props property this algorithm ensures accurate object detection even for curved objects.

VI. Robotic Arm Pick Place Task

The objects that are detected by image processing algorithm are transmitted towards the microcontroller unit through zigbee for performing Pick and place task. The microcontroller unit consists of the hand module motor unit for performing pick and place task and another motor unit for front and back movement of robotic arm. when the microcontroller receives the detected object it signals the motor unit to perform the robotic arm pick place task.

VII. Results discussion

The object recognition is done by using image processing algorithms in MATLAB software. The image processing algorithms used are linemod algorithm and Offline surface clustering algorithm.

VIII. Conclusion

This paper proposed a method for object detection using image processing algorithms, required for performing robotic arm pick place operation. The image processing algorithms that are used in this paper are Linemod algorithm and Offline

Surface Clustering algorithm. The objects were detected by image processing algorithm and the outputs from both the algorithms were noted. It is found that the offline surface clustering algorithm can detect more objects properly when compared to Linemod algorithm within shorter duration.

VLSI Design of High Speed Vedic Multiplier for FPGA Implementation

Mr v.venkatesan
Assistant Professor
Department of ECE
St. Anne's CET

Mr R.Radhakrishnan
Assistant Professor
Department of ECE
St. Anne's CET

Mr G. Mahindran
Assistant Professor
Department of ECE
St. Anne's CET

***Abstract*—Internet of Things (IoT) links the objects of the real world to the virtual world, and enables anytime, anywhere connectivity for anything that has an ON and OFF switch. It constitutes to a world where physical objects and living beings, as well as virtual data and environments, interact with each other. Large amount of data is generated as large number of devices are connected to the internet. So this large amount of data has to be controlled and converted to useful information in order to develop efficient systems. In this paper, we focus on to an urban IoT system that is used to build intelligent transportation system (ITS). IoT based intelligent transportation systems are designed to support the Smart City vision, which aims at employing the advanced and powerful communication technologies for the administration of the city and the citizens.**

I. INTRODUCTION

As the Wireless Sensor Networks have

technologically developed more rapidly and more efficiently, they have become the key source for the development of IoT. They find application in almost all

areas including smart grid, smart transportation systems, smart home, smart hospitals, and so on. The achievement of the above lead to the smart city development as mentioned by our Indian Prime Minister. The idea internet of things (IoT) was developed in parallel to WSNs. The term internet of things was devised by Kevin Ashton and refers to uniquely identifiable objects and their virtual representations in an internet-like structure. These objects may range from huge buildings, planes, cars, machines, any sort of goods, industries, to human beings, animals and plants and even their specific body parts. One of the major evolutions of WSNs will be after they are integrated with IoT. This paper aims to develop an intelligent transportation system. The future roads will be able to manage traffic congestion much better than today's networks. It has been imagined that in a span of around 20 to 30 years the existing traffic system would improve to an extent where cars can communicate with each other without any human interaction to control the traffic. Hence travel could be made smoother and safer. Sensors would be fitted in cars and these cars will be placed on the roads. These would monitor traffic and send the information wirelessly to a "central traffic control system," a hub that compiles data to feed back the information to vehicles on the road. For instance if there's lots of traffic, the central traffic control system would be told over WiFi and they in turn react by imposing speed limits that have to be followed by the vehicles in that congestion area. Since millions of money is spent on traffic congestion every year, it has been estimated that, by the implementation of smart transportation systems, the money spent will get reduced by at least 15

II. 2. PROPOSED SYSTEM

The flow diagram of the proposed system is shown in fig.1. The cars entering and leaving the parking slots are taken into count. The information thus gathered is sent to the garage management systems. Two types of sensors are employed here, Parking sensors and roadway sensors. In a similar manner two meters are used such as, existing parking meters and new parking meters. The information obtained from the sensors is passed to the sensor management systems. Parking meters send their respective data to the meter management blocks. All the information obtained above is sent to the central data management system where they are being collected and processed. They are in turn sent to the data warehouse for monitoring and storing. Hence this system helps the customers to make optimum use of the resources that are available for safer and smoother parking of their cars and vehicles. Hence there will be an orderly way of parking. Sensors identify the vacant parking spaces and send the information to the central server. On the other hand smart phone app requests for a parking space and the vehicle is directed to the available parking space. At the same time the parking fee is paid directly through the mobile app. This system can also be integrated to provide intelligent lighting of the streets. Here the street light is turned on when the street is being used by the vehicles and other times it remains switched off.

The parking assistance is provided using the following steps. Sensors detect whether a parking space is occupied and transmit data to the central server. Smart phone app requests a parking space and guides the drivers to that free space. Parking fee is directly paid through the smart phone app. Access to loading zones and residential parking zones are restricted. IoT traffic architecture comprises of RFID, Wireless sensor technologies, Ad Hoc networking and internet based information systems. Intelligent traffic IoT is divided into three layers such as Application layer, Acquisition layer and Network layer. Application layer is responsible for intelligent traffic management, intelligent driver management, information collecting

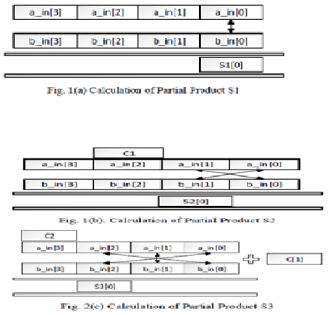

Fig. 1. Data flow diagram of IoT based smart parking assistance.

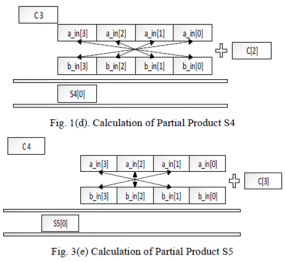

Fig. 2. Table 1 Intelligent Traffic Management:

and monitoring and information services. Network layer makes use of WiFi, 3G/4G and WiMax or GPRS. Acquisition layer employs RFID, RFID reader, WSN, Intelligent terminals.

The system makes use of wireless sensors to obtain real-time traffic information, such as traffic condition on each road, number of vehicles, and average speed. Utilization of wireless sensors is much appropriate due to their low power consumption and low cost. In order to achieve large-scale network layout, the system uses wireless cluster sensor network. Each cluster has a set of wireless sensors and each set is represented by the head node. Data at the head nodes are delivered to the backend system by means of a mobile agent. Already some new vehicles have been equipped with GPS and sensors capable of receiving and sending driving information. This information is sent to the monitor and control centre trough satellite communication facilities. GPS is connected to the wireless sensor networks which can be used for measuring driving speed and driving direction. The traditional traffic monitoring system based on image-processing technology has many limitations. The weather conditions have serious impact on this method. During heavy rain and thick fog the license plate is not clearly visible and hence the image cannot be captured. The development of e-plate based on RFID provides a better opportunity for intelligent traffic monitoring for identifying and tracking the vehicle. RFID can be used as a transponder in license plate equipped with a RFID tag and sensors. Here each car can get data it needs from the spot and deliver the data to assigned destination. The vehicle RFID tag stores information about the vehicle and the owner. Parameters such as vehicle plate number, vehicle type, speed of the vehicle, license number, the travelling location of the car are monitored and stored. This knowledge of information from every vehicle helps in estimating the number of vehicles on the road, average speed of the vehicles and the density of the vehicles on the road. The data from each vehicle is gathered or collected by means of a fixed or mobile RFID reader at each monitoring. Finally the information is sent to the central server for collecting, processing and storing. Once system connects to the internet, all information of vehicles on each road segment is immediately saved in database and can be used for any purpose and application. When a vehicle with an RFID tag passes through each monitoring station along the road, the RFID reader at those points will automatically read the tag data related to the vehicle and its owner and transmit to the wireless sensor active nodes. These nodes send accumulated data to the cluster head node. At the same time, a GPS receiver installed at the monitoring station can communicate with GPS satellites to obtain its position information that is taken as a position parameter of the vehicle. Then the data is transmitted using GPRS scheme to the real-time central database where the data is constantly updated to ensure data reliability.

III. 3. RESULTS AND DISCUSSIONS

This section describes the results obtained in the existing system. The survey is conducted for about 15 Km around Ooty. Here the location information is sent to the database every five minutes due to memory considerations and this can even be reduced. Processing system converted this raw information to meaningful data as shown in figure 2. The proposed system can function with less memory constraints and can send the location information continuously. The proposed system even provides parking assistance to the drivers on the road.

IV. 4. CONCLUSION

This paper presents a real time traffic monitoring system to solve the problem of real time traffic controlling and monitoring. The proposed system provides a new way of traffic control by the better utilization of resources. The traffic administration department can use this real time traffic monitoring information to detect the dangerous situations on the road and thereby react by imposing immediate actions. On the whole IoT will play an important role in traffic monitoring by improving the efficiency of traffic safety and travelling costs.

REFERENCES

[1] Andrea Zanella, Nicola Bui, et,al *Internet of things for smart cities* IEEE Internet of things journal vol.1, February 2014.
[2] Salim, et al. *Design and Implementation of Web-Based GPS-GPRS Vehicle Tracking System.* IJCSET December 2013.
[3] Zhu, et al. Intelligent transportation system based on Internet of Things. WAC 2012.
[4] L. Atzori, A. Iera, and G. Morabito, *The internet of things: A survey,* Computer. Networks., vol. 54, no. 15, pp. 27872805, 2010.

[5] Hasan Omar Al-Sakran *Intelligent traffic information system based on integration of Internet of Things and Agent technology*, IJACSA ,vol 6, 2015.
[6] Laisheng Xiao, Internet of Things: *a New Application for Intelligent Traffic Monitoring System, Journal of Networks*, vol 6, 2011.
[7] K. Ashton, That Internet of Things thing, *RFiD Journal*, 2009.
[8] D. Singh, G. Tripathi and A. J. Jara, A survey of Internet-of-Things: *Future Vision, Architecture, Challenges and Services*, IEEE World of Forum on Internet of Things.
[9] AnithaChepuru, Dr. K. VenugopalRao *A study on security of IoT in Intelligent Transport Systems Applications*, IJARCSEE, vol 5, September 2015.
[10] Y. Yin and J. Dalin Research and Application on Intelligent Parking Solution Based on Internet of Things, *5th International Conference on Intelligent Human-Machine Systems and Cybernetics (IHMSC)*,(2013).
[11] D. Bandyopadhyay and J. Sen, The internet of things - *applications and challenges in technology and Standardization"*, Springer International Journal of Wireless Personal Communications, 2011, vol. 58.
[12] V.Katiyar, P. Kumar and N. Chand, *An Intelligent Transportation System Architecture using Wireless Sensor Network, International Journal Computer Applications*, vol 14,2011
[13] D. Miorandi, S. Sicari, F. De Pellegrini and I. Chlamtac, Internet of things: *Vision, applications and research challenges,Ad Hoc Networks*, vol.10,2012.

EFFICIENT UTILIZATION OF ELECTRICALS IN A FORUM BY ANALYZING THE HUMAN MOVEMENTS

D.Kishore
PG scholar
Department of Mechatronics
Sri Venkateshwara College of Engineering,
Anna University,
Chennai.

***Abstract*—Wastage of electrical energy is a very big problem that is being faced by humans for a very long time. Still, in many places the energy is wasted by leaving the unused electricals switched on when there is no human present to use it. This can be reduced by monitoring each and every person in the hall so that the electricals that are not used can be switched off. In this project as soon as a person steps into the hall their entry is noted and their movements are being started to monitored. The hall is divided into different zones to locate the position of the humans by keeping track of the movements of the person in between the zones. The details are then used to find the position of every person who had entered the hall.**

I. INTRODUCTION

In the present scenario finding the positon of the human in the hall is done by the usage of infrared cameras which is too expensive as the manufacturing of the sensor is very high. Before which they used sensors which can detect the presence of the human by detecting the change in the surrounding due to the presence of the human. These are not very efficient and definitely has some condition at which it cant detect the presence of the humans in the hall. This results in faulty values and unable to control the electricals. The proposed system eliminates the drawback of the existing system by combining two existing systems which covers the disadvantages of the other system. One of them helps in finding the total no of persons present in the hall and the other is used to movements of the persons. By combining the results of both these systems we are able to find the no of persons present in a particular location of the hall. Using this information the electricals which will be needed in those particular locations can be switched on.

The system consists of Microcontroller, Entry Sensor, LCD Display, Motion Sensor, and Relay. Microcontroller: It is the main controller which processes the input received for the various sensors like IR Sensor, PIR Sensor, etc. and provides the control signal based upon the program in accordance with the received signal. Entry Sensor: It is used to sense the entry of a person. In this system IR Sensor is used to detect the entry or exit of the person in the hall. The IR Sensors consists of IR Transmitter and IR Receiver which are placed along the sides of entrance of the hall. There are two sensors placed parallel to one another to find if the person is entering or exiting the hall.

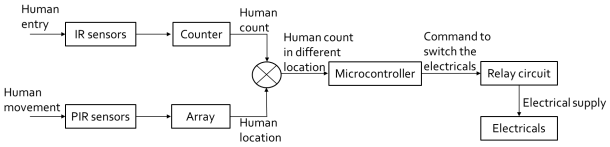

Fig. 1.

Motion Sensor: The motion sensor that is to be used in this is the Passive Infrared Sensor. The PIR Sensor is a pyro-electric sensor which is used to detect the infrared signal (Thermal signal) which helps in detecting the movements of human. All human body emits thermal energy. Human radiate at wavelength of 9-10 micrometers all time of the day. The movement in source of these waves are detected by the PIR Sensor and detects the movements of the human. LCD Display: It is used to display information in the form of texts, numbers, etc. In this system LCD module is used to display information about the entrance and exit of the human. Relay: It is an electrically operated switch. They are called as solid state switches as they are activated using electromagnets. In this system they are used to operate device of high power capacity with a low powered signal. Contents of subheading 2 goes here.

II. SIMULATION

The simulation of the project was decided to be done using the software Proteus due to its ease of use the following components were used. 2 Switches are used in the place of IR sensors which is used to give signals about the entry and exit of a person 2 Arduino boards are used as they are dont need any external power supply circuits which will make the circuit look complex 4 PIR sensors are used to find the movements of the people inside the hall 4 Relays are used to control the

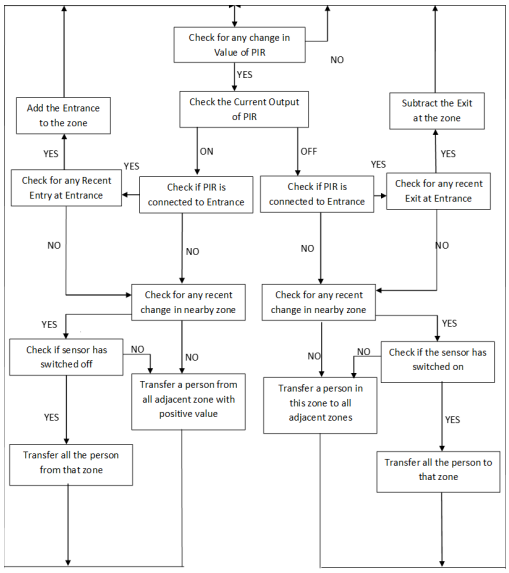

Fig. 2.

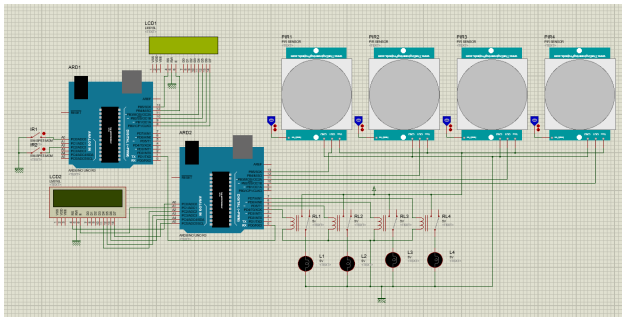

Fig. 3.

high voltage appliances using the low voltage signal received from the Arduino boards

REFERENCES

[1] Andrea Zanella, Nicola Bui, et,al *Internet of things for smart cities* IEEE Internet of things journal vol.1, February 2014.

[2] Eun Som Jeon, Jong-Suk Choi, Ji Hoon Lee, Kwang Yong Shin, Yeong Gon Kim,Toan Thanh Le and Kang Ryoung Park., www.mdpi.com/journal/sensors. *Human Detection Based on the Generation of a Background Image by Using a Far-Infrared Light Camera*. ISSN 1424-8220.

[3] karoly ronay, cristian dragos dumitru., 2015. 9th international conference interdisciplinary in engineering, inter-eng, tirgu-mures, Romania. *An approach to intelligent road lighting system with renewable energy based power supply*.

[4] Kazuya Murao, Tsutomu Terada, Ai Yano, and Ryuichi Matsukura., Graduate School of Engineering, Kobe University. *Detecting Room-to-Room Movement by Passive Infrared Sensors in Home Environments*.

Implementation Of Weed Detection System With Herbicide Sprayer Robot

Mr.A.Kumaraswamy
PG Scholar
Department of Mechatronics
Sri Venkateswara College of Engineering

Mr.S.Logesh
PG Scholar
Department of Mechatronics
Sri Venkateswara College of Engineering

***Abstract*—Over the past few years there was been a rising interest in using automation in agriculture as well as other fields. Weed control is one of the areas which demands automation. In conventional weed control systems, herbicides are sprayed uniformly all over the field. Apart from damaging consequences like negative impacts on soil and underground acquifers, Large amount of herbicides will be wasted, as only some parts of fields are covered with weeds. Finally based on the position of weeds, herbicides was sprayed on the weeds by sprayer robot. Alternatively robots are not only used to spray herbicides but also for spraying pesticides on the plants without any human help**

I. INTRODUCTION

Weeds are the main problem in the agriculture sector, weeds affects the plants growth and also the fertility of the soil, Using of automation have been increased in agriculture and other fields for the previous few years. The weed controller is one of the area that demanded for automation. In the predictable weed controller system the robot spray the herbicides evenly in the agriculture field. Separate from the negative significances like damaging plants, soil quality, underground water, huge herbicides are wasted because a few parts are enclosed with weeds in the field

In the Proposed system, In order to avoid or prevent these negative significances from happening a clever controller system can be employed. This weed controller need to be locate the weed plant in the field after that based on the weed position and robot spray that herbicide on the position of the weed. For this weed detection method crops should be grown in rows. Weeds are nothing but a unwanted plants which is grow between rows. In this situation weed and crop was mixed with each other so it is important to classify that with huge diversity of weeds

The system consists of PIC Microcontroller, DC motor, Sprayer motor, Relays. Software Section: The image was captured using webcamera (or) by any type of suitable camera which was suitable to capture the certain type of images, The certain type of captured image was stored in the Computer system, After the simulation of the entire process , System was connected to an Hardware section

Hardware Section: This section was connected to an UART (RS-232) to an controller unit, PIC micro controller was used as an entire processor for this system, Then by the relay it was used to control the process, Herbicides was stored in the container to spray on the weeds that were located on the specified location by using sprayer motor (Robot), DC motor was used as a wheel for moving the robot

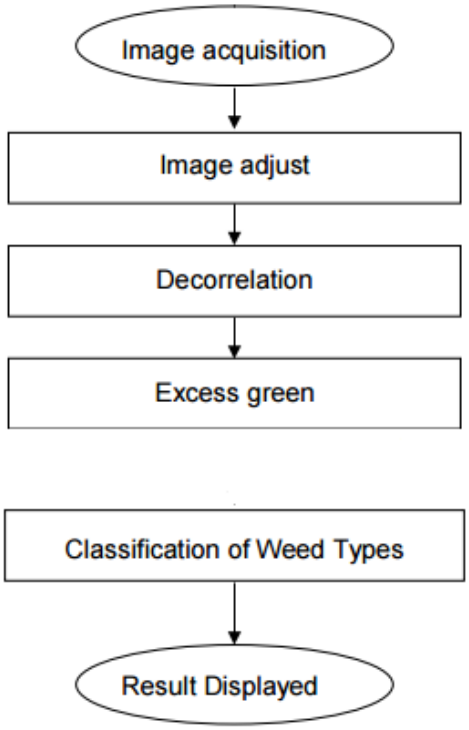

Fig. 1.

II. SYSTEM WORK CHART

III. SIMULATION

The simulation of the project was done using LABVIEW software. First of all is image acquisition that can be done by any types of digital cameras such as normal webcams. The camera should be installed perpendicular to ground. In this case a webcam was installed on the herbicide sprayer chassis at the height of 1.20 meters above the ground. At this height each output image covers nearly a row and two sides of that which is suitable for the purpose. The output images of the webcam were in RGB format with size of 640*480 pixels.

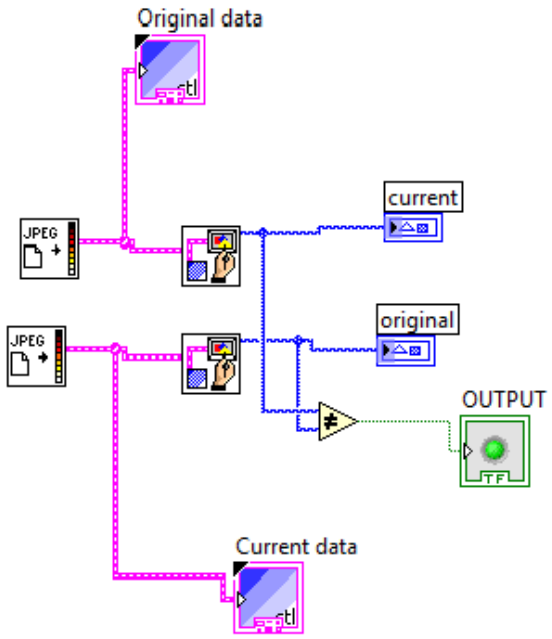

Fig. 2. Circuit Design in LABVIEW

After that the acquired images are processed in LABVIEW. Original image of the plant(without weeds) was already stored in the system , After capturing the image with the camera it was compared with the original image to check whether the weed was available or not If there is any type of weeds was available it was signaled and gives alert Software section was connected to serial communication in order to spray the herbicides to destroy the weeds in the particular area After giving the alert , command was given to the system whether to spray the herbicide on the desired spot.

REFERENCES

[1] Y. S. Tey and M. Brindal *Factors influencing the adoption of precision agricultural technologies: a review for policy implications, Precision agriculture, vol. 13, no. 6, pp. 713730, 2012*.

[2] R. B. Brown and S. D. Noble*Site-specific weed management: sensing requirements-what do we need to see Weed Science, vol. 53, no. 2, pp. 252258*, 2005.

[3] D. Slaughter *The Biological Engineer: Sensing the Difference Between Crops and Weeds, in Automation: The Future of Weed Control in Cropping Systems. Springer, 2014, pp. 7195*.

[4] F. M. De Rainville, A. Durand, F. A. Fortin *K. Tanguy, X. Maldague, B. Panneton, and M. J. Simard, Bayesian classification and unsupervised learning for isolating weeds in row crops, Pattern Analysis and Applications, vol. 17, no. 2, pp. 114*, 2012.

[5] J. P. Underwood, M. Calleija, Z. Taylor, C. Hung, J. Nieto, R. Fitch, and S. Sukkarieh *Real-time target detection and steerable spray for vegetable crops, in in proceedings, Workshop on Robotics in Agriculture at International Conference on Robotics and Automation (ICRA)*, 2015.

Daytime Brake Light Detection System Using Monocular Vision

Mr.A.C.B.YOKESH RAJ
Scholar
Department of Mechatronics
Sri Venkateshwara College of Engineering

Mr. A.Kumaraswamy
Scholar
Department of Mechatronics
Sri Venkateshwara College of Engineering

***Abstract*—Advanced Vehicle Safety is a recently emerging issue appealed from the explosive population of car owners. Increasing Driving Assistance system have been developed for warning drivers of potential hazards by analyzing surrounding with sensor or cameras. Issuing vehicle Deceleration and potential collision, brake lights are particularly important Signal, allowing of no neglect. In this project a Vision-Based Daytime Brake Light Detection System is proposed using a driving video recorder. First background subtraction is accomplished via the use of a Gaussian Mixture Model (GMM).Then number of foreground pixels are calculated and connected segment is said to be Brake Lights if this exceeds a threshold. If it is detected the vehicle(DC motor is taken as vehicle in this project) is stopped using interfaced Microcontroller. Initially vehicle will be in running condition when the brake light is detected the vehicle will be stopped. It reduces more accidents and collision of Vehicles.**

I. INTRODUCTION

Advanced Safety System are automotive functions, which purpose is to make traffic safer, by reducing the risk or accidents. These functions are continuously evaluating the traffic environment with the use of sensors like radar and cameras. Algorithms then use the sensor outputs to decide when the advanced safety system is to be activated in order to either warn the driver or to mitigate and try to avoid a collision or accident automatically. The output from the radar in the sensor system can be position, range and range-rate of other objects (vehicles) and the vision system can provide object recognition and detection of lane markers. The vision system has the possibility to provide detailed information about the surroundings and the detected objects regarding specific features, e.g. various traffic signs and lane markers, something that radar is incapable of.

II. BLOCK DIAGRAM

III. SYSTEM WORK CHART

IV. METHODOLOGY

A. HARDWARE REQUIREMENT

Camera is the first and the most important hardware in this system used for image acquisition purpose. Proper Selection of hardware is effective working of the system. A Good resolution will be implemented for this project which will capture the vehicle images on day. The camera can be mounted on the vehicle or we can fix somewhere so that the images are captured.

B. IMAGE COLLECTION

The second task in the Image processing Algorithm is to get live video feed from the camera connected.

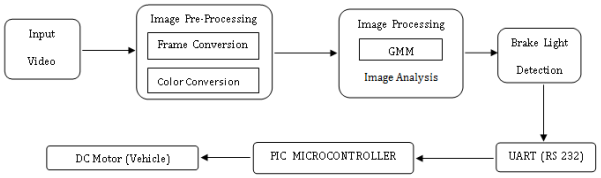

Fig. 1. The system Consists of PIC Microcontroller, DC Motor and Universal Asynchronous Receiver/Transmitter.

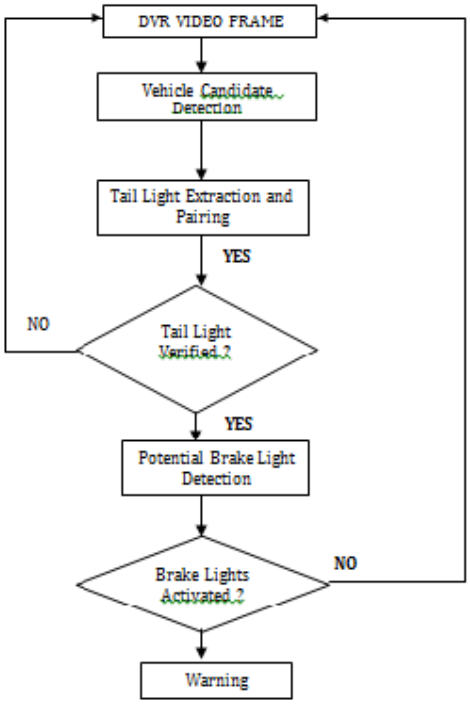

Fig. 2. The system Consists of PIC Microcontroller, DC Motor and Universal Asynchronous Receiver/Transmitter.

C. IMAGE PRE-PROCESSING

D. FRAME CONVERSION

The live video has been further converted into sequence of frames and these frames are used in order to apply further image processing algorithm. These converts image feed into video array. The input video is of the form mpeg, avi etc. Camera fitted in the car captures front vehicles. The captured video is converted into number of frames. The number of frames are based on the format of video.

E. COLOR CONVERSION :

The collected images are having different colors. So we have to do binarization, it converts RGB fames into the binary image. It converts the input image to a binary image. The output image BW replaces all pixels in the input image with luminance greater than level with the value 1 (white) and replaces all other pixels with the value 0 (black). It helps to identify important body parts of the vehicle for the system and we can easily spot the part having greater luminance.

F. IMAGE PROCESSING :

For removing the noise in the binary image, we calculate the weight of the object. Morphological operation is employed to reduce the noise. In Morphological Operation the technique such as erosion and dilation is used. Dilation adds pixels to the boundaries of objects in an image, while erosion removes pixels on object boundaries. The number of pixels added or removed from the objects in an image depends on the size and shape of the structuring elements used to process the image. Erosion is the processes of removing the noise in the input binary frame. Dilation is the process of reconstructing the interesting region that can be eliminated during the time of noise removal. So after this process we got an image having only required part of the vehicle i.e. we only got the image of the tail light.

G. IMAGE ANALYSIS :

H. TAIL LIGHT PAIRING

Pairing is done based on the size, and intensity of the light objects. In lamp pairing symmetry is check by the comparison of the aspect ratios of the light candidates. This is done to get objects of different shapes but similar size and position to be paired. Here similar lamp that is tail lights are to be paired and identified.

I. BRAKE LIGHT DETECTION

This is final step of Image Analysis where the highest threshold value of red color of preceding vehicle is taken as brake light .Thus the Brake Lights are detected.

V. SIMULATION

The simulation of project was done using MATLAB software.

Fig. 3. Brake Lights are Detected Conversion of Frames Conversion of Color

REFERENCES

[1] J. C. McCall and M. M. Trivedi *Video-based lane estimation and tracking for driver assistance: Survey, system, and evaluation, IEEE Trans. Intell. Transp. Syst., vol. 7, no. 1, pp. 2037*, Mar. 2006.

[2] C. Caraffi, T. Vojir, J. Trefny, J. Sochman, and J. Matas *A system for real-time detection and tracking of vehicles from a single car-mounted camera, in Proc. 15th Int. IEEE Conf. Intell. Transp. Syst., Sep. 2012, pp. 975982*.

[3] J.H. Park and C.S. Jeong *Real-time signal light detection, in Proc. 2nd Int. Conf. Future Generat. Commun. Netw. Symp., 2008, pp. 139142*.

[4] G. Siogkas, E. Skodras, and E. Dermatas *Traffic lights detection in adverse conditions using color, symmetry and spatial temporal information, in Proc. Int. Conf. Comput. Vis. Theory Appl., 2012, pp. 620627*.

[5] Y.L. Chen, Y.H. Chen, C.J. Chen, and B.F. Wu *Nighttime vehicle detection for driver assistance and autonomous vehicles, in Proc. IEEE 18th Int. Conf. Pattern Recognit., Aug. 2006, pp. 687690*.

A Hysteresis Comparator With Voltage Level Shifter Using Current Generators

Mrs. N Saraswathi
Scholar
Department of ECE
SRM University

Mr.Athira Dominic
Scholar
Department of ECE
SRM University

Mr. Mayank Kumar Singh
Scholar
Department of ECE
SRM University

Mr.Thejus Raj H
Scholar
Department of ECE
SRM University

***Abstract*—Among all the CMOS circuits, decreasing the supply voltage is one of the most effective ways to reduce their dynamic and short circuit power dissipation. In the case of analog circuits, the smaller supply voltage not only increases the sensitivity of the analog blocks to the noise by reducing their dynamic range but also it turns the required switches more challenging to implement. Therefore, in such circuits were separate blocks operate at different speeds, employing two or more different supply voltages will be advantageous from the power dissipation view point. However, instead of having a low supply voltage in one part and a high supply voltage in the other part, a voltage level shifter is needed to convert the logic levels from low to high with minimum power dissipation and propagation delay.The focus of this paper is to implement a power-efficient voltage level shifter that can convert very low levels of input voltage to higher levels and also to implement it in a hysteresis comparator. The proposed structure uses a current generator in order to avoid the static power dissipation. The design is implemented and simulated using the CADENCE Virtuoso tool in 90 nm technology and is suitable for the VLSI fabrication. IndexTermsVoltage Level Shifter,Power Efficiency, Propagation Delay. Hysteresis Comparator**

I. INTRODUCTION

Comparator ICs are designed to compare the voltages that appear at their inputs and to output a voltage representing the sign of the net difference between them. In a comparator circuit, if the differential input voltage is higher than the input offset voltage, plus the required overdrive, the output swings to a voltage representing logic 1[2]. In effect, a comparator can be thought of as a one-bit analog-to-digital converter. Capacitive strays from the output to an input or coupling of output currents into ground may cause the comparator circuit to become unstable. Guarding high impedance nodes and paying careful attention to layout and grounding can help to minimize these coupling effects. Latching is also helpful[3]. But it is not always possible to prevent instability by these measures. An often-effective solution is to use positive feedback to introduce a small amount of hysteresis. This has the effect of separating the up-going and down-going switching points so that, once a transition has started, the input must undergo a significant reversal before the reverse transition can occur. Voltage translators/level shifters are devices that resolve mixed voltage incompatibility between different parts of a system that operate in multiple voltage domains. They are common in todays complex systems, especially when interfacing with legacy devices. Systems often require voltage level translation devices to allow interfacing between integrated circuit devices built from different process technologies. The choice of the proper voltage level translation device depends on many factors and will affect the performance and efficiency of the circuit application[1]. In CMOS circuits, the dynamic energy is directly proportional to supply voltage. Higher the supply voltage, the more is energy consumption. Thus, the dynamic energy consumption can be reduced if we use low voltage supply in a circuit, without affecting its suitability for the desired purpose. However, when a low voltage circuit drives a high voltage circuit, the PMOS of the high voltage gate may not turn off completely by the low voltage high logic input. The requirement of level shifter arises here. The level-up shifters are used wherever low voltage gates drive high voltage gates. In present devices, it is required that more and more circuits can be designed on a single chip. This designing technique is called System on Chip (SoC) in which the entire system can be fabricated on a single chip[4]. However, the major concern is related to the fact that different gates can use different voltage levels. The output from a high voltage gate can be connected to the input of a low voltage gate and vice versa. Here the level shifter circuits have to be the major component of the CMOS devices. Another purpose to use the level shifter circuits is the difference between the voltage levels of core circuits and I/O circuits in multi-voltage devices. In multi-voltage level devices multiple blocks work on different voltages. Therefore, level shifters are necessary when signal passes from one block to another block. The integrated circuits may gain high packaging density if we scale down the size of transistors used. Together the hysteresis comparator and the voltage level shifter gives a scope to wide range of applications[5]. The rest of this paper is organized as follows. Section II presents voltage level shifter using current generators, Section III presents the hysteresis comparator with the basic voltage level shifter. In Section IV, hysteresis comparator with voltage level shifter using current generator is presented.The simulation results of the designs verifying the efficiency of the proposed design is presented in Section V and finally Section VI gives the conclusion.

II. VOLTAGE LEVEL SHIFTER USING CURRENT GENERATORS

Fig. 1. shows the schematic of the voltage level shifter using current generators. In this circuit, in order to reduce the strength of the pull-up devices, two current generators (i.e., MP3, MP4, MP5, MP6, MN3, MN4, MN5, and MN6) limit the currents applied to the pull-up transistors (i.e., MP1 and MP2). Consequently, by decreasing the strength of the pull-up devices, the pull down transistors (i.e., MN1 and MN2) would be able to overcome the mentioned contention at the nodes Q1 and Q2 and therefore discharge the output nodes to VSS even for the input voltages lower than the threshold voltage. In order to avoid the static power dissipation, the current generators are turned on only during the transition times, in which the logic level of the input signal is not corresponding to the output logic level[1]. The operation of the proposed structure is as follows. When the input signal IN is going from VSS to VDDL, MN1 is turned on and MN2 is turned off. Therefore, similar to the conventional counterpart, MN1 tries to pull down the node Q1,and consequently, MP2 is gradually turned on to pull the node Q2 up to VDDH. When IN changes from VSS to VDDL, there is an interval during which Q1 does not correspond to the logic level of IN. During this period, both MN4 and MN6 turn on, and therefore, transition current flows through MN4, MN6, and MP6. This current, which is mirrored to MP4, flows into MP2 and then charges the node Q2. At the same time, on the other side of the circuit, MN5 turns off because INB = VSS, and therefore, there is no current flowing through MP1 (i.e., IP1 0), meaning a weak pull-up device. This causes that MN1 be able to pull down the node Q1 even for the input voltage lower than the threshold voltage of MN1. Finally, when the node Q1 is pulled down to VSS and Q2 is pulled up to VDDH, MN4 is turned off, and therefore, no static current flows through MN4,MN6 and MP6.This means that the current generator

structures are turned on only during the transition times, in which the input and the output signals do not correspond, avoiding the static power dissipation. Similarly, when the input signal IN is switched from VDDL to VSS, the operation is forced to reverse states.

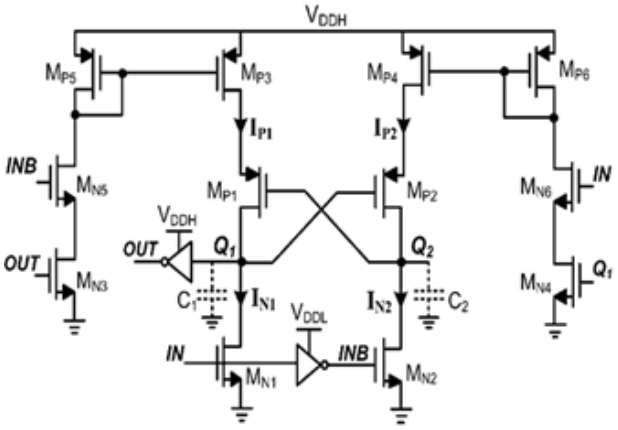

Fig. 1. Schematic of the Voltage Level Shifter using Current Generators.

III. HYSTERESIS COMPARATOR WITH BASIC VOLTAGE LEVEL SHIFTER

The existing hysteresis comparator with the basic voltage level shifter is shown in Fig. 2. above. The circuit consists of two parts the comparator and the level shifter. The output of the comparator is given as the input of the level shifter. In circuits where comparator plays the major role like in the analog to digital converters this circuit can be used. The comparator can work on a small supply voltage and the output can be level shifted as well as the instabilities due to the variation in the inputs can also be reduced[2]. Once the input signal is given the comparator compares these signals and provides the output at Vout1. When Vout1 is high M15 is ON and M16 is OFF and then the output is got. When Vout1 is low M16 is ON and M15 is OFF and then the corresponding output is got. In order to overcome the instability of the comparators hysteresis is used. It is the transistors M9 M10 that provides the hysteresis to the comparator. The level shift provided by the level shifter is very less.

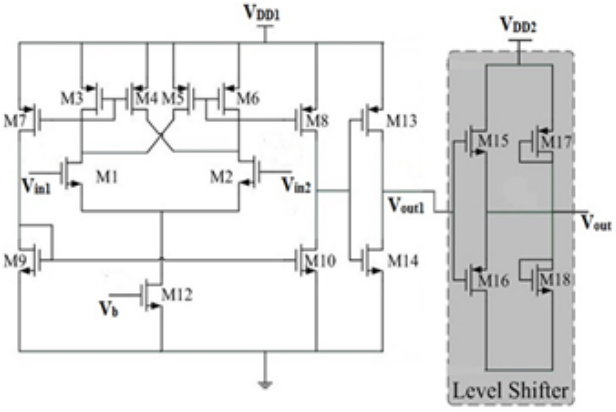

Fig. 2. Schematic of the Hysteresis Comparator with Basic Level Shifter.

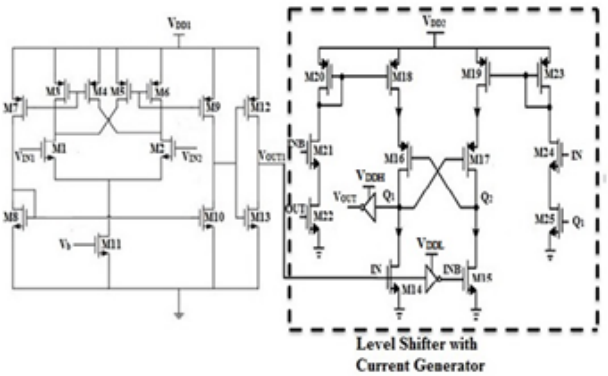

Fig. 3. Schematic of the Hysteresis Comparator with Voltage Level Shifter using Current Generators

IV. HYSTERESIS COMPARATOR WITH VOLTAGE LEVEL SHIFTER USING CURRENT GENERATORS

The Hysteresis Comparator with Voltage Level Shifter using Current Generators is shown in the Fig. 3. In the figure the basic level shifter is replaced with the proposed voltage level shifter and as a result the level shifting of the output of the comparator can be increased and can be used if different applications were the comparators are dominant. The operation of this circuit is similar to that of the existing system. The output of the comparator is given as the input to the level shifter. This shifter avoids the semiconductor process variations. This circuit gives a higher shift rather than the other comparator. The power consumption is also less. Gain is more. One drawback of the circuit is that it occupies more area since the no. of transistors used for the implementation of this circuit is more than the existing one.

V. SIMULATION RESULTS

The circuits are simulated in 90nm technology in order to verify the efficiency of the voltage level shifter using current generators and hysteresis comparator with voltage level shifter using current generators. All circuits are optimally designed for VDDH=1.8V and VDDL=0.4V.The Fig. 4. shown above refers to the transient response of the proposed voltage level shifter. The figure depicts a voltage level shift from 0.4V to 1.8V which is the optimum value. Compared to other structures the proposed voltage level shifter has better performance and can be implemented with high accuracy. The Fig. 5. shown above is the contention between the currents of transistors MP2 MN2.The contention rate is very less in the proposed voltage level shifter compared to all the existing systems. The Fig. 6. shown below is propagation delay of the proposed voltage level shifter. The figure depicts a propagation delay of 421 ps which is a less. All the above results shows that the efficiency of the proposed voltage level shifter is much better the existing structures. The Fig. 7.refers to the transient response of the Hysteresis Comparator with Basic Voltage Level Shifter. The figure depicts a voltage level shift from 400 mV to 434 mV which is a very less value. Gain of the Hysteresis Comparator with Basic Voltage Level Shifter is shown in Fig. 8.The value of the gain is 34.295 dB. The value is measured with respect to the AC response of the design and the got value is less compared to the Hysteresis Comparator with the Proposed Voltage level Shifter.The Fig. 9. shown below is the propagation time of the input signal of the existing hysteresis comparator. The propagation time value for the input signal is 49.8554 ns. The Fig. 10. refers to the propagation time of the output signal of the existing hysteresis comparator. The propagation time value for the output signal is 51.3005 ns. Hence, the propagation delay of the existing system is the difference of the propagation time of the output and the input signals, i.e. 51.301-49.855 = 1.445 ns. The Fig. 11. refers to the transient response of the Hysteresis Comparator with Voltage Level Shifter using Current Generators . The figure depicts a voltage level shift from 0.4V to 1.799 V which is the optimum value.The Fig. 12. shown above is the gain of the Hysteresis Comparator with Voltage

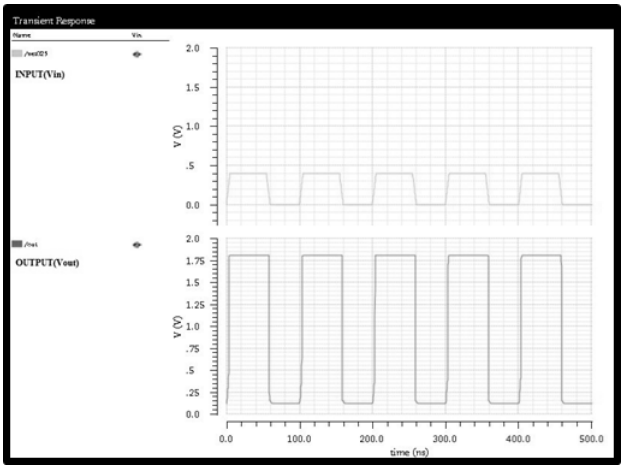

Fig. 4. Transient Response of the Voltage Level Shifter using Current Generators

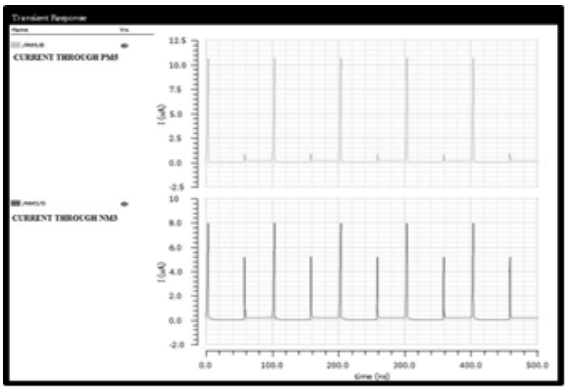

Fig. 5. Current through transistors MP2 MN2 in the Voltage Level Shifter using Current Generators.

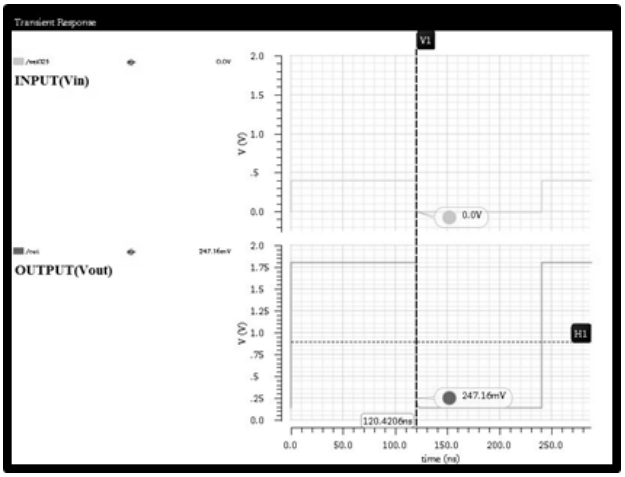

Fig. 6. Propagation Delay of the Voltage Level Shifter using Current Generators

Level Shifter using Current Generators .The value of the gain is 41.117 dB. The value is measured with respect to the AC response of the design and the got value is more compared to the existing Hysteresis Comparator. The propagation time of the input signal of the Hysteresis Comparator with Voltage Level Shifter using Current Generators is shown in Fig. 13. The propagation time value for the input signal is 49.635 ns. The Fig. 14. shown below is the propagation time of the output signal of Hysteresis Comparator with Voltage Level Shifter using Current Generators. The propagation time value for the output signal is 50.364 ns. Hence, the propagation delay of the output and the input signals, i.e. 50.364 - 49.635 = 729 ps. Performance of the structures is summarized in Table I. From the viewpoint of both delay and power it can be observed that the Voltage Level Shifter using Current Generators presents superior performance. This is because of the fact that in the structure the strength of the pull-up device is decreased when the pull-down device is pulling down the output node. Also, it is observed that the Hysteresis Comparator with Voltage Level Shifter using Current Generators show a better performance with respect to the power and gain.

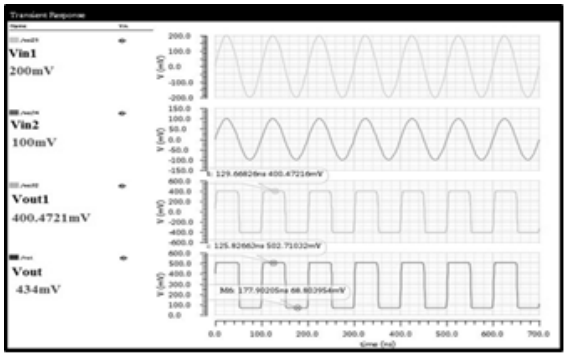

Fig. 7. Transient Response of the Hysteresis Comparator with Basic Voltage Level Shifter

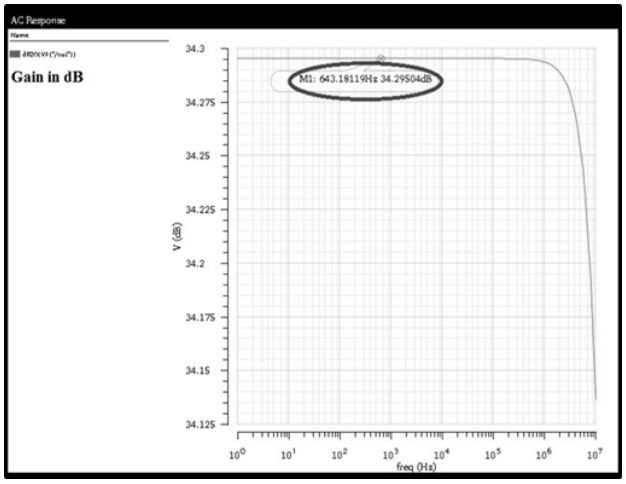

Fig. 8. Gain of the Hysteresis Comparator withBasic Voltage Level Shifter.

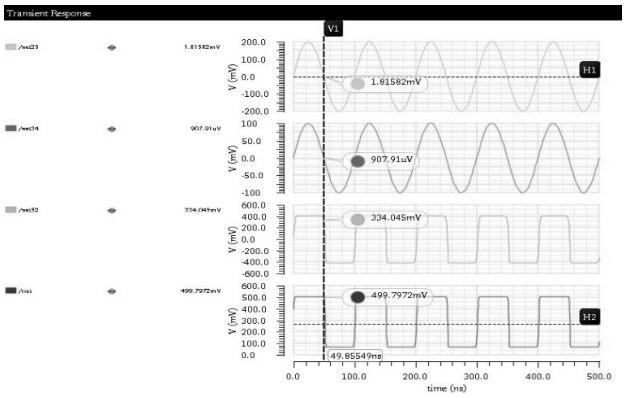

Fig. 9. Propagation time for the input signal of the Hysteresis Comparator with Basic Voltage Level Shifter.

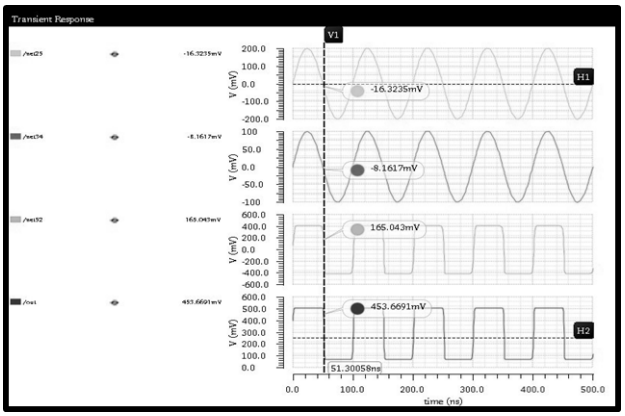

Fig. 10. Propagation time for the output signal of the Hysteresis Comparator with Basic Voltage Level Shifter.

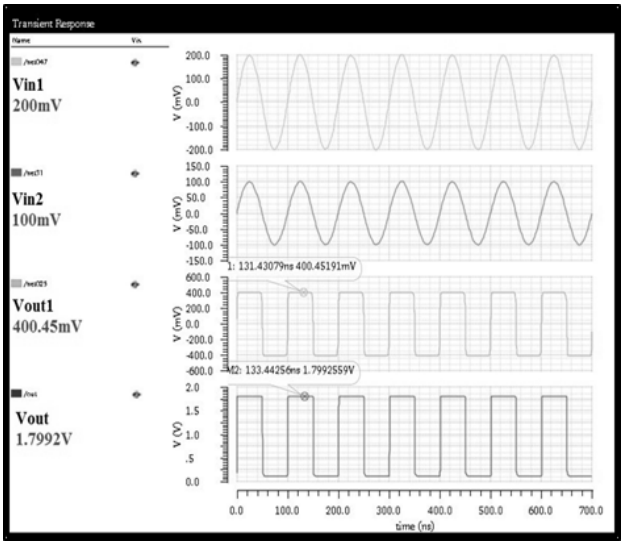

Fig. 11. Transient Response of the Hysteresis Comparator with Voltage Level Shifter using Current Generators

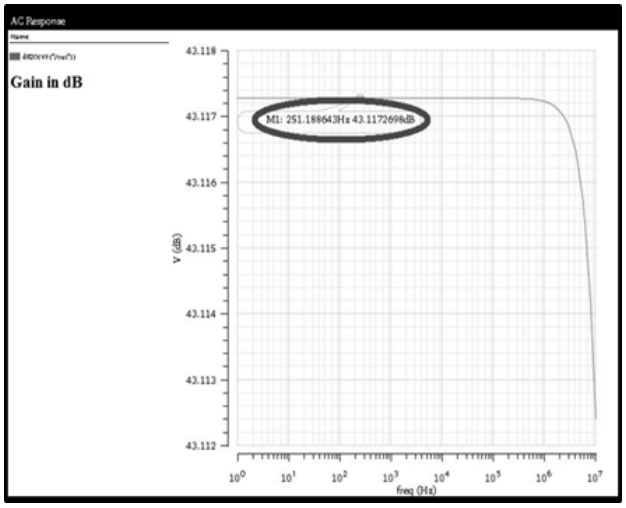

Fig. 12. Gain of the Hysteresis Comparator with Voltage Level Shifter using Current Generators

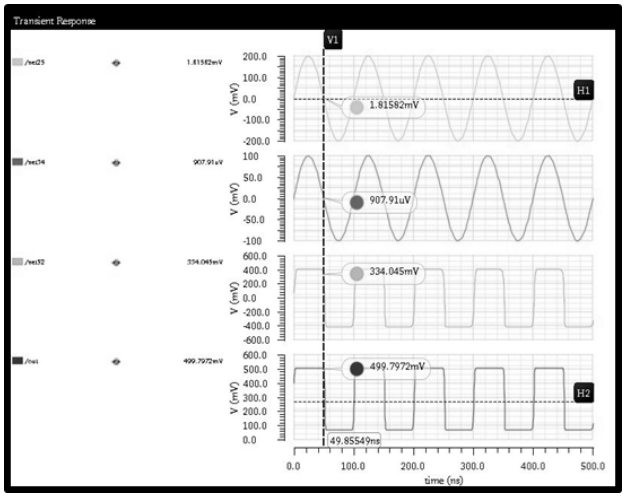

Fig. 13. Propagation time for the input signal of the Hysteresis Comparator with Voltage Level Shifter using Current Generators.

Fig. 14. COMPARATIVE SIMULATION RESULTS

Circuit	Output voltage level	Total Power	Propagation delay
Voltage Level Shifter using Current Generators	1.8V	161 nW	420 ps
Hysteresis Comparator with Basic Voltage Level Shifter	434mV	256 µW	1.445 ns
Hysteresis Comparator with Voltage Level Shifetr using Current Generators	1.8V	56.5 µW	729 ps

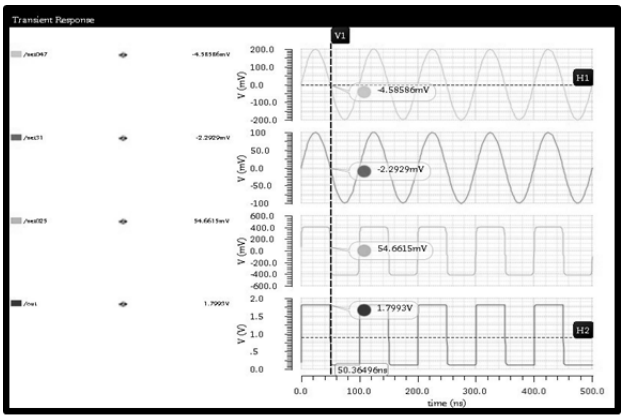

Fig. 15. Propagation time for the input signal of the Hysteresis Comparator with Voltage Level Shifter using Current Generators.

VI. CONCLUSION

In this brief,a power efficient hysteresis comparator with voltage level shifter using current generators is proposed which is able to convert extremely low inputvoltages. This is because of the fact that in the proposed structure the strength of the pull-up device is decreased when the pull-down device is pulling down the output node. Also, a static current path is not introduced between the supply rails in the proposed circuit. Simulation results using the 90nm CMOS technology shows the efficiency of the proposed circuit.

REFERENCES

[1] S.Rasool Hosseini, Mehdi Saberi and Reza Lotfi*A Low-Power Subthreshold to Above-Threshold Voltage Level Shifter, IEEE transactions on Circuits and Systems,Vol.61, No.10*, 2014.

[2] Chung-Yi Li, Chung-Len Lee, Ming-Hong Hu, and Hwai-Pwu Chou *A Fast Locking-in and Low Jitter PLL With a Process-Immune Locking-in Monitor, IEEE Transactions on Very Large Scale Integration (VLSI) Systems, Vol. 22, No. 10*, October 2014

[3] Y. Osaki, T. Hirose, N. Kuroki, and M. Numa *A low-power level shifter with logic error correction for extremely low-voltage digital CMOS LSIs,IEEE J. Solid-State Circuits, vol. 47, no. 7, pp. 17761783*, Jul. 2012.

[4] M. Lanuzza, P. Corsonello, and S. Pirri *Low-power level shifter for multisupply voltage designs, IEEE Trans. Circuits Syst. II, vol. 59, no. 12,pp. 922926*, Dec. 2012.

[5] S. Ltkemeier and U. Rckert *A subthreshold to above-threshold levelshifter comprising a Wilson current mirror, IEEE Trans. Circuits Syst. II,vol. 57, no. 9, pp. 721724*, Sep. 2010..

[6] S. Wooters, B. Calhoun, and T. N. Blalock *An energy-efficient subthreshold level converter in 130-nm CMOS, IEEE Trans. Circuits Syst.II, vol. 57, no. 4, pp. 290294*, Apr. 2010.

[7] Y. Kim, D. Sylvester, and D. Blaauw*LC : Limited contention level converter for robust wide-range voltage conversion, in Dig. Symp.VLSI Circuits, 2011, pp. 188189.*

[8] Y. Moghe, T. Lehmann, and T. Piessens *Nanosecond delay floating high voltage level shifters in a 0.35 m HV-CMOS technology, IEEE J. Solid-State Circuits, vol. 46, pp. 485497*, 2011.

[9] K.-H. Koo, J.-H. Seo, M.-L. Ko, and J.-W. Kim*A new level-up shifter for high speed and wide range interface in ultradeep sub-micron, in Proc. IEEE Int. Symp. Circuits Syst., Kobe, Japan,2005,pp.10631065.*

[10] [9] T.-H. Chen, J. Chen, and L. T. Clark, Subthreshold to above threshold level shifter design, J. Low Power Electron., vol. 2, no. 2, pp. 251258, Aug. 2006.

A WEARABLE PATIENT HEALTH MONITORING SYSTEM USING IOT

P.Tamilselvan
Assistant Professor
Department of EEE
Rajiv Gandhi College of Engg and Tech

T.Rahul
UG scholar
Department of ICE
Sri Manakula Vinayagar Engineering College

***Abstract*—Recently there has been a need to incorporate the use of mobile computing devices in hospital or clinical applications to enhance patient care. Internet of Things (IoT) makes all objects interconnected and it has been recognized as the next technical revolution. This paper presents a Internet of Things based system, aimed at improving healthcare and assistance to dependent people at their homes. In Internet of Things patient's parameters get transmitted through medical devices via a gateway, where it is stored and analysed. The significant challenges in the implementation of Internet of Things for healthcare applications is monitoring all patients from various places. Thus Internet of Things in the medical field brings out the solution for effective patient monitoring at reduced cost and also reduces the trade-off between patient outcome and disease management. Monitoring patient's Electrocardiogram(ECG) and Blood Pressure using Raspberry Pi board.**

I. INTRODUCTION

The unpredictable growth of the Internet of Things is changing the world and the rapid drop in price for typical IoT components is allow public to innovate new designs and products at home. IoT can be used in monitoring patients health, for making smart home and smart city. The unexpected occurrence in patients are monitored using IoT. In this paper specialized sensor is used to monitor patients ECG and Blood Pressure.

One of the key learning platforms for IoT is the Raspberry Pi. The Raspberry Pi is a popular platform became it offers a complete Linux server in a tiny platform for a very low cost. The Raspberry Pi also allows interfacing services and actuators through the general purpose I/O pins.

The combination of Raspberry Pi and IoT becomes a new innovation technology in healthcare system. Raspberry Pi is act as a small clinic after connecting these (ECG and Blood Pressure) sensors. Raspberry Pi is works as small clinic in many places. Raspberry Pi is collect

data from sensors and then it transfer wirelessly to IoT website. Raspberry Pi board is connected to the internet, that board MAC address is registered to the internet. After that in IoT website, add MAC address of this board. Then the sensors output is connected to the IoT website and GSM Module is provided to send the medical report via Text messages to the third party and doctors in case of emergency.

II. LITERATURE SURVEY

Modre-Osprian [1] monitors blood pressure level using Keep In Touch (KIT) and closed loop healthcare services. In KIT method, KIT is connected to the JAVA based mobile phone with the help of near field communication. It works on magnetic , inductive coupling and then the distance is short. After touching the KIT, the data is send to mobile phone. In closed loop services, the data is getting from mobile phone, then the data is send to the secure website. Using this website anybody can monitor patients blood pressure level.

Junaid Mohammed [2] monitors patients ECG wave anywhere in the world using IOIO- OTG Microcontroller. Android application is created for ECG Monitoring. IOIO-OTG microcontroller is connected to android phone using USB cable (or) Bluetooth dongle. After collecting data, the wave is send to android application. Monitor and store ECG waves in that android based application.

Mohammed S. Jasses [3] focused on body temperature monitoring using Raspberry pi board in cloud based system. In that paper, Raspberry pi is monitor body temperature and then these parameters are transfer by wireless sensor networks (WSN). Then these datas are added to the cloud based websites. Using this website monitor body temperature.

Hasmah Mansor [4] monitors body temperature using LM35 temperature sensor. The LM35 temperature sensor is connected to the Arduino Uno board. After that creating a website in SQL database format. Arduino Uno board is connected to that website. Then sensor output is send to the website. Using this website anybody can monitor body temperature in login process.

Mathan Kumar [6] discussed about monitors ECG, Respiration rate, heart rate and body temperature. These sensors are connected to PIC16F887A microcontroller. After

collecting data from sensors, the data is upload to the website manually. For monitoring purpose created an android application and webpage for monitoring health status.

Nithin P. Jain [8] monitors temperature, blood pressure, heart rate of patients. Microcontroller AT Mega 32 is used for connecting these sensors. GSM module is connected to this microcontroller. After collecting data, if the value is low SMS is send to the doctor.

Soumya Roy [9] monitors ECG waves of patients. AT Mega 16L microcontroller is used for monitoring ECG waves.

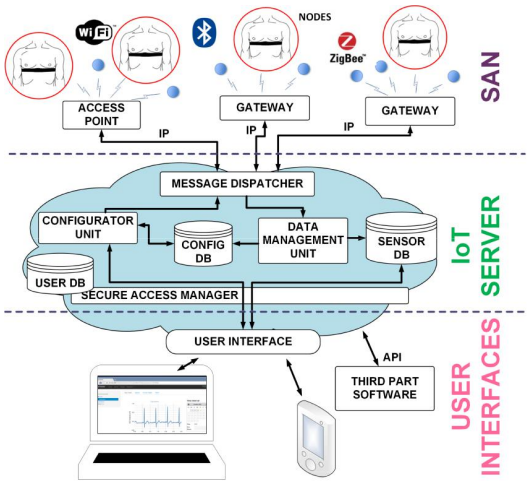

Fig. 1. Overview of ECG Blood Pressure Monitoring system using Raspberry Pi

ZigBee module is used for transferring ECG waves. ZigBee module is sends data to nearest connected sys tem for ZigBee.

Rajeev Piyare [10] implement controlling and monitoring home appliances using android b ased smart phone. Arduino uno board is connected to home app liances (light, fan, etc). Creating an android application for this smart home. Arduino uno board and android app is con nected by internet. Using this android app controlling and monitoring home appliances anywhere in the world.

Karandeep Malhi [7] monitors body temperature, heart rate using C8051F020 microcontroller. Wearable sensors are used to collect data and then send to micro controller. Zigbee module is connected to this microcontroller and then that module is transfer data to the nearest receiver .

In this paper we have ECG Blood Pressure reading results are monitored. These sensors signals send to the Raspberry Pi via amplifier circuit and signal conditioning unit (scu), because the signals levels are low (gain), so amplifier circuit is used to gain up the signal and transmit the signals to the Raspberry Pi. Raspberry pi is a linux based operating system works as a small pc processor system. Here patients ECG Blood Pressure is measured using respective sensors and it can be monitored in the monitor screen of computer using Raspberry Pi as well as monitoring through anywhere in the world using internet source. Raspberry Pi is programmed for the particular project need that via USB dongle (or) Ethernet for patient's health

monitoring through internet. It sends all the current health data of the particular patient to the web database. Anybody can access the web and can see the health of patients.

Sensor and actuator nodes (SANs). Lightweight wearable ECG sensors and other ambient sensors collect data and send them in real time via a wireless protocol (ZigBee, Bluetooth, WiFi) to a gateway connected to the home ADSL router (Fig. 1).

Both the gateway and the message dispatcher are transparent at the logical communication level between sensors and IoT server. The architecture has been developed with the aim of enabling the integration of sensor networks based on different networks protocols (WiFi, ZigBee, Bluetooth) The only component aware of the local sensor network protocol is the gateway, which runs a firmware that can manage the corresponding protocol. The gateway encapsulates the packets of the sensors in a universal format which preserves all the information present in the native format. Hence sensors send messages in their native format to the IoT server, where the data management unit extracts information and enters it in a universal format into the sensor database. When sensors need to be configured or interrogated, the configurator unit prepares a command according to the target sensor protocol. The IoT server converts the raw payload from heterogeneous nodes into a universal format, containing object identifier, object type, measurement unit, data field, geographical position, and timestamp. Then, it makes the data available to applications and users. In this way, data visualization and processing is separated from measurement and data collection, and does not need to take into account the communication protocol of the originating source. In addition, the IoT server receives data from users in order to configure and manage the SANs.

The main components of the IoT server are illustrated in the cloud of Fig. 1, since they can be part of a distributed information system. The message dispatcher manages the bidirectional communication with the sensor networks, using no information on the network protocol or on the type of application. The data management unit is a collection of software modules interpreting data from sensors and storing them in a universal format in the sensor database. The configurator unit receives inputs from users or applications and translates them into protocol-specific commands to the SANs, consulting the configuration database. Finally, the secure access manager provides access to stored information and SAN configuration only to authorized users and applications, according to information contained in the user database.. User interfaces. The entire system is configurable and controllable through an intuitive web interface from any computer, smart phone or tablet connected to the internet. In the IoT server, health data can be combined with other data, merged, processed by users and/or authorized clinicians.

Users with proper access rights can monitor the current sensor status, or query and visualize data in a specific time interval. In Fig. 2, the ECG data visualization thought the web interface is shown

An ECG device generally consists of an analog frontend (AFE) circuit and a signal processing circuit. The AFE circuit capabilities and requirements mainly depend on the ECG application. Many aspects of the design of an ECG AFE depend on the ECG signal characteristics. The ECG is a graphical representation of the electric potential difference created on the body surface by heart contraction, which can be detected at different body locations. ECG devices can have a different number of leads, from one to a maximum that is usually 12, depending on the target application. For monitoring purposes, a one-lead AFE is usually adequate, since only

Fig. 2. ECG user interface

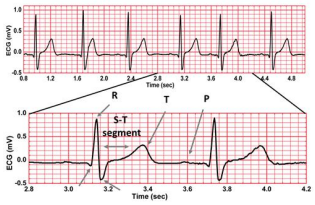

Fig. 3. Sensors output from Raspberry Pi board

macroscopic behaviours are of interest.

The ECG signal consists of three main components:

1. the actual differential ECG signal;
2. the differential time-varying ECG offset;
3. the common-mode signal.

The actual ECG signal has a bandwidth from 0.05 Hz to 150 Hz. It has a peak-to-peak amplitude of approximately 1 mV but can reach 3 mV. Blood pressure sensor is fixed with ECG in band for better communication with raspberry pi 3 model B board. Thus the simplified structure of the system has clearly explain that check the human physical parameters and send the signal to the raspberry board. That saved signal is transfer to the IOT and saved permanently. By using IOT, we can save data for many year and keeping records with safe. At the same time the message has to be transfer to the patient and doctor mobile through GSM module.

III. .RESEARCH AND DEVELOPMENTS

Technology plays an important role in today's world like industries, personal life's, environment and agriculture fields. Among these fields health care process is the most important field and crucial also. The improvement of medical equipments and devices also plays a significant contribution for technology development in health care devices. This process is produces doctor's for new technology to monitor private use. Patient's also connect video conference to the physicians for improving their health status. It also reduces patient's money and waiting time at hospitals. Using this technology development, patient's record their health status in their own mobile phone and then store the data.

IV. CONCLUSION AND FUTURE WORKS

We have proposed a wireless wearable ECG Blood Pressure monitoring system embedded in an IoT platform that integrates heterogeneous nodes and applications, has a long battery life, and provides a high-quality ECG signal. The system allows monitoring multiple patients on a relatively large indoor area (home, building, nursing home, etc.). Another remarkable feature of our system is a very low marginal cost per added sensor, since our architecture enables a single low-cost gateway to manage multiple sensors.

After connecting these sensors to the Raspberry Pi board, there are two ways to access the output. One is directly connected to the monitor, keyboard, mouse to the Raspberry Pi board and got output in monitor screen. The another method is Raspberry Pi board is connected to a laptop (or) computer using data cable After that install putty software to the respective system. Change IP address, Subnet mask, gateway to that system. Then open that putty software output will display in that screen.

Future work will focus on monitoring additional health-related parameters using a broader combination of transducers, sensors, and correlation techniques, and on improving system reliability and robustness to patient movement and connectivity losses.

REFERENCES

[1] Andrea Zanella, Nicola Bui, et,al *Internet of things for smart cities* IEEE Internet of things journal vol.1, February 2014.

[2] A. Dohr, R. Modre-Osprian, M. Drobics, D. Hayn, G.Schreier, *"The Internet of Things for Ambient Assisted Living*, Seventh International Conference on Information Technology, pp 804-809,2010.

[3] Junaid Mohammed, Abhinav Thakral, Adrian Filip Ocneanu, Colin Jones, Chung-Horng Lung, Andy Adler,*"Internet of Things: Remote Patient Monitoring Using Web Services and Cloud Computing*, 2014 IEEE International Conference on Internet of Things (iThings 2014), Green Computing and Communications (GreenCom2014), and Cyber-Physical-pp 256-263,2014

[4] Mohammad S. Jassas, Abdullah A. Qasem, Qusay H. Mahmoud,*" A Smart System Connecting e-Health Sensors and the Cloud A Smart System Connecting e-Health Sensors and the Cloud* Proceeding of the IEEE 28th Canadian Conference on Electrical and Computer Engineering Halifax, Canada, pp 712-716,May 3-6, 2015.

Diagnosis of Parkinsons Disease Using Retina Model

R.VINO
UG scholar
Department of ECE
ST.anne's CET

R.BHUVANA
UG scholarr
Department of ECE
ST.anne's CET

A.PUVIARASI
UG scholar
Department of ECE
ST.anne's CET

***Abstract*—The Human Visual System (HVS) model based image quality metrics, correlates strongly with the evaluations of image quality as well as with human observer performance in the visual recognition process. Physiological modeling of retina plays a vital role in the development of high-performance image processing methods for better visual perception. For image processing in medical diagnosis, one has to follow several steps like image preprocessing, image segmentation, feature extraction, image recognition, and interpretation. . The main aim of this work is to develop a model for retina, which has complex neural structure, capable of detecting the incoming light signal and transforms the signal before transmitting it through the optic nerve. This retinal model comprises of the photoreceptor, outer-plexiform and inner-plexiform layers exhibiting the properties of compression and spatiotemporal filtering in the processing of visual information. The spatial frequency value is evaluated using Discrete Cosine Transform (DCT) technique thereby enhancing the contrast visibility in the dark area and maintaining the same in the bright area using photoreceptor layer of the retina. Contour contrast enhancement is achieved by modeling outer-plexiform layer of retina and parvo channel of the inner-plexiform layer is modeled to extract finer details of the image. Clinical Diagnosis of Parkinsons disease [PD] leads to errors, excessive medical costs, and provide insufficient services to the patients. There is no particular method or a test to detect the PD. The diagnosis of the Parkinsons disease needs an accurate detection. Dopamine nerve terminals can be reduced in the brain parts such as Substantia nigra, Striatum, and other brain structures. This paper is used to classify the PD/normal patient based on retina model using digital image processing.**

I. INTRODUCTION

Imaging modalities like X-rays, Computed Tomograms, Ultra- sound, and Magnetic Resonance Imaging are used to assess the condition of an organ/full body. Proper diagnosis and treatment are aided by monitoring the physiological condition over an observation period. To make diagnosis simpler and accurate, the images obtained through the scanning modalities are subjected to processing. Medical image processing technique go through the following steps for disease diagnosis and to check for normal and abnormal conditions, (i) The first step is image preprocessing to filter noise and to enhance image quality. (ii) The next step is image segmentation where the region of interest is segmented using different segmentation algorithms. (iii) The third step is feature extraction, where different textures and statistical features are extracted to analyze the morphological behavior of the image. (iv) The final step is classification, where the image is classified as normal and abnor- mal image by comparing the values of the extracted features. The software can be used for simulation to evaluate strategies and to perform planned treatments. To extract the finer details of the image, the acquired image is subjected to several step by step processing, like image pre-processing, image segmentation, feature extraction, image recognition, and interpretation. Algorithms are written to process the image which makes the system more complex. The main scope of these algorithms is fairly expansive, ranging from automatically extracting Region of Interest (ROI) as in the case of segmentation thereby improving the quality of perceived image using image enhancement. Parkinson's disease is a second neurodegenerative disease which causes major threat to aged people and in the society as a whole and this is next to Alzheimers disease. Neurochemically, Parkinsons disease gets occurred due to the loss of dopamine nerve terminals in the region of striatum which are connects to the Substantia Nigra. Dopamine deficit may cause due to the loss of neurons in the midbrain of Substantia Nigra which will lead to the result that there occur changes within nigrostriatum neural conduction. Apart from that, PD can also characterize by the presence of intracytoplasmic inclusions called lewy bodies. Clinical diagnosis for each and every human may vary largely. Problems with imbalance, tremor, postural instability, rigidity are all the major symptoms for PD. Motor symptoms usually start at one side of the body and gradually it will progress to the opposite side. Other parkinsonian syndromes are mainly affected by these symptoms. Idiopathic PD diagnosis indicators are symptoms, move to advanced stage, and treatment response based on levadopa. Tremor symptoms lead to loss of voluntary movement. Tremor may happen at thumb and wrist, which is one of the most typical initial symptoms. The amount of resistance can be measured by limb rigidity when it is moved passively. PD disease patients have higher resistance in limb than normal person. Changes in muscle and joints properties can also contribute to the presence of parkinsonian rigidity. Bradykinesia symptoms lead to some of the familiar problems such as difficult to sit and stand in a floor, get in and out of a car, chair. Still there is no medical treatment to diagnose Parkinsons disease although medication is available while the symptoms are gets identified at early stages of this disease [3]. Early stage diagnosis can result in significant life saving. Parkinsons disease specialists

make correct decisions by evaluating their test results of their patients. Diagnosing Parkinsons disease may need experience and highly skilled specialists [4]. Improvement of diagnosis and assessment in early disease can gets resolved by functional neuro imaging. Statistical Parametric Mapping (SPM) is a popular Matlab based software package for performing neuro imaging studies that can be used to locate significant effects of statistical parametric models in images. There are number of nerve cells in human brain which are called as neurons where each neuron is connected to other neurons via stand of fiber called axons.Nerve impulses get transmitted from one neuron to other by axons, when the neurons are affected. Dendrites are the one which connects a neuron and axons of other neurons. The contact point between a dendrite and axon is called a synapse. Most of the medical diagnosis uses classifier that will get increasing gradually. Classification systems can be used to improve accuracy, reliability of diagnosis and minimizing possible errors, as well as making the diagnoses of the disease more time efficient. In this paper ,the svm classification is used to diagnosis the parkinsons diseases.

II. RETINAL STRUCTURE

Human retina contains nearly about 200 million nerve cells; it is less than a millimeter thick over most of its extent (. The retina detects light falling on it, and then con- verts the incoming light into its equivalent electrical signal and later performs initial processing of signal and finally the processed information is sent to the brain through optic nerve where this information is perceived as an image. Human retina acquires infor- mation from the outside world, performs sampling, compresses the information and sends the information to the brain.Path of information flow from the light source to the optic nerve fiber is derived from a three neuron chain which starts from the photoreceptor layer to bipolar cells to ganglion cells. The first and foremost layer of the retina is the photoreceptor layer which is responsible for visual data acquisition; this layer is also associated with local logarithmic compression of the image luminance. Photoreceptor layer is in-turn connected to the ganglion cell layer through a series of neurons. There are two main receptors in the photoreceptor layer namely, the cones responsible for color vision processing and are color sensitive. The rods are even more sensitive than cones and are responsible for dim light vision. Rods are responsible for producing low-level illumination that gives rise to scotopic vision. Rods and cones, in general, produce a nonlinear response. The retina cells are connected to each other for better visual perception, thereby forming two main layers namely, the Outer-Plexiform Layer (OPL) and the Inner-Plexiform Layer (IPL). In the Outer-Plexiform Layer (OPL), the signals are transmitted from the photoreceptors layer to two kinds of cells namely, the bipolar cells and the horizontal cells through a junction called synaptic triad. Connections between cones and bipolar cells are of a one-to-one type in the fovea region; several bipolar cells may be connected to the same cone . If a cone is excitatory to a bipolar cell, it is also excitatory to a horizontal cell, and this horizontal cell is, in turn, inhibitory to the bipolar one. In the Inner-Plexiform Layer (IPL), the bipolar cells are con- nected to ganglion cells and the amacrine cells, the axons of the ganglion cell constitute the optic nerve, and the amacrine cells play a similar role as the horizontal cells in the OPL.

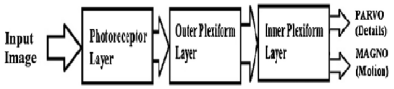

Fig. 1. Retinal layers in HVS model

III. RETINAL LAYER BASED HVS MODEL

The block diagram of the processed retinal layer model is shown in fig.1. In the proposed design of retinal layer model, the three main layers namely photoreceptor layer, outer-plexiform layer, and the inner-plexiform layer is considered.

The photoreceptor layer enhances the contrast value of the image for different values of compression parameters ranging from 0 to 1. Photoreceptor layer output is fed to the outer-plexiform layer. In the outer-plexiform layer, photoreceptor cell layer also interacts with the horizontal cell layer. The outer-plexiform layer is modeled considering the response of bipolar ON and OFF channel thereby enhancing the contours. The response of the outer- plexiform layer is passed to the inner-plexiform layer.The inner-plexiform layer provides us with finer details of the image and information on motion analysis for processing visual data. The out-put of the inner plexiform layer has two channels namely parvo and magno. Our work focuses only on parvo channel, which is concerned with the extraction of the finer detail of the image; magno channel is associated with motion analysis. In this study, only still images are considered, and only parvo channel is concentrated for processing visual information.

MATHEMATICAL MODELING OF RETINAL LAYERS As shown in fig.1, the main retinal layers involved in the signal processing are photoreceptor layer, outer-plexiform, and inner- plexiform. Based on their functionalities mathematical modeling is attempted and is presented in this section.

IV. PHOTORECEPTOR LAYER MODEL

A photoreceptor cell is modeled using the cone transfer function given by the expression in equation (1) Fph=1/[1+ph+2ph(1-cos(2fs))+j2phft] (1) where Fph denotes the cone transfer function which is a function of spatial frequency (f s) and temporal frequency (f t), ph is the gain of the photoreceptor, and its value is set to 0.7, ph denotes spatial cut-

off frequency, and its value is set to 7 . Spatial frequency (f s) is computed by applying discrete cosine transform (DCT) to the input image, and temporal frequency (f t) is considered to be merely dc value since for this work only static image is considered . The basic Michaelis Menten relation is modified so as to include a local adaption effect and normalized for a luminance range of [0, Vmax] A(p)=[C(p)/C(p)+C0(p)].Vmax+C0(p) (2) C0(p)=S0.L(p)+Vmax(1-S0) (3) Compression parameter Co(p) depends on L0(p) , the cone transfer function, static compression parameter value So and Vmax the highest pixel value in the image. Local luminance L0(p) is computed using the cone transfer function as shown in Eq. (1). In the human visual system, the static compression parameter value varies depending on the ambient light. A static compression parameter S0 of range (0, 1) is considered to increase flexibility and make the system more accurate. V max value is equated to 255 because that is the highest pixel value in the input image. In this study, the static compression parameter value So is adjusted between 0 and 1 to increase the flexibility and to make the system more perfect. The adjusted luminance A0(p) of the photoreceptor layer as shown in figure depends on the current luminance C0(p) and on the compression parameter Co(p) which is, in turn, linked linearly to the local luminance L0(p) of the neighborhood of the photoreceptor.

V. OUTER-PLEXIFORM LAYER MODEL

The outer plexiform layer is modeled using the spatial-temporal filter whose transfer function is given by the expression. FOPL(fS)=Fph(fs)[1-Fh(fs)] (4) Fh(fs,ft)=1/[1+h+2h(1-cos(2fs))+j2hft] (5) As shown in the spatial, temporal filter is derived as a difference in the low pass filter which models the photoreceptor network and a low pass filter which model the horizontal cell network h of the retina.

VI. INNER PLEXIFORM LAYER MODEL

Contour-Contrast-enhanced image from the outerplexiform layer is then passed to the inner-plexiform layer. Contour enhance- ment depends more on contours. Logarithmic transformation in Matlab is evaluated using the formula given in Eq. (6). Logarithmic transformation=K*Log(1+double(Input image)) (6) where K is a constant. The inpu image is doubled to convert the image into its decimal equivalent value. The natural logarithm is then applied as shown in the above equation. A logarithmic transformation is used to expand the value of dark pixel values in an image and to compress the dynamic range of the image.

VII. CONVENTIONAL IMAGE PROCESSING VS .HVS BASED IMAGE PROCESSING

Any digital image processing algorithm has the following sequence as shown in fig.2. A digital image is acquired by any imaging modalities, which includes image sensing, sampling, and quantization. In Pre-processing step image is improved by filtering that increase the chance of success of the other processes. It includes image enhancement, restoration, and morphological analysis, like noise removal, image sharpening.

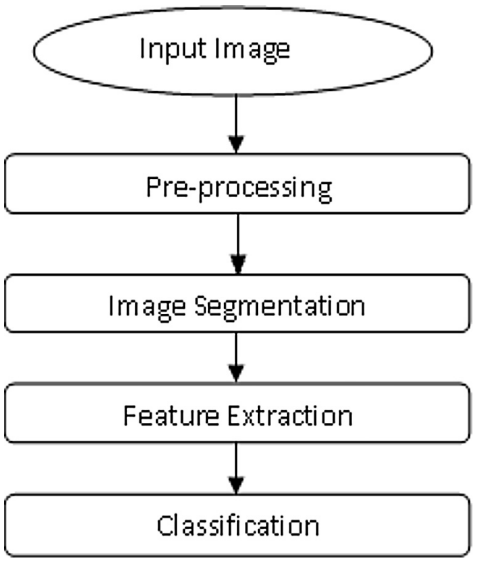

Fig. 2. Proposed block diagram

Segmentation is the process of breaking down an image into its constituent parts, i.e. to a meaningful form which is easier to analyze. Some of the most common segmentation techniques followed are edge detection, compression-based method, and boundary extraction. The objects and boundaries in an image are detected using image segmentation techniques. Feature extraction is the process of extracting features that result in some quantitative information of interest or features which are basic for differentiating one class of objects from another. It is used to analyze the texture of an image. Image textures are analyzed either by the statistical method or structural method. Feature extraction gives information on various properties of an image which leads to next step of Recognition and Interpretation. Recognition is the process of assigning a label to an object based on the information provided by descriptor (Feature Extractor). And, interpretation is the process of assigning meaning to an ensemble of recognized object called classification. Any medical images are subjected to the above-mentioned processing steps before diagnosis. The processing time involved in carrying out these steps is time-consuming, and moreover, the segmentation algorithm used is subjective to the application. These processes introduce computational complexity in any imaging modality unit and needs a specific algorithm function.

As an alternative, retinal model based Human Visual System for processing medical images is proposed which works with less computational effort. The acquired digital image from any imaging modality is passed through the modeled retinal layers for processing. The processed image features are analyzed based on the features described in next section and found to be better. Support Vector Machine(SVM) are supervised techniques for classification which finds a linear hyper plane by placing the largest margin by mapping input features to a higher dimensional space through either linear or nonlinear kernel functions. Prediction/Prognostic models gets developed

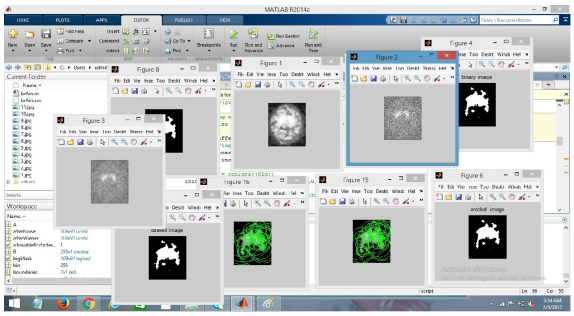

Fig. 3. Output image

that can be used to identify the purpose of risk prediction in PD with the help of multivariate logistic regression techniques. The probability occurrence of one out of two classes gets modeled by binomial logistic regression. Supervised learning algorithm which requires training data and one of the most powerful supervised classification algorithms is Support Vector Machine (SVM). The main intent of SVM classifier is to directly focus on finding classification boundary without probability estimation values. This classifier is also known as hard classifier. Moreover classification may be performed with the help of probability estimation and evaluate class-conditional probabilities are known as soft classifier.

VIII. RESULTS AND DISCUSSION

The proposed that diagnosis of Parkinsons disease done by the integration of information from a variety of imaging modalities. This is a method for processing and analysis of brain images. A MATLAB is a program for processing and analysis of brain images and molecular neuroimages. It gets run in an MATLAB environment and freely downloadable. Preprocessing can be done by using DCT and segmentation can be done by using spatial-temporal filter. The logarithmic transformation is applied for feature extraction. Finally SVM classifier is used to classify the PD/normal as shown in fig.3.

IX. 4. CONCLUSION

Human visual system is a very powerful system. The proposed retinal layer model imitates some parts of the retinal functionalities including its luminance, compression properties and spatial and temporal frequencies for visual processing. . Hence, the proposed HVS model can be used an alternative to the existing generic image processing technique and can be applied extensively in robotic vision or computer vision. Parkinsons disease caused by reduction of dopamine in nerve terminals and reduction cannot be diagnosed easily. This survey paper proposed for automatic recognition of Striatum, substantia nigra in brain stem. SPECT imaging test can be used to detect reduction of dopamine in brain. Classification algorithms are used to distinguish between normal and PD. Therefore accurate diagnosis of PD and number of wrong decisions gets reduced with the help of diagnosis algorithms. Extracting features and selecting appropriate features will yields good classification results.

REFERENCES

[1] Beaudot, W. H. A. (1996). Sensory coding in the vertebrate retina: *Towards an adaptive control of visual sensitivity. Network: Computation in Neural Systems*, 7 (2). 317-3.

[2] Benoit, A., Alleysson, D., Herault, J., Le Callet, P. (2009). *Spatio-temporal tone mapping operator based on a retina model. Lecture Notes in Computer Science*, 5646, 1222.

[3] Benoit, a. A., Caplier, b. A., Durette, b. B., Herault, b. J. (2010). *Using human visual system modeling for bio-inspired low level image processing. Computer Vision and Image Understanding*, 114, 758773.

[4] Brooks, A. C., Zhao, X., Pappas, T. N. (2008). *Structural similarity quality metrics in a coding context: Exploring the space of realistic distortions. IEEE Transactions on Image Processing*, 17, 8.

[5] Chen, Z., Zhang, L. (2009). *Multistage directional median filter. World Academy of Science, Engineering and Technology*, 59

Performance Analysis Based Modeling Of Induction Heating For Industrial Application Using Fem Tool

Ms.Anuradha D
Scholar
Department of ECE
Anna university,Puducherry.

Ms.Mayavady .K
Assistant Professor
Department of ECE
St. Pauls Engg. college

***Abstract*—The objective of this project is to develop a design and modeling of induction heating analysis was performed to detect the temperature distribution on mold surface used for industrial application using Fem tool. In this research FEA analysis is used which results more closely to prototype result . To perform 2-D static and transient analysis of electromagnetic and thermal analysis of induction heating which is used to obtain its steady characteristics such as magnetic flux density vector, joule heat generation, thermal heat generation using ANSYS software 17.2. The induction coils were placed in close to mold surface and coils excited by a large alternating current at high frequency. The AC current induced heat in the mold surface and the surface temperature was raised quickly. The analysis showed that the results of surface temperature distributions of the coil. This leads to the conclusion that increasing the number of coils and input current would be able to get uniform surface temperature distribution as well as rapid temperature increase.**

I. INTRODUCTION

Induction heating was first noted when it was found that heat was produced in transformer and motor windings, as mentioned in the chapter Heat treating of metal. Accordingly, the theory of induction heating was studied so that motors and transformers could be built form maximum efficiency by minimizing heating losses. The development of high-frequency induction power supplies provide a means of using induction heating for surface hardening. The early use of induction involved trial and error with built-up personal knowledge of specific applications but a lack of understanding of the basic principles. Throughout the year the understanding of the basic principles has been expanded, extending currently into computer modeling of heating application and processes. Knowledge of these basic theories of induction heating helps to understand the application of induction heating as applied to induction heat treating. Induction heating occurs due to electromagnetic force field producing an electrical current in a part. The parts heat due to the resistance to the flow of this electric current. Induction hearing is used for the direct heating of electrically conducting materials. The primary advantage is that the heat is generated within the material itself, giving very fast cycle times, high efficiency, and the potential for localized heating. The magnetic oscillations are sourced by a coil in which a large current passes with the same frequency. Assuming that there is an oscillation, the current through a loop of wire as the phase Current a FEM cross sectional simulation of magnetic field densities as Current passes through the relative loop of wire. As the number of loops increases, the intensity magnetic field localizes to the axis of the coil. The highest magnetic field B in the very centre which can be estimated by the equation.

Where is the magnetic permeability of the interior of the coil, N is the number of loops (or turns), l is the length of the solenoid.The number of loops increases in number and in density from left to right. The rightmost illustration estimates infinitely dense windings.When this oscillating magnetic field intercepts a conductive object, it will induce a current in it. The direction and velocity of the induced current will oppose that of the current of the inducing coil. Notice that the current density decreases exponentially as the distance from the surface of the steel increases. This is known as the skin effect and is defined as,

The skin depth is related to the frequency, conductivity, and permeability of the material. The reference depth is the theoretical minimum depth of heating that a frequency will produce at a given power and work piece temperature. The cross sectional size of the work piece being heated must be at least 4 times the reference depth, or current cancellation will occur. This comes from manipulation of the skin depth equation. As a rule of thumb, the reference depth is the depth where 86 of heating occurs from eddy currents and resistivity. The heat distribution and current distributions of a cylindrical work piece with diameter a. The voltage-source series resonant converter uses the natural resonance of an LCR network to generate high voltages across the reactive components. It consists of a series combination of an inductor (work coil), capacitor, and a lossy resistance. The resistance is the combination of losses from the work piece, resistance of the work coil, internal ESR of the capacitor, and any system losses. This is the simplest model used to represent induction heating, although more complicated analysis will assign specific losses to discrete resistor elements.

II. VOLTAGE LEVEL SHIFTER USING CURRENT GENERATORS

Fig. 1. shows the schematic of the voltage level shifter using current generators. In this circuit, in order to reduce the strength of the pull-up devices, two current generators (i.e., MP3, MP4, MP5, MP6, MN3, MN4, MN5, and MN6) limit the currents applied to the pull-up transistors (i.e., MP1 and

MP2). Consequently, by decreasing the strength of the pull-up devices, the pull down transistors (i.e., MN1 and MN2) would be able to overcome the mentioned contention at the nodes Q1 and Q2 and therefore discharge the output nodes to VSS even for the input voltages lower than the threshold voltage. In order to avoid the static power dissipation, the current generators are turned on only during the transition times, in which the logic level of the input signal is not corresponding to the output logic level[1]. The operation of the proposed structure is as follows. When the input signal IN is going from VSS to VDDL, MN1 is turned on and MN2 is turned off. Therefore, similar to the conventional counterpart, MN1 tries to pull down the node Q1,and consequently, MP2 is gradually turned on to pull the node Q2 up to VDDH. When IN changes from VSS to VDDL, there is an interval during which Q1 does not correspond to the logic level of IN. During this period, both MN4 and MN6 turn on, and therefore, transition current flows through MN4, MN6, and MP6. This current, which is mirrored to MP4, flows into MP2 and then charges the node Q2. At the same time, on the other side of the circuit, MN5 turns off because INB = VSS, and therefore, there is no current flowing through MP1 (i.e., IP1 0), meaning a weak pull-up device. This causes that MN1 be able to pull down the node Q1 even for the input voltage lower than the threshold voltage of MN1. Finally, when the node Q1 is pulled down to VSS and Q2 is pulled up to VDDH, MN4 is turned off, and therefore, no static current flows through MN4,MN6 and MP6.This means that the current generator

The voltage source va is pulsed at some frequency as a square wave. Charge and magnetic energy are interchangeable stored in the capacitor and inductor respectively act together to exchange voltages and currents. The result from this second order differential circuits is a sinusoidal circuit. The series resonant converter has a low input impedance, meaning that all of the current ia through the work coil must be supplied by the source. The voltage across the reactive components is directly related to the quality factor Q, through the equation.

Therefore if is very small, then the voltage across the capacitor will be very large. As the dual to the voltage-source series resonant converter, the current source parallel resonant converter has the same components connected in parallel branches. An input current ia source supplies a square wave of current at a frequency. The energy storage elements transform the voltage across them into a sinusoidal voltage with a peak.

The parallel resonant converter has a high input impedance, meaning that all of the voltage va across the work coil must be supplied by the source. The current through the reactive components is directly related to the quality factor Q, through the equation.

Therefore if RC is very small, then the voltage across the capacitor will be very large. Selecting the capacitance and the inductance to use in an induction heating system is critical. A specific frequency may be required for case hardening or optimal heating. One may have the luxury to choose the power source based on their application, but other cases may require the use of one specific resonant converter. The issue here is whether induction heating application should receive a high voltage or a high current. It is common to find work coils in voltage-source series induction heating systems to have a large number of turns. The voltage across the capacitor will be very high, suggesting that the voltage rating needs to be high as well. A large magnetic field is generated from the many number of turns of wire, though there may be less current traveling through it then in the parallel converter. Series systems are common in induction cooking where a household current is sufficient.

III. Overview of Induction Heating

Induction heating is a method of heating conductive objects by means of electromagnetic induction. This method of heating is of great interest to materials and manufacturing industries as it is fast, precise and controllable. Though an induction heating system may be more expensive, it is usually preferable to other types of processing methods such as open flame heating or chemical processes in most efficient and precise heating method in practice today. Heat treatment is a group of manufacturing techniques used to alter the hardness and toughness of a material. Heat treatment includes, but is not limited to annealing, case hardening, induction hardening, precipitation strengthening, tempering and quenching. A metal that has been heat hardened can be too brittle for a final product unless it is further conditioned with heat. Usually the metal is held at a temperature for a set amount of time, and then cooled slowly over a time period. Cooking by means of induction heating is a technology where cookware is heated by means of electromagnetic induction. The cookware is placed on top of a stovetop wherein directly beneath lies a coil. The effort is to create heating within the cookware itself and not within the stovetop. This is a more economical way of heating as it does not generate as much wasted heat through transfer of the stovetop. Because the heating is so evenly distributed. This method gives the cook incredible control over the heat. Most of the heat comes from hysteric losses due to magnetic materials, so cookware that contains ferric materials such as iron or stainless steel work best. Induction cooking is about 90 efficient compared to gas and standard electric cooking . The heating of the work piece arises from the ohms law, commonly referred to as ohmic heating. As a current passes

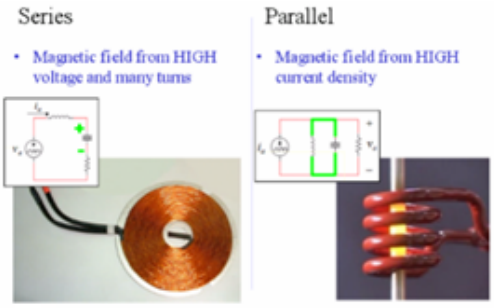

Fig Simple induction heater coils.

through a resistance, the power dissipated by the resistance is directly proportional to the square of the current times the resistance. Therefore a large current and a large resistance will dissipate more heat. Induction heating uses high oscillations of magnetic fields to induce a very large current into the work piece. Cooling may be required due to ohmic heating the work coil itself. It is most often desirable to choose a capacitance for a work coil. In the simplest form, the following relation exists for the driving frequency.

The energy transfer to the object to be heated occurs by means of electromagnetic induction. It is known that an alternating current is induced in a loop of conductive material when this loop is placed in an alternating magnetic field formula is as follows,

Where, U= Voltage (V) = magnetic flux (Wb) t= time (s) When the loop is short-circuited, the induced voltage U will cause a current to flow that opposes its cause the alternating magnetic field. This is the Faraday Lenz law. In many practical applications, a solenoid or coil is used to generate the magnetic field. When a current flow though a conductor with resistance R, the power is dissipated in the conductor.

In most applications of induction heating, the determination of resistance R is not a simple matter due to the non-uniform distribution of current in the conductor. A general characteristic of alternating currents are concentrated on the outside of a conductor. This is called the skin effect. In addition, the eddy currents induced in the material to be heated are greater on the outside. The skin effect is characterized by its so called penetration depth. Penetration depth is defined as the thickness of the layer, measured from the outside, in which 87 of the power is developed. The penetration depth can be deduced from Maxwells equations. For a cylindrical load with a diameter that is much bigger than, the formula is as follows, Where, = resistivity [m] = magnetic permeability [H/m] (= 0. r) f= frequency [Hz] On the one hand, the penetration depth depends on the characteristics of the material to be heated while on the other hand, it is also influenced by the frequency. This frequency dependence offers a possibility to control the penetration depth. As can be derived from the formula above, the penetration depth is inversely proportional

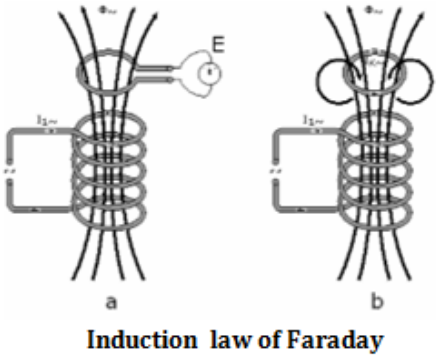

Fig. 1. Induction law of Faraday

to the square root of . For non-magnetic materials like copper or aluminium, the relative magnetic permeability is r =1. Ferromagnetic material like copper or aluminium, the relative magnetic permeability is r =1.

Ferromagnetic material (such as iron and many types of steel) on the contrary, has a r value that is much higher. Therefore, these materials generally show a more explicit skin effect. The magnetic permeability of ferromagnetic materials depends strongly on the composition of the materials and on the circumstances (temperature, magnetic field intensity, saturation). Above the curie temperature, r suddenly drops again to r =1, which implies a rapid increase of the penetration depth. The load of an induction installation is heated because of the Joule effect as a result of induced eddy currents. The simple formula P=R I cannot be used because the distribution of the currents over the conductor is not uniform. Where, d is diameter of the cylinder [m], h is height of the cylinder [m], H is magnetic field intensity [A/m], is resistivity [.m], o is magnetic permeabity of vacuum(4.10-7 H/m), r is relative permeability, f is frequency [Hz], C is coupling factor, F is power transmission factor. where, P is power, induced in the load and Pi is power, dissipated in the inductor.

IV. Finite Element Analysis

Finite Element Analysis (FEA) is a mathematical method used to solve various problems such as stress analysis, electric field, magnetic fields. It is a fundamental tool for design engineers. In FEA the object is divided into large number of elements composed of nodes. The geometry of the structure is defined by coordinates if nodes and connectivity of elements. Procedure for FEA is Pre-Processor: To define the geometry, loading and boundary conditions. Solver: System equations are constructed and solved. Post-Processor: Graphical display of data. Injection molding, injection compression molding and hot emboss forming are all plastics encloses specific structure of the mold and gets cooled down so as to duplicate mold structure. Generically plastics mean thermal plastic materials that can be applied in such processes include: plastic, glass, metal, composite material mainly based on plastic, glass and metal. Generally, the mold temperature is lower than the glass transition temperature of plastics, therefore, a condensation layer is created when melted plastic is in contact with mold cavity surface, the thickness ratio between condensation layer and product thickness rises as the increase while the reduction of the product thickness. When the proportion occupied by the condensation layer s too high, the filling of melted plastic becomes more difficult which leads to problems such as short-

δ in [mm]	Steel 20° C	Steel 20° C	Copper 20° C	Copper 20° C	Graphite 20° C
ρ [μΩm] →	0.16	0.16	0.017	0.086	10
μ_r [-] →	40	100	1	1	1
Frequency ↓					
50 Hz	4.50	2.85	9.31	20.87	225.08
100 Hz	3.18	2.01	6.58	14.76	159.15
1 kHz	1.01	0.64	2.08	4.67	50.33
10 kHz	0.32	0.20	0.66	1.48	15.92
100 kHz	0.10	0.06	0.21	0.47	5.03
1 MHz	0.03	0.02	0.07	0.15	1.59

injection, incomplete duplication of the structure and residual stress, etc.

Where E is the electric constant, C is the electric conductivity, j is the magnetic conductivity. The electromagnetic wave will induce eddy current in the conducting body, and the eddy current will decay according to exponential distribution from the surface to the inner. The calculation of the induced temperature within the work piece requires the solution of the heat equation with convection boundary conditions. For isotropic material, the transient heat equation under circular cylindrical coordinates for a solid with an internal source can be expresses as a Fouriers differential equations as follows from the below equation.

Where c is the specific heat capacity, k is the thermal conductivity, T is the transient temperature of the solid,

Is the rate of heat generation within work piece. The analysis procedure is composed of the modeling process, the analyzing process of the electromagnetic field and thermal analysis, and the calculation of the distribution of the solid fraction. Material data defined as solid model are presented by ANSYS parametric design language.

V. Results and Discussion

In this project ANSYS software is used for the modeling and designing of induction heating used for washing machine. This project focuses on the designing and analysis of induction heating. In this project ANSYS 17.2 is used. Main objectives of computer aided design for induction heating to meet the design specifications, improve the performance of heating element which is used to obtain its steady state characteristics such as magnetic flux density vector, joule heat generation, thermal heat generation using ANSYS software 17.2. This project is further extended to a hardware circuit of induction heater for industrial application Result is divided into five different steps. From the below figure represents the time verses temperature is plotted. When the time is increased temperature get increased. From the table 5.1 the different time and temperature value was given for example when the step time 2.000 for the corresponding temperature is 38.7288 o C. Similarly by using the same procedure the different value of time and temperature is noted down. When the step time is 30.000 for the corresponding temperature is 97.9129 o C.

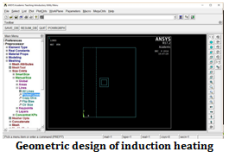

Geometric design of induction heating

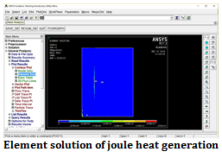

Element solution of joule heat generation

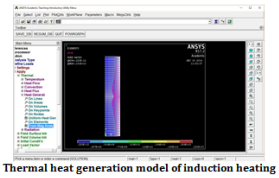

Thermal heat generation model of induction heating

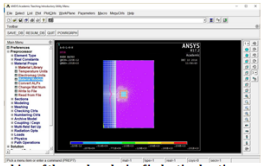

Meshing of thermal analysis of induction heating

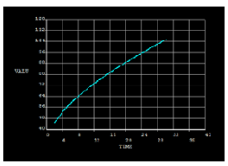

VI. Conclusion

Design and Modeling of induction heating analysis was performed to detect the temperature distribution on mold surface used for industrial application using FEM tool. The 2-D static and transient analysis of electromagnetic such a magnetic flux density vector, joule heat generation, and thermal heat generation using ANSYS software 17.2 was performed. Both numerical simulation and experimental observation were carried out on a mold plate for a rapid heating/cooling cycle development using induction heating combined with water cooling through cooling channel. The mold plate surface temperature raises at about 20'C/sec and cooling down at 2.5'C/sec. Mold plate temperature distribution exhibits good uniformity as well. The results show the feasibility of this technology to real injection molding process. The developed simulation algorithm also shows great success that can provide as a useful tool for system design. Based on thermodynamic theory, a basic equation for the multistage launcher temperature was set up using the load transfer method. The launcher transient temperatures field simulation problem was solved and the temperature distributions of the drive coil and the armature were analyzed. Simulation results showed that, when considering the magneto resistance effect and the skin effect, the temperature distribution of the drive coil was uniform and the armature temperature rise was mainly on the outer surface and tail. Finally, a launcher temperature measurement experimental platform was set up and the stimulation results were verified by temperature measurement at the key points.

References

[1] J. Acero, J. M. Burdio, L. A. Barragan, D. Navarro, R. Alonso, J. Ramon, F. Monterde, P. Hernandez, S. Llorente, and I. Garde*"Domestic induction appliances: an overview of recent research," IEEE Industry Applications Magazine, vol. 16, pp. 39-47*, Mar. 2010.

[2] C. Carretero, J. Acero, R. Alonso, J. M. Burdio, and F. Monterde*"Embedded ring-type inductors modeling with application to induction heating systems," IEEE Transactions on Magnetics, vol. 45, pp. 5333-5343*, Dec. 2009.

[3] O. Lucia, J. M. Burdio, L. A. Barragan, J. Acero, and I. Millan*"Series-Resonant Multiinverter for Multiple Induction Heaters," IEEE Transactions on Power Electronics, vol. 25, pp. 2860-2868*, Sep. 2010.

[4] J. Biela, A. Wirthmueller, R. Waespe, M. L. Heldwein, K. Raggl, and J. W. Kolar*"Passive and active hybrid integrated EMI filters," IEEE Transactions on Power Electronics, vol. 24, pp. 1340-1349*, May 2009. C. K. Lee, Y. P. Su, and S. Y. R. Hui*"Printed spiral winding inductor with wide frequency bandwidth," IEEE Transactions on Power Electronics, vol. 26, pp. 2936-2945*, Oct. 2011.

Digital Signal Processing in Modern Synthetic Aperture Radar

Mr.R.Radhakrishnan
Assistant Professor
Department of
Electronics & Communication Engineering
St.Annes CET

Mr. Venkatasan
Assistant Professor
Department of
Electronics & Communication Engineering
St.Annes CET

Mrs. M. Vaidehi
Assistant Professor
Department of
Electronics & Communication Engineering
St.Annes CET

***Abstract*—There has been an explosive growth in Digital Signal Processing theory and applications over the years. This seminar report explores the applications of digital signal processing in Radar. A survey on applications in Digital Signal Processing in Radar from a wide variety of areas is carried out. A review is done on basic approaching models and techniques of signal processing for different parameters and extracting information from the received signal. The various techniques adopted at different stages of radar to obtain the targets signature, is also briefed.**

I. INTRODUCTION

Flexibility and versatility of digital techniques grew in the front- end signal processing and with the advent of integrated digital circuitry, high speed signal processors were developed and realized. Radar continued to grow in the recent years by keeping the future developments in mind and with better digital capability. Significant contributions in DSP in Radar have been in MTI processing, Automatic Detection and extraction of signal, Image reconstruction, etc. A case study on Radar Synthetic Vision System for Adverse Weather Aircraft landing is discussed.

In this report an effort is made to identify the contribution of DSP in the advancement of Radars.

II. . MODERN RADAR

RADAR transmits radio signals at distant objects and analyzes the reflections. Data gathered can include the position and movement of the object, also radar can identify the object through its "signature" -the distinct reflection it generates. There are many forms of RADAR -such as continuous, CW, Doppler, ground penetrating or synthetic aperture; and they're used in many applications, from air traffic control to weather prediction.

In the modern Radar systems digital signal processing (DSP) is used extensively. At the transmitter end, it generates and shapes the transmission pulses, controls the antenna beam pattern while at the receiver, DSP performs many complex tasks, including STAP (space time adaptive processing) -the removal of clutter, and beamforming (electronic guidance of direction).

This document was created by Unregistered Version of Word to PDF Converter

The front end of the receiver for RADAR is still often analog due the high frequencies involved. With fast ADC convertors-often multiple channel, complex IF signals are digitized.

However, digital technology is coming closer to the antenna. We may also require fast digital interfaces to detect antenna position, or control other hardware.

The main task of a radar's signal processor is to make decisions. After a signal has been transmitted, the receiver starts receiving return signals, with those originating from near objects arriving first because time of arrival translates into target range.

III. BLOCK DIAGRAM OF MODERN RADAR SYSTEM

The signal processor places a raster of range bins over the whole period of time, and now it has to make a decision for each of the range bins as to whether it contains an object or not.

This decision-making is severely hampered by noise. Atmospheric noise enters into the system through the antenna, and all the electronics in the radar's signal path produces noise too.

A. Major blocks of modern radar system

The major components of modern radar are the antenna, the tracking computer and the signal generator. The tracking computer in the modern radar does all the functions. By scheduling the appropriate antenna positions and transmitted signals as a function of time, keeps track of targets and running the display system.

Tracking Computer :Even if atmospheric attenuation can be neglected, the return from a distant object is incredibly

weak. Target returns often are no stronger than twice the average noise level, sometimes even buried under it. It is quite difficult to define a threshold for the decision whether a given peak is noise or a real target. If the threshold is too high then existing targets are suppressed, that is, the probability of detection (PD) will drop. If the threshold is too low then noise peaks will be

This document was created by Unregistered Version of Word to PDF Converter

reported as targets, that is, the probability of false alarms (PFA) will rise. A common compromise is to have some 90% probability of detection and a false alarm rate of 10-6.

It maintains a given PFA known as CFAR, for Constant False Alarm Rate. Rather than keeping the threshold at a fixed point, CFAR circuitry inspects one range bin after the other and compares the signal level found there with the signal levels found in its neighboring bins. If the noise level is rather high in all of these (eg, because of precipitation) then the CFAR circuit will raise the threshold accordingly.

Further tasks of the signal processor are:

Combining information: Secondary surveillance radars like those located on

airports can ask an aircraft's transponder for information like height, flight number or fuel state. Pilots may also issue a distress signal via the transponder. The ground radar's signal processor combines this data with its own measurements of range and angular direction and plots them all together on the appropriate spot on the scope.

Forming tracks: By correlating the data sets which were obtained in successive scan cycles, the radar can calculate a flight vector which indicates an aircraft's speed and expected position for the next scan period. Airport radars are capable of tracking hundreds of targets simultaneously, and flight safety depends heavily on their reliability. Military tracking radars use this information for gun laying or guiding

missiles into some calculated collision point.

Resolving ambiguities in range or Doppler measurements: Depending on the radar's pulse repetition frequency (PRF), the readings for range, Doppler or even both are ambiguous. The signal processor is aware of this and selects a different PRF when the object in question is measured again. With a suitable set of PRFs, ambiguities can

be eliminated and the true target position can be determined.

Ground Clutter Mapping: Clutter is the collective term for all unwanted blips on a radar screen. Ground clutter originates from buildings, cars, mountains etc, and a clutter map serves to raise the decision threshold in areas where known clutter

sources are located.

Due to the astronomical increase in energy demand in the last few years, the state has a deficit of power and it is estimated to be around 15.4% as on Feb 2010.

SS

IV. Detection of Signals

V. Detection of Signals

Detection is the process by which the presence of the target is sensed in the presence of competing indications which arise from background echoes (clutter), atmospheric noise, or noise generated in the radar receiver. The noise power present at the output of the radar

receiver can be minimized by using filter, whose frequency response function maximizes the output peak-signal to mean-noise (power) ratio is called matched filter. we shall discuss the application of digital filtering to matched filters.

VI. Fast Convolution Filter implementation

Dual pipeline FFT matched Filter

In this system, FFTs are pipelined and both the forward and reverse radix-r FFTs are implemented in hardware. Initial recording of the data is done using input buffer (IB) memory and it takes N/r clock pulses to read N data points and r input rails. The amount of time

N/r is called as one epoch. It requires three epochs for the first data to be completely filtered, and is delivered by one epoch thereafter. In the dual FFT systems arbitrary data is filtered sequentially with arbitrary reference functions selected from reference memory.

Drawback

In many applications the same data set be filtered with several different filters, in this case only one forward transform is performed followed by several inverse transforms, it is possible to eliminate one of the pipeline FFTs. This is desirable since it would save a large amount of hardware.

Single forward FFT matched Filter

The data is first transformed and the result stored in the temporary storage memory [TSM]. The data is then multiplied by the filter function and inverse transformed. This allows multiple readouts of the forward transformed data from the TSM and multiple filtering of the same data set; the output of each filter will appear sequentially.

Drawback

The data at the output of the forward FFT are in digit reverse order, it is then corrected by reading the data out of the TSM in digit reversed order. The second FFT is performed the output is placed into an output buffer, and to be read in a bit reversed order from the output buffer. It requires five epochs for the first data to be completely filtered, and is delivered by one epoch thereafter.

Reconfigurable FFT Matched Filter

The FFT subsystem switches the interstage delay lines to realize both forward and reverse transforms. Forward Transform: By routing the data through the interstage delay memories [IDMs] in decreasing order Inverse Transform: by sending data through the IDMs in the increased order of size. The total memory of each stage is the number of delay lines memories. Comparison of 4 matched Filter systems The relative performance of Dual Pipeline matched Filter is fastest but requires two complete pipeline FFTs hence more hardware is required.

Single inverse transform matched Filter has better performance over Single forward transform matched Filter and also doesnt require a double buffered output memory. Reconfigurable FFT matched filter is preferred and chosen most of the times, it doesnt require digit reversed to the IB and also doesnt require digital recording of TSM.

VII. Doppler processing

Doppler processing is used to filter out clutter and thereby reveal fast moving targets. Such filters are implemented digitally, FFT or a set of transversal filters. Cancellers and few optimized methods are some of the Clutter rejection techniques:

VIII. Cancellers

Clutter rejection filter amounts to the design of FIR digital filter with stopbands to reject the clutter frequency component. A simple filter is a two-pulse canceller.

A two-pulse canceller is used if the clutter component [assuming DC only] remains constant in a given range bin and can be eliminated by subtracting the output from two

successive pulses. The transfer function of two -pulse canceller is equal to 1 - z-1 . And is equivalent to FIR digital filter with magnitude response sin (2w) .In practice, the clutter have a power spectrum that covers frequencies above DC. The two -pulse canceller will attenuate low frequency components but may not totally reject clutter.

IX. MTI Signal Processing

This document was created by Unregistered Version of Word to PDF Converter A major task in moving target indicator (MTI) radar is to obtain a time- domain filter, with the introduction of digital technology, these are achieved using digital transversal filters, recursive filters and filter banks.

X. Adaptive Thresholding and Automatic Detection

Digital processing permitted the reference level to be generated/internally from the observations themselves, thereby permitting more sensitive and faster thresholds. Most of the Radars employ automatic detection circuits to maintain, ideally, a constant false alarm rate [CFAR] by generating estimates of the receiver output. Automatic target detection for a search radar can be achieved by comparing the processed voltage in each cell to 1.A fixed threshold level.

2.Threshold levels based upon the mean amplitude of the ambient interference. 3.A level computed on the basis of partial [a prior] knowledge of the interference distribution.

XI. Adaptive Threshold CFAR processors

The Adaptive threshold CFAR processors is applicable to situations were the distribution of the processed data [in the no- signal case] is known generally and unknown parameters associated with the distribution can be estimated. It is often implemented as moving or sliding window through which estimates of the unknown parameters of the interference are formed

XII. Distribution free CFAR processors

These provide CFAR characteristics when the background return has a unknown distribution. These processors remain insensitive to variations in the distribution, and generally experiences additional detection loss their CFAR properties make their application advantageous.

This document was created by Unregistered Version of Word to PDF Converter

1. Double Threshold Detector 2. Modified double threshold Detector 3. Rank order Detector 4. Rank-sum double quantizer Detector

beginSCANNING Radar Applications

One of the solutions during the adverse weather landing is to use a radar imaging system. In this section we will discuss the prototype section for aiding pilots to land in zero visibility weather conditions. In this section we will describe a synthetic vision system (SVS). This system provides a runway image to the allow pilots to see through fog and adverse weather. The SVS system consists of an electro mechanically scanned antenna, transmitter, millimeter wave integrated circuit (MMIC) receiver, display processor and heads up display (HUD). Images are enhanced using beam sharpening, noise reduction, and motion compensation processing techniques prior to the critical transformation from radar coordinates to true pilot perspective for display on the HUD. In this system Versa module Eurocard (VME) platform is used. Single antenna operation by using a circular and isolating Positive-Intrinsic-Negative (PIN) diode switch in duplexer. The receiver system consists of a low noise GaAs Field-effect Transistor (FET) MMIC receiver. The received and amplified signal is down converted twice. The detected output is sent to display processor for digitization, signal processing and to the

display unit. SVS Display Processor and Raw Data Recording The raw digitizer radar video data recording obtains snapshots at 4s intervals with a total

recording time of 600s. During aircraft approach the control processor is interrupted by the IRIG Time Code Slave every 4s, which signals, to the control processor that a raw digitizer

frame acquisition are to be performed. The control processor stores the next immediate frame after antenna retraces.

beginCONCLUSIONS:

In this report a brief overview of applications of digital signal processing in Radar is presented. Matched filter implementation, echo cancellers and automatic detection and tracking are discussed in separate sections. In most of the modeling, Fast Fourier transform is

a very commonly used technique for analyzing and filtering digital signals. Also a case study is carried out on Radar Synthetic Vision System for Adverse Weather Aircraft Landing. Different techniques of detection of targets in foliage are discussed for SAR. The recent advances in signal processing are blended with many more algorithms to present an up-to date perspective and can be implemented in Digital Signal Processor because of their flexibility and the ability to attain high precisions.

A Survey on IOT Based Medical Records of a Patient

Mr. Babu.V
UG Scholar
Department of ECE
St.Annes CET,

Mr. A.AjithKumar
UG Scholar
Department of ECE
St.Annes CET,

Mr.Amstrong Michael Raj
UG Scholar
Department of ECE
St.Annes CET,

***Abstract*—Biometric measurements have the potential to improve both security and convenience in many areas of our daily lives, including in health care and social services. The objective of this project is to improve the security and health care performance in the Medical Report machine as well as to provide easy access to cast Medical Report the by using finger print. Fingerprint is one of the unique identities of a human being which is being used in the Aadhar system. By using arduino software and by using IOT we capture the finger print of every individual is being captured. The Medical of the Case Sheet is transmitted to PC through arduino communication. Finger print of the person captured is compared to Aadhar details using IOT. We also know about individual persons full details in the UIDAI and Medical Report Linked Database. Next-generation biometrics may well go beyond the human body. Several works point to the possibility of identifying individuals by looking at the bacteria that inhabit their bodies.**

I. INTRODUCTION

Biometric measurements have the potential to improve both security and convenience in many areas of our daily lives, including in health care and social services. The objective of this project is to improve the security and health care performance in the Medical Report machine as well as to provide easy access to cast Medical Report the by using finger print. Fingerprint is one of the unique identities of a human being which is being used in the Aadhar system. By using arduino software and by using IOT we capture the finger print of every individual is being captured. The Medical of the Case Sheet is transmitted to PC through arduino communication. Finger print of the person captured is compared to Aadhar details using IOT. We also know about individual persons full details in the UIDAI and Medical Report Linked Database. Next-generation biometrics may well go beyond the human body. Several works point to the possibility of identifying individuals by looking at the bacteria that inhabit their bodies.

comparison technique had not been totally satisfactory. Accordingly, one object of the present invention is to provide a demand controller having an improved forecasting technique. Another object of the present invention is to provide a demand control technique that can be implemented relatively simply without the need for excessive complex data processing and logic circuitry

II. III. HARDWARE CONFIGURATION

There are many different types of electronics hardware development boards featuring embedded processors and the most famous species like Raspberry pi, Beagle Bone, Arduino Galileo. The embedded world evolved very differently there were too many choices for processors, which were mainly chosen for price and features. The devices like Raspberry pi and Beagle Board are best for handling media such as video. They are designed to function on a much higher level with already integrated hardware that takes care of things like Ethernet, video processing, large quantities of RAM and an almost unlimited amount of storage space. In the other side the Arduino is an excellent choice if we have a project requiring sensors (and decent memory and processing power), monitoring, or have productivity-related applications (Galileo has a real time clock.) Galileo could be used to develop smart everyday "things" with lots of sensors, such as health monitoring, security system, home automation, fitness devices, or simply be an inexpensive personal computer running Linux sans all things by Arduino.

III. SOFTWARE CONFIGURATION

IoT devices can be used to enable remote health monitoring and emergency notification systems. These health monitoring devices can range from blood pressure and heart rate monitors to advanced devices capable of monitoring specialized implants, such as pacemakers Fit bit electronic wristbands or advanced hearing aids. Some hospitals have begun implementing "smart beds" that can detect when they are occupied and when a patient is attempting to get up. It can also adjust itself to ensure appropriate pressure and support is applied to the patient without the manual interaction of nurses. Specialized sensors can also be equipped within living spaces to monitor the health and general well-being of senior citizens, while also ensuring that proper treatment is being administered and assisting people regain lost mobility via therapy as well.[85] Other consumer devices to encourage healthy living, such as, connected scales or wearable heart monitors, are also a possibility with the IoT. More and more end-to-end health monitoring IoT platforms are coming up for antenatal and chronic patients, helping one manage health vitals and recurring medication requirementsTo satisfy the energy needs of the state, Tamil Nadu Electricity Board has a total installed

capacity of 10,214 MW which includes Central share and Independent Power Producers. Other than this, the state has installations in renewable energy sources like windmill up to 4300 MW.

Due to the astronomical increase in energy demand in the last few years, the state has a deficit of power and it is estimated to be around 15.4% as on Feb 2010.

IV. A. UIDAI and Medical Report Linked Database:

A Linked database is an organized collection of data. It is the collection of schemas, tables, queries, reports, views, and other objects. The data are typically organized to model aspects of reality in a way that supports processes requiring information

V. B. Finger Print Stage:

This system registered the users that consider as authority to access control in the enrollment model. Each user in this stage will take the Aadhaar ID number that is saved in the database. In fingerprint stage we used two important functions feature extraction and the matching function which has been discussed below.

VI. BLOCK DIAGRAM

VII. C. Feature Extraction:

The feature extraction is responsible for expressing fingerprint's unique characteristics adequately such as directions of the lines, terminals of lines, bifurcation and so on. To ensure the accuracy of comparison, the method of feature extraction must extract useful features as such as possible; meanwhile, filter false features for various reasons. There are two kinds of features in fingerprint images: global feature and local feature. Global feature can reflect overall shaper of fingerprint, which usually applies to fingerprints' classification, the process of extract global feature frequently belongs to procedure of fingerprint classification. The Local feature can reflect minutiae of fingerprint, usually applies to fingerprints' comparison. Strict feature extraction means local features' extraction. Two fingerprints often have the same global features, but their local features cannot be exactly the same. The important information of fingerprints' local feature is following: terminals, bifurcations, branch points, isolated points, enclosures, short lines and so on. In fact, not all the fingerprints have these two features, it often be used as fingerprints' sub-matches. This system uses terminals and bifurcations in feature extraction and matching algorithm.r can consume a maximum power supply for about 22 hours. But for the particular two hours, the power supply is limited by the controller. This helps the E.B to provide minimum power to the power instead of power cut. During this minimum supply how the consumer cant consume the excess power supply.

For normal 22 hours power from the energy meter is directly provided to the load. For that particular two hours the current flow path is changed by using relay. After that, current flow is directed to through the current limiter, which limits the output current.

Thus the current flow direction is changes by using Timer, Buffer and Comparator. The timer decides the timing of the limited current flow. It may be either three or four hours in future. The time when the power limit made is decided by the buffer and comparator. When signal from EB comes the comparator compares the signal and it holds the signal for some times after that the timer triggered with indicator now the current flow path is changed to MCB. After timing is finished, the controller will turn off immediately and normal power flow will occur.

VIII. D. Feature Matching:

The matching function, features extracted from the input fingerprint is compared against those in a database, which represents a single user (retrieved from the system database based on the claimed identity). The result of such a procedure

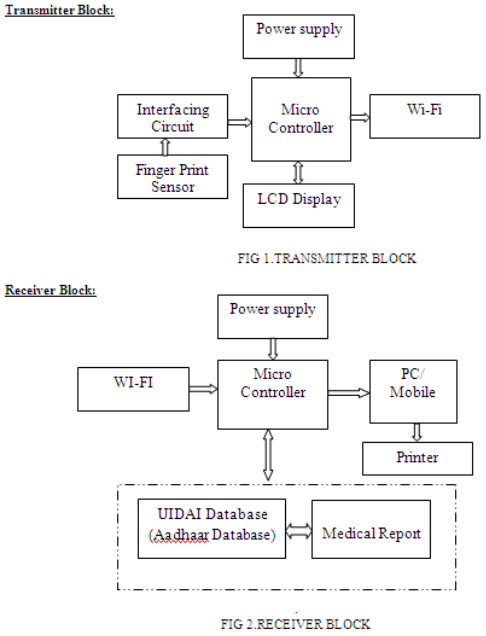

Fig. 1. INSTALLED CAPACITY

Microcontroller	ATmega328
Operating Voltage	5volts
Input Voltage(limits)	6-20V
Digital I/O pins	14
Analog input pins	6
DC current per I/O pin	40mA
Flash Memory	32kB(ATmega328)
SRAM	2kB(ATmega328)
EEPROM	1kB(ATmega328)
Clock	16MHZ

Table. 1. Specifications of Arduino Board UNO

Fig. 2. BLOCK DIAGRAM

is either a degree of similarity (also called matching score) or an acceptance/rejection decision. There are fingerprint matching techniques that directly compare gray scale images using correlation-based methods, so that the fingerprint template coincides with the gray scale image. However, most of the fingerprint matching algorithms use features that are extracted from the gray scale image. A large number of approaches to fingerprint matching can be found in previous work. In this proposed work we used the matching algorithm that support the optical fingerprint reader module SFG algorithm is specially designed according to the image generation theory of the optical fingerprint collection device. It has excellent correction tolerance to deformed and poor-quality fingerprint and work with both1:1 and 1:N.

IX. E. Face Recognition:

Every human could be identified by the faces and could be easily recognized by the faces. Early face recognition Algorithms used simple geometric models, but the recognition process has now matured into a science of sophisticated mathematical representations and matching processes. Thus the face recognized could be both verified and identified. Thus, by using face recognition here we could avoid the fraudulence.

Microcontroller	ATmega328
Operating Voltage	5volts
Input Voltage(limits)	6-20V
Digital I/O pins	14
Analog input pins	6
DC current per I/O pin	40mA
Flash Memory	32kB(ATmega328)
SRAM	2kB(ATmega328)
EEPROM	1kB(ATmega328)
Clock	16MHZ

Table. 1. Specifications of Arduino Board UNO

Fig. 3. VOLTAGE COMPARATOR

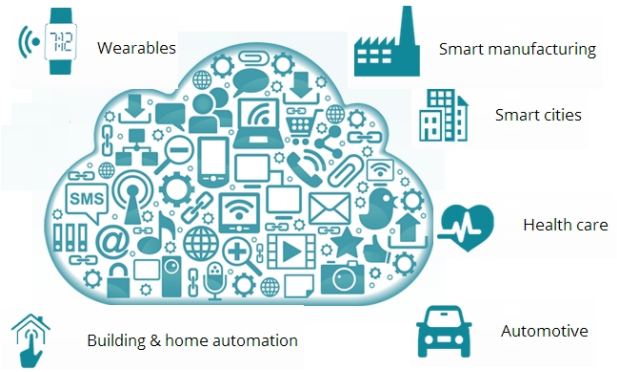

Fig. 4. BUFFER AND INDICATOR CIRCUIT

X. IV. Working

The finger print sensor is interfaced with the microcontroller. The processor activates the finger print sensor at the time of finger is placed in the sensor. Then the related data is stored in the microcontroller. The microcontroller transfers the related information to PC. When the human places the finger on the finger print sensor, the sensor sends the corresponding data to the microcontroller. Microcontroller receives the data from the finger print sensor. Then compared with the stored data if the person finger is valid for that Patient name mentioned in the Aadhaar ID card and Medical Report.

XI. Circuit Breaker

Magnetic circuit breakers use a solenoid (electromagnet) thats pulling force increases with the current. Certain designs utilize electromagnetic forces in addition to those of the solenoid. The circuit breaker contacts are held closed by a latch. As the current in the solenoid increases beyond the rating of the circuit breaker, the solenoid's pull releases the latch which then allows the contacts to open by spring action. The core is restrained by a spring until the current exceeds the breaker rating. During an overload, the speed of the solenoid motion is restricted by the magnet. The delay permits brief current surges beyond normal running current for motor starting, energizing equipment, etc. Short circuit currents provide sufficient solenoid force to release the latch regardless of core position thus bypassing the delay feature. Ambient temperature affects the time delay but does not affect the current rating

of a magnetic breaker. The circuit breaker contacts must carry the load current without excessive heating, and must also withstand the heat of the arc produced when interrupting the circuit. Contacts are made of copper or copper alloys, silver alloys, and other materials. Service life of the contacts is limited by the erosion due to interrupting the arc. Miniature and molded case circuit breakers are usually discarded when the contacts are worn, but power circuit breakers and high-voltage circuit breakers have replaceable contacts.

beginconclusion The internet has drastically changed the way we lived, as in scenario all the interaction is done over the internet. The IoT has the potential to add a new dimension to this process by enabling communication between smart objects. IoT should be considered as a part of future internet as everything is going to be connected in a network so that objects can interact with each other, but still there are lots of issues which are to be solved to make this a reality. Lot of research is required in this field, once implemented successfully; the quality of life is improved because of the reduction of the effort made by humans on unimportant things. In this paper, we presented the technologies and applications that can be used to make Internet of Things a reality. After that, we state some good examples where Internet of Things is of great use, and at last we discuss some open issues which are still to be solved before the wide acceptance of this technology.

REFERENCES

[1] Ambavarapu Bhavana, M.Jasmine*Fingerprint Based Authentication System Using Arm7 International Journal Of Science And Research ISSN 2319-7064*,vol 5, Issue 5, 2015.

[2]] Karthik Krishnamurthi,Suraj Thapa,Lokesh Kothari And Arun Prakash, *Arduino Based Weather Monitoring System International Journal Of Engineering Research And General Science ISSN 2091-2730*,vol 3, Issue 2, 2015.

[3]] N.Gopal, dr.R.K.Selvakumar*Multimodal Biometric Identification System- An Overview International Journal Of Engineering Trends And Technology ISSN 2231-5381*,vol 33, Issue 7, Mar 2016.

[4]] Rathna Prabha, Trini Xavier, Deepika, Iswaryaemph, A Survey on E-Voting System Using Arduino Software International Journal of Advanced Research in Electrical, Electronics and Instrumentation Engineering ISSN vol 5, Issue 2, Feb 2016..

[5]] Ruchi Parashar, Abid Khan, Neha*A Survey: The Internet Of Things International Journal of Technical Research and Applications e-ISSN: 2320-8163,* ,Volume 4, Issue 3 (May-June, 2016), PP. 251-257

Design of Cascade Topology Based Doherty Power Amplifier for Wireless Applications

P. Aruna Priya
PG Scholar
Department of ECE
SRM University

Rupali Singh
PG Scholar
Department of ECE
SRM University

Chirag Kasliwal
PG Scholar
Department of ECE
SRM University

Ann Merin Georgi
PG Scholar
Department of ECE
SRM University

The key role of the Power Amplifier (PA) in RF transmitter is to exhibit high output power. This paper presents design and comparison of cascode topology based Class AB PA and Doherty PA using 180nm CMOS technology. The input and output matching device is designed using Pi type matching network. The result shows that power amplifier achieves output power of 18.298 dBm at 2GHz cut off frequency. Further this amplifier has been combined with a Class C amplifier to produce an amplifier called as Doherty Power Amplifier. The comparison result shows that Doherty Power Amplifier achieves output power of 48.131 dBm. It amplifies signals effectively than Class AB power amplifier. These are implemented using Agilent Advanced Design System (ADS) simulation tool.

Keywords - Power amplifier, Doherty, Cascode, Efficiency.

I. INTRODUCTION

Power Amplifier is the most energy consuming block inside the RF transceiver. Therefore performance improvement is a critical point. In CMOS power amplifiers the main non-linearity is due to the non linear gate to source capacitance (Cgs), intrinsic non linear transconductance [1-2].The other non-linearities resulting from drain junction capacitor and output conductance can be neglected. Mostly power amplifiers use common drain and common source topology [3-4]. In this paper cascode topology is used to design a Class AB amplifier. The cascode topology is used as it provides good isolation with respect to the impedance effects at output and input. The supply voltage VDD can be increased to produce higher output power levels by dividing the voltage swing equally between the cascode transistors. This prevents the device from any damage. Also the voltage swing can be unequally divided between common gate and common source transistor. This leads to a higher PAE performance level. Further in this paper cascode structure is used to design a Class C amplifier and these two amplifiers are combined together to produce a system which has enhanced efficiency to about .This combined structure using two parallel amplifiers is called as Doherty Power Amplifier. One amplifier is called as Carrier or main amplifier biased in Class AB and the other one is called as peaking or auxiliary amplifier biased in Class C.The two power amplifiers are connected on the DPA structure using a power splitter. The power splitter is implemented with the help of

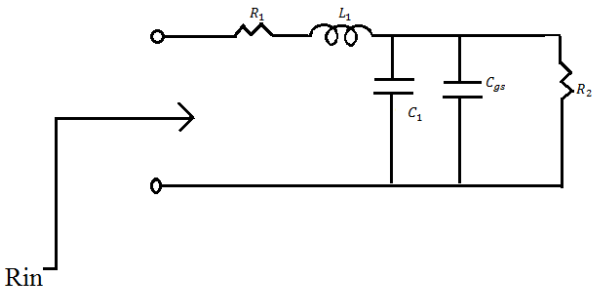

Fig. 1. Equivalent circuit (input)

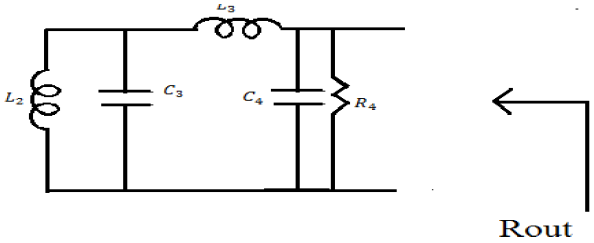

Fig. 2. Equivalent circuit (output)

3dB Coupler. The output of both the amplifiers are combined with the help of impedance inverter which ties main amplifier output to auxiliary amplifier and impedance transformer on the output. The impedance inverter is implemented with the help of microstrip line. Doherty power amplifier is efficient and can achieve very high linearity, so can be used in base station [5-6]. The proposed design is simulated in 180nm CMOS technology using ADS software tool.

II. DESIGN AND ANALYSIS OF CLASS AB POWER AMPLIFIER CIRCUIT

The power amplifier has been designed using cascode topology biased in Class AB. The gate to source voltage is 2.9 and drain voltage is 1.8V. The input and output resistance can be calculated from the following equivalent circuits as shown in Fig.1 and Fig.2 below

The output resistance of the circuit is described in the following equation

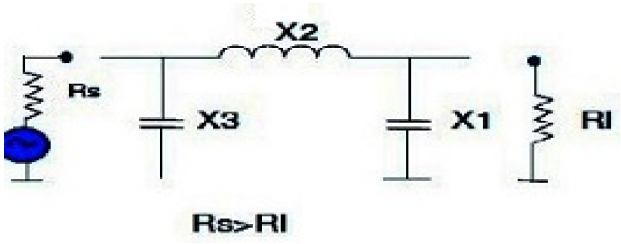

Fig. 3. Pi matching network

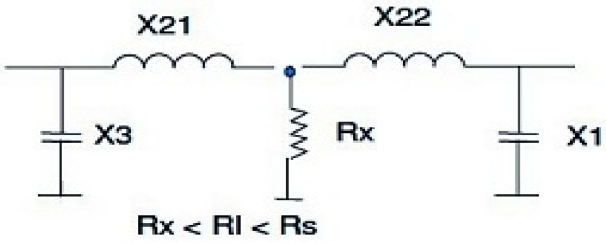

Fig. 4. Pi network with imaginary resistor Rx

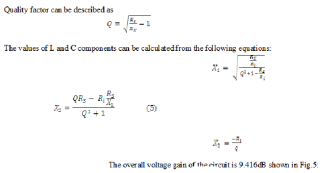

Fig. 5.

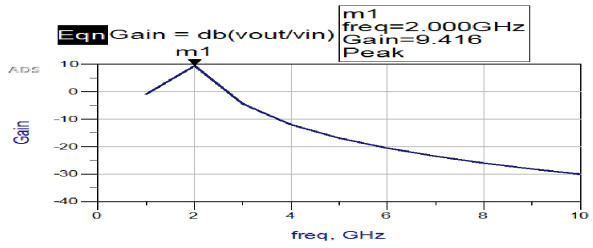

Fig. 6. 5 Gain vs. Frequency

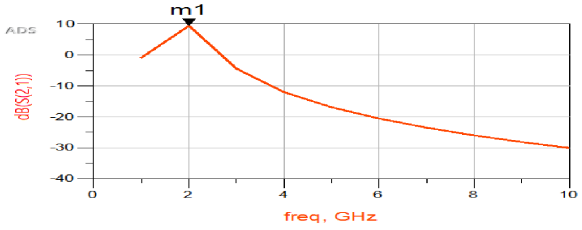

Fig. 7. 6 S (2, 1) vs. Frequency

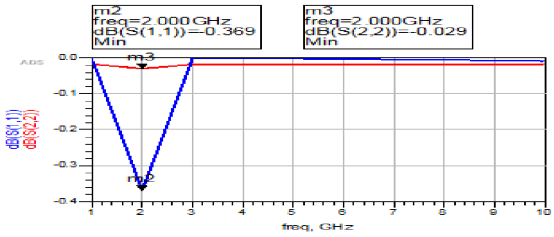

Fig. 8. 7 S (1, 1) dB, S (2, 2) dB vs. Frequency

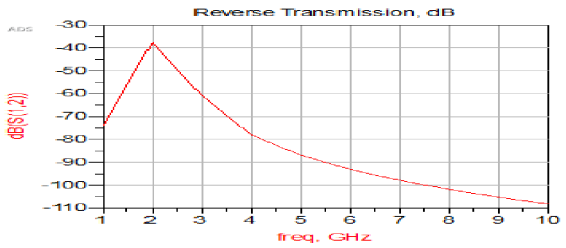

Fig. 9. 8. S (1, 2) dB vs Frequency

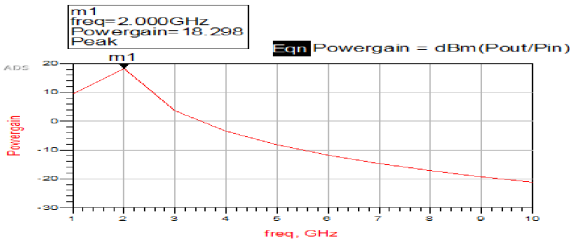

Fig. 10. 9. Power gain vs Frequency

The overall voltage gain of the circuit can be calculated from equation (2)

The input and output matching network is designed using Pi type matching network as shown in Fig.3:

This circuit can be represented as two L circuits connected together through their shunt component as shown in Fig.4 below. The imaginary resistor Rx has to be larger than both resistors Rs and Rl.

The overall voltage gain of the circuit is 9.416dB shown in Fig.5:

The S parameter simulation results are shown below

With the help of S parameter simulation we can obtain forward transmission gain 9.416dB.The input and output transmission coefficient is -0.369dB and -0.029dB respectively

The power gain of the circuit obtained is about 18.298dBm as shown above in Fig.9 The complete schematic is shown in Fig.10

III. DESIGN OF DOHERTY POWER AMPLIFIER

TThe increased use of Doherty power amplifier is due to the need to maintain amplifier efficiency and also due to the increasing peak to average power ratios found in new modulation format. When a signal modulator with an amplitude component is applied to a conventional PA, amplitude

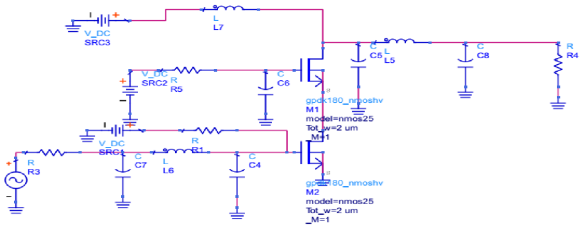

Fig. 11. Complete schematic of Class AB power amplifier

distortion occurs. When PAPR ratio increases amplifier has to accommodate the peaks while running at a low average power level. So this situation is overcome in Doherty power amplifier. It is able to accommodate signals with higher PAPR ratios. In addition to power amplifier it consist of combiner which matches the signals in phase between two halves such that both signals are added together to produce required output. Therefore the overall gain of the circuit is much greater than a conventional power amplifier. The proposed DPA consists of three parts i.e. design of sub power amplifiers, design of 3db Coupler and the design of combining network. The power splitter is implemented with the help of 3dB Coupler. The power splitter is designed with the objective of dividing input power equally and reducing the losses as maximum as possible. There are two power amplifiers used in the design. The main amplifier is biased in Class AB and the auxiliary amplifier is biased in Class C. The cascode topology is used for the design. The bias voltage of common gate is normally greater than common source amplifier. The drain voltage of main amplifier biased in Class AB and auxiliary amplifier biased in Class C is 20V and 6V respectively. The gate to source voltage is 3V for main amplifier and 0.4V for auxiliary amplifier. The input and output matching device is designed using L type matching network which consist of an inductor and capacitor. It can be designed either by using LC or CL matching network depending on downward and upward transformation. The output of both the amplifiers are combined with the help of impedance inverter which ties main amplifier output to auxiliary amplifier and impedance transformer on the output. In the proposed design impedance inverter is implemented with the help of microstrip line. The impedance transformer converts 50ohm load to 25ohm on input side. As the main amplifier saturates, its output impedance begins to drop. The impedance inverter converts main amplifier output impedance to a high value, thus allowing auxiliary amplifier to pump power into load. Therefore, impedance inverter in a way transforms saturated main amplifier into a current source. Both the amplifiers behave as two parallel current sources, thus providing power to output network. The overall schematic and simulation results are shown in Fig.11 below:

The overall voltage gain of the circuit is 30.343dB shown in Fig. (12). The measurement result shows that the proposed circuit achieves output power of 20dBm to 48dBm in the frequency range 1.5-2GHz

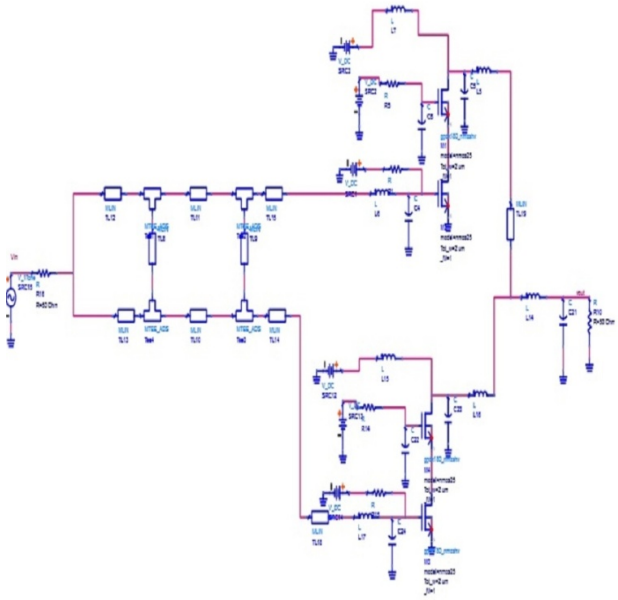

Fig. 12. Schematic of proposed Doherty power amplifier

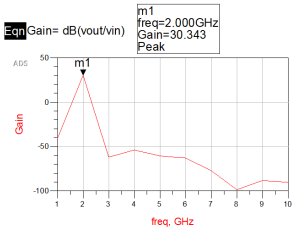

Fig. 13. . Gain vs. Frequency

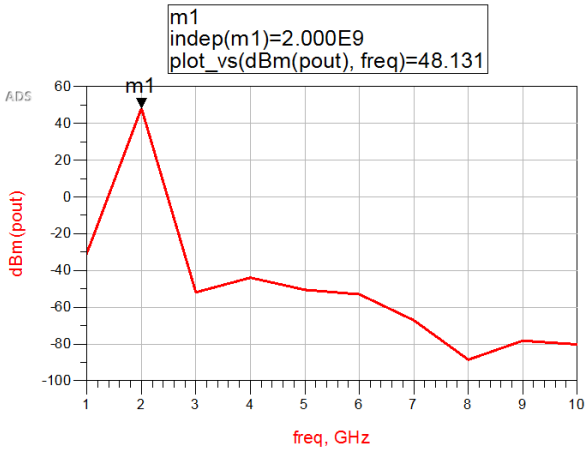

Fig. 14. . Pout (dBm) vs. Frequency

The table shown below describes the comparison between the two types of amplifiers proposed in this paper i.e. between Class AB power amplifier and Doherty power amplifier.

Type	Frequency (GHz)	Gain (dB)	Pout (dBm)	Efficiency (%)
Class AB PA	*2*	*9.416*	*18.298*	*40-42*
DPA	*2*	*30.343*	*48.131*	*55-64*

Fig. 15.

IV. CONCLUSION

The result shows that PA achieves output power of 20dBm at 2GHz cut off frequency. The comparison result shows that Doherty Power Amplifier achieves output power of 48.13dBm at cut off frequency. It amplifies signals effectively than a Class AB power amplifier. The efficiency achieved is around 55-64 which is greater than Class AB power amplifierBoth the designs have been simulated and implemented in ADS software tool using CMOS technology.

REFERENCES

[1] [1]T. Queries et al. *A CMOS Class-A 65 nm PA for60 GHz Applications,*, IEEE Silicon Monolithic Integrated Circuits in RF Systems Conference, Mar. 2010, pp. 120-123.

[2] [2] M. A. Khan, Danish Kalim, and Renato Negra *Study on load transformation networks for differential common drain class-B RF PA,*,Semiconductor Conference Dresden (SCD), 2011, pp. 1-4.

[3] [3] M. A. Khan, Danish Kalim, and Renato Negra *Analysis and design of an unconditionally stable common-drain class-B RF PA in 90 nm CMOS technology,*, Integrated Nonlinear Microwave and Millimeter-Wave Circuits Conference, 2011, pp. 1-4.

[4] [4] Jing Xia, Member, Mengsu Yang, Yan Guo, Student Member, IEEE, and Anding Zhu, Senior Member, IEEE, *A Broadband High-Efficiency Doherty Power Amplifier With Integrated Compensating Reactance*, IEEE Transactions on Microwave Theory and Techniques,Vol 64,No 7,July 2016.

[5] [5] Chen Xiao-qun, GuoYu-Chun, Shixiao-wei, *Design of a highly efficient Doherty power amplifier for the OFDM system*, Journal of Xidian university, China Vol. 35, No. 6 pp. 1020-1025, Dec2008

[6] [6] Bumman Kim, Ildu Kim, Junghwan Moon *Advanced Doherty Architecture*, IEEE Microwave Magazine, pp, 72-86, October 2010.

Garbage Management System for Smart City Mission using Internet of Things

BalaBasker.S
Assistant Professor
Department of ECE
St.Annes CET,Panruti, India.

***Abstract*—Smart city Mission in India has to be equipped with basic infrastructure and technological advancements to provide better ambience and comfort for living in those cities. To lead a smarter life, a cleaner and most hygienic environment should be assured, in order to achieve it cleaning the dustbin is an important process which has to be done at regular basis but due to unpredictability in filling of waste it gets overflowed before the next cleaning process date. It is also noted the employers do not remove garbage present in the dustbin regularly. So to ensure such a pristine environment, we have designed a project named Garbage Management System for Smart City Mission using Internet of Things for the municipal dustbins which intimates the Centre of municipality for immediate cleaning of dustbin with proper verification. Our model monitors the garbage level in the dustbin using ultrasonic sensor and sends the alert to the server once when the garbage gets filled. Once the municipal employee cleaned the dustbin he needs to confirm his work using RFID Tag. RFID reader reads the Tag and checks the level of the garbage in dustbin and sends the status of cleaning to the server. The municipal authorities can use this system to monitor the waste collection status in the smart cities in real time and measure the performance of the team. An Android application is developed to remotely monitor the cleaning process done by the workers and hence reducing the manual process of monitoring and verification.**

I. INTRODUCTION

The ultimate need of the hour for a developing nation is the key for Smart City Mission. The influential ecological factors that pose to be a threat to this may include: hazardous pollution and its subsequent effects on health of humanity, alarming global warming and depletion of ozone layer etc. Mostly Environmental pollution may be owing to the Municipal Solid Leftovers (MSL) [2]. A Proper maintenance becomes mandatory for an efficient and effective removal of the generated Municipal Solid Leftover [8]. It is perceived that often the waste space gets too much occupied due to irregular removal of garbage occupancy in the dustbin. This exposition proposes an e-monitoring system that putforths an embedded system and web based software assimilated with RFID and IoT technology. Using the anticipated system, monitoring of the waste collection status could be monitored effectively. This design designates a technique in which the garbage level could be checked at regular intervals which would prevent the undesirable overflow of the bin. In addition to this it also has facilitation sto intimate the authority to clean up in case of any overflows. The filling level of the garbage in the dustbin and its original level height could be sensed/ monitored by the ultrasonic sensor. Programming in the Arduino UNO is done in such a way that once a particular level of filling is sensed information message is sent requesting a clean-up. The practice of pervasive computing technology namely Radio Frequency Identification (RFID), and sensor networks offer a brand new channel to optimize the waste management systems in a better circumstances.

II. EXISTING SYSTEM

A single directional cylinder is suspended next to the lid of dustbin. The piston is free to move up and down vertically inside the dustbin to a certain level. A plate is attached to the cylinder for compressing the garbage. The shape of this plate depends upon the shape of the dustbin. The compressing plate consists of a side hole through which the leaf switch is suspended upside down. The level of leaf switch is placed lower to the maximum level to which the compressing plate can reach down thus even after the switch gets pressed, garbage can be dumped in the dustbin to a certain extent. The opening of the dustbin is located little higher to that of the threshold level. The opening of the dustbin is covered by a lid that is attached to the inner lateral surface of the dustbin. Thus when the compressor reaches the maximum level for compression, it blocks the inlet lid such that no garbage from outside can be dumped into the dustbin during the while. Preventive measure is taken in such a way that the garbage do not damage or block the functioning the leaf switch at any case. The materials used for designing the dustbin and the compressor is selected in such a way that it exhibits anti corrosive properties.

The conventional waste collection and management approach has the following problems [4]: Lack of information about the collecting time and area. Lack of proper monitoring system for tracking all activities related to solid waste management. Loss of productivity due to inefficient utilization and unauthorized use of vehicles. There is no quick response to urgent cases like truck accident, breakdown, long-time idling. There is no quick way to response to client's complaints about uncollected waste. There is no analysis of finding best route path of collecting waste.

III. SMART GARBAGE ALERT SYSTEM

The proposal in this dissertation focuses on the following objectives : To develop an electronic monitoring system for

Fig. 1. Flow Chart of proposed system

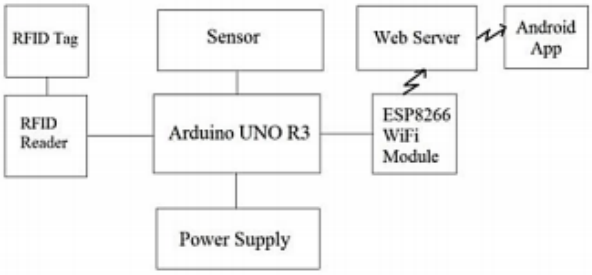

Fig. 2. Block diagram of proposed system

solid waste management. The system will have the facility to send SMS to the workers and supervisors.

To develop a web based GUI so that the system can be accessed from anywhere and information can be viewed by different group of people. The GUI will have the facility for the citizens to put their complaints and comments on the service.

The ultrasonic sensor sends the distance continuously to the Arduino. Arduino checks the level and sends the alert as FILLED when cm ¡25 and as CLEANED when cm ¿75.

When an RFID Tag Interrupts the Reader, the ultrasonic sensor checks the level again and sends the status of cleaning as CLEANED when cm ¿75 and as NOT CLEANED when cm ¡25. All the above conditions send the alert/status to the ThingSpeak webserver via WiFi Module and it is viewed in the Android App at the server end.

IV. SYSTEM DESIGN

The system is designed in such a way that it avoids the overflow of the dustbin by sending alerts to the municipality with help of a microcontroller linked with a webserver using IoT. It also includes the verification process after cleaning the dustbin.

A. Block Diagram

B. Ultrasonic Sensor Ultrasonic ranging module HC - SR04 provides 2cm - 400cm non-contact measurement function, the ranging accuracy can reach to 3mm. The modules includes ultrasonic transmitters, receiver and control circuit. The basic principle of work:

1) Using IO trigger for at least 10us high level signal, 2) The Module automatically sends eight 40 kHz and detect whether there is a pulse signal back. 3) IF the signal back, through high level , time of high output IO duration is the time from sending ultrasonic to returning. Test distance = (high level timevelocity of sound) (340M/S))/ 2

C. Arduino UNO R3

The Arduino Uno is a microcontroller board based on the ATmega328 (datasheet). It has 14 digital input/output pins (of which 6 can be used as PWM outputs), 6 analog inputs, a 16 MHz ceramic resonator, a USB connection, a power jack, an ICSP header, and a reset button. It contains everything needed to support the microcontroller; simply connect it to a computer with a USB cable or power it with a AC-to-DC adapter or battery to get started. The Uno differs from all preceding boards in that it does not use the FTDI USB-to-serial driver chip. Instead, it features the Atmega16U2 (Atmega8U2 up to version R2) programmed as a USB-to-serial converter. Revision 2 of the Uno board has a resistor pulling the 8U2 HWB line to ground, making it easier to put into DFU mode.

D. RFID Reader

RFID tag is a small device which stores and sends data to RFID reader. They are categorized in two types active tag and passive tag. Active tags are those which contain an internal battery and do not require power from the reader. Typically active tags have a longer distance range than passive tags. Passive tags are smaller and lighter in size than the active tags. They do not contain an internal battery and thus depend on RFID reader for operating power and certainly have a low range limited up to few meters. The microchip stores the unique ID and incorporates the necessary logic circuitry for functioning of the tag. It has an internal EEPROM to store the unique ID. The antenna receives power and RF signals from the RFID reader and sends those signals to the chip. The chip receives those signals, computes them and sends back the data to RFID reader.

E. ESP8266-01 WiFi Module ESP8266 offers a complete and self-contained Wi-Fi networking solution, allowing it to either host the application or to offload all Wi-Fi networking functions from another application processor. When ESP8266 hosts the application, and when it is the only application processor in the device, it is able to boot up directly from an external flash. It has integrated cache to improve the performance of the system in such applications, and to minimize the memory requirements. Alternately, serving as a Wi-Fi adapter, wireless internet access can be added to any microcontroller-based design with simple connectivity through UART interface .

F. Android Studio Android Studio is the official IDE for Android app development, based on IntelliJ IDEA. Android Studio offers even more features that enhance your productivity when building Android apps, such as:

A flexible Gradle-based build system Build variants and multiple APK file generation Code templates to help you build common app features A rich layout editor with support for drag and drop theme editing

Fig. 3. ESP8266-01 WiFi Module

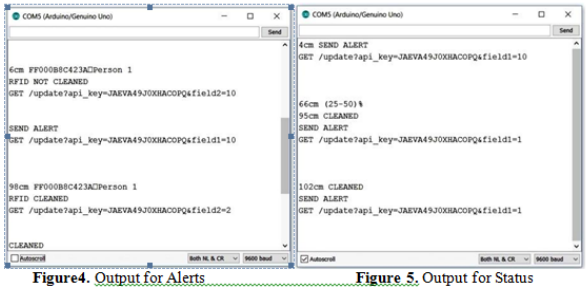

Figure4. Output for Alerts **Figure 5.** Output for Status

Fig. 4. ESP8266-01 WiFi Module

Fig. 5. a) Homepage of the App b) Alerts page of the App c) Status page of the App

V. RESULTS AND DISCUSSION

A.ARDUINO IDE OUTPUT

The Arduino is programmed based on the 4 levels set in the dustbin:

Level 1 (¿75 cm) Cleaned Level 2 (50 cm to 75 cm) (25 -50) Level 3 (25 cm to 50 cm) Above 50 Level 4 (¡25 cm) Send Alert

The Interrupt from the RFID Tag causes rechecking of the level and it displays the status of cleaning done by the cleaner (¿75 cm) Cleaned (¡25 cm) Not Cleaned

The chart (b) shows the level of the dustbin received from the Arduino. Value 10 denotes that the dustbin is Filled and the value 2 denotes that the dustbin is Cleaned. The chart (c) shows the status of the dustbin after cleaning at the time of interruption caused by the RFID Tag. Value 10 denotes that the dustbin is Not Cleaned and the value 2 denotes that the dustbin is Cleaned.

VI. CONCLUSION

So our project can be used for proper monitoring and maintenance of the garbage in real time and also turns the irregular cleaning of the dustbins by sending alerts to the concerned individual at regular intervals. It also further improves the system by additionally endorsing the status of cleaning in real time and measure the performance of the team. Thus our system comes in handy as an admirable solution in environmental maintenance. In addition to this it also aids to diminish the need for high human intervention in garbage maintenance of the municipality and pollution monitoring system.

REFERENCES

[1] Md. Liakot Ali, Mahbubul Alam, Md. Abu Nayeem Redwanur Rahaman, *RFID based E-monitoring System for Municipal Solid Waste Management, 2012 7th International Conference on Electrical and Computer Engineering*, Pg 474-477, December,2012

[2] [2] TWINKLE SINHA, K.MUGESH KUMAR, P.SAISHARAN, *SMART DUSTBIN, International Journal of Industrial Electronics and Electrical Engineering*, ISSN: 2347-6982, Volume-3, Issue-5, May-2015

[3] [3] L.Gogoi: (2012): *Solid Waste Disposal and its Health Implications in Guwahati City: A Study in Medical Geography, Lambert Academic Publishing, Germany*, ISBN 978-3-8454-0149-2

[4] [4] Hannan, M., A., Arebey, M., Basri, H. (2010). *Intelligent Solid Waste Bin monitoring and Management System, Australian and Applied Sciences*, 4(10): 5314-5319, 2010, ISSN 1991-8178

[5] [5] Visvanathan, C., Ulrich, G., *Domestic Solid Waste Management in South Asian Countries A Comparative Analysis, 3 R South Asia Expert Workshop, 30 August - 1 September*, 2006 Kathmandu, Nepal

[6] [6] Rahman, H., Al-Muyeed, A. (2010).*Solid and Hazardous Waste Management, ITN-BUET, Center for Water Supply and Waste Management*

[7] [7] Flora, A. (2009) *A proposal on sustainable and integrated solid waste management system for university Kebangsaan Malaysia- Towards a clean environment:*.

[8] [8] Daniel V., Puglia P. A., and M. Puglia, *RFID-A Guide to Radio Frequency Identification, Technology Research Corporation*, 2007

ONLINE EXAMINATION SYSTEMS FOR BLINDS

Ms.S.Jayasudha
Assistant Professor
Department of ECE
PEC

K.Arivarasi
UG scholar
Department of ECE
PEC

V.Kavitha
UG scholar
Department of ECE
PEC

***Abstract*—A number of developing countries continue to provide educational services to students with disabilities in segregated schools.Also all students, regardless of their personal circumstances, have a right of access to and participation in the education system, according to their potential and ability. However, with the rapidly growing population and increasing number of people with blindness along with other disabilities, need for use of technology in the field of education has become imminent.With existing system of competitive examination, students face problems while interacting with the system, misunderstandings arising due to human mediator and also an ability to cope-up with the other students. Our project, through the use of speech technology, attempts to provide solutions for some of these issues by creating an interactive system. Thus, the application will help in creating an environment that provides equal opportunities for all the students in taking up competitive exams. This will improve the current educational system for blinds career.**

I. INTRODUCTION

The growth of the Internet, and in particular the World WideWeb, is already influencing the way science is taught and willundoubtedly do so to greater extent in the future. In areas of education it offers a medium that has the potential to be more responsive to students. To encourage greater participation in their own learning, and to give greater access to different sources of information than traditional methods offers. In the future blind peoples also can do online exam like a normal human if our project is delivered in real time . For the Supervising Faculty: Marking the test is done automatically and instantaneously; the faculty is relieved fromthese, time consuming duties. Questions can be easily recycled from the question bank, easily edited and changed, Different versions of the same question can be generated for different students.

A. For the Blinds

Tests can be taken anytime. Tests can be taken anywhere. Blinds can login the exam using their image verification. Questions can be attempted in a stress-less environment Test can be taken using a simple personal computer, Here Questions and options are through voice.The Answer also can be submitted by the user through voice. The results are also delivered through voice.

B. For the Administration

The marks are automatically collected, analyzed, and disseminated for purposes like evaluation of teaching and learning process.

II. EXISTING SYSTEM

In this world blind peoples can get the knowledge using various interfaces. Such as one common method of the blind people have been intended to use is by voice recognition , that is which has a voice recording system. Where the content had recorded already in certain format, the blind people should be supposed to hearthe recorded content in that recording system based on this way they can easily know the content and learn in a preferred way and also they can interact with that system by giving their voice as an input. These common procedures have been used for the blind people to expose their talent in various platforms and to get compete with normal people through the help of many devices For example in iphone there is an facility which allows a blind people to get interact with that device as a normal man. If they touches any button or the display option in the iphone have been designed to react as soon as by giving voice output. So a blind people can use all the facility provided in that phone (they are able to access all the options like a normal man browsing,chatting,SMS,Music,streaming.etc).

Disadvantage: Major disadvantage is that they have to give a voice input in a clear manner, there should be some mismatch, while giving a long word as input, there may be noise suppression and also for different language other than English they are not feeling comfortable.

III. PROBLEM DEFINITION

The main aim is to propose a system that uses speech technology to provide students with access to information during exams. The key focus of application is to provide students with an ability to interact with the system through speech. The application automates the examination process through reading out questions to the user and receiving their input orally. Application also provides accessories for other requirements, like knowing the time remaining, during exams. Use of this application shall benefit students with: Learning disabilities, including dyslexia and dysgraphia. Poor or limited motor skills. Vision impairments. Physical disabilities. Limited English Language.

IV. PROPOSED SYSTEM

providing online examination for blind people. There has been no proper application for By considering the above

disadvantage we will be going to create an entire window application for blind people to admit in online examination like a normal people without any difficulties. (Hereall outputs are in voice) . The Exam Management System has been developed to support automatic grading, exam archiving, and exam administration. In most of them, the widely used questions are correspondence to courses, and it should be easily judged and evaluated online by comparing with the correct answers. The typical questions include yes/no questions, multiple-choice/ single-answer questions, multiple-choice/multiple-answer questions, matching questions, numeric questions, and essay questions. This system is built based on open source technology

V. SCOPE

This project proposes a system that will create a revolution in a world of education by providing an easier way for visually impaired people to take tests just as normal students do. The system acts as a mediator who converts the responses that are given orally to the system to acceptable and needed format i.e.Text. When user gives response orally speech to text converter is invoked and it converts the response in text to mark the appropriate option of all. Similarly, other essential things like timer and result can also be heard. Both the things can be invoked orally by just remembering few commands. There are different sections in the system. User can choose any one option through voice command. The whole system works on voice command so that everyone can use the same system including visually impaired people.

VI. TECHNIQUES USED

The project is a window application in .NET that can be used to conduct examination for physically challenged. The project has mainly used following techniques: Speech synthesis Speech recognition CBIR Speech synthesis is a technology used to output voice when given text as an input. Sometimes also known as text to speech conversion. Speech recognition is a technology used to output some text or an event when given speech as an input. Sometimes also known as speech to text conversion. Content based image retrieval is a technique use to match images.

VII. MODULE DESCRIPTION

A. Register

The very first module is registration module. In this module the visually impaired person or the blind person can have registration before giving exam. The details required are to be filled by a third person or a coordinator appointed .After all the details are filled properly a registration id will be provided to the examinee .The examinee can use this registration id to login and give exam. B. Login

The second module is login module. In this module the examinee can login using registration id provided during registration and password that will be candidates image. Then, candidates image will be matched with the one that he/she had provided during registration. If both the user id and image matches candidate will be allowed to login otherwise he/she will not to be redirected to exam window. For image matching we have used the CBIR technology. time expire or not. The systems end the exam if it is expired then C. Admin login

In this module the administrator having a secure id and password and can control the entire examination. Admin can also update the question database, can delete questions, update questions, can also maintain examinee database that is registered students database. Proper security is there for accessing question database and examinee database i.e proper authentication is there. D. Exam

In this module there is the window which appears after the successful login of them examinee. The very first window will be of rules and regulations which constitutes the necessary instructions that are needed to beremember by examinee while giving exam. The question that appears on screen is read out so that the visually impaired examinee can listen and give response of the question asked. The answer n be given by examinee by choosing right option verbally. And the given answer is marked and then answer can be submitted verbally. The answer can alsobe skipped. Meanwhile, the timer is running and after every 15minutes the remaining time is called out. The examinee can skip questions ,mark for review questions as per his requirement and can answer them whenever he/she wants. Candidate can also navigate to any of the questions by just speaking the question number. The result will be produced on the next window after all the questions are attempted.

Question database is to store data related to all questions and its four options along with correct answer of test paper. Subject database is to store different subject name and its id available for exam. Registration database is to store candidates information submitted by him during registration. Result database is to store information related to examinee result exmarks, question attempted ,no. of correct answers and so on. The logic is described as follows: The systems first match the images and verify the candidate details who have already registered. If they are. not correct the systemstarts again. If the images and details of the candidate are correct then the system allows candidates to begin their exam. While the candidate answering the questions the system check for the time if the exam time expire or not. The systems end the exam if it is expired then save the answers in the database. E.Examination engine: Examination Engine contains the logic used by the candidate to take exam and shows the results after they finish

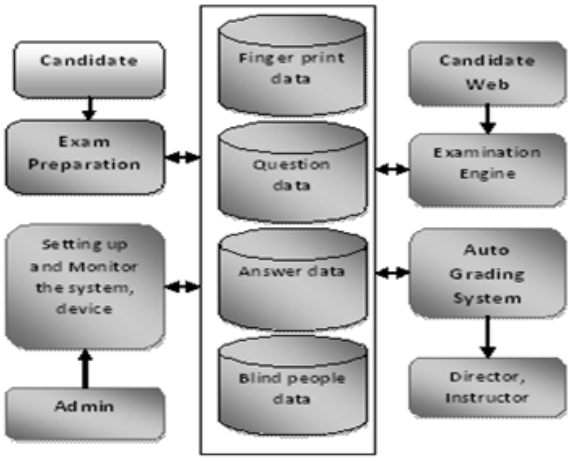

it. This logic is described as follows: The systems first match the fingers prints and verify the candidate details who have already registered. If they As shown in fig. 2 Examination Engine contains the logic used by

the candidate to take exam and shows the results after they finish it. This logic is described as follows: The systems first match the fingers prints and verify the candidate details who have already registered. If they are not correct the system starts again. If the finger prints and details of the candidate are correct then the system allows candidates to begin their exam. While the candidate answering the questions the system check for the time if the exam time expire or not. The systems end the exam if it is expired then save the answers in the database. F.Working: As in proposed system, we have seen that by giving voice as an input there are some disadvantages, By considering this we will be going to design a website in which an information (or) question have been delivered through voice as per the area and as per the language and we want the blind people to select their option through the arrow key and also providing many option by pressing an appropriate key provided that will be given in the instruction would be displayed in the website. The supervisor will read the appropriate instruction and based on that they should guide the blind candidates to admit. G.Advantages: They can easily give the answer by pressing a single key without get confused with the mismatching Words. It reduced candidates depressing.

VIII. VIII. CONCLUSION

This project would be a very useful one for every blind people and physically challenged to admire their talent easily through online exam like other humans. In our project we will be going to deliver an entire application for physically challenged people which can provide an interactive interface. Examinee can easily give exam by giving easy voice commands. Thus, physically challenged people can easily give exam like a common man without much difficulty. Through this they have been able to attend many exams in the future And also we will try to do as much as improvement in future as per the collection of feedback.

REFERENCES

[1] Brooks, D.W., *Web-teaching: a guide to designing interactive teaching for the World Wide Web.* 1998, New York: Plenum Press.

[2] De La Beaujardiere, J.F., Cavallo, J., Hasler, A.F., Mitchell, H.,OHandley, C., Shiri, R., White, R. *The GLOBE Visualization Project: Using WWW in the Classroom,* Journal of Science Education and Technology, 6(1), 15-22, 1999.

[3] I. Hernn-Losada, C. Pareja-Flores, and J. Velzquez-Iturbide*Testing-Based Automatic Grading: A Proposal from Blooms Taxonomy,* Eighth IEEE International Conference on Advanced Learning Technologies, 2010.

[4] S. Bonham, A. Titus, R. Beichner and L. Martin, *Education research using web-based assessment systems,* Journal of Research on computing.

[5] Sue J. Cho, Suk I. Yoo, *A Matching Algorithm for Content Based Image Retrieval,* International Conference on Information Technology, 2014.

IOT Based Student Attendance Monitoring System Using Arduino and Finger Scanner

V.Vinothkumar
UG scholar
Department of ECE
St.Anne's CET

S.Ranjithbabu
UG scholar
Department of ECE
St.Anne's CET

***Abstract*—Biometric student attendance system increases the efficiency of the process of taking student attendance. This paper presents a simple and portable approach to student attendance in the form of an Internet of Things (IOT) based system that records the attendance using fingerprint based biometric scanner and stores them securely over cloud. This system aims to automate the cumbersome process of manually taking and storing student attendance records. It will also prevent proxy attendance, thus increasing the reliability of attendance records. The records are securely stored and can be reliably retrieved whenever required by the teacher.**

I. INTRODUCTION

Attendance plays a major role in educational institutions. The most common means of taking attendance in the classroom is by calling out the roll numbers of students or asking the students to manually sign the attendance sheet, which is passed around during the lecture. The process of manually taking and maintaining the attendance records becomes highly cumbersome. Biometric systems have reached a sufficiently advanced stage wherein they can now be deployed in systems without hampering portability. With the recent development of various cloud based computing and storage systems, data can be securely stored and retrieved whenever required. Primarily, fingerprints and iris images are considered to be the most reliable for use in biometric systems [7], [8]. A system that records the attendance making use of biometric scanners and stores them securely over cloud in the form of Google Spreadsheet can help resolve issues. The system consists of a fingerprint scanner which is used for ascertaining a students identity. If the fingerprint scanned matches with records present in the database, attendance is granted to the student by updating to the Google Spreadsheet.

II. RELATED WORK

The RFID based attendance system simplifies the process of taking attendance and reduces the paper work and saves the lecture time. Student have to display their RFID card to the RFID reader in order to mark their attendance, and then the collected data will be sent to the professors cell phone via Bluetooth, in this way he/she can keep the record of attendance daily [1]. The iris based attendance system includes a small but very high resolution camera for taking the image of the iris, which is then compared with the data enrolled in the database. If the entered data matches with the already existing data, the attendance of particular person is marked present. This system is costlier because of the high resolution camera, but its the most fool proof system for the task, as the pattern and the colour of the iris is unique for every individual [2]. The wireless fingerprint attendance management is based on biometrics and wireless technique solves the problem of spurious attendance and the trouble of laying the corresponding network. It can make the users' attendances more easily and effectively [3][10]. Enrolment of fingerprints is done on the Server using Digital Persona Fingerprint USB Sensor and verification is done on the client with the transmission of fingerprint templates over the network. In this system attendance report is generated automatically and is further forwarded to faculty members via Email. In addition to this, SMS is also sent to parents mobile in case of short attendance of students

III. SYSTEM OVERVIEW

The proposed system involves a biometric attendance system that integrates an ESP8266 NodeMCU breakout board and a fingerprint scanner. The fingerprint scanner processes the users fingerprint to verify the students attendance. NodeMCU uploads the attendance data to Google Spreadsheet using a service called PushingBox API. A. ESP8266 NodeMCU ESP8266 NodeMCU is an open source development board based on ESP8266-12E chip and NodeMCU firmware that integrates GPIO, PWM, I2C and ADC all in a one board. It has 10 GPIO and every GPIO can be PWM. It has ISSN (Online) 2278-1021 ISSN (Print) 2319-5940 IJARCCE International Journal of Advanced Research in Computer and Communication Engineering ICRITCSA M S Ramaiah Institute of Technology, Bangalore Vol. 5, Special Issue 2, October 2016 Copyright to IJARCCE DOI 10.17148/IJARCCE 11 Arduino like hardware IO, which can effectively reduce the extravagant work for configuring and manipulating hardware. Due to its low cost, compact design and wireless connectivity, it helps to prototype an IoT product efficiently. NodeMCU can be programmed using Lua script. Programming NodeMCU firmware with Lua script has certain disadvantages like need to learn new language, reduced pin out and scarce documentation. Since, the board has Arduino like hardware IO; it can be programmed directly using Arduino IDE by erasing NodeMCU firmware. Arduino IDE is more familiar and has

vast documentation and support community. B. Fingerprint scanner Everyone in this world has marks on their fingers. These marks have a pattern and this pattern is called the fingerprint. Since, they are unique and cannot be removed or changed, they have become ideal means of biometric identification. An image of the users fingerprint is captured by fingerprint scanner. This captured image is called as live scan. The live scan is processed digitally to create a biometric template (a collection of certain extracted features) which is stored and used for matching [8]. Identification of fingerprints of individuals is done on the basis of both hardware and software techniques. C. Fingerprint Processing Fingerprint processing has three primary functions: enrolment, searching and verification. Out of these, enrolment plays an important role. It involves capturing an image of the users fingerprint. Searching involves sifting through a set of stored fingerprints and comparing them with the input fingerprint. Verification involves acknowledging a match between the input fingerprint and one already present in the stored fingerprints. D. Internet of Things The Internet of Things (IoT) is the scenario in which objects, animals or people are provided with unique identifiers, and the ability to transfer data over a network without requiring human-to human or human-to-computer interaction [9]. IoT revolves around increased machine-to-machine (M2M) communication and encompasses wireless embedded sensors and actuators that assist users in monitoring and controlling devices remotely and efficiently [5]. This innovation will be enabled by the embedding of electronics into everyday physical objects, which will allow them to integrate seamlessly with the existing infrastructure. E. PushingBox API API (Application Programming interface) is a set of routines and protocols for accessing a Web-based software application or Web tool. PushingBox is a cloud service that provides cloud notifications based on API calls. Using PushingBox API, it is easy to launch the scenario of notifications by simply attaching DeviceID as the only argument. These scenarios can be linked with anything from tweeting, receiving emails, uploading data to Google Docs, etc. PushingBox API provides the integrative functionality of the PushingBox service. F. Google Spreadsheet Google Sheets is a web based application that allows creating, updating and modifying spreadsheets and share data live online. Google sheet is based on Ajax that makes it dynamic. It allows storing and organising different types of data, much like Microsoft Excel. Google Sheets does not offer all advance features of Excel but, it's easy to create and modify spreadsheets ranging from the simple to the complex. Google Sheet is compatible with Microsoft excel and CSV (Comma-Separated Values) and can also be saved as HTML.

IV. IMPLEMENTATION

Fingerprint Enrolment In the enrolment process, the fingerprint of each student is recorded. The fingerprint of the student is scanned using the fingerprint scanner in the system. Each fingerprint is assigned an ID number. The ID number is stored on the NodeMCU board. This number is unique for each student. Enrolment of fingerprints is performed only once. The student IDs can be changed or replaced as and when required. The process is as shown in Fig. 2 and Fig. 3. ISSN (Online) 2278-1021 ISSN (Print) 2319-5940 IJARCCE International Journal of Advanced Research in Computer and Communication Engineering ICRITCSA M S Ramaiah Institute of Technology, Bangalore Vol. 5, Special Issue 2, October 2016 Copyright to IJARCCE DOI 10.17148/IJARCCE 12 Fig. 2 Enrolment Process Fig. 3 Enrolment Process B. Fingerprint Comparison and Recognition The system, being portable, can be passed around during the lecture from student to student to record attendance. During the fingerprint comparison and recognition process, the students fingerprint will be compared with the stored fingerprints in the NodeMCU board. During this process, a yellow coloured LED will glow, as shown in Fig.4. This will indicate to the student that the system is ready to take fingerprint input. The student then has to place his/her finger on the fingerprint scanner. The fingerprint input is then verified with the stored fingerprints. Fig. 4 Ready for Input C. Validation of Recognised Fingerprint In the previous process, the fingerprint input is compared with the stored fingerprints. If it matches a fingerprint present in the NodeMCU, a green coloured LED will glow, as shown in Fig. 5. This will indicate to the student that the fingerprint has been recognised successfully. Otherwise, a red coloured LED will glow, as shown in Fig.6. This will indicate that the fingerprint does not match any stored fingerprint. The student can then try again when the yellow LED glows, starting the Fingerprint Comparison and Recognition process again. Fig. 5 Fingerprint Matched Fig. 6 Fingerprint Not Matched D. Granting Attendance Uploading Data to Google Spreadsheet If the fingerprint is recognised, the attendance granting process starts. The unique ID number of the student is recognised. The attendance data is logged into Google Spreadsheet by uploading the students ID number in it, as shown in Fig.7. For uploading the ID number in Google Spreadsheet, PushingBox API is used. After the attendance is granted, i.e. the ID is stored in Google Spreadsheet, the Fingerprint Comparison and Recognition process starts. The system can then be passed on to another student. ISSN (Online) 2278-1021 ISSN (Print) 2319-5940 IJARCCE International Journal of Advanced Research in Computer and Communication Engineering ICRITCSA M S Ramaiah Institute of Technology, Bangalore Vol. 5, Special Issue 2, October 2016 Copyright to IJARCCE DOI 10.17148/IJARCCE 13 Fig. 7 Attendance Data on Google Sheets V. FUTURE SCOPE The system can be improved by encasing it in a plastic covering. This would make it more compact and easy to use in a classroom setting. The system can be configured to enable lecture-wise attendance taking. It can further be improved to automatically calculate attendance percentages of students and intimate the teachers if a students attendance is below a certain percentage. It can also be modified to fit the corporate environment.

V. 4. CONCLUSION

The traditional process of manually taking and maintaining student attendance is highly inefficient and time consuming.

The attendance monitoring system based on biometric authentication has a potential to streamline the whole process. An Internet of Things (IoT) based portable biometric attendance system can prove to be of great value to educational institutions in this regard as it proves to be highly efficient and secure. The cost involved in making this system is quite less, when compared to conventional biometric attendance system. The use of cloud computing to store the attendance records makes all the data easy to access and retrieve as end when required by the teachers. The use of fingerprint scanner ensures the reliability of the attendance record. The system, due to its lack of complexity, proves to be easy to use and user friendly.

REFERENCES

[1] Prashik S. Bhagat, Prof. D. S. Shilwant, Prof. S. P. Kharde, Praful S. Bhagat, Abhijit S. Andure, Prof. Amol A. Shirsath, *Iris based attendance system*, International Journal== of Advanced Research in Computer Engineering Technology (IJARCET), Volume 4 Issue 8, August 2015.

ESTIMATION OF PARKINSONS DISEASE RISK BY STATISTICAL MODEL

Sr. Anita
Assistant Professor
Department of ECE
St. Anne's CET

Dr.Aruna Priya
Professor
Department of ECE
SRM University

***Abstract*—The constant progress and complexity of clinical and non- clinical treatment of Parkinsons disease (PD) become very tough to diagnose the disease. This may lead to delayed diagnosis, misdiagnosis and excessive medical cost. Rapid advances in diagnostic techniques have offered an effective way for tracking the different stages of the disease. This paper focuses the early PD diagnosis and its progression is estimated by Gama Amino Butyric Acid (GABA) concentration level with the help of Striatal Binding Ratio (SBR) values. SBR values of Caudate and Putamen (left right) are calculated from Single Photon Emission Computed Tomography (SPECT) images as treated as input variables and the response variable is GABA concentration level. The mathematical model for GABA concentration level is developed by using the input variables like SBR values of Caudate and Putamen (left right). The performance of the model is analyzed using ANOVA (Analysis of variance), normal probability curve and residual plot. The coefficient of determination (R2) gives 99.3of fitness rate with the regression line. The progression rate of PD is measured for three consecutive years and it is compared with the threshold value of GABA to find the severity of the Parkinsons disease. Keywords: Parkinsons disease, SBR, level of GABA concentration, Mathematical model, progression rate**

I. INTRODUCTION

Parkinsons disease is a progressive movement disorder which constantly affects the mid brain neurons of human called substantia nigra. It is clinically defined by the major symptoms of resting tremor, rigidity, postural instability, bradykinesia, cognitive and psychiatric disturbances.The diagnosis of PD is easy when symptoms are full blown. But an accurate diagnosis is quite tough when the disorder is mild, which demands the formulation of an early detection technique for PD [1-3].The inhibitory neurotransmitter dopamine regulates and controls movements, motivation and cognition. Degeneration of these dopamergic nerve cells along the nigrostraital pathway affects the gait system of human, which in turn leads to Parkinsons disease [4]. SPECT images take the crucial role to discriminate PD patients from the healthy group by calculating dopamine deficit in Caudate and Putamen of the midbrain, even in the premature stage of PD. Thus, calculating dopamine deficiency (ie.SBR) in Caudate and Putamen of the human brain from the SPECT image is a valuable diagnostic tool for discriminating Parkinsons disease from the healthy control [5, 6]. Still the cases have high SBR value misdiagnosed as PD(supposed to be low) and the cases have low SBR value misdiagnosed as healthy control (supposed to be high). Hence the misdiagnosed rate is significant [3]. Gamma-Amino Butyric Acid (GABA) is also a most essential inhibitory transmitter in the central nervous system (CNS) and spinal card. GABA mediates pre-synaptic inhibition of primary blood vessels in the motor neuron system. The disturbances of the GABA concentration level in CNS influence the motor system [7]. Several neurological disorders including Parkinson's disease, anxiety, depression, insomnia, and epilepsy are negatively related with the level of GABA concentration in the human brain [8]. Hence the neurotransmitters dopamine and GABA are found to be a novel diagnostic tool for detecting PD. The model that the log of the odds states how the variables are related with prediction of the Parkinsons disease. Hence formulating the mathematical model is a new approach to diagnosis PD. In statistics regression analysis focuses on the relationship between a dependent variable and one or more independent variables. Primarily it supports to understand how the dependent variable changes when any one of the independent variable is varied while the remaining independent variables are held fixed. When the regression analysis has considerable overlap with the field of machine learning, it can predict the various disorders. It is also used to realize how the independent variables are related to the dependent variable, and to investigate the forms of these relationships [9]. The machine learning techniques such as Multivariate Logistic Regression (MLR), Artificial Neural Network (ANN), and Support Vector Machine (SVM) are effectively used to formulate a prediction model for diagnosing neural disorders. Machine learning techniques consent with individual level characterization rather than group level characterization. Hence high level of clinical translation is obtained. MLR aims at the determination of probability based on SBR values, which classify the subjects into different risk categories. SVM finds the hyper plane in order to classify the subjects and high accuracy was achieved [10-12]. In the present study, the level of GABA concentration of Parkinsons disease is calculated using SBR values. The developed mathematical model of GABA is to predict the early diagnosis of PD and its progression rate by using regression analysis. The developed model has potential to assist the clinician in the diagnostic process.

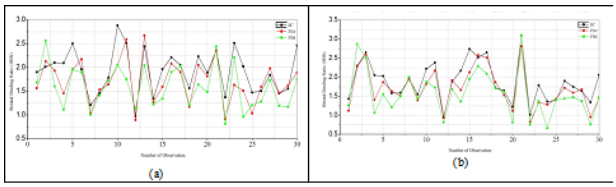

Fig. 1.

II. COMPUTATIONAL METHODOLOGY

A. Database

All PD subjects taken from the international PPMI database are in three stagesof Hoehn and Yahr (HY). The corresponding SBR values are taken for the analysis [13]. The SBR values are calculated as follows: Iterative reconstruction was performed on SPECT raw projection data using hybrid ordered subset expectation maximization (HOSEM) algorithm. Iterative reconstruction was done without any filtering to ensure consistency of the reconstructions. The HOSEM reconstructed files were processed for Attenuation correction, which was filtered and normalized to get the same anatomical alignment. Striatal uptake count densities of the region of interest (ROI) were extracted and used to calculate striatal binding ratios (SBRs) for each region of the four striatal regions.SBR is calculated by PPMI as follows and compared with Occipital cortex region below the Putamen as reference region [14].

SBR= (target region/reference region) 1 (1)

Where, Target region: left caudate, right caudate, left putamen, right putamen. Reference region: occipital cortex.

B. Statistical significance of SBR

All statistical analysis was carried out using Minitab software with 5significant level (95of confidence level). Histogram plots were drawn for three consecutive years and it is presented in Fig.1. The plots illustrate the different stages of SBR values distribution for Caudate and putamen (both left and right) of PD Patients. It also shows the amount of overlap between the three consecutive years. The overlap is higher in Caudate (left and right) than Putamen. Higher the overlap, difficult to discriminate the progress rate of the disease [3]. Hence the classification tool plays a major role as they integrate all the characteristics of disease, train the model and categorize them accordingly.

beginfigure[!t]

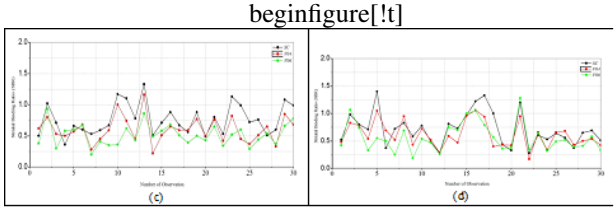

Histogram plots of the striatal binding ratio (SBR) values

C. The level of GABA concentration

The gradual changes of neurochemical lead to PD in the human body. The GABA and dopamine in Caudate and Putamen is interrelated to measure progression of PD. From the literature [15] it is found that the threshold level of GABA for PD. If the measured GABA lies below the cases are affected by PD. Similarly it lies above it is a healthy control. The Level of GABA concentration is measured using radio receptor array.

Predictor	B	SE	T	P value
Constant	0.114468	0.005631	20.33	0.00
Caudate(R)	0.008960	0.004785	1.87	0.062
Caudate(L)	0.025654	0.004956	5.18	0.000
Putamen(R)	-0.005756	0.006367	-0.90	0.367
Putamen(L)	-0.028090	0.007518	-3.74	0.000

Fig. 2. B is a regression coefficient for the predictors; SE is its standard error; T is test statistics; P value is the significance of the regression coefficient

III. 3. RESULTS AND DISCUSSIONS

A. Formulation of the mathematical model for the level of GABA concentration

The coefficients of regression analysis of the level of GABA concentration for PD are shown in table 1 along with their P value of the parameters. It is observed that the P value of the level of the GABA concentration for Caudate (L) and Putamen (L) are most significant, whereas Caudate (R) and Putamen (R) are not so significant. It indicates the reliability of the model.

Where S is the estimated standard deviation about the regression line, R-squared is the coefficient of determination. Adjusted R-squared is an approximately unbiased estimate of the population R-squared. The S value is the measurement of error.The model is better if it is smaller. The higher value of R-squared is better to determine the coefficients of a regression equation. The closeness of the adjusted R-squared with R-squared determines the fitness of the model [17]. In both cases, the adjusted R-squared value is closer to the R-squared value is shown in table 2. The mathematical model given in equation 4 is framed from the coefficient (B) value of the regression table 1.

It is observed from the model that the GABA is positively related with SBR values of left and right caudate and negatively related with left and right putamen. Hence high value of putamen has less likely have PD.

Overall model evaluation An analysis of variance (ANOVA) was performed for GABA to evaluate the model performance which is presented in table 3. The associated p-value for the model is lower than 0.05 (i.e. level of significance =0.05, or 95 confidence), which indicates that the model can be considered statistically significant better than a null model. The normal probability plot for GABA is presented in Fig.2. It can be noticed that the residuals fall on a straight line, which means that the errors are normally distributed and the regression model is well fitted with the observed values. Fig.

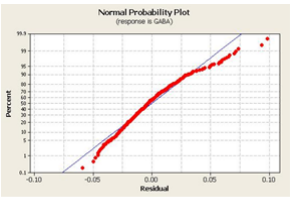

Fig.2 Normal probability plot for GABA for PD

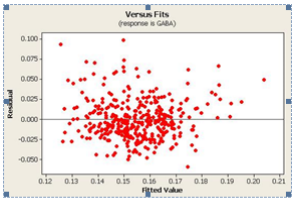

Fig. 3 Residual Vs fitted values for GABA for PD

Fig. 3.

3 shows the residual values with the fitted values for GABA. It indicates that the maximum variation of $-0.075 to 0.050$, which shows the high correlation that exists between fitted values and observed values.

B. Estimation of PD risk

The progression rates of PD for the three consecutive years are compared and its risk is shown in Fig.4. It shows less overlap between the GABA values, which has high discriminative power between them. The notched box plot shown in Fig.5 gives the outliers of the PD progression rate. Since all values lie between the ranges of the level of GABA concentration, it is evident that the high performance is observed from the developed model

beginfigure[!t]

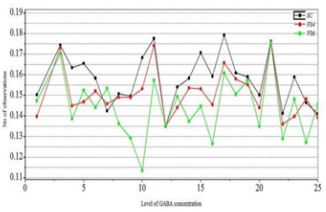

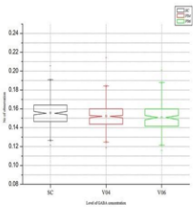

Fig. 4. Histogram plot for the level of GABA concentration Fig.5. Box plot for the level of GABA concentration

In each notched box plot, the central mark is the median (q2), the edges of the box are the 25th (q1) and 75th (q3) percentiles, the whiskers extend to the most extreme data points that are not considered outliers, and outliers are plotted individually. The extremes of the notches or the centers of the triangular markers correspond to q2 ± 1.57(q3 _ q1)/√n where n = 674 is the number of observations.

The SPECT images are again taken from the same patient for three consecutive years. The measured SBR values are applied to predict the early PD and its progress rate. The same procedure has been adopted for every three consecutive years to estimate the progression rate of PD. The Fig. 6 shows the progression rate of PD for three consecutive years. From the graph it is evident that the averaged GABA concentration level is increased for every year such as first year 0.1556, second year 0.15524 and the third year 0.1502.

IV. 4. CONCLUSION

The diagnosis of early PD and its progression rate is estimated for three consecutive years. The predictive mathematical models for the level of GABA concentration of PD patients are developed by using Regression analysis. These models have the potential to discriminate PD from healthy control. The model performance was tested using ANOVA, normal probability curve and residual plot. The residual plots of GABA for PD are generated and it is observed that regression model is well fitted and highly correlated with the observed values. The progression rate is measured for three years from the model; hence, the severity of the disease is estimated. The inference is that the prediction models for estimating GABA concentration level is a novel method to aid the clinicians for diagnosing PD. It overcomes the misdiagnoses of PD with high rate of accuracy compared with the related work.

REFERENCES

[1] de Lau, L. M and Breteler, M *Epidemiology of Parkinson's disease*, The Lancet Neurology, vol. 5, pp.525-535.

[2] Moore DJ, West AB, Dawson VL, Dawson TM *Molecular pathophysiology of Parkinson's disease.*, Annual Review Neuroscience 28 (2005): 57-87.

[3] Prashanth , R., Sumantra Dutta Roy Pravat and Mandal Shantanu Ghosh, K*Automatic classification and prediction models for early Parkinsons disease diagnosis from SPECT imaging*,Exepert system with Applications vol. 41, pp.3333-3342

[4] T.c. Booth.M, Nathan.A.D.waldman.A.Mquigley, A.H.Schapuria and J. Buscombe *The role of functional dopamine transporter AJNR AMJ neuroradial* ,36:229-35, Feb 2015

[5] Bairactaris, C., Demakopoulos, N., Tripsianis, G., Sioka, C., Farmakiotis, D., Vadikolias. K., Heliopoulos, I., Georgoulias, P., Tsougos, I., Papanastasiou, I., Piperidou, C. *Impact of dopamine transporter single photon emission computed tomography imaging using I-123 ioflupane on diagnoses of patients with parkinsonian syndromes*, Journal of Clinical Neuroscience, vol.16,pp. 246-252.

[6] Booij, J., Tissingh, G., Boer, G. J., Speelman, J. D., Stoof, J. C., Janssen, A. G., Wolters, E. C., van Royen, *[123I]FP-CIT SPECT shows a pronounced decline of striatal dopamine transporter labeling in early and advanced Parkinson's disease*, Journal of Neurology, Neurosurgery Psychiatry, vol. 62, pp.133-140.

[7] [7] (2007)American college for advancement in medicine, Monograph, Alternative Medicine Review, Vol. 12, pp-274-279

[8] [8] Acta Med Okayama and Kuroda H. (1983) Gamma-aminobutyric acid (GABA) in cerebrospinal fluid. vol.37 (3), pp. 67-77.

[9] [9]Douglas C. Montogomery, Elizabeth A. Peck and G.Geoffrey Vining (2001) Introduction to Linear Regression Analysis Arizona State University, fifth edition,576 pages.

[10] [10] Orru, G., Pettersson-Yeo, W., Marquand, A. F., Sartori, G., Mechelli, A.. *Using support vector machine to identify imaging biomarkers of neurological and psychiatric disease: a critical review. Neuroscience Biobehavioral Reviews*,

[11] [11] Shubhambind, arvind Kumar Tiwari, Anil Kumar Sahani, (2015). A Survey of Machine learning Based Approaches for Parkinson Disease prediction,vol6 (2),1648-1655

Dual Band Triangular Patch Antenna with SR in its Ground Plane

Dr. R. Gayathri Rajaraman
Assistant Professor
Department of ECE
Annamalai University

***Abstract*—A compact dual band triangular patch antenna using a novel metamaterial structure in its ground plane is presented in this paper. The role of the metamaterial structure is to miniaturize the antenna, inducing multi resonances. The antenna resonates at 5.46, 6.02 GHz with adequate gains of 3.2, and 5.6 dBs respectively. Key Antenna parameters obtained from the simulator are presented along with detailed discussions.**

Keywords: Microstrip patch antenna, linear polarization, wireless applications

I. INTRODUCTION

Microstrip patch antenna (MPA) has many remarkable features when compared with many wireless antennas like cheap, light weight, easy integration etc because of this features it finds application in almost all wireless system [1]. The design of such antennas is always a challenging task to designers as it should occupy minimum space but do the best performance during transmission and reception. There are many types of patches like rectangular, square, triangular, hexagonal, elliptical and so on. In this paper a triangular patch is modelled to resonate using a metamaterial (MTM) structure, Spiral Resonator which is found to create miniaturisation when designed properly. The basic details about triangular patches are available in [2-6]. Metamaterials are artificially synthesized materials supporting backward waves with negative permeability, permittivity. This was originally proposed by Vessalago in 1968. Some advancements in design of MPA with MTM are seen in [7-14]. This paper is presented as four sections; The

Conventional Design, Proposed Design, Analysis and Conclusions

A. Design of the Conventional Patch

The antenna is designed with RT Duroid substrate with relative permittivity of 2.2 and a thickness of 62 mils. The top view is shown in Figure1, while the dimensions are seen tabulated in Table 1.

The inset feed with a microstrip line of 50 ohm impedance is carried out to make the antenna resonate at 6.6 GHz with -12.74 dB as in Figure 2.

The ludwig radiation pattern and the polar plot of the conventional patch are shown in Figures 3,4. For the optimized Inset feed position various antenna parameters from the EM simulators are shown in Table 2. The gain has adequate co and cross po levels supporting linear vertical polarization. The directivity and VSwr are also adequate for the patch. This patch is modified and that is presented in the next section.

B. Design of the Proposed Antenna

The conventional patch antenna is etched with an inverted U shaped slot besides etching a spiral resonator in its ground this leads to dual resonance.The values are shown in Table 2. The model is shown in Figures 5,6.

The spiral resonators are found to create miniaturization up

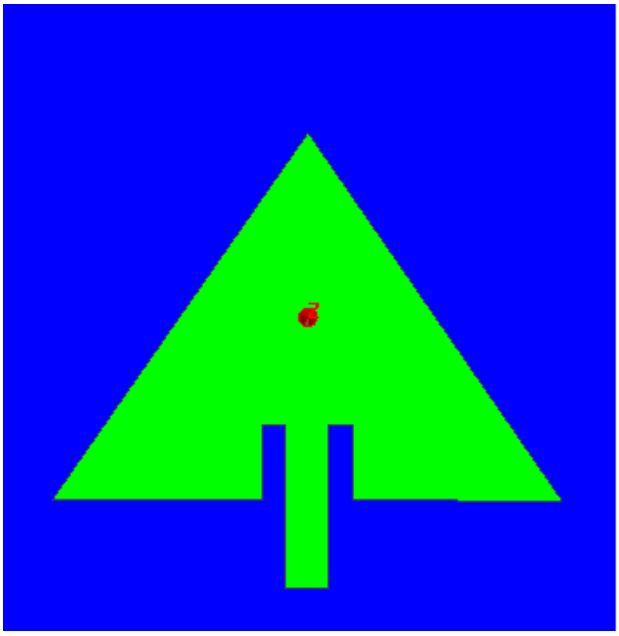

Fig. 1. Simulated MPA Model

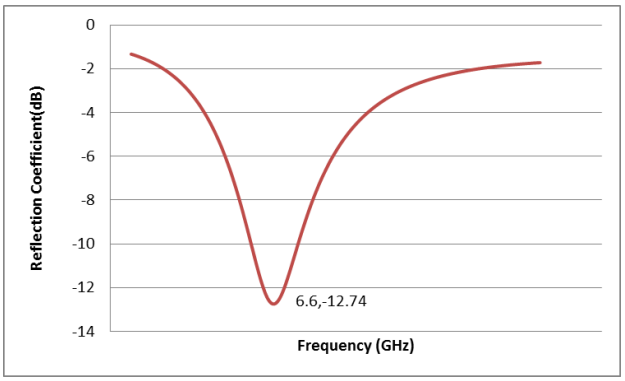

Fig. 2. Reflection Coefficient of Proposed Antenna.

to /30. The design equations presented in this section holds good only if value of N, which is the number of turns of resonator, does not exceed a predefined integer value as given below

The design equations for the spiral resonators are as follows

Where stands for width, s for spacing , N is an integer, n stands for number of turns, l stands for length while the expressions for lSRavg and Co are available in [9].

C. Analysis of The Proposed Antenna

The modified patch is found to resonate at two frequencies 5.46, 6.02 GHz with a return loss of -18.05, -13.15 dBs ;

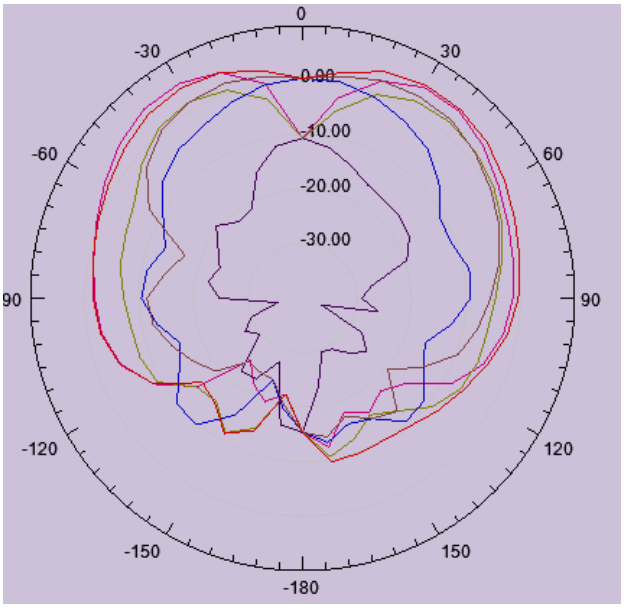

Fig. 3. Radiation Pattern of MPA

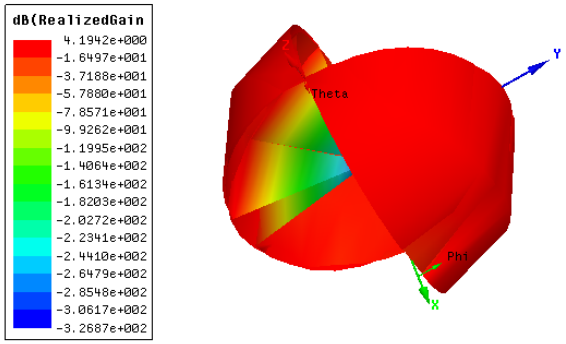

Fig. 4. Polar Plot (Gain) of the Proposed

Quantity	Value
Directivity	*3.9801*
Gain (dB)	*3.95*
Efficiency	*98.5*
VSWR	*1.2*

Fig. 5.

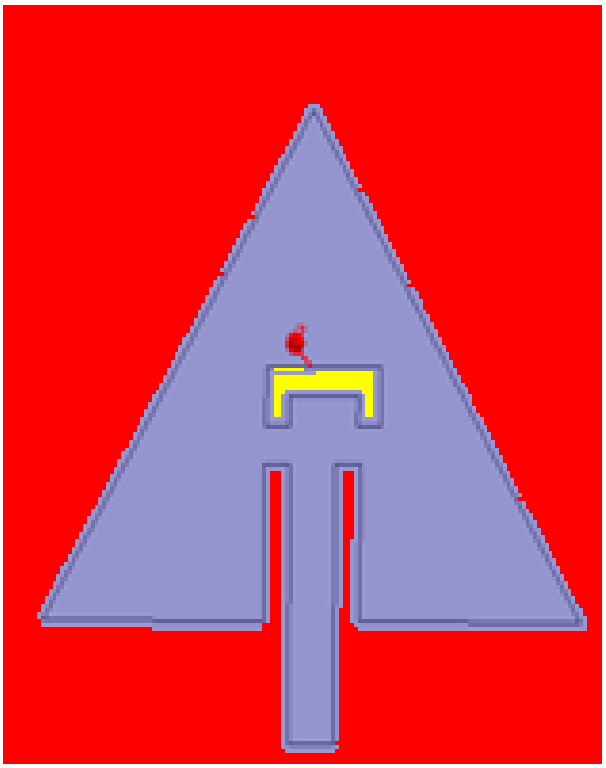

Fig. 6. Top View of the Proposed Antenna.

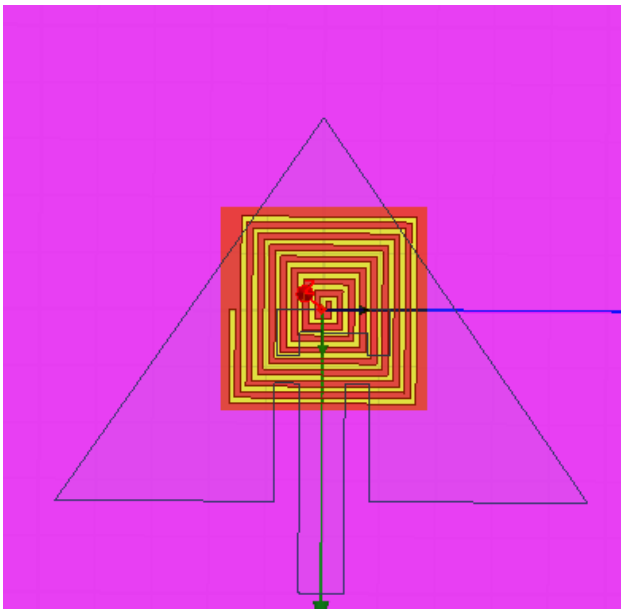

Fig. 7. Top View of the Proposed Antenna.

Parameters	Size (mm)
Substrate	*60 x60 x1.524*
Ground	*60x 60*
SR turns	*8*
Width	*0.5*
Distance	*1*
Thickness	*0.002*

Fig. 8. Dimension of the Proposed Antenna

This is depicted in Figure 7. Further at this frequencies polar plots are simulated and are shown in Figures 8,9. The antenna has FBR values hence may be some attempts may be done to curtail back radiation in further research.

II. Conclusion

Spiral resonator is used effectively in the design of this compact dual resonant antenna which can be easily fabricated using PCB techniques. The antenna is cheap and flexible in nature due to use of Rt Duroid in its design. The size reduced antenna has adequate gain, band width, directivity in its dual resonant frequencies.

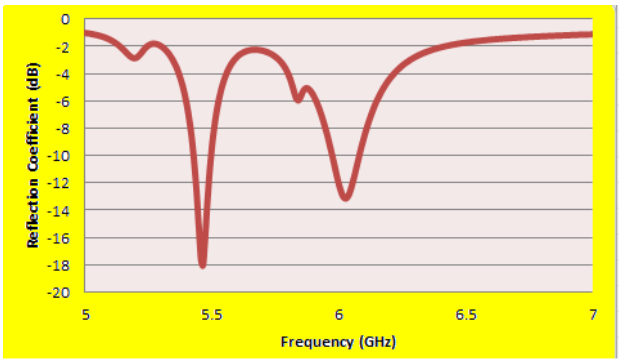

Fig. 9. Radiation Pattern of the Proposed Antenna

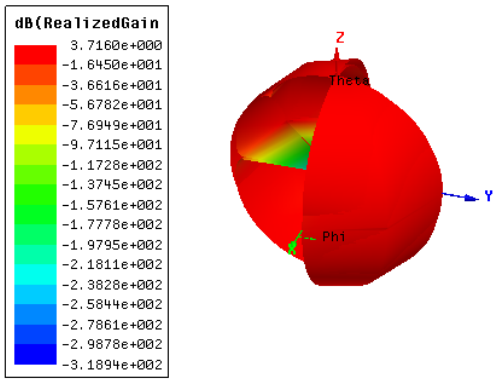

Fig. 10. Polarplot of the Proposed Antenna

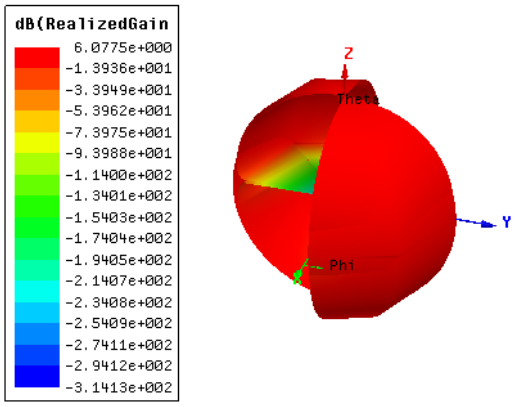

Fig. 11. Polar plot of the Proposed Antenna

Quantity	Value	Units
Max U	0.26101	W/sr
Peak Directivity	3.9128	
Peak Gain	3.332	
Peak Realized Gain	3.2801	
Radiated Power	0.83829	W
Accepted Power	0.9844	W
Incident Power	1	W
Radiation Efficiency	0.85157	
Front to Back Ratio	28.718	

Fig. 12. Simulated Antenna Parameters at 5.464 GHz

Quantity	Value	Units
Max U	0.44916	W/sr
Peak Directivity	6.0461	
Peak Gain	5.9445	
Peak Realized Gain	5.6445	
Radiated Power	0.93358	W
Accepted Power	0.94954	W
Incident Power	1	W
Radiation Efficiency	0.9832	
Front to Back Ratio	10.642	

Fig. 13. Simulated Antenna Parameters at 6.024 GHz

III. Acknowledgements

I thank the authorities of Annamalai university. I would like to thank my Guru, Dr. Khagindra Kumar Sood, Group Head, Satcom Systems and Technology Group (SSTG) Satcom and Navigation Applications Area (SNAA), Space Applications Centre, Indian Space Research Organization, Ahmedabad, India

References

[1] R. Garg, P. Bhartia, I. Bahl, A. Ittipiboon *Microstrip antenna design handbook*, Artech House, London; 2001.

[2] Jashwant S. Dahele and Kai Fong lee*On the Resonant Frequencies of the Triangular patch antenna*, IEEE Transaction on Antenna Prop. 1987;35,100-101p.1987.

[3] K.F.Lee, K.M.Luk, J.SDahele *Characteristics of the Equilateral Triangular Patch Antenna*, IEEE Transaction on Antennas Prop.1989; 36,1510-1518p.

[4] Nirun Kumprasert and Wiwat Kiranon. *Simple and Accurate Formula for the Resonant Frequency of the Equilateral TriangularMicrostrip Patch Antenna,*, IEEE Transaction on Antennas Propagation.1994; 42,1178-1179p.

[5] K. Sharma and B. Bhat*Analysis of triangular microstrip resonator. IEEE Trans. Microwave Theory Tech*, 1982; 30, 2029-2031p..

[6] Shyh-TirngFang , Kin-Luong , Tzung- Wern Chiou *Bandwidth enhancement of inset-microstrip-line-fed equilateral triangular microstrip antenna*, IEEE Transaction on Antenna Propagation, 1988; 34,2184-2186p.

[7] V.G.Veselago.The electrodynamics of substances with simultaneously negative values of , . Soviet Physics Uspeki. 1968; 10(4): 509514p.

[8] J.D.Baena, J.Bonache, F.Martin, R.Marques *et al. Equivalent circuit models for split ring resonators and complementary ring resonator coupled to planar transmission lines*, IEEE Transactions on Microwave Theory Techniques. 2005; 53(4): 14511461p.

[9] F.Billoti, A.Toscano, L.Vegni *Design of spiral and multiple split-ring resonators for realization of miniaturized metamaterial samples* IEEE Transactions on Antennas Propagation. 2007; 55(8): 2258 2267p.

[10] R.Gayathri, M.Anitha, K.K.Sood *Wideband gain-enhanced miniaturized metamaterial-based antenna for wireless applications* International Journal of Inventive Engineering and Sciences. 2014; 3(1): 2022p.

[11] R.Gayathri, M.Anitha, Alok K.Singhal *et al. Miniaturized patch antennas for wireless applications using slot-type complementary split ring resonator loading* International Journal of Applied Engineering Research. 2014; 9(22): 1737117381p.

Iris Recognizable Theft Controller with Robbery Notification Using GSM Modules

Divya
UG Scholar
Department of ECE
MRK Institute of Technology

Yogithai
Assistant Professor
Department of ECE
MRK Institute of Technology

Rajeswari
Assistant Professor
Department of ECE
MRK Institute of Technology

Sangeetha
Assistant Professor
Department of ECE
MRK Institute of Technology

Gandhimadhi
Assistant Professor
Department of ECE
MRK Institute of Technology

In this fast pacing world, the proportional to the development, crime and theft rate also on the high. In order to keep our data confidentially so that no other unauthorized person could have access on them. This paper is proposed for provides security which can be used for many banks, institutes, jewelry shops and various organization etc. Here theft controller design and development that uses the GSM modules to prevent the theft, it also includes iris recognition, GSM modules, and spray unit, auto dialing unit, 8051 microcontroller, and alert system. There are many methods of verifying authentication through password,RFID,digital locking, and figure print based security system but this system is most efficient and reliable. To prevent flee of thief automatic chloroform is sprayed when intruder found which affect the thieves who cannot do nothing. Automatic dialing unit informs the theft event to local police and to the important persons. Alert system is used to make emergency alarm to the other sides. This project mainly used as a device to avoid theft in houses, banks whenever security needs. Keywords: iris recognition,GSM, chloroform spray, Anti-Jammer, vibrating sensor.

I. INTRODUCTION

Security has been play a key role in many of our places. When we are opening the newspaper, we can see at least one robbery or burglary based news. This robbery and burglaries were done by breaking the windows, drilling, the walls and breaking the lockers. The goal of our project is to limit the crimes and robbery, this proposed work is used to secure an important properties (money, jewel, etc.).It should make a strong alert system to suppress theft rates at least to certain extent. The most secured system is Iris recognition because an iris of one person never matches the other. Biometrics Studies commonly include fingerprint, face, iris, voice, signature, and hand geometry recognition and verification. Many other modalities are in various stages of development and assessment among these available biometric traits iris proves to be one of the best traits providing good mismatch ratio, high accurate in terms of security. It should keep good communication with to arrest the thief who trying to stole the public and private properties. Hence we have made this project.

II. RELATED WORKS

Various attempts are made for providing the security for all domiciles. Up to date complex security is not discovered.

A. Lock and Key System

First step towards security was Lock and key system. Security protocol followed in this system was Single key for a single lock. Initially, this system was considered to provide at most security. But this belief was soon proved wrong by the fact that multiple keys can be easily made for a single lock. Hence this system is an outdated system to provide security.

B. Password Authentication

Next level of Security used password as an authenticating tool. This system stores password of authenticated users for the purpose of validation. System using password authentication provides considerable security to the users as it acts as a secret of authorized users. This system also have a pitfall that password can be acquired by unauthorized user by continuously trying all the possible combinations. This is also one among the hundreds of attempt made for providing security.

C. Authentication by RFID card

Next level of technological development for providing security was authentication by RFID card. This system enriched the level of security. Access is granted only for the user whose RFID code Matches with the authorized code. This system also have disadvantage of duplication of RFID card and anyone who possess this card can unlock the door.

D. Fingerprint based security system

In this finger print security system, in this mode, stored fingerprint images will be verified with the scanned images. When coming to our application the images of the persons fingerprint that are authorized to open the locker doo module with a unique id. But disadvantages of this system is it can be hacked easily.

III. Proposed work

Our proposed system overcomes all the security problems in existing system and provides high Security and efficiency. This is a perfect solution for saving/protecting one for an unauthorized entry. Iris recognition is a boon solution for these problems, which provides high level of recognition accuracy. It is more accurate and cost effective method and duplication is virtually impossible. An iris recognition System can easily perform verification. In verification, the system compares an input iris to the stored iris of a specific user to determine if they are from the same finger. Now the security of our home/office is literally in our vision.

IV. Burglary detection

Iris recognition technology uses the unique pattern of the human iris to recognize a given individuals. Iris recognition simply involves taking a picture of the iris, this picture is used solely for authentication. The iris is the annular region of the eye bounded by the pupil on the inside and the sclera (white of the eye) on the outside. Each iris is distinctive, and even the irises of identical twins are different. It is possible to detect artificial irises (e.g., designer contact lenses). In our project we are using IriShield USB MK 2120 with its capturing distance 2.5inches 3 inches from the front of camera lens. This irishield offers ultra-compact, lightweight, and low power consumption, auto capture, template generation and Matching, secure on board processing, secure data communication because of this device has its own 2048 bit RSA key securely generated on board for encryption and digital signature , and cost effective.

V. Auto dialing unit

This is an automatic alert unit. IT informs the theft event to OWNER, local police and to the important persons.

VI. Spray unit alert system

The spray unit which contains chloroform with concentration in the range of 1,500 to 30,000 ppm. When the microcontroller switches this unit, automatically chloroform will spread over the area, and the burglar gets unconscious. It leads to they cannot do anything. The alert system gives outer alert which makes emergency alarm sound to the other side.

VII. Conclusion future enhancement

The main goal of this work is to limit the crimes and robbery. There are many equipment that have designed till date. This system is cost effective, simple, and GPRS based anti-theft security has been successfully designed. It avoid the flee of thief and provides complete solution for house, banks and jewelry shops protect from the burglary or robbery. The main advantages of this security system are, Cost effective Automatic alert system Full secure for money Easy thief catcher Automatic dialing unit It used in reserved places The design that we have created very efficiently and will be best in future.for future iris recognition with face recognition also added to it thats why identification of theft is easy.

References

[1] [1]. G.Divya, A.Sabitha, D.Sai Sudha, K.Spandhana, N.Swapna, J.Hepsika*Advanced Vehicle Security System with Theft Control And Accident Notification Using GSM and GPS Modules*, IJIREEICE Vol 4 March 2016.

[2] [2]. Madhuri Lokare, Wrushali Mender *Android Based Elderly Assistive System Using Psoc*, International Journal For Innovative Research In Science Technology, Vol 3, June 2016.

[3] [3]. Kavitha, Sharma, Anand Mure *Advanced Woman Security System Based On Android,*, Internationsala Journal Of Innovative Research In Science Technology, Vol May 2016.

[4] [4]. Pritpal Singh, Tanjoit Sethi, Bihupti Bhusan Biswal, *A Smart Anti-Theft System For Vehicle Security*, International Journal Of Material And Mechanics And Manufacturing, Vol 3 No.4 November 2015.

[5] [5]. M.S.Joshi And D.V.Mahajan *ARM 7 Based Theft Control, Accident Detection And Vehicle Positioning System*, International Journal Of Innovative Technology And Exploring Engineering, Vol 4 July 2015

Performance Evaluation of Wireless Sensor Node Powered by RF Energy Harvesting

Kalaiselvi
UG Scholar
Department of ECE
MAILAM ENGINEERING COLLEGE

Sheelarani
UG Scholar
Department of ECE
MAILAM ENGINEERING COLLEGE

Kirthika
UG scholar
Department of ECE
MAILAM ENGINEERING COLLEGE

***Abstract*—Internet of Things (IoT) links the objects of the real world to the virtual world, and enables anytime, anywhere connectivity for anything that has an ON and OFF switch. It constitutes to a world where physical objects and living beings, as well as virtual data and environments, interact with each other. Large amount of data is generated as large number of devices are connected to the internet. So this large amount of data has to be controlled and converted to useful information in order to develop efficient systems. In this paper, we focus on to an urban IoT system that is used to build intelligent transportation system (ITS). IoT based intelligent transportation systems are designed to support the Smart City vision, which aims at employing the advanced and powerful communication technologies for the administration of the city and the citizens.**

I. INTRODUCTION

As the Wireless Sensor Networks have

technologically developed more rapidly and more efficiently, they have become the key source for the development of IoT. They find application in almost all

areas including smart grid, smart transportation systems, smart home, smart hospitals, and so on. The achievement of the above lead to the smart city development as mentioned by our Indian Prime Minister. The idea internet of things (IoT) was developed in parallel to WSNs. The term internet of things was devised by Kevin Ashton and refers to uniquely identifiable objects and their virtual representations in an internet-like structure. These objects may range from huge buildings, planes, cars, machines, any sort of goods, industries, to human beings, animals and plants and even their specific body parts. One of the major evolutions of WSNs will be after they are integrated with IoT. This paper aims to develop an intelligent transportation system. The future roads will be able to manage traffic congestion much better than today's networks. It has been imagined that in a span of around 20 to 30 years the existing traffic system would improve to an extent where cars can communicate with each other without any human interaction to control the traffic. Hence travel could be made smoother and safer. Sensors would be fitted in cars and these cars will be placed on the roads. These would monitor traffic and send the information wirelessly to a "central traffic control system," a hub that compiles data to feed back the information to vehicles on the road. For instance if there's lots of traffic, the central traffic control system would be told over WiFi and they in turn react by imposing speed limits that have to be followed by the vehicles in that congestion area. Since millions of money is spent on traffic congestion every year, it has been estimated that, by the implementation of smart transportation systems, the money spent will get reduced by at least 15

Fig. 1. Data flow diagram of IoT based smart parking assistance.

II. 2. PROPOSED SYSTEM

The flow diagram of the proposed system is shown in fig.1. The cars entering and leaving the parking slots are taken into count. The information thus gathered is sent to the garage management systems. Two types of sensors are employed here, Parking sensors and roadway sensors. In a similar manner two meters are used such as, existing parking meters and new parking meters. The information obtained from the sensors is passed to the sensor management systems. Parking meters send their respective data to the meter management blocks. All the information obtained above is sent to the central data management system where they are being collected and processed. They are in turn sent to the data warehouse for monitoring and storing. Hence this system helps the customers to make optimum use of the resources that are available for safer and smoother parking of their cars and vehicles. Hence there will be an orderly way of parking. Sensors identify the vacant parking spaces and send the information to the central server. On the other hand smart phone app requests for a parking space and the vehicle is directed to the available parking space. At the same time the parking fee is paid directly through the mobile app. This system can also be integrated to provide intelligent lighting of the streets. Here the street light is turned on when the street is being used by the vehicles and other times it remains switched off.

The parking assistance is provided using the following steps. Sensors detect whether a parking space is occupied and transmit data to the central server. Smart phone app requests a parking space and guides the drivers to that free space. Parking fee is directly paid through the smart phone app. Access to loading zones and residential parking zones are restricted. IoT traffic architecture comprises of RFID, Wireless sensor technologies, Ad Hoc networking and internet based information systems. Intelligent traffic IoT is divided into three layers such

Fig. 2. Table 1 Intelligent Traffic Management:

as Application layer, Acquisition layer and Network layer. Application layer is responsible for intelligent traffic management, intelligent driver management, information collecting and monitoring and information services. Network layer makes use of WiFi, 3G/4G and WiMax or GPRS. Acquisition layer employs RFID, RFID reader, WSN, Intelligent terminals.

The system makes use of wireless sensors to obtain real-time traffic information, such as traffic condition on each road, number of vehicles, and average speed. Utilization of wireless sensors is much appropriate due to their low power consumption and low cost. In order to achieve large-scale network layout, the system uses wireless cluster sensor network. Each cluster has a set of wireless sensors and each set is represented by the head node. Data at the head nodes are delivered to the backend system by means of a mobile agent. Already some new vehicles have been equipped with GPS and sensors capable of receiving and sending driving information. This information is sent to the monitor and control centre trough satellite communication facilities. GPS is connected to the wireless sensor networks which can be used for measuring driving speed and driving direction. The traditional traffic monitoring system based on image-processing technology has many limitations. The weather conditions have serious impact on this method. During heavy rain and thick fog the license plate is not clearly visible and hence the image cannot be captured. The development of e-plate based on RFID provides a better opportunity for intelligent traffic monitoring for identifying and tracking the vehicle. RFID can be used as a transponder in license plate equipped with a RFID tag and sensors. Here each car can get data it needs from the spot and deliver the data to assigned destination. The vehicle RFID tag stores information about the vehicle and the owner. Parameters such as vehicle plate number, vehicle type, speed of the vehicle, license number, the travelling location of the car are monitored and stored. This knowledge of information from every vehicle helps in estimating the number of vehicles on the road, average speed of the vehicles and the density of the vehicles on the road. The data from each vehicle is gathered or collected by means of a fixed or mobile RFID reader at each monitoring. Finally the information is sent to the central server for collecting, processing and storing. Once system connects to the internet, all information of vehicles on each road segment is immediately saved in database and can be used for any purpose and application. When a vehicle with an RFID tag passes through each monitoring station along the road, the RFID reader at those points will automatically read the tag data related to the vehicle and its owner and transmit to the wireless sensor active nodes. These nodes send accumulated data to the cluster head node. At the same time, a GPS receiver installed at the monitoring station can communicate with GPS satellites to obtain its position information that is taken as a position parameter of the vehicle. Then the data is transmitted using GPRS scheme to the real-time central database where the data is constantly updated to ensure data reliability.

III. 3. RESULTS AND DISCUSSIONS

This section describes the results obtained in the existing system. The survey is conducted for about 15 Km around Ooty. Here the location information is sent to the database every five minutes due to memory considerations and this can even be reduced. Processing system converted this raw information to meaningful data as shown in figure 2. The proposed system can function with less memory constraints and can send the location information continuously. The proposed system even provides parking assistance to the drivers on the road.

IV. 4. CONCLUSION

This paper presents a real time traffic monitoring system to solve the problem of real time traffic controlling and monitoring. The proposed system provides a new way of traffic control by the better utilization of resources. The traffic administration department can use this real time traffic monitoring information to detect the dangerous situations on the road and thereby react by imposing immediate actions. On the whole IoT will play an important role in traffic monitoring by improving the efficiency of traffic safety and travelling costs.

REFERENCES

[1] Andrea Zanella, Nicola Bui, et,al *Internet of things for smart cities* IEEE Internet of things journal vol.1, February 2014.

[2] Salim, et al. *Design and Implementation of Web-Based GPS-GPRS Vehicle Tracking System.* IJCSET December 2013.

[3] Zhu, et al. Intelligent transportation system based on Internet of Things. WAC 2012.

[4] L. Atzori, A. Iera, and G. Morabito, *The internet of things: A survey,* Computer. Networks., vol. 54, no. 15, pp. 27872805, 2010.

[5] Hasan Omar Al-Sakran *Intelligent traffic information system based on integration of Internet of Things and Agent technology*, IJACSA ,vol 6, 2015.

[6] Laisheng Xiao, Internet of Things: *a New Application for Intelligent Traffic Monitoring System, Journal of Networks*, vol 6, 2011.

[7] K. Ashton, That Internet of Things thing, *RFiD Journal*, 2009.

[8] D. Singh, G. Tripathi and A. J. Jara, A survey of Internet-of-Things: *Future Vision, Architecture, Challenges and Services*, IEEE World of Forum on Internet of Things.

[9] AnithaChepuru, Dr. K. VenugopalRao *A study on security of IoT in Intelligent Transport Systems Applications*, IJARCSEE, vol 5, September 2015.

[10] Y. Yin and J. Dalin Research and Application on Intelligent Parking Solution Based on Internet of Things, *5th International Conference on Intelligent Human-Machine Systems and Cybernetics (IHMSC)*,(2013).

[11] D. Bandyopadhyay and J. Sen, The internet of things - *applications and challenges in technology and Standardization"*, Springer International Journal of Wireless Personal Communications, 2011, vol. 58.

[12] V.Katiyar, P. Kumar and N. Chand, *An Intelligent Transportation System Architecture using Wireless Sensor Network, International Journal Computer Applications*, vol 14,2011

[13] D. Miorandi, S. Sicari, F. De Pellegrini and I. Chlamtac, Internet of things: *Vision, applications and research challenges,Ad Hoc Networks*, vol.10,2012.

THE KEY TO CONNECT SMARTHOME USING IOT

Mr.SATHYA MOORTHY.S
Assistant Professor
Department of Electronics and communication
MRK Institute Of Technology

Ms.K.POORANI
UG Scholar
Department of Electronics and communication
MRK Institute Of Technology

Ms.S.DHARANI
UG Scholar
Department of Electronics and communication
MRK Institute Of Technology

Ms.P.KEERTHIGA
UG Scholar
Department of Electronics and communication
MRK Institute Of Technology

Ms.D.ENIYA
UG Scholars
Department of Electronics and communication
MRK Institute Of Technology

***Abstract*—Automation systems are gaining popularity around the world. The use of these powerful technologies for home security has been proposed and some systems have been developed. Other implementations see the user taking a central role in providing and receiving updates to the system. We propose a system making use of an Android based smartphone as the user control point. Our Android application allows for dual factor (facial and secret pin) based authentication in order to protect the privacy of the user. The system successfully implements facial recognition on the limited resources of a smartphone by making use of the Eigenfaces algorithm. The system we created was designed for home automation but makes use of technologies that allow it to be applied within any environment. This opens the possibility for more research into dual factor authentication and the architecture of our system provides a blue print for the implementation of home based automation systems. This system with minimal modifications can be applied within an industrial application. IndexTermsAuthentication, Facial Recognition, Biometrics, Internet-of-Things, User Centric Automation.**

I. INTRODUCTION

Automation is rapidly becoming a mainstream part of the world in which we all live. People have begun to see the major advantages that this technology can bring. Houses and industrial buildings are becoming more and more focused towards being smarter than ever before. With the advances in the new technologies that are available and the new capabilities that have been created the automation of homes, buildings and working environments has become a reality. The expansion to allowing the implementation to be able to react to certain situations automatically or with some user input is something that could potentially have a huge effect on many peoples lives. People have gained an interest in making use of technology in order to make their lives easier. The main aim is to fast track the adoption of sensor technology. Making use of a mobile phone based device will hopefully allow for a rapid adoption rate, due to the popularity of these devices. With this adoption more and more people will become involved in the collection of sensor based data. This data can then be used to allow for the direct management of user centric systems, such as smart homes or within industrial applications. This use of user center /created sensor data is prejudiced by the inability of a system to impirically trust the source. Current designs of systems dont provide for a trust relationship to be created between the data (or instructions) that the user can submit and the system that will respond to this data/commands. A single PIN is no longer consider to be secure enough and a range of authentication methods have been proposed . The system that we will propose will allow for a user to submit two methods of authentication in order to provide for a more secure implementation. Inside the application the issue of privacy has also become a primary concern. The risk of external access to the system may discourage many users from making use of a automation system. Automation is an area that needs to careful consider security, especially if application involves user data. One technology that we believe could play a pivotal role in the creation of a home/industry automation system is the smartphone. The powerful operating system that has has been created and the advanced technology that is included will potentially mean that the smartphone device could act as the central technology that enables home or small industrial automation systems. These devices have also rapidly become the primary computing device for many people. The huge popularity of smartphone devices and their relative capabilities could make them the central technology for a small automation system. A well defined interoperable automation system could be created to work independent of any specific details relating to the smartphone . Our proposed system allows for the simple and effective use of an Android based smartphone to control a home in a home-based automation situation. We created both the Android application as well as the embedded

system within a home environment but designed the system to be capable of deploying within an industrial environment. The system was tested allowing control over home electrical devices (geysers, lights etc) in order to mimic a common embedded environment. The Android application provides for secure access by requiring two factor authentication. The use of biometric security features (facial recognition) as well as a user defined secret, in the form of a five digit pin code, were used to control access to the application. The user must at all times remain the primary focus of such systems and security of the system needs to be highly well thought out. The system was designed to be as interoperable with as many technologies as possible. In theory any system could be included with the current design allowing for a robust and capable implementation that focuses on ensuring easy use for the user.

II. SECURITY AUTOMATION

A number of potential security issues exist within the home. In order to help with the approach we decided to address a few key security scenarios that, we believe, affect many people on a daily basis. We do note, however, that the system we design is generic enough to be applied within almost any application with minimal additions. The security concerns that we are trying to address are listed below: Arriving late, to a dark residence, where no lights where switched on prior to arrival. Being away from the residence for extended periods of time, where criminals could be keeping an eye on the residence for activity or movement. Suspecting something suspicious inside or outside the residence Our belief is that security in these scenarios can be improved by granting the user the ability to manipulate the lights at his/her residence as well as controlling other electronic devices, such as a television or radio. The user should be able to control these devices from any remote location. The idea behind being allowed to control devices from remote locations will allow for the user to simulate activity at the residence. This will deter criminals from attempting to take advantage of the security situations seen above. Our system also takes advantage of the ability for the user to view their house from a distance, even on the other side of the world, and in some cases may be able to alert the required authorities by using the IP based camera. All the embedded devices are set to communic ate with the web server and then communicate with the Android application. The focus of our research will be on providing assistance to the home security system using the power of home automation and the advanced capabilities of the Android Platform. The aim is to produce an Android based application, providing a secure level of access, that allows for the user to monitor, control and simulate life in sections of his home. The operation of the system will be achieved using the combination of individual components as can be seen. The main component of the system will be a cellphone application running on a Android device. This will form one of the main parts of the system. The entire system will be comprised of: Web Server, Wireless Transmitter, Wireless Receiver, Switching Modules

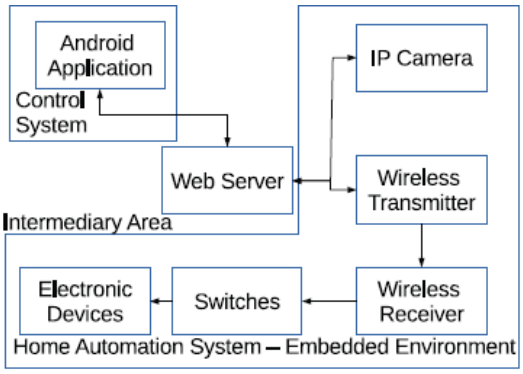

Fig. 1. Schematic of the used RF/DC rectifier

and Android Application. A. Web Server Implementing a web server is necessary to allow the user the feature of remote access to the switching and streaming devices. The web server will be the main interface between the hardware and software of the project. The main functionality of the webserver is to relay the switching commands from the application (on the cellphone) to the wireless transmitter (beginning of the embedded home automation network).

A. *Wireless Transmitter and Receiver*

A wireless transmitter is designed to transmit the data from the web server to a wireless receiver, which in turn will switch devices. Interfacing between the web server and wireless transmitter is achieved through the use of a UART interface. Data is transmitted and received by using a TCP socket connection between the two wireless modules. A maximum data transfer rate of 12 Mb/s can be achieved with the use of the wireless modules. A single byte of data is transmitted at a time so wireless transmission occurs instantly. The wireless receiver module was designed to create an access point to which the wireless transmitter can connect. On this module the TCP socket mentioned previously is opened and the device listens for an incoming connection on that socket. The data that represents the commands issued by the user via the application is received on the TCP socket. Depending on the received command the associated pin is switched.

B. *Switching Modules*

Switches were designed to switch 230V standard South African main voltage rails, using a 3V control signal set on the wireless receiver module. The switches consist of a 250V relay with a 5V DC coil, a NPN transistor switch and a 5V voltage regulator. Each switch is connected to a port of the wireless receiver as well as to the electronic device or light that needs to be switched. The use of this architecture allows for a standard guide to be followed for the implementation of home automation systems. Ensuring that the system can be used for both security as well as a number of other applications has been one of our goals.

C. Android Application

The Android application is designed as a secure user friendly interface to access the features of the product. This will be the users control mechanism for the hardware of the system. To ensure added security for the system the android application will require dual authentication for access control. The Android application is the only point of contact between the client and the embedded system.

D. Facial Recognition:

The first authentication method will be facial recognition based. The facial recognition has been implemented through the use of an Eigenface algorithm. The algorithm used to create the facial recognition system will be discussed in the next section. Performing facial recognition on board a Android based smartphone, has been a possibility for a number of Android Versions. Our system does not make use of the included API and has been created from known approaches/algorithms and have not made any use of existing libraries. The Android application will be secured making use of the facial recognition system designed. This is one piece of the two factor authentication that will be implemented in order to secure the application.

E. Pin Verification System:

As a second level of authentication, a 5-digit user specified pin was used. Implementing this second method allows two different methods of identification to be used, namely; who you are for the facial recognition implementation and what you know for the pin verification system. A 5-digit pin is used as with 5 digits, 2002 unique passcodes can be selected. This number is calculated as shown below, where n is the number of different numbers to choose and r is the number of digits that can be selected. In the chosen system 12345 and 54321 are considered to be the same, the order of the numbers is not considered. (n + r 1)!/ r!(n 1)! Through the application of both of the authentication systems to the application, a higher level of accuracy will be achieved. This will help with one of the key features of our application, which is to allow for the technology to be completely hidden from the user and still being able to provide the best experience. The application must ensure that the user has the easiest use of the entire system as possible. The technology must be able to fall to the background. This ability will allow for the user to completely experience the capabilities of the technology and not have to worry about the intricate details as to how the system achieves its goals

F. BIOMETRIC SECURITY - FACIAL RECOGNITION

Facial recognition is an ever-growing field of study in security systems. Facial recognition uses a specific algorithm to identify a person using his face through the use of an image or video feed. Various algorithms and techniques can be considered in facial recognition systems, some of the better known and computationally powerful algorithms that will be discussed here include Eigenfaces, Fisherfaces and correlation.

G. Options Available

A number of facial recognition algorithms exist. Each of the algorithms have their own strengths and weaknesses. The algorithms that we considered in the implementation of the authentication system were: Correlation, Fisherfaces and Eigenfaces.

H. Correlation and Fisherfaces

The technique of applying correlation is possibly the simplest of the recognition algorithms. This algorithm works by normalizing the training images to have unit variance and a zero mean. Using these normalized images distances on the images are measure and compared to that of the input image. Although this algorithm is the simplest to implement there are a number of drawbacks, the biggest of which is that it is computationally expensive to match the image to its closest match. Another drawback is that this algorithm is that it does not handle lighting variation well; it would need images of most of the lighting variations to work reliably. The correlation algorithm also requires large amounts of storage for all the training images under the varying conditions. The Fisherfaces algorithm relies on the principle of linear discriminant analysis (LDA) which is used to find a linear combination of features which can represent multiple classes of data. This works similar to the Eigenfaces method by computing a covariance matrix of the training images. This algorithm compares between-class scatter as well as within-class scatter where Eigenfaces mostly compares only the between class scatter. The within-class scatter is mostly due to the lighting variation in the images. This results in Fisherfaces performing much better under lighting variations as well as expression variation. Fisherfaces also functions as a dimensionality reduction method which reduces the amount of data needed to store the training images. However Fisherfaces is more computationally expensive than Eigenfaces, as more comparisons need to be computed. This makes the algorithm unfavourable for a low resource situation as is the case with many mobile devices. The use of a more computationally friendly algorithm will be greatly favoured as the user is not going to be expected to wait long periods of time for the facial recognition to be completed.

I. Eigenfaces

The Eigenface algorithm makes use of principle component analysis (PCA) which is a statistical procedure, it is used to replace original values with a smaller set of values comprised of linear combinations of the original variables(the principal components). By doing this the dimensionality of data can be greatly reduced. This is one large advantage of the Eigenface algorithm, especially in mobile applications where the available resources of the mobile device are limited. The smaller data set is used to represent the variability of the original data with the use of less data. For PCA to be implemented the data needs to be similar in size. To accomplish this some pre processing in the form of image normalization will need to be implemented. The images are captured using the front facing camera of a Samsung GT-I9300 smart phone. Implemented to

limit the effects of image orientation and background noise in the images. These images are resized to a resolution of 128128 as well as grayscaled, this forms the preprocessing step of the recognition process. The accuracy of the facial recognition implementation is affected by the number of images in the training set, as well as the threshold value used to determine recognition.

III. SYSTEM OPERATION

The facial recognition implemented on our Android based smartphone was the primary research concern for the system. Once the embedded system was created we attempted to provide added security by using two factor authentication for access to the controlling application. This was in order to assist in ensuring that the user feels safe and secure knowing that only they have access to the private details an application of this nature can provide.

A. Facial Recognition Operation

The Eigenfaces algorithm requires the use of assorted training images. These images should be captured with similar conditions and lighting. The images in the training set will be represented as vectors of the various training faces. The vectors contain the pixel intensities of the various images. A image with a resolution of N N will be represented as an image vector with a size of N2 1 In order to eliminate common data between the images, and improve the distinguishability, the mean data is subtracted, providing for a set of more distinguishable photos. Subtraction of the mean image results in a covariance matrix: C = AAT (2) where A is the matrix of the different image vectors after subtraction of the mean. This matrix then has the size of N2 N2 which, on a mobile device, is computationally infeasible. The concept of PCA allows us to reduce the dimensions of the covariance matrix by calculating C. By making use of PCA the dimensions of the covariance matrix are further reduced which results in a covariance matrix of size m M, with M being the original training set size. Making use of this the eigenvectors can then be calculated and be represented as vi, where i ranges from 1 to M. It can be seen from some matrix properties that by arranging the corresponding eigenvalues of the covariance matrix in descending order and only using some of the higher values, the more useful Eigenfaces can be used for recognition. This in turn allows for a smaller data set, increasing efficiency. Images to be recognized can be represented by a combination of the various Eigenfaces. The mean of the testing set is subtracted from the image to be recognized and multiplied with the eigenvector weights that each Eigenface contributes to the image. wk = uTk nk (3) where uT is the transposed matrix of the eigenvectors and k is the data of an image after the mean was subtracted. These weights contribute to an error value, which is compared to a threshold to determine recognition .

IV. TESTS

A number of tests were completed in order to determine the capabilities of the facial recognition system.

A. Facial Recognition Experimental Approach

The first set of tests were used to determine the most appropriate choice for the number of images to be used when training the image recognition classifier. Two key measurements were taken: the fail match rate (FMR) and the fail non match rate (FNMR). The FMR is calculated using the total number of images that get recognized. The FNMR is calculated using the number of images that do not get recognized. During the course of this test the threshold value used in the classifier is kept constant. The number of images used in the training set ranges from 25 to 50 images with a change of 5 images each time. The total accuracy of the algorithm was then calculated from these values. The next test was completed to calculate the most appropriate option for the threshold value that is used. The number of training images is kept at fifty for the duration of this test. The threshold value is calculated as a percentage of the maximum weight difference between the testing image and the Eigenfaces. The threshold value ranges between and with a change of between each test. The final test that was completed was to measure the performance of the algorithm against the number of training images that were used. Performance was measured directly by using execution time. The number of training images was compared against the total execution time for the algorithm.

B. Other Component Tests

The other components of the system were also tested. All of them successfully responded of the time. As an example the pin authentication component achieved a for the decryption of the stored pin and comparison to the entered pin only allowing access when they both matched. Multiple tests were completed on the other devices; all of which achieved perfect results.

C. Results

D. Number of Training Images Test

The result show that with an increasing number of images in the training set, the overall accuracy of the facial recognition algorithm is increased. This algorithm is run on a mobile device that has limited resources, so there has to be a trade-off between the accuracy of the algorithm and the execution time of the recognition process. An accuracy of could be achieved using images in the training set as seen in Table I. The decision on the number of images to use for training purposes is not an exact science and compromises need to be made between execution time and accuracy. It can be seen from the results that more images does not always mean a higher degree of accuracy but generally speaking the more images used allow for a greater degree of accuracy from the classifier. In order to circumvent this a more powerful device (phone) could be used, this could allow for a higher accuracy and not impact the user as much. We should also consider the effect this may have on users with older models as they should not be directly prevented from using our system, maybe a solution is to let the user decide which to favour, speed or accuracy.

E. Threshold Value:

It can be seen that in choosing a threshold value the best accuracy was achieved when using of the maximum error rate as the threshold as seen in table II. By increasing this threshold more images that were not trained on would be seen as recognized and decreasing this threshold will cause some correct images to not be recognized. As can be seen from the results the accuracy of the system begins and reaches a peak at and then begins the process of decreasing again. This is the best fit that we could achieve in order to have a high degree of accuracy for our system. It should be noted that the table has been shortened in order to limit space wastage. The testing involved continued until was reached and the highest values are shown in the table.

F. Performance Test:

The test that was run to compare the execution time, was done to find a good balance between accuracy and the time it takes to complete the recognition process. The execution time for larger numbers of training images however is quite large and would be infeasible in the system. The results for this test can be seen in figure These results show that the more training images used have a direct effect on the execution performance of the system. As the main aim of the system is usability a careful decision must be made as to what number of images to use. The user does not want to wait for an extended length of time in order to access the application.

G. General Comments

By storing the pin in an encrypted manner the security of the system is improved. One concern is the method is used to store the encryption key for encrypting the user pin. The key used for the encryption should not be hard coded into the application. This leads to the common concern area where the algorithm and methods used to secure the system are secure but the implementation is not. In future iterations of the Android operating system the requirement of encrypting the locally stored key will not be of as high an importance as Google has decided to encrypt by default all storage include on the mobile device, although this will not prevent an attack by a malicious application. In the meantime a more appropriate manner may be to use a secure certificate exchange with the web server, already included in the system, in order to retrieve the required key which is stored server side. By storing the key securely on the server it is inherently more secure, due to the fact that Android provides no fine grained permission management for external file. Facial recognition was chosen as the biometric access due to the relative ease of which other biometric systems (fingerprints) have been broken into and shown to be ineffective. A number of challenges are inherent in the current design of the system. Insufficient lighting or incorrect use of the orientation overlay of the system could negatively affect the operation of the system. The system is limited by the available resources of the device on which it is executed. If the battery power source of either the wireless transmitter or receiver is discharged. Both modules would need to be restarted for connection between them to be re-established. These problems need to be examined in future iterations of the system. The two way communication between the Android application and the web server could be used to inform the user of an alarm triggering. The web server can also implement image processing techniques and automatically record and forward a video to the user, which will come up as a simple notification, when movement is detected. A similar technique of facial recognition but applied on the web server could automatically analyze friend or foe scenarios when applied within the home. The level of security application that can be applied with the simple automation of a home using an Android mobile and a connected home is nearly boundless. Switching lights on and off, opening and closing curtains and turning music on and off at random times during the day, or night, can simulate the presence of the home owner and thereby deter criminals from assuming a easy target. With the increasing number of wireless sensor networks being deployed around the world the problem of user authentication and security is at the forefront of many implementers minds. Many approaches have been proposed to the problem of authentication of the participants within a system, one promising approach is the use of elliptic curve cryptography techniques to provide for the authentication of the communicators within the application. This approach provides for a number of advantages over our approach and is comparable to similar systems being developed. The advantage that our system provides is the use of dual factor authentication. We believe this is significantly more secure than the traditional authentication approaches Another advantage that our system can provide is the separation of the two sources of the authentication data. A separate camera from the one provided on a mobile phone can be used. This photo can then be processed and an alert on a mobile device can be used to provide the pin number on the phone for the second authentication. As an example this method will be perfect for any reconfiguration options performed on devices with cameras. The device takes my picture and submits it for authentication, while it requests the second authentication

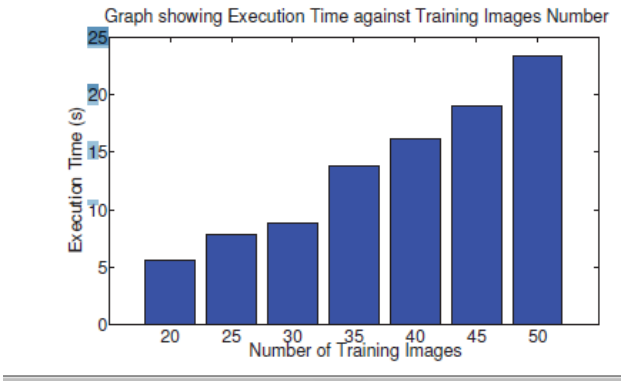

Fig. 2.

method. Once both authentications are successful the device accepts the reconfiguration settings.

V. CONCLUSION

The operation of the system is succesful and due to the design is both robust and interoperable with a range of applications within an automated home. The main aim of implementing reliable facial recognition to be used as a method of providing biometric security to the control application of a smart home has successfully been achieved. This makes the use of the smart application more enjoyable for the end user. Additionally, the implementation of a pin entry system allows for the secure access in conjunction with the biometric system and ensures secure operation of the application. From this implementation we have shown that it is possible to make use of biometric features in order to protect wireless sensor network system. Our system is also interoperable and could be deployed across a number of different application examples. The industrial application could allow employees to clock in at a given camera equipped device and providing their pin to assist with authentication. Another simple example is to enable employees to control environmental controls within their working environment from their mobile devices. Many different applications can be created from the simple application that we have shown. Some further work needs to be completed into the security of storing encrypted information on an Android smartphone. Additionally some research into new facial recognition techniques need to be completed. Although 80

REFERENCES

[1] H. Hassan, J. Martinez-Rubio, A. Perles, J. Capella, C. Dominguez, and J. Albaladejo, *Smartphone-based industrial informatics projects and laboratories,*, IEEE Transactions on Industrial Informatics, vol. 9, no. 1, pp. 557566, Feb 2013.

[2] C. Opperman and G. Hancke, *Using nfc-enabled phones for remote data acquisition and digital control,* in AFRICON, Sept 2011, pp. 16.

[3] C. Kruger and G. Hancke, *Implementing the internet of things vision in industrial wireless sensor networks,* in Industrial Informatics (INDIN),2014 12th IEEE International Conference on, 2014, pp. 627632.

[4] A. Ray, J. Akerberg, M. Gidlund, and M. Bjorkman, *A solution for industrialdevice commissioning along with the initial trust establishment,*in Industrial Electronics Society, IECON 2013 - 39th Annual Conference of the IEEE, Nov 2013, pp. 55705575.

[5] M. Jung, G. Kienesberger, W. Granzer, M. Unger, and W. Kastner,*Privacy enabled web service access control using saml and xascml*.

VHDL implementation for design of an I2C Interface for Temperature Sensor and an EEPROM Memory

Ms.Haripriya K M
Scholar
Department of Electronics and communication
CK College of engineering and technology

***Abstract*—This paper is mainly based on I2C bus controller which communicates or interface between both master and slave devices ie FPGA and temperature sensor (SE95), EEPROM memory (24C02) and SSD display for serial communication. The implementing I2C bus on Field Programmable Gate Array is more simple when compared to others because it requires only two wires and less number of connections pins. Thus in our paper we are going to design and implement I2C bus using VHDL code which interfaces FPGA board and with temperature sensor with EEPROM memory and displayed on application circuit ie SSD display and synthesized using Xilinx 13.1 platform.**

A. INDEX TERMS:

I2Cbus,Master,Slave,VHDL,EEPROM(24C0) Temperature Sensor(SE95),Xilinx

B. KEYWORD:

FPGA- Field programmable gate array., SDA Serial data line., SCL Serial clock line.,TWI Two wire interface .,I2C-Interconnect integrated circuit

I. INTRODUCTION

Communication on PCB board is achieved by using number of buses, here we are introducing I2C bus which was introduced in the year 1980 by Philips company. The main reason for using this was to reduce the connection between ICs. because it utilises two bus line signals ie SDA (serial data line) and SCL(serial clock line). By nature SDA is bidirectional and SCL is unidirectional. I2C (interconnect integrated circuit) or TWI (Two wire interface) bus is synchronous 8 bit oriented serial communication bus. I2C bus interfaces main processor and as many peripheral devices and it consists of more than one master and can have as many slaves devices such as ADC, Memory, Oscillator etc. Each devices on I2C bus have unique addresses and this address consists of 7 bit or 10 bit. In this paper we are interfacing FPGA board with Temperature sensor and the temperature sensed data can be stored in EEPROM memory and it can be displayed on SSD display.

II. INTRODUCTION

In many military network scenarios, connections of wireless devices carried by soldiers may be temporarily disconnected by jamming, environmental factors, and mobility, especially when they operate in hostile environments. Disruption Tolerant Networks (DTN) is a type of network that is designed to provide communications in the most unstable and intermittent connections, where the network would normally be subject to frequent and long lasting disruptions that could severely degrade normal communications. Also Disruption- tolerant network (DTN) technologies are becoming successful solutions that allow nodes to communicate with each other in these extreme networking environments. Typically, when there is no end to-end connection between a source and a destination pair, the messages from the source node may need to wait in the intermediate nodes for a substantial amount of time until the connection would be eventually established. Attribute-based encryption is a type of public-key encryption in which the secret key of a user and the cipher text are dependent upon attributes (e.g. the country in which he lives, or the kind of subscription he has). In such a system, the decryption of a cipher text is possible only if the set of attributes of the user key matches the attributes of the cipher text. A crucial security aspect of Attribute-Based Encryption is collusion-resistance. An adversary that holds multiple keys should only be able to access data if at least one individual key grants access.

III. I2C BUS PROTOCAL

A. I2C Specification

I2C is synchronous 8 bit oriented serial communication bus, which consists of two signal lines and one common ground. The two wires are SCL and SDA , by nature SCL is unidirectional and SDA is bidirectional, both lines are used in order to transfer the data along with the clock signal. I2C bus consists of two or more number of masters and have as many as slaves. The number of slave devices connected onto the I2C bus it is addressed by different address where address consists of 7 bit or 10 bit and can transfer any length of data . There is acknowledgment bit sent by slave to master or visa versa, to ensure the data is received after each data transfer. And it has four standardized speed modes, called standard (100 kbps), fast (400 kbps), fast- plus(1 Mbps) and high-speed(3.3 Mbps).

B. DATA TRANSFER

The data on SDA line it is stable when SCL line is high and when SCL line is low data can be exchanged. The data

which is transferred on SDA line begins with START bit and ends with STOP bit. START operation happens when SCL line is high and SDA line is at falling edge (ie from high to low) and STOP operation happens when SCL line is high and SDA line is at rising edge (ie from low to high). Once this START operation begins bus is considered to be busy, bus becomes free once STOP condition appears. This is followed by 8 bit of device address here the 8th bit is considered to be read/write. If this bit is low than it is considered to perform write operation or else read operation. This is followed by ACK signal (acknowledgement signal), which indicates that operation is successfully completed.

C. Case of Multiple Master situation

In this a problem arises -synchronization issue .

Therefore, devices are connected in such a way that they are connected as a wired AND conditions. The open drain /open collector characteristics of the FETs/Transistors/Gates in Wired AND used as the devices to control the data collision of two masters. This is obtained by Arbitration techniques. That is when one master is transmitting a High level signal, while the other is transmitting a low level signal on the SDA line, the high level signal is allowed the Low level signal is switched off. The reason being the SDA data must be in synchronous with the SCL while it is in High level. This is one way of arbitration. Another way, is that when two masters are trying to address the same device arbitration continues with the comparison of the data- bits to check the whether they are master transmitter or acknowledge bits if they are master-receiver. So the address and data is not lost during this arbitration process as it is determined by the winning master. A master that loses the arbitration can generate clock pulses until the end of the byte in which it loses the arbitration. If a master also incorporates a slave function and it loses arbitration during the address stage, its possible that the winning master is trying address it. Then the losing master should switch over to slave mode. However, the arbitration is not allowed in repeated start data, a stop condition data and a repeated start stop condition. Also the slave is not allowed in the arbitration procedure.

IV. PROPSED ARCHITECTURE

The design of this project consists of FPGA board which is interfaced with EEPROM memory and temperature sensor and the temperature sensor sense the value and those value will be written into EEPROM memory and it can be displayed on application circuit ie SSD display. This temperature sensor can be used in industry or in ovens etc in order to sense the temperature and indicate the value of the temperature. The interfacing is done using I2C bus protocol which consists two line SCL and SDA these two lines are connected to power supply using pull up resistor and these resistor values depends on number of slave devices connected to master. So if the number of slave device increase the resistor value decreases.

V. IMPLMENTATION OF I2C FOR EEPROM MEMORY (24C02)

EEPROM memory it is 256 byte ie 2k bit with 32pages each page consists of 8 byte.

A. FEATURES

Low-voltage and standard-voltage operation - 1.8(Vcc = 1.8V to5.5V). InternallyOrganized128x8(1K), 256x8(2K),512x8(4K), 1024x8(8K) or 2048x8(16K). Two-wire serial interface Write protect pin for hardware data protection

VI. DEVICE ADDRESSING OF EEPROM MEMORY

The address of all I2c bus are either 7 bits or 10 bits. The modules and all the common chips which we connect to I2c bus will have 7 bit address. This means that I2C bus can have up to 128 devices, since 7 bit number can be from 0 to 127. We always send 8 bit address , the extra bit is used to inform the slave if master is writing to it or reading from it, if bit is zero the master is writing to clave device. If bit is 1 then the master is reading from slave. For an EEPROM(24C02) device the 4 MSBs are fixed as 1010, the rest 3 bits ie A0 A1 and A2 are programmable, so we cannot maximum of 8 EEPROM(24C02) devices Figure shown below gives the clear idea of addressing byte. During transmission of data bits in I2C it transmit from MSB to LSB during implementation using VHDL .

A. Writing Data to EEPROM (24C02) Device

1. Send a start sequence 2. Send the I2C address of the slave with R/W bit low (even address) 3. Send the internal register number in which you want to write to 4. Send the data byte 5. Optionally send any further data bytes. 6. Send the stop sequence.

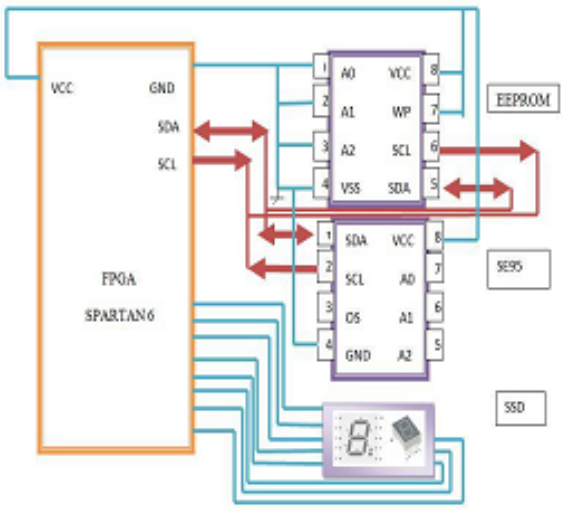

Fig. 1.

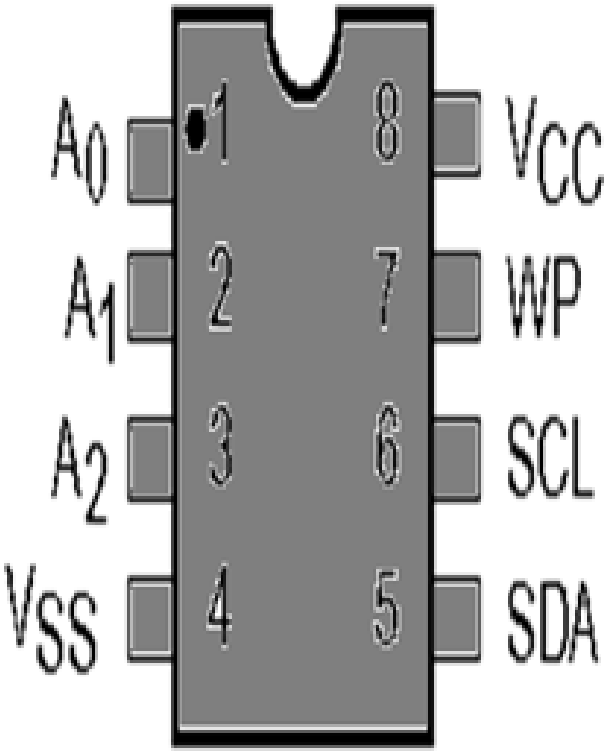

Fig. 2.

Pin Name	Function
A0, A1, A2	Device Address Inputs
SDA	Serial Data/Address
SCL	Serial Clock
WP	Write Protect
Vcc	+1.8V to +6V Power Supply
Vss	Ground

Fig. 3.

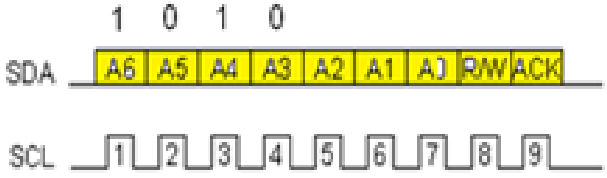

Fig. 4.

B. Reading Data from EEPROM(24C02) Device

Send a start sequence. Send 0xC0 (I2C address of the device with R/W bit low(even address). Send 0x01 (Any Internal address of the bearing register). Send a Start sequence again. Send 0xC1 (I2C address of the device with the R/W bit high (odd addresss). Read data byte from device Send the stop sequence.

VII. TEMPERATURE SENSOR (SE95)

A. General description

SE95 is a temperature sensor which converts temperature value into digital values by making use of an on-chip band gap temperature sensor with sigma delta analog-to-digital conversion techniques. And this device also consists thermal detector which detect over temperature and provides output. And by using controller via the 2 wire serial i2c bus interface can access the data registers contained in SE95. When temperature exceeds, an open-drain output (pin OS) which includes in device becomes active. And it consists three selectable logic address pins ie A0. A1, A2, so that bus can connect eight devices without address conflict.

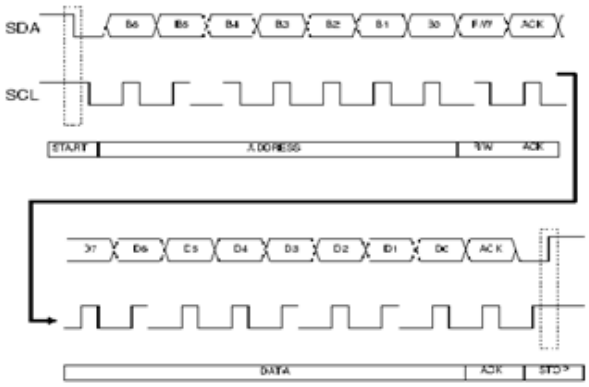

Fig. 5.

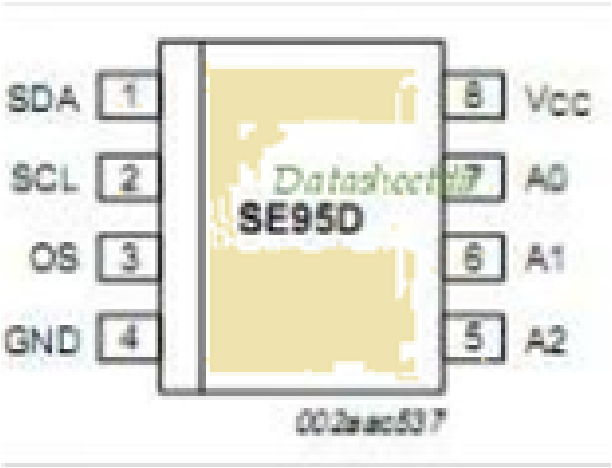

Fig. 6. PIN CONFIGURATION OF SE95

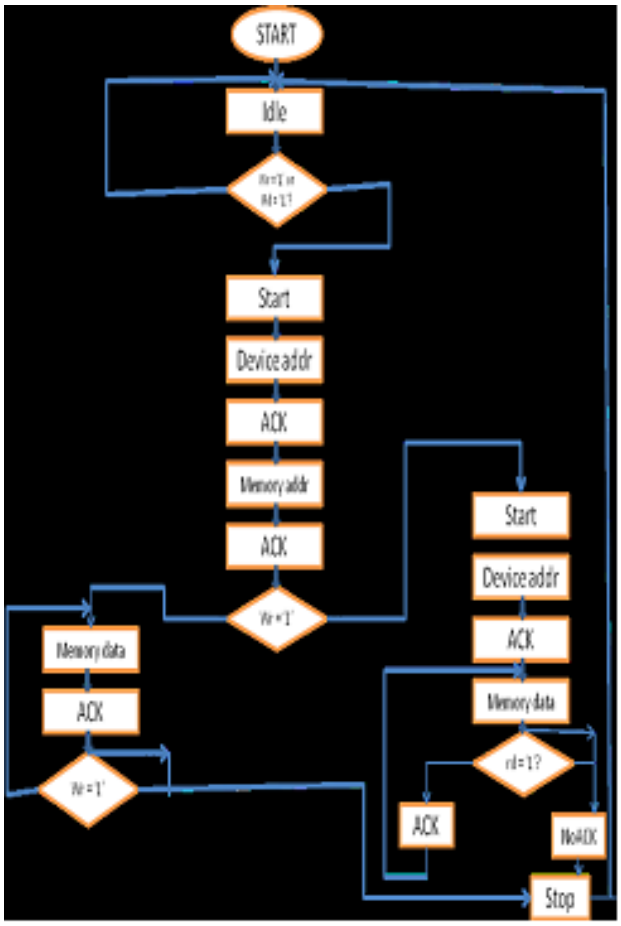

Fig. 7.

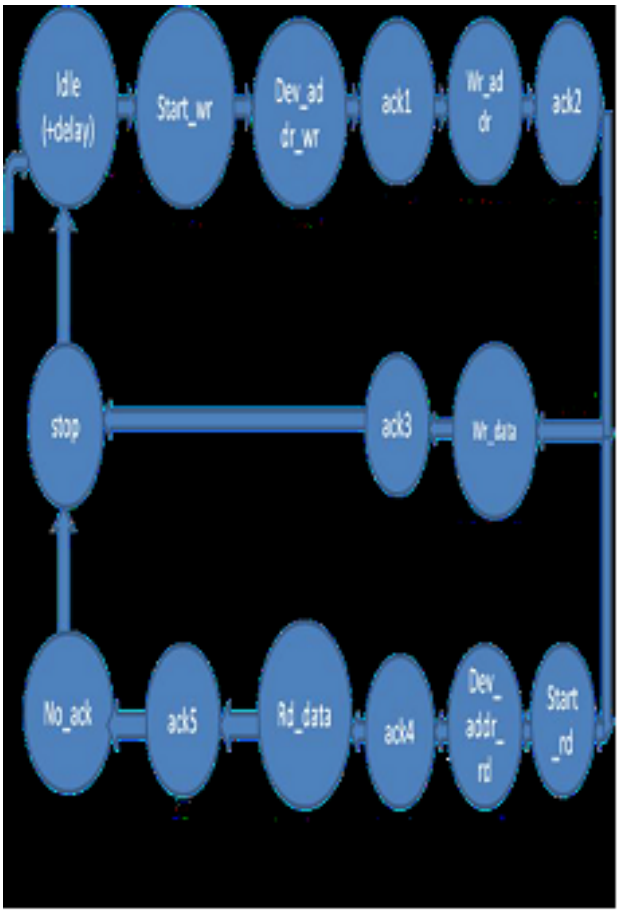

Fig. 8.

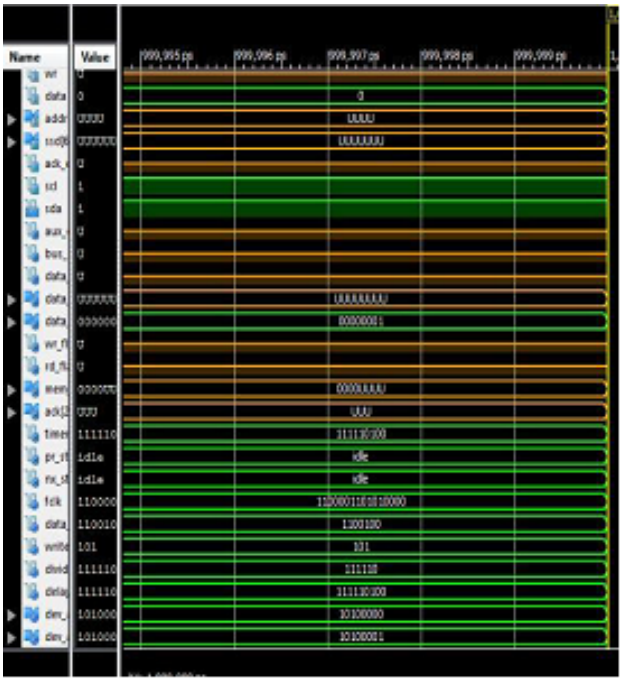

Fig. 9.

B. FEATURE

1. Temperature range from -55 C to +125C. 2. I2C-bus interface to 400kHz with 8 devices on the same bus 3. 13-bit ADC that offers a temperature resolution of 0.03125 C.

VIII. IMPLEMENTATION RESULT

I2C bus protocol is designed and implemented in VHDL using 13.1 Xilinx platform. The device waveform and device utilization summary is given below

IX. CONCLUSION:

In this Paper, we have more particularly focused on design features and utilization issues of high-quality I2C Master/Slave IPs based upon design-reuse methodology. The design process is simplified using VHDL and here 3 slaves been connected, this I2C protocol can handle as many number of slaves which helps in PCB or single board in order to connect as many peripheral devices. Therefore this protocol can be used in real time system where data cannot be lost and the design is simple because it make use of two wires.

REFERENCES

[1] *The I2c Bus Specification Version 2.1January 2000* .

A WEARABLE PATIENT HEALTH MONITORING SYSTEM USING IOT

Jeevanandham
Assistant Professor
Department of ICE
Sri Manakula Vinayagar Engineering College

T.Rahul
UG scholar
Department of ICE
Sri Manakula Vinayagar Engineering College

***Abstract*—Recently there has been a need to incorporate the use of mobile computing devices in hospital or clinical applications to enhance patient care. Internet of Things (IoT) makes all objects interconnected and it has been recognized as the next technical revolution. This paper presents a Internet of Things based system, aimed at improving healthcare and assistance to dependent people at their homes. In Internet of Things patient's parameters get transmitted through medical devices via a gateway, where it is stored and analysed. The significant challenges in the implementation of Internet of Things for healthcare applications is monitoring all patients from various places. Thus Internet of Things in the medical field brings out the solution for effective patient monitoring at reduced cost and also reduces the trade-off between patient outcome and disease management. Monitoring patient's Electrocardiogram(ECG) and Blood Pressure using Raspberry Pi board.**

I. INTRODUCTION

The unpredictable growth of the Internet of Things is changing the world and the rapid drop in price for typical IoT components is allow public to innovate new designs and products at home. IoT can be used in monitoring patients health, for making smart home and smart city. The unexpected occurrence in patients are monitored using IoT. In this paper specialized sensor is used to monitor patients ECG and Blood Pressure.

One of the key learning platforms for IoT is the Raspberry Pi. The Raspberry Pi is a popular platform became it offers a complete Linux server in a tiny platform for a very low cost. The Raspberry Pi also allows interfacing services and actuators through the general purpose I/O pins.

The combination of Raspberry Pi and IoT becomes a new innovation technology in healthcare system. Raspberry Pi is act as a small clinic after connecting these (ECG and Blood Pressure) sensors. Raspberry Pi is works as small clinic in many places. Raspberry Pi is collect

data from sensors and then it transfer wirelessly to IoT website. Raspberry Pi board is connected to the internet, that board MAC address is registered to the internet. After that in IoT website, add MAC address of this board. Then the sensors output is connected to the IoT website and GSM Module is provided to send the medical report via Text messages to the third party and doctors in case of emergency.

II. LITERATURE SURVEY

Modre-Osprian [1] monitors blood pressure level using Keep In Touch (KIT) and closed loop healthcare services. In KIT method, KIT is connected to the JAVA based mobile phone with the help of near field communication. It works on magnetic , inductive coupling and then the distance is short. After touching the KIT, the data is send to mobile phone. In closed loop services, the data is getting from mobile phone, then the data is send to the secure website. Using this website anybody can monitor patients blood pressure level.

Junaid Mohammed [2] monitors patients ECG wave anywhere in the world using IOIO- OTG Microcontroller. Android application is created for ECG Monitoring. IOIO-OTG microcontroller is connected to android phone using USB cable (or) Bluetooth dongle. After collecting data, the wave is send to android application. Monitor and store ECG waves in that android based application.

Mohammed S. Jasses [3] focused on body temperature monitoring using Raspberry pi board in cloud based system. In that paper, Raspberry pi is monitor body temperature and then these parameters are transfer by wireless sensor networks (WSN). Then these datas are added to the cloud based websites. Using this website monitor body temperature.

Hasmah Mansor [4] monitors body temperature using LM35 temperature sensor. The LM35 temperature sensor is connected to the Arduino Uno board. After that creating a website in SQL database format. Arduino Uno board is connected to that website. Then sensor output is send to the website. Using this website anybody can monitor body temperature in login process.

Mathan Kumar [6] discussed about monitors ECG, Respiration rate, heart rate and body temperature. These sensors are connected to PIC16F887A microcontroller. After

collecting data from sensors, the data is upload to the website manually. For monitoring purpose created an android application and webpage for monitoring health status.

Nithin P. Jain [8] monitors temperature, blood pressure, heart rate of patients. Microcontroller AT Mega 32 is used for connecting these sensors. GSM module is connected to this microcontroller. After collecting data, if the value is low SMS is send to the doctor.

Soumya Roy [9] monitors ECG waves of patients. AT Mega 16L microcontroller is used for monitoring ECG waves.

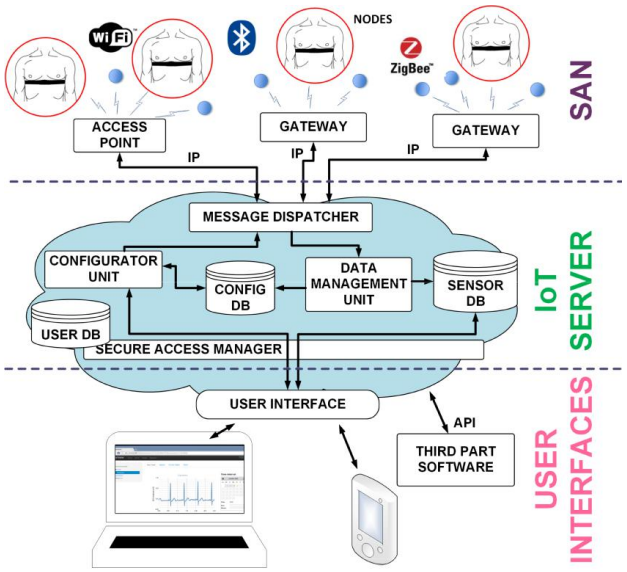

Fig. 1. Overview of ECG Blood Pressure Monitoring system using Raspberry Pi

ZigBee module is used for transferring ECG waves. ZigBee module is sends data to nearest connected sys tem for ZigBee.

Rajeev Piyare [10] implement controlling and monitoring home appliances using android b ased smart phone. Arduino uno board is connected to home app liances (light, fan, etc). Creating an android application for this smart home. Arduino uno board and android app is con nected by internet. Using this android app controlling and monitoring home appliances anywhere in the world.

Karandeep Malhi [7] monitors body temperature, heart rate using C8051F020 microcontroller. Wearable sensors are used to collect data and then send to micro controller. Zigbee module is connected to this microcontroller and then that module is transfer data to the nearest receiver .

In this paper we have ECG Blood Pressure reading results are monitored. These sensors signals send to the Raspberry Pi via amplifier circuit and signal conditioning unit (scu), because the signals levels are low (gain), so amplifier circuit is used to gain up the signal and transmit the signals to the Raspberry Pi. Raspberry pi is a linux based operating system works as a small pc processor system. Here patients ECG Blood Pressure is measured using respective sensors and it can be monitored in the monitor screen of computer using Raspberry Pi as well as monitoring through anywhere in the world using internet source. Raspberry Pi is programmed for the particular project need that via USB dongle (or) Ethernet for patient's health

monitoring through internet. It sends all the current health data of the particular patient to the web database. Anybody can access the web and can see the health of patients.

Sensor and actuator nodes (SANs). Lightweight wearable ECG sensors and other ambient sensors collect data and send them in real time via a wireless protocol (ZigBee, Bluetooth, WiFi) to a gateway connected to the home ADSL router (Fig. 1).

Both the gateway and the message dispatcher are transparent at the logical communication level between sensors and IoT server. The architecture has been developed with the aim of enabling the integration of sensor networks based on different networks protocols (WiFi, ZigBee, Bluetooth) The only component aware of the local sensor network protocol is the gateway, which runs a firmware that can manage the corresponding protocol. The gateway encapsulates the packets of the sensors in a universal format which preserves all the information present in the native format. Hence sensors send messages in their native format to the IoT server, where the data management unit extracts information and enters it in a universal format into the sensor database. When sensors need to be configured or interrogated, the configurator unit prepares a command according to the target sensor protocol. The IoT server converts the raw payload from heterogeneous nodes into a universal format, containing object identifier, object type, measurement unit, data field, geographical position, and timestamp. Then, it makes the data available to applications and users. In this way, data visualization and processing is separated from measurement and data collection, and does not need to take into account the communication protocol of the originating source. In addition, the IoT server receives data from users in order to configure and manage the SANs.

The main components of the IoT server are illustrated in the cloud of Fig. 1, since they can be part of a distributed information system. The message dispatcher manages the bidirectional communication with the sensor networks, using no information on the network protocol or on the type of application. The data management unit is a collection of software modules interpreting data from sensors and storing them in a universal format in the sensor database. The configurator unit receives inputs from users or applications and translates them into protocol-specific commands to the SANs, consulting the configuration database. Finally, the secure access manager provides access to stored information and SAN configuration only to authorized users and applications, according to information contained in the user database.. User interfaces. The entire system is configurable and controllable through an intuitive web interface from any computer, smart phone or tablet connected to the internet. In the IoT server, health data can be combined with other data, merged, processed by users and/or authorized clinicians.

Users with proper access rights can monitor the current sensor status, or query and visualize data in a specific time interval. In Fig. 2, the ECG data visualization thought the web interface is shown

An ECG device generally consists of an analog frontend (AFE) circuit and a signal processing circuit. The AFE circuit capabilities and requirements mainly depend on the ECG application. Many aspects of the design of an ECG AFE depend on the ECG signal characteristics. The ECG is a graphical representation of the electric potential difference created on the body surface by heart contraction, which can be detected at different body locations. ECG devices can have a different number of leads, from one to a maximum that is

Fig. 2. ECG user interface

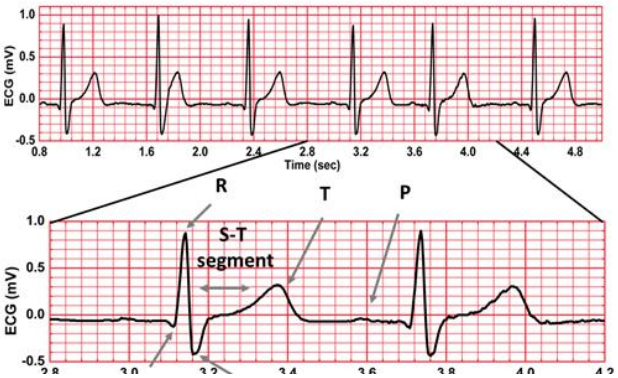

Fig. 3. Sensors output from Raspberry Pi board

usually 12, depending on the target application. For monitoring purposes, a one-lead AFE is usually adequate, since only macroscopic behaviours are of interest.

The ECG signal consists of three main components:

1. the actual differential ECG signal;
2. the differential time-varying ECG offset;
3. the common-mode signal.

The actual ECG signal has a bandwidth from 0.05 Hz to 150 Hz. It has a peak-to-peak amplitude of approximately 1 mV but can reach 3 mV. Blood pressure sensor is fixed with ECG in band for better communication with raspberry pi 3 model B board. Thus the simplified structure of the system has clearly explain that check the human physical parameters and send the signal to the raspberry board. That saved signal is transfer to the IOT and saved permanently. By using IOT, we can save data for many year and keeping records with safe. At the same time the message has to be transfer to the patient and doctor mobile through GSM module.

III. .RESEARCH AND DEVELOPMENTS

Technology plays an important role in today's world like industries, personal life's, environment and agriculture fields. Among these fields health care process is the most important field and crucial also. The improvement of medical equipments and devices also plays a significant contribution for technology development in health care devices. This process is produces doctor's for new technology to monitor private use. Patient's also connect video conference to the physicians for improving their health status. It also reduces patient's money and waiting time at hospitals. Using this technology development, patient's record their health status in their own mobile phone and then store the data.

IV. CONCLUSION AND FUTURE WORKS

We have proposed a wireless wearable ECG Blood Pressure monitoring system embedded in an IoT platform that integrates heterogeneous nodes and applications, has a long battery life, and provides a high-quality ECG signal. The system allows monitoring multiple patients on a relatively large indoor area (home, building, nursing home, etc.). Another remarkable feature of our system is a very low marginal cost per added sensor, since our architecture enables a single low-cost gateway to manage multiple sensors.

After connecting these sensors to the Raspberry Pi board, there are two ways to access the output. One is directly connected to the monitor, keyboard, mouse to the Raspberry Pi board and got output in monitor screen. The another method is Raspberry Pi board is connected to a laptop (or) computer using data cable After that install putty software to the respective system. Change IP address, Subnet mask, gateway to that system. Then open that putty software output will display in that screen.

Future work will focus on monitoring additional health-related parameters using a broader combination of transducers, sensors, and correlation techniques, and on improving system reliability and robustness to patient movement and connectivity losses.

REFERENCES

[1] Andrea Zanella, Nicola Bui, et,al *Internet of things for smart cities* IEEE Internet of things journal vol.1, February 2014.

[2] A. Dohr, R. Modre-Osprian, M. Drobics, D. Hayn, G.Schreier, *"The Internet of Things for Ambient Assisted Living*, Seventh International Conference on Information Technology, pp 804-809,2010.

[3] Junaid Mohammed, Abhinav Thakral, Adrian Filip Ocneanu, Colin Jones, Chung-Horng Lung, Andy Adler,*"Internet of Things: Remote Patient Monitoring Using Web Services and Cloud Computing*, 2014 IEEE International Conference on Internet of Things (iThings 2014), Green Computing and Communications (GreenCom2014), and Cyber-Physical- pp 256-263,2014

[4] Mohammad S. Jassas, Abdullah A. Qasem, Qusay H. Mahmoud,*" A Smart System Connecting e-Health Sensors and the Cloud A Smart System Connecting e-Health Sensors and the Cloud* Proceeding of the IEEE 28th Canadian Conference on Electrical and Computer Engineering Halifax, Canada, pp 712-716,May 3-6, 2015.

A Survey on Artificial Intelligence

Ms.C.Adithya
Assistant Professor
Department of Electronics and Communication Engineering
St.Annes College of Engineering and Technology

Mrs.C.Suganya
Assistant Professor
Department of Electronics and Communication Engineering
St.Annes College of Engineering and Technology

Ms.J.Revathi
Assistant Professor
Department of Electronics and Communication Engineering
St.Annes College of Engineering and Technology

***Abstract*—This paper reviews the meaning of artificial intelligence and its various advantages and disadvantages including its applications. It also considers the current progress of this technology in the real world and discusses the applications of AI in the fields of heavy industries, gaming, aviation, weather forecasting, expert systems with the focus being on expert systems. The paper concludes by analyzing the future potential of Artificial Intelligence.**

I. INTRODUCTION

Artificial intelligence (AI) is defined as intelligence exhibited by an artificial entity to solve complex problems and such a system is generally assumed to be a computer or machine. Artificial Intelligence is an integration of computer science and physiology Intelligence in simple language is the computational part of the ability to achieve goals in the world. Intelligence is the ability to think to imagine creating memorizing and understanding, recognizing patterns, making choices adapting to change and learn from experience. Artificial intelligence concerned with making computers behave like humans more human like fashion and in much less time then a human takes. Hence it is called as Artificial Intelligence. Artificial intelligence can be divided into parts according to philosophy of AI. a) Strong AI b) Weak AI

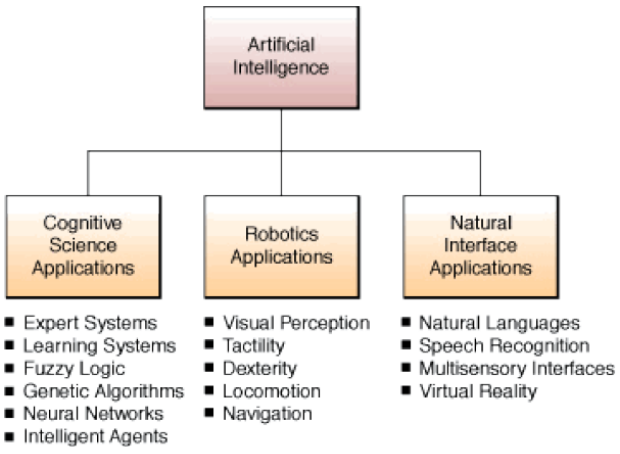

Fig. 1. Overview of Artificial intelligence

II. STRONG AI

The principle behind Strong AI is that the machines could be made to think or in other words could represent human minds in the future. Thus Strong AI claims that in near future we will be surrounded by such kinds of machine which can completely works like human being and machine could have human level intelligence. If that is the case, those machines will have the ability to reason, think and do all functions that a human is capable of doing. Current research is nowhere near creating strong AI, and a lively debate is ongoing as to whether this is even possible .

III. WEAK AI

The principle behind Weak AI is simply the fact that machines can be made to act as if they are intelligent. Weak AI simply states that thinking like features can be easily added to computer to make them more useful tools and this already started to happen. For example, when a human player plays chess against a computer, the human player may feel as if the computer is actually making impressive moves. But the chess application is not thinking and planning at all. All the moves it makes are previously fed in to the computer by a human and that is how it is ensured that the software will make the right moves at the right times. More examples of Weak AI are witness expert systems, drive by wires cars and speech recognisation systems Artificial Intelligence (abbreviated as AI) is the capability of a device to perform activities, which would otherwise only be expected of the human brain. These activities include the capacity for knowledge and the ability to acquire it. It also comprises of the ability to judge, understand relationships and last but not least produce original thoughts. Intelligence = perceive + Analyse + React Also, there is a huge different between short term memory and RAM. Short-term memory holds pointers to the long-term memory where all the information is actually stored while RAM stores data that is isomorphic to data being held on a hard disk. Also, RAM has a memory limit while there seems to be no capacity limit when it comes to short-term memory.

IV. TURING TEST

The Turing test is a test of a machine's ability to exhibit intelligent behavior. The test was introduced by Alan Turing

in his 1950 paper Computing Machinery and Intelligence. The original question behind this test was Can machines think? . The test proceeds as follows a human judge engages in a natural language conversation with one human and one machine, each of which tries to appear human. All participants are placed in isolated locations. If the judge cannot reliably tell the machine from the human, the machine is said to have passed the test. In order to test the machine's intelligence rather than its ability to render words into audio, the conversation is limited to a text-only channel such as a computer keyboard and screen. Sufficiently many interrogators are unable to distinguish the computer from the human being then it is to be concluded that the computer thinks.

V. ADVANTAGES AND DISADVANTAGES

One of the major advantages of artificial intelligence is that its decisions are based on facts rather than emotions. Even after our utmost efforts, it is a well-known fact that human decisions are always affected in a negative way by our emotions. Unlike humans, machines with artificial intelligence do not need any sleep, thus overcoming the inherent disadvantage of tiredness in humans. Easier spreading of knowledge. Once an artificial mind is trained for something, it can be very easily copied to the others reducing the time wasted in otherwise passing on knowledge to other humans through training. Lack of creativity in responses Inability to explain the logic and reasoning behind a certain decision. Current development is at a stage where the AI cannot know when there is no solution to a particular problem. Any malfunctioning can lead to the AI producing wrong solutions and since it cannot explain the reasoning behind its answer, blind reliance on AI can lead to problems. Lack of common sense in reasoning can also cause major problems. It can be used to cause mass scale destruction if given in the wrong hands.

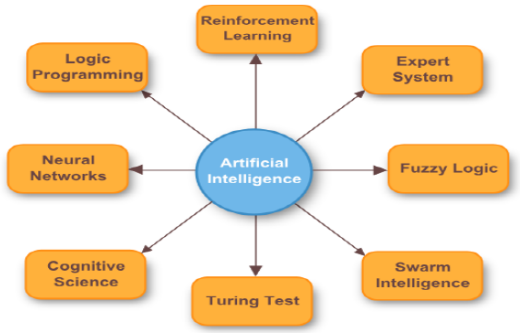

Fig. 2. Areas of Artificial Intelligence

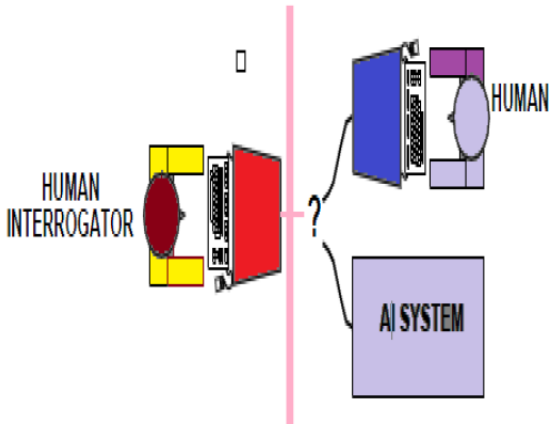

Fig. 3. Turning Test for Checking machine intelligence

All this being said, one of the most concerning problem with the development of AI is that it will soon start substituting humans in every field thus causing a high rate of unemployment, which would lead to depression, crime and poverty. Also, there are some fields that require the human touch and there is a growing sense of belief that machines will quite possibly never be able to replace humans. The caring behavior of nurses in hospitals is one example of a job that humans feel machines will never be able to do justice to.

VI. CURRENT PROGRESS

Artificial Intelligence was created with the sole aim of mimicking or even outperforming human minds. Thus it is very important we question the fact whether it has actually been able to do so. It cannot be ignored that the fact of AI is being used all around us especially in the fields of medicine, robotics, law, stock trading etc. It is being used in homes and big establishments. such as military bases and the NASA space station. NASA has sent out artificially intelligent robots to planets so as to learn more about their habitat and atmosphere, with the intention of investigating if there is a possibility of humans living on these planets. Expert systems have been used by Mercedes Benz and other auto manufacturers in the design of vehicle components, subway systems in Washington, D.C. use expert system software controllers to cause subway trains to stop within 3 inches of the right spot on the platform. These trains have motormen primarily to reassure passengers. AI has filtered into general applications in these fields and has become so common that it is not referred to as Artificial Intelligence anymore. Blind supporters of AI would point to the time when AI Deep Blue II defeated chess master Garry Kasparov to prove that Artificial Intelligence can in fact be smarter than humans. Though there is no doubt that the AI Deep Blue II won that game, it is still probably one of the dumbest software alive. The operators were programming the AI in every round depending on the oppositions last move. Also, the Deep Blue II had studied all of Kasparov? s previous games while the latter wasn? t given the same benefit. One can safely say that even though the Deep Blue II AI defeated Kasparov, it was never a fair fight to begin with. Latest technologies like Xbox 360? s Kinect and iPhone? s Siri use algorithms based on Artificial Intelligence, but it is a well-known fact that these technologies are a long way from being perfect. Thus we can safely conclude that though Artificial Intelligence has made a lot of progress in the past few decades, it is not at a level where in one can confidently state that it is now ready to completely replace the human mind. That being said, large-

scale research is now being conducted into the field of proper simulation of the human brain. Cortex is a project by Artificial Development Inc. and Swiss government's IBM sponsored Blue Brain Project, are two main ventures, whose goal is to simulate the human brain.

VII. APPLICATIONS

Artificial Intelligence in the form of neural networks and expert systems has applications in almost all human activities. The combination of high precision and low computation time makes AI a cutting edge technology. Robot ES? s are already taking over workshop level jobs in large industries, thus side lining humans into a more supervisory role. Stock brokerage firms are now using Artificial Intelligence to analyze data, make analysis and buy or sell stocks without the interference of any human beings. Some of the applications of Artificial Intelligence are as follows- A. Gaming Industry- One of the most commonly known applications of AI in the gaming industry is its use in chess. Even though these machines are not as intelligent as humans, they use brute force algorithms and scan 100? s of positions every second so as to determine the next move. As stated earlier, AI is also being used in Microsoft Xbox 360? s Kinect for body motion detection. But it is still in its infancy and requires a lot more advancement for it to be used in day-to-day applications. B. Heavy industries- Artificial Intelligence robots have become very common in heavy industries and are employed in jobs that are otherwise considered dangerous for humans. These robots also increase the efficiency, as they do not need any break while working thus overcoming the inherent disadvantage of tiredness in humans.

C. Weather Forecasting- Neural networks are nowadays being used for predicting weather conditions. Past data is provided to the neural network, which then analyses the data for patterns and predicts the future weather conditions. D. Expert Systems- Expert Systems are machines that are trained to have total expertise in specific areas of interest. They are developed to solve the problems in niche areas. These

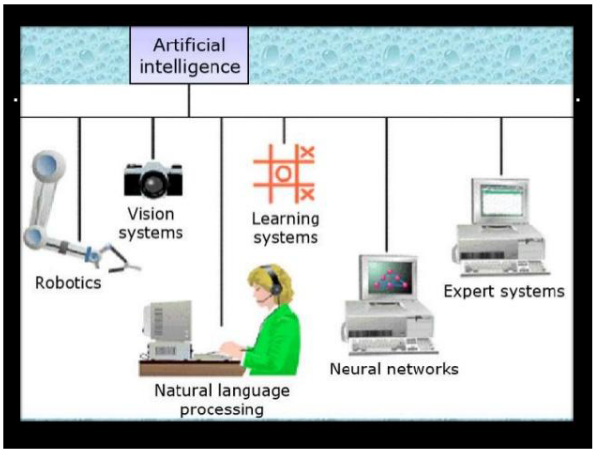

Fig. 4. AI Applications

Fig. 5. Pattern matching AI applications

systems use statistical analysis and data mining to solve these problems by deducing the solutions through a logical flow of yes-no questions. An expert system is made up of 3 parts- Knowledge base- It stores all the information, rules, data and relationships that are needed by the expert system to have total expertise in its area of interest Inference engine- It seeks information from the knowledge base on being presented with a query, analyses it and responds with a solution or recommendation in the way a human expert would Rule- It is a conditional statement that links the given conditions to the final solution E. Data Mining or Knowledge Extraction: Data mining is a fast-growing area. Data mining is a part of a process called KDD knowledge discovery in databases. This process consists basically of steps that are performed before carrying out data mining such as data selection, data cleaning, pre-processing of data, and data transformation. "Data Mining is the use of computer algorithms to discover hidden patterns and unsuspected relationships among elements in a large data set. AI is a broader area than machine learning. AI systems are knowledge processing systems. Knowledge representation, knowledge acquisition, and inference including search and control, are three fundamental techniques in AI.

F. Knowledge representation: Data mining seeks to discover interesting patterns from large volumes of Data. These patterns can take various forms, such as association rules, classification rules, and decision trees, and therefore, knowledge representation becomes an issue of interest in data mining.

VIII. FUTURE ASPECTS

The use of artificial intelligence will lead to production of machines and computers, which are much more advanced than what we have today. Speech recognition systems will reach much higher levels of performance and will be able to communicate with humans, using both text and voice, in unstructured English. There will be a great future some day for expert system applications in all aspects of health care, in both clinical and administrative areas, in improving patient care and in allocation of financial, social, and other resources.

But when it comes to the question of Artificial Intelligence creating machines, which are more intelligent than human beings, no one seems to have the answer. Also, even if it is possible, the amount of time it will take cannot be predicted. It is also expected to have human brain features like learning from experience, cognition and perception. Whether human consciousness will be incorporated in these machines is still not known. Robots in the future will be able to do everybodys work and will be faster and more efficient as compared to human beings in doing it. If one is ill, they can hire a robot nurse that will provide them with medicines at proper intervals. Thus it can be safely said that Artificial Intelligence is still in its embryonic stage and its future depends only and only upon the scientists solving the mystery of the human brain. Till that is done, no one can make a conclusion of whether our future will be affected positively or negatively by Artificial Intelligence.

IX. CONCLUSION

The computing world has a lot to gain or benefits from various AI approaches. Their ability to learn by example makes them very flexible and powerful. Furthermore there is no need to devise an algorithm in order to perform a specific task i.e. there is no need to understand the internal mechanisms of that task. They are also very well suited for real time systems because of their fast response and computational times which are due to their parallel architecture. The goal of artificial intelligence is to create computers whose intelligence equals or surpasses humans. Achieving this goal is the famous AI problems from last decade researchers are trying to close the gap between human intelligence and artificial intelligence.

REFERENCES

[1] George F Ludger *Artificial Intelligence - Structures and strategies for complex problem solving* ,5th Edition, Pearson, 2009.

[2] Girish Kumar jha *Artificial Neural Networks and its applications* ,international journal of computer science and issues 2005.

[3] Xindong Wu, Senior Member, IEEE *Data Mining: An AI Perspective* ,vol.4 no 2 (2004)

[4] Satvika Khanna et al. *Expert Systems Advances in Education* ,NCCI 2010 -National Conference on Computational Instrumentation CSIO Chandigarh, INDIA, 19-20 March 2010

[5] Kaijun Xu *Dynamic neuro-fuzzy control design for civil aviation aircraft in intelligent landing system* ,Dept. of Air Navig. Civil Aviation Flight Univ. of China 2011.

[6] Eike.F Anderson. *Playing smart artificial intelligence in computer games* ,The National Centre for Computer Animation (NCCA) Bournemouth University UK.

[7] K.R. Chaudhary *Goals, Roots and Sub-fields of Artificial Intelligence* ,MBM Engineering College, Jodhpur, India 2012

DATA BROADCAST IN MOBILE ADHOC NETWORKS USING SECURED KEY MANAGEMENT ALGORITHM

Ms.B.Mary Amala Jenni
Assistant Professor
Department of ECE
St.Annes's CET

Mrs. D. Umamaheshwari
Assistant Professor
Department of ECE
St.Annes's CET

Mrs. M. Vaidehi
Assistant Professor
Department of ECE
St.Annes's CET

***Abstract*—In recent trend, MANET (Mobile Adhoc Networks) plays a vital role in all applications. MANET is an infrastructure less network, it sends the information through intermediate nodes. It is for security issues the intermediate nodes cannot be a trusted one. Security plays a major role, it can be provided with the help of key management. Our aim is to provide secure methods for handling cryptographic keying algorithms. Key management includes generation, distribution and maintenance. Even if lot and lot of security techniques was proposed with small circumstances. In this paper, we proposed an algorithm for the purpose of sending the data in secured way in a mobile Adhoc network.**

I. INTRODUCTION

Mobile Adhoc network is a Self configuring network of mobile nodes connected by wireless links, to form an arbitrary topology. The network nodes are interconnected through wireless interfaces and unlike traditional networks lack specialized nodes. MANET having dynamic network topology, in which the network may change frequently. Nodes can be move around within the network but the network can also be split into many smaller networks, which can be merged with other networks.

MANET having limited bandwidth than other traditional networks. This may limit the size and usage of the message. MANET use batteries as a power source. The nodes consume high power, while using complex algorithms and operations.

MANET has a limited physical security. The use of wireless communication and the exposure of the network nodes increase the possibility of attacks against the networks. There are many security issues in MANETs like secure multicasting, secure routing, and privacy aware routing. Key management is to provide secure methods for handling cryptographic approaches.

The main role of key management schemes involves generation, distribution and maintenance. Cryptographic schemes involves in symmetric andasymmetricmechanisms.

Symmetric encryption involves, same keys are used by the sender and the receiver. Same key is used for both encryption and decryption of the data. Asymmetric encryption uses two party key. One of the key is public and the other key is private. Public key is known by all the users and the private is used by the specific sender and the receiver. The key management service must ensure that the generated keys are securely distributed to their owners. In public-key cryptography the key distribution mechanism must guarantee that private keys are delivered only to authorized parties. In MANET there are various Key Management Schemes proposed.

To secure communications in Mobile Ad Hoc Networks (MANETs), messages are often protected by encryption using a chosen cryptographic key, which, in the scenario of group communication is called the group key proposed in [1]. Multicast [2] is a communication service that provides data delivery from a source to a set of recipients, also known as multicast group. Secure group communication systems typically rely on a group key, a secret shared by all members of the group. Privacy is obtained by encrypting all data with the group key. The key management system controls access to the group key, ensuring that only authenticated members receive the key.

In mobile ad hoc network, it is little difficult to establish a secure connection between the source and the destination. The malicious nodes or the devices can counterfeit identified to make fake trust relations with each other and then it slowly started attacking the mobile Adhoc network. Such nodes would drop all the data packets which is received that they need to

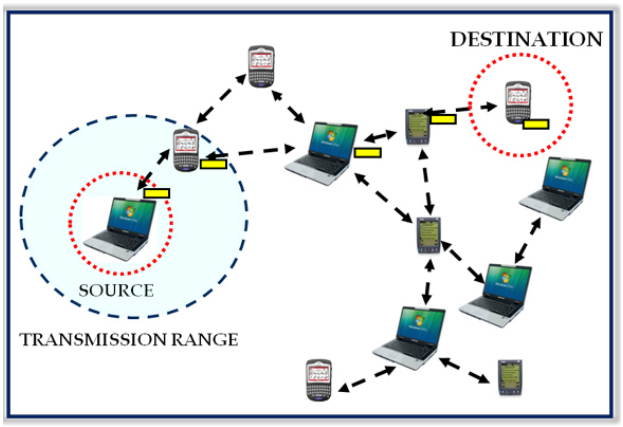

Fig. 1. Mobile Adhoc network

transmit the data towards the destinations.

II. OVERVIEW OF KEY MANAGEMENT SCHEMES IN MANET

Key management can be defined as a set of techniques and procedures supporting the establishment and maintenance of keying relationships between authorized parties.

2.1. Cryptographic Mechanisms Cryptographic mechanisms involves in encryption and decryption of datas. The process of converting plain text into cipher text is called as encryption and converting the cipher text into plain text is called as decryption. For the above two process we are in a need of secured information called as key. This key may be categorized into two types, private key and public key. Private Key is a random secret key; it uses some sort of algorithms to encrypt and to decrypt the data. Private Key plays important role in both symmetric and asymmetric cryptography. In Symmetric encryption mechanism, the sender and the receiver uses same key for encryption as well for decryption. The problem in symmetric encryption mechanisms is once if the key is missed or broken then the security is lost while exchanging the information. As in the case of asymmetric cryptography, two different mathematical mechanisms are used, based on the complexity and the length of the private key used, its security depends.

III. PROPOSED ALGORITHM

The main objective of this work is to communicate securely with each other in a mobile Adhoc network. This is possible only when the key is highly protected from the hackers. This algorithm involves in four different steps as follows: 1. Secret head Selection 2. Secret algorithm Selection 3. Secret keys determination 4. Group creation 5. Sharing of keys 6. Transmission of datas 7. Share verification of keys 8. Digital Signature 9. Reconstruction of datas.

The proposed techniques are as follows. Initially, in a mobile Adhoc network many nodes are actively participated without any infrastructure mechanisms. In order to provide the security, the base station which first selects the cluster head randomly. Then the cluster head decides the intermediate nodes involved in transmitting the data from source to destination, the intermediate nodes are decided based on the traffic, Payload , battery capacity etc., The working module is classified and categorized into nine modules as mentioned above. Initially the base station can select the cluster head based on some of the parameters like traffic, battery capacity, etc., and then the secret key determination is processed and shared between the authenticated nodes in order to transmit the data in secured way.

Digital signature is another secured way to transmit the data. Whenever the data is transmitted between the intermediate nodes, all the nodes which are involved in transmission of data must authenticate themselves by means of digital signature. The digital signature must be verified once it is processed. But it cannot be communicated with the intermediate nodes in prior. Then based upon the asymmetric mechanism a pair of private protective key is generated namely PPk1 and PPK2. PPk1 is a key which is shared only with the source node, intermediate nodes between source and destination and the destination node. Whereas PPK2 is a secondary private key this is shared only between the sender and the receiver. This PPK2 key is changed only after a particular seconds, that must be updated only between the sender and the receiver. PPk1 is a key which is shared only with the source node, intermediate nodes between source and destination and the destination node. This is key used between the intermediate nodes, only with the help of the key the users could able to find the information where the data is come from and where we need to send next. For every transmission of data, the nodes should be verified by the digital signature. So that we could able to find secure

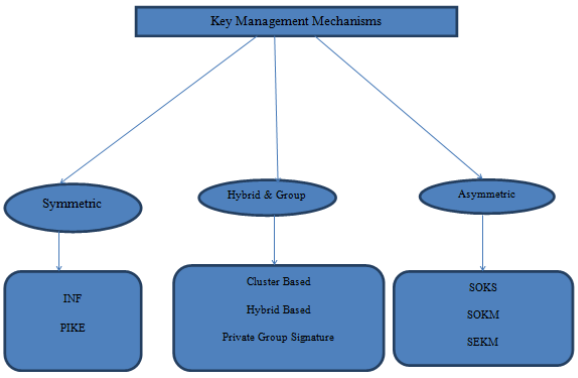

Fig. 2. Basic key management mechanisms

Fig. 3. Flow chart of proposed System

transmission of datas.

IV. CONCLUSION

In mobile Adhoc network, security plays a major role. Though various algorithms proposed they were small discrepancies present. In this paper a new methodology is proposed to transmit the data in secured manner by means of pair of protective key with a digital signature. This will transmit the data in more secured way, as we implement this type of mechanisms in military, cyber applications. By this methodology, we can secure the data in a major level in mobile Adhoc networks.

REFERENCES

[1] [1] Bing Wu, Jie Wu, Yuhong Dong *An efficient group key management scheme for mobile ad hoc networks*,Int. J. Security and Networks.Vol. 2008.

[2] [2] V. Palanisamy, P. Annadurai *Secure Group Communication using Multicast Key Distribution Scheme in Ad hoc Network*,2010 International Journal of Computer Applications (0975 - 8887) Volume 1 No. 25.

[3] [3] Valle, G. and Cerdenas, R. *Overview the key Management in Ad Hoc Networks*,ISSADS pp. 397 406, 2005.

[4] [4] Wu, B., Wu, J., Fernandez, E., Ilyas, M. and Magliveras, S. *Secure and Efficient key Management in mobile ad hoc networks*,v.

[5] [5] R. Pushpa Lakshmi, A. Vincent Antony Kumar *Cluster Based Composite Key Management in Mobile Ad Hoc Networks* ,International Journal of Computer Applications, vol. 4- No. 7, 2010.

[6] [6] CAPKUN, S., HUBAUX, J., AND BUTTYAN, L *Mobility helps peer-to-peer security*,IEEE Trans. Mobile Comput. 5, 1, 4351,2006.

[7] [7] ABDUL-RAHMAN, A. AND HAILES, S *A distributed tust model*,In Proceedings of the ACM New Security Paradigms Workshop,1997.

[8] [8] DAHILL, B., LEVINE, E., ROYER, E., AND SHIELDS, C *An efficient group key management scheme for mobile ad hoc networks*,Tech. rep. UM-CS-2001-037.University of Massachusetts, Amherst, MA.

[9] [9] S. Radha Rammohan *Anomaly Detection in Mobile Adhoc Networks (MANET) using C4.5 Clustering Algorithm*,International Journal of Information Technology Management Information System (IJITMIS), 7 (1), 2015, pp. 01-10.

[10] [10] Priyanka Yadav and Deepa Chaurse *Survey and Analysis of Security Issues in Vehicular Adhoc Network*,International Journal of Electronics and Communication Engineering and Technology (IJECET), 5(3), 2016, pp. 7078.

WITH BEST COMPLIMENTS FROM

VEDHA SYSTEMS

Contact us:
34-B, West Main Road,
Brindavanam,puducherry-605013

0413 224 0890, +91-9443 344 890
Email: info@vedhasystems.in
http://www.vedhasystems.in

Veda systems(vs)are one of the fastest and leading distributors of branded electronic products in Pondicherry. We are providing the best servics to customers so as we being ranked, one of the authorised product distributors. Our service and customer support has been specifically designed to solve the neds of our customer as quick as ossible. Our products are branded and delivered on time to its customers; we supply high quality brands of electronic products like Canon, Panasonic, Matrix,ESSI, Honeywell, Samsung to customer's satisfication.

Pacer
Innovative Power Solutions Since 1992

Contact us:
No. 242, Old No. 92/2, L. B Road,
Thiruvanmiyur Chennai - 600041, Tamil Nadu, India.
+91-8048601957
Email: info@pacerups.com
http://www.pacerups.co.in/

Pacer Power Solutions Private Limited is manufacturer, supplier and wholesaler of UPS Systems & Voltage Stabilizers. This whole range of products is made complying with the set norms and standard of the industry. Owing to follow an ethical business policy, we have garnered numerous customers in the market. Some of them are Anna University, Chennai, Tamil Nadu, Palmer and Laurie Limited, Chennai, Tamil Nadu and Haldia Petrochemicals Limited, Chennai, Tamil Nadu

WITH BEST COMPLIMENTS FROM

JAYAM ELECTRONICS

Contact us:
No:12/21,1st Main Road, Venkateswara Nagar, Velachery, Chennai-600 042, Tamil Nadu.
+91 96772 52848
Email: jayamelectronicsje@gmail.com
http://www.jayamelectronics.in/

Jayam Electronics hereby inform that we are manufacturing Electrical and Electronics lab equipments since 2005. Now we are supplying Electronic Instruments and Experimental trainer kits for (Electronics & Communication Engineering lab) and (Electrical & Electronics Engineering lab) for Engineering Colleges and Polytechnic Colleges in all over India. We had supplied our equipments for Central Government Institute CIPET (Central Institute of Plastics Engineering & Technology) in centers like Chennai, Ahmadabad, Lucknow and Bhubaneswar.

Contact us:
21, Raj Nagar,3rd Street,
Shanthi Nagar, Opp Vasantham Super Market,
Madurai.
9042129799
Email: asmiagi@yahoo.com
http://asmiassociates.com/

Asmi Associates leading marketing company in stationery in Tamilnadu. Our company was established in 2008. We started with caltrix electronic industries a calculator company and now we have spread our wings for more than 6 companies, such an stylish pens, lezing, mark pencils etc., In caltrix calculator last year we supplied more than 60 engineering colleges and more than 30 polytechnic colleges in Tamilnadu. Last year we sold out more than 60,000 scientific calculators for various student segments from our company. We have a strong sales network in Tamilnadu.

WITH BEST COMPLIMENTS FROM

WITH BEST COMPLIMENTS FROM

WITH BEST COMPLIMENTS FROM

WITH BEST COMPLIMENTS FROM

St. Anne's College of Engineering and Technology,
Anguchettypalayam, Panruti - 607 110,
Cuddalore dt.
www.stannescet.ac.in
stannescet@gmail.com
04142 - 241661, 242661

ISBN 978-93-5254-811-8